ASB American Society of Biomechanics

FOUNDED IN 1977

ABSTRACT BOOK

ASB Annual Meeting

AUGUST 5 - 8 2024

Monona Terrace Community and Convention Center

Madison, WI

www.asbweb.org

#ASB2024

DO ALTERED SPINAL LOADS AFTER LIMB LOSS INFLUENCE LUMBAR SPINE AXIAL CREEP DEFORMATION?

Steven D. Voinier[1-3*], Pawel R. Golyski[2,3], Brad D. Hendershot[2-4], Courtney M. Butowicz[2-4]
[1]Oak Ridge Institute for Science and Education; [2]Walter Reed National Military Medical Center; [3]Extremity Trauma & Amputation Center of Excellence; [4]Uniformed Services University of the Health Sciences, Bethesda, MD,
*Corresponding author's email: steven.d.voinier.ctr@health.mil

Introduction: Low back pain (LBP) is exceedingly prevalent after transfemoral limb loss (TFL), potentially resulting from alterations in trunk-pelvic motions and spinal loads during daily activities [1]. During walking, modeling and simulation work suggests that the combination of increases in trunk motions and muscle activations impose up to 60% greater mechanical loads on spinal tissues in persons with vs. without TFL [1]. Repeated exposures to increased spinal loads can induce a larger creep response in spinal tissues, increasing intervertebral joint and facet joint laxity [2], decreasing spinal stability [3] and ultimately adversely affecting spine health risk for LBP [4]. While simulations can provide estimates of the mechanical environment within the spine based on model assumptions, ex vivo mechanical testing allows for a more direct evaluation of actual tissue behavior. Thus, the objective of this study was to compare estimated differences in spinal creep characteristics, as a potential precursor to spinal injury or degeneration, of individuals with and without TFL using an ex vivo porcine model of the lumbar spine and axial loading trajectories derived from spinal loads estimated during walking among persons with and without TFL. We expected that the larger spinal loads experienced by persons with TFL during walking would increase the corresponding spinal creep deformation profiles compared to persons without TFL.

Methods: Four (4) cadaveric porcine lumbar spines were dissected from the T15 to sacrum ~15 minutes postmortem and stored at -30° C. Non-structural soft tissue and musculature were removed, preserving ligaments, facet joints, and intervertebral discs and the T15/L1 vertebrae and sacrum were potted. A servohydraulic materials testing system applied time-varying compressive load profiles, derived from walking simulations of persons with (peak: 901 N) and without (peak: 675 N) TFL [1], repeatedly at a frequency of 0.89 Hz for 90 minutes (corresponding to over 4800 gait cycles). Each spine sample underwent both loading conditions (in a randomized presentation order), and spines were submerged in 1X PBS solution for ~24 hr to normalize disc hydration levels between conditions. Deformation data (i.e., axial displacement) were sampled at 102 Hz. Specimens were initially ramp loaded (3 second ramp) to the first load in the gait cycle (0% gait) before continuing with the gait cycle loading. Deformation during the initial ramp load was considered the elastic deformation. Creep was calculated as the difference between measured deformation throughout the test and the elastic deformation. Creep data were smoothed via a moving median algorithm and down-sampled to 1 Hz. The relative ratio in creep deformation was calculated between sample-specific loading conditions (i.e., with vs. without TFL).

Results & Discussion: Axial creep deformation after the first gait cycle was ~1.5X higher in the TFL vs. control condition (Fig 1) but decreased to ~1.3X by 50 minutes. The initial creep response reflects strain after a fully hydrated condition, which unlikely occurs within a daily loading paradigm due to the slow disc rehydration rates [5]. As expected, the increase in TFL load increases poroelastic creep, but the long-term asymptotic creep is also controlled by the low permeability of the annulus fibrosis periphery [6]. Thus, the temporally insensitive ~1.3X increase likely represents the more realistic discrepancy between the TFL and control conditions. This increase in long-term strain from the TFL loading paradigm reflects the diminished ability for the disc to adequately pressurize the annulus to support load [7].

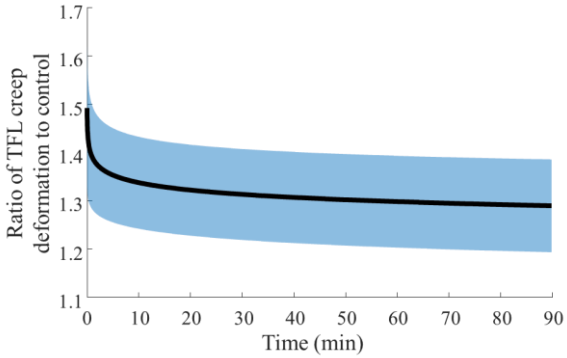

Figure 1: Mean relative ratio in axial creep deformation of transfemoral limb loss (TFL) vs. control loading condition, as a function of experimental time.

Significance: The increased creep and altered mechanical environment from repeated exposures to elevated spinal loads with TFL gait may be a predominant contributing factor that predisposes the lumbar spine to injury. This is the first known study to implement population and activity-specific load to evaluate the mechanical response of spinal tissues among persons with lower limb loss. While the current testing protocol did not account for the corresponding kinematic profiles commonly observed during walking in persons with TFL, which may exacerbate discal creep and introduce stress concentrators in spinal structures, future work will combine these population- and activity-specific load and kinematic (both multi-axial) profiles to determine their individual and interactive effects on spinal tissue characteristics (we expect these results by time of conference).

Acknowledgments: This research was supported in part by an appointment to the Department of Defense (DoD) Research Participation Program administered by the Oak Ridge Institute for Science and Education (ORISE) via an interagency agreement between the U.S. Department of Energy (DoE) and the DoD (contract number DESC0014664).The views expressed herein are those of the authors and do not necessarily reflect the official policy of the Uniformed Services University of the Health Sciences, DoD, nor the US Government.

References:[1] I. Shojaei *et al.*, *Clin. Biomech.*, 2016.; [2] I. Busscher *et al.*, *Clin. Biomech.*, 2011.; [3] M. Solomonow *et al.*, *Spine (Phila. Pa. 1976).*, 1999.; [4] J. Abboud *et al.*, *J. Neurophysiol.*, 2018.; [5] G. D. O'Connell *et al.*, *J. Mech. Behav. Biomed. Mater.*, Oct. 2011.; [6] P. P. A. Vergroesen *et al.*, *J. Biomech.*, 2016.;[7] P. P. A. Vergroesen *et al.*, *Osteoarthr. Cartil.*, 2015.

IN VIVO VERTEBRAL DISPLACEMENTS VIA DIGITAL TOMOSYNTHESIS AND VOLUME CORRELATION

Yener N. Yeni[1,2*], Daniel Oravec[2], Roger Zauel[2], Sudhaker Rao[1,2], Michael J. Flynn[2]
[1] Henry Ford Health + Michigan State University Health Sciences, Detroit, MI, USA
[2] Henry Ford Health, Detroit, MI, USA
*Corresponding author's email: yeni@bjc.hfh.edu

Introduction: Vertebral fractures are the most common type of osteoporotic fracture and associated with significant complications. Identification of at-risk individuals is important for timely intervention to prevent a vertebral fracture. The current standard assessment of bone quality based on bone mineral density (BMD), even supplemented with measures of bone texture and risk factors, is useful but not accurate. Digital tomosynthesis-based digital volume correlation (DTS-DVC) has recently been introduced as a biomechanics-based assessment for vertebral bone quality [1]. Inspired by a laboratory technique that combines microcomputed tomography with mechanical loading for mechanical assessment of extracted bone structures, DTS-DVC makes use of supine and standing DTS images of a patient in combination with DVC. In vitro studies have shown vertebral displacement and stiffness measured from DTS-DVC correlate well with those from microcomputed tomography and have ability to predict vertebral strength [2, 3]. In vivo studies are limited to a proof-of-concept demonstration of the method with one patient [1]. The purpose of the current study was to characterize in vivo measurement error of DTS-DVC-derived vertebral displacement metrics and to examine the extent to which DTS-DVC can measure differences in vertebrae due to loading and presence of vertebral deformity (vertebral fracture).

Methods: Nineteen patients, 7 with at least 1 confirmed vertebral fracture (Fx) and 12 with no vertebral fracture (NFx), were recruited with informed consent under IRB approval. The Fx and NFx groups were not significantly different in age (63.7 ± 11.9 vs 64.3 ± 7.1 yrs), BMI (25.6 ± 4.6 vs 25.4 ± 3.3 kg/cm^2), BMD (0.814 ± 0.096 vs 0.843 ± 0.092 g/cm^2) or T-score (-2.34 ± 0.90 vs -2.42 ± 0.98) ($p>0.52$ to $p>0.94$). The participants were imaged twice in supine (U, "nonloaded"), once in standing position (S, "loaded"), and once in standing position while holding a 3.78kg weight (milk jug) in each hand (SL, "standing with load"). Image acquisition was performed using DTS (Shimadzu Sonialvision Safire II) with the participant in the AP view (producing a stack of coronal plane images).

DVC analysis was performed as previously described [1]. From DVC, endplate-to-endplate displacement (D_{DVC}) and standard deviation of superior endplate displacements ($SD.D_{DVC}$) were calculated. Compliance (C_{DVC}) was estimated using D_{DVC} and previous relationships between patients' body weight and vertebral loads [4, 5]. Using repeat unloaded scans of 5 normal patients, accuracy, precision and total measurement errors were calculated. Statistical analysis was performed using the linear mixed model framework in JMP (Cary, NC), with significance set at $p<0.05$.

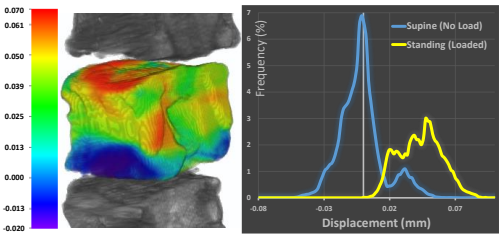

Fig. 1. In vivo 3D distribution of displacements in L1 vertebra of a 60 year old female patient, measured using DTS-DVC (left). Endplate-to-endplate displacement and noise distributions (right).

Results & Discussion: Displacements resulting from standing were well separable from the background noise and overall exhibited the expected gradients from the bottom to the top endplates (**Fig. 1**), allowing for the intended stiffness calculations. Based on repeat scans, accuracy, precision, and total measurement error was 0.0044 mm, 0.0758 mm, and 0.0759 mm, respectively. The top endplate displacement achieved by standing was 20 to 26 times the mean noise for the T12 and L1 levels. At the T12-L1 level of patients in the NFx group, load was significant for D_{DVC}, $SD.D_{DVC}$ and C_{DVC} ($p<0.0001$, $p<0.0001$, $p<0.004$, respectively), with no interaction between vertebral level and load ($p>0.06$ to $p>0.99$). Post-hoc analysis revealed that D_{DVC} was higher for SL than for S ($p<0.04$), and both higher than U ($p<0.001$) (**Fig. 2**). These results indicate that DTS-DVC measures meaningful displacements in response to perturbations to vertebral load in vivo.

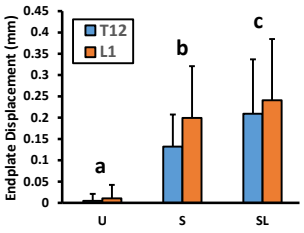

Fig. 2. D_{DVC} in intact vertebrae ("a", "b" and "c" different).

When the fractured and adjacent nonfractured vertebrae were compared within the Fx group, we found a significant interaction between load and group ($p<0.02$) for $SD.D_{DVC}$, post-hoc analysis indicating that $SD.D_{DVC}$ increases for S ($p<0.0001$) and SL ($p<0.0003$), only in the fractured vertebrae (**Fig. 3**). These results suggest that endplates deform more nonuniformly in fractured than intact vertebrae, and that DTS-DVC can detect mechanically compromised vertebrae. There were large differences in D_{DVC} (30%), $SD.D_{DVC}$ (55%) and C_{DVC} (11%) between intact L1 vertebrae of Fx and NFx groups; however, these were not statistically demonstrable. As such, while DTS-DVC may have diagnostic capability, further work is needed to establish its predictive capability for vertebral fracture.

Significance: This study demonstrates in vivo feasibility of the DTS-DVC method. A biomechanics-based assessment of vertebral bone quality is expected to improve our understanding and clinical assessment of vertebral fracture risk.

Acknowledgments: Supported by NIH R21AR070363.

References: [1] Oravec (2019), *Med Phys* 46:4553-62; [2] Oravec (2020), *Med Eng Phys* 84:169-73; [3] Yeni (2023), *J Biomech Eng* 145:041009; [4] Lee (2013), *Ergonomics* 56:832-41; [5] Iyer (2010), *Clin Biomech* 25:853-8.

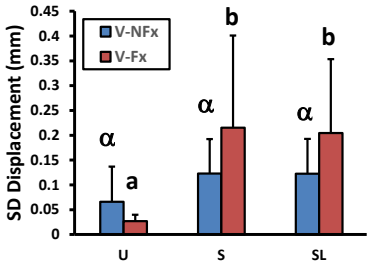

Fig. 3. $SD.D_{DVC}$ in fractured (V-Fx) and adjacent intact vertebrae (V-NFx) in the Fx group ("a" and "b" within V-Fx different, α in V-NFx not different).

LUMBAR SPINE POSTURAL CHANGE DURING PREGNANCY

Robert D. Catena[1*], Shenghai Dai[1], Brett T. Allaire[2], Jacob J. Banks[2], Dennis E. Anderson[2]
[1] Department of Kinesiology and Educational Psychology, Washington State University
[2] Beth Israel Deaconess Medical Center and Harvard Medical School
*Corresponding author's email: robert.catena@wsu.edu

Introduction: Understanding spine postural changes that occur during pregnancy could have a significant impact on clinical management of gestational pain and help address biological questions about pregnant hominin spine evolution. Attempts have been made to model musculoskeletal changes during pregnancy [1], however, the lack of vertebral angle adjustments between time points of pregnancy in these models may be a significant limitation. Perhaps due to the lack of available information, clinicians and researchers have ignored how spine posture influences gestational biomechanics, including loads on the low back and pelvis.

Little is known about whether and how the spine adapts to pregnancy because of imaging contraindications for this population. It remains common practice to rely on palpable bony landmark positions to approximate spine and pelvic changes during pregnancy. We recently published on how the wide range of changes to lumbopelvic posture influence balance control and gait energetics in the latter half of pregnancy [2]. However, this work was limited to examining only the end of 2nd and start of the 3rd trimesters. Questions remain about lumbopelvic adaptations throughout the majority of pregnancy.

Since many clinicians and researchers believe lumbar vertebrae are forced into a "gestational lordosis" (increased lumbar angle) during pregnancy [3], the first aim of this study was to track lumbar spine curvature over a more complete window of pregnancy. Second, since we suspect spine curvature to be unrelated to gestational time [2], we examined whether concurrent body and torso anthropometry changes through pregnancy moderate the spine posture change. And in our third aim, we examined if measures at earlier time points can be used by clinicians and ergonomists to predict low back angle change in their patients.

Methods: Eleven pregnant individuals were tested eight times in ~4-week intervals from ~10 to ~38 weeks gestation. Body and torso anthropometry was measured. Torso center of mass (tCOM) position [4] and vertebral spinous processes (Fig 1) were tracked by motion capture. Lumbar angle was estimated from marker data through three methods (see Fig 1 caption for definitions). Aim 1 was addressed with a standard regression between gestational time and lumbar angles. Aim 2 was addressed with forward-step multiple regressions between anthropometry and lumbar angles. Aim 3 was addressed with cross- and auto-correlations between different time points.

Results & Discussion: Aim 1: None of the lumbar lordosis angles were correlated with gestational time ($r<0.2$). But, consistent with our previous study [2], the (lack of) relationship seemed to mask that some individuals (n=7) increased, and some (n=4) decreased lumbar lordotic curvature throughout pregnancy. An intrinsic factor(s) seems to be moderating the relationship between gestational time and standing spine posture.

Aim 2: Lumbar angles during pregnancy were correlated with three anthropometric measures ($r>0.6$): BMI, torso depth, and tCOM height [4]. These results further indicate that what was classically thought of as "gestational lordosis" is more a product of the individual's anthropometry rather than pregnancy. tCOM relationships may indicate the importance of fetal positioning in the uterus affecting low back posture change.

Aim 3: Inter-session lumbar angle varied enough that there was little auto-correlation ($r<0.4$). However, both first testing (at 10 weeks) and immediately preceding testing (testing 4 weeks earlier) tCOM position and BMI were better correlated ($r>0.4$) with lumbar angle. These results further support individual anthropometry before pregnancy, and fetal positioning during pregnancy, as potential predictors of low back angle change, but future work is needed to actually determine the relationship between tCOM and fetal positioning.

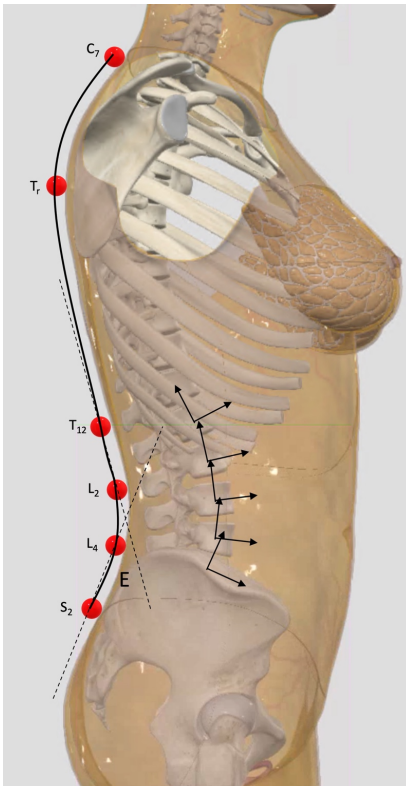

Figure 1: Dashed lines are vectors used to calculate the External (E) lumbar angle from motion capture markers (red dots). Solid line curve intersecting the motion capture markers is an example of Polyfit line (P). Axes intersecting the lumbar vertebrae represent the summation of angle changes used to calculate the Internal (I) lumbar angle [5].

Significance: Lumber angle increase does not always occur during gestation, but depends on individual characteristics. Perhaps, spine sexual dimorphisms did not evolve to simply accommodate for bipedal pregnancy, but additionally account for anthropometric variation in the population. Likewise, it seems that a single pregnancy musculoskeletal model set with prescribed spine angles over gestational time will not accurately account for the entire pregnant population. Since individual characteristics seem important, practitioners (clinicians and ergonomists) should consider an individualized approach to manipulating gestational lumbar postural modifications to allative back and hip related pains.

Acknowledgments: This collaboration was funded by an ASB research travel award.

References: [1] Haddox et al. (2020), *Gait Posture* v76; [2] Catena & Wolcott. (2021), *Gait Posture* v89; [3] Whitcome et al. (2007), *Nature* v450; [4] Catena et al. (2018), *J Biomech* v71. [5] Furlanetto et al. (2017), *JMPT* v40.

IN VIVO SUBJECT-SPECIFIC ESTIMATION OF CERVICAL SPINE DISC MATERIAL PROPERTIES

Soumaya Ouhsousou[1], Clarissa M. LeVasseur[2], Jeremy Shaw[2], William Anderst[2], and John C. Brigham[1]
[1]Department of Civil and Environmental Engineering, University of Pittsburgh, Pittsburgh, PA 15261, USA
[2]Department of Orthopaedic Surgery, University of Pittsburgh, Pittsburgh, PA 15203, USA
*Corresponding author's email: soo16@pitt.edu

Introduction: Progressive deterioration of the intervertebral discs of the cervical spine is related to aging and a variety of mechanical factors. Spinal fusion is the most common surgical procedure to treat symptomatic disc degeneration. However, post-surgery, patients may experience degeneration of another disc, which has been linked to altered mechanical stresses within the cervical spine due to the fusion. Yet, the specific mechanisms behind this phenomenon remain unclear. In order to elucidate how mechanical stresses change after fusion surgery and their impact on individual intervertebral discs, it is important to establish an approach for subject-specific mechanical analysis of cervical spine mechanics. Previously developed spine models have typically assigned the same stiffness values to each disc based upon measurements obtained from cadaver tissue [1], [2]. However, this assumption neglects the heterogeneity among discs which may result in inaccurate predictions. To address this shortcoming, an optimization-based approach has been developed to estimate the material properties of each intervertebral disc based on *in vivo* motion data. The purpose of this project was to non-invasively estimate the subject-specific material properties for the annulus and nucleus of each disc within the cervical spine.

Methods: Subject-specific cervical spine finite element analysis (FEA) process was established. CT scans of the cervical spine with an average resolution of 0.30×0.30×1.0 mm were utilized, and 3D geometries of the vertebral bodies were extracted for the cervical spine. Then, intervertebral disc geometries, including annulus with embedded fibers and nucleus, were approximated based on the spacing between the vertebrae. Facet cartilage was also included to simulate the articulation between the posterior elements of adjacent vertebrae (Figure 1). Each tissue component was assumed to be homogeneous with elastic and isotropic material properties, and initial material parameters were assigned to each component based on published values [1]. Boundary conditions were set such that the inferior endplate of C7 was fully constrained. Intervertebral motion data from multiple motion trials of a given subject, obtained from dynamic biplane radiography [3], were then used to calibrate the disc material properties and ultimately validate the calibrated spine mechanical model. The calibration was carried out using gradient-based optimization which minimized the difference between the measured flexion/extension of each spine motion segments and that estimated by the FEA.

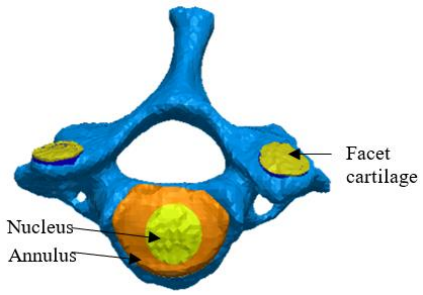

Figure 1: Three-dimensional geometry of the vertebra with intervertebral disc and facet cartilage.

Results & Discussion: The calibration process was performed for a female subject, 47 years of age, who was scheduled to undergo a C5-C6 anterior cervical discectomy and fusion surgery, and produced Young's moduli of 4.6, 4.0, 4.4, 6.3, 4.6 MPa for the annulus and 0.24, 0.25, 0.8, 3.3, 0.9 MPa for the nucleus of each disc from C23 through C67. The calibrated material properties were validated by comparing *in vivo* kinematics to the FEA kinematics using additional flexion and extension trials that were not used for calibration. An example flexion and extension trial used for validation is shown in Figure 2, which shows the position of two nodes on each vertebra of the FEA model compared to the *in vivo* kinematics. The validation results showed a mean absolute error of 0.99 mm and 2.4 mm posteriorly and anteriorly, respectively, within 61 frames of movement during flexion and extension. These promising results suggest it may be possible to estimate subject-specific material properties of the intervertebral discs non-invasively using an optimization-based approach with *in vivo* kinematic data and FEA. Future work includes expanding the cohort examined and adding ligaments to the model. Also, a more realistic calibration can be carried out by adding heterogeneity to each annulus of each disc (anterior, posterior, lateral disc properties).

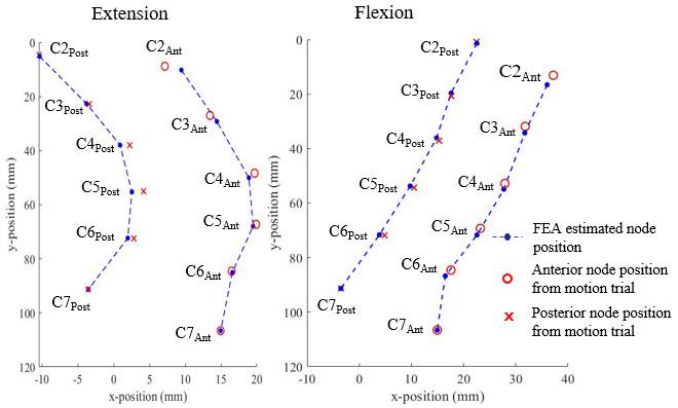

Figure 2: The unloaded and loaded position of the nodes predicted by the spine FEA compared with measured data.

Significance: Unlike traditional invasive methods, this preliminary study uses a non-invasive approach to estimate the discs material properties based on *in vivo* motion data. This method has the potential to enhance the accuracy and subject-specificity of spine mechanical models. Furthermore, incorporating heterogeneous subject-specific material properties will also potentially allow for identifying discs that are more susceptible to degeneration.

References:
[1] Y. H. Kim et al. (2018), *J. Mech. Sci. Technol.* 32(1);
[2] S.-H. Lee et al. (2011), *Spine* 36(9);
[3] LeVasseur CM et al. (2022), *Ann Biomed Eng.* 50(7).

ROLE OF THE POSTERIOR LIGAMENTOUS COMPLEX IN LUMBAR SPINE STABILITY – A FINITE ELEMENT STUDY

Isaac K. Kumi, Michael Polanco, Sebastian Bawab, Stacie I. Ringleb
Department of Mechanical and Aerospace Engineering, Old Dominion University, Norfolk, VA, USA
*Corresponding author's email: sringleb@odu.edu

Introduction: The lumbar spine supports the human body, facilitates movement, and protects the spinal cord. Integral to its stability and functionality is the network of ligaments that surround and interconnect its vertebral segments. The posterior ligamentous complex (PLC) is one of the most frequently injured ligament complexes in the spine. The PLC includes the interspinous ligament (ISL), capsular ligament (CL), supraspinous ligament (SSL), and the ligamentum flavum (LF).

Prior research has revealed that specific ligaments such as the SSL, LF, and CL contribute to the stability of the thoracolumbar spine. However, research into the contributions of each ligament in the PLC to the kinematics of the lumbar spine remains limited. Therefore, the purpose of this study was to explore how each ligament within the L4-L5 segment's PLC contributes to the lumbar spine's stability and integrity by simulating the progression of PLC ligament failures in the L4-L5 segment.

Methods: A finite element L1-L5 lumbar spine model, including the vertebrae, discs, and intervertebral ligaments, was obtained from SimTK [1]. Material properties were acquired from the literature [2-3]. The inferior endplate of the L5 vertebra was fixed in all degrees of freedom while allowing the superior endplate of the L1 vertebra to move freely.

Pure moment loads of 7500 N-mm were applied to the superior rigid endplate of the L1 vertebra, and kinematics were assessed in flexion, extension, lateral bending (LB), and axial rotation (AR). Next, two experiments were conducted. First, individual PLC ligaments were removed from the L4-L5 segment in isolation to simulate individual ligament failure. Additionally, the progressive failure in the PLC was simulated using a common injury mechanism to the PLC [4] in the L4-L5 by serially sectioning the CL followed by the ISL, SSL, and LF. Changes in ROM for the entire lumbar spine were analyzed for flexion, extension, lateral bending, and axial rotation. The ROM was expressed as a percentage of the intact model.

Results & Discussion: The intact model's predicted range of motion (ROM) aligned with the published data (Fig.1) for flexion/extension and lateral bending [5-7]. The differences observed in axial rotation between the FE model and experimental data might be attributed to the material properties assigned to the soft tissues in the FE model, such as the intervertebral discs (IVD). When contributions of the ligaments were examined individually, failure of the CL was the only ligament to have an impact on ROM in flexion and axial rotation (~ 7%). Conversely, there was little to no impact on the ROM in extension and lateral bending (Fig.2). This can be attributed to the posterior placement of these ligaments, which are meant to resist motion in the opposite (anterior) direction of the ligament's location hence having little to no effect on extension [8].

During the simulation of injury progression through the PLC, the most significant impact on ROM was observed in the failure of the CL in flexion and axial rotation (Fig. 3). However, following the sequence of injury progression, the failure of the SSL also resulted in a slight change in ROM of the lumbar spine in flexion (~ 4%). These outcomes confirm previous findings highlighting the critical role of the CL and SSL in maintaining lumbar spine stability [4,9-11].

While this study focused on the effects of ligament failure in the L4-L5 segment on range of motion, future research could investigate if injuries in other segments have different impacts on lumbar range of motion as well as how these injuries affect loading in the spine and intervertebral disks.

Significance: The findings from this study provide some insights into the kinematic significance of removing individual ligaments within the PLC. This knowledge is a first step toward understanding how ligament injuries can lead to long-term degeneration in the spine.

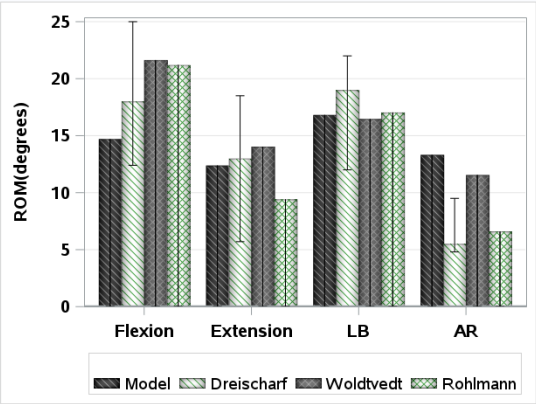

Figure 1: Comparison of predicted ROM to published studies; Dreischarf et al.; Woldtvedt et al.; Rohlmann et al.

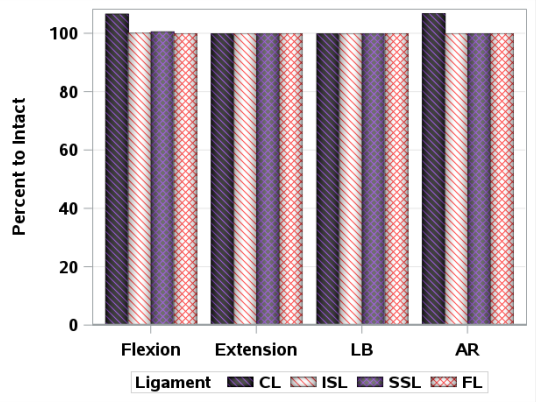

Figure 2: Percent of ROM to intact model for each individual PLC ligament failure.

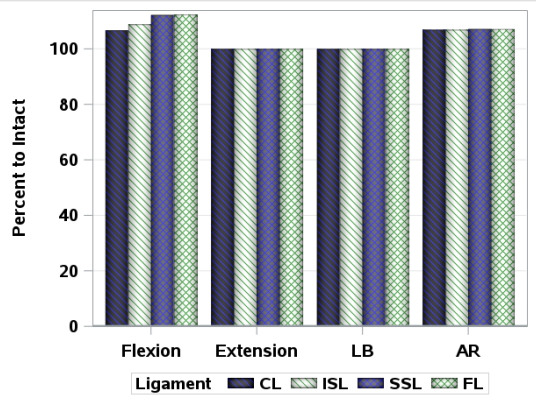

Figure 3: Percent of ROM to Intact model following the sequence of ligament failure in the lumbar spine.

References: [1] Finley et al. (2018), *Comp. Method in Biom*. 21(6); [2] Naserkhaki et al. (2018), *J Biomech* 70; [3] Rohlmann et al. (2016), *J Biomech* 39; [4] Pizones et al. (2012), *Spine*, 37(11); [5] Dreischarf et al. (2014), *J Biomech* 47(8). [6] Woldtvedt et al. (2011); [7] Rohlmann et al. (2001), *Spine* 26(24); [8] Muscolino (2015), *Wolters Kluwer Health*; [9] Kumi et al. ASB Conference (2023); [10] Heuer et al. (2007), *J Biomech* 40; [11] Li et al. (2017) *Medicine*, 96(35).

REDUCED MICROVASCULAR FUNCTION IN SUPRASPINATUS TENDON TEARS: INSIGHTS FROM POST-CONTRACTILE MRI-BOLD ANALYSIS

Kinyata J. Cooper[1*], Sean Forbes[1], Scott Banks[2], Tyler LaMonica[3], Bryce Gambino [3], Kevin Farmer[3], Federico Pozzi[1]
University of Florida [1]Department of Physical Therapy, [2]Department of Mechanical and Aerospace Engineering, [3]Department of Orthopaedics Surgery and Sports Medicine
*Corresponding author's email: kinyata.cooper@ufl.edu

Introduction: Rotator cuff tears are a common cause of pain and disability among adults. Over 4.5 million Americans seek medical care for rotator cuff tears each year[1]. Histological studies demonstrate that the degenerative process following a rotator cuff tear disrupts the vascularity of the shoulder muscles[2,3.] Quantitative magnetic resonance (MR) markers, on the other hand, offer a promising avenue to assess muscle vascularity without the need of invasive sampling. Post-contractile MR imaging-based blood oxygen level-dependent (MRI-BOLD) response is a marker that reflects the balance of oxygen delivery and utilization in skeletal muscle[4]. Inadequate delivery of oxygen to skeletal muscles can impede healing and recovery. This novel application of MRI-BOLD to rotator cuff tears in the shoulder may elucidate a contributing factor of degeneration. This will enable early detection and tracking subtle progressions of degeneration and regeneration, without invasive methodologies. Treatments targeting microvascular function may positively impact those recovering from rotator cuff tears.

This study aims to examine the MRI-BOLD response in individuals with full-thickness rotator cuff tears compared to those without tears. Due to histological vascular alterations in patients with rotator cuff tears[3] and alterations in MRI-BOLD response across other skeletal muscle injuries and conditions[5,6], we expect individuals with a rotator cuff tear to have a lower MRI-BOLD response (i.e., diminished oxygen delivery) compared to healthy individuals.

Methods: Eighteen participants enrolled in this study: 12 with full-thickness tears of the supraspinatus with or without involvement of the infraspinatus (66.5 ± 7.3 years, 4 males, 8 females), and 6 controls with intact rotator cuff confirmed by ultrasound imaging (63.2 ± 3.9 years, 2 males, 4 females). Using a 3T MR Phillips system, MRI-BOLD response was measured following five brief (2s) maximal isometric shoulder abduction contractions, each separated by 1 min of rest. A magnetic resonance compatible dynamometer was used to monitor abduction contraction during the scan. A single axial slice chosen at the maximal cross-sectional area of the supraspinatus muscle was used to draw the region of interest. These regions of interest were used to plot the MRI-BOLD signal intensity over 6 minutes (1 slice/s). The signal intensity was fitted to a sixth-order polynomial function[7] to determine the MRI-BOLD peak response, time to peak, and time to halfway recovery, which are markers of microvascular function. Unpaired, one-tailed t-tests compared indices of the MRI-BOLD response variables.

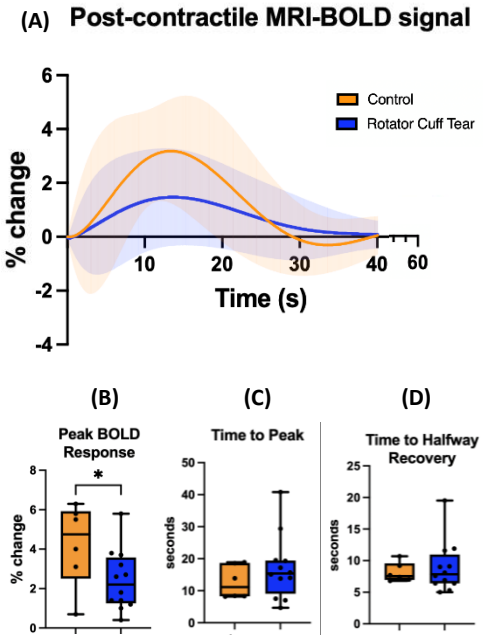

Figure 1: Microvascular function between the rotator cuff tear and control groups. Ensemble averages of the post-contractile MRI-BOLD response signal over the first 40 seconds of the 60 second acquisition period (A), average MRI-BOLD peak response (B), time to peak (C), and time to halfway recovery (D). Values are mean ± standard deviation.

Results & Discussion: Average peak MRI-BOLD response was lower in the rotator cuff tears compared to the control group (2.4 ± 1.5% vs. 4.3 ± 2.1%, Figure 1B). No significant differences were found between average time to peak response (17.0 ± 10.0s and 12.7 ± 5.2s, p = 0.17, Figure 1C) and average time to halfway recovery (8.9s ± 4.0s and 8.1s ± 1.5s, p = 0.33, Figure 1D) for the rotator cuff tear and control groups, respectively. Overall, our results indicate that individuals with rotator cuff tears had a reduced oxygen delivery relative to utilization than controls suggesting impaired microvascular function in the supraspinatus muscle.

Significance: These results advance the field of quantitative imaging of the rotator cuff by evaluating the post-contractile MRI-BOLD response in shoulder muscles for the first time. They highlight the potential of post-contractile MRI-BOLD as a non-invasive tool for characterizing degenerative changes in the supraspinatus muscles after tendon tears. Our findings support that microvascular impairments may be evident following rotator cuff injuries; and focusing on mechanisms of muscle degeneration (rather than structural) after rotator cuff tears, may provide additional insight. This knowledge can advance the understanding of the ability of rotator cuff muscle to heal and respond to treatment, offering value for future studies assessing healing capacity and novel therapeutic interventions.

Acknowledgments: NIH NIAMS R21 AR077231

References: [1] Mathiasen et al. (2018), *Curr Rev Musculoskelet Med. 11*(1); [2] Gibbons et al. (2017), *J Bone Joint Surg Am.* 99(3); [3] Matthews et al. (2006), *J Bone Joint Surg Am. 88*(4); [4] Towse et al. (2011), *J Appl Physiol. 111*(1); [5] Sanchez et al. (2011), *Am J Physiol Circ Physiol 301(2)*; [6] Ledermann et al. (2006), *Circulation 113(25).* [7] Lopez et al. (2021), *J Appl Physiol* 131: 83–94.

Using OpenCap to assess single- and dual-task single leg vertical jump performance

Fatemeh Aflatounian[1], Kaylan Wait[1], Brendan Silvia, [1] Alexandra C. Lynch[1], James N. Becker[1], Keith A. Hutchison[1], Janet E. Simon[2], Dustin R. Grooms[2], and Scott M. Monfort[1]
[1]Montana State University, Bozeman, Montana, USA, [2]Ohio University, Athens, Ohio, USA
Email : fatemehaflatounian@montana.edu

Introduction: Single-leg vertical jump (SLVJ) assesses upward jumping ability, emphasizing knee extensor power, particularly relevant to identifying altered function following an anterior cruciate ligament (ACL) reconstruction [1]. ACL injuries often happen during sports when visual attention is externally focused; however, common clinical assessments often neglect cognitive-motor deficits that lead to riskier movements [2]. Dual-task screening simultaneously tests cognitive and motor skills, aiding in identifying such deficits [3]. However, traditional motion analysis is costly and time consuming for data collection and processing [4]. OpenCap enhances clinical accessibility to full-body kinematics by using iOS devices and automated cloud processing, reducing both cost and time burden [4]. The purpose of this study was to demonstrate the ability of a clinically-feasible approach (i.e., OpenCap) to reflect similar kinematics obtained by standard marker-based motion capture during single- and dual-task SLVJ. Given OpenCap's success in capturing sagittal plane kinematics in other jumping movements, we hypothesized strong correlations between OpenCap and marker-based outcomes.

Methods: 10 healthy athletes (5F/5M, 19.8±2.3 yrs; 1.66±0.18 m; 67.8±11.0 kg; Tegner: 7.5±1.3; Marx: 10.6±3.6) completed the SLVJ task. Participants performed the SLVJ under both single-task (ST) and dual-task (DT) conditions on both limbs, with three trials each. DT involved two peripheral lights (FITLIGHT Sports Corp) for Go/No-Go cues and one overhead light for a memory task, adapted from a visual-cognitive triple hop [5]. Participants awaited a pre-defined 'Go' color on one of the peripheral lights before performing the SLVJ, focusing on the overhead light to recall three rapidly displayed colors. Full-body kinematics were simultaneously captured using both a marker-based motion capture system (MoCap) (10 cameras, Motion Analysis Corp; 5 AMTI force plates) and OpenCap with two iOS devices. MoCap data were processed in Visual3D using an inverse kinematics model [6], while OpenCap data were processed using the automated cloud processing within the OpenCap workflow. Kinematic trajectories from both methods were analysed in MATLAB to extract jump height and peak trunk, hip (pHFA), and knee flexion angle (pKFA), and pelvis tilt during the propulsive phase (from 0.4 sec before leaving the force plate until toe off) [1]. Toe-off was defined using force plate data for MoCap and when the pelvis vertical position exceeded a 5% increase from the standing position for the OpenCap data. Pearson correlations (or Spearman if data were not normally distributed) were used to compare outcomes between two approaches, with $p < 0.05$ indicating statistical significance.

Results & Discussion: There were strong correlations between MoCap and OpenCap values for both ST and DT variables jump height and joint kinematics during the propulsion phase of SLVJ (r = 0.6 to 0.92, p = 0.05 to <0.001, **Figure 1**). These results demonstrate a strong ability for OpenCap to capture trends in SLVJ outcomes (e.g., the individuals with higher jump height or joint flexion measured via MoCap were also identified with OpenCap). It is worth noting that these strong correlations were obtained after omitting OpenCap trials with unrealistic pose estimation from the automated OpenCap cloud processing. Out of the 120 good (i.e., hands remained on hips, clean landing, reacting to correct color for DT) trials collected, 10 were later omitted due to unrealistic OpenCap pose estimations. Opportunities to further enhance the ability to leverage OpenCap to assess SLVJ performance and minimize dropped trials include optimizing the number and position of the cameras for this movement as well as improving the color contrast between participants and their environment. Additional opportunities to refine the analyses pipeline to more robustly extract the variables with minimal manual effort also exists. In general, OpenCap captured essential variables related to ACL injuries during SLVJ, which has potential as a useful tool for clinicians. However, there is a still need for future studies with larger cohorts, including individuals with ACL reconstruction, and to streamline the workflow to optimize clinical feasibility.

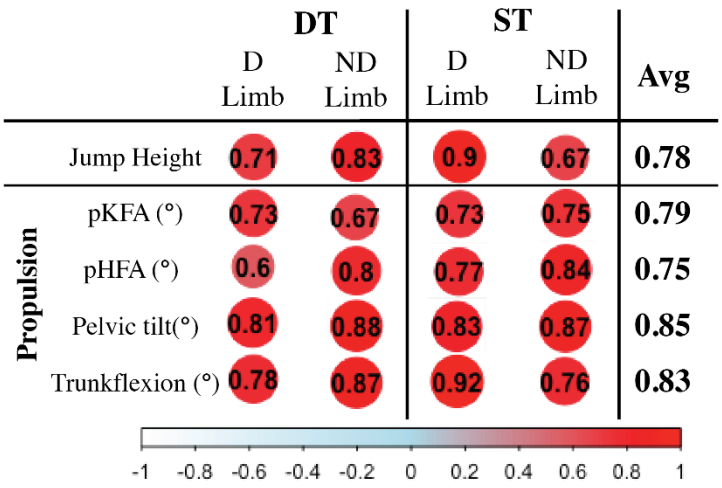

Figure 1: Correlogram of OpenCap and MoCap systems (DT: Dual task, ST: single task, D: Dominant, ND: nondominant)

Significance: Improving clinicians' access to high resolution, joint-level kinematics during return-to-sport tasks may provide a more comprehensive approach for clinicians to evaluate the readiness of their patients to return to sport. In this study, OpenCap strongly correlated with key kinematic outcomes across multiple joints during single- and dual-task SLVJ. Future efforts using this clinically-feasible approach to collect these data and relate to patient outcomes are needed to demonstrate the clinical relevance of these data.

Acknowledgements: This research was supported by the NIH award R03HD101093.

References: [1] Kotsifaki et. al. (2022) *Br J Sports Med* 56(9): 490-498, [2] Vargas et. al. (2023) *IJSPT* 18(1): 122-131, [3] Monfort et. al. (2019) *Am J Sports Med* 47(6):1488–1495, [4] Uhlrich et. al. (2023) *PLoS Comput Biol* 19(10): e1011462, [5] Farraye et. al. (2023) *J Sport Rehabil* 32(7): 802-809, [6] Fischer et al. (2021) *J Applied Biomech* 37(4)

CHANGES IN LANDING BIOMECHANICS AFTER CONCUSSION: A PROSPECTIVE LONGITUDINAL STUDY OF HIGH SCHOOL FEMALE ATHLETES

April L. McPherson[*1-3], Jennifer A. Hogg[4], Tessa C. Hulburt[1-3], Christopher D. Riehm[1-3], Taylor M. Zuleger[1-3], Jed A. Diekfuss[1-3], Kim D. Barber Foss[1-3], David R. Howell[5], Gregory D. Myer[1-3]

[1]Emory Sports Performance And Research Center (SPARC), Flowery Branch, GA; [2]Emory Sports Medicine Center, Atlanta, GA; [2]Emory University School of Medicine, Atlanta, GA; [4]University of Tennessee Chattanooga, Chattanooga, TN; [5]Sports Medicine Center Children's Hospital Colorado, Aurora, CO; *Corresponding author's email: April.mcpherson@emory.edu

Introduction: Sport-related concussion (SRC) elevates risk for future lower extremity musculoskeletal injury (LE MSKI).[1] Adolescent athletes are of particular concern for concussion-LE MSKI sequalae, since an estimated 1.1-1.9 million SRCs occur annually in US athletes under 18 years old[2] and recovery periods are often longer in adolescents compared to adults.[3] Adolescent athletes also demonstrate neuromuscular control deficits following SRC symptom resolution, which may contribute to elevated LE MSKI risk.[4]

Biomechanical deficits following SRC are theorized to contribute to elevated risk of LE MSKI. However, prior research is limited to retrospective study designs to characterize landing biomechanics following SRC. Adolescent athletes with SRC history landed with less ankle dorsiflexion and knee flexion compared to controls, movement patterns suggestive of greater LE MSKI risk.[5] A cross-sectional study indicated females with SRC history landed with greater knee abduction angle and performed a sidestep cut maneuver with less lateral trunk bending compared to controls.[6] While these retrospective studies indicate an association between poor movement patterns and SRC history, no prospective longitudinal study has evaluated changes in landing biomechanics after a concussion. Therefore, the purpose of this study was to prospectively evaluate changes in biomechanics in female adolescent athletes after they suffered a concussion and to compare with females who did not sustain a concussion. We hypothesized that athletes who suffered a concussion during their competitive season would demonstrate deleterious changes to biomechanics at post-season relative to matched controls.

Methods: 275 female athletes (12-18 years old) were recruited from high school athletic teams (soccer (n=105), basketball (n=62), volleyball (n=108)) prior to the start of the competitive season (15.4±1.2 years; height 1.60±0.3 m; mass 75.3±3.2 kg). Athletes completed drop vertical jump (DVJ) trials from a 31cm box prior to the start of the athletic season (PRE) and after completion of the season (POST) while 3D motion capture and ground reaction forces were collected. Injuries were recorded throughout the season, and athletes who reported a diagnosed concussion during the season were included in the concussion group (CONC, n=9). CONC athletes were matched by sport, age, height, and mass to three athletes who did not sustain a concussion (CTRL, n=27). Peak ankle, knee, and hip kinematics (°) and external joint moments ($Nm*kg^{-1}*m^{-1}$) were analyzed via 2 (Group; CONC, CTRL) × 2 (Time; PRE, POST) repeated measures ANOVA in R. Statistical significance was set *a priori* at $p<0.05$.

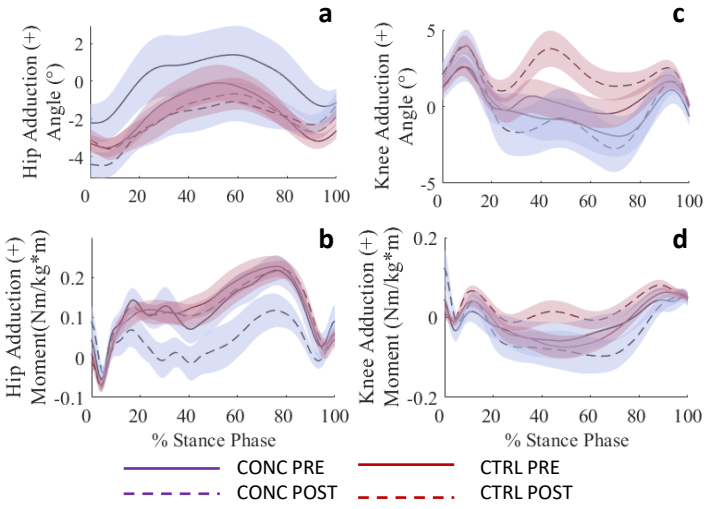

Figure 1: Average ± standard error curves for right leg Hip Adduction a) angle and b) moment and Knee Abduction c) angle and d) moment.

Results & Discussion: CONC athletes were not significantly different in age, height, mass, or athletic exposures from CTRL athletes ($p\geq0.19$). POST testing was completed an average of 69±34 days following concussion. There was a significant main effect of Time for left hip adduction angle and right hip adduction moment ($p\leq0.02$). Athletes had greater left peak hip abduction angle and lower right peak external hip adduction moment at POST compared to PRE. There was a significant main effect of Group for left peak hip adduction moment ($p=0.00$), where CONC athletes exhibited lower peak left external hip adduction moment than CTRL athletes. No significant interaction effects were observed ($p\geq0.09$).

This preliminary analysis found that female adolescent athletes who suffered a concussion demonstrated similar landing biomechanics to CTRL athletes when only peak discrete values are considered. However, CONC athletes appear to adopt altered frontal plane strategies at the hip and knee across the entire phase of a landing cycle (**Fig. 1**).

Significance: While biomechanical deficits have been theorized to contribute to elevated risk of LE MSKI post-concussion[4], this is the first prospective longitudinal analysis evaluating changes in landing biomechanics from pre- to post-concussion. This study indicates that CONC athletes may adopt altered loading strategies that may contribute to increased dynamic knee valgus loading strategies and elevate risk for LE MSKI. Further investigation is necessary to determine if the observed altered landing strategies in our cohort are consistent in a more acutely concussed population.

Acknowledgements: Research was directly supported by NIH/NIAMS research grants U01AR067997, R01AR077248, R01AR076153, and T32NS7453-20. This work was also partially funded by internal support from the Department of Orthopaedics at Emory University.

References: [1] McPherson (2019) *Am J Sports Med* 47(7); [2] Bryan (2016) *Ped* 138(1); [3] McCrory (2017) *Br J Sports Med* 51(11); [4] Chmielewski (2021) *J Sport Health Sci* 10(2); [5] Avedesian (2020) *J Appl Biomech* 36(5); [6] Shumski (2023) *J Athl Train*;

AMPLITUDE AND TEMPORAL DIFFERENCES IN COUNTERMOVEMENT JUMP GROUND REACTION FORCES FOLLOWING ANTERIOR CRUCIATE LIGAMENT RECONSTRUCTION

Katelyn S. Campbell[1*], Sierra D. Hastings [1], Eric L. Dugan[1,2]
[1]Motion Analysis Laboratory, Texas Children's Hospital, The Woodlands, TX, USA
[2]Department of Orthopaedic Surgery, Baylor College of Medicine, Houston, TX, USA
*Corresponding author's email: kscampbe@texaschildrens.org

Introduction: Studies have shown adolescents and young adults returning to a high level of activity after anterior cruciate ligament reconstruction (ACL-R) are at an increased risk of sustaining another anterior cruciate ligament injury, in either the ipsilateral or the contralateral knee [1]. Utilizing biomechanical analyses to assess injury risk and guide return to sport clearance can be beneficial.

Traditional methods of biomechanical analysis often focus on differences in amplitude with less focus on if or how the data are temporally aligned. Amplitude is often associated with mechanical capacity, while timing is often associated with coordination and control. Ignoring timing disregards variability in coordination and control during clinical interpretation and return to sport criteria. Therefore, the purpose of this study was to utilize nonlinear registration to assess amplitude and timing effects in ground reaction forces (GRF) in the involved and uninvolved limbs during the eccentric and concentric phases of countermovement jump (CMJ) in adolescents post ACL-R.

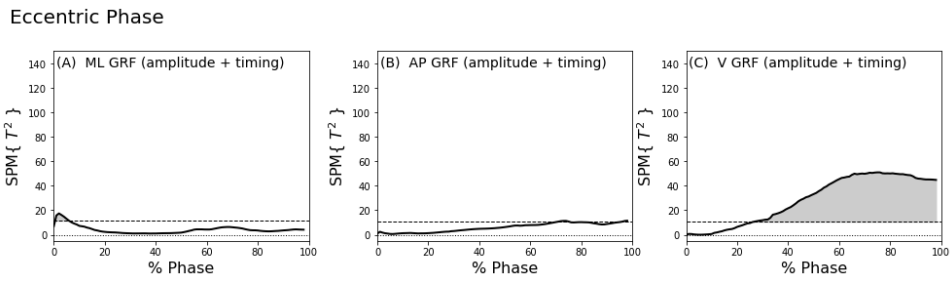

Figure 1. Hotelling's T^2 (SPM{T^2}) tests showing differences in ground reaction forces (GRF) between involved and uninvolved limb in the **(A)** mediolateral (ML), **(B)** anteroposterior (AP), and **(C)** vertical (V) directions during the eccentric phase.

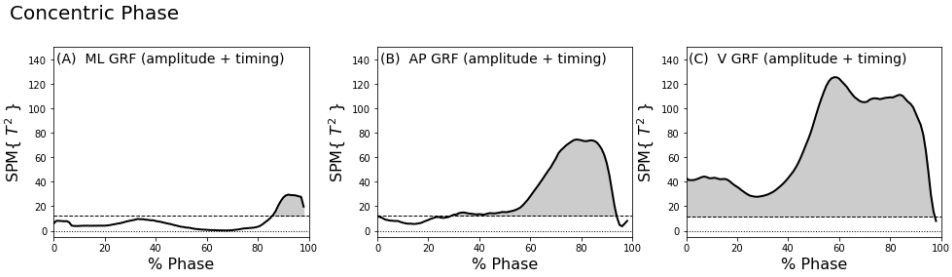

Figure 2. Hotelling's T^2 (SPM{T^2}) tests showing differences in ground reaction forces (GRF) between involved and uninvolved limb in the **(A)** mediolateral (ML), **(B)** anteroposterior (AP), and **(C)** vertical (V) directions during the concentric phase.

Methods: Sixty-three adolescents (76.7 ± 20.6 kg; 1.71 ± 0.11 m; 12-20 y; 39M/24F) 214.3 ± 66.3 days post ACL-R performed six CMJ. Two force platforms (1000 Hz; AMTI, Watertown, MA) were used to assess GRF of the involved and uninvolved limbs. Data were filtered using a zero-lag, fourth-order, Butterworth low-pass filter with cut-off frequency of 20 Hz and normalized to body mass.

Using a novel technique presented by Pataky and colleagues, data were first linearly registered for each phase of the CMJ (eccentric and concentric) and then these data for each phase were nonlinearly registered, resulting in nonlinearly registered data and optimal deformation fields (Python 3.9.13) [2]. These data were then analyzed using paired nonparametric Hotelling's T^2 (SPM{T^2}) tests. Post hoc univariate tests were also conducted on amplitude and displacement components separately. Significance for all tests was a priori set at $p < 0.05$.

Results & Discussion: Hotelling's T^2 revealed significant differences in GRF in all three directions between the involved and uninvolved limbs. In the eccentric phase, GRF in the mediolateral (ML), anteroposterior (AP), and vertical (V) directions were all significantly different from 1-6%, 72-75%; 97-100%, and 27-100% of the phase, respectively (Figure 1). Similarly, during the concentric phase, discrepancies were observed in the ML, AP, and V directions from 86-100%, 29-93%, and 0-99% of the phase, respectively (Figure 2). Subsequent post hoc t-tests revealed timing differences in the ML direction and amplitude differences in the AP and V directions between the involved and uninvolved limbs during both phases. These results suggest that there are asymmetries in both amplitude and timing of GRF during CMJ that exist even seven months post ACL-R. These findings are similar to previous findings that asymmetries in kinetics during the concentric phase of CMJ still existed at time of return to sport [3].

Significance: Measurement of force asymmetry between involved and uninvolved limbs allows clinicians to track progress and make return to sport decisions with athletes after ACL-R. Delineation between asymmetries in amplitude or timing in both the eccentric and concentric phases of a CMJ provides the clinician with the opportunity to address the appropriate deficit of either capacity or coordination. This leads to better targeted treatment plans to help an athlete return to sport safely after ACL-R.

References: [1] Wiggins et al. (2016), *Am J Sports Med* 44(7); [2] Pataky et al. (2022), *J Biomech* 136; [3] Kotsifaki et al. (2023), *Br J Sports Med* 57(20).

Comparing the impact of sports bras on breast acceleration in full busted women

Saba Yazdekhasti[1]* & Stacey Gorniak[1]
[1]Dept. of Health and Human Performance, University of Houston, Houston, TX 77204
email: *syazdekhasti@uh.edu

Introduction: Breast biomechanics and the effectiveness of sports bras in reducing discomfort during exercise form an important yet specialised area for addressing and alleviating physical barriers for participating women in exercise. Ill-fitting bras during daily activities and exercise can lead to musculoskeletal pain and discomfort [1], [2]. This situation is exacerbated by physiological changes in breast structure due to ageing, childbirth, and breastfeeding [3]. Effective sports bras significantly reduce breast motion [4], [5], yet accurately measuring this movement challenges researchers due to the hyper-elastic nature of breast tissue [6]. Motion capture systems, commonly used to study breast kinematics [7], [8], face limitations in accurately capturing the full range of breast motion, often relying on markers placed on the bra rather than the breast itself. Our study seeks to bridge these methodological gaps by comparing acceleration data from motion capture systems and direct-attached sensors, aiming to enhance our understanding of breast biomechanics across various activities and bra conditions.

Methods: In our study, 20 healthy female volunteers (33 ± 12 years of age, BMI = 30.2 ± 6.5 kg/m^2), spanning a range of D to G bra cup sizes, participated in a comprehensive breast motion analysis involving both Vicon motion capture system and Delsys Trigno sensors (built-in triaxial accelerometers) to assess breast acceleration during exercise (Figure 1). Participants underwent two assessment sessions: the first for body composition via DXA scans and basic health metrics, and the second for biomechanical evaluation. During a series of controlled physical activities, sensors were positioned on and underneath the bra, and passive reflective markers were used to measure breast acceleration relative to the torso. The activities included low to high impact exercises and a treadmill test to simulate varied physical exertion levels. This methodology allowed for precise measurement of breast displacement and acceleration, aiming to reconcile discrepancies in breast motion data capture.

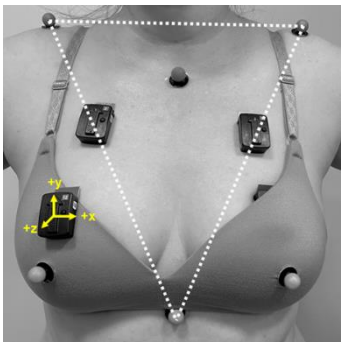

Figure 1: Vicon markers on the anterior thorax. Thorax plane denoted by white dashed lines; Vicon-based breast acceleration of areola markers calculated from this plane. Delsys Trigno sensors shown on upper and lower superior aspects of each breast shown; Trigno axes denoted in yellow.

Results & Discussion: Our study highlights significant differences between Vicon motion capture and Delsys Trigno sensors in measuring breast acceleration during various physical activities, with accelerometers showing consistently higher values of breast tissue acceleration during physical activities *($p < 0.05$)*. This discrepancy suggests accelerometers' superior sensitivity to localised breast movements not captured by motion capture's passive reflective markers. Despite these differences, our findings corroborate previous research indicating no significant disparity in breast movement between the right and left areolas *($p = 0.75$)* and the broader breast regions encompassed by the bra cup *($p = 0.17$)*, affirming the reliability of sports bras in providing uniform support. However, the significant difference in upper breast acceleration between right and left sides *($p < 0.05$)* detected by accelerometers underscores the necessity for a refined approach in assessing breast biomechanics, moving beyond the conventional reliance on nipple displacement as the sole indicator of overall breast movement. Our comparison between the Delsys Trigno sensors on the fabric and tissue suggests that well fitted sports bras allow external markers to accurately reflect breast motion. The study's approach underscores our commitment to enhancing sports bra design through meticulous biomechanical analysis, providing insight into the effectiveness of different sports bras designed for full-busted women compared to every-day bras in reducing unwanted breast motion during various physical activities. Future research should broaden participant demographics to include varied physiological backgrounds and activities, enhancing our understanding of breast dynamics and supporting the development of more effective sports bras.

Significance: This new approach can result in sports bras tailored to diverse body shapes and exercise routines. In contrast to previous studies that mainly examined breast biomechanics during running, this study evaluated breast motion during a range of physical activities with varying impact levels, ensuring optimal support and comfort for women engaging in a wide range of exercises.

Acknowledgments: This work was supported by summer funding to SY and materials loan by Bounceless (PI: Gorniak).

References:

[1] D. McGhee, 2009.
[2] T. Amin, T. Puntambekar, and D. Ravisankar, *Proceedings of ICoRD 2021*, Springer, 2021, pp. 97–105.
[3] S. Xu, J. Wang, H. Gong, X. Yao, and Z. Wang, *J. Eng. Fibers Fabr.*, vol. 16, p. 15589250211018196, 2021.
[4] B. R. Mason, K.-A. Page, and K. Fallon, *J. Sci. Med. Sport*, vol. 2, no. 2, pp. 134–144, 1999.
[5] M. Norris, T. Blackmore, B. Horler, and J. Wakefield-Scurr, *Ergonomics*, vol. 64, no. 3, pp. 410–425, 2021.
[6] J. Zhou, W. Yu, and S. Ng, *Text. Res. J.*, vol. 83, no. 14, pp. 1500–1513, 2013.
[7] D. W. Powell, H. B. Fong, and A. K. Nelson, *Front. Sports Act. Living*, vol. 5, 2023.
[8] A. L. Boschma, 1994.

CENTER OF PRESSURE AFFECTED BY FATIGUE DURING LATERAL CUTTING IN SOCCER ATHLETES: DIFFERENCES ASSOCIATED WITH KNEE KINEMATICS AND KINETICS

Alex N. Denton[1,2*], Emily Karolidis[2], Michael E. Hahn[2]
[1]Knight Campus for Accelerating Scientific Impact, University of Oregon, Eugene, Oregon, USA
[2]Bowerman Sports Science Center, Dept. of Human Physiology, University of Oregon, Eugene, Oregon, USA
*Corresponding author's email: adenton@uoregon.edu

Introduction: The 2023 Women's World Cup highlighted the destructive impact of lower limb injuries on female soccer athletes, as anterior cruciate ligament (ACL) injuries alone sidelined over two dozen professional athletes. The ACL is integral for maintaining knee joint stability and performing lateral cutting and rapid pivoting movements fundamental to soccer. However, the mechanics of these movements impose an inherent injury risk to the ACL, especially in female athletes [1]. While soccer remains a fast-growing sport among female athletes in the United States, female soccer athletes have a notably greater risk of sustaining an ACL injury compared to female athletes in other sports [2] and male soccer athletes [3]. The risk factors contributing to lower limb injuries in female soccer athletes are complex and multifactorial. Skeletal differences, such as variations in bone shape and alignment [4], coupled with changes in knee joint flexibility altered by the endocrine system [5], are natural risk factors influencing the likelihood of ACL injury in female athletes. Furthermore, high-intensity athletic performance can elevate neuromuscular fatigue leading to deficits in muscular strength and adverse movement coordination [6], thereby escalating the risk of lower limb injuries in female athletes. The biomechanical risk factors indicative of neuromuscular fatigue specific to female soccer athletes during on-field training and gameplay remain unidentified. Nevertheless, center of pressure (COP) measurements may provide insight into mechanical strategies at the knee during lateral cutting movements. Therefore, the purpose of this study was to explore the impact of COP trajectory during lateral soccer-specific movements on knee joint kinematics and kinetics in response to neuromuscular fatigue in male and female athletes. We hypothesized females would exhibit greater COP maximum displacement than males, due to a more posterior point of initial contact (IC), and greater COP asymmetry would occur with the onset of fatigue.

Methods: Nineteen competitive soccer athletes (9 female, 10 male; 21.1±2.4 yr; 67.6±9.6 kg; 172.3±8.1 cm) with no prior traumatic lower limb musculoskeletal injuries provided informed consent. Participants performed a series of unanticipated lateral cutting steps targeting 120° from a running approach at 80% of perceived maximum velocity in an indoor artificial turf laboratory. Lateral cutting kinematics and kinetics were recorded before and after a fatigue-based protocol involving a modified Gauntlet fitness test. The goal of the fatigue-based protocol was to attain the fastest completion time across five consecutive stages of running (1600, 800, 400, 200, and 100 m) with a lateral cutting step every 50 m and one minute of rest between each stage. Footwear was standardized among participants with a standard firm ground cleat and elliptical stud shape (Adidas Copa Sense). Participants were equipped with pressure-measuring insoles (Novel Pedar) during the fatigue-based protocol. Differences in COP maximum displacement and IC (mediolateral (x) and anteroposterior (y)) among groups were evaluated during 1600 and 400 m trials using a series of two-way mixed effect ANOVAs (sex X fatigue). The relationships among IC and maximum COP displacement on knee kinematics and kinetics were separately examined using multiple linear regression.

Results & Discussion: Fatigue had a main effect on COP_x displacement, whereas sex had a main effect on COP_y displacement ($p<0.05$) (Fig. 1). Neither factor had an impact on asymmetry. The $COP_{x\&y}$ displacements were predictive of knee valgus angle and moment ($p<0.05$). Greater COP_x displacement will lower knee valgus angle and moment; however, greater COP_y displacement will produce the opposite outcome. Additionally, greater COP_x displacement was also predictive of lower knee extensor moments. The IC_x was predictive of knee joint flexion angle, extensor moment, and valgus moment, but IC_y was only predictive of knee extensor moment ($p<0.05$).

A lateral and anterior shift in IC location will lead to greater knee joint flexion angle, extensor moment, and valgus moment. Although the mechanics of the knee are closely related, it is possible female soccer athletes may benefit from striking on the medial aspect of the heel during lateral cutting to achieve preferred landing mechanics for preventing ACL injury.

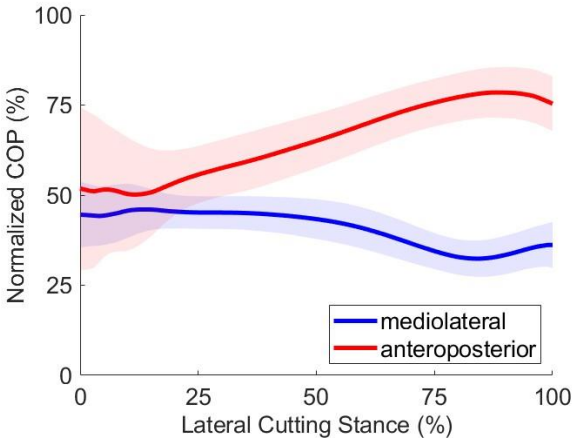

Figure 1: Average and standard deviation mediolateral and anteroposterior center of pressure (COP) trajectory during a lateral cutting step normalized to insole width and length, respectively. Larger COP values represent lateral or anterior movement.

Significance: Preventing lower limb injuries in female soccer athletes is not only beneficial for improving athletic performance and physical fitness but also for overall health and well-being.

Acknowledgments: This work was supported by the Wu Tsai Human Performance Alliance and the Joe and Clara Tsai Foundation.

References: [1] Donelon et al. (2020), *Sport Med Open* 6(53); [2] Allen et al. (2016), *AJSM* 44(10); [3] Ireland (2002), *Orthop Clin North Am* 33(4); [4] Beynnon et al. (2014), *AJSM* 42(5); [5] Heitz et al. (1999), *J Athl Train* 34(2); [6] McLean et al. (2009), *MSSE* 41(8).

Lower-Extremity Response to Soccer Cleat Stud Shape and Fatigue State: Considerations for Female-Centric Traction Design

Emily C. Karolidis[1*], Michael E. Hahn[1]
[1]Department of Human Physiology, University of Oregon, Eugene, OR, USA
*Corresponding author's email: ekarolid@uoregon.edu

Introduction: Anterior cruciate ligament (ACL) tears occur at a 3-time higher rate in female soccer athletes than males [1]. This sex-based disparity is associated with differences in neuromuscular control, joint laxity, and anatomical alignment, altering kinetic and kinematic performance profiles [2]. These differences widen with fatigue, furthering the risk of injury in females [3].

Despite mechanical differences between sex, soccer footwear is designed for male users. With known sex differences in movement patterns and joint loading, it should not be assumed that females are able to withstand the same amount of traction as males. High traction footwear may exacerbate female susceptibility to torsional injury mechanisms, such as those of ACL injury, if rotational resistance exceeds ligament loading capacity [4]. Cleat outsole properties, such as stud shape, are direct moderators of rotational resistance at the shoe-surface interface [4]. However, the effect of stud shape on female mechanics remains unknown. This study investigates the influence of soccer cleat stud shape, elliptical and bladed, on the knee kinetics and kinematics of athletes pre- and post-fatigue. It is hypothesized that bladed cleats, offering greater rotational resistance than elliptical cleats, will increase knee loading patterns in female athletes only, while it is predicted that cleat type has no effect on males. Furthermore, it is hypothesized that fatigue will negatively influence the lower extremity mechanics of females only, while there is no discernable effect of fatigue on males.

Methods: College-aged soccer athletes (n = 20 in progress; 10 male, 8 female reported; 21.2±2.3 yr; 68.6±9.0 kg; 171.7±7.5 cm) provided informed consent and performed two data collections. For each visit, cleated footwear of different stud shapes was worn: bladed (adidas Predator .2), or elliptical (adidas Copa Sense .3). Cleat order was randomized for each subject.

Athletes performed unanticipated cutting tasks in a turfed facility before and after a fatigue protocol. A 19-camera system (Vicon, 100 Hz) collected the trajectories of 28 retroreflective markers, while 4 force platforms (AMTI, 1500 Hz) recorded ground reaction force data. Athletes performed 6 cuts (80% maximum speed to unanticipated 120° cut, 3 trials each direction), representing the pre-fatigue state. A field-based fatigue protocol, developed to challenge aerobic and anaerobic energy systems, was then completed. After, the athlete repeated the cut tasks, representing mechanics observed in a fatigued state. Knee flexion angle at initial contact (KFA), peak knee valgus angle (KVA), peak internal knee extensor moment (KEM) and peak anterior tibiofemoral shear force (ASF) were calculated using inverse dynamics in Visual3D, pre- and post-fatigue, and compared across cleat conditions in male and female athletes. Mixed effects ANOVA examined main and interaction effects of sex, cleat condition, and fatigue state at an alpha level of 0.05.

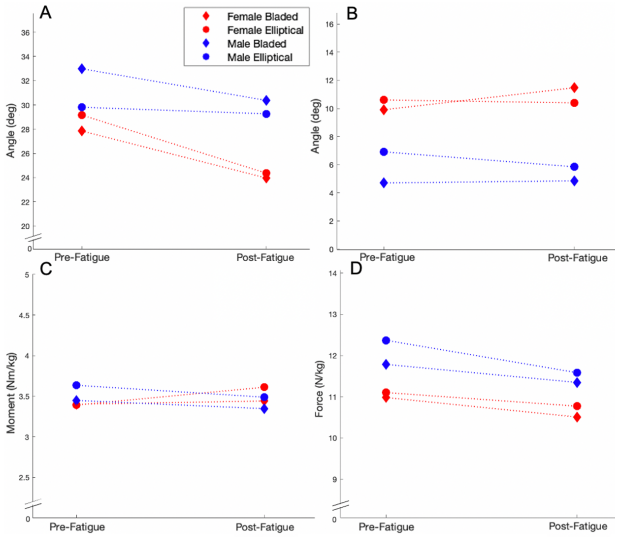

Figure 1: Interaction plots of knee mechanical parameters averaged across sex, cleated condition, and fatigue state. (A) knee flexion angle at initial contact, (B) peak knee valgus angle (C) peak knee extensor moment (D) peak anterior shear force

Results & Discussion: There were no significant 3-way interactions of sex, cleat condition and fatigue state on the aforementioned knee kinetic or kinematic variables. However, there was a significant 2-way interaction of sex and fatigue state on KEM ($p = 0.0404$), revealing that fatigue detrimentally increased KEM in females, while protectively decreased KEM in males . Main effects were observed for sex on peak KVA ($p = 0.0147$), with females effecting greater valgus angles than males across all fatigue states and cleat conditions. Main effects were also observed for fatigue state on KFA ($p = 0.0143$), with fatigue decreasing KFA for both sexes in either cleat condition.

Interim trends suggest fatigue to negatively influence the cutting mechanics of female athletes more so than male athletes. In comparison, the fatigue response of male athletes instead may offer joint protective strategies. This difference in fatigue response amplifies existing differences in sex-based mechanical cutting strategy, further elevating the risk of female injury, comparatively. While no significant effects of cleat condition are reported, the elliptical cleat appears protective against the fatigue-induced knee valgus increases observed with the bladed cleat. The difference in rotational traction offered between elliptical and bladed cleat types may be the source of this difference.

Significance: Female-specific biomechanics is notably under-investigated, despite its importance in understanding female injury mechanics. This ongoing project seeks to re-evaluate the existing standards for soccer cleat design, inclusive of the needs of female athletes. Results demonstrate the importance of female-centric cleat design, moderating traction according to mechanics observed during a fatigue state.

Acknowledgments: This work is supported by the Wu Tsai Human Performance Alliance, and the Joe and Clara Tsai Foundation.

References: [1] Waldén et al., *Knee Surg Sport Tr A*, 2010 [2] Decker et al., *Clin Biomech*, 2003 [3] Kernozek et al. *Am J Sports Med*, 2007 [4] Butler et al., *Scan J Med Sci Sport*, 2012

HIP MUSCLE FORCE CHANGES AFTER TRANSFEMORAL BONE-ANCHORED LIMB IMPLANTATION

Mitchell Ekdahl[1*], Nicholas Vandenberg[2], Danielle Melton[2], Cory Christiansen[2], Jason Stoneback[2], Brecca Gaffney[1,2]
[1]University of Colorado Denver, [2]University of Colorado Denver Anschutz Medical Campus
*Corresponding author's email: mitchell.ekdahl@ucdenver.edu

Introduction: People with unilateral transfemoral amputation (TFA) experience pain and discomfort at the limb-socket interface, which contributes to compensatory movement patterns [1]. Asymmetric kinematics result in altered joint loading [2] which has been linked to the development and progression of osteoarthritis. Bone-anchored limbs (BALs) alleviate socket issues by directly connecting the prosthesis to the residual bone [3]. We have shown that sagittal plane joint loading is normalized and abductor muscle force is increased when using a BAL [4, 5]; however, the directional relation between the two is not well understood. Hip joint motion changes the direction of muscle line of action relative to the hip joint center, which influences the relative magnitudes of anteroposterior (AP), superoinferior (SI), and mediolateral (ML) muscle force. Resolving muscle forces into these components would improve understanding of how muscle function may be related to observed changes in hip joint loading after BAL implantation. The purpose of this study was to evaluate changes in AP, SI, and ML force generation of the hip musculature before and after transfemoral BAL implantation.

Methods: Overground walking motion data were collected from 12 participants at two timepoints relative to BAL implantation: ~2 days prior to implantation using a socket prosthesis and 12-months post implantation as previously described [5]. Musculoskeletal models for each participant at each timepoint were developed within OpenSim [5], and muscle force magnitudes were estimated with static optimization [6]. The 3-dimensional line of action of each hip muscle was calculated [7] and used to resolve amputated limb muscle forces into ML, AP, and SI components within the pelvis reference frame. Muscles included in analysis were gluteus maximus, gluteus medius, gluteus minimus, tensor fasciae latae, iliacus, psoas, rectus femoris, and biceps femoris long head. Ensemble averages of muscle force components over the stance period of gait were compared between timepoints using statistical parametric mapping ($\alpha = 0.05$) [8].

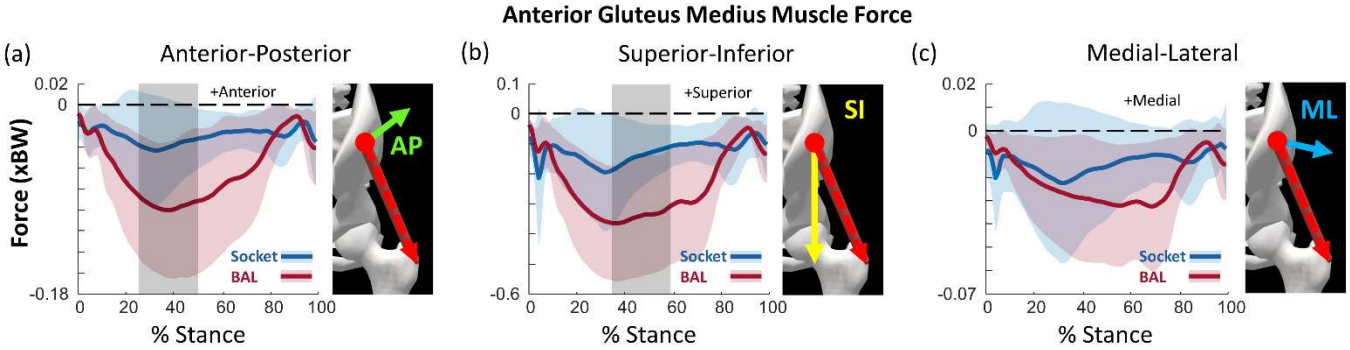

Figure 1: Anterior gluteus medius muscle force generation in the (a) AP, (b), SI, and (c) ML directions before (blue) and after (red) BAL implantation. Grey shaded regions indicate significant differences between the two timepoints.

Results & Discussion: Force production of hip spanning muscles in all three cardinal planes of motion were altered following BAL implantation, with a representative muscle shown in Figure 1. Anterior muscle force was increased for the posterior gluteus medius (pre-swing, $p=0.001$). Posterior muscle force was increased for the anterior gluteus medius (mid-stance, $p<0.001$) and biceps femoris long head (terminal stance and pre-swing, $p<0.001$), but was decreased for iliacus and psoas (terminal stance and pre-swing, $p<0.001$). Inferior muscle force generation was increased for the anterior (mid-stance, $p<0.001$) and middle (terminal stance and pre-swing, $p<0.001$) gluteus medius, gluteus minimus (mid-stance, $p<0.001$), and tensor fasciae latae (mid-stance, $p<0.001$). Lateral muscle force direction for the middle gluteus medius (terminal stance and pre-swing, $p<0.001$) and posterior gluteus minimus (mid-stance, $p<0.001$).

Hip joint loading following BAL implantation is decreased in the anterior direction during pre-swing, but is not changed during mid-stance and terminal stance [5]. Hip flexor muscle forces decreased in the anterior direction during terminal stance and pre-swing, which suggests a more normalized propulsion strategy and may be driving the observed reduction in anterior hip joint loading. However, hip abductor muscle forces were increased in all three cardinal planes of motion during mid-stance, terminal stance, and pre-swing. As many muscles spanning the hip have functions in multiple planes, changes in force production following BAL implantation may affect joint loading in directions other than that of the primary function of the muscle. Therefore, discrepancies between changes in muscle force production and joint loading following BAL implantation may be a result the directional force components of hip abductor muscles and hip flexor muscles offsetting each other. We conclude that directional components of force must be considered to understand how muscle function may be affecting hip joint loading.

Significance: The results of this study provide a better understanding of how muscle function is related to observed changes in hip joint loading following BAL implantation and may help to inform post-surgical muscle rehabilitation practices to produce more normalized hip joint loading in this population.

Funding: University of Colorado Bone-Anchored Limb Research Group and the National Institutes of Health (K01AR080776).

References: [1] Buter (2014), *J Tissue Viability*; [2] Struyf (2009), *Arch Phys Med Rehabil*; [3] Brånemark (2014), *Bone Joint*; [4] Gaffney (2022), *Clin Biomech*; [5] Vandenberg (2023), *J Biomech*; [6] Anderson (2001), *J Biomech* [7] van Arkel (2013), *J Orthop Res*; [8] Pataky (2015), *J Biomech*

PAIN, FORCE, AND MOTION DURING GRASP IN FEMALES WITH CARPOMETACARPAL OSTEOARTHRITIS

Alexis R. Benoit[1*], Tamara Ordonez Diaz[1], Yenisel Cruz-Almeida[2], Jennifer A. Nichols[1]
[1]J. Crayton Pruitt Family Department of Biomedical Engineering, University of Florida, Gainesville, FL
[2]Department of Community Dentistry and Behavioural Science, University of Florida, Gainesville, FL
* Corresponding author's email: abenoit1@ufl.edu

Introduction: Movement evoked pain (MEP), or pain during physical activity, is an area of interest for the musculoskeletal research community [1]. Yet, to our knowledge, few studies robustly evaluate the complex interplay of kinematic, kinetic, and pain variables. Understanding these interactions could provide a greater understanding of the pathophysiological mechanisms driving diseases, hereby leading to more effective, targeted treatments. In this context, we decided to examine MEP, force production, and range of motion (ROM) in women with carpometacarpal osteoarthritis (CMC OA) during maximal and submaximal cylindrical grasp. Studying CMC OA is important as it affects 85% of postmenopausal women and can negatively impact overall quality of life [2]. We analyzed cylindrical grasp because it mirrors real-life scenarios requiring dynamic thumb stability and force production. Evaluating maximal and submaximal grasp enabled the examination of adaptive movement strategies in response to changing task demands. We hypothesized that increases in CMC OA severity would be associated with (i) heightened levels of MEP, (ii) reduced force, and (iii) smaller ROM.

Methods: This exploratory analysis is part of an ongoing IRB-approved study (IRB #201900693) of women with CMC OA. To enable examination of different metrics of disease severity, two cohorts were defined: one by radiographic severity (Eaton-Littler scale, severity increases across four stages) and one by pain severity (AUSCAN, self-reported pain). Twelve participants were included, with three per radiographic stage (stage I: 58.7 ± 11.8 years, stage II: 70.7 ± 19.5 years, stage III: 67.3 ± 4.6 years, stage IV: 60.0 ± 19.3 years). Among them, seven (64.7 ± 11.0 years) had self-reported hand pain, while five (63.4 ± 18.7 years) reported no pain. External thumb-tip forces were recorded at 3,000 Hz using a multi-axis force sensor. Simultaneously, motion capture data was collected at 100 Hz with a 12-camera Vicon system using a custom hand marker set. Each participant performed cylindrical grasp with their thumb on the force sensor for two tasks [maximal (100% effort) and submaximal (50% effort)] with three trials per task. MEP ratings were recorded based on a 101-point Visual Analog Scale (VAS) before, during, and after each trial. Scaled models were generated in OpenSim v4.4, and inverse kinematics was applied to the motion capture data to obtain joint angles for ROM. Unpaired t-tests of all variables were performed in GraphPad.

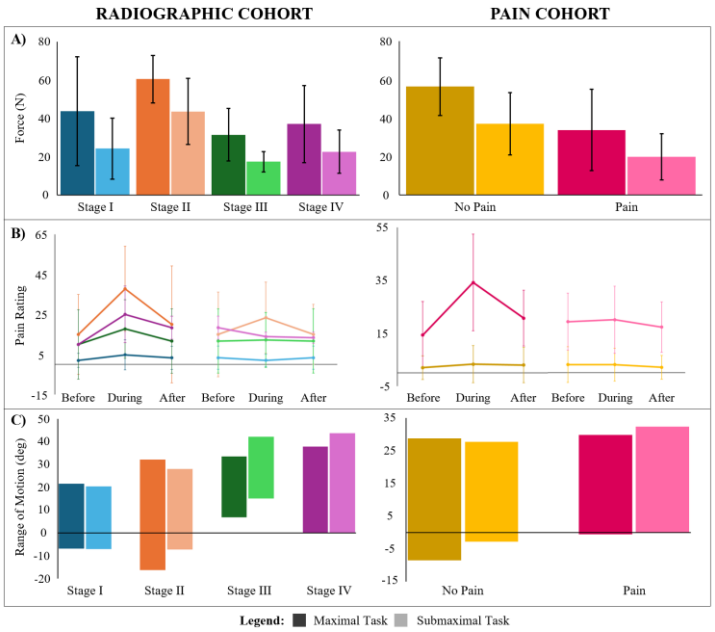

Fig. 1: (A) Maximum thumb-tip force, (B) movement evoked pain ratings, and (C) range of motion were analyzed separately for the radiographic (left) and pain (right) cohorts. Maximal (darker colors) and submaximal (lighter colors) tasks are reported. Error bars represent standard deviation.

Results & Discussion: Individuals with Stage II CMC OA exhibited both the highest forces (Fig. 1A) and the highest MEP ratings (Fig. 1B) during both tasks, suggesting that those with early joint degeneration have not yet adapted their movement strategy to eliminate or avoid pain. Consistent with prior work, ROM during flexion of the carpometacarpal joint varied with radiographic stage [3-4]. Interestingly, individuals with Stage II CMC OA exhibited the greatest ROM, whereas individuals with Stage III CMC OA demonstrated the lowest ROM (Fig. 1C). Those experiencing pain produced less force than individuals without pain (Fig. 1A). MEP was larger during maximal tasks compared to submaximal tasks across all cohorts, with significant differences between pain cohorts [maximal ($p < 0.01$), submaximal ($p < 0.05$)] (Fig. 1B). Together, these results indicate that individuals may compensate for pain by adopting a weaker grasp.

The relationship between force production and MEP is more evident in pain cohorts (Fig. 1B), while ROM differences seem to be more pronounced among radiographic stages (Fig. 1C). These findings underscore the importance of considering different participant groupings to gain a comprehensive understanding of the multifaceted nature of this disease and its functional limitations. Study limitations include a small sample size and uneven distribution of participants across pain cohorts. Future work will expand the sample size and analyze force variability to explore force control strategies across cohorts and task demands.

Significance: This study is a first step toward understanding the interplay between pain, force production, and joint mechanics associated with CMC OA. Elucidating this interplay will allow us to integrate CMC OA phenotypes (i.e., symptom presentation, radiographic evidence) into targeted treatments to restore joint function and reduce overall pain.

Acknowledgments: Funding from National Institutes of Health (R01 AR078817, KL2 TR001429, F31 AG074645).

References: [1] Corbett et al. (2019), *Pain* 160(4); [2] Becker et al. (2013), *CORR* 471(12); [3] Gehrmann et al. (2010), *J Hand Surg Am* 35(9); [4] Ordonez Diaz et al. (2024), *J Orthop Res*. epub ahead of print.

FEASIBILITY OF IN-SILICO GAIT RETRAINING FOR PATIENTS WITH UNILATERAL TRANSFEMORAL BONE-ANCHORED LIMBS

Nicholas W Vandenberg[1*], Benjamin Wheatley, R. Dana Carpenter, Cory L Christiansen, Jason W Stoneback, Brecca M M Gaffney
[1]University of Colorado – Denver, Denver, CO
*Corresponding author's email: nicholas.vandenberg@ucdenver.edu

Introduction: Patients with unilateral transfemoral (TF) amputation using socket prostheses utilize aberrant movement patterns as a compensatory strategy for the loss of biological joints and in response to problems related to socket fit [1,2]. Bone-anchored limbs (BALs) are alternatives to socket prostheses that rely on bony ingrowth from osseointegration to directly fix an implant within the residual bone, which a prosthetic limb can then attach to [3]. Rehabilitation following BAL implantation surgery is a crucial step in patient recovery and typically includes gait retraining to target movement and loading symmetry [4]. However, these processes lack standardization, and the potential impact of enforcing symmetry on an inherently asymmetrical system (represented by patients with TF amputation) is not well understood. Combining optimal control theory with musculoskeletal modeling yields a method for simulating potential rehabilitative interventions in a dynamically consistent manner, without causing physical stress to an individual [5]. To our knowledge, likely due to the computational complexity, these methods have not yet been used to investigate a movement pattern retraining intervention in TF BAL users. Therefore, our objective was to establish the feasibility of implementing a gait retraining intervention for patients with TF BAL, using a combination of optimal control and musculoskeletal modeling.

Methods: A musculoskeletal model with 10 degrees of freedom (DOF) and 18 muscles was used to model an able-bodied individual. An optimal control problem using OpenSim Moco [5] was solved to predict a solution trajectory of 'ideal' 2D gait dynamics by minimizing muscle activity and using generic healthy kinematics as an initial guess for the solver to converge. The musculoskeletal model was then adapted to simulate an individual with a right TF amputation using a BAL by removing uniarticular knee musculature and all ankle musculature, creating a simulated myodesis by adjusting the insertion sites of hip flexor and extensor muscles (rectus femoris and hamstrings), and adding ideal torque actuators to the prosthesis joints, resulting in a model with 10 DOF and 13 muscles. A gait retraining intervention was then simulated for the TF BAL model using another optimal control problem which tracked the previous able-bodied kinematics while minimizing muscle activity. Muscle activations, for the amputated limb and analogous able-bodied limb, from each solution were qualitatively compared to determine the changes in muscle activity that are required to produce the 'ideal' movement patterns in a patient with unilateral TF BAL.

Results & Discussion: Gait retraining of the TF BAL model resulted in decreased activity from the hip extensors during the loading response as compared to the able-bodied solution (Fig. 1), when these muscles would typically be eccentrically active to help decelerate the body during weight acceptance. Additionally, hip extensors activity in the TF BAL were increased during terminal stance (Fig. 1). Coupled with the burst of activity from the hip flexors in early swing period, this may be indicative of an adapted compensation for swing limb advancement where the extensors 'prime' the amputated limb into extension at the end of stance before relying on the hip flexors to advance the limb in the absence of propulsion from ankle plantarflexors. In able-bodied gait, the ankle plantarflexors generate a large propulsive force during terminal stance that allows the swing limb to semi-passively advance through the transfer of momentum [6]. To achieve an able-bodied gait pattern without these muscles, the TF BAL model relied on increased hip flexor activity throughout the swing phase in order to fully advance the limb, with significantly increased activity observed from the iliopsoas (Fig. 1).

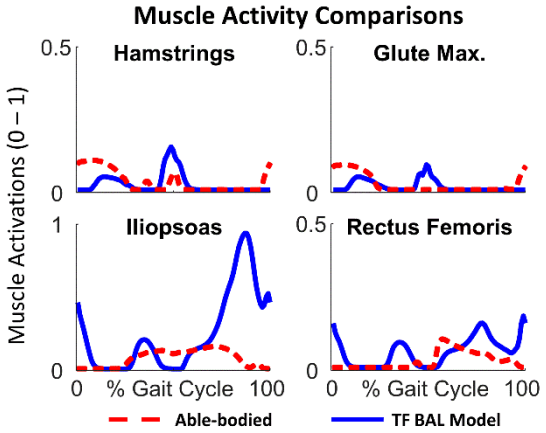

Figure 1. Muscle activation comparison between able-bodied predictions (red, dashed) and TF BAL model tracking (blue, solid) during a right limb gait cycle.

An important limitation in this study is the 2D gait dynamics restricted to the sagittal plane. As common aberrant movement patterns observed in individuals with TF amputation occur in the frontal and transverse planes (i.e., circumduction of the amputated hip or the compensated Trendelenburg pattern) and muscles act in three-dimensions, it is not clear if the current results would be feasible to achieve an able-bodied gait pattern. Our future work is implementing a more complex musculoskeletal model with 3D DOFs and an expanded muscle set to better estimate synergistic muscle activity required for the TF amputee model to replicate the able-bodied gait in our simulated retraining intervention.

Significance: Establishing the feasibility of *in silico* methods for modelling gait retraining interventions in patients with TF BALs may help to determine the changes in muscle demand that are required to produce a more optimal movement pattern. This framework has the potential to inform subject-specific targeted movement pattern rehabilitation following TF BAL.

Acknowledgments: This work is supported by the University of Colorado Bone-Anchored Limb Research Group and the National Institutes of Health (R03HD111012).

References: [1] Gilliss et al *JAOA* (2010) [2] Morgenroth et al *PM&R* (2012) [3] Branemark et al *JRRD* (2001) [4] Leijendekkers et al *Physiotherapy Thry & Pract.* (2017) [5] Dembia et al *PLoS* (2020) [6] Gronley & Perry *Phys Therapy* (1984).

THE IMPACT OF PERIACETABULAR OSTEOTOMY ON THE CONTRALATERAL HIP

Madison M. Wissman*, Molly C. Shepherd, Michael D. Harris
Washington University School of Medicine in St. Louis
*Corresponding author's email: m.wissman@wustl.edu

Introduction: Developmental dysplasia of the hip (DDH) is characterized by a shallow acetabulum and insufficient coverage of the femoral head that causes instability of the joint and increases risk for early osteoarthritis [1]. The abnormal bone shape of DDH increases stabilization demands on the hip abductor muscles, which results in higher-than-normal medially and superiorly oriented joint reaction forces (JRFs) during walking [2]. Periacetabular osteotomy (PAO) is a surgical approach to correcting DDH by reorienting the acetabulum to better cover the femoral head and to medialize the hip joint center [3]. Although research indicates that PAO is able to decrease the magnitude of detrimental JRFs on the surgical hip, 80% of individuals have radiographic evidence of bilateral DDH and are still at risk of developing symptoms and osteoarthritis on the contralateral hip [4, 5]. Ongoing research from our institution has found that 51% of patients report pain in the contralateral hip and 33% undergo contralateral PAO within 5 years of their first PAO surgery. An important step in understanding why individuals develop contralateral hip pain is to assess biomechanical changes that may occur after a patient undergoes PAO. The current study investigated the effects of PAO on hip joint angles and JRFs of the contralateral limb during walking and how they compare to changes on the surgical hip. We hypothesized that the surgical hip would experience a reduction in superiorly and medially oriented JRFs after PAO, and the contralateral hip JRFs would be elevated in the medial direction before surgery and experience no change after PAO.

Methods: Six female participants with DDH were included in this study. Gait kinematics were captured before and four months after unilateral PAO using an instrumented treadmill and a 10-camera motion capture system. Participants were tracked using 70 reflective markers while walking at their pre-PAO self-selected speed. Kinematics were captured at 100 Hz and ground reaction forces (GRFs) at 2000 Hz. Magnetic resonance imaging from before surgery was used to make subject-specific models, which were later updated using post-op imaging to create the post-surgery models [6]. Kinematics and GRFs were used to run computed muscle control and joint reaction analysis in OpenSim on representative gait cycles for the surgical and contralateral limbs pre- and post-PAO. All forces were normalized to bodyweight and statistical parametric mapping with paired samples t-tests was performed across the normalized gait cycle at an alpha level of 0.05.

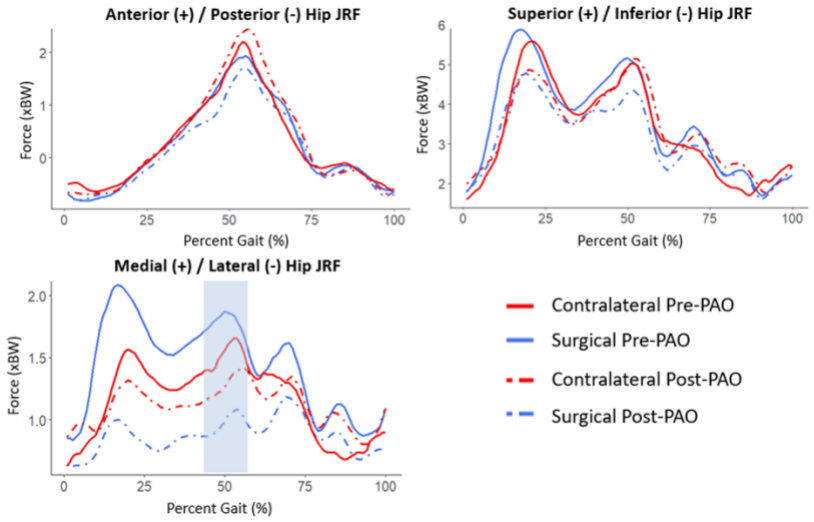

Figure 1: Surgical hip and contralateral hip JRFs during walking. Shaded areas indicate significance at $p < 0.05$.

Results & Discussion: There were no significant changes to joint angles after PAO on either the surgical or contralateral hip. Comparing JRFs before and after PAO indicated a modest decrease in superiorly directed JRFs in the surgical and contralateral hips, and a decrease in medial JRF in the surgical hip. The only significant pre-to-post PAO change was a decrease in the medial JRF during late stance in the surgical hip (Fig. 1). This partially supported our hypothesis. Interestingly, the medial JRF in the surgical hip decreased enough after PAO that the average value was lower than that of the contralateral hip (Fig 1). These results suggest that PAO can substantially change JRFs in the surgical hip, while causing only minor biomechanical changes in the contralateral hip. If so, it may not be biomechanical changes from PAO that instigate eventual contralateral pain in 51% of PAO recipients. Instead, contralateral pain may be part of natural DDH disease progression that depends on contralateral bony anatomy. However, the current sample of patients is small and there could be biomechanical changes that were not detectable. It is likely that multiple factors (bony anatomy, activity level, biomechanics) contribute to both surgical and contralateral hip outcomes after PAO. This study begins an important effort to understand what leads to contralateral pain and damage, and to inform clinicians about how to advise and treat their patients.

Significance: This study is one of the first to examine the biomechanical influence of PAO on the contralateral limb in patients with DDH. Understanding the impact of PAO and the factors that contribute to symptom onset is crucial for effective management of DDH and preservation of the hip joint.

Acknowledgments: Funding provided by the National Institute of Arthritis and Musculoskeletal and Skin Diseases K01AR072072 and R01AR081881.

References: [1] Wyles et al. (2017), *Clin Orthop Relat Res*. 475(2); [2] Harris; [3] Ganz et al. (1988), *Clin Orthop Relat Res*. (418):3-8; [4] Gaffney et al. (2020), *J Biomech.* 98; [5] Jacobsen et al. (2006), *Clin Orthop Relat Res.* 446:239-246 ; [6] Song et al. (2019), *Comput Methods Biomech Biomed Engin*. 22(3)

THE INFLUENCE OF LOAD CARRIAGE AND PROSTHETIC FOOT TYPE ON PLANTARFLEXOR AND PROSTHETIC FOOT CONTRIBUTIONS TO BODY SUPPORT AND PROPULSION DURING WALKING

Aude S. Lefranc[1, 3, *], Krista M. Cyr[2], Glenn K. Klute[2], Richard R. Neptune[1]
[1] Walker Department of Mechanical Engineering, The University of Texas at Austin, Austin, TX
[2]Center for Limb Loss and MoBility, Department of Veterans Affairs, Seattle, WA
[3] Enovis, DJO Surgical, Research & Innovation Biomechanics Team, Austin, TX
*Corresponding author's email: Lefranc@utexas.edu

Introduction: Individuals with unilateral transtibial amputation (TTA) display reduced self-selected walking speeds, increased bilateral asymmetry and incidence of osteoarthritis relative to non-amputees[1,2]. These walking deficits can be attributed in part to the loss of the ankle plantarflexors, which are essential to providing body support, forward propulsion, leg-swing initiation and balance control[3,4]. Studies have shown that the plantarflexors also play a critical role during load carriage[5]. However, transtibial amputees cannot modulate their ankle power on the residual side, as the properties of passive prosthetic feet, such as stiffness, are constant and cannot adapt to changing load conditions. Further, the relative effects of various commercially available prosthetic feet, as well as different load carriage positions, remains unclear. Thus, the purpose of this study was to use modeling and simulation to investigate the effects of a range of prosthetic feet and load conditions on plantarflexor and prosthetic foot contributions to body support and forward propulsion.

Methods: Kinematic, kinetic and EMG data were collected from five individuals with TTA. Twenty trials were collected for each individual, consisting of five loading conditions (no load; 13.6 kg (30 lbs) carried as a front load, back load, intact-side load and residual-side load) while wearing four prosthetic feet: a passive clinically prescribed foot (PR), a passive foot one category stiffer than prescribed (SF), their prescribed foot with a heel stiffening wedge (HW), and a dual-keel foot (DK). Two participants also wore a powered-ankle foot prosthesis (PW; Empower, Ottobock, Austin, TX) for all loading conditions, thus completing an additional five trials each. A generic musculoskeletal model (OpenSim gait2392[6,7]) was modified to create a 3D TTA model. To model the various loading conditions, a body was attached with a spring-damper interface to either the front, back, intact- or residual-side of the torso segment of the model. For each subject, a gait cycle was simulated from each loading and prosthesis condition using OpenSim 4.1[6,7]. A ground reaction force decomposition[8] was used to determine plantarflexor and prosthetic foot contributions to body support and propulsion.

Results & Discussion: Wearing a clinically non-prescribed foot (DK, HW, SF, PW) typically resulted in an increased contribution to support from the prosthetic foot relative to the prescribed foot (Fig 1A). The addition of a load resulted in increased foot contribution to support across all loading conditions and prostheses (Fig 1A). In particular, the intact-side load resulted in the largest increase in prosthetic foot contribution, followed by the back load condition. Increases in gastrocnemius (GAS) and soleus (SOL) contributions to support were observed during loading relative to the no load condition, which was consistent with other modeling studies[9]. For most conditions, the combined contribution to forward propulsion from GAS and SOL was greater than the prosthetic foot (Fig 1B). In contrast, the prosthetic foot contributed more to braking across all conditions. GAS contributed most to forward propulsion for the back and residual-side load conditions; however, SOL and the prosthetic foot contributed the most during the intact-side loading condition. When wearing stiffer passive feet (i.e., SF, DK and HW), the contributions of GAS and SOL to propulsion notably increased. This suggests that individuals wearing clinically non-prescribed feet may depend more on their intact limb than their prosthesis to generate propulsion, potentially due to unfamiliarity with the stiffer foot.

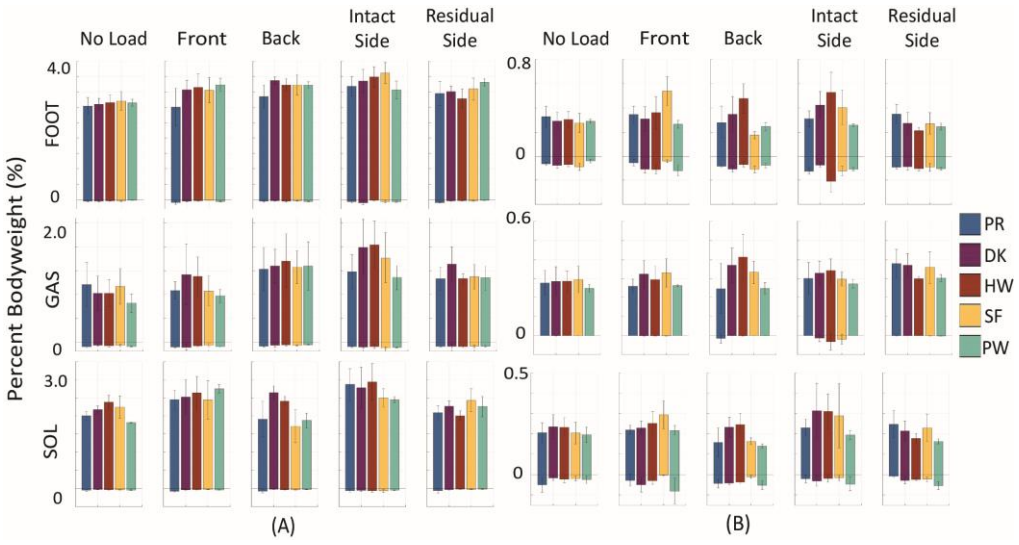

Figure 1: Prosthetic foot (FOOT) and plantarflexor (SOL and GAS) contributions to (A) support and (B) propulsion. Foot types investigated include a passive clinically prescribed foot (PR), a passive foot one category stiffer than prescribed (SF), their prescribed foot with a heel stiffening wedge (HW), a dual-keel foot (DK) and a powered-ankle prosthesis (PW).

Significance: This study provides insight into the effects of load carriage and prosthetic foot selection on plantarflexor and prosthetic foot contributions to support and propulsion. Further studies with more participants are needed to generalize these findings.

Acknowledgments: Supported by VA awards RX003138 and RX002974.

References: [1] Struyf et al. (2009), Arch Phys Med Rehabil 90(3); [2] Robinson et al. (1977), Phys Ther 57(8); [3] Neptune et al. (2001), J Biomech 34(11); [4] Neptune et al. (2016), J Biomech 49(13); [5] McGowan et al. (2008), J Appl Physiol 105(2); [6] Delp et al. (2007), IEEE Trans Biomed Eng 54(11); [7] Seth et al. (2018), PLoS Comput Biol 14(7); [8] Liu et al. (2006), J Biomech 39(14); [9] Silder et al. (2013), J Biomech 46(14)

TOWARD AN UNDERSTANDING OF THE RESULTANT ENDPOINT FORCES THAT SMALL MUSCLE GROUPS PRODUCE THROUGHOUT THE PLANE OF LATERAL PINCH: APPLICATION TO RESTORATION OF GRASP FOLLOWING NEUROLOGIC IMPAIRMENT

Oliver Garcia, Joseph Towles*
Engineering Department, Swarthmore College, Swarthmore PA
*Corresponding author's email address: joseph.towles@swarthmore.edu

Introduction. The quality of life of up to 135,000 persons around the world, who annually suffer a cervical spinal cord injury [1, 2], is severely affected due to loss of hand function. Tendon transfer surgeries that engage the paralyzed flexor pollicis longus (FPL) muscle are commonly performed to enable lateral pinch grasp [3]. Functional outcomes, however, have been mixed [4, 5], we think, in part, due to FPL's inability to produce a well-directed force at the thumb-tip that would promote stable grasp [6]. This work builds on our previous work [7] where we investigated whether small groups of muscles could produce better-directed endpoint forces than FPL alone (i.e., endpoint forces directed less than 54 deg relative to the palmar direction three dimensionally (3D), Fig. 1) during lateral pinch grasp throughout the plane of flexion-extension (FE). The goal of this simulation study was to further explore whether small groups of paralyzed muscles could produce better-directed endpoint forces than that of FPL, throughout the range of motion of lateral pinch grasp, however, this time allowing for the possibility of each muscle to transmit different levels of donor muscle force. Following a tendon transfer surgery, different levels of donor muscle force transmitted to the paralyzed recipient muscles would naturally happen because thumb movement would produce geometrical changes between the line of action of the donor muscle force and those of the forces transmitted to the recipient muscles.

Methods. We simulated 3D lateral pinch force production following tendon transfer surgery in which the donor muscle was attached to small groups of paralyzed muscles using nonlinear optimization and in-situ, 3D measurements of individual muscle endpoint forces previously published [6, 7]. Additionally, we accounted for lateral pinch force production throughout the plane of FE by incorporating muscle endpoint force vectors that were measured (flexed and extended postures) and estimated (mid-flexed posture) in multiple thumb postures (Fig. 1) that spanned the lateral pinch range of motion [6, 7]. Twenty small muscle groups were formed and consisted of all possible pairs and triplets of muscle combinations consisting of the thumb's chief flexor muscle, FPL, and its four intrinsic muscles, the radial and ulnar heads of the flexor pollicis brevis (FPBr, FPBu), adductor pollicis (ADP) and abductor pollicis brevis (APB). The optimization algorithm searched for all muscle combinations across all three postures that maximized palmar force production and that produced resultant, 3D endpoint force vectors that were directed less than 54 deg relative to the palmar direction at the thumb-tip (defined in Fig. 1). Each muscle could generate a force up to its maximum isometric force capacity [7].

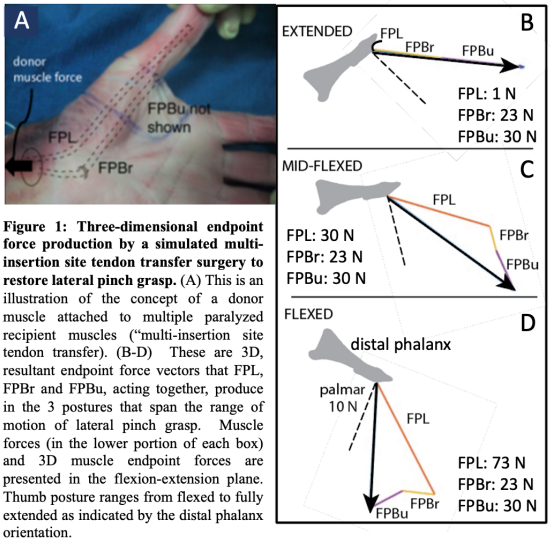

Figure 1: Three-dimensional endpoint force production by a simulated multi-insertion site tendon transfer surgery to restore lateral pinch grasp. (A) This is an illustration of the concept of a donor muscle attached to multiple paralyzed recipient muscles ("multi-insertion site tendon transfer). (B-D) These are 3D, resultant endpoint force vectors that FPL, FPBr and FPBu, acting together, produce in the 3 postures that span the range of motion of lateral pinch grasp. Muscle forces (in the lower portion of each box) and 3D muscle endpoint forces are presented in the flexion-extension plane. Thumb posture ranges from flexed to fully extended as indicated by the distal phalanx orientation.

Results & Discussion. We found that every muscle group was able to produce a better-directed force than FPL in at least one posture. Specifically, 4 groups produced such a force in 1 posture, 10 groups in 2 postures, and 6 groups in all 3 postures (a representative muscle group is presented in Fig. 1). Pertaining to the latter 6 groups, FPBr and FPBu participated in 5 such groups, ADP participated in 3, FPL in 2, and APB in 1. From the standpoint of individual postures, 16 of the 20 muscle groups were able to produce better-directed endpoint forces than FPL in the flexed posture, 19 in the mid-flexed posture, and 8 in the extended posture. The finding that FPBr and FPBu most frequently occurred in muscle groups that produced better-directed endpoint forces than that of FPL could be due to complementary endpoint force characteristics [6]. Additionally, both, as biarticular muscles, are less affected by thumb extension than FPL, a triarticular muscle. Thumb extension causes endpoint force vectors to rotate farther away from the palmar force direction [6, 7]; endpoint force production in that direction is key for producing stable grasp [6]. Lastly, muscle force values (Fig. 1) that the optimization algorithm found to achieve desired endpoint force directions can be used to determine the required portion of donor muscle force that must be transmitted to recipient muscles. For example, in Fig. 1D, FPL would receive 3 times as much donor muscle force as both FPBr and FPBu, and FPBr and FPBu would receive nearly equal amounts.

Significance. As far as we know, this simulation study is the first to apply an endpoint force-based biomechanics approach to the design of tendon transfers aimed at restoring lateral pinch grasp following cervical spinal cord injury throughout the FE plane and highlights the possibility of employing "multi-insertion site tendon transfers." Investigating the surgical feasibility of engaging multiple recipient muscles, including intrinsic muscles, in a tendon transfer surgery and determining how to implement the appropriate coordination of donor muscle force across recipient muscles are next steps to consider.

References: [1] Lee BB et al (2014), *Spinal Cord*, 52: 110-116. [2] National Spinal Cord Injury Statistical Center, Facts and Figures at a Glance (2015). [3] Fox KI et al (2018), *Topics Spinal Cord Inj Rehabil*, 24(3): 275-287. [4] Johanson ME et al (2016), *Arch of Phys Med Rehab*, 97:S144-53. [5] Waters R et al (1985), *J Hand Surg [Am]*, 10A: 385-391. [6] Towles et al. (2008), *Clin Biomech* 23(4): 387-94. [7] Towles (2023), *Annu Int Conf IEEE Eng Med Biol Soc*, 1-5.

A GENERATIVE DEEP LEARNING MODEL PREDICTS GROUND REACTION FORCES AND FUTURE KINEMATICS

Tian Tan[1*], Tom Van Wouwe[2], Keenon F. Werling[3], Scott L. Delp[2], Jennifer L. Hicks[2], Akshay S. Chaudhari[1]
[1]Radiology, [2]Bioengineering, and [3]Computer Science, Stanford University, Stanford, CA, USA
*Corresponding author's email: alanttan@stanford.edu

Introduction: Deep learning models can predict 3-D gait kinematics and kinetics from sparse kinematics measurements [1]. However, such models require large datasets for training, a rarity in the biomechanics field where datasets typically contain a small number of subjects tested in a single laboratory. We recently created a large human dynamics dataset using the AddBiomechanics tool [2], which standardized marker-based motion capture data and ground reaction force (GRF) data from fifteen studies conducted by twelve different laboratories. Our dataset has more than 50 hours of gait dynamics data collected from 273 subjects, mitigating the biases of individual datasets. We used our large dataset to train a diffusion-based, general-purpose generative model, which represents human gait dynamics and can generate unknown biomechanical parameters that are harmonious with known ones. As such, unlike prior regressive deep learning models that have strict specifications regarding inputs and outputs, our model allows flexible input-output pairs, thus adaptable to various prediction tasks. In this abstract, we present the performance of our unified generative gait model on three example tasks: 1) predicting GRF using kinematics, 2) predicting future lower-limb joint angles using past kinematics, and 3) reconstructing pelvis and trunk kinematics using lower-limb kinematics.

Methods: The AddBiomechanics dataset was split into training and test sets. The test set consists of walking and running gait data for fifteen randomly selected subjects (one from each of the fifteen constituent datasets); the remaining subjects' data, regardless of motion type, were used for training. The motion states in each trial (i.e., kinematics of an OpenSim Rajagopal model [3] and 3-D body weight (BW) normalized GRF of each foot) were linearly resampled to 60 Hz and randomly segmented into 1.5s windows, creating 2-D matrices with dimensions of time and states. We added iteratively increasing noise into each data window and trained a transformer-based generative model to recognize the noise [4]. This trained model was used for all three downstream prediction tasks during testing. For each task, the portion of the data windows corresponding to the desired model output was masked by random noise whereas the input portion was preserved. Then, the model used the input portion as guidance to remove noise from the output. The unmasked inputs for the three tasks were: 1) full-body kinematics of all the time steps, 2) full-body kinematics of the first 1,480ms, 1,460ms, …, and 1,300ms of each 1.5s window, and 3) combinations of lower-limb joint angles (Table 2) of all the time steps. For each constituent dataset, its average GRF and kinematics curves across all the gait cycles were used as the baseline. Specifically, gait cycles of the training set were segmented based on GRF, resampled to 100 points, averaged, and resampled to match the lengths of test set gait cycles.

Results & Discussion: For GRF prediction, our model outperformed the baseline across all three axes (Table 1). For future joint angle prediction, our model outperformed the baseline for predicting motion states up to 160ms in the future (Figure 1). By providing different inputs to the model, we observed the need for 3-D Hip angles to reconstruct pelvis and trunk angles with maximal accuracy, compared to solely using ankle and knee flexion angles (Table 2).

In summary, our deep-learning-based gait model trained on a large biomechanics dataset outperformed the baseline across multiple tasks, including GRF prediction, future kinematics prediction, and missing kinematics reconstruction. Unlike previous models, our model is adaptable to a range of input combinations and prediction targets due to its generative nature.

Significance: Our general-purpose generative gait model can be used to predict current and future kinematics and kinetics, thus potentially enabling applications such as exoskeleton control and gait training.

Acknowledgments: This work was supported by the Joe and Clara Tsai Foundation through the Wu Tsai Human Performance Alliance.

References: [1] Zago et al. (2021), *Front. Bioeng. Biotechnol.* 638793; [2] Werling et al. (2023), *Plos One* 18(11); [3] Rajagopal et al. (2016) *IEEE TBME* 63(10); [4] Van Wouwe et al. (2023), arxiv:2308.16682

Table 1: RMSE of GRF Estimation When Using Full-Body Kinematics as Model Input.

Axis		RMSE (BW)
Medio-lateral GRF	Baseline	0.27 ± 0.07
	Proposed	**0.22 ± 0.06**
Anterior-posterior GRF	Baseline	0.46 ± 0.16
	Proposed	**0.32 ± 0.13**
Vertical GRF	Baseline	2.18 ± 1.25
	Proposed	**1.16 ± 0.64**

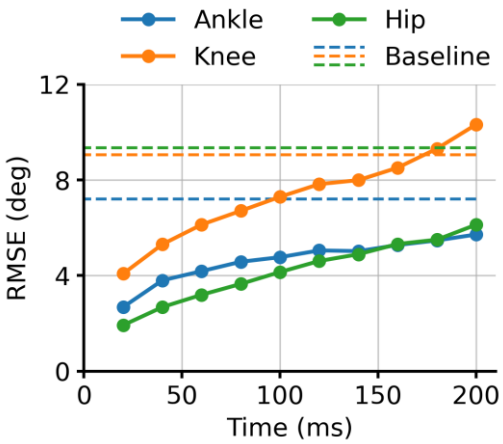

Figure 1: RMSE of Future Ankle, Knee, and Hip Flexion Angle Prediction When Using the Past Full-Body Kinematics as Model Input. Predictions were made from 20 ms to 200 ms ahead of the input.

Table 2: RMSE of Pelvis and Trunk Kinematics Reconstruction When Using Combinations of Joint Angles as Model Input.

Input			RMSE
Ankle Flexion	Knee Flexion	3-D Hip	
✓			8.03 ± 4.16
	✓		8.03 ± 4.09
✓	✓		7.44 ± 3.93
		✓	4.74 ± 3.19
✓	✓	✓	**3.76 ± 2.32**
Baseline			5.07 ± 2.64

DATA-DRIVEN DEEP LEARNING OF HUMAN BIOLOGY ENABLES PERSONALIZED GENERALIZATION OF CONTROL FOR WEARABLE ROBOTICS

Aaron. J Young[1*], Dean Molinaro[1]
[1]Georgia Institute of Technology, Atlanta, GA
*Corresponding author's email: aaron.young@me.gatech.edu

Introduction: One of the major barriers that prevents wearable lower limb robotic systems, such as powered prostheses and exoskeletons, from being adopted ubiquitously is the lack of control systems that handle real-world multi-task locomotion activities. Studies show mobility is strongly linked to quality of life, participation and depression, and these technologies have significant ability to enhance human ambulation, reduce fall risk, and improve overall quality of life [1]. However, current state-of-the-art systems tend to struggle to be useful in more than 1 or 2 tasks due to the difficulty of hand engineering systems to perform well across both heterogeneous human populations as well as highly varied real-world use in numerous tasks such as multi-speed walking, stairs, ramps, sit-to-stand and start/stops. The advent of end-to-end deep learning offers a new solution to this problem but requires massive datasets to be effective. We have engineered a new class of training datasets for exoskeleton users focused on physiological state estimation, such as biological joint moment, which enables user-independent and task agnostic control capability [2].

In this study, we test the hypothesis that a deep learning-based control system trained to human biological moment can unify control across a variety of locomotion modes to reduce metabolic cost and joint work compared to not using an exoskeleton [3].

Methods: We first collected a series of training data (N=24) which consisted of exoskeleton users walking in a custom powered hip exoskeleton weighing 4.5 kg and providing up to 18 Nm peak torque (Fig 1A) [4]. Users completed trials consisting of standing, level walking at different speeds, transitions, ramps at different inclines, and stairs at different heights. Motion capture and force plate data were collected for all these tasks and standard inverse dynamics was run to compute net joint torques. We trained a temporal convolutional network (TCN) to estimate joint torques in real time and scale assistant to 20% biological moment [2]. We performed tests in a new cohort (N=10) to test the accuracy of the unified deep learning system in real-time. We also performed outcomes testing which included metabolic cost and joint work to localize energy changes to joints. For metabolic testing, we also compared to gold standard human-in-the-loop (HIL) optimized spline based control in which the controller had previously been optimized on a task specific basis, which in theory represented the ceiling of what could be achieved. We also compared to a zero impedance condition.

Results & Discussion: The unified control system enabled by deep learning human physiological state provided reliable and accurate assistance both within and across task transitions. Average R^2 values for estimating biological hip moment across level walking, ramps and stairs was above 0.8 (representative tracking curves shown in Fig. 1B), which enabled a highly controllable system for all testing subjects during real-time operation. Human outcomes matched our hypothesis with the unified controller significantly ($p<0.01$) reducing metabolic cost by over 5% level walking and over 10% in ramp ascent compared to the no exoskeleton condition. The unified controller also matched HIL optimized spline control in level walking and surprisingly exceeded it's performance by 5% ($p<0.01$) in ramp ascent.

Total positive joint work (compared to no exoskeleton) was reduced with unified control in level walking by 17.5%. Unsurprisingly, this was primarily due to the human users reducing their hip-level joint efforts (by 29.2%), but smaller reductions were observed at both the knee (9.7% reduction) and ankle (7.7%), indicating some level of redistribution of effort occurred across lower limb joints.

Significance: We demonstrate, for the first time, a novel unified control system based on deep learning of human physiological state capable of real-time estimation and control for exoskeleton applications [3]. Key significance is that we can now enable reliable and useful control without the need for estimating tasks explicitly (typically achieved through either a state machine or mode classifier) or the need to estimate gait phase for control. In addition, all deployments were user-independent (no training data from the test subject) and absolutely no hand tuning or user-specific configurations were allowed in this study. This new style of control has the potential to enable exoskeleton technology to be deployed in real-world and community ambulatory environments.

Acknowledgements: This project was funded by NSF FRR, NSF NRI and NIH New Innovator Award (DP2).

References: [1] Metz (2000), *Transport policy* 7(2); [2] Molinaro et al., (2022). *IEEE TMRB* 4(1); [3] Molinaro et al. (2024), *Science Robotics* (in press); [4] Kang et al. (2021) *Robotics and Automation Letters* 6(2).

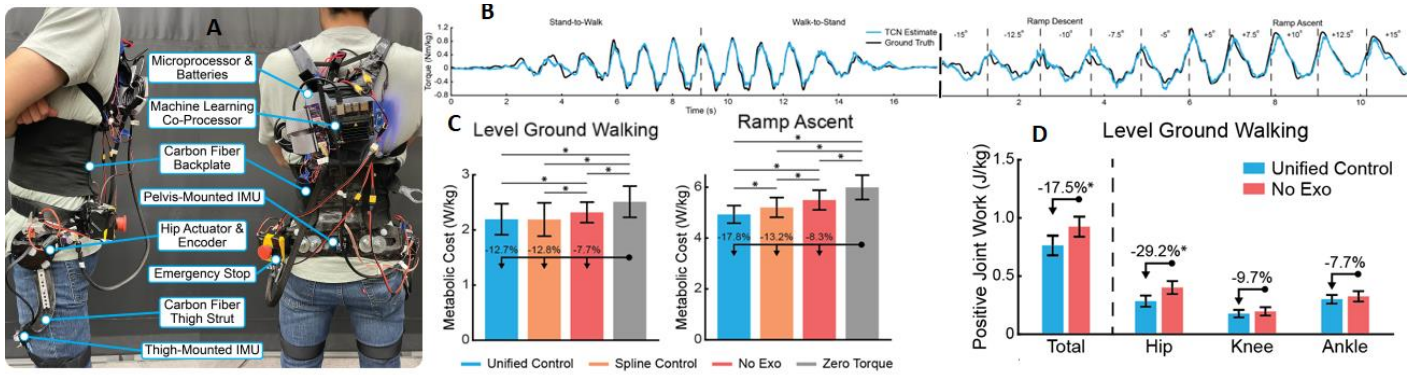

Figure 1: This N=34 study was conducted with an autonomous robotic hip exoskeleton designed at Georgia Tech (A). Representative tracking of the deep learning system (B) showed an average R^2 of 0.84 across walking, ramps and stairs compared to ground truth inverse dynamics. Our unified control system reduced both metabolic cost (C) and joint work (D) significantly compared to the no exoskeleton baseline.

GAIT EVENT DETECTION IN OLDER ADULTS WITH AND WITHOUT PARKINSON'S DISEASE VIA SHANK-WORN INERTIAL MEASUREMENT UNITS AND CONVOLUTIONAL NEURAL NETWORKS

Anthony J. Anderson[1*], Michael Gonzalez[1], Siegfried Hirczy[2], Kimberly Kontson[1]
[1]US Food and Drug Administration, Office of Science and Engineering Laboratories, Division of Biomedical Physics
*Corresponding author's email: anthony.anderson@fda.hhs.gov

Introduction: Parkinson's Disease (PD) is a progressive neurodegenerative disorder that impairs gait and balance, diminishing mobility and increasing fall risk. Current PD management relies on infrequent clinical assessments, which results in long periods of suboptimal care. Continuous monitoring technologies may allow for more frequent therapy changes and thereby maximize function, even when using the same treatment modalities. There is significant interest in using wearable inertial measurement units (IMUs) for assessing PD patients. Wearables like smartwatches have shown promise in detecting symptoms such as tremor, providing clinicians with quantitative data on patients' daily symptoms. Extending wearable technologies to gait assessment could transform PD care by offering detailed insights into gait and mobility from lower limb IMU data via spatiotemporal gait metrics, allowing for more precise treatment.

Accurate gait event detection is essential for analyzing spatiotemporal gait metrics from IMU signals. Traditional methods, based on expert-crafted algorithms with multiple open parameters [1], are often brittle and fail to generalize to complex pathological gait signals. Advances in deep learning (DL) present new opportunities for enhancing detection accuracy. However, much of the existing DL research addresses simple walking tasks, such as straight-line or treadmill walking. This pilot study investigates the use of temporal convolutional neural networks (TCNs) for detecting initial contact (IC) and final contact (FC) gait events in individuals with and without PD, covering various tasks like walking, turning, and sit-to-stand and walk-to-sit transitions. We hypothesize that TCNs can accurately detect initial and final contact events, even amid complex movements, providing an important building block in remote gait assessment.

Methods: Data collection occurred at Johns Hopkins School of Medicine in Baltimore, MD, and the VA Puget Sound Healthcare System, in Seattle, WA, involving 60 participants split into PD-diagnosed (34 participants, age 67±10) and control groups (26 participants, age 75±8). Both sites used uniform protocols with participants wearing a set of IMUs (Xsens, MTw Awinda) during gait tasks on a pressure-sensing walkway (Protokinetics, Zeno), capturing foot contact timing for IC and FC gait event validation. Tasks included self-paced and hurried pace walks with 180-degree turns, and the timed-up-and-go (TUG) task, providing a dataset that included periods of standing, sitting, walking at several speeds, turning, and sit-to-stand and walk-to-sit transitions with annotated gait events.

The dataset was divided into equal sized training, validation, and testing sets with no participant overlap. IMU signals from the right lateral shank, specifically three-axis acceleration and gyroscope data, were cut into two-second windows for the TCN model, following the methods of Romijnders et al. [2]. Training targets were 1-dimensional arrays, marking right-foot gait events (IC or FC) with 1s and 0s elsewhere. Separate TCN models for IC and FC events were trained. Overfitting was prevented with iterative evaluation on the validation set during model training. A peak-finding algorithm post-training isolated gait events, using an F-score-optimized magnitude threshold on validation data. Outputs from each model were counted as true positives if they were above the peak-finding threshold and within 50 ms (5 frames) of a labeled event. Performance on the test set was evaluated via precision, recall, and F-score, assessing the TCNs' gait event detection accuracy.

Results & Discussion: The evaluation of the TCN model on the unseen testing dataset demonstrates its potential in gait event detection (Table 1). Overall, the model showed strong performance detecting gait events. Comparatively, Romijnders et al. [2] achieved superior precision and recall values of ≥97% and ≥92%, respectively, in a related study employing similar methodologies for gait event detection. The discrepancies in model performance between our study and theirs could be attributed to three main factors: 1) the larger participant pool in their study, which included 157 participants, 2) the less complex gait tasks (straight-line walking) they analyzed, and 3) the use of a higher sampling frequency in their IMUs (200 Hz compared to our 100 Hz). These differences underscore the potential impact of participant number, movement complexity, and sampling rate on model efficacy. Future research should aim to systematically investigate how variations in training data volume and task complexity influence the performance of deep learning models in the context of gait event detection.

Significance: This study provides insights into the applicability of temporal convolutional neural networks for detecting gait events in complex movements in a population of participants with and without PD. While deep learning methods show promise as a foundational technology for wearables-based digital health tools, clinical translation will benefit from further research into the limits of model performance, as well as research into validation methods in the free-living environment.

Acknowledgments and Disclaimer: Funding was provided by the FDA Critical Path Initiative and FDA Division of Biomedical Physics. The mention of commercial products, their sources, or their use in connection with material reported herein is not to be construed as either an actual or implied endorsement of such products by the Department of Health and Human Services. This article reflects the views of the authors and should not be construed to represent FDA's views or policies.

References: [1] Niswander and Kontson (2021), *Sensors 21*(12), [2] Romijnders et al., (2022), *Sensors 22*(10)

Model	True Positives	False Positives	False Negatives	Precision	Recall	F Score
Initial Contact	1,532	108	182	0.93	0.89	0.91
Final Contact	1,544	113	287	0.93	0.84	0.88

ELECTROMYOGRAPHY AND ACCELERATION DATA COMPARISON FOR HAND GESTURE CLASSIFICATION

Samira Afshari*, Rachel Vitali, Deema Totah
Department of Mechanical Engineering, University of Iowa, IA, USA
*Corresponding author's email: samira-afshari@uiowa.edu

Introduction: The design of efficient, intuitive, powered upper-limb prostheses capable of performing multi-degree of freedom hand gestures requires an understanding of the most salient signals for intuitive control. In recent years, there has been a significant increase in using wearable sensors, such as EMG [1-3], IMU [4, 5], FMG [6], and flex sensors [7], for classifying hand gestures due to their ease of use outside labs. With many wearable sensors available for biomedical applications, a major issue in this area is optimizing sensor use and the data collection process. There is a need to identify the most informative wearable sensors in gesture classification, so that they can be used in the design of efficient, cost-effective, and accurate active prostheses. Electromyography (EMG) sensors and accelerometers are among the most common ones being used for hand gesture prediction. Improving gesture recognition accuracy means more accurate identification of the user's intended grasp type, which is required for intuitive control of hand prosthetics. Studies show the addition of acceleration signals to EMG effectively improve classification accuracy [8], however, the classifier performance has not been studied enough using only accelerometers for gestures with fine movements. Studies show that using IMU sensors, which include both accelerometer and gyroscope signals, can be efficient enough with prediction of specific command-type gestures [5]. The main purpose of this study is to investigate which sensor type, either EMG or acceleration, results in better subject-specific gesture recognition accuracy.

Methods: Forearm EMG and acceleration data previously collected from 28 able bodied and 13 subjects with amputation [9] were used to train a Linear Discriminant Analysis (LDA) model to classify 10 hand gesture types. For each subject, three models were trained: 1) using only EMG data (EMG), 2) using only acceleration data (ACC), and 3) using a combination of both signals (EMG&ACC). The data were collected while subjects held gestures *statically* and interacted with objects to form *dynamic* gestures. Data was time windowed with a window length of 400 samples and 95% overlap between successive windows. Four time-domain features (mean absolute value, waveform length, slope sign changes, and zero crossings) were extracted from the windowed EMG signals [10] and four other features (mean, standard deviation, root mean square, and mean absolute deviation) were extracted from the 3-axis accelerometer (ACC) signals [11]. Finally, classification accuracy was calculated for each subject using 4-fold cross validation.

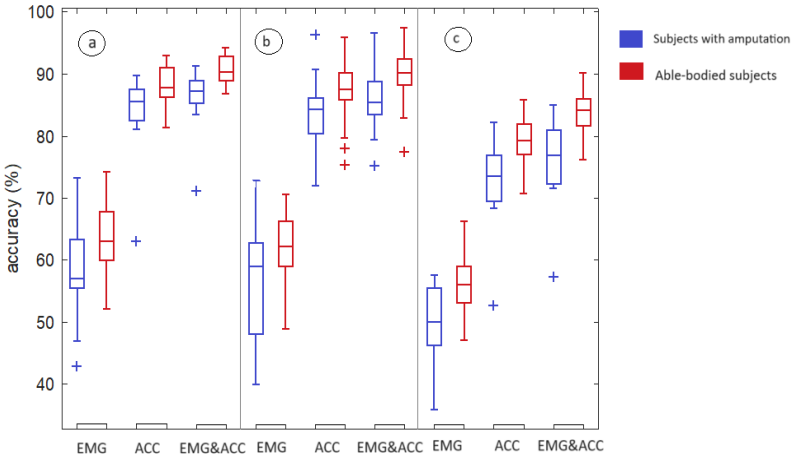

Figure 1. Classification accuracy comparison between EMG, ACC, and both, when the classifier is trained and tested with a) static gesture data only, b) dynamic data only and c) both static and dynamic data.

Results & Discussion: The results show that acceleration data is playing a more important role to correctly predict hand gestures, compared to EMG data. Adding acceleration data to EMG noticeably improved hand gesture classification accuracy (Fig. 1). Using only EMG has been shown before to be effective for gesture prediction [5], however, with the ten hand gestures in this study, acceleration is more informative for gesture classification. Additionally, comparing two groups of subjects, it seems that the classification accuracy is always higher in able-bodied subjects than in subjects with amputation. Nonetheless, ACC signals alone had classification accuracies comparable with ACC and EMG combination for both subject groups. This is informative as ACC sensors are generally cheaper and more easily integrated into prosthetic devices, as they do not require the skin contact EMG sensors require and are less location-sensitive than EMG sensors. Future work will investigate optimal features for each sensor data set to identify a minimal sensor and feature set for efficient, optimal gesture recognition with wearable sensors.

Significance: Identifying that acceleration signals are more informative than EMG for hand gesture recognition reduces the number of sensors needed to achieve high classification accuracy, which can lead to a better design of hand prosthetic devices with less complexity.

Acknowledgments: This work was funded by start-up funds from the University of Iowa.

References: [1] Lv et al. (2021), *Biomedical signal processing and control* 68; [2] Murciego et al. (2022), *J NeuroEngineering and Rehabilitation* 19(1); [3] Tripathi et al. (2023), *IEEE trans on Instrumentation and Measurement* 72; [4] Moschetti et al. (2016), *J Sensors* 16(8); [5] Guimarães et al. (2021), *IEEE ISC2*; [6] Sadeghi Chegani et al. (2018), *BME online*, 17(1); [7] Calado et al. (2022), *IEEE trans on Systems, Man, and Cybernetics*, 52(10); [8] Gijsberts et al. (2014), *IEEE TNSRE* 22(4); [9] Cognolato et al. (2020), *J Scientific Data* 7(1); [10] Englehart et al. (2013), *IEEE trans on BME* 50(7); [11] Moschetti, et al. (2016), *J Sensors* 16(8);

EVALUATION OF AN AUTOENCODER FOR COMPUTING MUSCLE SYNERGIES

Siddharth R. Nathella[1*], Aaron J. Young[1], Lena H. Ting[1,2]
[1]George W. Woodruff School of Mechanical Engineering, Georgia Institute of Technology, Atlanta, GA
[2]Wallace H. Coulter Department of Biomedical Engineering, Georgia Institute of Technology, Emory University, Atlanta, GA
*Corresponding author's email: snathella@gatech.edu

Introduction: Muscle synergies are a set of commonly recruited muscle coordination patterns that can be used to describe more complex patterns of motor control. The analysis of muscle synergies has been an important tool in the evaluation of human motor control. The typical approach to computing muscle synergies is to use non-negative matrix factorization (NMF), a dictionary learning algorithm, which is iteratively performed with increasing numbers of synergies until a reconstruction threshold is reached, typically 90% variance accounted for (VAF) [1]. While this approach has been effective in producing interpretable synergies, it has significant limitations, specifically regarding the selection of an appropriate number of synergies to reproduce data (synergy count), and the functional relevance of muscle synergies extracted using low synergy counts. Because the reconstruction threshold can be essentially arbitrary, it is hard to know if a "correct" number of synergies has been selected, and synergies computed via NMF at lower synergy counts will often split at subsequent synergy counts, making the "true" structure difficult to determine. Often the VAF by one synergy (VAF_1) has been used to evaluate overall motor control complexity, and there is not a clear relationship between this synergy and the "true" synergy. We propose using an autoencoder, a machine learning technique for data dimensionality reduction, as an alternative method for computing muscle synergies with greater biomechanical relevance and stronger agreement of synergy structure at different synergy counts.

Methods: An autoencoder (AE) is a machine learning technique used to compress data to a lower dimensional representation, and then reconstruct the data through a symmetric decoder. In contrast to NMF, the AE can take advantage of additional terms, including a bias term and non-linear activations, to encode the data. The AE presented here was constructed as a simple 1-layer neural network, with the size of the hidden layer determining the number of muscle synergies. Each input to the AE was a single time sample of electromyography (EMG) data, with the network trained to reconstruct that same data. The network was constrained to have non-negative weighting components, with no constraints on the biases, and a rectified linear unit activation function on the output layer. To extract muscle synergies from a trained AE, we extracted the *weights* term from the hidden layer of the trained model. This gives a resulting matrix of shape *synergy count* × *muscles*, which can be directly compared to the dictionary matrix computed through NMF. N=21 subjects' EMG data (11 muscles walking at 1.3 m/s) from an open-source dataset was used for both approaches [2]. The synergy count was swept from 1-5 for each approach. To determine agreement in synergy structure across synergy counts, the mean cosine similarity of the most similar synergies between subsequent synergy counts was computed for every subject (structures of synergy count *i* compared to structures of synergy count *i-1*).

Results & Discussion: Comparing the synergy structures produced by the two approaches, the AE shows a clear improvement in the similarity of corresponding synergies at different selected number of synergies (Figure 1A). Importantly, in a representative subject, muscle synergy structure is much more reflective of a biomechanical function (e.g. weight acceptance), even when only 1 synergy is computed. The NMF synergies at each subsequent synergy count show up as a previous synergy split in two (Figure 1A, red), whereas the AE adds unique information with each added synergy. This gives a clear point at which new information has not been added, and thus is a much more definitive point for selecting the "correct" synergy count. Using NMF, it is clear how different conclusions could be made if 2, 3, or 4 synergies were computed. In contrast, AE shows substantially higher agreement of muscle synergy structure across synergy counts (Figure 1B, green vs red), meaning the information contained with one synergy extracted is nearly identical to the information contained in the corresponding synergy at every other synergy count. The AE can achieve this through the inclusion of a bias term, which allows for good reconstruction of the original data without compromising the interpretability of the synergy.

Significance: This work provides a new framework for computing muscle synergies in human movement. By providing a method with less synergy structure variance at different synergy counts, researchers can have a higher confidence in the conclusions they draw from synergy analysis, with less concern with their selection of synergy count. As addressed earlier, VAF_1 has been used as a metric of motor control complexity without regard for "true" muscle synergy structure. Our AE method improves the interpretation of this approach as the single muscle synergy selected is more indicative of a functional synergy underlying the overall muscle coordination pattern.

Acknowledgements: *The authors would like to thank the Georgia Tech Woodruff School of Mechanical Engineering for their support through the Interdisciplinary Research Fellowship.*

References: [1] Ting & Chvatal (2010), *Decomposing Muscle Activity in Motor Tasks*. [2] Camargo et al. (2021), *J Biomech*.

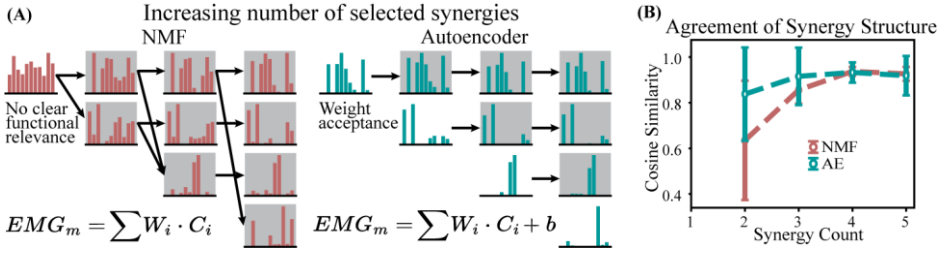

Figure 1: A) Structure of the muscle synergies for a representative subject across up to four selected synergies. The formulae describe the equation of synergy weights and activation to produce reconstructed EMG data. **B)** Agreement of synergy structure with the previous selected number of synergies. Synergies at *i* selected synergies were compared to the most similar synergy at *i-1* selected synergies.

A KINEMATICALLY-INFORMED APPROACH TO NEAR FUTURE JOINT ANGLE ESTIMATION AT THE ANKLE

Ryan Pollard[1], David Hollinger[1], Ivan E. Ulloa-Nail[1], Michael Zabala[1]
[1] Department of Mechanical Engineering, Auburn University, Auburn, AL, USA
*Corresponding author's email: rzp0051@auburn.edu

Introduction: Informing joint angle estimation algorithms with recorded biological signals has shown benefit for assistive device control [1,2,3,4], resulting in increased synchronization between a user and an assistive device [5] as their kinematic trajectories are aligned [6]. Due to the often-nonlinear relationship between recorded biological signals and measured joint angles, machine learning models are often used when performing future joint angle estimation [5]. While machine learning and neural networks thrive at finding solutions to highly complex relationships, the necessary computation time required to solve for these future joint angle estimations likely limit the useful inclusion of these models in real time assistive device control. As such, implementing simple, analytically-governed models may provide benefit in future joint angle estimation as an alternative to the computationally expensive nature of machine learning. Due to their simplicity, we hypothesized that a kinematically-informed joint angle estimation model would demonstrate a lower estimation runtime than machine learning models trained and tested on an identical dataset. Likewise, although the kinematically-informed are more simplistic than their machine learning counterparts, we secondly hypothesized that for near-future estimation horizons ($t_{pred} \leq$ 100ms) the future joint angle estimation errors of kinematically-informed models would be comparable to those of machine learning models. Finally, due to the potentially significant effect of the length of the estimation horizon on estimation error, we thirdly hypothesized that the estimation error of the kinematically-informed models would increase as the estimation horizon increased.

Methods: A ten camera Vicon motion capture system was used to record the lower-limb joint kinematics at a 120 Hz sampling rate of twenty-four healthy individuals (12 males, 12 females; age 21.8 ± 2.9 years; height 170.9 ± 10.1 cm; body mass 69.5 ± 10.9 kg) in the Auburn University Biomechanical Engineering (AUBE) Laboratory. Each participant provided informed consent, and the study protocol was approved by the Auburn University IRB (no. 17-279-MR 1707). Subjects were asked to perform three level-ground walking trials at a self-selected speed through the center of the AUBE Lab. Motion capture data was post-processed and filtered to determine sagittal-plane ankle angles for each trial. Five kinematically-informed models were developed for joint angle estimation at three distinct estimation horizons: t_{pred} = 50 ms, 75 ms, and 100 ms. The estimation error and elapsed runtime for each model at each estimation horizon was evaluated using an *optimal* sliding window size (a model-specific window size that returned a minimum estimation error for the given model – sliding windows evaluated in this study ranged from Δt_{sw} = 25 ms to 200 ms). Two Random Forest (RF) machine learning models were also developed to serve as the baseline for model comparison. RF models were trained on two randomly selected walking trials and tested on the third remaining walking trial for each participant, while the analytically-governed kinematic models were tested on the same walking trial as the RF models for each subject. Model performance, specifically runtime and estimation error, was compared between model types at each estimation horizon and subsequently between estimation horizons for each model type.

Results & Discussion: Results indicated that kinematically-informed models yielded significantly lower estimation runtimes for each of the evaluated estimation horizons (Fig. 1 - kinematic models: t_{run} < 0.62 ms, RF models: t_{run} > 8.19 ms for all estimation horizons). Additionally, RF models performed with significantly lower estimation error for the t_{pred} = 75 ms and 100 ms estimation horizons, but no significant differences were found between the most accurate kinematic models and the RF models for the t_{pred} = 50 ms estimation horizon (Fig. 2). Likewise, results indicated that the estimation error of each model type increased as the estimation horizon increased. Such results show that kinematic models can be used as a baseline for joint angle estimation model comparison for near future applications, given these models' minimal required runtimes and comparable estimation errors at these estimation horizons.

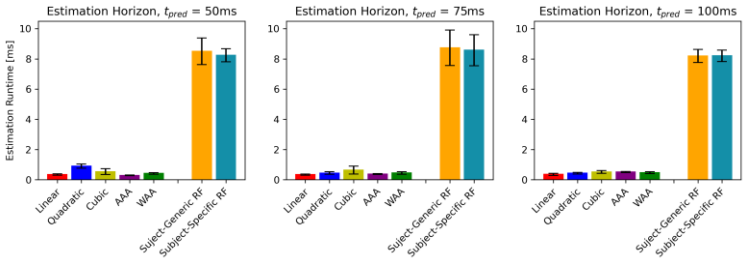

Fig. 1: Estimation runtime for each model at three distinct estimation horizons.

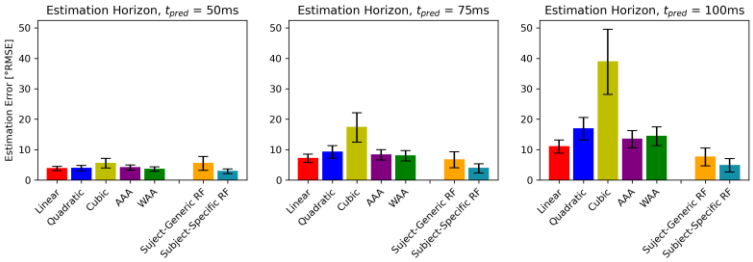

Fig. 2: Estimation error for each model at three distinct estimation horizons.

Significance: This study presents a novel, yet simplistic, approach to near future joint angle estimation for assistive device applications. Because of their reduced computational demand, deploying kinematically-informed models at near future estimation horizons would allow an assistive device additional time to actuate without compromising on estimation accuracy. Additionally, because kinematically-informed models are analytically governed and are not trained like machine learning models, they can be considered both task and subject agnostic. Therefore, kinematically-informed models may be beneficial for assistive devices applications that promote free-ambulation rather than laboratory-restricted actions.

References: [1] Ngeo (2013), *35th IEEE EMBC*; [2] Ghosh (2019), *IEEE/ASME AIM*; [3] Chen (2023), *IEEE Sensor*, *23*; [4] Lee (2021), *Sensors*, *21*; [5] Jimenez-Fabian (2012), *Med. Eng. & Phys.*, *34*; [6] Chisty (2021), *IEEE TMRB*, *3*; [7] Coker (2021), *Sensors*, *21*; [8] Andriacchi (1998), *J. Biomech. Eng.*, *28*; [9] Grood & Suntay (1983), *J. Biomech. Eng.*, *105*.

RELIANCE ON VISION FOR WALKING BALANCE IS RELATED TO SOMATOSENSORY DEFICITS IN INDIVIDUALS WITH CEREBRAL PALSY

Ashwini Sansare[1*], Hendrik Reimann[2], John Jeka[2], Samuel C.K. Lee[3]
[1]Dept of Kinesiology and Sports Management, Texas A&M University
[2]Kinesiology and Applied Physiology, University of Delaware; [3]Dept of Physical Therapy, University of Delaware
*Corresponding author's email: ashwini@tamu.edu

Introduction: Individuals with cerebral palsy (CP) rely on vision over other senses for balance control, as evidenced by increased postural sway during standing when their visual input is manipulated [1,2]. With respect to walking balance, our previous work [3] has shown that visual perturbations led to a magnified and delayed center of mass (COM) response in the CP group compared to their age- and sex-matched peers. While it is hypothesized that the increased sway with visual perturbations is due to the reliance on vision to compensate for deficits in somatosensory system, such as difficulty in perceiving touch, vibration, position of joints and limbs, and in discriminating between two points in space (two-point discrimination), there is currently no evidence for this hypothesis. None of the prior work has directly investigated the link between response to perturbations and somatosensory deficits.

Here we performed a secondary analysis of our prior study [3] in individuals with and without CP to investigate the relationship across subjects between their response to visual perturbations during walking and their somatosensory deficits, specifically ankle and hip joint position sense, two-point discrimination, and vibration. We hypothesized that individuals with degraded sensory processing will have a larger response to visual perturbations.

Methods: Twenty-eight individuals (14 with CP, 14 age-and sex-matched typically developing (TD) controls) walked on a self-paced treadmill inside a virtual reality cave that induced a visual fall stimulus in the frontal plane every 10-12 steps. Each trial lasted two minutes and was repeated ten times, with intermittent rest breaks. We measured the response to visual perturbations as area-under-the-curve of the COM (AUC COM), where higher values imply a magnified response to the visual perturbations and, in turn, a greater reliance on vision for walking balance. We tested the participant's performance on four sensory tests, (1) ankle joint position sense, (2) hip joint position sense, (3) two-point discrimination, and (4) vibration. We analysed our data through (1) bivariate correlations using Pearson's coefficient, and (2) multiple regression analysis (MRA) using all four sensory tests as predictors and the COM response to visual perturbations as the outcome.

Results & Discussion: First, we found significant ($p<0.05$) and strong correlations between the response to visual perturbations and performance on all four sensory tests (Figure 1). Out of the four somatosensory tests, ankle joint position sense showed the strongest correlation ($r = 0.878$, $p < 0.001$) with the response to visual perturbations. These results support our hypothesis that those individuals with degraded sensory processing are more affected by visual input during walking.

Second, while our results showed a strong correlation between sensory deficits and a response to a visual perturbation for both the CP as well as the healthy control i.e. the TD group, the relationship was stronger for CP (r=0.88, 0.69, 0.78, and -0.80 for ankle and hip joint position, 2-point discrimination and vibration, respectively).

Lastly, with respect to MRA results, multicollinearity, i.e. the correlation between somatosensory predictors themselves, was so high that it precluded inclusion of two or more predictors in any model, indicating that performance on any of the sensory tests, irrespective of which one it was, was enough to predict the response to visual perturbations, and in turn, predict those that likely rely on vision over other senses for walking balance control.

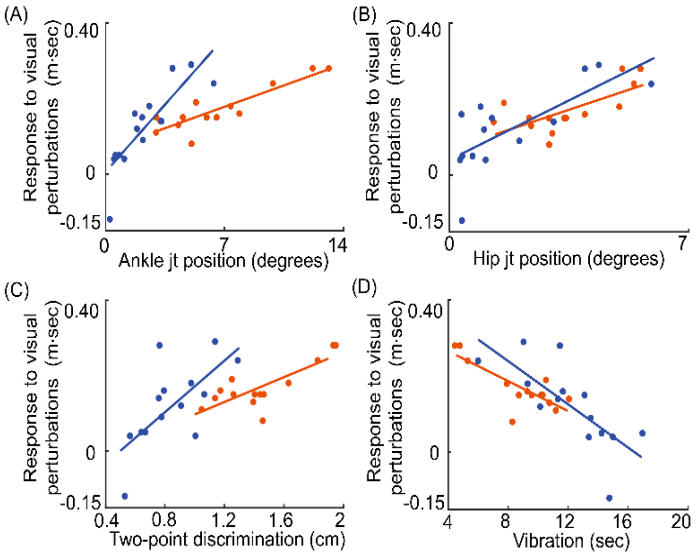

Figure1. Bivariate correlations between the four somatosensory predictors (horizontal axes) and the CoM excursion in response to the visual perturbations (vertical axes) for CP (orange) and TD (blue) group.

Significance: Overall, our findings suggest a direct link between sensory deficits and visual reliance during walking. While most assessments as well as treatments for balance rehabilitation in CP address motor deficits, our findings highlight the importance of considering sensory regulation of walking balance in rehabilitation protocols. This study is an initial step in identifying sensory tests as potential markers for predicting patients that are most likely to rely on vision for balance control and hence, are most likely to be affected when receiving altered or reduced visual input (such as stepping into a dark room). Results from MRA suggest that performing a simple battery of sensory tests or even a single test can help identify individuals that are most likely to be perturbed by altered visual input as "at-risk" individuals for balance rehabilitation.

Acknowledgments: This work was supported in part by the American Society of Biomechanics Grant-in-Aid 2022-23 and by the Foundation for Physical Therapy Research Promotional of Doctoral Studies (PODS) II Scholarship.

References: [1] Barela et al. (2011), *Res in Dev Dis*; [2] Yu et al. (2020), *J Mot Beh*; [3] Sansare et al. (2022), *Front. Hum. Neurosci.*

SUSCEPTIBILITY TO UNRELIABLE VISUAL INPUT MAY INFLUENCE REACTIVE STEPPING THRESHOLD

Hannah D. Carey[1*], Tom Van Wouwe[2], Friedl De Groote[1]
[1]KU Leuven, Department of Movement Sciences, Leuven, Belgium
[2]Department of BioMechanical Engineering, Delft University of Technology, Delft, The Netherlands
*Corresponding author's email: friedl.degroote@kuleuven.be

Introduction: Potentially destabilizing conditions, such as a jostling bus, cracked pavement, or dim lighting, are a common feature of daily life. Healthy people can typically withstand most of these disturbances, but changes in sensory and motor function that occur with normal aging leave older adults more vulnerable to falls. Over one-third of older adults fall every year, leading to injury, death, and reduced quality of life [1]. To avoid falls, people typically respond to disturbances with a combination of three well-described kinematic strategies: ankle movements, hip movements, or stepping [2]. Older adults are known to resort to hip and stepping strategies earlier than young adults [3], but the underlying reasons are unclear. Older adults could step more often because they lack sufficient muscle strength, have changes in musculoskeletal structure that reduce passive stability, have changes in sensory acuity that inhibit detection of a disturbance, or simply opt for a safer strategy due to fear of falling. Additionally, studies of reactive balance commonly investigate the effects of a single type of perturbation, but changes in sensory acuity may have a different impact on different types of perturbations. For example, decay of the vestibular system might influence responses to rotational more than responses to translational perturbations. Accordingly, we had two objectives: to compare the kinematic responses of young and older adults to a broad array of standing perturbations, and to look for relationships between sensory function and perturbation response. We hypothesized that older adults would step more often and at lower thresholds, exhibit larger trunk and ankle movements, and score lower than young adults in measures of sensory function. Our investigation of associations between balance response and sensory function were exploratory, but we expected lower sensory scores to be correlated with balance response, such as lower stepping thresholds.

Methods: Ten healthy young adults (7F, 22.9±1.3 yrs) and 29 healthy older adults (12F, 71.2±4.4 yrs) participated. We collected motion capture and ground reaction force data during backward translations (6 difficulty levels), forward translations, plantarflexion, and dorsiflexion rotations (4 levels each). To assess sensorimotor function, participants also performed the Sensory Organization Test (SOT); we compared SOT scores (composite and 4 sub-scores) between groups using rank-sum or t-tests, as indicated by the Shapiro-Wilk test.

To quantify balance response, we calculated step incidence, stepping threshold (maximum extrapolated center of mass, XCOM, deviation), ankle response (maximum center of pressure deviation), and hip response (maximum trunk lean deviation) for each perturbation level. We took the average of each balance variable across all trials and difficulty levels for each perturbation direction, and compared between age-groups with rank-sum or t-tests. We then used linear regressions, including the effects of age group, to compare the balance response and sensory function variables.

Results & Discussion: Consistent with our hypothesis, we found intergroup differences in balance performance. Older adults stepped more often in all but plantarflexion perturbations, where few people stepped in either group. Older adults also had lower stepping thresholds than young adults during translations, but higher thresholds during rotations. Only dorsiflexion perturbations elicited differences in hip and ankle movements between young and older adults. Because stepping incidence was generally low during rotations, larger XCOM deviations together with larger hip and ankle responses likely mean older adults were more disrupted by these rotations than young adults, who showed mostly ankle responses, with little deviation in XCOM or hip movement.

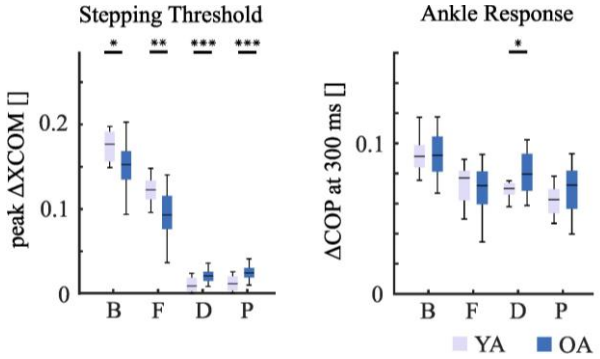

Figure 1: Stepping thresholds (peak ΔXCOM in non-stepping trials) and ankle response (peak ΔCOP at 300ms) in backwards (B), forwards (F), dorsiflexion (D) and plantarflexion (P) perturbations. Stars indicate significant differences between age groups.

Older adults scored lower than young adults on all SOT scores except one, SOM, which measures the effect of absent vision. The PREF score compares postural sway between absent and sway referenced vision, and indicates how well a person may filter out unreliable sensory information. PREF was significantly correlated with stepping threshold for all perturbation directions, with higher scores associated with larger stepping thresholds; however, the correlation was weak for translations ($r^2 = 0.17$) and moderate during rotations (r^2=0.36 in D, 0.3 in P). For forwards and rotational perturbations there was an interaction effect of age, showing a stronger positive correlation in young adults, but little in older adults. For other SOT scores, we found few significant relationships with balance response variables, and none that showed a moderate or strong correlation.

Significance: Here we provide further evidence that different perturbation types can elicit different types of responses, and illustrate the importance of carefully selecting perturbation magnitudes to elicit differences in young and older adults. We have also found some preliminary correlations between the ability to disregard unreliable sensory input and balance response; however, more thorough evaluations of sensory function and task prioritization are likely needed to establish clear relationships.

Acknowledgments: This work was funded by FWO (Research Foundation Flanders) Research Project G088420N

References: [1] Tinetti et al. (1988), *N Engl J Med* (319); [2] Hof (2007) *J Biomech.* 40(2); [3] Pai et al. (1998) *J Biomech.* 31(12)

Can Young Adults Flexibly Shift Attentional Focus when Texting While Walking: Effects of Different Cognitive and Motor Tasks

Chi-Whan Choi[1], Kejing Yan[2] Simone V. Gill[1]*
[1]Rehabilitation Sciences PhD Program, Sargent College of health and Rehabilitation Sciences, Boston University, Boston, MA
[2]Department of Mathematics and Statistics, College of Arts and Sciences, Boston University, Boston, MA
*Corresponding author's email: simvgill@bu.edu

Introduction: Texting while walking is common among people of all ages, and mobile phone use during walking is associated with pedestrian injury [1]. While texting, individuals notice significantly fewer objects in their surroundings [2], [3]. Furthermore, recent studies have shown that young adults reduce their gait speed and weave more by prioritizing the texting task when texting while walking [4]. However, it is presently not known how young adults prioritize their attention during texting while walking when faced with cognitive tasks or motor tasks of increasing difficulty or both. Understanding how young healthy adults react during different levels of cognitive loads and motor tasks may provide a benchmark for future studies in populations with cognitive and locomotor impairments. Therefore, the objective of this study was to evaluate how young adults prioritize cognitive or motor performance during different levels of cognitive and motor tasks. To examine these questions, we quantified texting speed, accuracy, and walking performance as participants walked with or without two levels of texting difficulty, walked with crossing three different heights of obstacles and while doing both tasks. We hypothesized that each texting condition, obstacle condition and the combination would contribute to performance differences in cognitive and motor tasks.

Methods: Twenty participants took part in this study (N = 20; Female = 12; mean age = 21.5 years old ± SD 2.8; BMI range = 18.0—45.4 kg/m^2). Participants were asked to report their familiarity with texting while walking (FTW) on a scale from 1 to 5 (5 meaning most familiar). Then, we assessed their baseline texting performance while seated by asking them to retype a sentence and to type in answers to questions with their own smartphone. Autocorrect and autofill functions were turned off. While the retyping task was focused on attentional resources, the answering task required attention and recall. The questions were standardized texting questions from previous literature [5] and randomly determined. Participants walked for 3 trials for each condition: flat ground walking (initial baseline), obstacle condition (crossing obstacles of low, medium, and high heights), cognitive task condition, Typing (retyping sentence via text) or Texting (answering questions via text), combined condition, Typing or Texting with obstacle crossing of the 3 heights, and flat ground walking (final baseline). The condition order was randomized except for baseline trials. Dual task costs (DTC) using each accuracy and speed of Typing or Texting compared to the baseline tests were calculated and, spatio-temporal gait parameters including (Step Length, Stride Length, Stride Width, Step Time Stride Time, Total Double Limbs Support Time, Velocity, and each coefficient of variation (CV) of the parameters) using gait carpet were measured. XGBoost, a powerful machine learning algorithm, was performed to identify the most important gait parameters for the dependent variables, then two-way ANCOVAs were utilized to investigate the effects of each cognitive task and obstacles, and their interaction on dependent variables while controlling for FTW as a covariate.

Results & Discussion: CV Step Time was the feature that contributed the most to XGBoost's performance in gait parameters. Cognitive task ($F_{2,38}$=43.048, p<.001), obstacle condition ($F_{3,38}$=454.197, p<.001), and their interactions ($F_{6,38}$=7.736, p<.001) were significant for CV Step Time (R^2(20) =.712). FTW had no significant effect on CV Step Time. Post-hoc Tukey analysis showed a significant difference between Typing and Texting when crossing a high obstacle on CV Step Time (p=.014), with the reduced accuracy in Typing and increased accuracy in Texting (CV Step Time-accuracy tradeoff) reflected by DTC. There was no significant difference among the two tasks in other obstacle conditions (Fig.1).

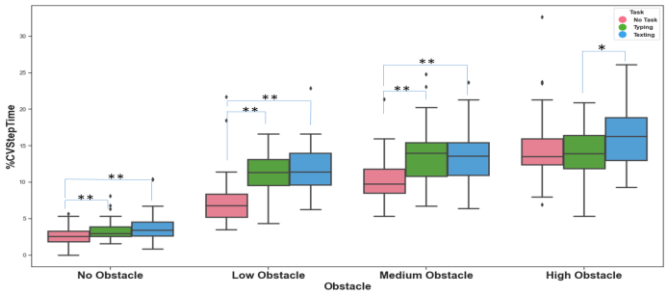

Figure 1: The differences in CV Step Time across cognitive tasks in each obstacle conditions. Each pink, green and blue indicates No task, Typing and Texting. * indicates a significant difference (p < 0.017) with significance level at .017 (ie, .05/3 [where 3 is the number of comparisons]) and ** indicates p < 0.001.

Significance: This study extends existing research about the effect of texting on spatiotemporal gait parameters while walking. The additional cognitive load had a significant effect on gait variability represented by CV Step Time while crossing the highest obstacle. There was little change between mid and high obstacle in gait variability with reducing Typing accuracy while Typing condition. In contrast, gait variability significantly increased in the Texting condition compared to the mid obstacle while crossing a high obstacle with increasing Texting accuracy (Fig 2). When young adults faced different environment, gait variability was affected by the additional cognitive load. In other words, young adults can modify their texting and walking behaviour with respect to different environmental demands when less cognitive load, but the addition of a cognitive load such as recalling to answer questions may lend credibility to growing concerns about mobile phone use. This is closely related to pedestrian safety due to the fact that young adults may prioritize their texting activity even when they are facing risky circumstances in real-world. Thus further research is needed regarding the effects of cognitive load and environmental demand during texting while walking.

References: [1] Gary et al. (2014), *J Trauma Acute Care Surg* 85(6); [2] Nasar et al. (2008), *Accid Anal Prev*, 40(1); [3] Hyman et al. (2010), Appl Cogn Psychol 24(5); [4] Plummer et al. (2015), *Gait Posture* 41(1); [5] Demura et al. (2009), *Eur J Sport Sci* 9(5).

A LOW-COST AND MOVEMENT-BASED TOOL FOR CONCUSSION DIAGNOSIS

Jacob M. Thomas[1*], Jamie B. Hall, Rebecca Bliss, Stephen P. Sayers, Emily Leary, Trent M. Guess
[1]School of Health Professions, University of Missouri
*Corresponding author's email: jmt2mb@missouri.edu

Introduction: Currently, sport-related concussions are diagnosed using a combination of self-reported symptomology and visually scored movement tasks [1]. Investigations using gold standard tools such as force plates and marker-based motion capture systems, have found significant increases in center of mass (CoM) and center of pressure (CoP) velocity and displacement during eyes closed (EC) Romberg balance tasks [2]; slower reaction time [3]; as well as reduced gait speed and increased medial-lateral (ML) CoM velocity during simple and dual task gait [4] in individuals with concussion (CC), as compared to healthy (H) individuals. A low-cost tool which uses a combination of these identified variables to diagnose concussion may provide a more accurate and comprehensive alternative to current diagnosis methods [5]. Therefore, the purpose of this study was to assess the classification accuracy of a machine learning model using these outcome measures measured by a low-cost movement assessment system between individuals with and without concussion.

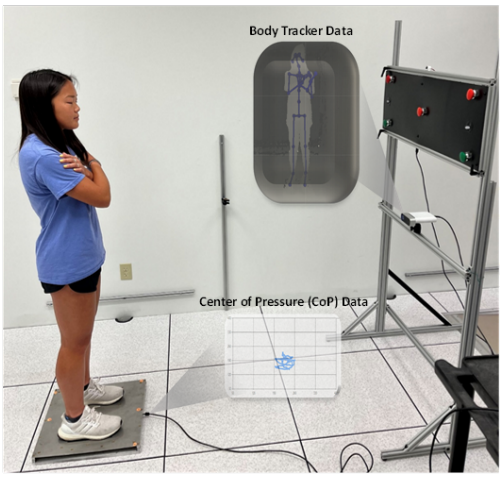

Figure 1. Participant performing a static balance task with MPASS force plate and body tracker data represented visually.

Methods: Forty collegiate athletes were recruited for this study. Twenty athletes (19.45±1.20 yrs., 11 females) who had suffered a concussion within 2-weeks (5.40 ± 3.68 days) prior to data collection were placed in the CC group. Twenty healthy sport, sex, and position-matched teammates (19.7 ± 1.19 yrs.) who had no concussions in the past year were recruited for the H group. All participants performed 3 trials of each of the following tasks: walking (normal, serial subtraction by 7 (SS), and head shaking (HS)), Romberg balance (eyes open (EO)/EC on both firm/foam surfaces and with/without SS), and reaction time. All tasks were assessed using the Mizzou Point-of-Care Assessment System (MPASS; target cost less than $1,500), which is comprised of a custom force plate for measuring kinetics, a depth camera with body tracking for measuring kinematics, and custom interface board for interfacing with the participant and measuring reaction time (Figure 1). Discrete MPASS outcome measures were used as inputs for an XGBoost machine learning model. Data were divided into an 80/20 training-testing split. Due to this study's relatively low sample size, model parameters were tuned to avoid overfitting and minimize model complexity. Following model training and prediction of the testing set, 5-fold cross-validation was performed to assess the generalizability of the model.

Table 2. Feature Importance by Number of Model Appearances

Feature	Number of Appearances in Cross-Validation Models
Mean Total Velocity of ML CoM: EC SS Firm Balance	3
95% Ellipse area of CoP: Firm EC SS Balance	1
Stride Time: Normal Gait	1
95% Ellipse area of CoM: Firm EC SS Balance	1
Mean Total Velocity of ML CoP: EC Firm Balance	1
Mean Total Velocity of ML CoP: EC SS Firm Balance	1
Number of Correct Buttons Pressed: Reaction Time	1
Mean Total Velocity of CoM: EC SS Foam Balance	1
Mean Total Velocity of ML CoM: EC Foam Balance	1

Results & Discussion: Cross-validation of the model resulted (Table 1) in a mean: accuracy of 82.5%, sensitivity of 75%, specificity of 90%, positive predictive value of 88.2%, and negative predictive value of 78.3%. Feature importance for this model (determined by a variable's frequency of appearance in both cross-validation and initial models) are presented in Table 2. These performance measures are higher than other studies using xgBoost and biomechanical outcome measures for classification [6-7]. Though our sample size is limited, thereby limiting the generalizability of this model, results demonstrate promise for using machine learning in combination with MPASS measurements for concussion diagnosis.

Table 1. Cross-Validation Confusion Matrix

	Reference	
Prediction	CC	H
CC	15	2
H	5	18

Significance: These findings demonstrate the potential usefulness of combining machine learning and low-cost movement assessment tools to improve concussion diagnosis.

Acknowledgements: This study was funded by the American Society of Biomechanics' Grant-in-Aid award.

References: [1] Echemendia et al. (2017), *British Journal of Sports Medicine* 51(11); [2] Qiao et al. (2021), *Annals of biomedical engineering* 49(10); [3] Lempke et al. (2020) *Sports medicine* 50 (7); [4] Fino et al. (2018), *Gait & Posture* 62; [5] Buckley et el. (2016), *Journal of sport and health science* 5(1); [6] Noh et al. (2021), *Scientific Reports*; [7] Calderon-Diaz et al. (2023), *Sensors* 24(119)

INSTRUMENTED TIMED TANDEM GAIT IN COLLEGE ATHLETES AFTER CONCUSSION

Cecilia Monoli[1*], Amanda Morris[2], Regan Crofts[1], Christina Geisler[1], Tessa L. Petersell[1], David Quammen[1], Adam Hollien[1], Leland E. Dibble[1], Peter C. Fino[1]
[1]University of Utah, Salt Lake City, UT
[2]California State University, Department of Kinesiology, Sacramento, CA
*Corresponding author's email: cecilia.monoli@utah.edu

Introduction: The Timed Tandem Gait (TTG) test is frequently used to assess dynamic balance after concussion [1,2]. The TTG test entails walking heel to toe as quickly as possible, timed with a stopwatch, with the primary outcome being task completion time. While this task is designed to test balance and coordination after concussion [3], clinical scoring only considers the completion time; no measures of postural control are considered or evaluated. The purpose of this study was to longitudinally investigate postural control during the TTG after concussion using inertial measurement unit sensors to measure mediolateral (ML) sway during the TTG task.

Methods: A total of 27 NCAA Division I athletes (Table 1) provided informed written consent for this IRB-approved study. Participants completed testing at three timepoints: within 72 hours after a concussion (Acute); within 72 hours of beginning the Return To Play protocol [4] (Pre RTP); within 72 hours of being cleared for return to competition (Post RTP). Concussed athletes and matched healthy controls were tested on the same day. Not all participants were able to attend every timepoint. Participants completed the TTG task wearing an inertial measurement unit (IMU; APDM Inc., Portland, OR), sampling at 128Hz, at the lumbar region of the spine (~L3/L4). Subject completed the TTG three times and were instructed to walk heel to toe, as quickly and as accurately as possible down a line (3-m long), turn 180°, and return to the starting point using the same tandem gait. The task was timed using a stopwatch, and the results of the fastest completion were retained for analysis [5]. Acceleration and angular velocity data from the IMU were processed through custom algorithms in MATLAB (r2023b; MathWorks, Natick, MA) to obtain the mediolateral (ML) root mean squared (RMS) sway of the walking portions of the trial, and the peak turning speed. Pearson's correlation coefficients assessed the relationship between ML sway and completion time, and independent t-tests with Bonferroni adjustments (α=0.05/3) assessed differences between groups at each timepoint.

Table 1. Demographics of the athletes enrolled at each timepoint and Timed Tandem Gait results, reported as mean and standard deviation. *Statistically significant (p≤0.017).

Participants		Assessment timepoints		
		Acute	Pre RTP	Post RTP
N (F, M)	Concussed	16 (13, 3)	10 (10, 0)	13 (11, 2)
	Control	10 (7, 3)	7 (7, 0)	9 (6, 3)
Age, years mean (SD)	Concussed	19.4 (1.5)	19.9 (1.6)	19.5 (1.6)
	Control	19.6 (1.8)	20.0 (2.0)	19.8 (1.8)
Timed Tandem Gait				
Completion time, s mean (SD)	Concussed	14.34 (2.50)	12.38 (1.30)	11.71 (1.10)
	Control	13.02 (1.99)	11.96 (1.28)	11.44 (1.64)
RMS ML sway, m/s^2 mean (SD)	Concussed	1.09 (0.30)	1.09 (0.19)*	1.31 (0.26)
	Control	1.28 (0.37)	1.41 (0.33)*	1.34 (0.30)
Turning velocity, °/s mean (SD)	Concussed	273.57 (43.13)	296.04 (46.01)*	326.24 (43.70)
	Control	316.55 (78.80)	385.74 (78.06)*	332.23 (75.98)

Results & Discussion: Acutely, the concussion group was slower compared to the controls (Fig. 1a) but improved to control speeds over time. The concussion group exhibited less ML RMS sway and reduced turning velocity (Fig.1b & 1c) acutely and at Pre RTP. There was a strong negative correlation (r < -0.580) between completion time and ML RMS sway at every timepoint for the control group and at Pre RTP (r = 0.674) for concussed athletes. The lower ML RMS sway in the concussed group may indicate a stiffening strategy [6], where the central nervous system reduces the degrees of freedom to simplify balance control. While the TTG completion time improved across assessments, the stiffer movement indicates a potential lingering impairment with the balance control strategies utilized by concussed participants. Similar trends in sport-relevant tasks, where performance outcomes improve but neuromuscular control remains impaired, may contribute to musculoskeletal injury risk post-concussion.

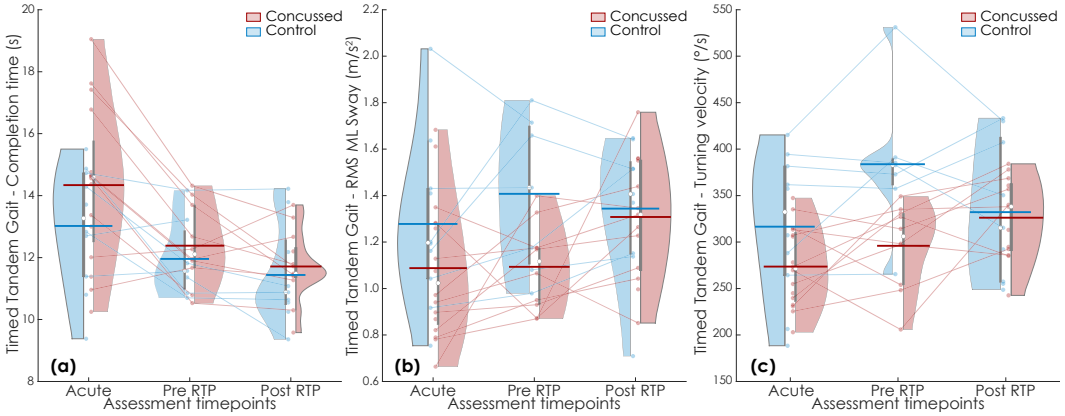

Figure 1: Violin plot of Timed Tandem Gait completion time (a), sway (b), and turning velocity (c) results for concussed (red) and controls (blue) at each assessment timepoint (Acute, Pre RTP and Post RTP).

Significance: Instrumenting TTG test with IMUs allows for the investigation of postural control strategies, and suggests that resolution on performance outcomes (i.e. completion time) may not indicate recovery of neuromuscular control.

References: [1] Howell et al. (2017) *J Sci Med Sport* 20(7); [2] Davlin et al. (2004), *Percept Mot Skills* 98; [3] Oldham et al. (2018) *Med Sci Sports Exerc* 50(6); [4] Morris et al. (2020) *Front Sports Act Living* 2; [5] Morris et al. (2024), *J Athl Train.* 59(1). [6] Carpenter et al. (2004) *Journal of Neurology, Neurosurgery & Psychiatry* 75.

STOCHASTIC OTIMAL CONTROL WALKING SIMULATIONS OF A MODEL WITH FEET

Dhruv Gupta[1*], Wouter Muijres[1], Lars D'Hondt[1], Friedl De Groote[1]
[1]Department of Movement Sciences, KU Leuven, Leuven, Belgium
*Corresponding author's email: dhruv.gupta@kuleuven.be

Introduction: Optimal control simulations have shown that both musculoskeletal dynamics and sensorimotor noise are important determinants of movement [1]. However, due to the high computational cost of solving stochastic optimization problems, the effect of noise has mainly been studied in reaching and standing based on simple models [2, 3]. We recently introduced a computationally efficient framework for stochastic optimal control that enables the use of more complex models of musculoskeletal dynamics and applied it to generate simulations of walking for a five-link walker [4]. The control policy consisted of feedforward and time-varying joint- and task-level feedback and thereby captured important components of human motor control. Yet, due to the absence of feet in this model, realism of the predicted kinematics was limited. Alternatively, stochastic optimal control simulations of walking have been generated based on a more detailed 2D musculoskeletal model with a very simple control policy of feedforward and joint-level feedback with constant gains [3]. Here, we present stochastic optimal control simulations of walking based on a 2D skeletal model with feet and a control policy consisting of feedforward and full-state time-varying feedback. These simulations are the next step towards gait simulations that account for the complexity of both the musculoskeletal system and neural control.

Methods: We simulated gait based on a torque driven 2D model with 7 segments (head-arms-trunk-pelvis, upper legs, lower legs, and feet). The model was defined in OpenSim (simtk.org). inertial properties and joint definitions were derived from OpenSim's gait1018 model but we defined the kinematic chain with the foot as the root segment. We did not model compliant foot-ground contact but assumed that the feet were rigidly connected to the ground during stance. We modelled gait in three phases. The first phase (double support) started with heel strike and ended with foot flat of the right foot. During this phase, the heel of the right foot and the toe of the left foot were connected to the ground with a pin joint. During the second phase (initial single stance), the right foot was welded to the ground and the left foot was constrained to be above the ground. The last phase (terminal single stance) began when the right foot's heel lifted and lasted until heel strike of the left foot. In this phase, the right foot's toe was connected to the ground with a pin joint and the left foot was constrained to be above the ground except for the last time instance, where its heel was constrained to be on the ground and have zero velocity.

Torques consisted of feedforward and time-varying linear feedback of the deviations of the state (angular positions and velocities) from the reference state. We assumed that the torque was corrupted by zero mean Gaussian motor noise. The reference state was chosen to be the state obtained by the feedforward torques in the absence of noise. To solve for feedforward torques and feedback gains, the variables of our control policy, we minimized expected effort (sum of squared torques). We solved the resulting stochastic optimal control problem using our recently proposed framework that is based on a deterministic approximation [2]. The state distribution was approximated by a normal distribution and could therefore be described by its mean and covariance. The mean state dynamics were described by the nonlinear skeleton dynamics in the absence of noise. The dynamics of the state covariance was described by the continuous Lyapunov differential equation based on a local first order approximation of the nonlinear dynamics around the mean state [2]. To obtain stable steady-state walking, we imposed symmetry of the mean state and state covariance, i.e. uncertainty does not grow over time.We imposed a speed of 1.1 m/s and stance time of 0.57 s and let the simulation choose the time spent in each phase. Problems were formulated in Matlab using skeleton dynamics from OpenSim. All problems were solved using direct collocation. We used CasADi (casadi.org) to formulate the problems and for algorithmic differentiation. Non-linear programming problems were solved with ipopt. We compared the experimental kinematics of one subject to those predicted from stochastic and deterministic simulations.

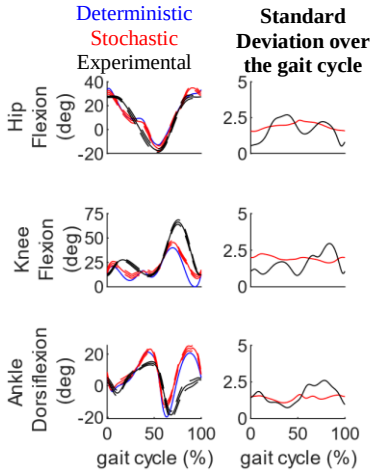

Figure 1: Exp and predicted kinematics from deterministic and stochastic frameworks.

Results & Discussion: The mean kinematics of the stochastic and deterministic simulations differed illustrating that noise shapes the mean trajectory. Kinematics obtained with both deterministic and stochastic simulations differed from the experimental data although the main features were captured (Fig. 1). Differences between simulations and experimental data are likely due to the use of a simple skeleton model as deterministic simulations based on more detailed 3D musculoskeletal models predict walking kinematics that are very similar to experimental data [5]. Kinematic variability predicted by the stochastic optimal control simulations had a similar order of magnitude than experimentally observed variability but did not capture how variability varied within the gait cycle (Fig 1). This discrepancy might suggest that we did not correctly model uncertainty. It is likely that sensory noise also shapes the variability. We are currently exploring how different levels of motor and sensory noise shape the variability.

Significance: Our framework has the potential to become an important tool to understand the effect of uncertainty, e.g. due to sensorimotor noise, on gait mechanics and control. This might be especially important when we try to understand gait deficits in neurological disorders that affect sensorimotor control.

Acknowledgments: We acknowledge the support of Marie Curie OpenAIRE ID – 101068850 and FWO research project G088420N.

References: [1] van Beers et al. (2002), *R Society. B: Bio Sciences*, 357(1424); [2] Van Wouwe et al. (2022), *PLOS Comp Bio*, 18(6); [3] Koelewijn & Van Den Bogert (2020), *J Biomech*, 104; [4] Muijres et al (2023). *TGCS*; [5] D'Hondt et al. (2023), *bioRxiv*, 2023-03.

WALKING WITH A TRANSFEMORAL BONE-ANCHORED LIMB RESULTS IN GREATER KINEMATIC SYMMETRY AND PROSTHETIC LIMB CONTROL ACROSS SELF-SELECTED WALKING SPEEDS

James B. Tracy[1*], Brecca M. M. Gaffney, Peter B. Thomsen, Mohamed E. Awad, Danielle H. Melton, Cory L. Christiansen, Jason W. Stoneback
[1]University of Colorado, Anschutz Medical Campus, Aurora, CO *Corresponding author's email: james.tracy@cuanschutz.edu

Introduction: Daily living requires individuals to walk at varying speeds to avoid obstacles, interact with others, and exercise. After a transfemoral amputation, these tasks are complicated by between-limb kinematic asymmetries (e.g., step length, trunk lateral bend) that are associated with reductions in walking efficiency and functional performance [1,2]. Bone-anchored limbs (BALs) involve fixing within the intramedullary canal of the bone a titanium implant which protrudes from the residual limb through an aperture or stoma to which the prosthesis componentry attaches [3]. BAL use may improve prosthetic limb control by having an interiorly fixed interface to the residual limb, as opposed to an exteriorly fitted socket, providing a consistent prosthetic-residual limb interface. BAL use has been shown to improve vibrotactile sensation compared to socket prosthesis users [4] which may improve proprioceptive capacity and further support prosthetic limb control. As a result, BAL use may improve gait symmetry through increased sensation of and response to walking ranges of motions. The purpose of this analysis was to describe the relationships between kinematic symmetry and self-selected walking speed walking with a socket prosthesis and one-year later walking with a BAL. We hypothesized that (1) between-limb symmetry would be greater when using a BAL compared to using a socket prosthesis and (2) that prosthetic limb control would be greater for BAL users across self-selected speeds evidenced by smaller correlations of between-limb symmetry and gait speed.

Methods: Twenty individuals scheduled for BAL implantation surgery walked 5 times overground at self-selected speeds within 5 days before surgery (SOCKET) and 1 year after implantation (BAL). Spatiotemporal parameters (cycle/stance/swing time, step/stride length) and joint angles (ankle, knee, hip, pelvis, and trunk) were calculated (Visual 3D) from whole-body motion capture (Vicon). Individual limb gait parameter metrics and the maximum and minimum angles in each plane for each joint were used to calculate the between-limb symmetry using the Normalized Symmetry Index (NSI) [5]. SOCKET and BAL symmetry were compared with paired t-tests adjusted for multiple comparisons (Bonferroni, $p \leq 0.001$). Each trial's NSI absolute value was correlated to gait speed using Pearson correlations (r) at each time point. Absolute r values of 0.1 to 0.3 represented small correlations and 0.3 to 0.5 medium correlations [6].

Results & Discussion: Self-selected walking speeds ranged from 0.64–1.46 m/s (n = 100 trials) and 0.71–1.45 m/s (n = 99 trials) for SOCKET and BAL, respectively (p = 0.44, Cohen's d = 0.08). Seven of the 35 measures showed significantly greater symmetry for BAL use ($p \leq 0.001$, d = 0.35–0.81) and two showed greater asymmetry ($p \leq 0.001$, d = 0.35–0.36). SOCKET and BAL walking resulted in a mixture of measures showing positive correlations (i.e., increased asymmetry across self-selected speeds) and negative correlations (i.e., increased symmetry across self-selected speeds) initially suggesting no clear relationship with between-limb movement symmetry across self-selected speeds for this cohort of participants ($-0.48 \leq r \leq 0.42$). The direction of the correlation (i.e., positive or negative) should not be ignored as this provides insight into how symmetry changed across self-selected speeds. Fifteen measures changed from either a negative correlation to speed with a socket prosthesis to a positive correlation with a BAL (n = 10) or vice versa (n = 5). A trend showed measures that changed signs at the ankle and knee joints (i.e., prosthetic joints) changed from negative to positive correlations (n = 8) while changes at the pelvis and trunk (i.e., anatomical joints) tended to change from positive to negative correlations (n = 5). Considering notable absolute changes in correlations from SOCKET to BAL walking ($|\Delta r| \geq 0.2$), 5 measures had weaker correlations to gait speed and only 2 measures had stronger correlations to gait speed (Table 1). Decreasing the absolute magnitude of correlation (i.e., absolute correlations closer to 0) suggests that BAL use improves prosthetic limb control while walking because the symmetry of those with a BAL walking at faster self-selected speeds was comparable to the observed symmetry for those with a BAL walking at slower self-selected speeds. Across self-selected walking speeds, the dynamic interactions of the residual limb with a socket prosthesis likely increase due to the relative motion of the socket, liners, skin, and underlying tissues. This dynamic interaction unique to an individual with a lower-limb amputation could contribute to between-limb asymmetry as gait speed changes and the range of motion and forces driving this relative movement are altered. Because the BAL interface between the residual limb and the prosthetic components is fixed, it follows that between-limb symmetry and prosthetic limb control would be greater with BAL use.

Significance: The results of this study suggest that BAL use produces more between-limb kinematic symmetry and greater prosthetic limb control as between-limb symmetry is more consistent across self-selected walking speeds. Walking speed influenced between-limb symmetry for some of these kinematic measures and influenced some measures differently between prosthesis types. Therefore, rehabilitation focused on modifying gait asymmetries may need to consider a range of walking speeds, especially for individuals with a socket prosthesis, and alter rehabilitation for individuals with a BAL to focus on their distinct symmetry needs. For example, since hip abduction asymmetry increased as self-selected speed increased with BAL use but not with a socket prosthesis (Table 1), emphasizing hip abduction control during rehabilitation may provide benefits unique to BAL users for walking at faster speeds. A notable limitation is that this analysis was limited to the participants' self-selected walking speeds, which was wide, but it is still unknown how asymmetries may change within individuals walking at different speeds.

Table 1: Correlations of between-limb symmetry (|NSI|) to gait speed for 7 measures with notable absolute changes ($|\Delta r| \geq 0.2$).

MEASURE	SOCKET	BAL
Stance Time	-0.26	-0.01
Knee - Max Flexion Angle	-0.48	0.18
Knee - Max Extension Angle	0.03	0.28
Knee - Max External Rotation Angle	-0.33	-0.01
Hip - Max Abduction Angle	0.01	0.42
Trunk - Max Internal Rotation Angle	-0.23	0.03
Trunk - Max External Rotation Angle	-0.24	-0.01

Funding/Refs: CU Bone-Anchored Limb Research Group. **[1]** Carse (2020), *Gait Post* 75; **[2]** Devan (2015), *Rehab Res Dev* 52; **[3]** Brånemark (2001), *Rehab Res Dev* 38; **[4]** Häggström (2013), *Rehab Res Dev* 50; **[5]** Queen (2020), *J Biomech* 99. **[6]** Cohen (1988), *Stat Power Analysis* 2nd ed.

HOW IS LOAD DISTRIBUTED ACROSS LIMBS DURING PROLONGED BOUTS OF WALKING IN PERSONS WITH TRANSFEMORAL OSSEOINTEGRATION?

K.F. Ash[1,2*], P.R. Golyski[1,3], C.L. Dearth[1,3,4], J.A. Forsberg[1,4], B.K. Potter[1,4], B.D. Hendershot[1,3,4]
[1]Walter Reed National Military Medical Center, Bethesda MD, [2]Henry M. Jackson Foundation for the Advancement of Military Medicine, Inc., Bethesda, MD, [3]Extremity Trauma & Amputation Center of Excellence, Falls Church, VA, [4]Uniformed Services University of the Health Sciences, Bethesda, MD
*Corresponding author's email: kiichi.f.ash.ctr@health.mil

Introduction: Asymmetric gait is common among individuals with unilateral transfemoral amputation (UTFA) due to movement strategies that compensate for deficient residual limb strength while maximizing stability and comfort [1]. During walking, one common compensatory strategy is biasing limb loading toward the intact limb, which over time can lead to complications such as knee/hip osteoarthritis or lower-back pain [2]. Osseointegration (OI), the direct skeletal attachment of the prosthesis, aims to eliminate socket-related complications, improving overall mobility and perhaps movement quality (e.g., reducing reliance on the intact limb and/or arms and assistive devices). The aim of this work was to compare load distribution across upper and lower limbs in Service members with UTFA during prolonged walking, before and 24 months after OI. With an improved prosthesis interface and functional capacity [3], we hypothesized OI would facilitate increased loading of the prosthetic leg and reduced loading of the contralateral (intact) leg and arms.

Methods: Eleven Service members with UTFA (9M/2F, mean±SD age: 37.4±9.4yr, body mass: 96.1±15.1kg, stature: 177.4±9.1cm) completed a five-minute bout of walking on an instrumented split-belt treadmill (Bertec, Columbus, OH) with instrumented handrails at their self-selected walking (SSW) speed (0.8±0.2m/s). If able, participants walked at three additional speeds (0.7m/s, 1.0m/s, and 1.3m/s). Bilateral ground and handrail reaction forces were collected before OI while using their traditional socket and again at 24 months after OI. Force distribution as percent bodyweight (%BW) was calculated for each limb during each stride. Walking speed during each stride was calculated by integrating anteroposterior handrail and ground reaction forces divided by mass with respect to time and assuming the mean speed was the commanded treadmill speed. A linear mixed model with fixed effect of prosthesis interface (pre vs. post OI, covariate of walking speed, and random effect of participant assessed the main and interaction effects for each limb ($p<0.05$).

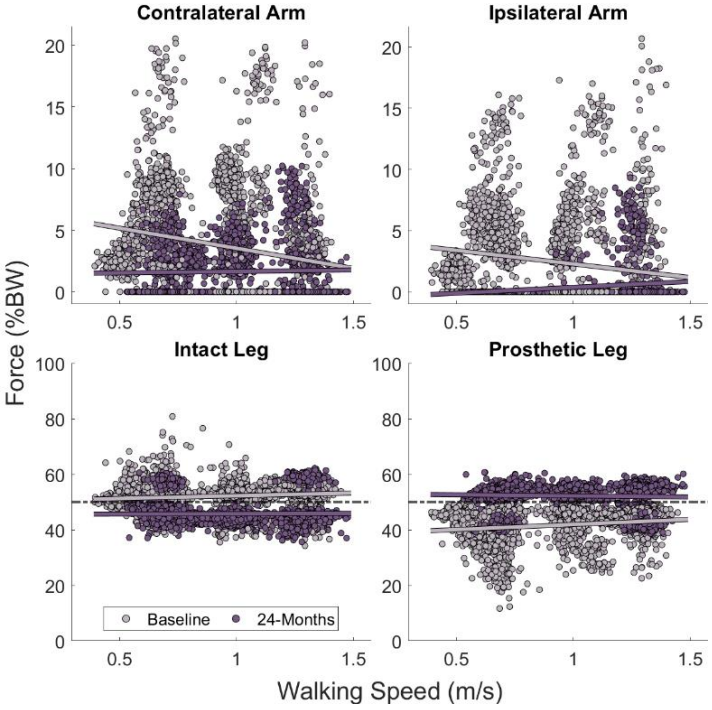

Figure 1: Loading distribution across limbs during a 5-minute walk on an instrument treadmill, before and after osseointegration. All data, including walking speeds, were calculated on a stride-by-stride basis.

Results & Discussion: Individuals loaded their prosthetic leg to a greater extent ($p=0.026$) after OI (51.3±6.2%BW) vs. before OI (40.2±5.5%BW); the intact leg tended to be loaded less after OI (47.2±0.75%BW) vs. before OI (51.3±3.0%BW), although this difference was not significant ($p=0.321$). Similarly, the contralateral and ipsilateral arms tended to be loaded less after OI (1.9±2.5%BW and 0.5±0.9%BW) vs. before OI (5.0±3.9%BW and 3.4±3.1%BW), although also not significant ($p=0.196$ and $p=0.072$). As walking speed increased, both the intact and prosthetic legs were loaded more ($p<0.001$ and $p=0.031$) while each arm loaded less ($p<0.001$). Overall, our hypothesis was partially supported, suggesting that OI increases loading of the prosthetic leg while offloading the other limbs during prolonged walking.

Significance: In this work, we used a first-principles approach to determine loading across all limbs among individuals with OI on a stride-by-stride basis. This analysis suggests that OI facilitates greater loading on the prosthetic limb with less reliance on the intact leg and arms, potentially improving gait quality and thus long-term outcomes (e.g., reducing risk of secondary complications). Our findings contrast that of recent literature showing reduced loading on the prosthetic leg after OI [4]; such differences may be attributed to force sensation related to surface compliance (i.e., treadmill vs. overground) or walking confidence (i.e., presence of handrails), additional work should explore temporal relationships in limb loading throughout prolonged bouts of walking and with time since OI.

Acknowledgements: Supported by DoD award #W81XWH-17-2-0060 and the EACE. The authors also acknowledge the Limb Optimization and Osseointegration Program, and numerous others who supported biomechanical and functional evaluations. The views expressed are those of the authors and do not necessarily reflect the policies of HJF, USUHS, DoD, nor the U.S. Government.

References: [1] Sagawa et al. (2011) *Gait & Posture* [2] Butowicz et al. (2018) *Adv Wound Care* [3] Van de Meent et al. (2013) *Arch Phys Med Rehabil* [4] Bluementritt et al. (2023) *Clin Biomech*

CONSIDERING SELF-SELECTED WALKING SPEED NULLIFIES THE EFFECT OF PROSTHETIC FOOT TYPE ON CONTRALATERAL KNEE LOADS AMONG INDIVIDUALS WITH UNILATERAL TRANSTIBIAL LIMB LOSS

Pawel R. Golyski[1,2*], John M. Chomack, David V. Herlihy, Jason T. Maikos, Brad D. Hendershot
[1]Extremity Trauma and Amputation Center of Excellence, Falls Church, VA, [2]Walter Reed National Military Medical Center, Bethesda, MD
*Corresponding author's email: pawel.golyski.civ@health.mil

Introduction: Individuals with lower limb loss are highly heterogeneous, particularly in terms of functional ability (e.g., Medicare K-level), challenging the generalizability of research findings to inform clinical care and optimize long-term health. For individuals with unilateral transtibial limb loss (UTTLL), reducing long-term osteoarthritis risk in the contralateral knee is a major health optimization objective [1], which may be achieved through prescription of advanced biomimetic prosthetic feet that reduce contralateral limb loads [2]. Here, we investigated the effects of three types of prosthetic feet (energy storing and returning [ESR], articulating energy storing and returning [ART], and powered [POW]) on limb loading in a diverse cohort of Service members and Veterans with UTTLL, considering self-selected walking speed (SSWS) as a statistical covariate representative of functional ability. We hypothesized that POW prosthetic feet would be associated with lower maxima and loading rates in contralateral vertical limb ground reaction forces (vGRF), knee adduction moments (KAM), and tibiofemoral contact forces (TCF), independent of functional ability.

Methods: Twenty-nine individuals with UTTLL (25 males/4 females, mean±SD age: 51±13yr, stature: 181±8cm, body mass: 91.8±19.0kg, time since amputation: 120±122mo, etiology: 22 trauma, 3 cancer, 4 diabetes) wore three different prosthetic feet (ESR, ART, POW), in a randomized sequence with approximately 1 week to acclimate to each foot. After each acclimation period, full-body motion (120 Hz) and GRFs were collected as participants walked overground. Individual trials were post-hoc binned into three speeds: slow (0.8-1.1 m/s), medium (1.1-1.4 m/s), and fast (1.4-1.7 m/s). A full-body OpenSim model with UTTLL was scaled to each participant [3]. Tibiofemoral contact forces were estimated using a custom static optimization procedure [4] in conjunction with OpenSim's joint reaction analysis tool. Overall maxima and loading rates in vGRF, KAM, and TCF were evaluated using a repeated measures ANOVA with within-subject effects of prosthetic foot type and trial speed together with a between-subject effect of self-selected walking speed (SSWS). SSWS was estimated using 6MWT distances in each participant's prescribed foot type (range: 272 to 704 m, spanning the lowest K3 to the highest K4; [5]). Significance was determined when $p \leq 0.05$. All activities were approved by the local IRB, and participants provided informed consent.

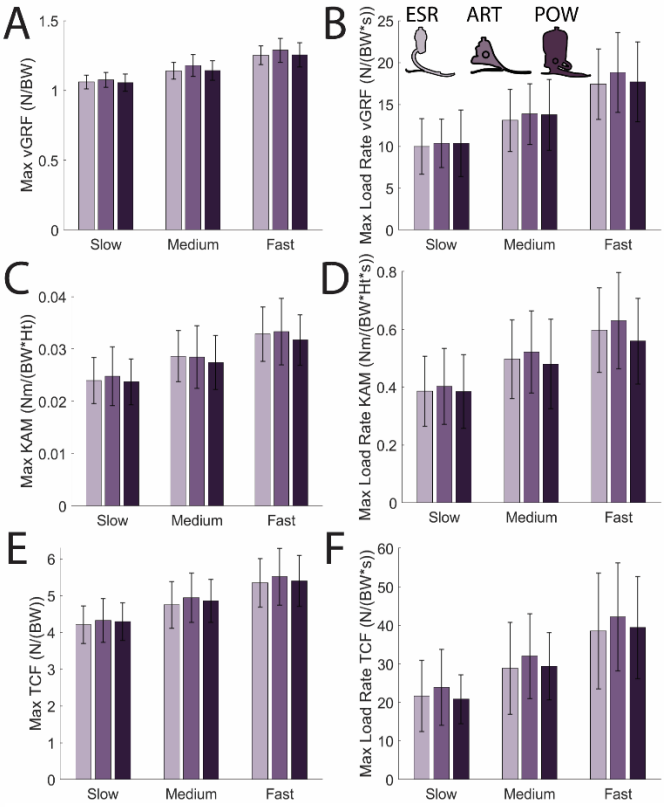

Figure 1: Maxima and loading rates of (A-B) vertical ground reaction force, (C-D) knee adduction moment, and (E-F) tibiofemoral contact force, normalized to bodyweight or bodyweight*height. Error bars represent ±1 standard deviation.

Results & Discussion: Across all loading metrics, there were no significant effects of SSWS ($p>0.24$), prosthetic foot type ($p>0.14$), or interaction between prosthetic foot type and trial speed ($p>0.08$; Fig. 1), which did not support our hypothesis. Faster trial speeds were associated with larger loads for all metrics ($p<0.04$) except for KAM loading rate ($p=0.18$). Considering a post-hoc analysis without inclusion of SSWS as a covariate resulted in significant effects of prosthetic foot type on max vGRF ($p=0.03$, ART>ESR, $p=0.039$) and KAM loading rate ($p=0.05$, with no significant pairwise effects), our findings suggested that relative to conventional ESR feet, more advanced biomimetic prosthetic feet may not reduce contralateral limb loads across walking speeds, independent of functional ability among K3 to K4 individuals with UTTLL.

Significance: This study represents one of the most comprehensive biomechanical investigations of the effects of prosthetic foot type on contralateral limb loading, with implications on clinical decision making and device design. Future studies should extend outside the laboratory to characterize these relationships across different environments and tasks of daily living.

Acknowledgments: Support was provided by the Congressionally Directed Medical Research Programs, Orthotics and Prosthetics Outcomes Research Program (Award #W81XWH-17-2-0014). The views expressed in this abstract are those of the authors, and do not reflect the official policies of the Uniformed Services University of the Health Sciences, U.S. Departments of the Army, Navy, Defense, Veterans Affairs, nor the U.S. Government.

References: [1] Struyf et al. *Arch Phys Med Rehabil* 2009. [2] Grabowski & D'Andrea *JNER* 2013. [3] Willson et al. *Comput Methods Biomech Biomed Engin* 2022. [4] Uhlrich et al. *Sci Rep* 2022. [5] Sions et al. *Arch. Phys. M.* 2018.

EVALUATING PHYSICAL AND PHYSIOLOGICAL LOADS DURING LOADED MILITARY TRAINING HIKES

Ethan Wong[1,2*], Matthew Hoch[3], Brian Green[1,2], Nicole Heimark[1,2], Amy Silder[2]
[1]Naval Health Research Center, San Diego, CA
[2]Leidos Inc, San Diego, CA
[3]University of Kentucky, Lexington, KY
*Corresponding author's email: ethanjwong29@gmail.com

Introduction: Inertial measurement units (IMUs) allow easy access to raw data and enable measurements of segmental motion and acceleration. Improvements in sensor technology have resulted in greater onboard data storage capacity, a smaller form factor, and decreased sensitivity to drift. Yet, as highlighted in recent review articles, most studies on walking and running have been limited to indoor settings [1] or were not able to investigate how changing factors such as terrain, gait speed and distance may be considered in outdoor settings [2]. In contrast, commercially available wearables (e.g. Fitbit, smart watches) enable easy-to-measure activity features such as heart rate and location in the real world. Unfortunately, restrictive commercial contracts and proprietary algorithms have limited the development of methods that allow for the synchronization of data from multiple sensor types and/or public repositories. In our study, we overcome these limitations by introducing methods to easily and accurately collect and analyze tibial accelerations and spatiotemporal gait data from long distance outdoor hikes over varied terrain features. The purpose of this abstract is to demonstrate and elaborate on the methods and processes used to collect data from various wearable technologies while presenting an example of results that can be obtained through automated data analysis techniques.

Methods: Data were collected from 91 Marines (mean ± standard deviation, 34M, 20±3y, 70±11kg, height 168±10cm), who completed a 10km ruck hike in combat uniform. Participants carried 27±8kg, which including a 3.3kg weapon. Prior to the hike, each participant was equipped a Garmin Solar Instinct 2 GPS watch and two Xsens DOT IMUs, secured on the anterior-medial tibia immediately above the boot. Equipping each participant required approximately one minute, as no synchronization or calibration was necessary during the setup process. Data from the IMU and GPS were stored locally to each device then transferred to a computer via a direct cable. All data processing was fully automated using custom code written in MATLAB. Exact calibration of IMU orientation relative to the tibia was done using gravity during the longest bout of standing and the first principal component of angular velocity during the longest continuous bout of walking. Activity (e.g. walking, running, non-movement) throughout the hike was classified using speed, with walking defined as 0.45–1.00m/s. To simplify data collection procedures, IMU and GPS global time were synchronized post hoc using the time stamp created by each sensor. After data synchronization, tibial accelerations were extracted for each foot contact during walking. Corresponding cadence and step length were estimated by combining gait cycle times with speed from the GPS watch. High resolution terrain features (e.g., slope, aspect, surface) were obtained from ArcGIS (Esri) and combined with each participants' direction of travel (calculated from changes in latitude-longitude location) to estimate the ground slope on which the participants were walking. Together, these methods resulted in synchronized data for axial and anterior-posterior (AP) tibial accelerations, walking speed, incline, cadence and step length for the duration of the hike. Proof-of-concept results are presented using data from a 3km gently sloping mountain pass [3] on a predominantly fanglomerate trail. Paired t-tests were used for all demonstrative analyses (α=0.05), without correcting for covariates.

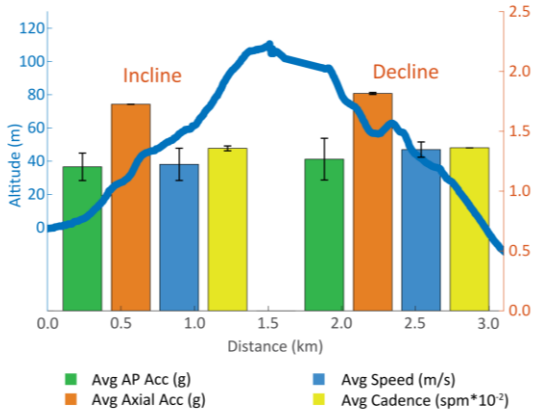

Figure 1: Altitude profile along the gently sloping mountain pass. Incline and decline metrics of interest are shown on their respective sides. Values of each metric are scaled to the right y-axis.

Results & Discussion: As expected, participants walked slower uphill (1.73±0.41m/s), compared to downhill (1.82±0.37m/s, p<.001, d=0.67). Without controlling for speed, we also found no significant difference in cadence, whereas step lengths were shorter travelling on an incline (uphill 0.52±0.22m, downhill 0.58±0.36m, p=.003, d=0.23). This is in comparison to laboratory-based load carriage studies that found no significant effect of incline on cadence or step length during treadmill walking at fixed speeds [4,5]. Tibial accelerations in the axial direction were less when walking uphill, compared to downhill (uphill 1.73±0.41g, downhill 1.82±0.38g, p=.022, d=0.23) but the AP (i.e. braking/propulsive) direction showed no significant differences (uphill 1.20±0.39g, downhill 1.27±0.43g, p=.120, d=0.16). These combined data from different wearable technologies demonstrate a brief overview of how our methods can examine differences in several gait parameters during the variable terrain in the ascent and descent of a mountain pass.

Significance: Data presented here represent ~1,100km and over 12,000 steps and were collected and processed using methods that can easily be adapted to any outdoor gait assessment. Our data collection setup is fast and requires no calibration. Unlike previous studies, we synchronized location and IMU data, which enabled us to explore the interaction between the many environmental and human factors that influence performance, fatigue, and injury risk.

References: [1] Brenson et al., (2022), *Sensors*; [2] Edwards et al., (2023) *Appl Ergonomics*; [3] Shoeneberger et al, USDA-NRCS (2017) *Soil Survey Manual*; [4] Silder et al., (2012) *J Biomech*; [5] Sturdy et al., (2023*), J Electromyogr Kinesiol*.

Impact of Exertion on Metatarsophalangeal Joint Loads During Prolonged Load Carriage

Ankur Padhye[1*], Stacey Meardon[1], Junfei Tong[2,3], Jaques Reifman[2], and John Willson[1]
[1]Department of Physical Therapy, East Carolina University, Greenville. NC
[2]Department of Defense Biotechnology High Performance Computing Software Applications Institute, Telemedicine and Advanced Technology Research Center, U.S. Army Medical Research and Development Command, Fort Detrick, MD, USA
[3]The Henry M. Jackson Foundation for the Advancement of Military Medicine, Inc., Bethesda, MD, USA
*Email: padhyea20@students.ecu.edu

Introduction: The high volume and intensity of physical training faced by military Service members during training tasks contributes to a high incidence of lower extremity overuse injuries, especially in females.[1] Metatarsals are a common injury site in Service members and may be linked with a proximal shift in ground reaction force (GRF) under the toes to the metatarsal region during military tasks like prolonged rucking.[2,3] This shift may affect metatarsophalangeal (MTP) joint contact forces (JCF). However, to date, MTP JCF changes experienced over the course of military training activities are unknown. Thus, the purpose of this study was to compare MTP JCF at the beginning and at the end of a 5km rucking task in physically active females and to evaluate toe flexor muscle force contributions to MTP JCF estimates.

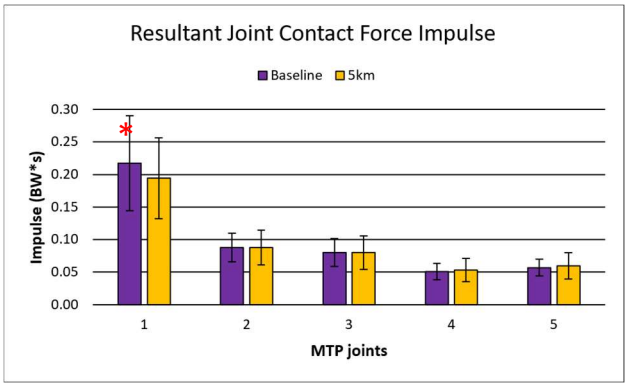

Figure 1: Body weight normalized RJCF impulse for all 5 MTP joints. Error bars represent standard deviation. *p < 0.05.

Methods: Time synchronized left foot 3D marker data (200 Hz), ground reaction forces (2000 Hz), and in-shoe plantar pressure data (100 Hz) were recorded at the beginning and end of a 5 km rucking task in 21 females (22.4 yr, 1.65 m, 58.2 kg, physical activity rating 7.4/10). The rucking task was performed at 1.5 m/s with 22.7 kg of symmetrical load carriage. Plantar pressure data recorded in computed tomography (CT)-informed foot regions (masks) were used to assign GRF to metatarsal and toe regions for MTP joint moment and joint reaction force inverse dynamics calculations at each MTP joint. Toe flexor muscle force contributions to MTP JCF were estimated using subject-specific moment arms from CT images. The resultant JCF (RJCF) at each MTP joint were calculated and peak RJCF, RJCF impulse, and RJCF loading rates averaged over 5 stance phases were compared at the beginning (baseline) and end (5km) of the rucking task using paired t-tests (α=.05).

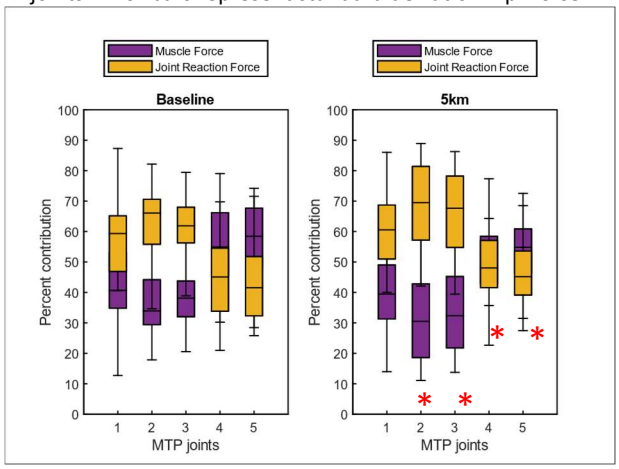

Figure 2: Percent contribution of muscle force and joint reaction force to the RJCF. Error bars represent maximum and minimum values. *p < 0.05 in comparison with baseline.

Results and Discussion: Following the rucking task, 1st MTP RJCF impulse decreased 10% (p=.03) (Figure1) and RJCF loading rate decreased 14% for the 2nd (p=.02) and 15 % at 3rd (p=.02) MTP joints. Peak RJCF at the 1st MTP joints also decreased by 8% but the change was not statistically significant (p=.06). Toe flexor muscle contributions to the RJCF at Baseline (Figure 2) and were significantly lower at the 2nd (p=.01), 3rd (p=.01), 4th (p=.01), and 5th (p=.02) MTP joints after 5km of rucking compared to baseline. The toe flexor contributions lowered by 15 and 16% respectively at the 2nd and 3rd MTP joints. The reduction in MTP RJCF with exertion may represent decreased MTP joint contributions to forward propulsion and is consistent with existing literature reporting lower toe pressures following exertion.[3,4]

Significance: This study used CT-informed plantar pressure masks to estimate changes in MTP JCF during a military-relevant training task. Results of this study may contribute to metatarsal injury prevention efforts in female Service members. For example, the large muscle contributions to MTP JCF, and largest of the significant reductions in these contributions at 2nd and 3rd MTP joints with exertion, may increase the risk of bone stress injuries[5] and underscore the value of toe flexor endurance in female Service member MTP injury prevention efforts.

Disclaimer: The opinions and assertions contained herein are the private views of the authors and are not to be construed as official or as reflecting the views of the U.S. Army, the U.S. Department of Defense, or The Henry M. Jackson Foundation for the Advancement of Military Medicine, Inc. This abstract has been approved for public release with unlimited distribution.

References: [1] Jones et. al. (1989), Ex. & Sports Sci. Rev. 17, 379-422. [2] Ross et.al. (2002) Mil. Med. 167(7), 560-565. [3] Nagel et.al. (2008), Gait & Posture 27, 152-155. [4] Willson & Kernozek (1999), Med. Sci. Sports. Exerc. 31(12), 1828-1833. [5] Sharkey et.al. (1995), Bone Joint Surg Am. 77(7):1050-7.

A NOVEL BIOMARKER FOR DETECTING FATIGUE IN SOLDIERS DURING LOADED WALKS

Kolby J. Brink*[1], Kari L. McKenzie[2], Chad R. Straight[2], Kevin S. O'Fallon[2], Seung K. Kim[1], & Aaron D. Likens[1]
[1]Department of Biomechanics, University of Nebraska at Omaha, Omaha, NE USA
[2]US Army Combat Capabilities Development Command Soldier Center, Natick, MA
*Corresponding author's email: kolbybrink@unomaha.edu

Introduction: In the context of Soldier well-being, the detection and management of injuries are vital due to their potential to disrupt careers or jeopardize lives[1]. This study introduces Recurrence Quantitative Analysis (RQA), a promising nonlinear analysis that monitors system behavior over time, as an auspicious biomarker to indicate movement changes due to fatigue and distinguish injured from non-injured Soldiers[2]. The purpose of this study was to use RQA to assess Soldiers' movement dynamics during multiple bouts of load carriage, focusing on 1) fatigue effects and 2) comparing Soldiers removed from the study due to undisclosed injury exacerbation with Soldiers who completed the protocol.

Methods: Twelve male Soldiers (age: 24.0 ± 3.4 years, weight: 88.9 ± 11.8 kg, completed N=7) participated in a four-day protocol designed to simulate the demands of a three-day mission, followed by one day of recovery. Data is presented only for mission days (MIS1-3), during which Soldiers engaged in either a two-hour (MIS1 & MIS3) or 30-minute (MIS2) ruck march on a treadmill, carrying an additional 50% of their body mass in a weight vest. Sternum acceleration was derived from inertial measurement units. Recurrence plots were constructed using the sternum acceleration and the mean line length (MLL) was used as the dependent measure. Multilevel models (MLMs) were used to determine the rate of change in MLL during load carriage tasks.

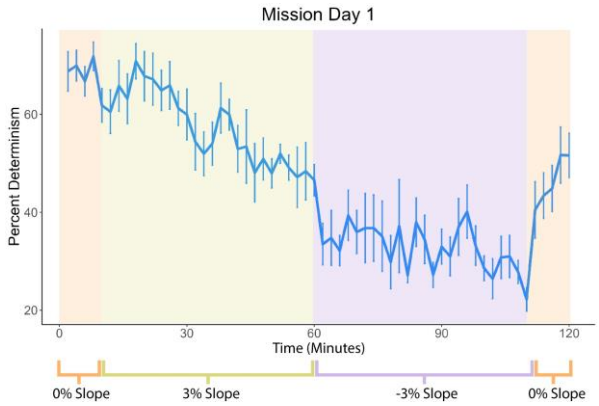

Figure 1: Line graph depicting percent determinism from the recurrence plots generated for every 2-minute segments of the loaded walking trials during Mission Day 1. Shades of panels depict the slope of the treadmill throughout the 2-hour long trial.

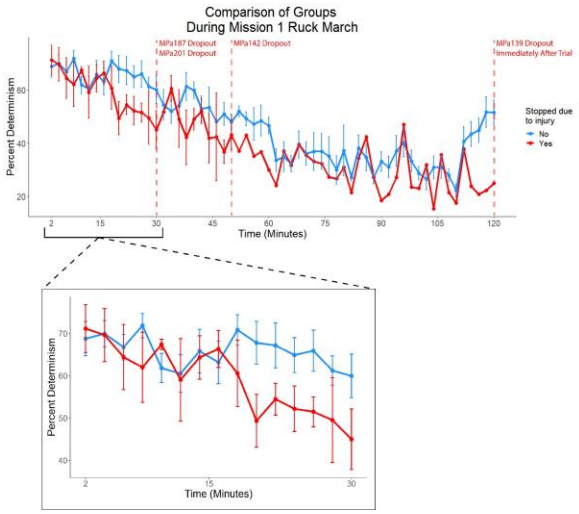

Figure 2: Line graph depicting percent determinism for 2-minute segments during the loaded walking trial on Mission Day 1. The blue line represents the group that completed the trial without stopping due to injury exacerbation, while the red line represents the group that stopped. The top graph covers the entire 2-hour walking trial, indicating dropout points. The bottom graph focuses on the initial 30 minutes when all soldiers were still participating, allowing for a direct comparison between the two groups.

Results & Discussion: MLMs revealed that MLL decreased by .13 SDs/10 min during MIS1 load carriage, $t(404.11)= -7.36$, $p<.001$. MLL decreased by .39 SDs/10 min during MIS2 load carriage, $t(76.0)= -3.668$, $p<.001$. MLL decreased by .11 SDs/10 min during MIS3 load carriage, $t(446.02)= -7.28$, $p<.001$. Also, when averaging across the first 30-minutes of the MIS1 loaded march (when all Soldiers were still participating), Soldiers who eventually discontinued due to an injury exhibited an MLL .64 SDs lower than that of the healthy Soldiers $t(7.79)= -2.77$, $p=.025$. In conclusion, the decline in MLL signifies a shift in the predictability and regularity of Soldiers' movements during load carriage. This change may be indicative of increased instability attributed to accumulated fatigue. Furthermore, the diminished MLL observed in injured Soldiers suggests that MLL may serve as a promising biomarker of injury onset or the onset of fatigue.

Significance: RQA proves to be a non-invasive biomechanical biomarker capable of detecting both the onset of fatigue and injuries in Soldiers during loaded walking. This novel approach to assessing Soldier readiness holds promise as a practical method for use in the field, contributing to the health and safety of military personnel.

Acknowledgments: This work was supported by the National Strategic Research Institute and the Department of Defense (U2-20-F0101) and the U.S. Army DEVCOM Soldier Center under the Measuring and Advancing Soldier Tactical Readiness and Effectiveness (MASTR-E) program. AL is also supported by awards from the National Institutes of Health (P20GM109090) and the National Science Foundation (2124918). The authors would like to acknowledge the exceptional contributions of the data collection team on this project. For every one participant in this study there was a team of 7 researchers required for the 30hrs data collection per week.

Supported by US Army MASTR-E Program and NSRI

References: [1] Anderson KA et al. *Sports Med. 2*016; 10.1186/s40798-016-0046-z. [2] Webber Z. *Tutor Contemp Nonlinear Methods Behav Sci.*. 2005;591:402–9.

TENDON INJURY MODELS IN *EX VIVO* BOVINE TENDON PRODUCE DIFFERENT MECHANICAL PROPERTIES

Zoe M. Moore[1*], Grace Wood[2], Jake Elliott[2], Julianna C. Simon[1,2], Meghan E. Vidt[1,3]
[1]Biomedical Engineering, The Pennsylvania State University, University Park, PA, USA
[2]Graduate Program in Acoustics, The Pennsylvania State University, University Park, PA, USA
[3]Physical Medicine and Rehabilitation, Penn State College of Medicine, Hershey, PA, USA
email: *zmm5238@psu.edu

Introduction: Pain associated with shoulder injuries is the 3rd most common musculoskeletal complaint in adults [1]. Shoulder pain is often caused by a tendon overuse injury (tendinosis) that breaks down the collagen fibers of the tendon [2]. Current treatments for tendon overuse injury produce inconsistent results, suggesting that tendon injury needs to be studied further [3]; however, there is no consistent model for studying tendon injury. Specifically, a common *in vivo* model used to study tendon injury involves the injection of collagenase into the tendon to create microdamage [4]. Other *ex vivo* studies apply mechanical overloading to the tendon to induce microdamage within the tissue [5]. While both injury models aim to mimic tendon injury, it is unknown how these two injury models influence the resultant mechanics of the tissue. Therefore, the objective of this work is to compare the effects of collagenase injection and mechanical overload on mechanical properties in an *ex vivo* bovine tendon model.

Methods: Twelve bovine superficial flexor tendons were obtained from a local abattoir. Tendons were assigned to an injury group: healthy non-injured (n=4); collagenase injection (n=4); and mechanical overload (n=4). All healthy tendons experienced no injury prior to mechanical testing. The collagenase injected tendons were injected with 1 mL of collagenase in a fibrin gel along the long axis and allowed to rest in phosphate buffered saline for 24-hours prior to testing. The mechanically overloaded tendons were loaded with an MTS-858 Mini Bionix mechanical testing machine (MTS Systems Corp., Eden Prairie, MN). Loading was applied in tension along the long axis of the tissue at 0.1 mm/s until the slope of the force displacement curve was approximately 0. The tendons were then ramped down at 0.1 mm/s until tendon displacement returned to 0; this was repeated 5 times. Mechanical testing was performed using the MTS instrument following injury, using a protocol previously established by our group, with slight modifications to accommodate the larger animal model [6,7]. For mechanical testing, tendons in all groups underwent cyclic loading between 1-5% strain, followed by stress relaxation at 5% strain, then load-to-failure at 0.1mm/s. The tests were video recorded at 30 frames/second using a Panasonic Lumix (Panasonic. Newark, NJ) camera for analyses.

The length, width, and thickness of the tendons were measured using digital callipers and the cross-sectional area was calculated by estimating the tendon cross-section at the midpoint of the tendon length as an ellipse. Stiffness was calculated as the slope of the force displacement curve recorded by the MTS instrument from the load-to-failure test. Ultimate tensile stress (UTS) was calculated by obtaining the maximum force achieved during the load-to-failure test and dividing this by the cross-sectional area. A one-way ANOVA was used to determine differences between injury group for each of the mechanical parameters using SAS Studio software (SAS, INC., Cary, NC) with significance set at $p<0.05$.

Results & Discussion: The maximum loads achieved for the healthy (1346±181 N) and collagenase (1351±298 N) injected tendons were comparable to that found in literature for healthy tendons (1559±176 N) [8]; the loads achieved for the mechanical overload tendons (511±199 N) were less than what has been previously reported. There were no differences found in UTS between the healthy (30±6 kPa) and collagenase (21±7 kPa) groups, ($p=0.077$); or the collagenase and mechanical overload groups, ($p=0.056$), but there was a difference in UTS between the healthy and mechanical overload (11±6 kPa) groups ($p=0.002$) (Fig. 1). There were no differences in stiffness between the groups (Fig. 1): healthy (159±45 N/mm) and collagenase (169±26 N/mm) ($p=0.750$); collagenase and mechanical overload (164±11N/mm) ($p=0.848$); or healthy and mechanical overload ($p=0.859$).

These results suggest that tendon overuse injury models produce different tissue mechanical properties in an *ex vivo* bovine model. There are emerging trends in differences in UTS between the 2 injury models, suggesting that they may represent different stages of injury progression. These trends are being further examined in a larger sample, as well as being used to assess the mechanical effects of emerging treatments, such as focused ultrasound, for tendon overuse injuries.

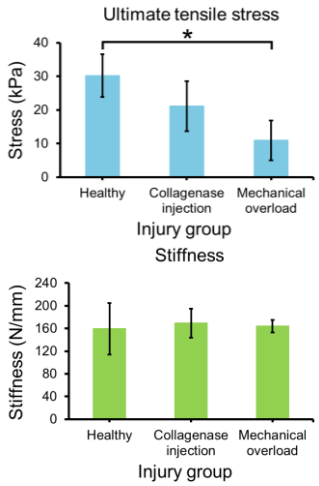

Figure 1: A) Ultimate tensile stress (UTS) for each injury groups. UTS was different between healthy and mechanical overload groups ($p=0.002$). B) Stiffness for each injury group. There was no difference between groups for stiffness ($p=0.935$). *indicates $p<0.05$.

Significance: Comparing the mechanical effects of these tendon overuse injury models help us understand how they relate to different stages of injury progression. Understanding the different mechanical responses will allow researchers to make more informed decisions when selecting a tendon injury model.

Acknowledgments: NIH-NIBIB R01EB032860 (PI: Simon)

References: [1] Lucas et al., 2022. BMC Musculoskelet Disord. 23(1). [2] Mitchell et al., 2005. BMJ. 331(7525):1124-28. [3] Dunning et al., 2014. Phys Ther Rev. [4] Gong et al., 2018. Connect Tissue Res. [5] Veres et al., 2012. J Orthop Res. 31(5):731-7. [6] Khandare et al., 2022. J Biomech. [7] Abraham et al., 2018. Mech Engr and Mat Science Independent Study. (75). [8] Colaco et al., 2017. J. Biomech (53):144-147.

THE EFFECT OF CALCIFICATION ON ELASTIC AND VISCOELASTIC PROPERTIES OF TENDONS

Joshua T. Bland[1,2*], Alexander W. Hooke[1,2], Elameen A. Adam[2], Chunfeng D. Zhao[2]
[1]Biomechanics Core Facility, Mayo Clinic, Rochester, MN
[2]Department of Orthopedic Surgery, Mayo Clinic, Rochester, MN
*Corresponding author's email: bland.joshua@mayo.edu

Introduction: A relatively common shoulder disorder which primarily affects the tendons in the rotator cuff is calcific tendinitis. Calcific tendinitis is characterized by an accumulation of calcium deposits in the affected tendon. The occurrence of calcific tendinitis has been recorded as being anywhere between around 3-10% of adults [1]. Symptoms can include pain and stiffness and may be acute or chronic. Although less common, calcific tendinitis can occur in other areas besides the shoulder such as the hip joint, rectus femoris, biceps femoris, and gluteus maximus [2]. This study used turkeys as a model to investigate the effect of calcification on the mechanical properties of tendons. Turkey flexor tendons have been shown to be a clinically relevant model for tendon research [3] and the tendons of older turkeys are known to be calcified. Turkeys rapidly increase in weight as they develop, thereby the load demand on their flexor tendons increases in tandem. For this reason, it is hypothesized that the increased loading of the tendons has a crucial function in the calcification of the tendons. Furthermore, it would be expected that the tendons become stiffer, and their viscoelastic properties decrease as the turkeys develop due to increased calcification.

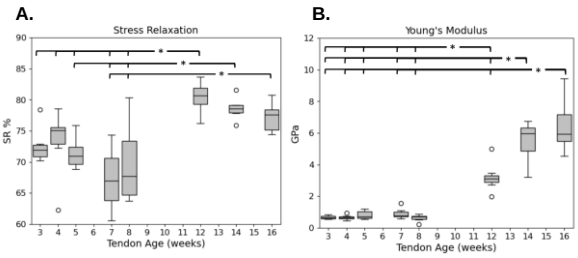

Figure 1: Box plots grouped by age for A) stress relaxation, B) Young's modulus. Significant post-hoc Tukey HSD test results shown with comparison bars (alpha = 0.05).

Methods: 52 turkey flexor tendons were tested. The tendons came from turkeys sacrificed at 3 (n=6), 4 (n=6), 5 (n=6), 7 (n=7), 8 (n=6), 12 (n=7), 14 (n=7) and 16 (n=7) weeks. Prior to testing, each tendon sample was fixed to a servohydraulic test machine (MTS Systems, Eden Prairie, MN) with clamps. After fixation, the gauge length was be recorded. Depth and width measurements were taken at mid gauge length to estimate the cross-sectional area (approximated as an ellipse). The 7–16-week-old samples went through the following preload and testing sequence: 1.) Cycled between 5N and 15N of tension for 10 repetitions at a rate of 0.3mm/s (preconditioning); 2.) 30 second position dwell at end of precondition displacement; 3.) Ramped to 40N at 0.3mm/s; 4.) Held initial 40N position for 60 seconds (stress relaxation); (5) Unloaded to 0N; (6) Dwelled for 30 seconds; 7.) Loaded to failure at 0.3 mm/s. Tendons from birds under 7 weeks followed a similar testing sequence as described above with loads and rates normalized to their cross-sectional areas.

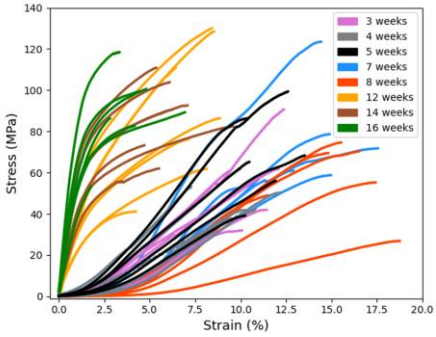

Figure 2: Stress-strain curves for the failure test of each tendon. Curves are color coded by age.

Results & Discussion: The stress relaxation data and load to failure data were analyzed for each specimen. Percent stress relaxation was calculated as the percentage of total stress remaining at the end of 60 seconds. Stiffness and Young's modulus values were calculated using the linear elastic region of the load to failure curve. Box plots illustrating the spread of data in each age group are shown in Figure 1. One-way ANOVA tests for stress relaxation, Young's modulus, and stiffness showed that tendon age had a significant effect. The results of post-hoc Tukey HSD test is also shown in Figure 1 (alpha =0.05). There were distinct differences between the percent stress relaxation values of the 3 through 8-week-old tendons and the older tendons. The older tendons had greater average percent stress relaxation values than the 3 through 8-week-old tendons and there was minimal interquartile overlap. The stress-relaxation component of our procedure allowed us to investigate the extent to which the mechanical response of the tendon was affected the viscoelasticity of the tendon. This time dependent nature appeared to decrease with the age of the tendons. The older tendons had strikingly greater Young's modulus values when compared to under 8-week-old tendons. Furthermore, the 14 and 16-week-old tendons had greater modulus values than the 12-week-old tendons. The stiffness values of the older tendons were also greater than the younger tendons. The stiffness values for each sequential age group were more dependably increasing than the Young's modulus values. A stress-strain curve for each tendon's load to failure region is shown on single plot in Figure 2. The stress-strain curves of the load to failure tests revealed a loss of the toe region after week 8. The loss of the toe region may indicate a changing role in the uncrimping of collagen fibers on the response but needs to be explored further. The slopes of the linear elastic regions for these tendons are greater than the younger tendons and the average slope appears to get progressively steeper from ages 12 to 16. Yielding also appeared to occur at higher stresses for the 14 and 16-week-old tendons.

Significance: By studying normal physiological calcification effects in turkeys, we may gain valuable insights into the overall physiological mechanisms involved. Further research in this area could provide significant contributions to our understanding of calcification processes across species.

Acknowledgments: This work was supported by the Mayo Clinic Biomechanics Core.

References: [1] Sansone et al. (2018), *Orthop Res Rev.* 10:63-72; [2] Paik. (2014), *Semin Arthritis Rheum.* 43(6); [3] Kadar et al. (2017), *J Surg Res.* 216:46-55.

THE THREE-DIMENSIONAL MORPHOLOGY OF MID-PORTION ACHILLES TENDINOPATHY EXHIBITS SLOW RECOVERY FOLLOWING ECCENTRIC EXERCISE, IN CONTRAST TO A HEALTHY TENDON

Leila. Nuri
Oakland University, School of Health Sciences, Department of Physical Therapy, Rochester, MI, US
Email: leilanuri@oakland.edu

Introduction: Mid-portion Achilles tendinopathy (MAT) adversely affects the structure, composition, and normal three-dimensional (3D) morphology of the Achilles tendon (AT) at rest and under load [1]. Eccentric heel drop exercise has become the treatment of choice for MAT. However, the acute response of MAT 3D morphology compared to a healthy tendon and the recovery process following eccentric exercise have not been thoroughly investigated. Previous studies have only focused on one tendon morphological parameter immediately after eccentric exercise and found conflicting results. Only one study has investigated the recovery process of MAT morphological properties (i.e., thickness) at two time-points: immediately and 24 hours after the exercise, and full recovery was observed after 24 hours for both healthy and MAT tendons [2]. Understanding how MAT 3D morphology changes after eccentric exercise and closely monitoring the recovery process for the first few hours after eccentric exercises could increase our knowledge about tendinopathic tendon physiology, mechanics, and clinical implications for recommending exercise frequency to patients with MAT. The aim of this study, therefore, was to evaluate MAT 3D morphology (i.e., volume, length, and CSA) and compare it to the healthy tendon response immediately and up to 3 hours following eccentric exercise. Due to a lack of information in the literature, we hypothesized that there would not be any significant difference between the healthy and tendinopathic tendon 3D morphology during recovery.

Methods: Ten male adults with unilateral Achilles tendinopathy and ten age-matched healthy male adults participated in the research. The ATs were scanned using freehand 3D ultrasound at rest prior to and immediately following the eccentric exercise protocol (6 sets of 15 repetitions of heel drops with a 1-minute rest between sets), and then at 30 minutes, 60 minutes, 90 minutes, 2 hours, 2.30 hours, and 3 hours post-exercise. A two-way (2 × 8), repeated-measures general linear model was used to examine the main effects and interactions of tendon type (tendinopathy and healthy) and time point (pre-eccentric exercise, 0 min, 30 min, 60 min, 90 min, 2 h, 2.30 h, 3 h) on tendon volume, CSA, and length. Planned contrasts were used to compare tendon normalized values for volume, length, and CSA between the tendons during recovery and at each post-eccentric exercise testing time relative to the values measured during pre-exercise and 0 min post-exercise testing times for each tendon.

Results & Discussion: Both MAT and healthy tendons underwent similar changes in volume, CSA, and length following eccentric exercise (at 0 minutes). During the recovery process, healthy tendons exhibited gradual recovery in volume, CSA, and length up to three hours. However, MAT showed recovery up to 90 minutes, after which the recovery plateaued. From 90 minutes onwards, there was a significant difference in the recovery percentages of healthy and MAT tendons, with MAT showing slower recovery compared to healthy tendons (Fig. 1). Overall, the normal slow recovery process of tendons is impaired 90 minutes after eccentric training in MAT, which may indicate that the MAT has less permeability under a lower gradient of fluid between the periphery and the tendon core, possibly due to impairment in the material properties of the MAT membrane or the reduced sensitivity of the tendon membrane pores to fluid influx into the tendon core. This may provide a basis for explaining why giving sufficient recovery time between eccentric exercise sets for patients with MAT is useful for alleviating their clinical symptoms. However, this study has limitations. Tendon recovery was measured only up to 3 hours, and neither type of tendon fully recovered within that timeframe. Further studies are required to investigate the recovery process of healthy and MAT tendons for longer periods during recovery.

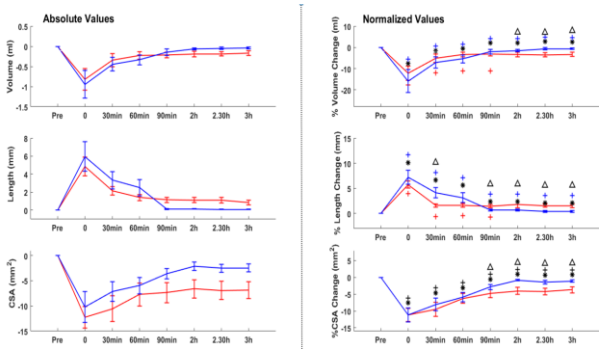

Fig. 1: Changes in 3D morphology of tendinopathic (red line) and healthy (blue line) tendons following eccentric exercise.

Significance: This study provided insight into the MAT physiology during the recovery process after an important clinical intervention for patients with Achilles tendinopathy (i.e., eccentric exercise). MAT recovers slowly and requires more time than a healthy tendon to recover. In clinical settings, when physical therapists prescribe eccentric exercises to patients with MAT, they should ensure that the timeframe between repetitions allows enough time for the tendon to fully recover.

Acknowledgments: We would like to thank all the participants who voluntarily participated in this study.

References: [1] Nuri et al. (2018), *Exp Physiol* 103:358–369; [2] Girgg et al. (2012), *MSSE* 44:12-17.

Gait symmetry in individuals with insertional Achilles tendinopathy

Hayley Powell Smitheman[1*], Richard Zell[2], Jeffery Brodie[2], Stephanie Cone[3], Karin Grävare Silbernagel[1]
[1]Biomechanics and Movement Science, University of Delaware, Newark, DE
*Corresponding author's email: hpowell@udel.edu

Introduction: Insertional Achilles tendinopathy is a painful injury resulting in reduced function and quality of life. Pain is caused in part from compression of the Achilles tendon on the proximal calcaneus in positions of dorsiflexion, resulting in impaired ability to walk and participate in activities of daily living. Gold standard exercise treatment is not effective in all individuals with insertional Achilles tendinopathy, perhaps secondary to altered gait mechanisms resulting in increased compression and pain. However, it is unknown if gait asymmetries, such as increased dorsiflexion and reduced ankle eccentric power, exist in this population, and further, if they relate to structural alterations including tendon thickening or symptom severity. Therefore, the primary purpose of this study was to assess differences in gait mechanics between limbs in individuals with insertional Achilles tendinopathy. We also aimed to assess the relationship between gait mechanics and symptoms and structure in this population. We hypothesized individuals with insertional Achilles tendinopathy would demonstrate gait asymmetries and gait biomechanics would relate to structure and symptom severity.

Methods: Eighteen individuals with a clinical diagnosis of insertional Achilles tendinopathy[1] (12 F, 52±13 years, 1.7±0.1 m, 93.7±20.1 kg) were included in this study. Ankle biomechanics were sampled from 3D trajectories of 39 reflective markers recorded with eight high-speed optical cameras (Vicon, Oxford, UK, 100Hz) during self-selected speed gait trials over a single floor-embedded force plate (Bertec, Columbus OH, 1000Hz). A kinematic model with lower extremity segments created from a static recording. Data were processed using Visual 3D (C-Motion, Rockville, MD). Peak dorsiflexion angle and eccentric ankle power normalized to subject mass and height were calculated. B-mode ultrasound imaging was performed with the subjects in prone to quantify tendon thickening at the insertion as the difference between the thickness of the tendon at the most prominent aspect of the proximal calcaneus and the thickness of the tendon at the soleus musculotendinous junction. Symptom severity was assessed with the Victorian Institute of Sport Assessment-Achilles (VISA-A) with lower scores indicating worse symptoms.[2] Paired t-tests were performed to assess for differences between the involved and uninvolved limb and Pearson's correlations were performed to assess for relationships between gait variables and structure and symptoms.

Results & Discussion: There were no observed differences in peak dorsiflexion angle, ankle eccentric power, or Achilles tendon thickening (p's>0.05) between limbs (Table 1) despite the most symptomatic limb having significantly worse symptoms (VISA-A $p<0.001$) compared to the least symptomatic limb. However, 50% of subjects reported bilateral symptoms with the VISA-A score indicating symptoms on the least symptomatic limb. When assessing the relationship between ankle biomechanics and structure and symptoms, peak dorsiflexion angle was moderately negatively correlated with VISA-A ($r=-0.635$, $p=0.005$) (Figure 1) but not correlated with tendon thickening ($r=0.368$, $p=0.133$). Eccentric ankle power was not correlated with VISA-A ($r=0.357$, $p=0.145$) but moderately negatively correlated with tendon thickening ($r=-0.620$, $p=0.006$). These findings suggest that increased dorsiflexion during gait was associated with worse symptom severity while increased eccentric power was associated with increased tendon thickening.

Significance: Increased dorsiflexion, a position of increased compression and pain, was associated with worse symptom severity while increased eccentric ankle power was associated with increased tendon thickening, a pathological structural finding. These findings suggest that individuals with insertional Achilles tendinopathy do not alter gait on the most symptomatic side but gait mechanics are related to symptoms and structure. Combining the propensity for development of bilateral symptoms in individuals with Achilles tendinopathy with the findings of this study suggest that gait biomechanics bilaterally may be driving structural and symptomatic changes. Further analyses are needed to confirm directionality of these relationships.

Acknowledgments: Research reported in this abstract was supported by the NIH awards R01AR078898 and R21AR077282, the Foundation for Physical Therapy Research, and the Rheumatology Research Foundation.

References: [1] Maffulli et al. (2003), *Clin J Sport Med* 13(11-15); [2] Robinson et al. (2001), *Br J Sports Med* 35(335-341).

Table 1. Difference between Most and Least Symptomatic Limbs

	Most Symptomatic	Least Symptomatic	p-value
Peak Dorsiflexion Angle (°)	14.1±6.1	13.3±3.5	0.400
Ankle Eccentric Power (W/kg·m)	-10.9±3.0	-10.2±2.3	0.183
Achilles Tendon Thickening (mm)	1.4±1.9	1.1±1.8	0.421
VISA-A	40.3±19.9	70.7±22.5	<0.001

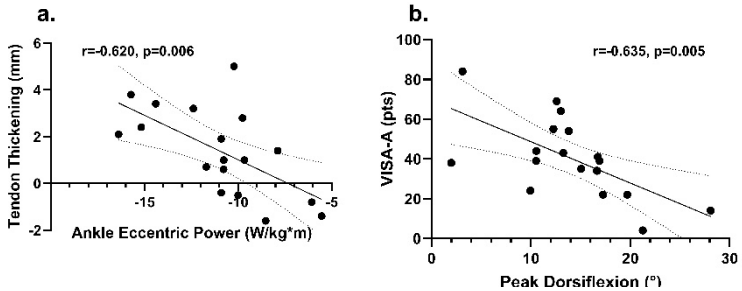

Figure 2. Correlations between eccentric ankle power and tendon thickening (a) and peak dorsiflexion angle and VISA-A (b).

Impact of forefoot biasing footwear on peak Achilles tendon force and ankle range of motion during rehabilitative exercises

Sara M. Magdziarz, Molly S. Pacha, Ruth L. Chimenti, David M. Williams, Jason M. Wilken*,
Department of Physical Therapy and Rehabilitation Science, The University of Iowa, Iowa City, IA
*Corresponding author's email: jason-wilken@uiowa.edu

Introduction: Achilles Tendinopathy (AT) is a common painful condition limiting daily mobility and athletic performance. AT is primarily treated conservatively through physical rehabilitation, where it is thought that incrementally loading the Achilles tendon promotes tendon healing and avoids further injury.[1,2] Exercise programs for AT often incorporate a variety of exercises selected to progressively load the Achilles tendon in a lengthened position with the ankle dorsiflexed, which may maximize tendon remodelling.[3-5] Footwear that biases loading to the forefoot (e.g., Figure 1) has been used in plyometric training with the goal of increasing maximum vertical jump[6] and may facilitate both increased ankle range of motion and tendon loading during AT rehabilitation activities. The purpose of this research, therefore, is to determine the effects of forefoot biasing footwear on peak Achilles tendon load and ankle kinematics during rehabilitation exercises commonly used in the treatment of AT.

Methods: Twenty healthy individuals (11 male/9 female, 25.1(9.2)yrs, 1.74(0.11)m, 71.4(15.5)kg) without a history of lower extremity injury, and an average Activities-Specific Balance Confidence Scale (ABC) score > 7, participated. Participants completed testing in two different conditions: with athletic shoes (NoJS) and with athletic shoes and forefoot biasing platforms attached to the distal end of the shoes (JS, Figure 1), in a randomized order. Participants completed overground walking at a self-selected walking velocity (SSWV) and the following activities bilaterally and unilaterally using only the right leg: heel-raises at 60Hz (2HR/1HR), heel-raises at 110Hz (2POGO/1POGO), and vertical hops (2HOP/1HOP). All activities were demonstrated for the participant prior to data collection. Activities were chosen to represent a range of tendon loading.[3] Sagittal plane ankle angle, ankle moment, and ankle power were calculated for the right leg. Peak data were identified for all activity repetitions and averaged for each participant. The peak Achilles tendon force was calculated by dividing participant peak sagittal plane ankle moment by the Achilles tendon moment arm of 5 cm.[3] Freidman tests were performed to test the main effects of the condition (NoJS, JS) for each activity. If the main effect was significant, Wilcoxon signed rank tests were performed (α=0.05 for all statistical comparisons).

Figure 1: Forefoot biasing footwear worn in addition to athletic shoes to augment Achilles tendon loading.

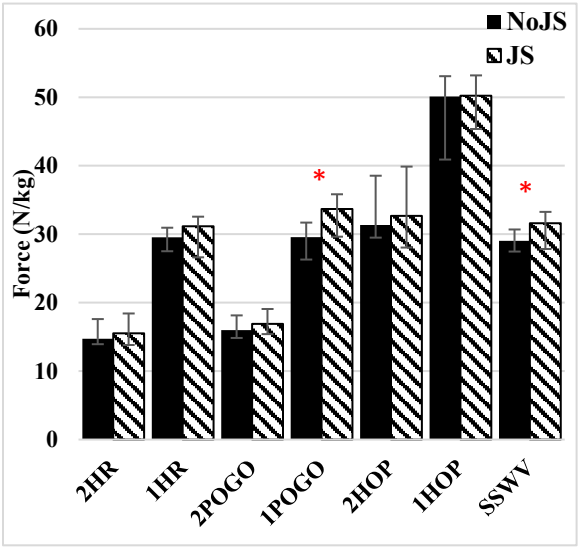

Figure 2: Median peak Achilles tendon force normalized to BW. * = significant ($p<0.05$)

Results & Discussion: Differences in median ankle angle range of motion were < 6.1 degrees for all activities with significant differences only in 2HOP and SSWV (2.0% and 22.1% difference, respectively). Forefoot biasing footwear showed significant differences in peak plantarflexion and dorsiflexion for most activities with increased dorsiflexion (>16% difference) and reduced plantarflexion (>26.5% difference) in all statistically significant differences. Forefoot biasing footwear had limited effect on peak Achilles tendon force and peak sagittal plane ankle power. Significant differences between conditions were only found for 1POGO and SSWV for peak Achilles tendon force (13.1% and 8.5% difference, respectively; Figure 2) and 2HOP and SSWV for peak sagittal plane ankle power (21.5% and 55.7% difference, respectively). Compared to overground walking, peak Achilles tendon force was < 8% different for 1HR, 1POGO, and 2HOP in both the NoJS and JS conditions.

Significance: The use of footwear intended to bias loading toward the forefoot had limited effect on peak Achilles force and sagittal plane ankle power for multiple activities used in the treatment of AT. However, despite most activities maintaining similar ankle angle range of motion between footwear conditions, forefoot biasing footwear shifted the range in which the activity was performed, reducing peak plantarflexion angle and increasing peak dorsiflexion angle for most activities. This forefoot biasing footwear may provide a means of increasing tendon strain throughout a variety of rehabilitation exercises, offering another strategy for loading progression. These data suggest that footwear alterations are unlikely to meaningfully alter peak forces but may alter ankle kinematics to positively promote tendon healing. Variables including loading rate and the cumulative loading of the tendon over the duration of the activity are under investigation.

Acknowledgements: We would like to acknowledge the contributions of, Maya Deuso, Bennett Goettsch, Max Kleinschmit, Jordan Klonne, and Emily Ramseyer for their efforts in support of data collection and Justin Alpers and Alexander Gaffney for their efforts in support of both data collection and processing.

References: [1] Sancho et al. 2023. Phys Ther Sport 60:26-33. [2] Head et al. 2019. Musculoskeletal Care 17(4):283-299. [3] Baxter et al. 2021. Med Sci Sports Exerc 53(1):124-130. [4] Alfredson et al. 1998. Am J Sports Med 26(3):360-6. [5] Devaprakash et al. 2022. J Appl Physiol 132:956-965. [6] Voisin et al. 2019. Int J Exerc Sci 12(6):491-504

Polyester suture-based artificial Achilles tendon: effect on muscle mass and length

Obinna P. Fidelis[1], Katrina L. Easton[1], Gabriela Bastos[2], Darryl Millis[2], David E. Anderson[2], Dustin L. Crouch[1]
University of Tennessee, Knoxville – [1]Tickle College of Engineering, [2]College of Veterinary Medicine
Corresponding author's email – ofidelis@vols.utk.edu

Introduction: Polyester (PET) suture-based artificial tendons [1] may be an effective alternative to tendon grafts for repairing critically sized tendon defects and would permit robust attachment of muscles to prostheses. Previous in vivo studies demonstrated the durability of the PET tendon interface with muscle and bone, but did not report the effect of the PET artificial tendon on muscle properties [1]. Our study objective was to investigate the effect of the PET artificial tendon on the mass and length of the involved and adjacent uninvolved muscles in New Zealand White (NZW) rabbits.

Methods: PET artificial tendons were fabricated from double-armed strands of USP size 0 polyester microfiber suture and coated with biocompatible silicone (LSR BIO M340, Elkem Silicones). All animal procedures were approved by our Institutional Animal Care and Use Committee. Two groups of NZW rabbits (mean age at surgery = 18.2 ± 1.9 weeks) underwent surgery on the left hindlimb. In one group, (EX, n=4), the Achilles tendon was excised; in a second group (ER, n=5), the Achilles tendon was excised and replaced with a PET artificial tendon. All rabbits underwent formal rehabilitation. At 8 weeks post-surgery, both hindlimbs were harvested, fixed in formalin for 5 days, then stored in ethanol. The involved muscles [lateral gastrocnemius (LG), medial gastrocnemius (MG), and soleus (Sol)] and select uninvolved muscles [tibialis cranialis (TC), extensor digitorum (ED) and superficial flexor digitorum (FD)] crossing the ankle were dissected from their origin to the myotendinous junction. For each muscle, mass and length were normalized by body mass and tibia length, respectively. These data were compared with a 3-way ANOVA with factors 'side' (operated vs non-operated), 'group', and 'muscle'; the Tukey HSD test was used for post-hoc pairwise comparison, with $p<0.05$ considered significant. We hypothesized that there would be a significant effect of treatment (group) on muscle mass and length.

Results & Discussion: ***Muscle Mass:*** In the EX group, muscle mass was significantly less for the involved muscles (LG, MG, Sol) in the operated limb than in the non-operated limb (Figure 1, left). In the ER group, even with the PET artificial tendon, muscle mass of LG, MG, and Sol were 16.7 ± 21.0% (p=0.503), 39.2 ± 9.1% (p<0.001), and 53.9 ± 15.7% (p=0.333) less, respectively, in the operated limb than in the non-non-operated limb. Mass of FD was greater (p=0.006) in the operated limb for the EX group, possibly because of increased biomechanical output (e.g., forces) to compensate for decreased output of LG, MG and Sol, as these muscles are all considered ankle plantar flexors [2]. ***Muscle Length:*** In the operated limb, muscle length was significantly less for MG and Sol in the EX group but only for MG in the ER group, compared to the non-operated limb (Figure 1, right). We expect that the involved muscles were shorter in the operated limb due to passive forces and unopposed muscle contraction; that involved muscles were retracted in the ER group suggests that the artificial tendons may have been longer than the biological tendons they replaced. There was no significant effect of group for either mass (p=0.267, F = 1.245) or length (p=0.941, F = 0.006), although there was a consistent trend of fewer bilateral differences in the involved muscles of the ER group (Figure 1). The post-surgery study duration (8 weeks) was relatively short; future studies are needed to determine long-term effects of tendon replacement. The muscle data are part of a larger dataset that includes longitudinal in vivo hindlimb kinematics and ground contact pressure during hopping gait, and muscle cross-sectional area (ultrasound); thus, ongoing analysis will reveal if the artificial tendon provided functional benefits over tendon excision only.

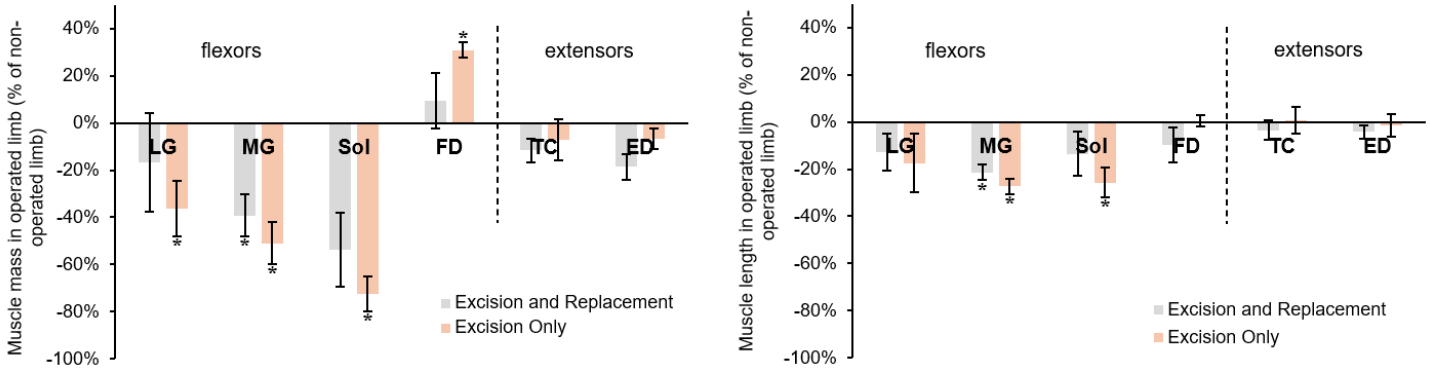

Figure 1. Mass (left) and length (right) of muscles in the operated limb as a percentage of values in the non-operated limb. *Differences between sides were significant (p<0.05). LG = lateral gastrocnemius; MG = medial gastrocnemius; Sol= soleus; FD = superficial flexor digitorum; TC = tibialis cranialis and ED = extensor digitorum.

Significance: Degeneration of muscle mass and length are expected to diminish muscle force-generating behavior, which could impair patient motor function. To establish artificial tendons as a viable treatment option, future studies are needed to identify artificial tendon designs, surgical techniques, and rehabilitation protocols that may better preserve or restore muscle properties.

Acknowledgement: Research was funded by the NIH (R61AR078096). Thanks to the UTK Office of Lab Animal Care, Jalen Barker, Elizabeth Croy, Lori Terrones, and Anne Wandishin for assisting with animal care and data collection.
References: [1] Melvin et al., (2011), *Ortho Res.* 29 (11). [2] Lieber and Blevins, (2003), *J Morphol*. 199.

VERTICAL GROUND REACTION FORCE LOADING RATES INFLUENCE TIBIOFEMORAL CARTILAGE T1ρ RELAXATION TIMES 1 MONTH POST-ACL RECONSTRUCTION

Justin D. Dennis[1*], Alex E. Nilius[1], Thomas Birchmeier[1], J. Troy Blackburn[1]
[1]University of North Carolina at Chapel Hill
*Corresponding author's email: jddennis@unc.edu

Introduction: Post-traumatic knee osteoarthritis (PTOA) is highly prevalent and develops rapidly after anterior cruciate ligament reconstruction (ACLR),[1] thus identifying early contributors to cartilage degeneration is imperative for mitigating PTOA risk. Lesser vertical ground reaction force (vGRF) magnitude and loading rate 6 months post-ACLR are associated with lesser tibiofemoral cartilage proteoglycan density (i.e., longer T1ρ relaxation times).[2] However, it is unclear how limb loading influences cartilage composition 1 month post-ACLR, which may identify early intervention targets. The purpose of this study was to determine the associations between tibiofemoral T1ρ relaxation times and vGRF magnitude, instantaneous loading rate, and linear loading rate in the ACLR limb 1 month post-ACLR. As lesser vGRF is associated with longer T1ρ relaxation times 6 months post-ACLR,[2] we hypothesized lesser vGRF magnitude and loading rates would be associated with longer T1ρ relaxation times 1 month post-ACLR.

Methods: Thirteen individuals with primary unilateral ACLR (46% female; age: 23±6 years; height: 1.74±0.09 m; mass: 71.5±13.75 kg; patellar tendon autograft: 10; quadriceps tendon autograft: 3) underwent magnetic resonance imagining with a Siemens Magnetom 3T scanner and 4-channel Siemens knee coil 1 month post-ACLR. Voxel by voxel T1ρ relaxation times were calculated using a five-image sequence in MATLAB (Mathworks) and images were manually segmented in ITK-SNAP software. Cartilage was divided into lateral and medial regions based on the peak of the tibial intercondylar eminence and was further subdivided into posterior, middle, and anterior weight-bearing regions based on the anterior and posterior horns of the meniscus (Figure 1). Participants also completed five barefoot walking trials at their preferred speed with a 10-camera motion capture system synchronized with 3 floor embedded force platforms. Peak vGRF was calculated from heel strike (i.e., vGRF>20N) to 50% of stance, vGRF instantaneous loading rate was calculated as the peak of the 1st time derivative of the vGRF waveform from heel strike to peak vGRF, and vGRF linear loading rate was calculated as the slope from heel strike to peak vGRF. Peak vGRF and vGRF loading rates were normalized to body weight in Newtons (×BW and ×BW•s^{-1}, respectively). Partial Pearson correlations while controlling for preferred gait speed were performed to determine the associations between T1ρ relaxation times and vGRF magnitude and loading rates in the ACLR limb ($\alpha = 0.05$).

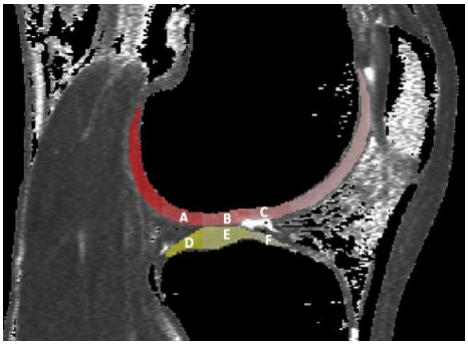

Figure 1: Segmented T1ρ relaxation time map of the lateral weight-bearing regions of the posterior femur (A), middle femur (B), anterior femur (C), posterior tibia (D), middle tibia (E), and anterior tibia (F).

Results: Preferred gait speed and peak vGRF were not associated with femoral or tibial T1ρ relaxation times (p>0.05). However, lesser vGRF instantaneous loading rate was associated with longer lateral femur anterior T1ρ relaxation times (ρ=-0.605, p=0.037) (Figure 2A). Lesser vGRF linear loading rate was associated with shorter lateral tibia posterior (ρ=0.628, p=0.038) and anterior (ρ=0.654, p=0.021) T1ρ relaxation times as well as shorter medial femur middle (ρ=0.588, p=0.044) and anterior (ρ=0.633, p=0.027) (Figure 2B) T1ρ relaxation times.

Discussion: Lesser vGRF instantaneous and linear loading rates influence femoral and tibial cartilage proteoglycan density differently in the ACLR limb. Supporting our hypothesis, lesser vGRF instantaneous loading rates were associated with worse ACLR limb femoral cartilage health. However, contrary to our hypothesis, lesser vGRF linear loading rates were associated with better ACLR limb femoral and tibial cartilage health.

Significance: The magnitude of vGRF was not associated with femoral or tibial cartilage health, thus future interventions should target the rate at which the limb is loaded during gait to augment cartilage health 1 month post-ACLR. Specifically, greater loading immediately after heel strike (i.e., instantaneous loading rate) may serve to improve cartilage health while rapid limb loading during the first half of stance (i.e., linear loading rate) may contribute to cartilage degeneration. Longitudinal analyses are necessary to elucidate the influence of loading rates on cartilage health over time.

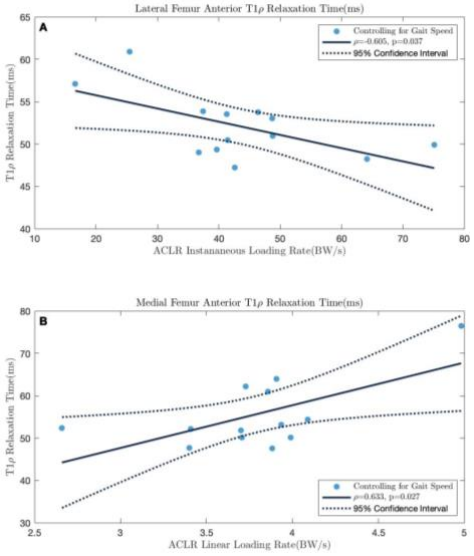

Figure 2: ACLR limb associations between lateral femur anterior T1ρ relaxation times and instantaneous loading rate (A) and medial femur anterior T1ρ relaxation times and linear loading rate (B).

Acknowledgments: This study was supported by the Department of Defence Award Number W81XWH21C00490011582719.

References: [1] Ajuied et al. (2014), *Am J Sports Med* 42(9). [2] Pfeiffer et al. (2019), *Med Sci Sports Exerc.* 51(4).

The relationship of patellar tendon and vastus lateralis shear-wave velocity with knee mechanics and quadriceps strength following ACL reconstruction

Tereza Janatova[1]*, Brian Noehren[1], and McKenzie White[1]
[1]Department of Physical Therapy, University of Kentucky, Lexington, KY
*Corresponding author's email: t.janatova@uky.edu

Introduction: Previous work has shown quadriceps weakness is associated with a reduced knee extensor moment (KEM) and lesser knee flexion excursion (KFE) during the stance phase of gait following anterior cruciate ligament reconstruction (ACLR) [1, 2]. However, quadriceps weakness alone does not fully describe the extent of quadriceps dysfunction in this population. Changes in tissue composition, such as extracellular matrix expansion resulting from increased collagen deposition, have been observed after an ACLR [3]. Excessive collagen within muscle alters muscle stiffness [4], which plays a crucial role in force production and may affect subsequent joint loading. Importantly, the force generated by the quadriceps muscles is transmitted through the patellar tendon, which serves as a common graft donor site for ACLR. Early evidence utilizing ultrasound elastography, a non-invasive modality that provides an indirect assessment of passive stiffness via shear-wave velocity (SWV), suggests the vastus medialis and the patellar tendon undergo substantial changes in post-operative rehabilitation, as evidenced by changes in cross sectional area and shear modulus via SWV [5, 6]. However, stiffness of the vastus lateralis has not yet been assessed following ACLR. Additionally, considering that both muscle and tendon stiffness are important for force production and transmission, it is plausible that differences in stiffness underlie the common strength deficits and alterations in gait biomechanics seen post-ACLR. Therefore, the aims of this study were to I) determine if there were between-limb differences in muscle and tendon stiffness following ACLR and II) assess their association with quadriceps strength and common gait metrics known to be affected in individuals engaged in early ACLR rehabilitation.

Methods: Sixteen individuals (7 females, age: 20.1±5.7 years, body mass index: 26.3±5.2 kg/m^2), evaluated 3.9±0.7 months after a primary ACLR via patellar tendon (n=14) or quadriceps autograft (n=2), participated in a single session consisting of ultrasound elastography, walking biomechanics, and quadriceps strength testing. Stiffness measurements were conducted using a GE Logic Fortis^{TM} ultrasound unit with a 50 mm linear-array transducer placed over the mid-belly of vastus lateralis and the central portion of the patellar tendon. Standardized settings (Frequency = 15 MHz, Gain = 56, Depth = 4 cm) and patient positioning (90 degrees of knee flexion) were employed. Data analysis was performed using a custom-built MATLAB Application (MathWorks Inc.). SWV was computed in a region of interest across the three most consistent consecutive images identified through normalized cross-correlation. Sagittal plane knee joint kinematic (200 Hz) and kinetic (2000 Hz) data at self-selected walking speed were collected using a 13-camera motion capture system (Motion Analysis Corp.) and 2 force plates (Bertec Corp.). Data were filtered using a 4th order Butterworth low-pass filter with a cutoff frequency of 8 Hz for kinematic data and 35 Hz for kinetic data. Peak KEM and KFE were calculated from the first 75% of stance. Quadriceps peak torque (QPT) was determined from four maximal voluntary isometric contractions performed at 90 degrees of knee flexion using an isokinetic dynamometer (Biodex System 4 Pro). Peak KEM was normalized to height and body weight, while QPT was normalized to body weight. Between-limb differences for all variables were compared via paired t-tests. Linear regressions explored the associations between vastus lateralis and patellar tendon SWV and peak KEM, KFE, and QPT.

Results & Discussion: Vastus lateralis SWV of the ACLR limb was on average 8.7% (or 0.28 m/s) slower than the uninjured limb (p=0.045), indicating less stiff tissue (Figure 1). No differences in patellar tendon SWV were observed (p=0.695; Figure 1). Vastus lateralis SWV was not associated with QPT, peak KEM, or KFE (p=0.093-0.911). Patellar tendon SWV was positively associated with QPT (R^2=0.295, p=0.030; Figure 2). These findings suggest there are early changes in stiffness properties of the vastus lateralis 4 months following ACLR, which can occur with alterations in muscle composition such as fibrosis and may not be immediately reflected in gait or QPT. Although patellar tendon SWV did not differ between limbs, results show that stiffer tendons are able to produce greater QPT emphasizing their importance in force transmission.

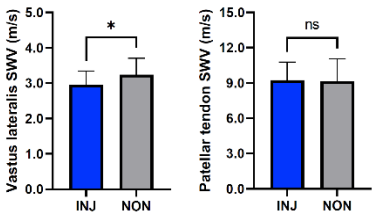

Figure 1. Between-limb differences in shear-wave velocity (SWS).

Significance: These results add to the body of literature revealing changes in muscle tissue quality post-ACLR and substantiate elastography as a modality that can be used to understand muscle and tissue remodeling post-ACLR. Future work would benefit from longitudinal studies with increased sample sizes exploring muscle and tendon stiffness throughout ACLR recovery as it may provide avenues for targeted interventions.

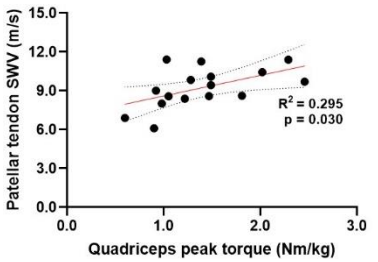

Figure 2. Association between patellar tendon shear-wave velocity (SWS) and quadriceps peak torque.

Acknowledgments: This study was supported by the National Institutes of Arthritis and Musculoskeletal and Skin Disease through grants R01AR072061 and R01AR07831602.

References: [1] Davis-Wilson et al. (2019), *Med Sci Sports Ex*; [2] Lin and Sigward (2018), *Gait & Posture*; [3] Noehren et al. (2021), *J Physiol*; [4] Konno et al. (2022), *Frontiers in Physiology*; [5] Gulledge et al. (2019), *Knee*; [6] Ito et al. (2023), *J Ortho Res*

TIBIOFEMORAL JOINT CHANGES SEEN ON FLEXED VS. EXTENDED WEIGHT BEARING CT AFTER ACL RECONSTRUCTION: ALTERED SCREW HOME MECHANISM?

Tyce C. Marquez*, Shelby Hulsebus, Shannon Ortiz, Brian R. Wolf, Donald D. Anderson
University of Iowa, Iowa City, IA
tyce-marquez@uiowa.edu

Introduction: Changes in the load-bearing pose of the knee following anterior cruciate ligament reconstruction (ACLR) have been linked to early compositional MRI changes in cartilage consistent with post-traumatic osteoarthritis (PTOA) [1]. Weight bearing CT (WBCT) enables evaluation of 3D joint space width (JSW) in the knee, and it shows promise for detecting OA earlier than plain radiography [2]. WBCT also offers loaded knee pose information comparable or superior to MRI that could be collected more affordably/easily across a network of clinical sites. 3D JSW distributions provide insight into both location/magnitude of any joint space narrowing and indicators of altered joint positioning as might be expected from graft misplacement or over-tensioning. These capabilities provide a means for quantifying joint alignment and how it changes with flexion, a direct indicator of knee joint laxity. Specifically, the screw-home mechanism (SHM) may cause 3D JSW distributions in the tibiofemoral joint to be different in flexed vs. extended poses. The aim of this study was to investigate differences in tibiofemoral joint mechanics in flexed vs. extended WBCT scans.

Methods: Thirty-one individuals (15M/16F, age: 24.0±10.4 years) with a unilateral isolated partial or complete ACL tear reconstructed by one of four surgeons were recruited to participate in this IRB-approved study. Bilateral WBCT scans of the knee in ~20°flexed [4] and fully extended positions were acquired 3.6±0.9 months after ACLR. Maps of the 3D JSW were generated for both intact contralateral and ACLR knees using fully automated measurement methods [3]. The center of contact (CoC) for each compartment was defined as the centroid of the narrowest 10% of JSW values. The location of the CoC was measured in the anterior-posterior (AP) direction relative to the overall compartment centroid. Each compartment was also separated into five distinct regions following methods previously published to regionally separate tibia surface articular cartilage [4] to compare average JSW between the flexed and extended scan pose.

Results & Discussion: The anterior translations of the CoC observed were consistent with the external rotation of the tibia and ACL tensioning that define the SHM. The tibia rotates externally approximately 15° during terminal extension, causing anterior tibial glide on the medial compartment due to its oblong articular surface [5]. The ACLR knee in the lateral compartments demonstrated larger anterior CoC translations moving from flexion to extension compared to the intact contralateral knee for both male and female groups (Table 1). On the medial side, only females demonstrated substantial differences in CoC translation, which may be due to graft placement and tensioning following ACLR. The regional JSW maps showed similar trends with the anterior, central, and posterior regions showing the biggest changes between scan poses (Fig. 1). The ACLR knees for both male and female groups demonstrated smaller anterior changes and more posterior changes compared to the intact knees, which may be related to the position and peripheral curvature of the apposed articular surfaces relative to one another. The female group demonstrated slightly larger differences compared to males in the anterior region for their respective ACLR and intact contralateral knees.

Table 1: Anterior CoC translation (mm) between scan poses (n = # knees).

Female	Medial	ACLR (n = 14)	7.63 ± 2.81
		Intact (n = 15)	5.37 ± 3.69
	Lateral	ACLR (n = 14)	4.98 ± 1.88
		Intact (n = 15)	3.74 ± 2.43
Male	Medial	ACLR (n = 13)	6.00 ± 3.56
		Intact (n = 13)	5.95 ± 3.68
	Lateral	ACLR (n = 13)	4.21 ± 3.14
		Intact (n = 13)	3.19 ± 2.82

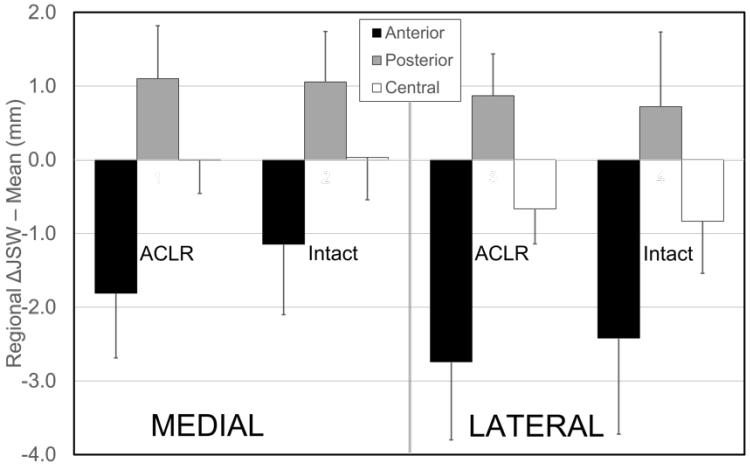

Figure 1: Regional changes in average JSW moving from flexed to extended knee pose.

Significance: Knee joint kinematics play a role in imaging markers assessed in monitoring PTOA risk and degenerative joint changes. WBCT provides 3D JSW and pose data in functional poses to assess variations and provide a more complete picture of PTOA risk. Additional WBCT scans are being obtained at 1-year post-ACLR visits, when the influence of any biomechanical changes associated with the surgery are more likely to be observed.

Acknowledgments: This research as supported by a grant from the Arthritis Foundation (Award #851789).

References: [1] Lansdown DA, et al. J Orthop Res. (2020), 38(6):1289-95. [2] Segal NA, et al. Osteoarthritis Cartilage. (2023), 31(3):406-13. [3] McFadden EJ, et al. Osteoarthritis Cartilage. (2022), 30(S1):S284-5. [4] Wirth W & Eckstein F. IEEE Transactions on Med. Imaging. (2008), 27(6):737-744. [5] Kim HY, et al. Clin Orthop Surg. (2015), 7(3):303-9.

MRI ANALYSIS OF BIOMECHANICAL RESPONSE AND T1ρ ALTERATION DUE TO EXTERNAL LOADING IN THE CARTILAGE OF ACL RECONSTRUCTED KNEE: A LONGITUDINAL CASE STUDY

Hongtian Zhu[1], Emily Y. Miller[2], Woowon Lee[1], Timothy W. Lowe[1], Corey P. Neu[1,2*]
[1]Paul M. Rady Department of Mechanical Engineering, University of Colorado Boulder, Boulder, CO, USA
[2]Biomedical Engineering Program, University of Colorado Boulder, Boulder, CO, USA
*Corresponding author's email: cpneu@colorado.edu

Introduction: The anterior cruciate ligament (ACL) is one of the most frequently injured structures in human knees. Even though ACL reconstruction (ACLR) is commonly used to repair torn ACL, on average 50% would go on to develop post-traumatic osteoarthritis (PTOA). With the point-of-onset joint injury known, ACLR provides a unique opportunity to characterize the development of PTOA. OA is characterized by biochemical and mechanical property changes to articular cartilage. MRI methods have sought to identify tissue changes in pre-OA, an early stage prior to radiographic detection or patient pain, when emerging disease-modifying interventions may be most effective. In this case study, we investigated alterations of the tibiofemoral cartilage throughout the injury and recovery processes after ACL reconstruction (ACLR) in one participant. We acquired T1ρ relaxometry maps before and after cyclic loading, as well as the intratissue displacement and strain of knee cartilage [1] at four different imaging sessions to track the alterations through time.

Methods: The scanning was done at healthy, after ACL tear injury but before ACLR, 4 months and 6 months after ACLR timepoints, using a clinical 3T MRI system (SIEMENS Prisma^{fit} 3T, with QED 15-channel knee coil). For each scanning session, we first collected the proton density-weighted double echo steady state (DESS) images to establish a common imaging plane, and then T1ρ-weighted images at the selected slice were acquired. After that, we captured a set of time-frame images using spiral Displacement ENcoding with Stimulated Echo (DENSE) sequence, to obtain full-field displacement and strain maps. During DENSE sequence, a 0.5Hz cyclic loading (1s loading, 1s unloading, equivalent to 0.5× body weight compressive load at the medial condyle [2]) was applied to the patient's ankle in the varus direction via a customized loading device (**Fig. 1A**) [3]. After DENSE, another set of T1ρ-weighted images was taken with the same parameters as the previous scan. The T1ρ map was calculated by fitting a monoexponential decay curve on each voxel of the weighted images at each spin-lock time. Then, the T1ρ data was averaged within each region of interest (ROI), based on the thickness of the cartilage (**Fig. 1B**). For the DENSE data, the medial tibial and femoral cartilage area was collectively selected as one ROI, where the displacement and 2D Green-Lagrange strain maps were calculated on a pixel-by-pixel basis.

Results & Discussion: Here, we found that the averaged T1ρ value (**Fig. 1C**) was lower at the ACL tear timepoint and increased to above healthy level at 6-month timepoint, indicating the knee homeostasis had been disrupted and excessive fluid could be observed due to the injury [4,5], and ACLR would be helpful to regain homeostasis within the knee. Zonal analysis showed a similar trend, and the value would indicate that the superficial zone would receive the most influence from the injury. When comparing the T1ρ values before and after load, we first found that the load would induce excessive fluid content on the medial side of the cartilage (**Fig. 1D**). The value difference showed that the cartilage would react differently to the loading throughout the recovery process, which could imply that ACLR could partially restore the functionality of the knee, but the dynamics of the knee had altered progressively and permanently. The averaged displacement fluctuated during recovery, and eventually resumed to a healthy level. However, for averaged strain, even though *Exx* and *Eyy* resumed to a level similar to the healthy timepoint, the elevated *Exy* could imply that the early stage of cartilage degeneration had already occurred even with ACLR [2,6].

Significance: We believe this work is the first to track biochemical and biomechanical changes of knee cartilage before and after ACL injury, as well as before and after cyclic loading, in a clinical 3T MRI setup. The initial decrease of T1ρ shows the cartilage component and microstructure disruption occur due to the injury. The increased T1ρ value throughout recovery may be positively linked to the onset of PTOA [7]. The difference in the T1ρ value before and after loading shows that the cartilage reaction to the load varies through time, suggesting compositional and structural changes in cartilage. Meanwhile, the elevated shear strain value, *Exy*, suggesting it could be an alternative biomarker for cartilage degeneration. This study shows the feasibility of using T1ρ and DENSE MRI to track biochemical and biomechanical changes in knee cartilage after ACL injury and through recovery, and its potential to be used for the identification of early-stage PTOA.

Acknowledgements: This work was supported by NIH grant 2 R01 AR063712.

Reference: [1] Lee+ Magn. Reason. Med. (2023). [2] Chan+ Sci Rep (2016). [3] Zhu+, SSRN (2023). [4] Souza+, J Orthop Sports Phys Ther (2012). [5] Le+, Ann. N. Y. Acad. Sci. (2016). [6] Griebel+ Magn. Reason. Med. (2014). [7] Li+, Osteo Carti. (2007)

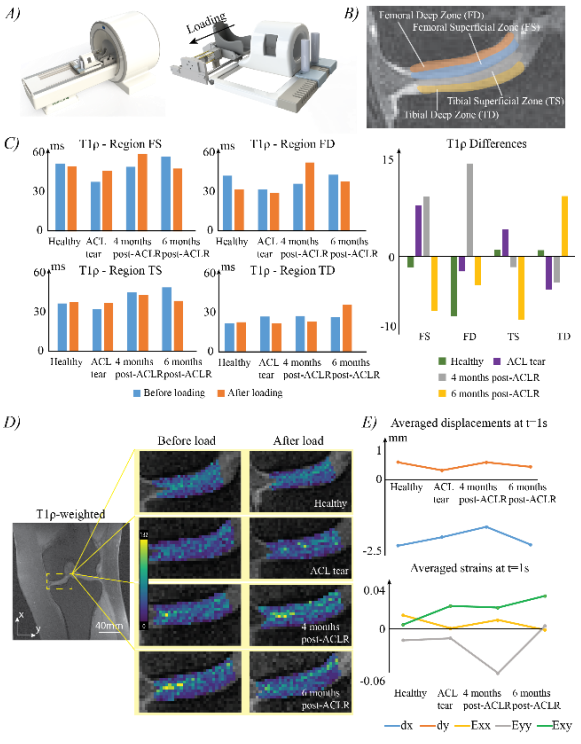

Figure 1: A) Customized loading device. B) ROI selection. C) Averaged T1ρ value within each ROI before and after cyclic loading, and differences. D) T1ρ map within medial cartilage. E) Averaged displacement and strains.

NOVEL ROBOTIC BIOMECHANICAL ASSESSMENT OF RODENT ACL INJURY MODELS

Stephanie G. Cone*[1]
[1]University of Delaware, Newark, DE, USA
*sgcone@udel.edu

Introduction: Preclinical small animal models are common in orthopaedic research, including injury studies of acute and chronic impacts of anterior cruciate ligament (ACL) rupture [1]. Recent innovations have prioritized imaging, biological, and behavioral analyses [1] with relatively little recent change in biomechanical methods. However, clinical outcomes in ACL injuries primarily focus on functional impacts like joint destabilization, altered range of motion, and aberrant loading [2]. Previous biomechanical studies in rodent knees used uniaxial testing, but to accurately replicate native movement we need a multi-axial mechanical testing framework. This study describes a first-of-its-kind miniature 6 degree-of-freedom (6DOF) robotic system used to determine rat knee biomechanics in intact and injured (ACL rupture) conditions. Given prior studies using uniaxial testing, we hypothesized that ACL rupture would result in translational and rotational destabilization. This novel development greatly enhances the translational capacity of preclinical small animal models in the ACL injury research space, with future applications in other joint biomechanics questions.

Methods: Knee joints were collected from female Long Evans rats (n=6) from a separate IACUC approved study and stored at -20°C in saline-soaked gauze. Soft tissue was dissected away from the joint, and bones were set in custom clamps. Robotic testing involved a tabletop 6-degree-of-freedom universal force sensing robotic testing system comprised of a Meca500 robotic arm (Mecademic), a multiaxial load cell (ATI Nano25 IP65), and commercial software (simVITRO) (Fig. 1) [3]. Knees were fixed to the robotic arm and load cell, and an anatomic joint coordinate system was established [4]. Passive flexion-extension (20°-60°) and varus-valgus demands (± 0.05 Nm varus torque, @ 40° flexion) were applied and a functional coordinate system was determined [5]. Functional tests including anterior-posterior (AP) drawer (peak loads: 2.5N at 20°, 40°, and 60° flexion) and varus-valgus (VV) torque (peak applied torques: 0.025N*m at 40° flexion) were performed with hybrid kinetic-kinematic controls. 6DOF kinetics and kinematics were recorded to develop "intact paths". The ACL was transected and the exams were again performed. Injured kinematics were recorded for "injured paths". Serial dissections were performed with the remaining tissues, and the "intact paths" and "injured paths" were performed in kinematic control between dissections. The principle of superposition determined functional contributions of each tissue. Statistical analysis included repeated measures ANOVA testing of joint kinematics and tissue function between states (alpha = 0.05).

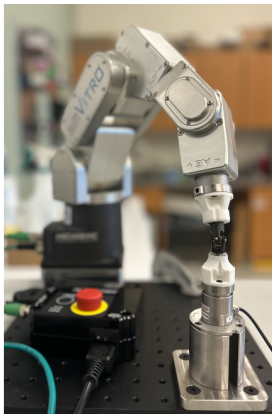

Figure 1: Robotic system for rodent joint testing.

Results & Discussion: Joint laxity in response to anterior (2.5N) loads and varus-valgus (0.025N*m) torques revealed translations of 1.3±1.1 mm and 10.4°±1.74° of rotation in healthy joints (Table 1). Joint laxity decreased with greater flexion within specimens ($p<0.05$ across states). The ACL was a primary restraint against anterior tibial force across flexion angles (percent of total joint force: 51% @ 20°, 94% @ 40°, 97% @ 60°) and contributed significantly under varus-valgus demands. Joint laxity increased with ACL rupture in all cases, more than doubling anterior tibial translations, tripling varus rotation, and doubling valgus rotations (Fig. 2). The MCL and the menisci were the primary functional backups for the ACL after injury. This study shows that in physiologically tests, the rat ACL retains functional relevance to its human and large animal counterparts. Our findings agree with and build upon prior findings in rat knee function. While this study was limited in number and range of specimens, ongoing work aims to further assess sex- and age-dependent differences and the functional effects of various injury models in both rats and mice. This novel approach in preclinical robotic joint testing establishes a new baseline for small animal biomechanics and will greatly enhance future work in translational research.

Anterior translation laxity (mm)			
Flexion angle	20°	40°	60°
Intact	1.30±1.13	1.29±1.10	0.76±0.37
ACL-injured	2.77±1.37	3.31±0.93	2.19±0.79
Rotational laxity at 40° flexion			
Direction	Varus		Valgus
Intact	5.64°±1.74°		4.71°±1.48°
ACL-injured	15.34°±5.77°		7.58°±2.94°

Table 1: Average joint laxity values (mean±std).

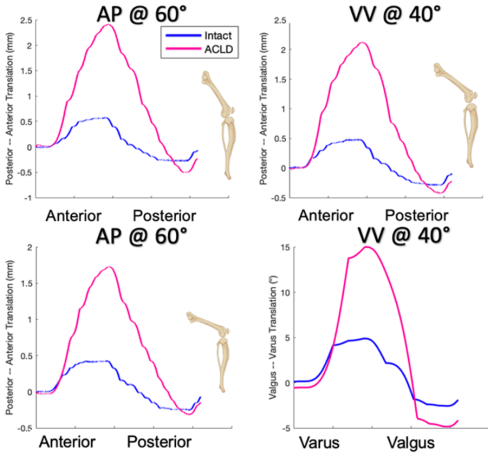

Figure 2: Representative force-deformation curves.

Significance: This preclinical work is highly valuable in translational research, providing functional context for preclinical models by establishing a framework for robust characterization of the biomechanics of small animal joint models. These small animal models are commonly used in preclinical work where functional outcomes are pivotal in the target clinical population, and as such having the capacity to assess physiologically relevant loading conditions is of great importance.

Acknowledgments: This project received support from the Delaware Center for Musculoskeletal Research (NIH P20GM139760), Olivia Dyer, and Tara Nagle.

References: [1] Little, D et al., J Orthop Res, 2023. [2] Woo, SLY et al., J Orthop Res, 2006. [3] Cone, S et al., Clin Orthop Rel Res, 2019. [4] Pennock, G et al., J Biomech, 1999. [5] Nagle, T et al., J Biomech, 2021.

PATIENT REPORTED AND BIOMECHANICAL OUTCOMES FOR SERVICEMEMBERS WITH ANTERIOR CRUCIATE LIGAMENT RECONSTRUCTION UNDERGOING REHABILITATION AT A MILITARY TREATMENT FACILITY

Andrew Plows[1]*, Julia A. Lytle[1], Tyler Cardinale[1], Patrick Desrosiers[1], Trevor Kingsbury[1]

[1] Naval Medical Center San Diego, San Diego, CA, USA

*Corresponding author's email: andrew.c.plows.ctr@health.mil

Introduction: Return to duty following anterior cruciate ligament reconstruction (ACLr) can be challenging and many Servicemembers (SMs) may experience long term dysfunction [1]. Within a Military Treatment Facility (MTF), the ACLr treatment protocol has a focus on early weightbearing and range of motion [2]. However, patients following ACL injuries often demonstrate lower-limb asymmetries during functional movements [3]. The purpose of this study was to assess Patient Reported Outcomes (PRO) and biomechanical outcomes in SMs during rehabilitation following ACLr.

Methods: 72 SMs (17 Females, 55 Males) underwent clinical evaluations every 3 months (3, 6, 9, and 12) following ACLr. SMs completed the Tampa Scale for Kinesiophobia (TSK-11), Knee Injury and Osteoarthritis Outcome score (KOOS), the Y-balance test (YBT), and a biomechanical assessment consisting of five cued body weight squats on two force plates (Kistler Instrument Corp, Novi, MI, USA). The variables of interest included compound scores for the TSK-11 and KOOS, Y-balance limb asymmetry, and squat concentric and eccentric phase asymmetry. A one-way ANOVA examined the effect of time on PROs and biomechanical outcomes. Significance was set at alpha < .05.

Results and Discussion: There was no significant difference between TSK-11 scores at any time point. This could indicate that apprehension to physical activity post injury isn't related to time spent in rehab. There were significant improvements in KOOS Sport & Recreation (S&R), Quality of Life (QOL), and Pain scores. S&R and Pain score differences occurred between the 3 (38.7 S&R, 64.7 Pain) and 6-month (63.6 S&R, 81.9 Pain) groups (p=0.00 S&R, p=0.001 Pain), and the 3- and 12-month (64.1 S&R, 81.0 Pain) groups (p=0.00 S&R, p= 0.005 Pain). Additionally, there was a significant difference in the S&R scores between the 3 (38.7) and 9-month (58.6) groups (p=0.01). QOL differences occurred between the 3 (38.3) and 6-month (55.4) groups (p=0.024) as well as the 3- and 12-month (58.2) groups (p=0.011). These improvements in patient reported outcomes later in the rehabilitation process mean that SMs are experiencing less pain, enjoying a higher quality of life, and can engage in more sports and physical recreation. Y-balance limb differences significantly improved between the 3 (12.0%) and 9-month (6.4%) groups (p=0.02) as well as between 3- and 12-month (5.2%) groups (p=0.004). Significant improvements in concentric and eccentric force asymmetry were observed during squatting between the 3 (21.8% Concentric, 16.8% Eccentric), and 12-month (9.9% Concentric, 9.1% Eccentric) groups (p=0.00 Concentric, p=0.01 Eccentric). Additionally, concentric force asymmetry significantly improved between the 9 (19.5%) and 12-month (9.9%) groups (p=0.01). These differences indicate that over time, SMs were able to more equally utilize their injured and non-injured limb for force production and balance.

Significance: Rehabilitation at the MTF often becomes inconsistent or stops completely after the 6–9-month mark. However, significant improvements in PRO and biomechanical outcomes during this period suggest that continued engagement with rehabilitation services, even after cleared for duty, are imperative to an optimal recovery. Utilizing a comprehensive clinical assessment can assist in patient retention and engagement with rehabilitation services as well as provide improved overall outcomes.

Acknowledgements: The views expressed herein do not necessarily reflect those of the Department of the Navy, Department of Defense, DHA, or the US Government. Thank you to Fedpoint Systems for support.

References: [1] Antosh (2018). Military medicine, 183(1-2), e83-e89. [2] Peebles, Liam (2019). Sports Medicine and Arthroscopy Review. 27. 10.1097/JSA. [3] Sanford BA (2016). The Knee, 23(5), 820–825.

EXPLORING DIFFERENCES IN ARM MOVEMENT DURING AN ANXIETY-INDUCTION TASK IN CHILDREN WITH MENTAL HEALTH DISORDERS

Jenna G. Cohen[1*], Bryn C. Loftness, Ellen W. McGinnis, Ryan S. McGinnis
[1]Biomedical Engineering, University of Vermont
*jenna.g.cohen@uvm.edu

Introduction: Externalizing (e.g., ADHD) and internalizing (e.g., anxiety, depression) disorders are common in children [1]. Current screening relies on parent-report surveys as children cannot reliably report on their emotions [2]. However, even the most attentive caregivers may underreport since many symptoms are unobservable [1]. When presented with emotional stimuli, children with ADHD and internalizing disorders exhibit distinct bio-behavioral responses as compared to children without these disorders [3], [4]. Furthermore, children with ADHD and anxiety exhibit differential stimuli reactivity than children with ADHD alone [5]. In this analysis, we consider children's arm movement as a bio-behavioral measure of reactivity during an anxiety-inducing task with two buzzers, serving as stimuli. We hypothesized that children's reactivity to emotionally-laden stimuli would indicate the presence of a disorder, and would differentiate amongst children by disorder type. Overall, this study aims to enhance our ability to detect mental health disorders in young children by identifying objective biomarkers.

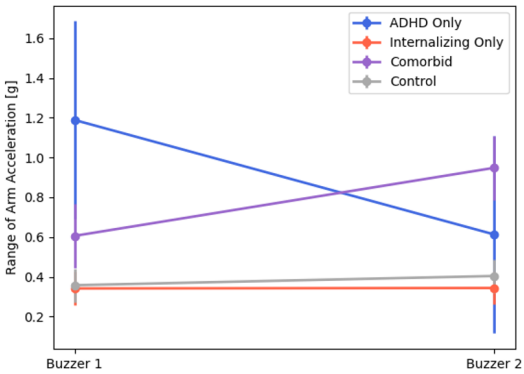

Figure 1: Mean and standard error of range in arm acceleration during the 15 second period after buzzers 1 and 2 by diagnostic group.

Methods: We present arm movement data from children ages 4-8 (N=73, 44% female, 7 ADHD only, 22 internalizing disorders only, 8 comorbid ADHD and internalizing disorders, 36 controls) during the three phases of the Trier Social Stress Task adapted for kids. In this three-minute task, children are told they will be judged while telling an impromptu story. Two startling buzzers sounded halfway through the task and with 30 seconds remaining, at which point children were told the amount of time remaining, increasing contextual fear. Child mental health diagnoses were determined via a gold-standard semi-structured interview (KSADS-PL) with clinical consensus. Range in arm acceleration was considered in 15 second periods after each buzzer. Change in arm movement from 15 seconds before and 15 seconds after each buzzer was also studied. Participants with more than a 20% increase in range were considered "reactors" to the stimuli. Cross tabulations were performed to compare the percentage of reactors in the control and any disorder (ADHD and/or internalizing) groups. One-way and repeated measures ANOVAs were performed to examine movement after the buzzers by diagnostic groups.

Results & Discussion: Cross tabulations of "reacting" to buzzers was significantly more common for children with a mental health diagnosis than without. For controls, 33.3% reacted to buzzer 1 and 36.1% to buzzer 2. For children with a diagnosis, 59.5% reacted to buzzer 1 and 40.5% to buzzer 2. We then analyzed post-buzzer movement further by diagnostic group. Children with ADHD exhibited significantly greater arm movement at buzzer 1 compared to those with internalizing disorders ($p=.009$) and controls ($p=.007$). There were significant interactions between arm movement across the two buzzers and diagnostic group. Children with ADHD exhibited relatively *smaller* movement following the second buzzer than the first, whereas children with internalizing disorders ($p=.030$) and controls ($p=.038$) exhibited a similarly small movement to both buzzers (Fig 1). While children with mental health disorders demonstrated greater likelihood of reactivity to the buzzers overall, the effect appeared to be driven by children with ADHD. Inconsistent with previous literature, children with internalizing disorders only did not appear different than controls. This could be due to types of anxiety and depression being collapsed in our group, which have been shown to have some opposing startle effects [6], or in the reactivity measurement being gross motor and not physiological. Children with ADHD had greater movement to buzzers overall, and this pattern differed depending on whether the child had comorbid anxiety, consistent with previous works. The differential patterns over time could be indicative of differential fear learning, wherein adults with internalizing disorders learn to anticipate aversive stimuli and become more sensitive over time [7] whereas adults with ADHD only do not [8]. Future work should examine physiological reactivity, such as heart rate and galvanic skin response, and further explore changes in reactivity over time by diagnostic group.

Significance: Arm movements surrounding surprising stimuli during a short anxiety-induction task provide potential biomarkers of mental health conditions in young children, supported by theory-driven hypotheses related to hyperarousal and fear learning.

Acknowledgments: Research supported by the US National Institutes of Health (MH123031) and the US National Science Foundation (2046440).

References: [1] K. B. Madsen et al. (2018), *Eur Child Adolesc Psychiatry*; [2] B. C. Loftness et al. (2023), *IEEE JBHI*; [3] M.G. Melegari et al. (2020), *J Atten Disord.*; [4] L. S. Wakschlag et al. (2005), *Clin Child Fam Psychol Rev* 8(3); [5] S. J. Lane et al. (2019), *Frontiers in integrative neuroscience* 13(40); [6] L. M. McTeague et al. (2012), *Depression and anxiety* 29(4); [7] A.R. Naudé et al. (2022), *Cogn Affect Behav Neurosci* 22; [8] D. Feifel et al. (2009), *Journal of psychiatric research* 43(4).

SHOULDER MUSCLE ACTIVITY INCREASES AFTER ACUTE BUT NOT CHRONIC PAIN RELIEF

Taylor J Wilson[1*], Motoki Sakurai[1], Phil McClure[2], Andy Karduna[1]
[1]University of Oregon, Eugene, Oregon, US, [2]Arcadia University, Glensdale, Pennsylvania, US
*Corresponding author's email: twilson8@uoregon.edu

Introduction: Subacromial pain syndrome (SPS; often referred to as shoulder impingement syndrome) is defined as chronic pain that arises from a broad set of pathologies localized to the subacromial space [1]. There is no consensus on how pain affects shoulder musculature. One of the leading hypotheses about muscular adaptations to pain includes the pain adaptation model (PAM). The PAM proposes that pain ridden muscles involved in movement (agonist muscles) decrease their activity, as measured by electromyography (EMG) while muscles that oppose the movement of agonists (antagonists) increase their activity, acting as a protective mechanism during movement [2].

The aim of the present study was to determine the effects of pain on muscle activity in patients with SPS, both before and after pain relief. In line with the PAM, we hypothesized that shoulder muscle activity will be higher in agonist muscles (lower in antagonist muscles) after pain relief, compared to pre-pain relief.

Table 1. Instances where muscle activity was larger in T2 compared to T1 ($p<0.05$) during movement from 40º (0%) to 110º(100%) HE.

T1 EMG < T2 EMG					
Muscle	Percentage of Movement				
AD	0-44%	50-70%	72-73%	90-91%	99-100%
MD	5-8%	15-18%	27-32%	35-36%	
UT	25-27%	55-60%	63-65%	70-73%	94-100%

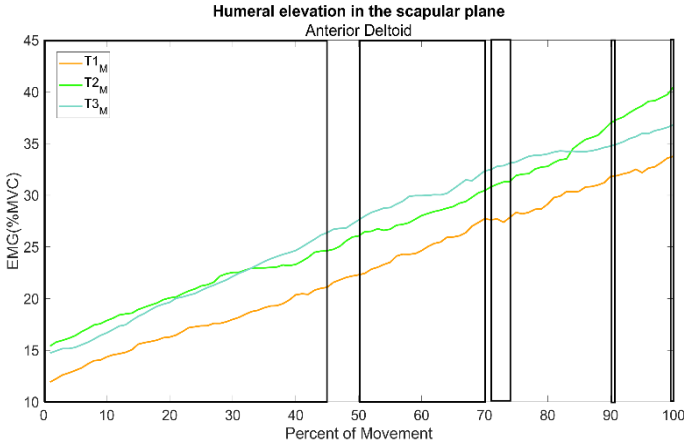

Figure 1. Mean anterior deltoid (AD) activity in the scapular plane before pain relief (T1), after subacromial injection (T2), and after physical therapy (T3). Muscle electromyography (EMG) activity is represented as a % of maximum voluntary contraction (%MVC). Black boxes indicate the ranges of HE where T2 EMG is significantly higher than T1 EMG ($p<0.05$).

Methods: Twenty-two patients were recruited from a local orthopaedic clinic. Inclusion criteria were ages 21 – 65 years (mean ± SD; 47.9 ± 10.3 years), experienced pain during passive (assisted) provocative manoeuvres (Hawkins or Neer), active elevation, and/or isometric resisted movements and planned to receive a subacromial injection.

The subject's affected side was instrumented with wireless Delsys Trigno EMG electrodes and wireless Xsens MTi inertia measurement unit (IMU) sensors to collect muscle activity and kinematic data, respectively. Surface EMG sensors were placed on the anterior, middle, and posterior deltoid (AD, MD, and PD, respectively), and upper trapezius (UT). Two IMUs were placed on the lateral aspect of the affected arm, superior to the elbow and on the torso at the level of the xiphoid process.

The subject was then instructed to complete three bouts of humeral elevation (HE) at an angle ~30 degrees forward of the frontal plane with an externally rotated arm for block one (T1). Block two (T2) was the same, and performed on the same day, as T1 but after a subacromial injection (6 cc 0.5% Marcaine and 1 cc DepoMedrol) applied by a physician and the subject's qualitative indication of pain-relief during an arm raise. For the last block (T3), subjects completed 6-weeks of physical therapy aimed at increasing range of motion and strength on the affected side and then repeated the same HE from T1/T2.

Multiple One-Dimensional Statistical Parametric Mapping (SPM1d) two-tailed paired t-tests were used to compare the activation of each muscle under analysis (AD, MD, PD, and UT) from 40º(0%) to 110º(100%) of HE: T1 vs. T2 and T1 vs. T3.

Results & Discussion: Partially agreeing with our hypothesis, AD, MD, and UT EMG activity increased after acute pain relief ($p<0.05$), but only for specific percentages of HE (Table 1), with a visual representation for AD (Figure 1). However, no differences in muscle activity were apparent in PD after acute pain relief (T1 vs T2) or for any muscle after chronic pain relief (T1 vs T3).

Increases in the muscle activity of the AD, MD, and UT in T2 compared to T1 are not surprising, as these muscles aid in shoulder flexion (AD,UT) and abduction (MD), while the PD aids in adduction and extension [3]. Additionally, the body may overcompensate muscle activity after acute relief of pain, whereas it returns to normal muscle activity after rehabilitation.

Significance: Our results partially support the PAM. Impaired deltoid activity could upregulate UT activity [4] and cause further injury or denervation of the muscles. Therefore, other muscles and structures may be affected by the decreased deltoid activity due to pain, which could lead to irregular scapular and humeral movements. Future studies could look at how deltoid activity pre- and post-pain relief affects functional alternations in and around the subacromial space. Others could compare post-pain relief deltoid activity in the affected versus unaffected shoulder. If differences are found, rehab modalities may need different approaches for those after acute versus chronic pain relief.

References: [1] Mitchell et al. (2005). *BMJ.*, 331(7525), 1124-28; [2] Hodges & Smeets (2015). *Clin. J. Pain.*, 31(2), 97-107; [3] Moser et al. (2013). *Skeletal Radiol.,* 42(10), 1361-75; [4] L. Ettinger et al. (2021). *J. Sport Rehabil.,* 30(8), 1144-50.

AN INERTIAL SENSOR-BASED COMPREHENSIVE ANALYSIS OF SCI MANUAL WHEELCHAIR USER MOBILITY DURING DAILY LIFE

Kathylee Pinnock Branford[1], Meegan G. Van Straaten[2], Omid Jahanian[2], Melissa M. B. Morrow[3], and Stephen M. Cain[1]*
[1]West Virginia University, Morgantown, WV, [2]Mayo Clinic, Rochester, MN, and [3]Univ. of Texas Medical Branch, Galveston, TX
*stephen.cain@mail.wvu.edu

Introduction: Decreased mobility can impact the health status of manual wheelchair (MWC) users. A detailed understanding of daily mobility in MWC users can help in determining associations between patterns of movement, physical activity, and health issues such as shoulder pathology. Studies conducted on MWC propulsions have mainly focused on investigating mobility characteristics obtained from using sensors on the wheels. These characteristics include distance, speed, activity hours, accumulated movement, the maximum period of continuous movement, maximum distance of continuous movement, and number of bouts of mobility per day [1-3]. Short and slow bouts of active propulsion dominate daily MWC usage, highlighting the frequent starts and stops during the day. [2]. Initiating movements, stopping, and maneuvering require higher inertial changes and dominate the physical demands on a MWC user during mobility. Stress on the upper extremities is higher during acceleration than constant velocity propulsion [4]. MWC users perform around 900 turns daily on average [5]. Laboratory-based approaches that utilize analyses of straight-line propulsion for long periods at higher speeds [6] have limited use for understanding real-world MWC mobility. Therefore, we aim to develop a comprehensive mobility analysis to assess and quantify detailed characteristics of MWC mobility during daily life to understand the relationship between daily arm use and shoulder pathology.

Methods: We utilized eight IMUs (Axivity-AX6; range ±16 g and ±2000 deg/s, sampling frequency 100 Hz): one on each wrist, upper arm, torso, wheel hub, and wheelchair frame. Data were collected from six MWC users with spinal cord injury (2F, 4M) over seven continuous days. Instantaneous wheelchair speed was calculated using the known radius of the rear wheel and the measured angular velocity of the wheels. We initialized bouts of mobility when the wheelchair speed was greater than 0.12 m/s and at least one wheel completed one revolution and ended when no movement was detected for a period greater than one minute. Outcome measures were obtained for each bout, including duration, mean speed, total distance (total distance traveled in a bout), maximum distance (furthest distance traveled from the starting point of the bout), and continuity (ratio of movement time to bout duration). We also calculated the number of starts, stops, and turns for each day. A k-means cluster analysis was used to identify three primary types of bouts of mobility based on bout characteristics.

Results and Discussion: Participants had between 305 to 500 bouts during a week, 313 to 920 starts and stops, and 460 to 1182 turns per week. The high number of turns and starts/stops during the week indicates that initiating movements dominate daily MWC usage, regardless of the employment status or physical activity levels of our participants. Bout duration had the most significant effect on the clustering results. It was used to classify bouts into three categories (Figure 1): short, medium, and long, with mean durations of 86.4s, 397.8s, and 1198.8s, respectively. Short bouts were highly continuous (56%), covered a mean maximum distance of 6.15 m, and had a mean speed of 0.25 m/s. Medium bouts were less continuous (38%), covered a mean distance of 15 m, and had a mean speed of 0.19 m/s. The continuity for the long bouts was (40%), covered a mean distance of 44 m, and had a mean speed of 0.22 m/s. Shorter-duration bouts account for almost 80% of the total bouts compared to more prolonged bouts, which account for only 5% per week. Our results differ slightly from previous research, but this is mostly due to our definition of a bout that allows stops for up to one minute within a bout. Further research is needed to quantify the impact of turns, starts, stops, and shorter-duration bouts on shoulder pathology progression.

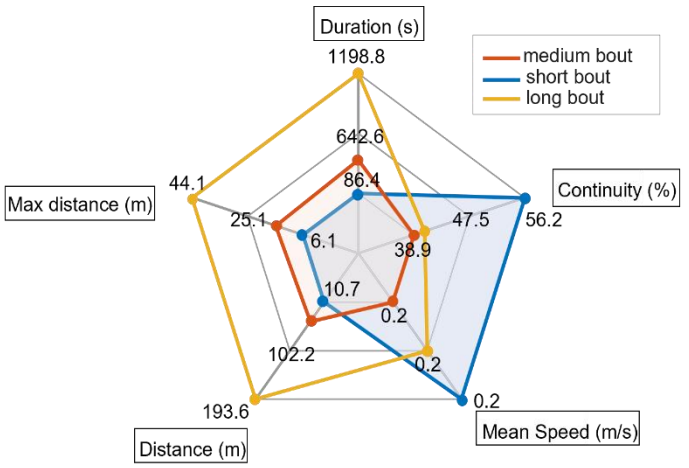

Figure 1. Comparison of the mean bout characteristics for short (blue), medium (red), and long (yellow) duration bouts of mobility. Short bouts were the fastest and most continuous, whereas medium duration bouts were the slowest and least continuous.

Significance: This analysis offers a distinctive understanding of the weekly mobility habits of individuals who use MWCs through bout characterization. Short-duration bouts and start/stop/turn maneuvers dominated daily MWC-related mobility. These findings have implications for understanding overall physical activity of MWC users and the demands imparted to the shoulder and upper extremity.

Acknowledgments NIH Eunice Kennedy Shriver National Institute of Child Health and Human Development (R01HD084423)

Reference: [1] Tolerico (2007) J of Rehabilitation Research; [2] Sonenblum (2012) Rehabil Res Pract; [3] Poop (2015) Med Eng Phys; [4] Koontz et al. (2005) J Rehabil Res Dev; [5] Togni (2022)) Front Bioeng Biotechnol; [6] Sosnoff (2015) Front Bioeng Biotechnol

KINEMATIC SMOOTHNESS ASSESSMENT FOR INDIVIDUALS WITH FUNCTIONAL MOVEMENT DISORDER BEFORE AND AFTER A ONE-WEEK INTENSIVE TREATMENT

Garrett Weidig[1*], Ava Carson[1], Josh France[1], Alysha DeMay[2], Cheris Grasse[2], Olivia Risko[2], Tamara Reid Bush[1]
[1]Michigan State University, East Lansing, MI, USA
[2]The Recovery Project, Lansing, MI, USA
*Corresponding author's email: weidigga@msu.edu, reidtama@msu.edu

Introduction: Functional Movement Disorder (FMD) is a debilitating disorder associated with involuntary movements that affect the quality of life and independence of individuals [1]. Symptoms of FMD often include involuntary, hyperkinetic movements such as jerks or tremors (jerks being larger in magnitudes and less frequent in comparison to tremors). Further, FMD is associated with long diagnostic periods (average 6.6 years) and FMD healthcare costs of over $1 billion in the U.S. annually [1]. Current treatment protocols of FMD consist of a one-week intensive rehabilitation with physical, occupational, and behavioral therapies, but success is determined using self-reporting questionnaires [2]. Having the ability to quantify movement quality, particularly hyperkinetic movements, is critical not only for tracking rehabilitation progress, but also for understanding characteristics of FMD in the diagnostic process. Kinematic smoothness is a metric that has been used to measure movement quality for populations that have 'shaky' movements such as Parkinson's Disease or those post-stroke, but has not been used for populations like FMD that can have greater variance in movement magnitude and frequency [3]. Thus, the goal of this work was to quantify movement smoothness in healthy, pre-treatment FMD, and post-treatment FMD groups using a mathematical analysis called SPARC (Spectral Arc Length) during a simulated drinking task to determine the efficacy of a one-week rehabilitation program. We expect that persons with FMD will have significantly smoother movements post-treatment, but may not attain the smoothness values exhibited by a healthy control group.

Methods: Eight healthy (4 female, mean age 20.6 years (S.D. 2.6)) and twelve FMD participants (8 female, mean age 49.8 years (13.6)) completed a simulated drinking task. All consented to testing (IRB #00008685). A six-camera motion capture system (Qualisys, Gothenburg Sweden) was used to obtain position data on 21 markers placed on bony prominences of the upper extremities, trunk, and head. Velocity was calculated using the ulnar styloid marker (Fig. 1). Smoothness was calculated using the SPARC approach, which was the negative of the arc length of the Fourier Transform of the velocity profile [4]. More complex profiles would result in more complex arc lengths and less smooth movement (values closer to zero are smoother). A paired t-test was conducted for the pre- and post-treatment groups to determine the effect of treatment. Also, unequal-variance t-tests were performed between both FMD groups and the healthy.

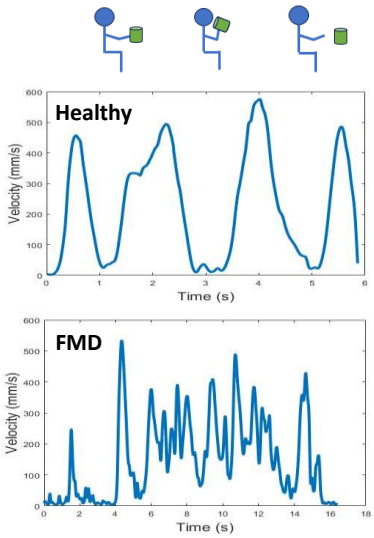

Figure 1: Velocity profiles of a healthy and pre-treatment FMD individuals during simulated drinking. Key points in the movement (grasping, drinking, and release) are labeled at the top. The pre-treatment FMD individual displays more frequent changes in velocity, which would result in greater SPARC.

Results & Discussion: The average SPARC value for the healthy group was -2.36 (0.19) whereas the average for the pre-treatment and post-treatment groups were -5.07 (1.68) and -3.49 (1.03), respectively. The post-treatment increase in smoothness (i.e., a decrease in SPARC), was significant ($p<.01$). Of the 12 FMD participants, 11 had increased smoothness (Fig. 2). Additionally, significant differences between the healthy and pre-treatment group ($p<0.01$), and between the healthy and post-treatment group ($p<.05$) were identified. Three participants were able to decrease their SPARC value to within one standard deviation of the healthy mean (Fig. 2).

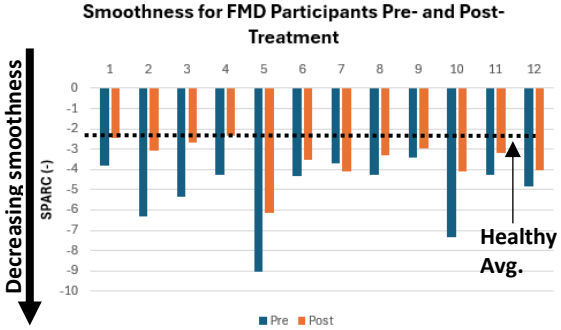

Figure 2: SPARC for each FMD participant pre- and post-treatment, plotted with the healthy average (dotted line). Smoothness improved following treatment for 11/12 participants. Participants who had the least smooth movements (highest value) pre-treatment saw greater changes to their smoothness value after treatment.

Significance: This research is one of the few quantitative studies to analyze FMD pre- and post-treatment. SPARC was able to determine differences in overall movement quality with a lower value indicative of improved function. One limitation was it did not differentiate between hyperkinetic symptoms (low versus high frequency and amplitude) and may require further investigation for best use. One advantage was that SPARC was only dependent on the velocity profile, which could be measured by a wearable accelerometer, such as a smart watch, instead of a motion capture system; thus, making it a directly translatable clinical tool. Being able to actively quantify complex, hyperkinetic movements can assist with monitoring symptoms through rehabilitation or throughout the diagnostic period, which may lead to quicker diagnosis of FMD.

Acknowledgments: We thank the therapists at The Recovery Project in Lansing for their collaboration and help in recruiting.

References: [1] Tinazzi et al. (2021), *Euro J Neuro* 28(5); [2] Czarnecki et al. (2012), *Parkinsonism & Related Disorders* 18(3); [3] Refai et al. (2021), *J NeuroEng & Rehab* 18(154); [4] Balasubramanian et al. (2015), *J NeuroEng and Rehab* 12(112).

Assessing the contributions of pain and pain-related psychological factors on gait quality in chronic low back pain

Bailes AH[1,2], McKernan GP, Redfern M, Cham R, Greco C, Brach JS, LB3P Investigators, Sowa GA
[1] Department of Bioengineering, University of Pittsburgh; [2] Department of Physical Therapy, University of Pittsburgh
anb254@pitt.edu

Introduction: Gait deviations are common in individuals with chronic low back pain (cLBP) [1]. Impaired gait contributes to decreased mobility, quality of life, and life expectancy [2]. While pain may be large contributor to the gait deviations observed in this population, it is likely that other factors also contribute to the gait impairments seen in cLBP. For example, beyond pain itself, pain-related psychological factors (i.e., fear-avoidance, pain catastrophizing) may impact trunk movement in individuals with cLBP [3]. Although fear-avoidance and pain catastrophizing have been studied in relation to trunk-specific movements [3], the impact of these pain-related psychological factors on gait has not been sufficiently studied. Given the strong association between gait and health outcomes [2], as well as the poor prognosis of individuals with cLBP and pain-related psychological factors [4], it is important to identify the distinct contributions of pain and pain-related psychological factors on gait quality in this population. It is hypothesized that both pain and pain-related psychological factors—specifically fear-avoidance and pain catastrophizing—will be significant predictors of gait quality in cLBP.

Methods: Five hundred (n=500) individuals with cLBP [5] completed a 4-meter walk test and two-minute walk test (2MWT) as part of a larger cross-sectional study (U19AR076725-01). Gait speed was measured during the 4-meter walk test, and a single low-back accelerometer (Lifeware, Inc) was used to derive additional gait-quality metrics from the 2MWT [6]. Participants completed the Fear-Avoidance Beliefs Questionnaire-Physical Activity subscale (FABQ-PA) and the 6-item Pain Catastrophizing Scale (PCS-6) to quantify fear-avoidance and pain catastrophizing. Participants also completed the Numeric Pain Rating Scale (NPRS) and Oswestry Disability Index (ODI) to quantify pain and disability. Multivariate multiple regression modeling was used to assess the impact of pain and pain-related psychological factors on several different gait quality metrics simultaneously. Gait speed, step time, step time asymmetry, step time variability, and within-stride gait symmetry as measured by harmonic ratio [7] were the dependent variables in the model. Demographic factors (i.e., age, sex, BMI) and disability as measured by the ODI were included as independent variables in the model due to their known associations with gait quality. To assess the contributions of pain, fear-avoidance, and pain catastrophizing, NPRS, FABQ-PA, and PCS-6 scores were included as additional independent variables in the model. F-tests were used to test the significance of individual model coefficients. Alpha values were adjusted for multiple comparisons.

Results and Discussion: NPRS ($F(7,491)=3.67$, $p<0.001$) was significant across all gait metrics when considered together using multivariate methods. Individually, NPRS was a significant predictor of gait speed ($\beta=-0.01$, $p=0.002$) and harmonic ratio (within-stride gait symmetry) in the anterior-posterior direction ($\beta=-0.04$, $p=0.003$). FABQ-PA was a significant predictor of gait speed ($\beta=-0.004$, $p=0.003$). FABQ-PA and PCS-6 were not significant for any other gait metrics, nor were they significant across all gait metrics when considered together using multivariate methods.

Taken together, these results suggest that pain and fear-avoidance both negatively impact gait speed. Interestingly, pain drives differences not only in temporal measures of gait quality (i.e., gait speed), but also in harmonic ratio, which is an accelerometry-based metrics that is understood to suggest subtle impairments in the neuromotor control of gait [8]. On the other hand, the impacts of fear-avoidance are limited to gait speed alone. Therefore, although both pain and fear-avoidance impact gait quality, it appears as though pain may influence neuromotor control of gait more so than fear-avoidance. Furthermore, pain catastrophizing does not appear to play any role in predicting gait quality.

It is important to note that this analysis excluded individuals who required an assistive device to complete the 2MWT and may therefore not be representative of the most gait-impaired population. In addition, participants may have had additional comorbidities, and therefore, participants' gait performance may have been influenced by factors other than cLBP. This concern is somewhat mitigated by the large sample size and inclusion of age, sex, BMI, and ODI in statistical modeling.

Significance: Pain and fear-avoidance both influence gait speed. Pain may have an additional impact on neuromotor control of gait as indicated by its influence on gait symmetry as measured by harmonic ratio. Clinicians should consider the ways in which pain and fear-avoidance impact overall mobility through gait assessments for patients with cLBP. Not only should pain be addressed during treatment, but interventions addressing fear-avoidance should be further explored to improve gait-associated health outcomes in cLBP.

Acknowledgements: The Back Pain Consortium Research Program is administered by the National Institute of Arthritis and Musculoskeletal and Skin Diseases. This research was supported by the National Institutes of Health through the NIH HEAL Initiative under award number U19AR076725-01. Research reported in this abstract was also supported by the Eunice Kennedy Shriver National Institute of Child Health and Human Development of the National Institutes of Health under Award Number F30HD112110. The content is solely the responsibility of the authors and does not necessarily represent the official views of the National Institutes of Health of its NIH Heal Initiative. We acknowledge the assistance of Chat GPT, developed by OpenAI, in the development of this abstract title, for assistance with literature searching, and for providing clarifications on statistical analyses used.

References: [1] Hicks GE, et al., *Gait Posture (*2017), 55; [2] Fritz S, Lusardi M, *J Aging Phys Act* (2015), 23(2); [3] Ippsersiel P, et al. *Phys Ther*. (2022), 102(2); [4] Stevans JM et al., *JAMA Netw Open* (2021), 4(2); [5] Deyo RA, et al., *J Pain* (2014), 15(6); [6] Zijlstra W, Hof AL, *Gait Posture* (2003), 18(2); [7] Menz HB, et al., *Gait Posture* (2003), 18(1); [8] Bellanca JL, et al., *J Biomech* (2013), 46(4).

INDIVIDUAL VARIABILITY IN PAIN AND QUALITY OF LIFE FOLLOWING SCOLIOSIS CORRECTION

Cole R. Grant[1], Mike J. Blake[1], Haven M. Hill[1], Scott S. Russo[2], Yunju Lee[1,3*]
[1]Department of Physical Therapy and Athletic Training, Grand Valley State University, Grand Rapids, MI, USA
[2]Orthopaedic Associates of Michigan, Grand Rapids, MI, USA
[3]School of Engineering, Grand Valley State University, Grand Rapids, MI, USA
*Corresponding author's email:leeyun@gvsu.edu

Introduction: Scoliosis is a common condition that is characterized by a lateral spinal curvature that exceeds 10 degrees [1]. In some cases, surgical intervention may be necessary. Spinal fusion is a prevalent approach for scoliosis correction, despite historical complications associated with immobilization [1]. Newer techniques, such as spinal fusion with pelvic fixation, aim to improve outcomes by minimizing post-surgical complications. Understanding the short- and long-term effects of spinal fusion is crucial for patients, physical therapists, and healthcare professionals involved in the decision-making process. This information can significantly impact treatment choices and patient expectations. The aim of this study was to provide clinical data to adult scoliosis patients regarding potential changes in physical function, pain levels, and overall well-being following corrective spinal fusion surgery.

Methods: Thirteen individuals from the Grand Rapids, Michigan area were enrolled in this unblinded, non-randomized, controlled clinical trial. The average height and weight were 161.6 cm and 73.9 kg, respectively. The average age of the participants was 63.9 years, with an 11:2 female-to-male ratio. All participants underwent spinal fusion surgery involving multiple vertebrae for scoliosis correction with pelvic fixation. Three outcome measures were completed. The Oswestry Disability Index (ODI), Visual Analogue Scale (VAS), Short Form Survey (SF-36), and Scoliosis Research Society questionnaire (SRS-30) were administered at baseline, 3 months, 6 months, 1 year, and 2 years post-surgery to assess function, pain, and functional ability [2,3]. Lower ODI and VAS scores indicate improved function and pain, while higher SF-36 and SRS-30 scores reflect better functional ability. Data analysis was performed using Excel and SAS JMP to compare quality of life measures and pain levels pre- and post-surgery.

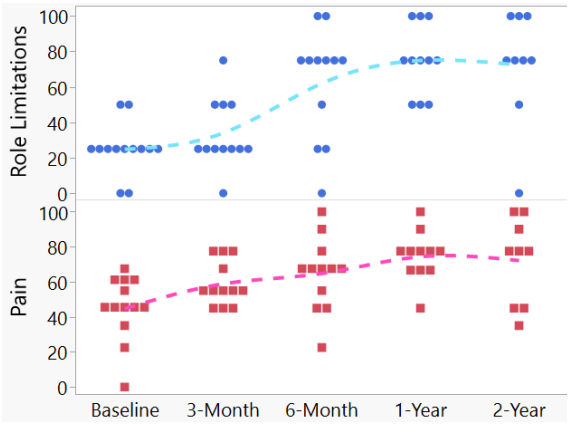

Figure 1: Longitudinal comparison of SF-36 scores for role limitations related to physical health (blue, circle) and pain (red, square) at multiple time points, at baseline, 3 months, 6 months, 1 year, and 2 years post-surgery. Dot-lines represent trends, points represent individual scores.

Results & Discussion: The SRS-30 scores showed a consistent improvement after surgery, with the most significant increase occurring between baseline and 3 months (67.5 to 96.5). This early improvement suggests potential benefits in terms of perceived disability and health-related quality of life. However, it is important to acknowledge that these self-reported measures may be influenced by post-surgical pain management and positive expectations associated with the procedure.

The SF-36 scores in Figure 1 show improvements in various categories. Furthermore, the ODI scores decreased at each time point, with the most significant reduction occurring 3 months post-surgery (27.15 to 16.92). Similarly, the Visual Analogue Scale (VAS) scores exhibited a downward trend, with the most significant decrease in average pain observed three months following surgery (57.3% to 26.3%). These findings suggest positive outcomes, such as improved function and pain management, especially in the early post-operative period. However, the significant score variations observed at six months, one year, and two years post-surgery emphasize the individual variability in long-term outcomes after spinal fusion. While some participants experienced sustained improvements in quality of life and pain management, others encountered setbacks. This highlights the intricate nature of recovery and the impact of multiple factors beyond surgical intervention. It is crucial to take into account the potential influence of factors such as adherence to the program, pre-operative health status, and sociocultural determinants on individual recovery paths.

Additionally, the notable reduction in the SF-36 physical functioning category after 3 months is likely due to the temporary restrictions on movement that are typically imposed after spinal fusion surgery. It is important to consider these findings in the context of the patient's rehabilitation process and recognize the possible impact of short-term limitations on self-reported physical function.

Significance: This study aims to improve understanding of the long-term effects of spinal fusion on the quality of life and pain experienced by individuals with scoliosis. It is important to acknowledge the variability in pain and quality of life outcomes among individuals, as this has implications for rehabilitation management [4]. Furthermore, our findings highlight the potential impact of sociocultural factors on post-operative outcomes. This information allows physical therapists to tailor interventions for areas frequently impacted by this procedure and work with other healthcare providers when rehabilitation progress is hindered. Limitations include the use of subjective patient-reported outcome measures, the small sample size, and the observed variability in individual recovery.

Acknowledgements: We appreciate the study participants for their cooperation and B.H., G.A., M.P., and L.B. for contributions.

References: [1] Gummerson et al. (2010), *Skeletal Radiol* 939-942; [2] Glassman et al. (2006), *Spine J* 6(1) 21-26;
[3] Kyrölä et al. (2019), *Disability and Rehabilitation* 43(1) 98-103; [4] Miyagishima et al. (2017), *Phys Ther Res 20:* 36-43

ACHILLES TENDON SHEAR WAVE SPEED DURING GAIT RELATES TO LOWER LIMB FUNCTION AND STRENGTH IN ADOLESCENTS

Kayla D. Seymore[1,2*], Stephanie G. Cone[1,3], Josh R. Baxter[4], Karin Grävare Silbernagel[1,2]
[1]Biomechanics and Movement Science Program, University of Delaware, Newark, DE, USA
[2]Department of Physical Therapy, University of Delaware, Newark, DE, USA
[3]Department of Biomedical Engineering, University of Delaware, Newark, DE, USA
[4]Department of Orthopaedic Surgery, University of Pennsylvania, Philadelphia, PA, USA
*Corresponding author's email: seymorek@udel.edu

Introduction: How physical activity influences Achilles tendon loading is important for understanding healthy and maladaptive calf muscle-tendon development during adolescence, as both overloading and underloading the Achilles tendon can be detrimental for tendon health [1]. Advancements in technology allow Achilles tendon loading to be measured during physical activities via wearable devices. Shear wave tensiometry is a wearable-based approach that directly measures shear wave speed as a proxy for tendon force through skin-mounted mechanical actuators and accelerometers [2]. Though functional Achilles tendon loads have been estimated in healthy adults, these load predictions cannot be generalized to adolescents, due to structural differences and changes in the calf muscle-tendon unit during growth. The purpose of this study was to (1) assess the variability in Achilles tendon shear wave speed during stages of growth and (2) determine the relationship between Achilles tendon shear wave speed and lower limb function and strength in adolescents.

Methods: Twenty adolescents (8 F, 10-17 years, 15 healthy, 5 with heel pain) were divided into groups based on estimated age at peak height velocity (PHV, age of fastest height increase during the adolescent growth spurt) for girls and boys in the United States [3]: before PHV, during PHV, after PHV. Each participant had Achilles tendon shear wave (SW) speed recorded during 30-sec bouts of walking and running using a tensiometer that consisted of a mechanical actuator (SparkFun Electronics, 100Hz tapping rate) and two mini accelerometers (PCB Piezotronics, 50 kHz sampling rate) secured over the midportion of the Achilles tendon on the involved limb (dominant or most symptomatic by self-report). Walking and running were performed at self-selected speed on a treadmill after a 2-minute warm-up. Achilles tendon SW speed was calculated from the tensiometer using the distance (8 mm) and difference in SW arrival time from between accelerometers [2] across approximately 15 strides. To assess lower limb function related to the Achilles tendon, total repetitions, maximum height, and total work from a maximum endurance single-leg heel-rise test were measured using a linear encoder affixed to the heel [4]. Bilateral peak isometric plantarflexor torque was measured at 0° plantarflexion on a HUMAC Norm isokinetic dynamometer (CSMi, Stoughton, MA) and normalized (Nm/kg/m) from the average of five 5-sec trials. The during PHV group was removed from analysis due to an n of 1 (female). Variability in Achilles tendon SW speed between the before and after PHV group was determined using univariate ANOVAs and White's test of heteroscedasticity (unequal variance between groups), controlling for sex, weight, limb, physical activity level (self-reported via questionnaire), and gait speed. Multiple regression determined the relationship between Achilles tendon SW speed and limb symmetry index (LSI=dominant [or most symptomatic]/non-dominant [or least symptomatic limb]*100) function and strength measures, while controlling for age, sex, weight, limb, physical activity level, and gait speed. Alpha was set at $p<0.05$.

Results & Discussion: Achilles tendon peak SW speed during gait did not vary between stages of adolescent growth ($p>0.05$). Additionally, walking and running peak SW speed did not differ between groups after controlling for covariates ($p=0.420$ and $p=0.458$, respectively) (Fig. 1a); though the sample was reduced due to missing data (before PHV=3, after PHV=9). Achilles tendon SW speed was related to lower limb function and strength. Less heel-rise work and peak isometric plantarflexion torque in the dominant/most symptomatic limb was associated with higher peak SW speeds during walking ($_{adj}R^2=0.728$, $p=0.005$ and $_{adj}R^2=0.636$, $p=0.0005$, respectively) and running ($_{adj}R^2=0.597$, $p=0.041$ and $_{adj}R^2=0.595$, $p=0.004$, respectively) (Fig. 1b). No relationship was observed for heel-rise repetitions or height ($p>0.05$).

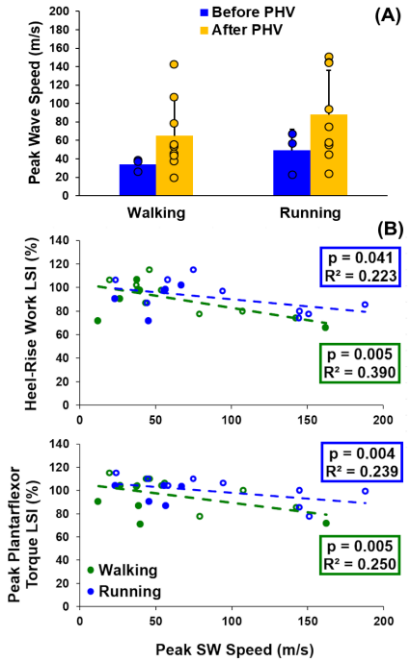

Figure 1: (A) Mean (SD) walking and running peak shear wave speeds. (B) Correlation of function and strength measures to peak shear wave speed. Closed circles (●) indicate before PHV group. Open circles (○) indicate after PHV group.

Significance: A short treadmill gait assessment of SW speed via tensiometry can quantify changes in Achilles tendon mechanics during adolescence, and relates to limb symmetry of lower limb function and strength. Improving calf strength and endurance may be a pathway for decreasing Achilles tendon loading and avoiding overuse injury in adolescents, though future research with a larger sample size is warranted to compare force-derived metrics of Achilles tendon loading to tensiometry SW speed.

Acknowledgments: Research reported in this abstract was supported by the National Institute of Arthritis and Musculoskeletal and Skin Diseases of the National Institutes of Health under award number F31AR081663.

References: [1] Docking & Cook. (2019), *J Musculoskelet Neuronal Interact* 19:300-310; [2] Schmitz et al. (2023), *Micromachines (Basel)* 15:32; [3] Sanders et al. (2017), *Sci Rep* 7:16705; [4] Silbernagel et al. (2006), *Knee Surg Sports Traumatol Arthrosc* 14:1207-17.

THE INFLUENCE OF SEX AND ARM DOMINANCE ON THE BALANCE OF GLENOHUMERAL MUSCLE VOLUME

Denali M. Hutzelmann[1], Colleen M. Vogel[1], Heath B. Henninger[2], Joshua M. Leonardis[1,3]
[1]College of Applied Health Sciences, [2]Department of Orthopaedics, University of Utah, Salt Lake City, UT, [3]Beckman Institute for Advanced Science and Technology, University of Illinois Urbana-Champaign, Urbana, IL
*Email: denalih2@illinois.edu

Introduction: The distribution of musculature about the glenohumeral joint plays a critical role in actuating movement of the humerus while simultaneously maintaining dynamic glenohumeral joint stability. Specifically, stability is maintained by the rotator cuff muscles, which generate a compression force to maintain the position of the humeral head within the glenoid amidst shear forces generated by muscles moving the humerus like the deltoid, pectoralis major, and latissimus dorsi [1]. An imbalance in the anterior-posterior distribution of rotator cuff muscle volume can result in humeral head migration during the generation of this compression force, potentially leading to glenohumeral instability and osteoarthritis [2]. A sex-related disparity in multidirectional glenohumeral instability exists, with the assumption that this is driven solely by greater generalized joint laxity in females [3]. We suspect that sex-differences in the balance of glenohumeral musculature may also contribute to this sex-related disparity. Therefore, this pilot study quantified sex-related differences in the bilateral distribution and balance of glenohumeral musculature.

Methods: Twelve individuals (6 M, 6 F, ages: 18-30 years) underwent magnetic resonance imaging (MRI) (3T Prisma-Fit, Siemens) of the bilateral upper extremities using a two-point Dixon sequence (field of view: 380mm, 1.2mm isotropic voxel size). Water-only images were transformed into the scapular plane and cross-sectional areas (CSAs) were obtained from the supraspinatus (SSP), subscapularis (SSC), combined infraspinatus and teres minor (INF-TMin), combined latissimus dorsi and teres major (LD-TMaj), deltoid (DELT), and pectoralis major (PEC), using slices in the axial or sagittal planes whose locations were defined by specific scapular anatomical landmarks (Fig. 1A). Volumes were then calculated from CSAs using established methods (Fig. 1B) [4]. The distribution of musculature was computed as the ratio of individual muscle volume to the summed volume. Muscle balance was calculated using ratios of absolute anterior-posterior rotator cuff and abd-adductor muscle volumes. Analyses of variance (α=0.05) tested the interaction between sex and arm dominance on absolute muscle volume, relative muscle distribution, and balance.

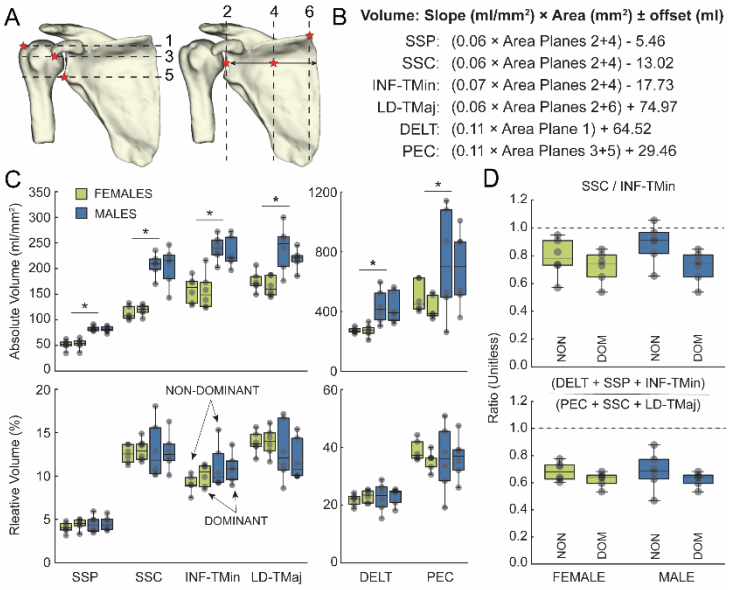

Figure 1: (A) CSAs were obtained in planes defined by key anatomical landmarks. (**B**) Volumes were computed using established equations. Sex and arm dominance-related differences in (**C**) absolute and relative muscle volumes, and (**D**) the balance of glenohumeral musculature, using muscles whose role was defined by their primary moment arms. Box plots represent median ± IQR. Non-dominant data on the left of each cluster. Individual participant data are represented by opaque dots. * p<0.05.

Results & Discussion: Females possessed lower absolute volume across all muscles (all p<0.001) (Fig. 1C). We observed no effect of arm dominance for any muscle in females or males (all p>0.52). This contrasts with previous work that revealed arm dominance-related differences in shoulder strength. Our results suggest that these may be driven by factors like neuromuscular control or individual muscle orientation relative to the joint. The observed sex-differences in absolute muscle volume disappeared when normalized to total muscle volume (Fig. 1C). The PEC accounted for the largest percentage of total muscle volume in males (mean±standard deviation: 36±9%) and females (37±4%) but did not differ by sex (p=0.09) or arm dominance (p=0.59). Similarly, the SSP represented the smallest percentage of total muscle volume for both sexes (females: 4.2±0.6%, males: 4.5±0.8%) and did not differ by sex or arm dominance (both p>0.34). No other sex or arm-dominance related differences were observed (all p>0.09).

In general, males and females possessed greater posterior than anterior rotator cuff muscle volume ((females: 0.75±0.12), males (0.88±.14)) as evidenced by a ratio below 1 (Fig. 1D). While the impact of sex on this measure did not reach significance (p=0.07), it did trend in a way that suggests a sex-difference may be discovered with a larger sample size. Nevertheless, our finding is far different from that of previous work, which found that the ratio of anterior to posterior rotator cuff musculature was close to 1 in healthy individuals [2,5]. Based on that previous work, our sample possessed a balance of rotator cuff musculature like that of someone with posterior glenohumeral instability. However, that previous work computed this balance using CSAs alone, which are sensitive to the transformation of data and the slice at which the CSA is taken, or by deriving muscle volumes from computed tomography, which is less optimal than MRI for the isolation of muscle. We also found that males and females generally possessed a greater volume of abductor muscles (females: 0.65±0.06), males (0.69±.19)), but that these measures did not differ by sex (p=0.40) or dominance (p=0.50). This finding may provide insight into the sex-specific etiologies of subacromial impingement and rotator cuff pathology through its potential effect on the superior-inferior migration of the humeral head.

Significance: The emerging trends of this pilot study indicate potential sex-differences in the muscular morphology of the shoulder joint complex. Our ongoing work aims to establish sex-specific etiologies of shoulder pain and pathologies with emphasis on the role of glenohumeral muscular balance.

References: [1] Ackland, *J Anat*, 2008; [2] Ishikawa H, *J Shoulder Elbow Surg.,* 2023; [3] Magnuson, J, *Journal of Shoulder and Elbow Surgery*, 2019; [4] Henninger HB, *Clin Orthop Relat Res.*, 2020; [5] Espinosa-Uribe, *Surg Radio Anat.*, 2017

VARIATION IN MUSCLE FORCE-LENGTH DYNAMICS IN NON-STEADY LOCOMOTION

M. Janneke Schwaner[1], Monica A. Daley[2]
[1]Department of Movement Sciences, Katholieke Universiteit Leuven, Leuven, Belgium
[2] Department of Ecology and Evolutionary Biology, University of California, Irvine, Irvine CA
*Corresponding author's email: madaley@uci.edu

Introduction: *In vivo* muscle force-length dynamics have been measured in relatively few muscles, species and conditions [1,2,3], and mainly during steady locomotion on a treadmill. It therefore remains a challenge to characterize dynamic muscle function over a realistic range of in vivo behaviors. Characterizing natural variation and relationships between activation, strain, force and work output in non-steady locomotor conditions is important for informing benchtop protocols to characterize dynamic muscle function, and for developing and validating muscle models for simulations. Here, we explore co-variation in force-length, activation and workloop dynamics in the guinea fowl lateral gastrocnemius (LG) muscle during running with treadmill belt speed perturbations. Under dynamically varying *in vivo* locomotor conditions, we expect strain transients and the phase relationship between activation and strain to have a substantial influence on the force and work output over the course of a stride cycle.

Methods: We collected *in vivo* muscle length, force, and activation (5000 Hz) from 6 guinea fowl LG muscles during level running (1.56 ms^{-1}) on a treadmill in steady conditions and with belt-speed perturbations (±0.5 ms^{-1}) resulting in deceleration and acceleration of foot speed [4]. We analyzed 2079 strides, with an average of 374 strides per bird. We normalized *in vivo* force relative to maximum isometric stress (F/F_{max}) and muscle strain relative to optimal isometric length (L/L_0). We measured muscle force magnitude, impulse and work produced per cycle. We used a principal components analysis (PCA) to analyze co-variance among strain, velocity, force and work variables, and used kmeans clustering to characterize strides with similar strain, force and work output characteristics.

Results & Discussion: The strain, force and activation trajectories were relatively consistent across individuals, but exhibited variation in average strain, velocity transients, and time course of force development in the speed-perturbed non-steady conditions. The first 5 principal components explained 80% of the variation in the dataset and were used in a kmeans cluster analysis. Four clusters were identified, characterized by differences in magnitude of velocity transients, magnitude of EMG intensity, average strain, and the timing and magnitude of force output. Strides in the cluster with the highest EMG intensity had low average strain, rapid shortening before foot contact, a force depression transient at foot contact, later peak force, lower mean velocity, and low work output. Strides in the cluster with high positive work output had the lowest EMG intensity, yet earlier and more rapid force development at time of foot contact, with intermediate strain and velocity transients. The results highlight nonlinear relationships between activation and force development in muscle. Variation in the timing of loading during stance can elicit complex changes in force development relative to the strain trajectory, leading to variation in work output over the stride cycle.

Significance: Measures of unsteady *in vivo* muscle dynamics help characterize the operating space of muscle mechanical function in realistic locomotor conditions. These data will help us to identify intrinsic mechanical factors contributing to variation in force and work output, including strain and velocity transients, and phase relationships between strain and activation. In the future, we aim to use these findings to develop new methods to characterize muscle contraction dynamics in controlled in situ and ex vivo conditions and provide data to help inform and validate the development of novel muscle models.

Acknowledgements: This work is funded by the National Science Foundation (NSF), grant number: 2016049 (to M.A.D).

References: [1] Roberts & Scales (2004), *J Exp Biol* 207(23); [2] Daley & Biewener (2003), *J Exp Biol* 206(17). [3] Biewener et al., (2014). *ICB* 54(6). [4] Schwaner et al., (2022), *ICB* 64(32).

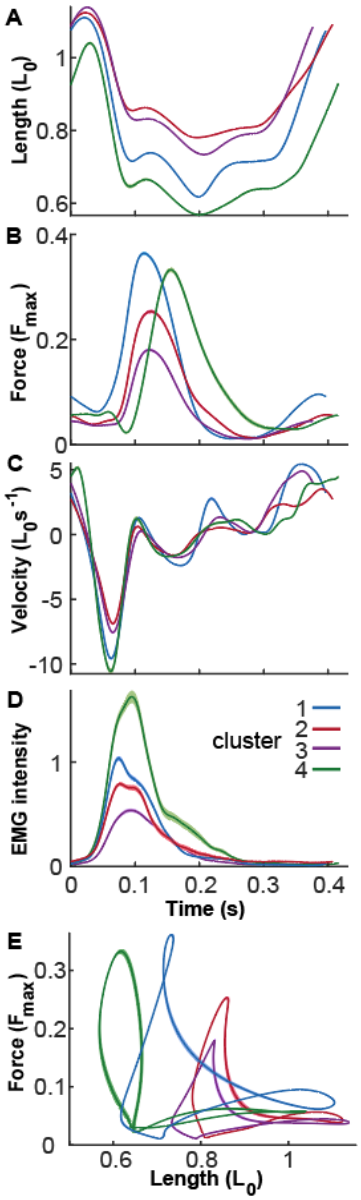

Figure 1 (A-D): *In vivo* trajectories (mean±95%c.i) for each stride category identified from the kmeans cluster analysis, representing the variation observed in muscle dynamics during speed-perturbed treadmill running. **(E)**. Workloops for each cluster-based stride-category (mean±95%c.i) , showing the variation in force-length dynamics over the stride cycle.

MUSCULAR DEMAND IS ENHANCED IN WOMEN AFTER POST-MASTECTOMY PREPECTORAL IMPLANT-BASED BREAST RECONSTRUCTION

David B. Lipps[1*], Susann Wolfram[1], Paige Myers[2], Adeyiza O. Momoh[2]
[1]School of Kinesiology, University of Michigan – Ann Arbor; [2]Section of Plastic Surgery, University of Michigan – Ann Arbor
*Corresponding author's email: dlipps@umich.edu

Introduction: Mastectomy rates in the U.S. are increasing, driven by more breast cancer patients opting for a mastectomy with breast reconstruction to manage future cancer recurrence and restore the natural breast mound [1]. An emerging approach to breast reconstruction is the use of a prepectoral placement of an implant above the pectoralis major muscle that is covered and held in place with an acellular dermal matrix [2]. This reconstructive method is less invasive than prior implant-based procedures with subpectoral implant placement, as no muscle disinsertion is involved. The short and long-term functional benefits of prepectoral implant-based breast reconstruction have yet to be objectively assessed. The current study presents the first prospective examination of neuromuscular control of the shoulder in women undergoing mastectomy with prepectoral implant placement. We hypothesized that prepectoral implant placement after mastectomy would not increase the muscular demand required to generate shoulder torque over the first year of recovery.

Methods: Nine women (mean age: 50.1 years, height: 1.64 m; mass: 79.1 kg) undergoing mastectomy with immediate prepectoral implant-based breast reconstruction were assessed at two time points: pre-operatively and at 12-month follow-up. All participants provided written informed consent. Participants had their treated arm (7 dominant/2 non-dominant) placed in a plastic cast attached to a 6-D load cell with their arm abducted 90 degrees and supported against gravity. Participants were asked to stabilize the shoulder using 3-D isometric torque production while surface electromyography (EMG) electrodes recorded the muscle activity from 12 superficial upper extremity muscles (sternocostal and clavicular regions of pectoralis major; anterior, middle, and posterior deltoid heads; upper, middle, and lower trapezius, latissimus dorsi, teres major, infraspinatus, and serratus anterior). They performed two maximum voluntary contractions (MVC) at the beginning of the experiment. Each subsequent trial had each torque component scaled to 15% MVC to ensure that participants repeatedly matched the prescribed torque without fatigue. The participants maintained 3-D isometric torques in 8 different combinations of torque production for 5 seconds. Each 3-D torque included an equal component of torque in each degree of freedom of the shoulder: flexion/extension, internal/external rotation, and vertical abduction/adduction. A real-time display of 3-D shoulder torques was provided. The recorded EMG data was detrended, high-pass filtered with a 4th order Butterworth filter with a 30Hz cutoff, full-wave rectified, and RMS filtered over a 200 ms window, and normalized to MVC. Muscular demand was also computed, a singular weighted measure of total muscle activity determined from surface EMG recordings of 12 upper extremity muscles scaled to each muscle's physiological cross-sectional area [4]. A repeated measures ANOVA model examined how muscular demand and individual EMG data differed with time and between the eight prescribed 3-D torque targets. A p-value < 0.05 was considered significant.

Results & Discussion: Muscular demand was significantly increased at 12-month follow-up compared to baseline ($F_{1,64} = 9.1$, $p = 0.004$), but there was no significant main effect of torque target on muscular demand ($F_{7,64} = 0.1$, $p = 0.99$). Further examination of individual muscle EMGs found significantly increased activation of the pectoralis major sternocostal region, middle trapezius, latissimus dorsi, and serratus anterior (all $F_{1,64} > 4.8$, $p < 0.033$) and decreased activation of the posterior deltoid ($F_{1,64} = 6.2$, $p = 0.015$) between pre-operative assessment and 12-month follow-up (Fig. 1).

These results directly oppose our hypothesis and instead suggest women undergoing prepectoral implant-based breast reconstruction experience altered neuromuscular control of the shoulder despite undergoing a less invasive reconstructive procedure. Further work is needed to delineate the source of this dysfunction. One possibility is the removal of the pectoral fascia during standard mastectomy procedures may alter the modulation of muscle contraction [3]. While the study is currently underpowered (71% power), ongoing recruitment will yield additional participants to achieve 80% power (*a priori* sample size = 12). While it's difficult to prospectively assess surface EMG muscle activity given its sensitivity to the electrode location over the muscle belly, we mitigated these concerns by standardizing electrode placement to anatomical structures.

Significance: Women undergoing mastectomy with prepectoral implant-based breast reconstruction exhibit altered neuromuscular control of the shoulder at 12-month follow-up, suggesting post-operative physical therapy focuses on retraining the activation of muscles around the shoulder.

Acknowledgments: American Cancer Society RSG-20-016-01-CCE

References: [1] Kummerow et al. (2015) *JAMA Surgery* 150. [2] Becker et al. (2015), *Plast Reconstr Surg Glob Open* 6. [3] McFarland et al. (2018) *Appl Ergon* 73. [4] Stecco et al. (2014) *Curr Phys Med Rehabil Rep* 2.

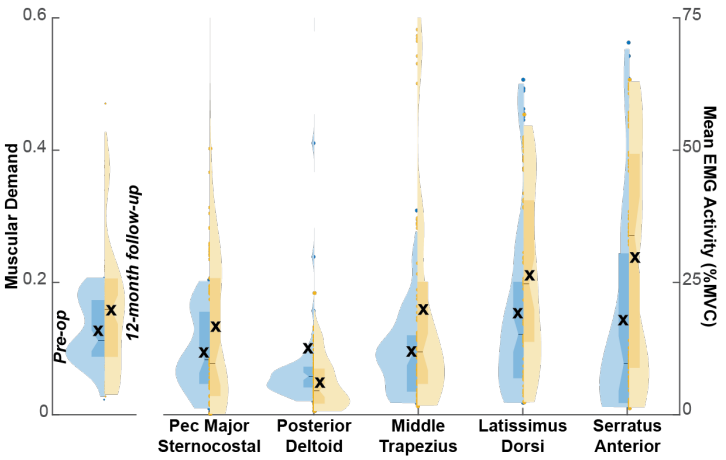

Figure 1: Violin-box plots for muscular demand (left) and mean EMG activity for the five muscles (right) with the greatest difference between the pre-operative visit (blue) and 12-month follow-up (yellow). The notch line indicates median and 'x' indicates mean values.

SEATED INFANT PRODUCTS ALTER BODY POSITION AND MUSCLE UTILIZATION

Danielle N. Siegel[1], Sarah M. Goldrod[2], Holly Olvera[1], Andrew Bossert[2], Christopher Wilson[2], Trevor J. Lujan[2], Brandi Whitaker[3], John L. Carroll[3], Erin M. Mannen[1,2*]

[1]Biomedical Engineering Doctoral Program, Boise State University [2]Mechanical & Biomedical Engineering Department, Boise State University [3]Arkansas Children's Research Institute *Presenting author's email: ErinMannen@BoiseState.edu

Introduction: The musculoskeletal and motor development of infants is greatly affected by their environment [1], which varies from being held in arms, lying on a firm flat surface, to spending time in various nursery products. In the U.S., infants spend an average of 5.7 hours (range 0-16 hours) per day in seated products like car seats used outside of a motor vehicle (infant carrier), bouncers, rockers, and swings [2,3]. Excessive time in these types of products, specifically car seats, has been shown to alter an infant's development and muscle utilization [4-8]. Additionally, previous research has found that increased suffocation-related hazards exist when lying in inclined products due to the changes in body position, particularly with their head and torso [9-11]. While many different injuries can occur involving seated products, infants zero to six months are more likely to suffer breathing-related injuries caused by suffocation compared to older children [12], in part due to their less-developed respiratory system and arousal response [13,14]. Because of the design features present in seated products, infants may be forced into higher head-neck flexion and a slouched position, increasing their risk for a breathing-related incident. The purpose of this study was to assess how an infant's muscle activation and body position are altered while lying supine in four commercial infant products (carrier, bouncer, rocker, and swing) compared to a firm flat playmat.

Methods: Thirteen healthy infants (4.2±1.4 mos; 7M/6F) participated in this IRB-approved study. Surface electromyography (EMG) electrodes (Delsys, 2000Hz) recorded muscle activity from the cervical paraspinals (CP), erector spinae (ES), abdominal muscles (AB), and quadriceps (QUAD) (**Fig. 1A**). A retroreflective marker-based motion capture system (Qualisys, 100Hz) tracked infant kinematics using custom 3-marker (6.5mm) rigid body clusters on the head, torso, and pelvis and 9.5mm markers on the shoulders and anterior superior iliac spine (ASIS) (**Fig. 1A**). Infants laid supine on a firm flat playmat (**Fig. 1B**) and unrestrained in a commercial infant carrier, bouncer, rocker and swing (**Fig. 1C**), each for three minutes. Using MATLAB, the EMG signal was filtered, and the mean was taken over 60 seconds for each condition and muscle group, then normalized to a percent of the playmat condition. The kinematic data was analyzed using MATLAB to determine the head-neck and torso-pelvis flexion by finding the angular orientation between adjacent body segments from the local coordinate systems defined by rigid body clusters on each segment in an ideal position (head, torso, and pelvis visually aligned in the sagittal plane). The trunk flexion was determined using the law of cosines between the shoulder and ASIS markers. All angles were normalized to the playmat condition to account for each infant's anatomical differences. Paired t-tests ($p<0.05$) were completed to compare the carrier, bouncer, rocker, and swing results to the playmat.

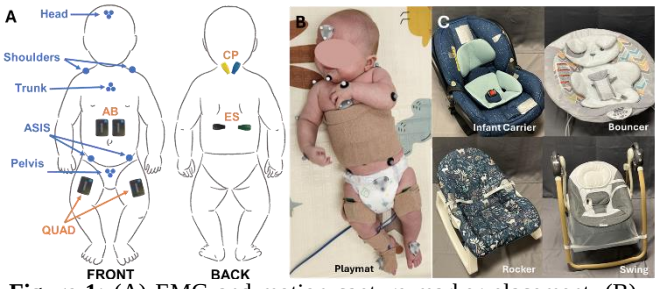

Figure 1: (A) EMG and motion capture marker placement, (B) experimental setup on playmat, and (C) four seated products.

Results & Discussion: In all seated products tested, infants exhibited increased head-neck and torso flexion of up to 21° and 27° above the playmat, respectively (**Fig. 2)**. Previous research has determined that head-neck flexion angles of just 15° to 30° can alter infant breathing patterns significantly [15]. Trunk flexion was significantly higher for all products (between 23° and 27° on average) compared to the playmat which relates to the conformity and/or concavity of the product in the longitudinal direction. For most products, infants exhibited higher abdominal muscle activity, which may indicate that infants use their diaphragmatic muscles at a higher level to overcome breathing challenges related to the flexed posture [16,17].

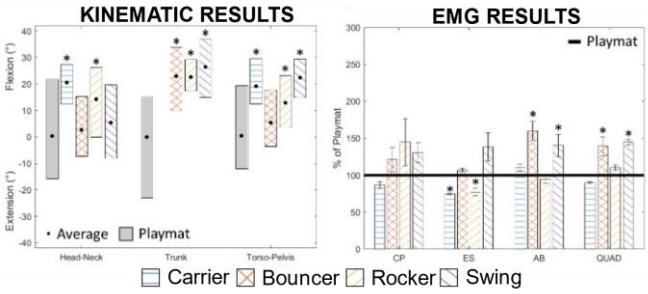

Figure 2: Kinematic results (left-mean, min, and max) and EMG results (right-mean ± stdev). *$p<0.05$ compared to the playmat.

Significance: This research quantified body posture and muscle activity of infants lying in a variety of seated products. Our results suggest that infants should avoid prolonged use to prevent respiratory-related hazards and musculoskeletal or motor developmental delays.

Acknowledgments: This research was part of a larger study funded by the U.S. Consumer Product Safety Commission (CPSC, Commission) under contract number 61320620D00002/61320621F1014. It has not been reviewed or approved by, and may not necessarily reflect the views of, the Commission. We acknowledge support from NIH NIGMS IDeA award P20GM148321.

References: [1] Hadders-Algra 2018, *Neuro & Biob Revs*; [2] Little 2019, *Inf Beh & Dev*; [3] Callahan 1997, *Arc Peds & Ado Med*; [4] Littlefield 2003, *JOP J Prosth & Orthot*; [5] Pin 2007, *Dev Med & Child Neuro*; [6] Jiang 2016, *Ped Phys Ther*; [7] Siddicky 2020, *J Biomech*; [8] Siddicky 2021, *J Ortho Res*; [9] Mannen 2019, *U.S. CPSC Report on Incl Sleepers*; [10] Wang 2020, *J of Biomech*; [11] Wang 2021, *J of Biomech*; [12] Gaw 2017, *Peds*; [13] Horne 2002, *Ear Hum Dev*; [14] Trachsel 2022 *Ped Anesth* [15] Wilson 1980, *J Appl Physio*; [16] Lee 2010, *Resp Phys & Neurobio* [17] Lin 2006, *Arch Phys Med & Rehab*.

MULTISCALE COMPUTATIONAL MODELING OF SOLEUS MUSCLE MECHANICS DURING SIT-TO-WALK

Katherine R. Knaus*, Michael F. Miller, Anne K. Silverman
Department of Mechanical Engineering, Colorado School of Mines
*katherine.knaus@mines.edu

Introduction: Sit to walk (STW) transitions are critical for independent living. Often, individuals select different foot placements to facilitate this transition [1], but how these placements are related to underlying muscular function is unclear. Foot placement can affect ankle angles and therefore musculotendon operating lengths, which will influence muscle force output. Muscle function is also likely to change with injury, across individuals, and throughout the lifespan. Modeling approaches are ideally suited to determine the mechanistic relationship between muscle function and whole-body movement. Whole-body musculoskeletal models can predict muscle coordination during transitional tasks, but often only include simplified, one-dimensional musculotendon representations. Tissue-level finite element models can overcome this limitation but require inputs from whole-body tasks to drive and validate output results. Combining these two model scales provides insight into muscular force generation, dynamic tendon interactions, and how tissue function results in observable whole-body movement. The purpose of this study was to determine how initial foot placement affects muscle behavior during STW. We hypothesized that an initial position in which the stepping limb is posteriorly offset from the other with the ankle in dorsiflexion will stretch the stepping limb soleus which will increase initial passive force and alter active soleus force generation in transition to walking.

Methods: Whole-body kinematic (200 Hz, Qualisys), ground reaction force (2000 Hz, AMTI), and surface electromyography (2000Hz, Delsys) data were collected on 15 healthy adult volunteers (7M/8F, 24.3±4.4 yrs, 72.7±13.2 kg, 1.73±0.10 m, 15 right foot dominant). Each participant began seated on a backless stool, without shoes and with socks, with arms folded across the chest in one of two initial foot positions (1) Symmetric, with knees at 90° and the feet hips-width distance apart and (2) A/P (anterior/posterior) offset, where the dominant foot was shifted posteriorly ⅔ of the foot length distance. Volunteers rose and transitioned to walking at a self-selected speed. Bilateral ankle angles and moments were determined from a 12-segment dynamic model with six degree of freedom joints in Visual3D. Ankle angles were imported into OpenSim v4.4 to calculate soleus musculotendon lengths from the gait2392 model [2] for STW from the initiation of torso movement to the second toe-off of the stepping foot. Bilateral soleus EMG data were digitally band-pass filtered with a 4th order Butterworth filter (20-500 Hz), full wave rectified, low pass filtered (fc=6 Hz), and magnitude normalized by the peak processed signal during functional heel-raises. Average soleus EMG data and musculotendon lengths were converted to apply as varying activation and length change inputs, respectively, to an image-based 3D finite element model (FEM) of the soleus muscle [3]. The FEM included distinct structures for the soleus muscle compartments and aponeuroses, which were both represented as transversely isotropic materials, and were meshed as tetrahedral elements with assigned fiber directions. Model predictions of passive architecture changes and eccentric tissue displacements were validated with diffusion and dynamic imaging [3]. STW simulations were performed in FEBio with passive prescribed soleus length changes for the (a) Stepping and (b) Stance limb in the (1) Symmetric and (2) A/P offset conditions [Fig. 1], beginning with an initialization phase to stretch the soleus to its length in the seated position. Simulations were repeated for each case with prescribed activation changes applied during STW.

Results & Discussion: In the A/P offset condition, the soleus of the stepping limb was stretched in the seated position and began STW with greater force than in the stance limb, unlike the Symmetric case where initial soleus force was equal in both limbs [Fig. 1A]. While initial soleus force was greater in A/P offset, forces during walking were lower than in the symmetric case. Further, the soleus force in the stepping limb had a greater active contribution during the start of walking in the Symmetric case [Fig. 1B].

Significance: This work builds on existing understanding of musculotendon function in steady-state tasks by investigating muscle contributions to non-steady-state transitional tasks that are critical in daily living. Multiscale modeling demonstrates variable muscle behavior in the context of movement strategy, providing insight into how passive and active mechanisms of tissue function relate to whole-body biomechanics. The results provide a baseline to compare muscle mechanics and energetics in populations with injury or musculoskeletal deficits, elucidating how muscles facilitate forward movement and contribute to stability when force production and energetic capacity is altered.

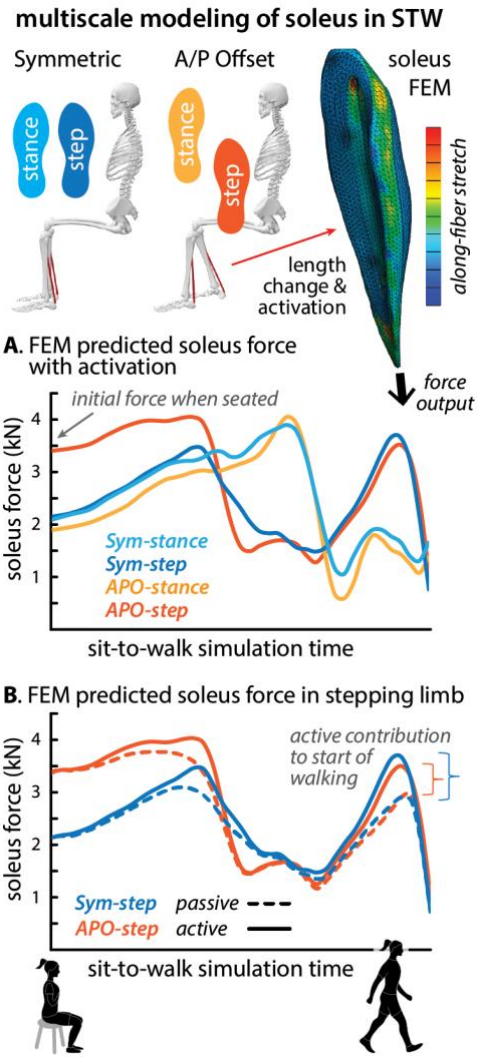

Figure 1: Multiscale model predicted soleus function in the stance and stepping limb during STW with Symmetric and A/P Offset initial foot placement. **A.** Soleus force was predicted from FEM simulations in each case with prescribed length change and activation. **B.** Predicted soleus force is shown for the step limb during STW with activations prescribed (active) or set to 0 (passive).

References: [1] van der Kruk et al. *npj Aging*, 2022; [2] Delp et al. *IEEE Trans Biomed Eng*, 1990; [3] Knaus et al. *J Biomech*, 2022

ENHANCING HIP EXTENSION MOMENTS DURING GAIT INITIATION FOR STUDYING ABNORMAL HIP EXTENSION -ADDUCTION COUPLING IN STROKE

Mounika Pasavula[1], Julius P.A. Dewald[2], Myunghee Kim[1*], M. Hongchul Sohn[2*]
[1]Department of Mechanical and Industrial Engineering, University of Illinois at Chicago
[2]Department of Physical Therapy and Human Movement Sciences, Northwestern University
*Corresponding authors' email: myheekim@uic.edu, hongchul.sohn@northwestern.edu

Introduction: Lower limb motor deficits after stroke pose significant challenges to balance during gait initiation, particularly in the frontal plane [1]. While studies have largely focused on behavioral aspects of these impairments, there remains a notable gap in understanding the underlying neural mechanisms. This study aims to elucidate the impact of stroke-induced neural constraints in controlling various degrees of freedom in the paretic leg following a stroke, which likely stems from an increased reliance on brainstem motor pathways in place of the injured corticospinal pathways [2]. Specifically, we focus on the abnormal coupling between hip extension and adduction torques previously found in individuals with stroke during isometric torque generation tasks [3,4]. We hypothesize that when stepping with the nonparetic limb, the reduced ability in the paretic standing limb to abduct while extending will impact frontal plane behavior/balance. To test our hypothesis, we propose to induce the abnormal hip extension-adduction coupling by increasing hip extension torque demand in the stance limb during gait initiation with a longer step and/or by applying resistance through a passive exosuit. In this case, study with one healthy participant, our goal was to validate the experimental design in demanding the level of hip extension torque that will fall within the range for inducing coupling in future experiments with the stroke participants.

Methods: A healthy female subject (age 28) performed gait initiation (a step with non-dominant (left) leg, arms crossed), under two-step length conditions (*normal* and *long*) × two exosuit conditions (*with* and *without* resistance), each repeated 7 times. *Normal* and *long* step lengths were determined by the preferred and maximum comfortable (80% of height) steps for the participant, respectively, and were controlled during the experiment by marks on the floor. The soft, passive hip exosuit (Hurotics Inc., Seoul, Korea) exerted pulling force at the thigh when engaged with an elastic band, and thereby resisting hip extension. The force was measured with a 1-DoF loadcell. Three-dimensional motion (legs and trunk) and ground reaction forces (stance and stepping legs) were measured with motion capture and force plates, respectively, with which joint angles and moments were calculated; band forces were excluded from inverse dynamics. By our experimental design and protocol, we expect to: 1) control sagittal plane kinematics (increased flexion/extension in the *long* step; same *with* vs. *without* resistance within each step length); 2) increase hip extension torque demand in the *long* step, and to a greater extent *with* resistance (greater tension); 3) that is sufficient to induce hip extension-adduction torque coupling in individuals with stroke.

Results & Discussion: Our experimental setup successfully controlled sagittal plane movements and increased hip extension torque demand both by increasing step length and adding resistance. However, resistance did not further increase torque in *long* steps compared to *normal* steps. Hip flexion in the stepping leg and extension in the stance leg increased with *long* step, regardless of resistance (Fig. 1A). Hip extension moment in the stance leg was greater in the *long* step compared to *normal*, step; however, resistance had the same effect in both step lengths, contrary to our expectation (Fig. 1B). We found that increased right-ward trunk rotation at peak hip extension in the stance leg (12.26±3.09º) and (28.74±3.86º) in *normal* and *long* step *with* resistance, respectively) mainly canceled out the additional tension that would have occurred by increased step length. We also found that lateral stance foot displacement was highly variable in *long* step *with* resistance (20.15±20.03cm; CV=0.99), compared to *normal* (20.12±14.32cm; CV=0.72), indicating frontal plane balance challenge even for the participant. These results suggest that future experiments with stroke participants must better control for trunk and frontal plane behavior to not confound the effect of the abnormal coupling induced by increased hip extension demand.

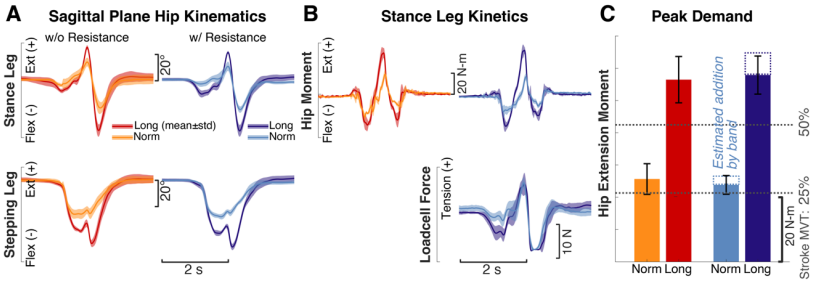

Figure 1. A) Sagittal plane hip joint angles in the stepping (top) and stance (bottom) legs. **B)** Sagittal plane hip moment (top) and resistance force (bottom) in stance leg. **C)** Hip extension moment with respect to the levels (horizontal dotted lines) known to induce abnormal extension-adduction coupling in a previous study [4].

Nevertheless, our protocol's hip torque demand is expected to induce abnormal hip extension-adduction torque coupling in individuals with stroke. Specifically, mean peak hip extension torques we observed fall within the range of 28.2-68.5% of maximum voluntary hip extension torques (MVT) for individuals with stroke (n=12), as reported in previous studies [3,4] (Fig. 1C). These studies present that at 25% and 50% of hip extension torque reduced the ability to produce abduction torque by 85% and even result in net adduction, respectively [4]. While individuals with stroke are likely to generate less extension torque (smaller/slower steps) during gait-initiation. However, the added resistance by the exosuit (simplified estimation shown in Fig. 1C), set to be factored into future inverse dynamics analysis, alongside the balance challenge will further heighten the manifestation of the abnormal coupling.

Significance: This case study validated an experimental protocol aimed at investigating the effect of abnormal hip extension-adduction coupling on gait initiation after stroke. The forthcoming main study with individuals with stroke using the protocol revised from these findings will reveal the effect of the altered neural control (upregulated reticulospinal pathways) of the lower limb after stroke on functional tasks such as gait initiation and may inform mechanistic approaches for more effective therapeutic interventions.

References: [1] Ryo et al., *J Rehab Med* (2021); [2] Macpherson et al., *J Physiol* (2018); [3] Sánchez et al., *Neurorehab and Neural Repair* (2017); [4] Sánchez et al., *Front in Neurol* (2018); [5] Yang et al., *J NeuroEng and Rehab* (2021).

SHORT-TERM EFFECTS OF PROPULSION FUNCTIONAL ELECTRICAL STIMULATION ON WALKING SPEED AND THE ENERGY COST OF WALKING AFTER STROKE

Ashlyn Aiello[1], Johanna Spangler[1], Kimberly Ang[1], Ashley Collimore[1], Dabin Choe[2], Ruoxi Wang[1], Conor Walsh[2], Louis Awad[1*]
[1]Sargent College of Health and Rehabilitation Sciences, Boston University, Boston Massachusetts, USA
[2]John A. Paulson School of Engineering and Applied Sciences, Harvard University, Cambridge, Massachusetts, USA
*Corresponding author's email: louawad@bu.edu

Introduction: The slow and energetically inefficient walking that is commonly observed after stroke is associated with impaired gait propulsion [1]. A reduced ability to produce paretic plantarflexor force is a key contributing factor to impaired gait propulsion [2]. We developed a functional electrical stimulation (FES) neuroprosthesis to safely assist post-stroke gait propulsion during overground walking by coordinating stance-phase plantarflexor neurostimulation needed for push off with swing-phase dorsiflexor neurostimulation needed for foot clearance [3]. Building on prior report of a variable therapeutic response to *treadmill*-based gait training with propulsion FES [4], the primary objective of this study was to evaluate short-term therapeutic effects of this *overground* intervention across patient subgroups prospectively identified by walking speed and degree of plantarflexor neuromotor impairment [5]. Although we expect faster and more energetically efficient walking after the overground gait training with the propulsion FES neuroprosthesis, given the heterogeneity of post-stroke gait impairments, we hypothesize that there would be differences in the intervention's effects across subgroups.

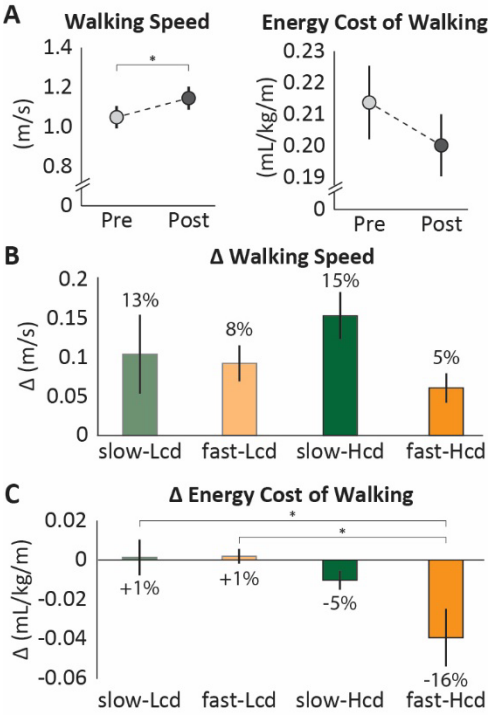

Figure 1: A) Group-level pre-to-post training changes. Subgroup analysis of **B)** walking speed and **C)** energy cost of walking.

Methods: Seventeen individuals with chronic post-stroke hemiparesis (mean ± SD: age 57.5 ± 10.9 years; time since stroke 6.5 ± 4.3 years; 3 female; 13 left side paretic) completed two study visits: a baseline evaluation session that measured walking speed and plantarflexor central drive [5] used to classify individuals into subgroups, and a gait training session that provided 30-minutes of overground walking practice with propulsion FES. The therapeutic outcomes measured before and after the 30-minutes of gait training included overground walking speed from timed walks around a 26.6-meter track and energy cost of walking from breath-by-breath metabolics (COSMED K5, Rome, Italy) collected during 3-minute treadmill walks. Using the SPSS software package, group-level therapeutic effects were assessed using paired t-tests of pre- and post-training data with alpha = 0.05. Between-subgroup differences were assessed using one-way ANOVA with least significant difference post-hoc tests. Group and subgroup data are reported in text as mean ± standard deviation (SD) with Cohn's d effect sizes (ES) and presented in the figures for comparison as mean ± standard error (SE).

Results & Discussion: After the 30 minutes of walking practice with propulsion FES, we observed large (ES = 1.46) and statistically significant ($p < 0.001$) group-level improvements in fast walking speed (0.10 ± 0.07 m/s, **Fig. 1A**). Moderate (ES = -0.51) group-level improvements in the energy cost of walking were also observed (-0.013 ± 0.026 mL/kg/m) that did not reach statistical significance ($p = 0.054$, **Fig. 1A**). We then assigned subjects to one of four *a priori* subgroups by applying median cutoff thresholds to their baseline paretic plantarflexor central drive (median = 47.79%) and walking speed (median = 0.89 m/s): slow individuals with i) low and ii) high central drive and fast individuals with iii) low and iv) high central drive (slow-L_{cd}: N=4, slow-H_{cd}: N=4, fast-L_{cd}: N=4, fast-H_{cd}: N=5). The intervention-induced improvement in walking speed did not differ significantly across the subgroups ($F = 1.526$, $p = 0.255$, ES = 0.26, **Fig. 1B**); however, the intervention-induced change in energy cost of walking was significantly different ($F = 3.949$, $p = 0.033$, ES = 0.26, **Fig. 1C**). Post-hoc testing revealed that the fast-H_{cd} subgroup had the greatest reduction in the energy cost of walking (-0.039 ± 0.033 mL/kg/m, ES = -1.20), which was significantly larger than the modest *increases* observed in the fast-L_{cd} (+0.002 ± 0.007 mL/kg/m, $p = 0.012$) and slow-L_{cd} (+0.001 ± 0.018 mL/kg/m, $p = 0.013$) subgroups. A baseline threshold for plantarflexor central drive may be required for patients to benefit energetically from propulsion FES gait training. Adjunctive pre-interventions that increase plantarflexor central drive may be a promising way to convert energetic non-responders to responders. Similarly, if plantarflexor central drive improves with repeated training visits, more individuals may experience concurrent speed and energetic benefits in the long-term.

Significance: A single session of overground gait training with propulsion FES is effective across patient subgroups in improving walking speed in the short-term. Fast individuals with high plantarflexor neuromotor control also demonstrate a marked reduction in the energy cost of walking. Baseline evaluation of paretic plantarflexor function can provide prognostic insight into the magnitude of recovery in walking quality, beyond improvements in speed, that can be expected with overground propulsion FES gait intervention.

Acknowledgments: Funding sources (AHA #830019, NSF #CMMI-1925085, NIH Blueprint subproject #15922).

References: [1] Awad et al. (2015), *Neurorehabil Neural Repair* 29(6); [2] Nadeau et al. (1999), *Clin Biomech* 14(2); [3] Choe et al. (in review), *OJEMB*; [4] Kesar et al. (2015), *Phys Med Rehabil Int* 2(10); [5] Collimore et al. (2024), *Bioengineering (Basel)* 11(2).

IMPROVEMENT IN FUNCTION FOR PATIENTS WITH BRACHIAL PLEXUS INJURIES USING A POWERED ELBOW ORTHOSIS

Sandesh G. Bhat, PhD[1]*, Emily J. Miller[1], Paul Kane[1], Kevin Hollander, PhD[2], Claudio Vignola, Ph.D.[3], Alexander Y. Shin, MD[1], Thomas G. Sugar, PhD[3], Kenton R. Kaufman, PhD[1]
[1]Mayo Clinic, Rochester, MN; [2] Augspurger Komm Engineering Inc., Phoenix, AZ; [3] Arizona State University, Tempe, AZ
*Corresponding author's email: bhat.sandesh@mayo.edu

Introduction: Navigating the path to recovery from a brachial plexus injury (BPI) poses significant challenges, involving intricate surgeries and extensive physical rehabilitation. Muscle strength takes up to 2 years to mature [1]. About 30% patients are unable to overcome gravity after the typical recovery period. In such cases, orthotic devices may be used to facilitate movement in the affected limb. Current commercially-available powered orthotic devices use the weak elbow flexor's activity to assist with flexion and are criticized for their bulky form-factor, inducing fatigue and reducing function during use in daily life [2]. The current commercially-available orthosis requires a sustained muscle activation to maintain the elbow position in flexion, which results in fatigue. To address this limitation, an innovative, lightweight powered myoelectric elbow orthosis has been developed. The orthosis utilizes a brake mechanism to hold the elbow in a flexed position, allowing the user to relax their muscle. Laboratory testing was performed to assess the fatigue and improvement in function, based on EMG activation, during activities of daily living when using the new orthosis.

Methods: 11 subjects with a BPI were studied under IRB no. 20-006849 (Age: 35 ± 13 years; BMI: 30.3 ± 6.3 $kg.m^{-2}$; Time since surgery: 44 ± 26 months). Manual muscle testing grades were used to assess their elbow flexion capabilities prior to testing. A certified orthotist fit the subjects with a custom attachment for the exoskeleton. A surface electromyography (EMG) sensor (EMG500, Motion Lab Systems, Inc., Baton Rouge, LA) was placed on the elbow flexor and signal activation thresholds were established. A 19-camera motion capture system (Raptor-12, Motion Analysis Corporation, Santa Rosa, CA) was used to obtain the elbow kinematics. 3 subjects were excluded due to technical issues during data collection. 2 subjects had a substantially low elbow flexor signal (MMT < 2) so, an alternate EMG sensor placement location (muscle belly of the upper trapezius) was used. The raw EMG data collected was band-pass filtered (4th order Butterworth filter with half powers at 20 Hz and 450 Hz) and full wave rectified. The subject performed three repetitions of four activities of daily living (ADLs), with and without the orthosis. The subjects were instructed to move their affected arm as if they were going to eat a granola bar (Hand to Mouth), move their affected arm as if they were going to scratch the top of their head (Hand to Head), stabilize an object (a clay ball) with their affected arm and slice it like a potato three times with their unaffected arm (Object Stabilization), and pick up the basket (with weights in it) with their unaffected arm, flex their affected arm and slide it under the basket handle to carry the basket 10 feet (Carry Task). The weights were increased until the subjects failed to lift the basket. Frequency domain analysis was performed on the EMG data using the median frequency [3] and the average power [4] when elbow flexion was held.

Results & Discussion: Despite the difference in time of recovery, all the subjects were able to flex and extend the orthosis. 83% of the subjects were observed to have either a higher average power or lower median frequency, associated with fatigue, during some or all of the activities without the orthosis (Fig 1). This preliminary data indicated the amount of fatigue experienced by the subjects might be reduced while using the orthosis. During the carry task, the subjects lifted significantly more weights with the orthosis (1 ± 0.8 kg more than without the orthosis), notably, the 2 subjects at MMT < 2 were able to lift an average weight of 0.4 kg with their weak elbow flexor signal. Hence, the orthosis improved function in the BPI subjects. It was also observed, via the EMG data, that the subjects did not relax their elbow flexors to rest their forearm on the orthosis during the activities. Similar observations were made in a prior study, where the BPI subjects, 17 months post-op, were shown to be incapable of relaxing their elbow flexors on command [5]. The subjects spent only 30 mins with the orthosis before data collection in the current study. Hence, further orthotic training might improve their ability to relax their elbow flexor and gain better functionality with the orthosis.

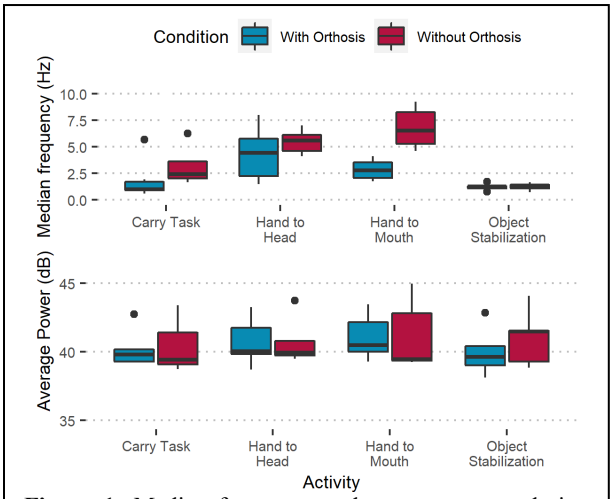

Figure 1: Median frequency and average power during activities of daily living.

Significance: The orthosis improved the subjects' elbow function during activities of daily living. Using the orthosis was observed to reduce fatigue in the subjects' elbow flexor. The subjects' inability to relax their elbow flexor on command highlights the importance of proper orthotic training.

Acknowledgements: The study was supported by the Department of Defense Grant No. W81XWH-20-1-0923.

References: 1. Noland, S.S., et al.(2019) JAAOS, 27(19): 705-716. 2. Webber, C.M., et al.(2021) Prosthet. Orthot. Int., 45(6): 526-531. 3. Roy, S.H., et al.(2009) IEEE Trans. Neural Syst. Rehabil. Eng., 17(6): 585-594. 4. Octavia, J.R., et al.(2015) Mult. Scler. Int., 2015. 5. Bhat, S.G., et al.(2023) Clinical Biomechanics: 105951.

THE EFFECT OF ANKLE EXOSKELETONS ON TIBIOFEMORAL FORCE IN PEOPLE WITH CEREBRAL PALSY

Ying Fang[1,2*], Zachary F. Lerner[1,3]
[1]Department of Mechanical Engineering, Northern Arizona University, Flagstaff, AZ 86011, USA
[2]Department of Physical Therapy, Rosalind Franklin University, North Chicago, IL 60064, USA
[3]Department of Orthopaedics, the University of Arizona College of Medicine-Phoenix, Phoenix, AZ 85004, USA
*Corresponding author's email: ying.fang@rosalindfranklin.edu

Introduction: Many people with cerebral palsy (CP) have gait pathology that may change joint loads, which lead to pain and joint degeneration [1]. Joint pain affects 44% of children with CP and 70% of adults with CP, limiting their daily function and activity level [2]. Ankle exoskeleton can improve gait patterns in people with CP [3]. The purpose of this study was to quantify compressive tibiofemoral force in people with CP during level walking with and without ankle exoskeleton assistance using two modeling approaches. We hypothesize that both approaches would indicate that the ankle exoskeleton would reduce tibiofemoral force in CP.

Methods: Eleven participants with CP (age: 20 ± 9 years; mass: 55 ± 9 kg, gross motor function classification system: I – III) completed two one-minute walks at preferred speed on a treadmill: one wearing normal shoes and one with ankle exoskeleton assistance. We collected motion, force, and muscle activity of eight lower limb muscles for the more affected limb. Joint angles and moments were derived in OpenSim 3.3, and the stance phase of three representative gait cycles were used to estimate tibiofemoral force. Muscle force was estimated using two approaches: the static optimization uses cost function that minimizes the sum of squared muscle activation; the EMG-informed approach minimizes the difference between estimated and measured EMG for all eight muscles [4]. Joint contact force was calculated using Joint Reaction Analysis in OpenSim [5]. Two-way repeated measures analysis of variance (ANOVA) were used to detect the main effects of ankle conditions and modelling approaches, and their interactions ($a < 0.05$).

Results & Discussion: There was a main effect of modelling approach on the early-stance and late-stance peak tibiofemoral forces, and stance-phase average tibiofemoral force ($p < 0.001$). There was no effect of ankle condition on tibiofemoral force, contrary to our hypothesis. Even though the group-level results suggested that ankle assistance did not reduce tibiofemoral force, we observed a reduction in average tibiofemoral force in the majority (7 of 11 based on static optimization and 8 of 11 based on EMG-informed approach) of our participants when walking with compared to without ankle assistance (**Fig. 1**). The lack of group-level difference could be attributed to the short walking time, as we did not find any group-level differences in lower limb kinematics or muscle activities between walking with and without the exoskeleton. The exoskeleton has been found to improve posture and reduce muscle activities in people with CP with longer walking trials [3], suggesting that a longer period may be required for users with CP to walk with smaller joint loads. Estimated tibiofemoral force was greater using EMG-informed approach compared to static optimization. This was consistent with previous findings [6]. It makes sense that static optimization often results in the most "efficient" solution that cannot represent people with neurological impairment like CP, therefore, would underestimate joint loads. However, the two approaches produced similar group-level results, indicating that static optimization may be used to estimate exoskeleton effect when EMG data are not available.

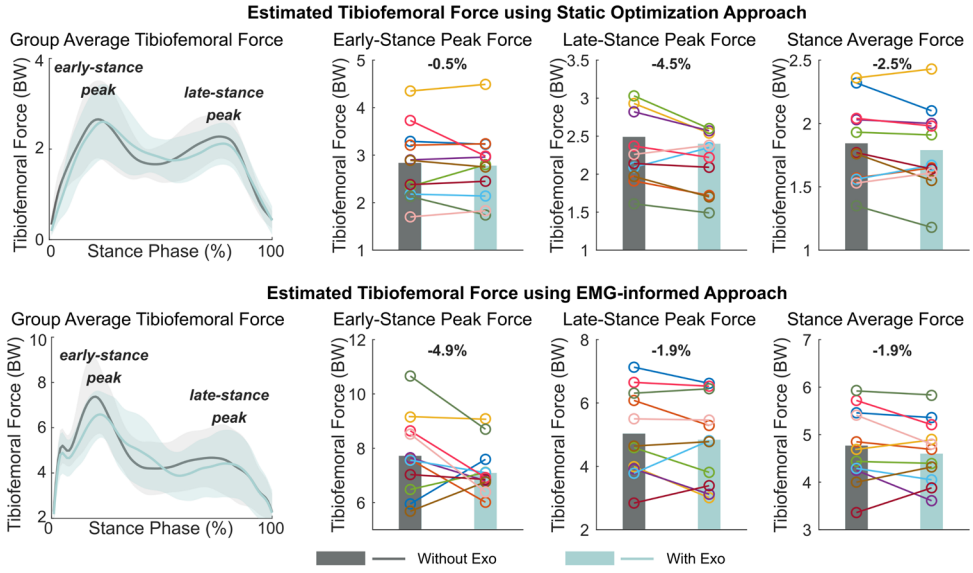

Figure 1: Stance-phase tibiofemoral force estimated using static optimization and EMG-informed approach during walking with and without ankle exoskeleton assistance in 11 participants with CP.

Significance: People with CP have a higher risk of joint pain and degeneration compared to the healthy population, and exoskeletons have potential to address this issue by improving their gait pattern and mobility. Our data indicate that ankle exoskeleton assistance can reduce tibiofemoral force in some, but not all, people with CP. Future research will focus on identifying neuromuscular and demographic characteristics of those who are more likely to benefit from the device.

Acknowledgments: This project was supported by National Institutes of Health under Awards F32HD109018 and 1R01HD107277.

References: [1] O'Connell et al. (2019), *Bone* 125; [2] van der Slot et al. (2021), *Ann Phys Rehabil Med* 64(3); [3] Lerner et al. (2019), *Ann Biomed Eng* 47(6); [4] Sartori et al. (2014), *J Biomech* 47; [5] Steele et al. (2012), *Gait Posture* 35(4); [6] Davico et al. (2020), *Clin Biomech* 72.

TARGETING PUSH-OFF MUSCLE RECRUITMENT IN CEREBRAL PALSY: COMPARING POWERED VS PASSIVE WEARABLE RESISTANCE

Emmanuella A. Tagoe[1*], Karl Harshe[1], Collin Bowersock[1], Zachary F. Lerner[1,2]
[1]Department of Mechanical Engineering, Northern Arizona University, and [2]College of Medicine-Phoenix, University of Arizona
*Corresponding author's email: eat277@nau.edu

Introduction: Effective recruitment of the ankle plantar flexor muscles is crucial for propulsion and forward progression during walking [1]. Individuals with mobility impairments like cerebral palsy (CP), the most prevalent childhood physical disability, often experience ankle muscle weakness that results in debilitated propulsion and forward progression necessary for efficient walking [2]. Targeted resistance training with powered robotic systems *(Figure 1A)* can elicit meaningful improvements in ankle muscle recruitment and strength for individuals with CP [3], [4]. However, these systems can be expensive, bulky, and often require expert knowledge to operate, which pose as barriers to clinical translation and practical at-home training. Thus, there is a clinical need for a simple and affordable tool that remains effective for training for CP rehabilitation. In this validation study, we sought to determine whether a simple passive device with adjustable spring stiffness would elicit similar improvement in push-off muscle recruitment as a powered systems with motorized resistance.

Methods: Pictured in *Figure 1B*, we developed a simple ankle device that used a leaf spring to provide adjustable plantarflexion resistance during walking to elicit improved push-off muscle recruitment. Peak resistance delivered by the spring was 0.08 Nm/kg. Our device utilized onboard sensors and a microcontroller with BLE to provide real-time audiovisual biofeedback of estimated ankle power. To validate the effectiveness of this passive ankle device, individuals with cerebral palsy (n=7, all male) tested both the passive ankle device *(Passive)* and a powered ankle exoskeleton *(Powered)* at a matched resistance and with identical biofeedback in a block-randomized order *(Figure 1A & B)*. Participants also walked without either device *(Baseline)*. Participants walked at their preferred speed on a treadmill for all conditions. Soleus muscle activity was recorded for all conditions to evaluate its mean and peak activations. Prior to any data collection, participants walked in both devices for ~15 minutes each to acclimate to each device and the biofeedback system. We performed a one-way repeated measures ANOVA to assess if any of the conditions was different. Pairwise comparisons with Holm-Bonferroni correction for multiple comparisons (adjusted significance level set at 0.05) was performed after significant main effects were seen.

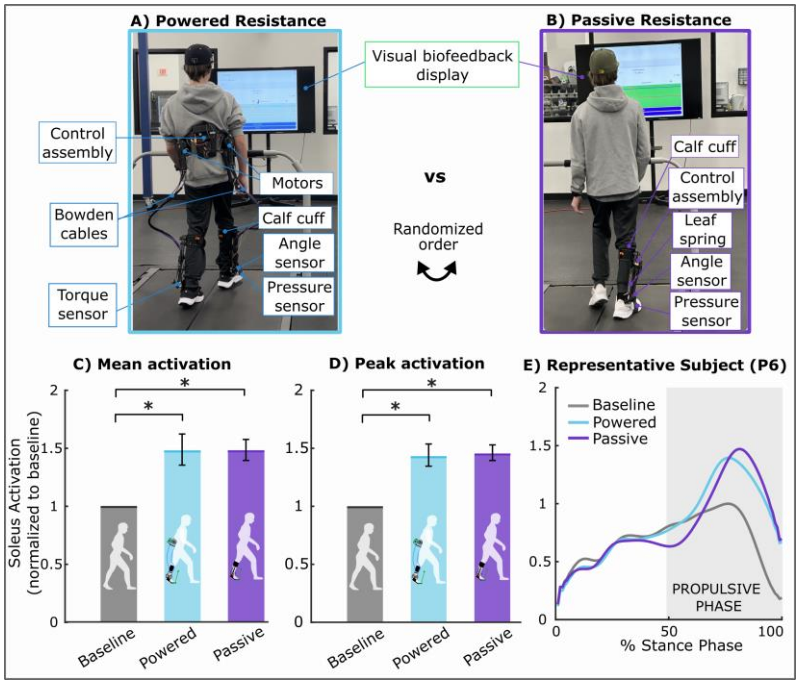

Figure 1: Pictures of A) Powered and B) Passive ankle device on a participant during study. C) Mean and D) Peak propulsive phase soleus activation relative to baseline walking for baseline walking, walking with the powered device and walking with the passive device at the group level. E) Mean soleus activation curve for baseline (gray), powered resistance (blue), and passive resistance (purple) walking conditions for one participant. Error bars represent standard error of the mean, brackets represent pairwise comparisons between respective conditions and * indicates statistical significance at 0.05 level.

Results & Discussion: Gait training with passive resistance increased mean soleus activation by 45.4% ± 6.8% (mean ± standard error of the mean; p = 0.002, *Figure 1C*) and peak soleus activation by 47.8% ± 9.1% (p = 0.006, *Figure 1D*) relative to baseline walking. Improvements in mean (p = 0.999) and peak (p = 0.999) soleus activation were similar during gait training with the powered resistance system compared to the new passive resistance device *(Figure 1C, D & E)*. These results suggest that that individuals with CP can quickly (after ~15 minutes of acclimation) increase their push-off muscle recruitment by almost double when walking with a passive resistance relative to their baseline walking and in a similar manner as motorized robotic devices. These improvements seen with the passive ankle device are encouraging and set the stage for future work to explore if multi-week gait training with this passive device will elicit functional improvements in ambulatory ability.

Significance: The findings from this study demonstrates that a simple, passive ankle device providing targeted plantarflexion resistance with ankle power biofeedback is capable of effectively improving functional push-off muscle recruitment in individuals with CP. This supports future research on the long-term effects of functional training with passive ankle devices that lower barriers for clinical translation and practical at-home training by reducing cost and complexity.

Acknowledgments: The authors would like to thank the participants and their families for their participation in the study.

References: [1] Sutherland et al. (1980), JBJS 62(3) [2] Dietz and Berger (1995), Dev. Med. Child Neurol. 37(2) [3] Conner et al. (2020), IEEE Open J. Eng. Med. Biol., 1 [4] Conner et al. (2021) J. Biomech. 126

GIVE YOURSELF A HAND: A PASSIVE EXOSKELETON FOR SELF-ASSISTED PHYSICAL REHABILITATION

Julia Manczurowsky[1], Blake Karavas[1], Henry Mayne[2], David Nguyen[3], John Peter Whitney[3], Christopher J. Hasson[1*]
Departments of [1]Physical Therapy, Movement and Rehabilitation Sciences; [2]Electeical and Computer Engineering; [3]Mechanical and Industrial Engineering; Northeastern University; *Corresponding author's email: c.hasson@northeastern.edu

Introduction: Rapid progress in the field of rehabilitation robotics has produced increasingly complex devices. However, mechatronic sophistication may not always be necessary, for example, in the case of self-assistance. Here, we test a novel hand exoskeleton that allows an individual to use an unimpaired hand to assist their impaired hand with a functional task. Conceptually, this is similar to mirror therapy, an intervention where an individual performs motor actions with their unimpaired limb while observing the behavior in a mirror. This approach can promote neuroplastic changes in the brain that reduce limb impairment [1]. However, unlike mirror therapy, using an exoskeleton to self-assist provides additional relevant somatosensory feedback to the affected limb, which may help learning. In this study, we artificially impair one hand of healthy individuals using dysfunctional electrical stimulation (DFES) and then ask them to perform a reach-to-grasp-and-lift task. First, we evaluated the effect of just wearing the exoskeleton. Then, we tested the hypothesis that participants using the exoskeleton to self-assist would improve faster than those who could not self-assist.

Methods: Twenty healthy right-handed adults (26 ± 3 yrs, 16 males/4 females) participated. While sitting, participants were instructed to reach, grasp, and lift a wooden cylinder to a target height of 5 cm as fast as possible. During the reach, DFES activated their left wrist and hand flexor muscles to make their hand close involuntarily, starting 0.5 s before a "go" command that signaled they should begin reaching and ending when the trial was completed. This perturbation required participants to activate their extensor muscles to oppose the DFES-induced flexor activation and successfully grasp and lift the object. In some conditions, participants wore a passive (i.e., does not produce energy) exoskeleton (Fig. 1) on both hands so they could use their right unaffected hand to assist their left affected hand. The exoskeleton transferred force from one hand to the other with a hydrostatic transmission that used a hybrid air-water configuration [2]. The exoskeleton's weight was offloaded with a 50-foot-long elastic band (the length minimized fluctuations in the offload force from band length changes). Optical motion capture was used to track hand and object motion and calculate movement times and task success.

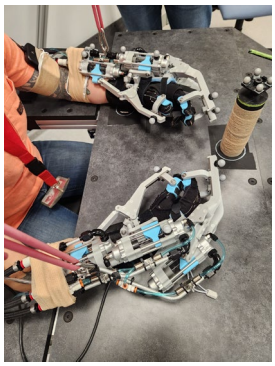

Figure 1: Passive exoskeleton.

The experiment was divided into two phases. Phase I evaluated the effects of the artificial impairment and wearing the exoskeleton. All 20 participants completed four conditions in a randomized order: 1) control, 2) artificial impairment, 3) exoskeleton, and 4) artificial impairment and exoskeleton together. Participants completed 20 trials in each condition. Phase II tested the self-assistance hypothesis. Participants were randomly assigned to either a self-assist group (n = 10) or a control group (only wore the exoskeleton on the left/impaired hand and could not self-assist; n = 10). Participants performed four practice blocks of 20 trials. The self-assist group performed a de-adaptation block where their ability to self-assist was removed, while the control group kept practicing the same no-assist condition. The primary outcome was reaching time (RT), defined as the time from the start of forward hand motion towards the object to when the object was lifted 2 cm off the table since this assured a functional grasp on the object was achieved.

For the Phase I analysis of RT, a two-way repeated measures ANOVA was performed with impairment state (on, off) and exoskeleton state (on, off) as independent factors. For Phase II, baseline performance was defined as the average RT during Phase I/Condition 4, and this was subtracted from each participant's data in Phase II to adjust for skill/impairment level. Exponentials were fit to each participant's adjusted RT data over the 80 Phase II trials, with two variables extracted: horizontal asymptote and rate of improvement; the latter was log-transformed due to non-normality (data from two people in the self-assist group were excluded because of poor exponential fits; they exhibited a slow linear increase in RT over practice). For de-adaptation (n = 10/group), the mean RT in the first 10 de-adaptation trials was used. Potential Phase II group differences were assessed using independent samples t-tests. Significance was set at $p < .05$.

Results: For Phase I, there were main effects of impairment state and exoskeleton state and no interaction. With or without wearing the exoskeleton, reaching was slower with the impairment compared to no impairment ($F = 26.5$; $p < .001$). With or without the artificial impairment, reaching was slower with the exoskeleton compared to no exoskeleton ($F = 112.9$; $p < .001$). For Phase II, the self-assist group decreased RT faster than controls ($p = .016$), but the horizontal asymptote (final extrapolated RT) was not different between the groups ($p = .329$). The de-adaptation RT was not different between the groups ($p = .450$).

Discussion: As expected, the artificial impairment (DFES) disrupted motor function by slowing reaching times. Wearing the exoskeleton also slowed reaching times. However, despite the exoskeleton encumbrance, participants who self-assisted with the exoskeleton to counter DFES improved their performance faster than controls and arrived at the same performance level. This does not include two participants who self-assisted but did not improve at all during the adaptation phase. Finally, there wasn't a performance penalty when self-assistance was removed during de-adaption, suggesting that participants did not become dependent on self-assistance.

Significance: This work suggests that a passive exoskeleton that transmits force and motion from one hand to the other may be useful for rehabilitation. A limitation of the approach is that it requires at least one limb to be functional for self-assistance; however, a caregiver or therapist could wear one side to assist instead. Since there are no electronics or motors, no specialized training is needed to use such a device, which may facilitate implementation in rehabilitation practice.

References: [1] Bhasin et al. (2012), *Neurology India*; [2] Whitney et al. (2016), *IEEE* (*ICRA).* **Funding:** Northeaster Univ. TIER 1

The effect of carbon fiber custom dynamic orthosis type on kinematics and kinetics of lower extremity joints in individuals with lower limb traumatic injuries

Jason M. Wilken[1], Sapna Sharma*, Kirsten M. Anderson, Molly S. Pacha, Kierra J. Falbo, Clare Severe, Andrew H. Hansen, Brad D. Hendershot, CARBON (CARBon fiber Orthosis research Network)
[1]Department of Physical Therapy and Rehabilitation Science, Carver College of Medicine, University of Iowa, Iowa City, Iowa
*Corresponding author's email: sapna-sharma@uiowa.edu

Introduction: Carbon-fiber custom dynamic orthoses (CDOs) have been used to improve gait mechanics during walking in individuals with lower limb trauma.[1] Most studies evaluating the effect of CDOs on gait mechanics focus on a single CDO that is commonly used in a military setting.[2] Multiple CDO designs are now used in civilian clinical practice, including stiff modular (MOD) devices with a rigid footplate (Figure 1. Reaktiv, FabTech Systems, Everett, WA) and more compliant monolithic (MONO) devices (Figure 1. PhatBrace, Biomechanical Composites, Des Moines, IA). The effect of apparent design differences between these civilian variants on lower limb mechanics in individuals with lower limb trauma is not well understood. The objective of this study was to compare the effect of civilian CDO variants on lower limb kinematics and kinetics, relative to each other and no CDO, after lower limb trauma.

Figure 1: Modular (left) and Monolithic (right) CDOs.

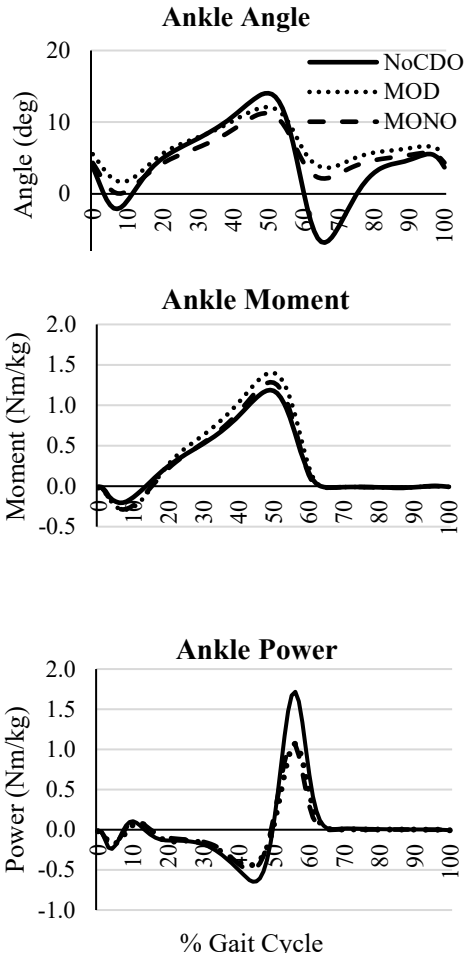

Figure 2: Ankle joint angle, moment, and power in the sagittal plane across the entire gait cycle for the three study conditions (NoCDO = no device, MOD = modular CDO, MONO = monolithic CDO). Positive angle values represent ankle dorsiflexion. Positive moment values represent internal ankle plantarflexor moment. Positive power values represent power generation.

Methods: Twenty-three individuals (mean age = 42.1[11.4] years) with a history of unilateral lower extremity traumatic injury, at least two years prior to testing, with persistent pain, weakness, and/or mobility deficits, participated. Biomechanical gait data were collected as participants walked on an over ground walkway at a controlled speed, based on the participant's leg length,[3] in three conditions: without a CDO (NoCDO) and with MOD or MONO CDO in a randomized order. Prior to data collection, participants accommodated to each CDO for at least three months. Sagittal plane ankle, knee and hip angles, net internal joint moments, joint powers, and ground reaction forces were calculated for the injured limb.

Results & Discussion: The MOD was significantly stiffer than MONO (stiffness: MOD=8.7[2.7] Nm/degree, MONO=4.6[2.4] Nm/degree). Both MONO and MOD CDOs reduced total sagittal plane of ankle motion and push-off power as compared to NoCDO (Figure 2). However, push-off power with the MONO and MOD CDOs was more than 25% greater than previously reported with military CDOs.[4] Peak power generation at the knee was over 20% greater with MONO as compared to MOD, however, both MONO and MOD CDOs generated about 50% higher peak knee flexor moments as compared to NoCDO. The two study CDOs did not affect the hip joint mechanics, however, the peak power generation at the hip with these devices was about 50% less than previously reported with military CDOs.[4]

Significance: Despite multiple design differences, including orthosis stiffness and geometry, the CDOs did not differentially effect ankle biomechanics. Both commercially available civilian CDOs reduced ankle joint range of motion and peak power generation during walking in a manner consistent with previous studies with CDOs used with military service members.[4] The two civilian CDO variants included in this study had a limited effect on joint mechanics of more proximal joints in individuals with lower limb trauma.

Acknowledgements: Research reported in this publication was supported in part by a Department of Defense grant under award W81XWH-18-2-0073 and by the National Center for Advancing Translational Sciences of the National Institutes of Health under Award Number UM1TR004403. The content is solely the responsibility of the authors and does not necessarily represent the official views of the U.S. government, federal agencies, organizations, or foundations.

References:
[1] Highsmith et al. 2016. J Rehabil Res Dev 53:157-184. [2] Grunst et al 2023. Prosthet Orthot Int. [3] Gates et al. 2012. Gait Posture 36:33-39. [4] Russell Esposito et al. 2017. Gait Posture 54:167-173.

CAPTURING FOOT SHAPE FOR ACCOMMODATIVE INSOLE DESIGN: COMPARING THREE TECHNIQUES

Kimberly A. Nickerson[1*], Scott Telfer[1], and Brittney C. Muir[1]
[1]RR&D Center for Limb Loss and MoBility (CliMB), Department of Veterans Affairs, Seattle, WA
*Corresponding author's email: kanick@uw.edu

Introduction: Custom accommodative insoles are used to offload and redistribute high plantar pressures in individuals with diabetes who are at high risk for plantar ulceration and subsequent lower limb amputation [1]. An important component of an accommodative insole's design is the surface geometry, which matches the three-dimensional shape of the bottom of an individual's foot to create full contact. Most commonly, a seated foam crush box impression is used to obtain foot shape for insole design. However, recent advances in scanning technologies have made a digital in-clinic workflow possible, which replaces the foam crush box impression with direct 3D scans of the foot that can be taken in various positions under differing loads. The shapes obtained from direct 3D scanning versus a foam crush box impression of the foot should be compared as differences may affect the form of the custom insole and the resulting pressure redistribution in the foot. Small differences in one-dimensional measurements such as foot length, width, and arch height between methods have been found, but a three-dimensional comparison of the shapes, particularly the plantar surface, would provide a more complete understanding of the differences [2]. The purpose of this study is to provide a preliminary assessment of three-dimensional differences in foot shape as captured by a foam crush box impression and direct 3D scanning.

Methods: A certified orthotist captured the right and left foot shapes of 10 individuals with diabetes using each of the following foot shape capture devices: 1) a foam crush box (Bio-Foam Foot Impression Box, Kent, OH, USA), 2) a flatbed 3D foot scanner (Tiger 3D Foot Scanner, Go 4-D Inc., ON, Canada), and 3) a handheld 3D scanner (Structure Sensor, XRPro LLC (Structure), MI, USA). During the foam crush box impression and flatbed scan, the participant was seated with the foot held in sub-talar neutral. For the handheld scan, the participant laid in a supine position with their feet hanging freely over the side of the bed. For digital comparison of the foot shapes from each method, the foam crush box impressions were digitally scanned (Creaform, Quebec, Canada). The three-dimensional triangular meshes from each scan were aligned to simulate the position of the foot in a Brannock device and cropped to isolate the plantar surface excluding the toes [3], [4]. One-dimensional measurements of foot length, width, and arch height were measured for each processed mesh. Arch volume was calculated as the volume between the plantar surface and the ground plane in the middle third of the foot [5]. Differences in foot shape parameters measured from the foam crush box and direct scanning methods were assessed with a repeated measures ANOVA with a within-subjects factor of capture method and Bonferroni corrections ($p<0.05$) applied. Mesh-to-mesh distances between the foam crush box mesh and the direct scanning method meshes for each subject were calculated as the Euclidean distances between 1480 mesh landmarks. A multiple template 3D elastic matching algorithm was used to place the landmarks on each mesh and create landmark correspondence [6]. For each of the landmark distances, a 1-sided t-test was used to test significance with a false discovery rate of $q=0.05$ to account for the large number of comparisons.

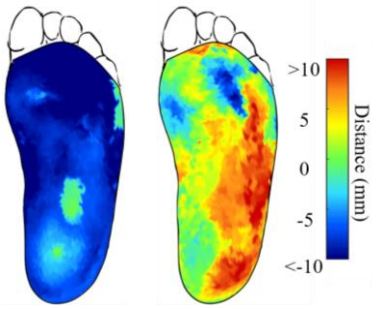

Figure 1: Colormap of average mesh-to-mesh distance for the foam crush box to the flatbed scanner (Left) and foam crush box to the handheld scanner (Right).

Results & Discussion: The measured foot shape parameters (Table 1) and mesh-to-mesh distances (Figs. 1 & 2) indicate a number of differences between the foot shapes captured by each method. Compared to the foam crush box, the handheld scanner captured a more similar medial-longitudinal arch shape than the flatbed scanner captured. In the arch region, the mesh-to-mesh distances between the foam impression and flatbed scanner were significant (Fig. 2) as the flatbed scanner significantly underestimated arch volume and arch height (Table 1). The glass surface of the flatbed scanner likely resulted in more soft tissue compression than the compliant foam box, contributing to these differences in shape. Additional differences in shape may be attributed to the variation in body/foot positioning across capture methods (i.e. seated vs. supine, sub-talar neutral).

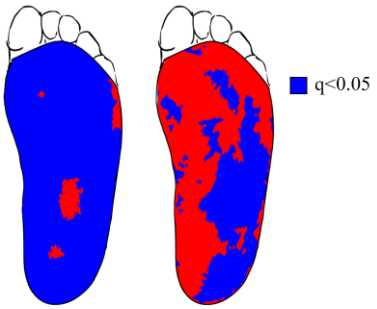

Figure 2: Significant differences in mesh-to-mesh distance (indicated in blue) for the foam crush box to the flatbed scanner (Left) and foam crush box to the handheld scanner (Right).

Table 1: Mean foot shape parameters for each capture method (n=20 feet)

	Foot Length (mm)	Foot Width (mm)	Arch Height (mm)	Arch Volume (mm^3)
Foam Box	231.0	99.1	26.7	57009.2
Flatbed Scan	**222.2**	98.0	**23.3**	**29669.7**
Handheld Scan	**222.8**	**93.9**	**29.6**	61431.2

bold indicates a significant difference from foam crush box measurement at $p<0.05$

Significance: Appropriate arch support and a full-contact geometry in an accommodative insole is essential to redistributing pressures from high-risk areas of the foot. The different methods used to capture foot shape result in different plantar surface shapes which may affect the designed insole's surface geometry and subsequent performance.

Acknowledgments: Funding was provided by VA Award A3539R.

References: [1] Mohamed et al. (2004), *Prosthet Orthot* 16(20); [2] Laughton et al. (2002), *J Am Podiatr Med Assoc* 92(5); [3] Witana et al. (2006), *Int J Ind Ergon* 36(9); [4] Rogati et al. (2021), *J Foot Ankle Res* 14(1); [5] Zhao et al. (2022) *Foot Ankle Surg* 28(7) [6] Zhang et al. (2022), *PLoS One* 17(12).

CAMERA-BASED SYSTEM TO TRACK ARCH HEIGHT INDEX DURING PREGNANCY AND POSTPARTUM

Michelle N. Meyers[1*], Casey Jo Humbyrd, M.D., M.B.E.[1], Josh Baxter, Ph.D.[1]
[1]Department of Orthopaedic Surgery, University of Pennsylvania, Philadelphia, PA
*Corresponding author's email: meyersm9@seas.upenn.edu

Introduction: Musculoskeletal pain is a frequent symptom in pregnancy in which 71% of patients report low back pain, 38% report hip pain, 22% report knee pain, and 40% experience foot pain [1,2]. This pain also extends into the postpartum period in which two-thirds of patients report pain in multiple parts of the body [2,3]. Foot structural changes and pain are one of the most common musculoskeletal conditions experienced during pregnancy and postpartum, yet these patients rarely receive specialized care. One of the key stabilizers of the foot is the spring ligament. Insufficient support from this ligament leads to flatfoot deformity and painful foot symptoms. Symptomatic flatfoot during pregnancy is hypothesized to result from increased body mass and circulating hormones that promote ligament laxity in preparation for childbirth.

Accurately and reliably tracking foot structure is critical to understand the effects of pregnancy on foot structure and to identify patients at increased risk of long-term pain and disability. The Arch Height Index (AHI) is a reliable research tool that quantifies foot structure using a custom measurement jig. However, the Arch Height Index Measurement Systems consists of sets of calipers to make key foot measurements to calculate AHI, which is time consuming and requires a trained investigator to make reliable measurements. This study developed a camera-based method to quantify AHI with the goal of reducing experimental time and increasing anatomical data by using a trained convoluted neural network model (DeepLabCut) to identify key landmarks of the foot. This method offers an inexpensive, reliable, and quick technique to track and study changes in foot structure throughout pregnancy and postpartum.

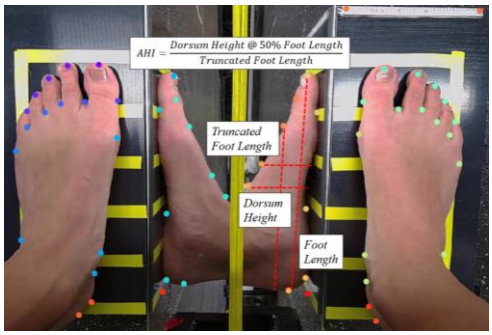

Figure 1. Camera-based AHI measurement photo with 58 DeepLabCut trackers on key landmarks of the foot. Dashed lines represent key measurements.

Methods: Our camera-based AHI measurement used mirrors at 45°angles and a webcam to capture the top and side view of both feet simultaneously (Fig. 1). We collected foot images from five non-pregnant female participants (25.8 ± 1.6 years) and three pregnant female participants (36.0 ± 1.4 years) at 12 weeks of pregnancy. We did not expect to detect foot structure differences during this stage of pregnancy [2]. We acquired photos while participants were sitting and standing with feet approximately shoulder width apart to detect changes in foot structure due to loading. We used these measurements to train a convoluted neural network (DeepLabCut) to identify 58 key landmarks of the foot and calculated foot structure including AHI – which is the ratio of the dorsum height at 50% of the foot length and truncated foot length (Fig. 1). We compared our camera-based AHI measurements against a recent report that used the caliper-based AHI measurement and tested for left-right and sit-standing differences within our data using paired t-tests.

Table 1. Camera-based AHI Measurements and Literature Comparison

Measurement	**Present Study**		**Weimar and Shroyer, 2021[4]**	
Sitting	*Left Foot*	*Right Foot*	*Left Foot*	*Right Foot*
Dorsum height (cm)	6.58 ± 0.50	6.73 ± 0.53	6.23 ± 0.44	6.40 ± 0.49
Truncated foot length (cm)	17.62 ± 0.66	17.56 ± 0.79	17.60 ± 0.92	17.37 ± 0.86
Total foot length (cm)	23.00 ± 0.82	22.88 ± 0.93	23.81 ± 1.11	23.80 ± 1.10
Arch Height Index	0.374 ± 0.026	0.383 ± 0.027	0.355 ± 0.031	0.369 ± 0.034
Standing	*Left Foot*	*Left Foot*	*Left Foot*	*Left Foot*
Dorsum height (cm)	6.15 ± 0.43	6.30 ± 0.38	6.00 ± 0.47	6.05 ± 0.47
Truncated foot length (cm)	17.89 ± 0.70	17.59 ± 0.72	17.79 ± 0.84	17.70 ± 0.87
Total foot length (cm)	23.29 ± 0.89	23.12 ± 0.91	24.1 ± 1.11	24.1 ± 1.10
Arch Height Index	0.344 ± 0.023	0.359 ± 0.022	0.338 ± 0.031	0.343 ± 0.033

Results & Discussion: Our camera-based AHI measurements compared favourably to caliper-based measurements reported by Weimar and Shroyer's study of foot structure within 79 females (21.53 ± 1.5 years) (Table 1.) [4]. Our camera-based AHI measurements also fell within one standard deviation of results of Butler's study using a caliper-based AHI measurements on 50 female recreational runners [5]. We detected significant differences ($p<0.05$) between left and right foot upon standing position dorsum height and AHI measurements. We also detected differences ($p<0.05$) between sitting and standing position measurement comparisons. Our preliminary data demonstrates 1) camera-based AHI measurements produce foot structure measurements that strongly agree with caliper-based measurements in larger female cohorts and 2) camera-based AHI measurements are sensitive to foot side and foot loading. These findings support using camera-based AHI measurements to longitudinally track foot structure throughout pregnancy.

Significance: This study provides clinicians with an easy to use and low-burden tool to longitudinally measure foot structure and potentially administer into clinics to screen for risk factors of foot pain. This technique is simple to implement, independent of investigator, takes less than 3 minutes, and does not require ionizing radiation.

Acknowledgments: We would like to thank the Ruth Jackson Orthopaedic Society (RJOS) and the American Orthopaedic Foot & Ankle Society (AOFAS) for their funding in this project.

References: [1] Kesikburun et al. (2018), *Ther Adv Musculoskelet Dis* 10(12); [2] Vullo et al. (1996), *J Fam Pract* 43(1); [3] Ponnapula et al. (2010), *J Foot Ankle Surg* 49(5); [4] Weimar et al. (2013), *J Am Podiatr Med Assoc* 103(3); [5] Butler et al. (2008), *J Am Podiatr Med Assoc* 98(2).

THE ROLE OF THE LATERAL ANKLE JOINT LIGAMENTS ON THE STABILITY OF THE SYNDESMOSIS

Ana V. Figueroa*, Edward O. Rojas, Wyatt M. Sailer, Bopha Chrea, Jessica E. Goetz
University of Iowa, Iowa City, IA
*anavictoria-figueroa@uiowa.edu

Introduction: High-ankle sprains involve injury to the syndesmotic ligaments: the anterior tibiofibular ligament (AITFL), interosseus ligament (IOL), and posterior tibiofibular ligament (PITFL) [1]. Conversely, low-ankle sprains are injuries to the lateral ligaments: anterior talofibular ligament (ATFL) and calcaneofibular ligament (CFL) [2]. Injury to the syndesmotic ligaments in high-ankle sprains are considered more destabilizing [1]. However, stability provided by the lateral ankle ligaments has not been elucidated in the literature. Sequelae of ligamentous injuries include multidirectional instability and posttraumatic arthritis, likely from altered joint mechanics, impingement, and changes in ligamentous strain [3]. This study aimed to determine the role of individual lateral and syndesmotic ankle ligaments on ankle tissue mechanics and joint stability. We hypothesized that ligament strain and relative bony ankle motion would increase with sequential ligamentous injury.

Methods: 22 through-knee lower extremity specimens underwent mechanical testing with an axially loaded external rotation (ER) stress. Specimens were randomized into either a high sprain (n=11, AITFL, IOL, PITFL, ATFL, CFL) or low sprain (n=11, ATFL, CFL, AITFL, IOL, PITFL) ligament transection sequence. The ankle ligaments were exposed by removal of skin and superficial subcutaneous tissues. Specimens were mounted on an MTS load frame (MTS Inc. Eden Prairie, MN), axially loaded to 750 N, and 5 Nm of ER torque stress was applied. Degrees to target ER torque were compared between sequences using linear regression modeling. AITFL and ATFL strain was measured throughout load application using an optical digital image correlation system (ARAMIS, GOM, Braunschweig, Germany). Mean strain was measured for loading tests after each sequential ligament transection. Signed rank tests were utilized to compare the mean strain in the AITFL or ATFL referencing the intact specimen.

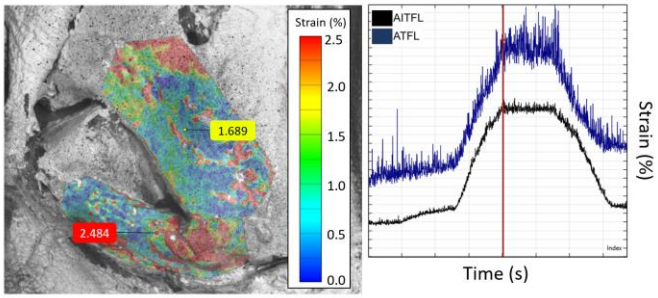

Figure 1: Digital image correlation analysis was conducted on the AITFL and ATFL to track the strain throughout the application of the 5 Nm of torque. Ligament strain is shown in both the heat map and graph form.

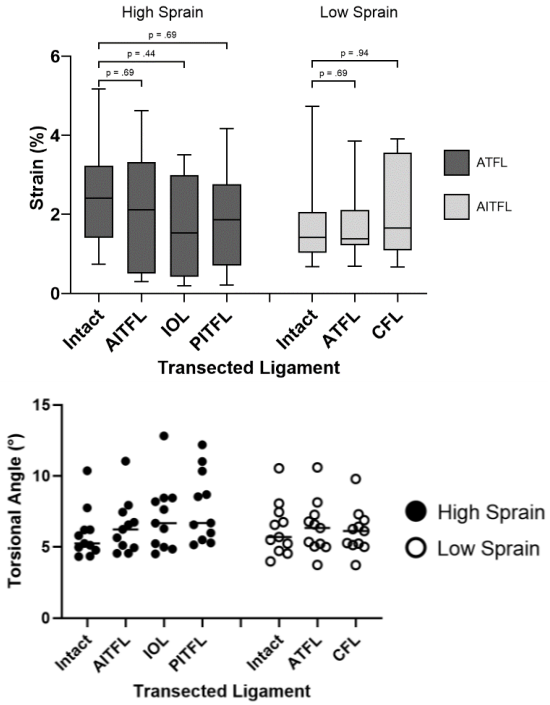

Figure 2: Median strain on both the ATFL (n=11) and AITFL (n=11) for each transection sequence upon application of 5 Nm of torque (top), and MTS-measured ankle rotation (bottom). There were no statistically significant differences in measured rotation angles.

Results & Discussion: Upon application of 5 Nm of torque in intact specimens, the mean ATFL strain was consistently higher than the AITFL strain. In the high sprain group, ATFL strain gradually decreased after each syndesmotic ligament was cut. However, no statistical differences were identified in this trend when compared back to intact specimens (p=0.69, p=0.44, and p=0.69, for AITFL, IOL, and PITFL transection, respectively). Torsional angle progressively increased with each ligament transection within the high sprain group. In contrast, in the low sprain group, both AITFL strain and torsional angle remained relatively constant after each lateral ligament transection, with no significant difference of strain on the AITFL in the (p=0.69 and p=0.94 for ATFL and CFL transection, respectively). For both sprain groups, there was no statistically significant difference in the rotation angle resulting from 5 Nm of applied ER force after any individual ligament transection.

Significance: This study used a novel strain tracking approach to quantify the ligament strain in high and low ankle sprains. Contrary to the initial hypothesis, it was found that ATFL strain decreased, and ankle rotation increased with increasing severity of high sprain. AITFL strain and ankle rotation angles remained consistent through increasing severity of low sprains. While the differences in rotation and strain were not statistically significant, larger ankle rotations could amplify the trends identified in ligament strain behavior. It is expected the reduction in strain results from bony impingement under greater rotation in the ligament deficient ankles.

Acknowledgments: The authors would like to acknowledge funding from the Orthopedic Research and Education Foundation. The authors would also like to thank Dr. Natalie Glass and Krit Petrachaianan for assistance with statistical testing.

References [1] Hunt et al. (2015), *J AAOS* 23(11); [2] Cawley PW, France EP. (1991), *Foot & Ankle* 12(2); [3] van Dijk CN, Vuurberg G. (2017), *Br J Sports Med* 51

ESTIMATED LIGAMENT STRAINS DURING JUMPING AND LANDING TASKS IN PEOPLE WITH CAI AND MATCHED CONTROLS

Renee M. Alexander[1*], Stacey A. Meardon[2], & Tim R. Derrick[1]
[1]Department of Kinesiology, Iowa State University
[2]Department of Physical Therapy, East Carolina University
*Corresponding author's email: rma24601@iastate.edu

Introduction: A lateral inversion ankle sprain is the most common type of ankle sprain [1], with ankle sprains accounting for >80% of all ankle injuries [2]. A lateral inversion sprain is characterized by damage to one or more of the lower ankle lateral collateral ligaments. Individuals have as great as 73% chance of having a subsequent or recurrent ankle sprain following an initial sprain and developing the condition of chronic ankle instability (CAI) [3]. Episodes of excessive inversion, a higher likelihood of having an ankle sprain, and an increased risk for development of ankle osteoarthritis are characteristics of having CAI as compared to a person with no history of CAI or ankle sprains [4]. Investigating where these individuals with CAI have higher lateral ankle ligament strains than their matched controls may help provide an indication of where they are more susceptible to subsequent or recurrent ankle sprains. Previously no statistically significant differences were found between the groups during dynamic trials of cutting, running, walking, and sprinting. The purpose of this study was to use musculoskeletal modelling to compare lateral ankle ligament strains between individuals with and without CAI during four dynamic tasks: single leg jumping, single leg landing, double leg jumping, and double leg landing.

Methods: Twenty people with CAI (average age 23 ± 4.1 years, height 172.4 ± 9.3 cm, and mass 67.4 ± 11.0 kg) and twenty matched controls (average age 21 ± 1.9 years, height 170.4 ± 8.5 cm, and mass 67.7 ± 11.5 kg) were recruited for the study and groups created based on the International Ankle Consortium position statement for patients with CAI in controlled research. Ground reaction forces (2000 Hz) and 3D kinematics (200 Hz) were collected during six trials of single leg jumping and landing and double leg jumping and landing while wearing standardized footwear. Reflective markers were placed on the proximal, distal, and lateral calcaneous and 4 clustered on the tibia and tracked using an 8 camera Qualisys system. Foot markers were used to measure the ankle angle based on the relative motion of the tibia markers to the calcaneous markers. These experimentally derived ankle angles were decomposed into 3D tibiotalar and subtalar joint motions based on literature-derived angular joint ratios [5,6,7]. A musculoskeletal model of the lower limb was created [8,9]. The model was animated using the 3D kinematics in MATLAB. Strains for the anterior talofibular ligament (ATFL), posterior talofibular ligament (PTFL), and calcaneofibular (CFL) were calculated relative to a standing trial. Ligament strains for each motion were compared between groups using independent t-tests with an $\alpha = 0.05$ and statistical parametric mapping (SPM).

Results & Discussion: The greatest peak strains were seen in the ATFL during double leg jumping (CAI 11.6% at 100% stance and Control 9% at 100% of stance). Comparatively, peak strains in the PTFL reached 3.4% at 72% of stance and 3.1% at 80% of stance during double leg jumping for CAI and control groups respectively. Peak strains in the CFL reached 4.2% at 48% stance for the CAI group and 3.6% at 66% stance for the control group. Peak strains were lower in the ATFL during double leg landing (7.2% at 1% stance for control and 9.3% at 1% stance for CAI) but were higher in landing than jumping for the PTFL and CFL (4.7% at 99% stance for CAI, 5.8% at 98% stance for control, and 8.6% at 98% stance for CAI and 9.1% at 97% stance for control respectively). Peak strains were the same or lower for both single leg jumping and landing for the ATFL, PTFL, and CFL in both groups (Fig. 1). No statistically significant differences were detected between groups.

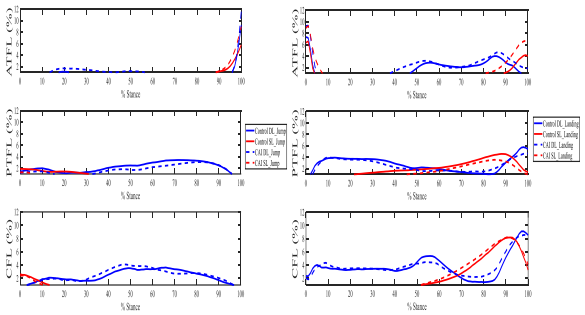

Figure 1: Peak average ensemble ligament strains for the ATFL, PTFL, and CFL. CAI group is denoted with dashed lines and controlled match groups with solid lines. Jumping tasks are on the left, landing tasks on the right.

For jumping and landing tasks, the highest peak estimated ligament strains tended to occur during early and late stance, suggesting a stabilizing role of the lateral ankle ligaments during the take-off and landing phase. Despite self-reported instability, minimal group differences in ligament strains were seen. The maximum peak average ensemble strains do not approach yield strains for ligament damage either [10]. Either our task demands were not high enough to elicit strain differences between groups, or the CAI group may be compensating for any instability with altered kinematics.

Significance: Overall, estimated peak ensemble ligament strains were higher during landing tasks than jumping tasks with ligament strains generally higher during the second half of stance. Landings are potentially more risky for new ankle sprains than jumps and especially for double leg landings than single leg landings.

Acknowledgments: Funding provided by East Carolina Physical Therapy Research Fund.

References: [1] Garrick (1977), *Am J Sport Med* 5(6); [2] Fong et al. (2007), *Sports Med* 37(1); [3] Yeung et al. (1994), *Brit J Sport Med* 28(2); [4] Valderrabano et al. (2006), *Am J Sport Med* 34(4); [5] Arndt et al. (2004), *Foot Ankle Int* 25(5); [6] Lundgren et al. (2007), *Gait Posture* 28(1); [7] Nester et al. (2007), *J Biomech* 40(9); [8] Malaquias et al. (2016), *Comput Method Biomec* 20(2); [9] Peña Fernández et al. (2020), *Sci Rep-UK* 10(1); [10] Siegler et al. (1988), *Foot Ankle Int* 8(5).

PASSIVE HINDFOOT KINEMATICS AS A FUNCTION OF ANKLE AND FOREFOOT PERTURBATIONS

Anthony H. Le[1,2]*, Andrew C. Peterson[1], Jordy A. Larrea Rodriguez[3], Takuma Miyamoto[1], Florian Nickisch[1], Amy L. Lenz[1,2]
[1]Department of Orthopaedics, [2]Deparment of Biomedical Engineering, [3]Deparment of Electrical and Computer Engineering,
University of Utah, Salt Lake City, UT
*Corresponding Author Email: anthony.le@utah.edu

Introduction: Accurate measurement of bony motion can aid our understanding of how individual joints in the foot and ankle compensate and interact with each other in response to injury, surgical intervention, or abnormality. Common *in vivo* foot models with skin-mounted retroreflective markers often oversimplify individual bone movements and assume the tibiotalar joint is the primary contributor to sagittal foot and ankles mobility [1-3]. Recent work underscores significant individual movement of the tarsal and midtarsal bones in healthy feet [4, 5]. While gait simulation in cadavers has yielded insights into dynamic foot and ankle bone motions, there has been limited focus on quantifying the passive adaptability of the foot and ankle. Therefore, the purpose of this study was to elucidate the passive hindfoot joint kinematics during robotically prescribed tibial motions with various ankle and forefoot perturbations.

Methods: Five fresh-frozen tibia-to-toe tip cadaveric specimens (5 males; 53 ± 13 yrs old) with no history of foot and ankle injury/surgery were procured under University of Utah Institutional Review Board approval. Proximal tibias were rigidly affixed to a 6-DOF robot end-effector via specimen specific mounting. Marker clusters mounted to the tibia, fibula, talus, calcaneus, navicular, cuboid, 1st metatarsal, and 5th metatarsal were tracked using motion capture. Weight-bearing CT scans were used to register individual transformations between marker clusters to bone coordinate systems defined by our Automatic Anatomical Foot and Ankle Coordinate Toolbox (AAFACT) [6]. Each specimen was loaded to 25 % body weight in a neutral position and prescribed tibial dorsiflexion/plantarflexion (DPF), internal/external rotation (IER), and varus/valgus alignment (VVS) motions under six perturbation conditions: flat, 45° toe wedge, 0.5-in block under 1st metatarsal, 0.5-in block under 5th metatarsal, 10° eversion, and 10° inversion. Subtalar (ST), talonavicular (TN), and calcaneocuboid (CC) joint rotations were calculated and normalized to initial joint angles measured in the loaded, neutral position on the flat surface. One-way repeated measures ANOVA statistical parametric mapping (SPM) analysis ($\alpha = 0.05$) compared joint rotations across conditions followed by post hoc comparisons with Bonferroni correction using the spm1d MATLAB package [7].

Results & Discussion: During prescribed tibial DPF, ST and TN joints compensated significantly for perturbations in the transverse and coronal planes during transition periods between peak prescribed dorsiflexion and plantarflexion (Fig. 1 Top). CC joint compensated significantly for perturbations in the sagittal and coronal planes throughout most of the prescribed motion (Fig. 1 Top). During prescribed tibial IER motion, ST and TN joints compensated for perturbation in the transverse and coronal planes during transition periods between peak prescribed internal and external rotation (Fig. 1 Middle). CC joint showed significant compensation for perturbations in the sagittal and coronal planes throughout most of the prescribed motion (Fig. 1 Middle). During prescribed tibial VVS motion, ST, TN, and CC joints showed minimal compensation for ankle and forefoot perturbation in the sagittal, transverse, and coronal planes (Fig. 1 Bottom). Hindfoot motion is intricate and pivotal for various aspects of gait biomechanics and overall foot and ankle function. This study demonstrated how the hindfoot joints compensate for ankle and forefoot perturbations, emphasizing their significant roles in foot and ankle mobility. Hindfoot motion facilitates adaptation to varying terrain, such as slopes or uneven surfaces. For instance, this study illustrated how the ST joint adjusted to the orientation of the ankle and forefoot, while the CC joint, which is usually believed to have little motion, exhibited significant compensatory motion in both the sagittal and coronal planes in response to perturbations.

Significance: Data presented in this study can enrich our understanding of individual joint function and their interplay within the foot and ankle complex. Examining individual bone motions can serve as crucial metrics for exploring pathologies and guiding surgical outcomes.

Acknowledgments: Support was provided by Paragon 28.

References: [1] Khazzam et al., 2006. *Gait Posture*, 24:85-93; [2] Jenkyn et al., 2009. *J Biomech Eng*, 131:034504; [3] Leardini et al., 2007. *Gait Posture*, 25:453-462; [4] Whittaker et al., 2011. *Gait Posture*, 33(4):645-650; [5] Aubin and Ledoux, 2023. *Foot and Ankle Biomechanics*, 351-363; [6] Peterson, A. et al, 2023. *Front Bioeng Biotechnol*, 11; [7] Pataky et al., 2010. *J Biomech*, 43(10):1976-1982.

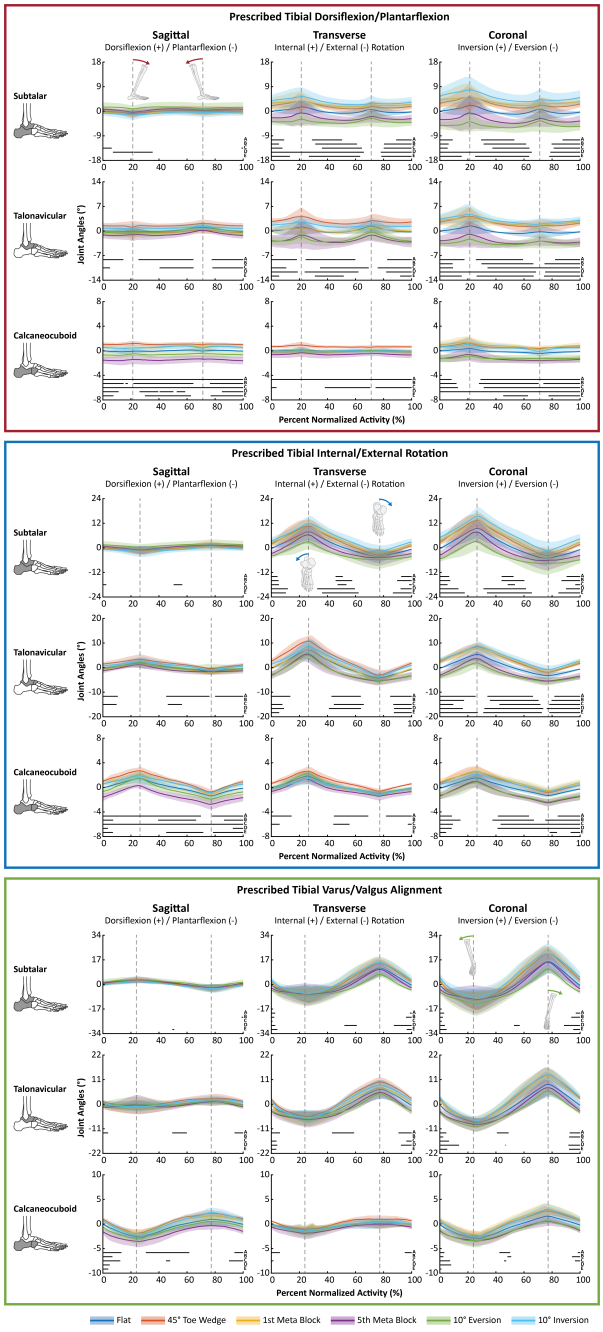

Figure 1: Mean (± SD) ST, TN, and CC joint kinematics in the sagittal, transverse, and coronal plane during prescribed tibial motions. Shaded regions indicate 95% CIs. Black horizontal bars indicate portions of prescribed motion where joint kinematics were significantly different between flat versus (A) 45° toe wedge, (B) block under 1st metatarsal, (C) 0.5 block under 5th metatarsal, (D) 10° eversion, and (E) 10° inversion via SPM analysis. Grey vertical dashed lines indicate peak prescribed motions.

OPTIMIZING SIT-TO-STAND ASSISTANCE FOR HIP-KNEE EXOSKELETONS WITH DEEP REINFORCEMENT LEARNING

Neethan Ratnakumar[1], Kübra Akbaş[1], Rachel Jones[1], Zihang You[1], Xianlian Zhou[1*]
[1]Department of Biomedical Engineering, New Jersey Institute of Technology, Newark, NJ 07102
*Corresponding author's email: alexzhou@njit.edu

Introduction: Executing sit-to-stand (STS) motion presents considerable challenges for individuals with movement disorders, including muscle weaknesses, osteoarthritis, balance issues, and other conditions [1]. Numerous experimental [2] and musculoskeletal simulation [3] studies have focused on understanding STS biomechanics, with additional efforts directed towards developing STS assistive devices [4]. However, the specific impacts of integrating exoskeleton assistance into STS movements are not thoroughly understood due to the complex interplay of sensory inputs, physiology processes, and the exoskeleton assistance, posing challenges in providing optimal STS assistance with proper timing without compromising the user's balance or stability. The goal of this study is to explore whether using a deep reinforcement learning (DRL) framework to optimize assistive hip and knee joint torque profiles can lead to considerable reduction in muscle activations during STS movements, without compromising stability. This approach is informed by targeted STS motion tracking and DRL reward functions that emphasize stability and aim to minimize power consumption by the joints. Four cases of STS are studied: 1) unassisted, 2) hip assistance (H-Exo), 3) knee assistance (K-Exo) and 4) hip plus knee assistance (H+K-Exo).

Methods: We have implemented a DRL framework to train STS controllers with and without exoskeleton assistance. These controllers are engineered to mimic a target STS motion (obtained without exoskeleton) while fulfilling additional task objectives, steered by specifically designed rewards (maintaining extrapolated center of mass [5] alignment, encouraging low power through minimizing joint moments, encouraging upright posture and minimum velocity at end standing position). Our training environment employs the two-level imitation learning structure by Lee et al. [6], which include a trajectory mimicking control policy network (CPN) that outputs desired joint angles and a muscle coordination neural network (MCN) that produces individual muscle excitations to generate desired torques, as shown in Fig 1(A). A key innovation in our work is the integration of idealized exoskeleton assistive torques into the control networks. These assistive torques work in conjunction with the muscle forces to generate the desired joint torques. A 2D, 10-DOF model (featuring 9 lower limb muscles per side, one back muscle, and one abdominal muscle) is modified by removing the left side, halving the torso mass, and adding additional contact spheres to the ischial tuberosity and the femur. Muscles are modeled as MuJoCo type [7] with rigid tendons to improve computational and learning efficiency.

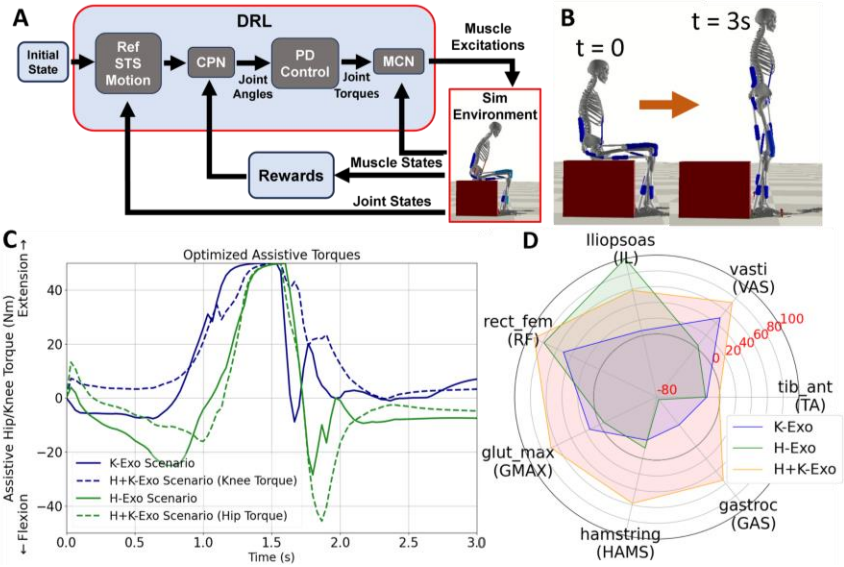

Figure 1: (A) The overall DRL framework. (B) STS motion from sitting at t=0 to standing at t=3s. (C) Mean assistive torques obtained for different assistive scenarios. Torques were limited to 50 Nm. (D) Percentage reduction in mean muscle activities, values below zero indicate an increase in muscle activity verses the unassisted baseline.

Results & Discussion: Larger lumbar flexion was observed when the hip joint was assisted (H-Exo & H+K-Exo), and smaller ankle angle range and a slightly increased forward lean were noted in all STS cases compared to experimental STS motion. Percentage reductions in mean muscle activations for the assistive cases compared to unassisted is presented in Fig 1(D). Particularly, considerable activation reductions in the major hip and knee extension contributors are noticed for the H+K-Exo case (VAS by 73.2%, GMAX by 68.6%, HAMS by 58.2%, & RF by 92.3%). However, the H-Exo and K-Exo cases resulted in slightly increased muscle activations in the HAMS, GAS and TA muscles (all with less than 0.025 in average activation magnitude increase). Assisting the hip joint or knee joint alone seems to introduce some instability after seat-off that is countered by additional muscle activations in the GAS and TA muscles. Soleus and biceps femoris muscles were excluded from the figure due to small activation observed for all cases. The mean assistive hip and knee joint torques for STS scenarios, presented in Fig. 1 (C), showcase mostly smooth torque profiles with occasional sudden changes, suggesting feasibility for real-world implementation via assistance profile parameterization.

Significance: The proposed DRL framework is a promising approach for creating STS assistive controllers. It offers an innovative solution for the complex challenges of testing control strategies and understanding neuromuscular control in real-world settings. We believe this work will significantly enhance mobility for those with mobility disorders, making it more accessible and inclusive for all.

References: [1] van der Kruk et al. (2021), *J Biomech 122*; [2] Norman-Gerum et al. (2020), *J Biomech 112*; [3] Muñoz et al. (2022), *PLOS ONE*; [4] Mungai et al. (2021), *IEEE Access 9*; [5] Hof et al. (2005), *J Biomech 38(1)*; [6] Lee et al. (2019), *SIGGRAPH*; [7] Todorov et al. (2012), *IROS*.

SPATIOTEMPORAL AND BIOMECHANICAL EFFECT OF A BILATERAL HIP-FLEXION EXOSUIT DURING TURNING IN INDIVIDUALS WITH PARKINSON'S DISEASE

Christina Lee[1], Chih-Kang Chang[1], Nicholas Wendel[2], Teresa Baker[2], Andrew Chin[1], Franchino Porciuncula[2], Terry Ellis[2*], Conor Walsh[1*]
[1]John A. Paulson School of Engineering and Applied Sciences, Harvard University, Boston, MA
[2]College of Health and Rehabilitation Sciences, Sargent College, Boston University, Boston, MA
*walsh@seas.harvard.edu, tellis@bu.edu

Introduction: Individuals with Parkinson's Disease (PD) experience various motor impairments caused by a loss of dopamine-producing neurons, including bradykinesia, tremors, and rigidity. Some individuals with PD experience freezing-of-gait (FoG), which is characterized by an inability to move the feet forward despite an intention to walk. While the neurological origin of FoG is unclear, individuals experience breakdown of spatiotemporal features of gait preceding FoG from a biomechanical perspective [1]. While activities that provoke FoG are individual-specific, common activities associated with FoG episodes include turning and gait initiation. Currently available treatments for FoG include pharmacological and surgical interventions that often have modest effects, which diminish with disease progression [2]. Recently, a bilateral hip-flexion assisting wearable exosuit has shown to effectively eliminate FoG for a single individual with PD during straight-line walking in a laboratory setting [3]. Subsequently, in this work, we investigated the spatiotemporal and biomechanical effect of this hip-flexion exosuit on multiple individuals with PD during various types of turns.

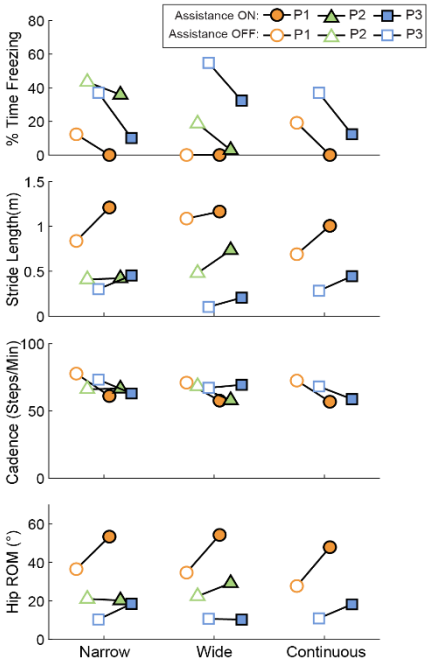

Figure 1: % Time freezing, spatiotemporal gait measures, and hip ROM with and without exosuit assistance during narrow, wide, and continuous walk-to-turn trials for three participants.

Methods: Three individuals with PD (average age 73 years, males) who experienced FoG during turning participated in this study. All participants wore an exosuit that provided 50-78N of force through the cable connecting the thigh and the waist belt to assist bilateral hip flexion. Assistance was applied at maximum hip extension during terminal stance of the gait cycle detected using thigh-mounted inertial measurement units (IMU; XSens, Enschede, Netherlands). The participants completed a 6-m walk followed by three different turns with and without exosuit assistance– narrow turn around a single cone, wide turn around a 0.75-m radius, and a continuous turn during which they walked around a 1-m radius path continuously for 40 seconds. During the turns, we also collected data from pressure insoles (XSENSOR, Calgary, Canada) and IMUs from bilateral shank and foot, and tracked lower extremity kinematics using optical motion capture (Qualisys, Gothenburg, Sweden).

We obtained % time spent freezing as an objective measure of freezing severity by identifying FoG episodes using data from pressure insoles and shank IMUs and validating with video annotation from a physical therapist. We also calculated stride length (m) and cadence (steps/min) as spatiotemporal gait measures from foot IMUs after identifying gait events using pressure insoles. For each stride, we obtained sagittal plane range-of-motion (ROM) of the hip, knee, and ankle. Given the relatively small sample size of individuals with heterogeneous impairment, we obtained the effect of exosuit assistance on our outcome measures using hedge's g effect size, which may be interpreted as the proportion of the group who benefited from the exosuit [4]. Effect sizes were considered small ($g \geq 0.2$), medium ($g \geq 0.5$), or large ($g \geq 0.8$) [5].

Results & Discussion: On average across all walk-to-turn trials, the participants walked with reduced % time freezing of $11.1 \pm 4.6\%$ (mean $\pm$ stdev) with exosuit assistance compared to $27.8 \pm 3.2\%$ without exosuit assistance ($0.54 \geq g \geq 2.0$). This reduction in freezing severity was accompanied by increased stride length of 0.70 ± 0.02 m and decreased cadence of 61.0 ± 2.9 steps/min with exosuit assistance, compared to stride length of 0.52 ± 0.04 m ($0.69 \geq g \geq 0.30$) and cadence of 70.5 ± 1.8 steps/min ($5.3 \geq g \geq 1.5$) without assistance. Average hip, knee, and ankle ROM also increased to $31.5 \pm 17.7°$, $46.2 \pm 18.1°$, and $16.8 \pm 4.9°$ with assistance, compared to $21.8 \pm 10.6°$, $35.9 \pm 15.0°$, and $13.7 \pm 5.3°$ without assistance, respectively ($1.1 \geq g \geq 0.35$).

Despite heterogeneous baseline impairment of the participants, the exosuit assistance reduced freezing severity in all participants during turning, an activity commonly known to provoke FoG episodes. Based on the exosuit effect on spatiotemporal gait measures and movement kinematics, we interpret the exosuit has a gait biomechanics preservation effect, which may be preventing the reduction in stride length that precipitates FoG episodes. Further investigation is necessary to explore how the modulation of exosuit parameters impact its effectiveness in addressing FoG and identify responder characteristics of our exosuit.

Significance: A bilateral hip-flexion exosuit that was previously demonstrated to avert FoG in an individual during straight-line walking reduced FoG in multiple individuals during turning as well. The exosuit may be successfully addressing FoG by preserving gait features that degrade during bouts of walking in individuals with PD.

Acknowledgments: This work was supported by the National Institutes of Health (U01 TR002775) and the Massachusetts Technology Collaborative.

References: [1] Chee et al. (2009), *Brain.* [2] Cui et al. (2021), *Front. Hum. Neurosci.*[3] Kim, Porciuncula et al. (2024). *Nat Med.* [2] Lipsey et al. (1990), Design sensitivity: statistical power for experimental research. [3] Hedges et al. (1985), *J. Educ. Stat.*

PAIRING LIMB POSTURE BIOFEEDBACK WITH AN ANKLE EXOSKELETON TO AUGMENT LIMB PROPULSION

Steven A. Thompson[1*], Emily E. Foley[1], Jason R. Franz[1], Gregory S. Sawicki[2], Michael D. Lewek[1,3]
[1]Joint Dept. of Biomedical Engineering, University of North Carolina at Chapel Hill & NC State University, Chapel Hill, NC
[2]George W. Woodruff School of Mechanical Engineering, Georgia Institute of Technology, Atlanta, GA
[3]Division of Physical Therapy, Department of Health Sciences, University of North Carolina at Chapel Hill, Chapel Hill, NC
*Corresponding author's email: sathom22@ad.unc.edu

Introduction: Limb propulsion deficits contribute to gait impairment following stroke and may arise from reduced ankle plantarflexor torque and/or trailing limb angle (TLA). Ankle exoskeletons (exo) can augment plantarflexion torque, but their use has not necessarily translated into enhanced gait performance in people post-stroke [1-2]. Instead, people post-stroke often *reduce* their TLA when using ankle exos, such that any increase in ankle torque fails to translate to improved limb propulsion [1-2]. Fortunately, people with stroke can use visual feedback to increase TLA, and consequently limb propulsion, *without* the use of an exo [3]. However, the feasibility of being able to adjust TLA via visual feedback while walking with a powered ankle exo remains unknown. Additionally, we sought to determine the interaction between TLA magnitude and exo torque assistance on limb propulsion. With unimpaired participants walking at a fixed speed, we hypothesized that increasing TLA would yield increased propulsion, independent of exo torque. In addition, based on prior literature demonstrating kinetic coupling between the ankle and hip [4], we hypothesized that increasing TLA would cause a transfer of positive mechanical work from the ankle to the hip; because ankle torque requirements should decrease as TLA increases.

Methods: Ten unimpaired adults walked on a dual-belt, instrumented treadmill (Bertec) at 1 m/s while wearing a bilateral powered ankle exo (Biomotum). Plantarflexion torque was provided to one limb only (training limb). Participants' baseline TLA (Fig. 1A) was obtained from a 50-s walking trial while wearing the exo unpowered (control condition). Using a block-randomized design, we provided real-time visual feedback of training limb TLA (baseline, baseline + 5°, or baseline - 5°) via a TV monitor (Fig. 1B), as participants were instructed to reach the target band (with a ± 1° height). Within each TLA block, participants walked with different levels of exoskeleton assistance (0%, 15%, and 35% BW plantarflexion torque). Each trial lasted 50 s following a brief accommodation period. We collected kinematic data using marker-based motion capture (Vicon) and treadmill ground reaction forces. Propulsive impulse, and the ratio of ankle-to-hip positive mechanical work were computed for the training limb and compared across conditions with a 2-way (TLA vs. exo torque) repeated measures ANOVA. Paired t-tests with Bonferroni corrections were used for post-hoc comparisons.

Results & Discussion: Despite no interaction effect between TLA and exo torque on propulsive impulse ($p=0.732$), we observed significant main effects of both TLA ($p<0.001$, $\eta_p^2=0.913$) and exo torque ($p=0.008$, $\eta_p^2=0.417$). Specifically, propulsive impulse increased significantly with each increase in TLA (all $p<0.001$) (Fig. 1C), and was slightly increased in the 35% BW torque condition compared to the 0% BW condition ($p=0.033$). We also did not observe an interaction effect for the ratio of ankle-to-hip work ($p=0.505$), although main effects were observed for both TLA ($p=0.003$, $\eta_p^2=0.475$) and exo torque ($p<0.001$, $\eta_p^2=0.172$). Each increase in TLA resulted in an unexpected *distal* transfer of work from the hip to the ankle (Fig 1D, all $p<0.002$). Furthermore, when exo torque was provided, we observed a shift in mechanical work from the hip to the ankle (all $p<0.018$). This redistribution of joint work has implications for people post-stroke who typically have reduced ankle work performance. Finally, all participants reached each TLA target while the exo was unpowered and powered, suggesting our method of visual biofeedback is effective at inducing alterations in limb posture while walking with the exoskeleton powered.

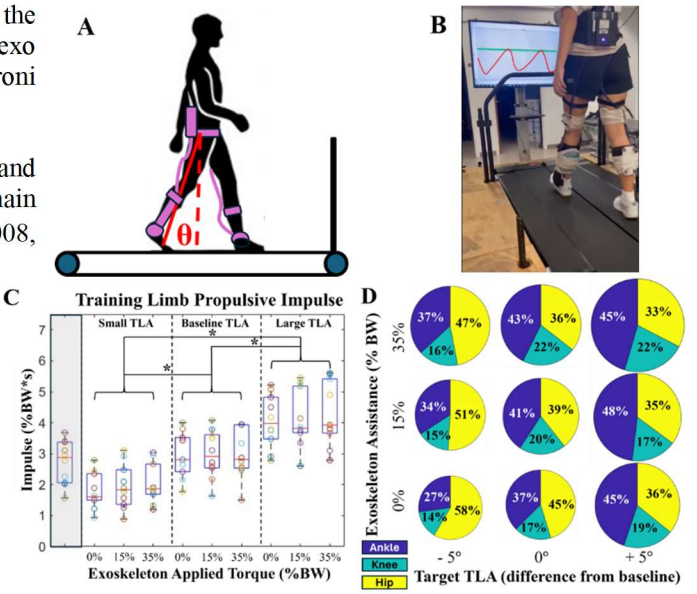

Fig. 1: (A) Measurement of TLA. (B) Participant walking with the exo with real-time visual feedback of TLA. (C) Resultant propulsive impulse for each TLA and torque combination condition, grey region represents initial unpowered control condition (* $p<0.05$). (D) Individual joint contributions to the total work done by the lower limb. Pie radius reflects magnitude of total work.

Significance: Physical assistive devices, such as exoskeletons, are increasingly being used in humans' daily lives for rehabilitation, performance enhancement, and injury prevention. To fully integrate humans with assistive devices, it is necessary to ensure people make best use of the device. Our results show that people can alter their TLA through visual biofeedback while walking with a powered exoskeleton to enhance forward propulsion. We interpret our findings thus far to suggest that users, to potentially include those with clinically-significant deficits in limb propulsion, can be taught to more effectively use these assistive devices.

Acknowledgments: NIDILRR – RERC: REGE22000170: Assisting Stroke Survivors with Engineering Technology (ASSET)

References: [1] McCain, E.M. et al. J Neuroeng Rehabil 2019;16(57). [2] Takahashi, K.Z., et al. J Neuroeng Rehabil 2015;12(23). [3] Lewek, M.D. et al., A. Neurorehabil Neural Repair 2018;32(12). [4] DeVita, P. & Hortobagyi, T. J Appl Physiol 2000; 88(5).

CHARACTERIZING THE EFFECT OF ANKLE EXOSKELETONS ON STANDING BALANCE IN OLDER ADULTS

Daphna Raz[1*], Varun Joshi[2], Necmiye Ozay[1], Brian Umberger[2]
[1]Department of Robotics and [2]School of Kinesiology, The University of Michigan, Ann Arbor
*Corresponding author's email: daphraz@umich.edu

Introduction: Humans rely on ankle torque to maintain standing balance, particularly in the presence of small to moderate perturbations. Reductions in maximum torque (MT) production and rate of torque development (RTD) occur at the ankle during aging, diminishing stability. Ankle exoskeletons are powered orthotic devices that may assist older adults by compensating for reduced muscle force and power capabilities. They may also be able to assist with ankle strategies used to maintain balance. However, an experiment on able bodied young adults showed that ankle exoskeletons using a gravity compensating feedback control strategy do not affect stability, even in the presence of perturbations directly applied to the center of mass (CoM) [1]. Two more recent studies have shown that ankle exoskeletons may have a destabilizing effect in the presence of delay [2] and visual perturbations [3]. No studies have investigated these effects in older adults. Here, we study the effect that ankle exoskeletons have on feasible boundaries of stability in physics-based models of healthy young and old adults, focusing on age-related deficits such as reduced MT and RTD. Analyzing feasible boundaries allows us to characterize constraints on standing balance without having to make assumptions on the specific form of the human controller.

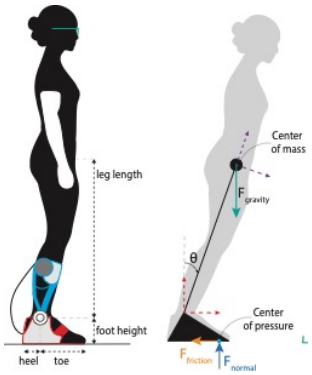

Figure 1: Human-exo free body diagram.

Methods: Bounds on human stability for feet-in-place activities such as standing may be characterized by the set of body CoM positions and velocities from which it is possible to stabilize to quiet standing. In prior work, we introduced a framework for analytically determining the complete boundaries on stability for general nonlinear models of human dynamics [4]. We use this method here to compute regions of feasible stability for a two-link model of a human wearing an exoskeleton (Fig. 1). We account for dynamic constraints on torque arising from the foot-ground contact. We also enforce biologically realistic limits on the MT and RTD, which are set in the model to values representing younger and older adults [5]. We first compute baseline stable regions without the addition of an exoskeleton torque. We then consider two exoskeleton controller strategies: a controller that compensates for gravity (GC) and a proportional-derivative controller (PD). We assume the torque is provided bilaterally and that both controllers saturate at 25 N m per side for a total of 50 N m about the ankle.

Results & Discussion: We found that ankle exoskeleton assistance does not notably increase or decrease the feasible stability of young adults. In a model corresponding to a young female, the feasible region is increased by 3% with the GC controller and 4% with the PD controller. The baseline and GC regions in the angle vs angular velocity plane are shown in Fig. 2a. In an older female model, the exoskeleton also has little effect on the total area, reducing the size of the feasible region by -1% for the GC (Fig. 2b) and PD controller. However, inspection shows that in some regions of the phase plane, the feasible stability boundary shrinks, while in other regions it grows. The dashed green line is the zero-torque trajectory (ZTJ), the unique combination of ankle angle and angular velocity that stabilizes over the foot even without ankle torque. Below the ZTJ, a dorsiflexion torque is required to generate enough momentum to stabilize over the foot and prevent a backward fall. Above the ZTJ, plantar flexion torque provides braking to prevent a forward fall. The plane can be divided into three regions separated by the ZTJ and a vertical line representing perfectly upright standing, where the gravitational torque is zero. In regions I and III, the torque due to gravity acts opposite the direction required to stabilize the system. However, in region II (shaded green in Fig. 2b), gravity provides an assistive breaking torque in the same direction as the plantar flexion torque. This is where the exoskeleton causes major reductions in the stabilizable region. Compensating the torque due to gravity via exoskeleton control can therefore have a destabilizing effect under certain conditions, which is more pronounced in older models with reduced MT and RTD.

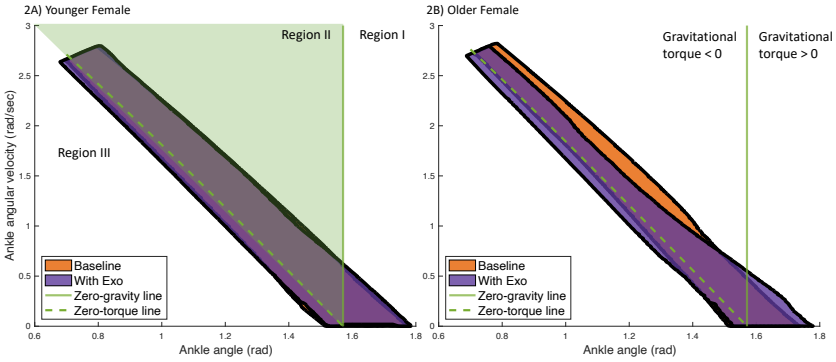

Figure 2: Boundaries of feasible stability for a younger female model, (A), and an older female model (B). No-exo baseline (orange) and gravity compensation (purple) conditions are shown. The two regions approximately overlap in the young female model.

Significance: Our initial results show that a GC and PD controlled ankle exoskeleton does not significantly affect feasible stability in users who have full ankle strength. For individuals with age-related deficits, there may be a trade-off. While exoskeletons can augment stability in portions of the phase plane, they can reduce stability in others. Our results suggest that the safety of well-established control strategies must still be experimentally validated in populations that have musculoskeletal deficits.

Acknowledgments: This work was supported by the NIH (NIBIB) under Fellowship Number F31-EB032745.

References: [1] Emmens et al. (2018), *J NeuroEng & Rehab* 15(1); [2] Beck et al. (2023), *Science Rob* 8(75); [3] Canete et al. (2023), *IEEE-TNSRE*; [4] Raz et al. (2023), *Proc. of the European Control Conf*; [5] Thelen et al. (1996) *J Gerontol A*

EXCESS EXOSKELETON "ASSISTANCE" DISRUPTS STANDING BALANCE BY ALTERING SENSORY FEEDBACK

Joon Han Kim[1*], Rish Rastogi, Giovanni Martino, Owen N. Beck, Max K. Shepherd, Gregory S. Sawicki, Lena H. Ting, Kristen L. Jakubowski
[1]College of Arts and Sciences, Emory University, Atlanta, GA, USA
*Corresponding author's email: joon.kim@emory.edu

Introduction: Wearable robotic exoskeletons are a promising tool for augmenting balance to address the urgent need for solutions that decrease the risk of falling [1-3]. Previously, we showed that providing ankle exoskeleton plantarflexion torque (30 Nm) to able-bodied participants during large backward support surface perturbations improved standing balance capacity [3]. Moreover, to be helpful, the timing of the exoskeleton torque needed to be faster than the physiological muscle activation response. However, in less challenging perturbations, increasing exoskeleton assistance (from 15 to 30 Nm) did not improve balance in all participants. Why larger amounts of assistance improved balance in some but not all remains unknown. In our prior study, we observed that artificially fast exoskeleton torque disrupted plantarflexor fascicle kinematics, altering the initial local sensory feedback [3]. Therefore, we hypothesize that individual variations in response to greater exoskeleton assistance are driven by differences in the sensory feedback generated by the perturbations. In this study, we examined whether altered plantarflexor muscle fascicle kinematics, a proxy for the sensory feedback response, was related to the response to greater exoskeleton assistance. We predict that individuals whose balance was improved with more assistance experienced a smaller increase in plantarflexor fascicle length as exoskeleton assistance increased (e.g., more assistance disrupted plantarflexor fascicle kinematics more).

Methods: Six healthy adults were instructed to maintain standing balance during backward support surface perturbations (15 cm over 500 ms) while wearing ankle exoskeletons (Dephy ExoBoot; Fig 1A). The exoskeletons were activated via an onboard accelerometer that detected the onset of the perturbation and initiated a plantarflexion torque within ~40ms, commanding either 15 or 30 Nm (50ms rise time, followed by a decline to 0 Nm over 150 ms), or no torque (Off). Conditions were randomized to prevent the participant from adapting to the exoskeleton assistance. Right soleus muscle fascicle lengths deep to the medial gastrocnemius were recorded via B-mode ultrasound. Fascicle lengths were tracked offline (Ultra Track) [4], and the lengthening of fascicles within the first 100ms was computed (Fig 1B-purple shaded). CoM kinematics were calculated based on motion capture and force plate data. To dissociate the effects of the exoskeleton torque and the later physiological response, the displacement of CoM (calculated as the integral of CoM velocity) was estimated in two-time windows: 0–200ms (initial phase Fig 1B-grey shaded) and 200–500ms (late phase Fig 1B-green shaded) after perturbation onset. We evaluated the relationship between the change in CoM displacement and the change in fascicle lengthening between the 15 Nm and 30 Nm conditions to determine if altered fascicle kinematics, and thus, sensory feedback, was associated with individual differences in the response to increased exoskeleton assistance.

Results & Discussion: We found a trend where participants who performed better with 30 versus 15 Nm of assistance (e.g., a negative ΔCoM Displacement) had a decrease in the initial stretch of the fascicles between the 30 and 15 Nm conditions (e.g., a negative Δ Fascicle length), whereas, participants who performed worse with more assistance, exhibited more initial stretch of the fascicles during the 30 versus 15 Nm condition (Fig 1C; $R^2 = 0.652$, $p = 0.052$). More sensory disruption with higher assistance levels may be beneficial for the balance-correcting response.

Significance: The same assistance from wearable robotic exoskeletons benefited some while negatively impacting others. Considering differences in physiological processes, such as how sensory feedback was altered because of exoskeleton assistance may be important when selecting the assistance strategy. Further understanding of the interactions between physiological processes and exoskeleton assistance strategies is an important step in developing a successful balance-augmenting exoskeleton controller.

Acknowledgements: NSF: ASEE #2127509, NIH F32 AG063460, R01 HD46922, R01 AG058615, R01 HD90642, McCamish Parkinson Disease Innovation Program

References: (1) Afschrift et al. *J Neuroeng Rehabil* **20**: 82, 2023; (2) Bayon et al. *J Neuroeng Rehabil* **18**: 1, 2022; (3) Beck et al. *Sci Rob* **8:** 75, 2023; (4) Farris and Lichtwark *Comput Meth Prog Bio* **128** 2016

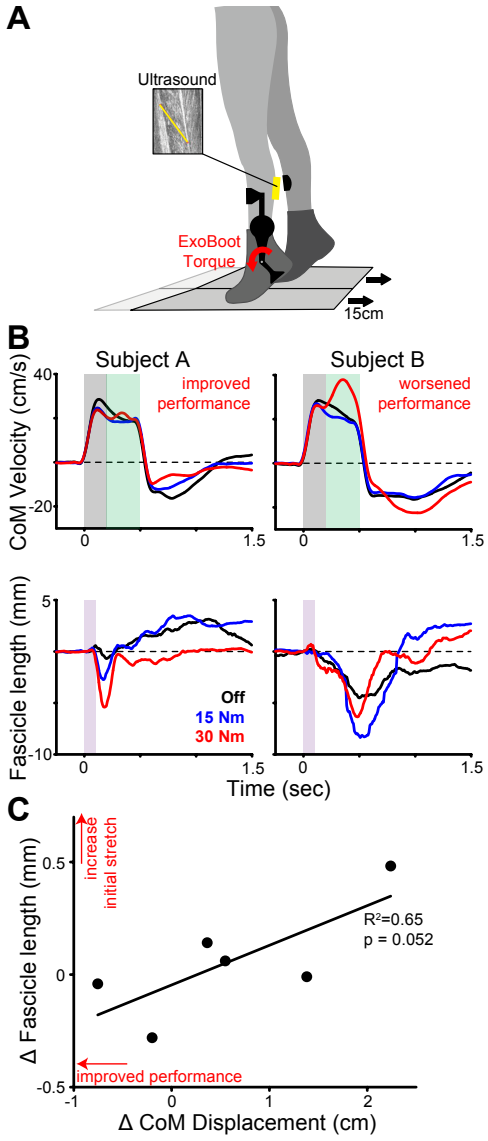

Figure 1: A) Experimental setup. B) Center of mass (CoM) velocity (top) and fascicle length (bottom) for two representative participants for the off (black), 15 Nm (blue), and 30 Nm (red) conditions. C) Relationship between the change in CoM displacement in the late phase between the 30 and 15 Nm conditions and the difference in the initial stretch of the fascicles between the 30 and 15 Nm conditions. Altered soleus fascicle kinematics was related to how balance performance was altered by more exoskeleton assistance.

SIX MONTHS OF EXOSKELETON-ASSISTED WALKING IMPROVES LOWER LEG MUSCLE MASS IN ADULTS WITH SPINAL CORD INJURY

[1]Elizabeth Bowman, Megan Pinette, [2]Leslie R. Morse, [2]Nguyen Nguyen, [2]Ricardo A. Battaglino, [3]Clas Linnman, [2]Jesse Kowalski, [1]Karen L. Troy*

[1]Dept. Of Biomedical Engineering, Worcester Polytechnic Institute, Worcester, MA *ktroy@wpi.edu

[2]Dept. Of Physical Medicine and Rehabilitation, University of Minnesota, Minneapolis, MN

Introduction: Individuals with SCI experience rapid muscle and bone loss [1-2], most of which can be attributed to disuse. Loss of muscle is linked to negative metabolic changes including cardiovascular deconditioning, lower resting metabolic rate [3], increased body fat, and a high rate of secondary conditions [4]. Bone loss associated with SCI results in a high rate of fractures [5-6]. Muscle and bone are tightly coupled both mechanically and physiologically [7]. Interventions that improve muscle can potentially improve cardiovascular health and may improve bone quality.

Exoskeleton devices allow a person to walk with assistance by providing stability and generating motion. We recently completed a clinical trial to investigate the effects of exoskeleton-assisted gait training in people with SCI. Here, we investigated the degree to which gaiting was associated with improvements to muscle, and the relationship between muscle and bone. We hypothesized that gait trianing would improve leg muscle volume and density due to mechanisms of passive stretch, improved blood flow, and mechanical loading of the skeleton. We also hypothesized that improved muscle would be associated with improved bone.

Methods: Thirty-four adults with AIS grades A-C (non-ambulatory) SCI gave written informed consent to participate in a 12-month clinical trial (NCT02533713; age: 37.2 ± 12.3 years, height: 181.4 ± 9.6 cm, mass: 73.7 ± 15.0 kg). The intervention consisted of 6 months of exoskeleton-assisted gait training performed 3 days per week, in 1-hour sessions. Gait training was performed with either an Indego or Ekso exoskeleton. Seventeen of the 20 participants who had pre/post gait data available at the end of the trial completed all 78 planned gait training sessions.

Bilateral CT data were collected on a 30 cm length cantered at the knees before and after 6 months of gait training. A calibration phantom with known hydroxyapatite equivalent density rods was included in each scan. Unilateral CT reconstructions were analysed quantitatively to obtain bone parameters in the proximal tibia and distal femur as previously described [1]. We quantified integral bone mineral content (BMC; g), bone volume (BV; cm^3) and bone mineral density (BMD; g/cm^3) for the epiphysis and metaphysis. Muscle was defined based on a voxel Hounsfield Unit (HU) value of -50 to 135 HU. Primary dependent variables were muscle volume (cm^3) and density for each of the four regions of interest (left, right, upper lower leg). Paired T-tests were used to compare pre/post gaiting data in each region. Pearson correlations and univariate linear regressions were used to examine relationships between baseline and change values, considering body size.

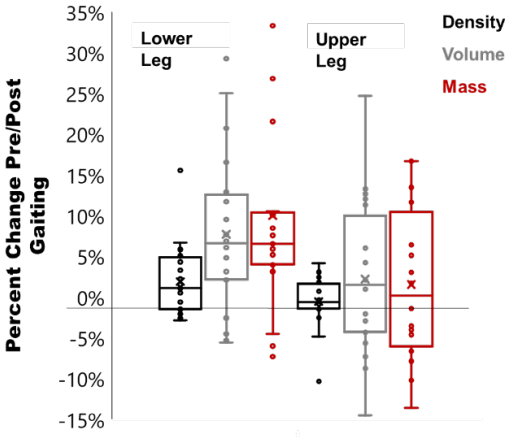

Figure 1 Percent change in lower and upper leg muscle after 6 months of gaiting.

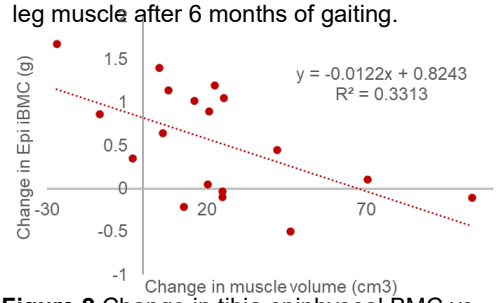

Figure 2 Change in tibia epiphyseal BMC vs. change in lower leg muscle volume

Results & Discussion: Gait training was associated with a 7.5±10.4% increase in lower leg muscle volume (p=0.005), and slight (1.6±3.5%) increases in lower leg muscle density (p=0.053). This resulted in significant increases of 9.7±11.3% in lower leg muscle mass (p=0.002; Figure 1). In general, BV was related to height and BMC related to mass. At baseline, lower leg muscle volume was correlated with tibia epiphyseal and metaphyseal BV ($r \geq 0.432$, $p \leq 0.011$) even after normalizing to height ($r \geq 0.395$, $p \leq 0.021$). In contrast, raw values of BMC were correlated with lower leg volume ($r \geq 0.443$, $p \leq 0.011$) but this relationship disappeared after normalizing to body mass. Similar relationships were observed for the femur. Pre/post changes in lower leg muscle mass were significantly and negatively associated with changes in epiphyseal bone mass and density at the tibia (Figure 2). This may be because people with the lowest BMC have difficulty adding bone new bone but may be able to recover lost muscle. Our hypothesis that muscle would improve with gait training was partly supported, in that we observed significant increases to lower leg muscle volume pre/post gaiting. We observed that body mass was strongly related to muscle volume and BMC, while body height was more closely related to BV. In other words, taller people generally have larger bones, while heavier people have bigger muscles and denser bones.

Significance: Small-scale studies have reported that people experience reductions in spasticity and neuropathic pain after exoskeleton walking [8]. This study adds to the body of evidence about the benefits of exoskeleton walking by demonstrating measurable improvements to lower limb muscle volume and mass after 6 months. Although it is unclear whether these improvements have a measurable impact on overall metabolism, increased muscle mass is associated with a higher resting metabolic rate.

Acknowledgments: This study was supported by DOD award W81XWH-15-2-0078.

References: [1] Edwards et al. *Ost. Int. (2013)* [2] Roberts et al. *J Clin End Metab (1998)* [3] Zurlo et al. *J Clin Invest. (1990)* [4] Drasites et al *Brain Sci. (2020)* [5] Bethel et al. *J Spin Cord Med (2016)* [6] Frotzler et al *Spin Cord (2015)* [7] Brotto and Bonewald, *Bone (2015)* [8] Mekki et al *J Am. Soc. Exp NeuroTher. (2018)*

ADVANCING THE USE OF IMUS FOR ASSESSING SPRINTING PERFORMANCE

Gerard Aristizábal Pla[1,*], Douglas N. Martini[1], Michael V. Potter[2], Stephen M. Cain[3], Wouter Hoogkamer[1]
[1]Department of Kinesiology, University of Massachusetts, Amherst, MA
[2]Department of Physics and Engineering, Francis Marion University, Florence, SC
[3]Department of Biomedical Engineering, West Virginia University, Morgantown, WV
*Corresponding author's email: gea62@pitt.edu

Introduction: Athletes and coaches aiming to enhance sprint performance can assess different key performance indicators (e.g., stride frequency, stride length and speed) across sprint phases and then use those to evaluate races and training runs. Inertial measurement units (IMUs) are gaining popularity for assessing sports performance. However, the accuracy of IMU-based estimates of stride parameters at sprinting speeds remains largely unknown. In addition, these key performance indicators may not offer precise actionable methodologies to improve an athlete's sprint performance. A typical actionable method used by coaches for improving sprint performance focuses on increasing negative foot speed (i.e., the speed of the backward and downward motion of the foot at ground contact). Significant correlations have been observed between the anteroposterior (AP) component of negative foot speed and peak sprinting speed [1,2,3]. However, it remains unknown if IMUs can be used to determine the relationship between negative foot speed and peak sprinting speed. In this study we set out to advance the use of IMUs for sprinting by: (1) assessing the accuracy of IMU-based stride parameters for 80m sprints; and (2) investigating the relationship between negative foot speed and peak speed attained during an 80m sprint. Following Potter et al. [4], we hypothesized that the difference between IMU-based stride estimates and stride estimates obtained with a camera-based capture system would be within 5%. In addition, based on [1,2,3] we hypothesized that faster peak speeds would be achieved with greater AP and vertical (VT) components of negative foot speed.

Methods: Seventeen participants performed 80m sprints on an outdoor track while wearing a shoe-mounted Blue Trident IMeasureU IMU. For aim 1, two cameras, at 20 and 70 meters from the start, were used to validate stride length calculated with the zero-velocity update (ZUPT) method for a single stride at 70 m and on a cumulative distance basis (i.e., from 0 to ~20 m, from ~20 to ~70 m and for the whole sprint). Gold standard measures of stride length and cumulative distance traveled were obtained by tracking the IMUs position with Kinovea. We employed Bland-Altman analysis to assess the agreement between the individual stride and cumulative distances measured using Kinovea and those obtained with the IMU. For aim 2, we calculated estimates of the runner's stride speeds by dividing stride lengths by stride times. These speeds were then subtracted to aligned foot velocities at time of initial foot contact, yielding the AP and VT components of negative foot speed. Peak speeds were determined as the fastest stride speed. We employed simple linear regressions to explore the correlation between each negative foot speed component and peak sprinting speed.

Results & discussion: (1) We obtained single stride and cumulative distance errors within -6 to 3% and -4 to 2%, respectively. Without accelerometer saturation for top speeds of 8.00 ± 0.88 m/s, we obtained a bias of -0.27 ± 4.61% (average bias ± limits of agreement). Our results provide improved accuracy beyond earlier studies on sprinting (a bias of -2.51 ± 8.54% for top speeds of 8.42 ± 0.85 m/s [5]). de Ruiter et al. [5] provided an alternative approach of the traditional ZUPT method [4] because their accelerometers exhibited saturation due to insufficient g-ranges for sprinting speeds. Our findings suggest that without the presence of accelerometer saturation, the traditional ZUPT method provides accurate estimates for sprinting speeds beyond the modified ZUPT method. (2) We also found that faster top speeds were achieved with greater AP and VT components of negative foot speed. Specifically, for peak stride speeds of 7.98 ± 0.78 m/s the adjusted R^2 values were 0.27 and 0.42 for the AP and VT component of negative foot speed, respectively. Our findings align with prior studies, confirming that negative foot speed is a key performance indicator of sprinting [1,2,3].

Significance: Shoe-mounted IMUs can be used to assess sprint performance by providing key performance indicators such as estimates of stride length, running speed and negative foot speed (Fig.1). Compared to traditional methods for assessing sprint technique, shoe-mounted IMUs offer key advantages such as cost-effectiveness, ease of setup, minimal interference with running performance, and the ability to provide immediate feedback. Consequently, our work aims to enhance the effectiveness of IMUs for sprint coaching and performance assessment compared to conventional techniques.

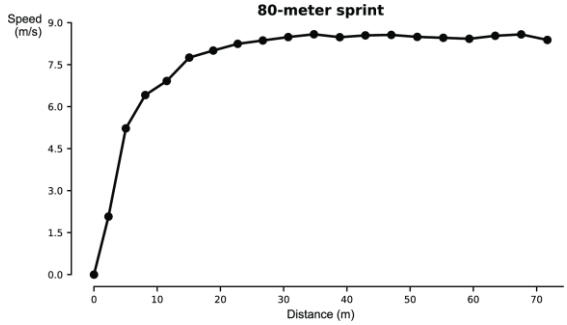

Figure 1: Speed calculated from an IMU on a stride-by-stride basis over the course of an 80-meter sprint for a representative subject as a function of distance covered.

Acknowledgments: The authors thank UMILL lab members who helped with data collections, Dr. Alex Shorter and Dr. Loubna Baroudi for sharing their insights and Dr. Leia Stirling for her help provided with software development and ZUPT implementation.

References: [1] Clark et al. (2023), *J Human Kinet* 87(1-9); [2] Murphy et al. (2021), *J Clin Transl* 7(5); [3] Haugen et al. (2018), *Int J Sports Physiol Perform* 13(4); [4] Potter et al. (2019), *Sensors* 19(11); [5] de Ruiter et al. (2022), *Sensors* 22(1); [6] Martín Fuentes et al. (2022), *Int J Environ Res Public Health* 19(11).

RELATIONSHIP BETWEEN RUNNING SYMMETRY AND INJURY IN DIVISION III DISTANCE RUNNERS USING THE NORMALIZED SYMMETRY INDEX: A PROSPECTIVE STUDY

Kathleen C. Madara[1*], Sarah A. Wright[1], Racheal McCoach[1], Michael Steimling[1,2]
[1]Moravian University
[2]St. Luke's University Health Network
*Corresponding author's email: madarak@moravian.edu
ASB#: 6788

Introduction: There is a lack of consensus on how running symmetry relates to running-related injuries, even though biomechanical variables have been identified as risk factors for injury.[1] Historically, asymmetry has been defined as a >10-15% difference between limbs and used as an indicator for return to sport. However, recent work has shown much higher asymmetry, around 11-37% in healthy runners.[2] We hypothesize that symmetry's conflicting findings and relationship to injury derive from the methods used to calculate symmetry.[3] Recent reviews have attempted to identify best practices for determining/defining asymmetry; however, what is considered asymmetrical differs depending on the symmetry equation.[2–4] This project uses the normalized symmetry index (NSI) [5], which was recently developed and allows for comparison between different types of variables due to how the equation normalizes to the available ranges irrespective of the limb. Therefore, this study aimed to identify the magnitude of "normal" symmetry using the NSI in division III distance runners. In addition, we aimed to assess the relationship between running symmetry and injury by comparing pre-season symmetry between those who sustained a running-related injury and those who did not during the cross-country season and over the entire running season, which included winter and spring track.

Methods: This study was a secondary analysis of an ongoing prospective study to assess the relationship between pre-season biomechanics and injury rates in Division III collegiate distance runners. Of the 50 runners assessed over two years, 30 runners who completed one year on the team were included in this analysis (14F, 16M). All runners were free of injury at the start of the running season when they were assessed. Motional analysis was completed using nine inertia measurement units (Noraxon) placed on the foot, shank, thigh, pelvis, and trunk, as well as accelerometers on each tibia. Participants completed a warm-up on a treadmill for 5 minutes at their self-selected training speed and then continued for an additional 4 minutes. 60 seconds of data were collected during the last minutes of running, and 30-foot strikes were processed using Noraxon's MR3 software to calculate lower extremity kinematics of the hip, knee, and ankle, max vertical tibial acceleration (VTA), max resultant tibial acceleration (TA), and vertical oscillation (VO). Kinematic variables were assessed during initial contact (IC), mid-stance (MS), and late stance (LS). The normalized symmetry index (NSI) was used to calculate symmetry, which returns a 0 for perfect symmetry to 100 (or -100) for total asymmetry. After the year, runners were divided into injured vs. non-injured groups. Those with injuries were defined as any athlete with a running-related overuse injury that resulted in lost training time.

Table 1. Normalized Symmetry Index Values (N=30)

	Variables	Mean	SD	Min	Max
IC	Max VTA	10.5	8.1	1.0	30.3
	Max Resultant TA	8.0	6.8	0.6	27.1
	Max Hip Abd	33.3	20.5	1.9	75.7
	Max Hip Ext Rot	31.7	14.4	1.5	58.7
	Max Knee Flex	34.9	15.7	1.1	69.2
	Max Ankle DF	47.8	21.4	1.2	79.7
MS	Max Hip Abd	32.3	18.3	6.7	72.7
	Max Hip Ext Rot	37.0	15.2	5.1	56.6
	Max Knee Flex	40.5	20.7	5.0	79.4
	Max Ankle DF	39.4	18.1	1.6	71.6
	Max Ankle Inv	48.0	19.3	9.5	72.0
LS	Max Hip Flex	25.3	16.0	1.9	64.2
	Max Hip Abd	35.2	18.7	3.4	77.6
	Max Ankle DF	20.9	16.1	0.5	66.3
	Max VO	24.4	15.5	2.1	58.7
	VO Excursion	14.1	11.1	0.1	37.6

Results & Discussion: NSI values across the variables (Table 1) show more symmetry with kinetic and spatiotemporal variables than kinematic variables (Table 1). Our findings show a larger "normal" movement symmetry range (NSI 8-47%) for kinematic, kinetic, and spatiotemporal variables than previously reported. Our secondary aim was to assess preseason symmetry differences between runners who sustained an injury during the cross-country season (n=11) and those who did not (n=19). There was a statistically significant difference between max knee flexion at IC (43% vs. 29%, p=0.016), max hip abduction at MS (42% vs. 26%, p=0.024), and max dorsiflexion symmetry at MS (48% vs. 34%, p=0.029). There were no statistically significant differences between groups when assessing for differences between runners who sustained an injury over the entire year (n=16) and those who did not (n=14). Only one variable approached significance, max knee flexion at IC (p=0.06). These findings suggest clinicians should consider the time between assessing running mechanics and when an injury occurs. As we found in the shorter timeframe from pre- to post- cross country season, there is a difference in symmetry for injured runners. In contrast, injuries seen over an entire running season may be related to other aspects of health that impact performance or movement changes happened after the initial evaluation.

Significance: Contrary to current suggestions, we would not recommend using a one-size-fits-all cut score for asymmetry. Instead, a reference library should be developed using the NSI to identify "normal" symmetry depending on the assessed variable. In addition, this work does not see consistencies in symmetry and its relationship to injury over time; the multifactorial aspects of running-related injuries could explain this. Therefore, symmetry may not be essential in injury prevention screening and rehabilitation. A more all-encompassing health analysis should be considered in addition to symmetry as well as re-evaluations throughout the running season.

References: [1] Vannatta CN. (2020) Clin Biomech. 75 [2] Stiffler-Joachim MR, (2021) Med Sci. Sports Exerc. 53 [3] Vannatta CN. (2023) Phy Ther in Sport 59 [4] Wayner RA. (2023) Phys Ther in Sport. 59 [5] Queen R, (2020) J Biomech. 99.

Test-retest reliability of pelvis and lower limb coordination during running

Rodrigo Paiva[1], Eliane C Guadagnin[2], Talissa Oliveira Generoso[1,3], João Emilio de Carvalho[2], Leonardo Metsavaht[2], Maykel D Martinez[2], Cauã Neves[2], Gustavo Leporace[1,2,*]

[1]Instituto Brasil de Tecnologias da Saúde (IBTS), Rio de Janeiro, Brasil

[2] Departamento de Diagnóstico por Imagem, Escola Paulista de Medicina, Universidade Federal de São Paulo, São Paulo, Brasil

[3] RUSH Medical Center, Chicago, USA

*Corresponding author's email: gustavo@biocinetica.com.br

Introduction: Kinematic analysis of running has become essential for rehabilitation and injury prevention, yet a lack of consensus on primary risk factors persists [1,2]. Many studies focus on discrete angular values, neglecting joint interdependence [3,4]. The modified vector coding (VC) technique offers continuous, precise angle-angle measures to quantify intersegmental movement [5,6]. Previous research identified differences in running kinematics between injured and non-injured individuals [7-9], highlighting the need for reliable results across different days, to guarantee that the observed changes do not arise from inherent measurement errors. This study aimed to assess the test-retest reliability of intersegmental coordination during running using VC in healthy runners.

Methods: The study involved 25 healthy runners (14 male / 11 female) aged 37.3±7.8 years, with specific inclusion criteria including a minimum weekly running volume of 10 miles/week, the absence of injuries in the last year, and a heel-strike running pattern. Data were collected over two sessions separated by two weeks to assess inter-session reliability. Data collection utilized a movement analysis system with high-speed cameras (Vicon, Oxford, UK; sampling rate: 250 Hz) and marker configurations on participants' thighs, legs, pelvis, trunk, and footwear. Participants ran on a treadmill at 2.92 m/s for four minutes. We utilized the VC technique to analyze intersegmental coordination and coordination variability during running in healthy individuals. This technique employs precise angle-angle measures to quantify movement between two segments over a specified period. The coupling analysis was done using the bin frequency [6]. The coordination variability was calculated as the circular standard deviation of the coupling angles across cycles, for the entire stance phase [10]. The following couplings were determined during the early, mid, and late stance phase: Foot (frontal plane) – Tibia (transverse plane); Foot (frontal plane) – Knee (sagittal plane); Foot (frontal plane) – Pelvis (frontal plane); Foot (sagittal plane) - Tibia (sagittal plane); Foot (sagittal plane) - Femur (sagittal plane); Tibia (sagittal plane) – Femur (sagittal plane); and Knee (sagittal plane) – Pelvis (frontal plane). The intraclass correlation coefficient (ICC) was calculated to determine the reliability between sessions. A significance level of 5% was adopted.

Results & Discussion: The results indicated that couplings generally showed moderate to excellent test-retest reliability across early, mid, and late stance phases. In the early stance, couplings generally exhibited moderate to excellent reliability, with ICC values ranging from 0.613 to 0.928. However, only the Foot (frontal plane) - Tibia (transverse plane) coupling showed moderate to good reliability, with ICC values of 0.613 and 0.824. In the mid stance, couplings demonstrated moderate to good reliability, with ICC values ranging from 0.521 to 0.899. Notably, the foot (frontal plane) - Tibia (transverse plane) coupling exhibited moderate reliability. In the late stance, couplings showed moderate to excellent reliability, with ICC values ranging from 0.632 to 0.979. However, the Foot (frontal plane) - Knee (sagittal plane) coupling displayed only moderate reliability. Variability analysis revealed a range of reliability from poor to excellent across early, mid, and late stance phases, with ICC values ranging from 0.248 to 0.996. In the early stance, the reliability of the tibia (sagittal plane) - femur (sagittal plane) coupling was poor (ICC: 0.248), while in the mid stance, the knee (sagittal plane) - pelvis (frontal plane) coupling exhibited poor reliability (ICC: -0.055). Similarly, in the late stance, the tibia (sagittal plane) - femur (sagittal plane) coupling also showed poor reliability (ICC: 0.215).

Significance: The main finding of this study was that out of a total of 42 investigated couplings, 33 showed good to excellent reliability in the test-retest. Additionally, 9 couplings showed poor to moderate reliability. These couplings should be used with caution in longitudinal studies to avoid errors in interpretation and comparison of the measures. The analysis suggests that the couplings with the poorest reliability predominantly occur in the sagittal plane, more specifically in the coupling between tibia and femur. This coupling is often a source of investigation in studies involving lower limb load absorption strategies and in the study of knee injuries. Therefore, we must be careful when analyzing results of studies involving this coupling, considering that the results found may not be reproducing reality. Another coupling frequently used in studies that investigate risk factors for ankle and knee injuries is the coupling between foot (frontal plane) - tibia (transverse plane). Our results showed moderate reliability in this coupling and, therefore, we must be careful when analyzing it. Overall, this study expands the horizons of knowledge in the field, opening avenues for further investigation and potentially reshaping how researchers and practitioners approach the analysis and interpretation of running kinematics.

References: [1] Blyton et al. (2023), *Gait & Posture*, 101; [2] Hollander et al. (2021), *Sports Med*. (2021); [3] Mousavi et al. (2019), *Gait & posture*, (69); [4] Pelegrinelli et al. (2020), J Biomechanics (101); [5] Hamill et al. (2000), *J App Biomechanics* (16); [6] Needham et al. (2015), *J Biomechanics* (48); [7] Langley et al. (2020), *Journal of Applied Biomechanics* 36(6); [8] Takabayashi et al. (2021), *J Orth Research* (39); [9] Hafer et al. (2017), *Gait & Posture* (51); [10] Rodrigues et al. (2015), *J App Biomechanics* (31).

ALTERNATIVE PREPROCESSING TECHNIQUES MAY UNVEIL DISTINCTIVE GROUND REACTION FORCE DYNAMICS RELATED TO THE PRESENCE OF RUNNING-RELATED INJURY

Ryan M. Nixon[1,2*], Melanie Beceiro, Michelle McGrath, Aiden Villasuso, Kevin R. Vincent[1,2], Heather K. Vincent[1,2]
[1]Department of Physical Medicine and Rehabilitation, [2]UF Health Sports Performance Center
*Corresponding author's email: ozswinem@ufl.edu

Introduction: Running is a popular global sport; however, it is accompanied by a high prevalence of running-related injuries (RRI). Despite extensive research, the precise relationship between RRI and kinetic biomechanical variables, such as ground reaction forces (GRFs), remains unclear (Milner et al., 2023; Senevirathna et al., 2023). Conventional preprocessing methods for running gait analysis may contribute to disparate findings: their significant data smoothing, focus on the vertical component of GRF, and specific GRF regions of interest may eliminate real biomechanical phenomena relevant to soft tissue or bony injuries during the early or late stance in the gait cycle. We aim to address previous methodological issues by introducing alternative pre-processing approaches and investigating GRFs among runners with different RRI histories. Significant differences in the GRFs may provide deeper insights underlying specific RRI than previously published.

Methods: 534 runners participated in the study and ran on an instrumented treadmill at self-selected speeds. Runners with a specific soft tissue injury (Achilles Tendinopathy [AT]) and bony injury (tibial stress fracture [TSF]) were selected as a sub-analysis for this study. Net GRFs were collected at 1200 Hz, and kinematic data were obtained using 3D motion capture. Runners were categorized by injury status (recently injured with AT or TSF, non-injured) and foot strike (rearfoot or non-rearfoot). Net GRFs and three GRF components were processed using four different low-pass filter cutoffs (600, 100, 60, 10Hz). We tested whether alternative pre-processing reveals differences in Net GRFs during the entire stance phase for all dimensions. Raw normalized data was fitted with a double Gaussian function to model the biphasic behavior of running GRFs. The two Gaussian peaks model the impact phase when the lower extremity strikes the ground and the active phase when the remainder of the body weight is loaded and unloaded.

Results & Discussion: For all runners, low-pass filtering cutoffs 60 and 10Hz had strong edge effects, near the beginning and end of each step, for all runners combined: lengthened stance times, smoothed waveforms, and altered Net GRF in the early (1-14%) and the late (85-100%) stance phase (all $p<0.05$); in comparison, frequencies ≥100 Hz maintained better signal integrity during the entire stance phase than the lower cutoffs. See Figure 1.

We normalized and frame-averaged raw, unfiltered, data for RRI subsets of runners with AT and TSF to case-matched, non-injured runners. Compared to non-injured runners, AT had shorter stance times, as well as higher Net GRFs in the early (14-18%) stance phase. Medial-lateral GRF forces during 20-23% stance were higher for AT on the right side. Runners with AT had 55% higher maximal lateral GRF forces and differing lateral and medial impulses. Also, runners with AT had 33% higher impact amplitude asymmetry than case-matched non-injured runners ($p\leq.05$).

Runners with TS showed higher Net GRF in the late (94-96%) stance phase ($p\leq.05$). Anterior-posterior GRFs (braking/propulsion) were 55%-106% higher in the late (86-100%) stance phase for the left limb and 64%-740% higher in the late (83-100%) stance phase for the right limb ($p<.05$). Runners with TSF showed higher impact amplitude (1.04 vs 0.66 BW: $p=.05$) and duration on the left limb (22.8±27.2 ms vs 9.3±4.8 ms; $p=.06$). Active impulses were lower for TSF on both limbs ($p<.05$).

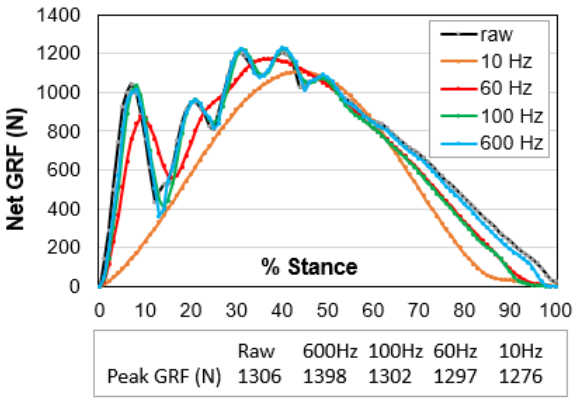

Figure 1: Net GRF with different filtering cutoffs.

Significance: The key finding was that GRF signal filtering affects the accuracy of GRF in regions necessary to find differences among RRI subgroups, such as AT and TSF. A reconsideration of how gait analysis GRF data are processed is important to improve our understanding of the relationships between loading during the entire stance and the injury experience of the patient. Clinically, this approach is critical for improving the precision of gait retraining approaches during therapy. Moreover, this alternative pre-processing may enhance the discriminative capacity of GRF for RRI prediction.

Acknowledgments: This work was supported by the UF Health Sports Performance Center and the UF Strategic Funding Initiative, Sports Collaborative.

References:

Milner, C. E., Foch, E., Gonzales, J. M., & Petersen, D. (2023). Biomechanics associated with tibial stress fracture in runners: A systematic review and meta-analysis. *Journal of Sport and Health Science*, *12*(3), 333–342. https://doi.org/10.1016/j.jshs.2022.12.002

Senevirathna, A. M., Pohl, A. J., Jordan, M. J., Edwards, W. B., & Ferber, R. (2023). Differences in kinetic variables between injured and uninjured rearfoot runners: A hierarchical cluster analysis. *Scandinavian Journal of Medicine & Science in Sports*, *33*(2), 160–168. https://doi.org/10.1111/sms.14249

FOOTWEAR REDUCES FOOT TORSION DURING RUNNING

Evan M. Day[1], Megan Saftich[1], Ed Nyman[1], Jennifer Sumner[1]
[1]Brooks Sports, Seattle, WA, USA
*Corresponding author's email: evan.day@brooksrunning.com

Introduction: Torsion of the foot (frontal plane movement of the forefoot relative to the rearfoot) is a natural motion of the foot during running, in which the forefoot and rearfoot are believed to move relatively independent of each other [1]. As the heel lifts off the ground in the second half of stance, the calcaneus/ankle joint begins inverting, increasing foot torsion as the forefoot remains relatively level on the ground [1]. While previous research has demonstrated that footwear influences the amount of foot torsion [1-3], such work has primarily focused on the extent to which torsional stiffness of a shoe affects foot torsion. The purpose of this research was to evaluate how different footwear constructions affect foot torsion during running.

Methods: Data from two human participant product testing rounds were aggregated (n=22, 11 females/9 males/2 non-binary, age: 21-61yr, height: 157-180cm, weight: 51-96kg). To assess the influence of footwear on foot torsion, a non-footwear condition, a sock shoe (5mm EVA sock-liner with rubber outsole an affixed sock) and three different footwear conditions (Brooks Ghost Max, Ghost 16, and Launch 4) were assessed. These products were chosen because of their various construction techniques, spanning a range of mechanical properties consistent with the breadth of running footwear on the market today (Peak acceleration during impact testing (G-max): 7.9-10.9, Forefoot Bending Stiffness: 3.8-9.6 N-m, Rearfoot Stack Height: 27-39mm, Forefoot Stack Height: 17-33mm, Heel-Toe Offset: 6-12mm). Three-dimensional kinematic data of the lower limb segments (forefoot, rearfoot, shank, thigh) were acquired using optical motion capture (Motion Analysis Corporation, Rohnert Park, CA, USA) and vertical ground reaction forces from an instrumented treadmill (Bertec, Columbus, OH, USA), collected for 10 running gait cycles at 3.35 m/s for each footwear condition. Using a two-segment foot model, foot torsion was calculated as the rotation, in the frontal plane, of the forefoot relative to the rearfoot. Positive foot torsion corresponds to forefoot eversion. One-dimensional, one-way repeated measures Statistical Parametric Mapping (SPM) (α = 0.05) was used to assess differences in foot torsion throughout stance. Follow up pairwise comparison analyses between each condition were conducted using SPM repeated measures t-tests.

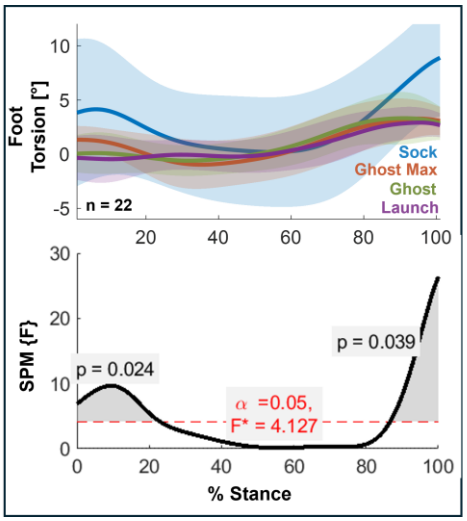

Figure 1: Top: Foot torsion kinematics for each footwear condition during stance phase; Bottom: running F-critical value (solid line) and F-critical threshold (dashed line). Shaded region represents significant main effect of footwear condition.

Results & Discussion: There was a significant main effect of footwear condition on foot torsion from 0-23% and 87-100% of stance (Fig 1). Post-hoc pairwise comparison revealed that this effect is largely driven by significant differences between the sock condition and each of the footwear conditions. Post-hoc comparisons of specifically the footwear conditions revealed the Ghost Max as different from the Ghost 16 and Launch 4 at the beginning of stance (0-23%). This is likely attributed to different landing angles of the foot and ankle influenced by shoe parameters, such as stack height, heel-toe offset, or cushioning stiffness. Of greater interest is the difference during late stance (87-100%), as the forefoot pushes off the ground. Results demonstrated that the sock condition allowed for a greater torsion range of motion than the footwear conditions, while there were no post-hoc differences between the Ghost Max, Ghost 16, or Launch 4 in the 87-100% phase; suggesting that most market available footwear may reduce foot torsion relative to how the foot moves without the resistance of a shoe (sock condition). This change in torsion during push-off suggests that footwear influences a different preferred movement path, corroborating previous results showing negligible differences between footwear conditions in kinematics at the ankle and knee compared to barefoot running [4]. Potential changes in one's kinematics as a result of footwear choice may affect other performance and injury mechanisms, such as spring function of the foot [5] or general comfort and experience in footwear [6]. While the habitual motion path theory research has focused exclusively on the ankle and knee [7], these results suggest a potential new area for considering how footwear influences someone to move similarly or differently from that which is habitual for their body.

Significance: Previous foot torsion research has focused almost exclusively on the influence of footwear torsional stiffness. This research broadened the scope to evaluate the influence of various footwear constructions on foot torsion. Regardless of footwear construction, foot torsion was reduced during push-off compared to the use of a sock shoe. This may have key implications for performance or injury mechanisms, and/or on-foot experience of footwear choice.

Acknowledgments: Thank you to all Brooks' Run Research Team members who assisted with data collection and processing.

References: [1] Stacoff et al. (1991), *MSSE*, 23(4), 482-490; [2] Graf & Stefanyshyn (2012), *Footwear Sci*, 4(3) 199-206; [3] Morio et al. (2009), *J. Biomech.* (42) 2081-2088; [4] Nigg et al. (2017), *MSSE*, 49(8), 1641-1648; [5] Asmussen et al. (2022), *JAB*, 38, 221-231; [6] Nigg et al. (2015), *BJSM*, 49, 1290-1294; [7] Sumner et al. (2023), *Footwear Sci* 3(sup1) S161-163

Does Running Speed Affect the Magnitude of Race Performance Improvement Experienced by Distance Runners Wearing "Super" Spikes?

Bradley Needles[1*], Alena M. Grabowski[1]
[1]University of Colorado Boulder
*Corresponding author's email: Bradley.Needles@colorado.edu

Introduction: Compared to traditional track spikes, "super" spikes are track spikes constructed with increased underfoot cushioning, highly compliant and lightweight midsole foams, and rigid spike plates spanning the length of the shoe's sole [1]. The stiffness of footwear, like "super" spikes, and running surfaces, that act as in series springs with a runner's legs, can positively affect running performance by reducing metabolic cost [2]. McMahon and Greene developed a "tuned" compliant track at Harvard University to optimize performance based on a runner's leg stiffness in combination with the in-series running surface stiffness. During the 1977 indoor track season, Harvard track runners achieved 2.91% faster race times on the "tuned" track compared to other track venues [3]. Thus, in-series stiffness properties of footwear and running surfaces likely affect the overall race performance of competitive runners. Despite runners achieving race performance improvements running on "tuned tracks", McMahon and Greene assumed that leg stiffness did not change with running speed and used constant leg stiffness values to design their "tuned" track [3]. Arampatzis et al. found that at faster running speed from 2.5 to 6.5 m/s leg stiffness increased [4]. A positive relationship between running speed and leg stiffness suggests that optimal running footwear and surface stiffness may change depending on running speed. "Super" spikes were introduced in 2020 and include midsole materials that are more compliant than materials used in previous generations of track spikes [5], and this reduced stiffness may improve athlete's race times differently depending on running speed. Based on the potential differences in race performance across track running events conducted at differing running speeds after the introduction of "super" spikes, we hypothesized that, at faster running speeds, the magnitude of race performance improvement compared to historical race time trends will decrease for professional male and female distance runners wearing "super" spikes.

Methods: We collected the top 100 male and female race times achieved during the 2001 to 2023 (omitting 2020) track seasons in the 800 m, 1500 m, 5000 m, and 10 km from the World Athletics Top Lists. We analyzed race times and assumed that all athletes wore "super" spikes from the 2021 season onwards. We then fitted regression equations to the average top 100 race times for each sex and event category per year from 2001 to 2019. We calculated race performance improvement (RPI) as the percentage difference between the 2001 to 2019 regression equation predictions for 2021 to 2023 race times and the actual average top 100 race times from 2021 to 2023 for each sex and event category.

$$\text{RPI (\%)} = \left(\frac{\text{Predicted Average Time - Actual Average Time}}{\text{Predicted Average Time}}\right) * 100$$

Then, after accounting for year to year variation in average top 100 race times, we compared RPI across average running speed for each distance with a second order polynomial regression equation (Fig. 1). Differences in RPI based on sex and event were assessed by one way Anova tests and Tukey's post hoc tests with a significance level of 0.05.

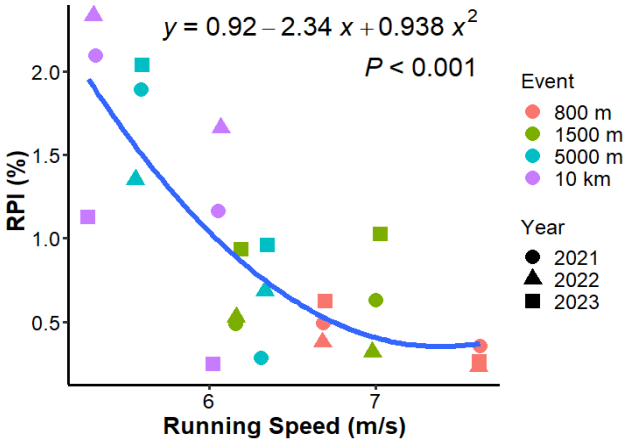

Figure 1: Race performance improvement (RPI) (%) across average running speed (m/s) for the top 100 male and female professional runners in the 800 m, 1500 m, 5000 m, and 10 km from 2021 to 2023. At faster running speeds, RPI decreases ($p<0.001$). Thus, effects of using of "super" spikes on RPI likely depends on average running speed.

Results and Discussion: We found that after accounting for historical trends in race times from 2001 to 2019, the use of "super" spikes improved average RPI for all sex and event combinations by 0.92 ± 0.66% (Fig. 1; $p < 0.001$), which corresponds with a race time improvement of roughly 2 sec per mile (1609m). We also found that women had a greater RPI than men (1.18 ± 0.73% vs. 0.65 ± 0.46%, respectively; $p = 0.042$) and that RPI was less for the 800 m compared to the 10 km race distance (0.39 ± 0.15% vs. 1.43 ± 0.76%, respectively; $p <= 0.014$). Thus, "super" spikes may not affect race performance uniformly. We found that RPI is negatively associated with average running speed for the top 100 male and female professional runners at distances of 800 m to 10 km (Fig. 1; $p < 0.001$). For example, the average RPI for the men's 800 m (average speed of 7.62 m/s) during the 2021 to 2023 track seasons, was six times lower than that of the women's 10 km (average speed of 5.29 m/s; Fig. 1). The potential reason for the association between RPI and running speed may be due to the midsole stiffness of the current generation of "super" spikes and the effects on overall leg stiffness while running at a given speed.

Significance: A negative relationship between RPI and average running speed could mean that "super" spikes disproportionately improve running performance based on the race distance and average speed. To maximize performance, future product development of "super" spikes may require midsole compliance and energy return values to be tailored to the race speed of the runner.

References:[1] L. Healey, Sports Med, 52(6), 2022; [2] McMahon and Greene, Journal of Biomechanics, 12(12), 1979; [3] McMahon and Greene, Sci Am, 239(6), 1978, [4] Arampatzis, Journal of Biomechanics, 32(12), 1999; [5] Kram, Footwear Science, 14(3), 2022.

RISK OF LATERAL INSTABILITY WHILE WALKING ON WINDING PATHS

Anna C. Render[1*], Joseph P. Cusumano[2], Jonathan B. Dingwell[1]
[1] Department of Kinesiology, Pennsylvania State University, University Park, PA, USA
[2] Department of Engineering Science & Mechanics, Pennsylvania State University, University Park, PA, USA
*Corresponding author's email: acr313@psu.edu

Introduction: People with balance impairments often struggle to perform turns and other lateral maneuvers while walking [1], leading to an increased risk of falls and injuries. Therefore, we asked how healthy people modify their mediolateral balance to walk on winding pathways, and how such non-straight walking tasks affect their stability. Here, we tested the stability-maneuverability hypothesis and predicted that people would exhibit greater risk of lateral instability to maneuver pathways of higher sinuosity.

Methods: We tasked 24 young healthy people (12F/12M; 25.8 ± 3.5 yrs) to walk on six unique paths projected onto the treadmill in an "M-Gait" virtual reality system (Motek Medical). We created three pseudo-random path oscillation frequency combinations: straight (STR), low frequency (LOF), and high frequency (HIF); each presented at two widths, wide (W = 0.60 m) and narrow (N = 0.30 m). We instructed people to "stay on the path" and encouraged them to minimize stepping errors during each of two 4-minute trials.

We extracted stepping data, and within each step, we found the minimum mediolateral Margin of Stability (MoS_L) [2], i.e., the distance between the extrapolated center of mass (XCoM) and lateral base of support. This yielded time series of MoS_L for all steps $n \in \{1, \dots, N\}$ throughout a trial from which we calculated the mean (μ) and standard deviation (σ) of MoS_L. To quantify the likelihood of taking an unstable step while walking based on Hof's condition [2], we used the $\mu(MoS_L)$ and $\sigma(MoS_L)$ to calculate the statistical probability that any step will exceed the stability boundary ($MoS_L < 0$), which we call lateral Probability of Instability (PoI_L) [3]:

$$PoI_L = \boldsymbol{P}(\boldsymbol{MoS_{Ln}} < \mathbf{0}) = \frac{1}{2}\left[1 - erf\left(\frac{\mu(MoS_{Ln})}{\sigma(MoS_{Ln})} \cdot \frac{1}{\sqrt{2}}\right)\right] \times 100\%$$

We used 2-factor ANOVAs to evaluate effects of path oscillation frequency and width on each variable: $\mu(MoS_L)$, $\sigma(MoS_L)$, and PoI_L.

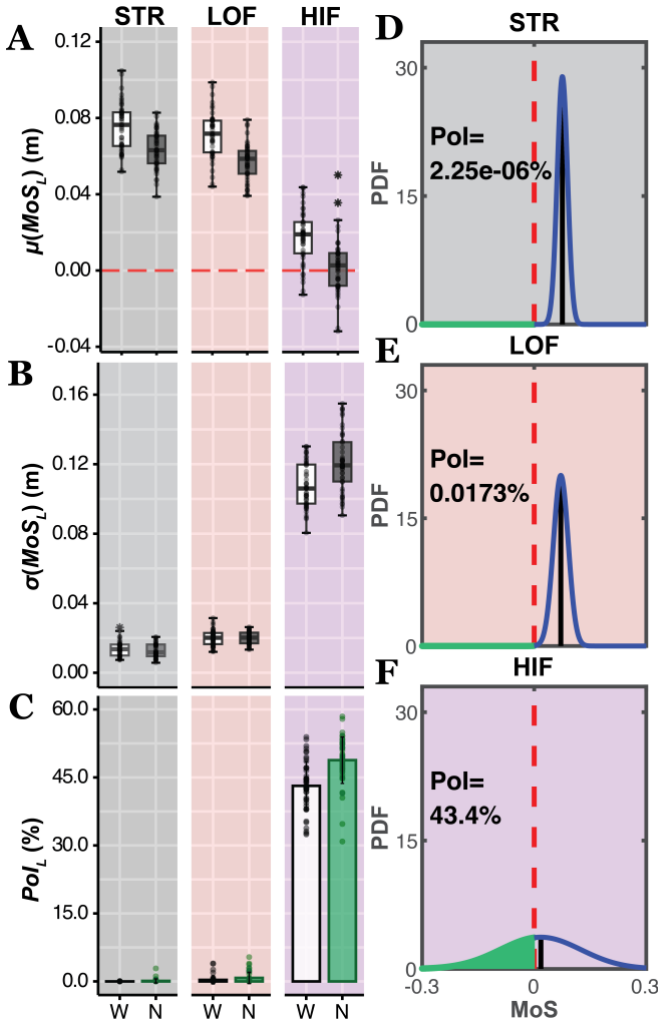

Figure 1: A) $\mu(MoS_L)$, **(B)** $\sigma(MoS_L)$, and **(C)** PoI_L on the W and N STR, LOF, and HIF paths. **D-F)** Example PDFs of the group average μ and σ MoS values where PoI is the cumulative probability (green area) over the range $MoS < 0$. **D)** For STR: μ=7.536cm, σ=±1.378cm. **E)** On the LOF path, $\mu\downarrow$ (7.125cm), $\sigma\uparrow$ (±1.992cm) thus, PoI↑. **F)** On the HIF path, $\mu\downarrow\downarrow$ (1.778cm), $\sigma\uparrow\uparrow$ (±10.762cm) thus, PoI↑↑.

Results & Discussion: People exhibited smaller $\mu(MoS_L)$ on paths of narrower width ($p<0.001$) and increased oscillation frequency ($p<0.001$) (Fig. 1A), indicating a smaller distance between their XCoM and base of support on average. Path width only influenced $\sigma(MoS_L)$ on HIF ($p=0.003$). However, at increased path oscillation frequencies for both widths, people also exhibited more variability ($\uparrow\sigma$) in their MoS_L (all $p<0.001$) (Fig. 1B). Thus, at higher path oscillation frequencies for both widths, people exhibited higher PoI_L, (all $p<0.001$), i.e., their instability risk increased walking on paths of higher sinuosity.

To visualize how PoI_L estimates risk of instability [3] that depends on *both* μ and σ, we generated example probability density functions (PDFs) (Fig. 1D-F) with group average $\mu(MoS_L)$ and $\sigma(MoS_L)$ values to represent a typical subject. For STR as baseline ($PoI_L \approx 2\times10^{-6}$%; Fig. 1D), $\downarrow \mu(MoS_L)$ and $\uparrow \sigma(MoS_L)$ on LOF (Fig. 1E), indicate the participant would be *more* likely to exceed the stability boundary ($PoI_L \approx 0.02$%). Whereas drastically $\downarrow \mu(MoS_L)$ and $\uparrow \sigma(MoS_L)$ on HIF (Fig. 1F), results in a likelihood of $MoS_L < 0$ once every ~2 steps ($PoI_L \approx 43.4$%)! Overall, to navigate more frequently winding pathways, people adapted smaller and more variable MoS_L that considerably increased their risk of taking an unstable step.

Significance: We demonstrate that people increase their risk of lateral instability while walking on winding paths, thereby trading-off stability for maneuverability. However, as no one fell, this highlights the importance of adaptability during locomotion as people enacted active rebalancing mechanisms [2], such as adjusting their steps, to mitigate falls in these destabilizing environments.

Acknowledgments: NIH / NIA Grants # R01-AG049735 & R21-AG053470, and Sloan Foundation Grant # G-2020-14067.

References: [1] Robinovitch et al. (2013), *Lancet*; [2] Hof et al. (2005), *J Biomech*; [3] Kazanski et al. (2022), *J. Biomech.*

QUANTIFYING WALKING STABILITY CONTROL MECHANISMS FROM FORCE PLATE DATA ALONE

Nancy T. Nguyen[1*], Elisa S. Arch[1], Jeremy R. Crenshaw[1]
[1]University of Delaware, Newark, DE
*Corresponding author's email: nanguy@udel.edu

Introduction: The lateral trajectory of the whole-body center of mass (COM) is controlled during walking, in part, through push-off and foot placement mechanisms that alter the magnitude and location of the vertical ground reaction force (GRF) [1-2]. Previous studies measured these mechanisms as a total center of pressure contribution to the acceleration of the COM [1]. However, identifying these mechanisms independently can provide insight on how walking stability is controlled. We propose a method to quantify such limb- and phase-specific contributions. The purpose of this study was to determine if we can accurately quantify these mechanisms from force plate data alone.

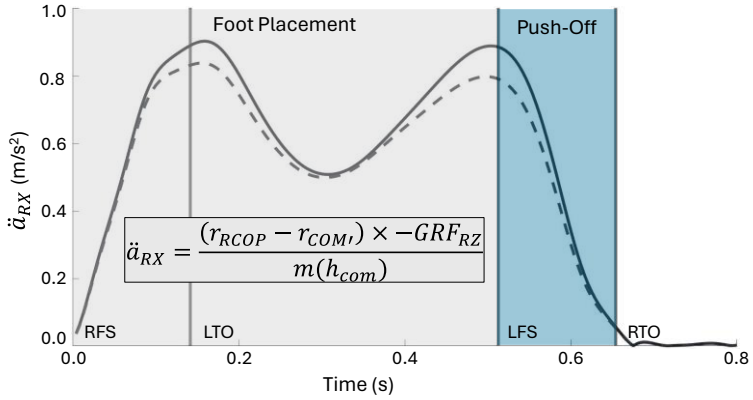

Figure 1. Example of **marker-based** (solid) and **force-plate-only** (dashed) contributions of the right-limb ($\ddot{a}_{RX}$) to lateral COM acceleration. The **foot-placement** contribution was evaluated from right foot strike (RFS) to left foot strike (LFS). The **push-off** contribution was evaluated from LFS to right toe off (RTO). r represents the lateral position of the **COP** or **COM'** (vertical COM projection on the treadmill surface). GRF_Z represents the vertical ground reaction force, m is mass, and h_{com} is COM height. Positive accelerations are directed medially (i.e. to the participant's left).

Methods: This is a secondary analysis of data from nine neurotypical participants (4 female; age 24.9 (2.80) years; BMI 24.0 (2.62) kg/m^2) walking on an instrumented treadmill (Bertec, 1200 Hz) at 0.6, 0.8, and 1.0 statures/s. Markers on the pelvis and lower extremities were also recorded (Qualisys, 240 Hz).

We focused this analysis on the right limb. The COM lateral acceleration specifically induced by the vertical GRF under the foot was determined from its magnitude and location relative to the COM (Figure 1; modified from [1]). This contribution was determined using two methods: 1) A **marker-based** method estimating the COM location as the midpoint of the iliac crest markers, and 2) a **force-plate-only** method. In this latter approach, the COM lateral and vertical location was determined from a method of double integrating the net shear and vertical GRFs [3]. We assumed the average lateral and vertical velocity over a stride was 0 m/s. In the lateral direction, we assumed the COM was above the net COP when lateral acceleration was 0 m/s^2. Peak COM height was assumed to be that of standing height. For both methods, we averaged the contribution (in m/s^2) during **foot-placement** and **push-off** phases (Figure 1) separately for three strides at each speed. Agreement between motion-based and force-plate-derived approaches was assessed with intraclass correlation (ICC(2,1)) and Bland-Altman plots.

Results & Discussion: We observed moderate-to-good agreement between the marker-based and force-plate-derived methods (Figure 2), with a trend of underestimating contributions with the force-plate-only approach. We are optimistic that we can improve agreement by repeating this analysis with a full-body marker set and reaction-board techniques to have more valid indicators of COM location (in progress). We will also test other approaches to estimating lateral COM location from force-plate data [4], and we will add left-limb and counter-rotation mechanisms of balance control [1].

Significance: We introduced an innovative method to characterize the limb- and phase-specific mechanisms of balance control during walking. We may be able to quantify these measures through force plate data alone. This method would allow us to analyze walking quickly and focus our studies on populations with atypical body sizes (e.g., obesity).

Acknowledgments: We acknowledge Luke Nigro for recording data for this study.
References: [1] van den Bogaart et al (2022), *J. Biomech. (136)* ; [2] Reimann et al (2018), *Kinesiol. Rev. (7)*; [3] Gutierrez-Farewik et al (2006), *Hum. Mov. Sci (25)*; Buurke et al (2023), *J. Biomech. (146).*

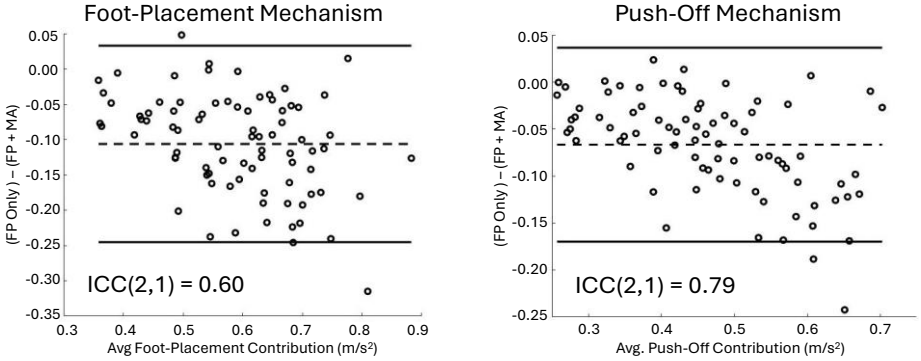

Figure 2. Bland-Altman plots and ICC values for the agreement between marker-based (Force Plate + Motion Analysis; FP + MA) and force-plate only (FP Only) approaches of estimating the foot-placement (left) and push-off (right) contributions to lateral COM acceleration. Each of nine participant is represented by nine data points, with three strides at three gait speeds.

ARE YOUR BALANCE DATA TELLING TALL TALES? IMPACT OF HEIGHT ON STABILITY ASSESSMENTS

Kevin D. Dames[1*] & Sutton B. Richmond[2]
[1]Biomechanics Laboratory, Kinesiology Department, SUNY Cortland, Cortland, NY, USA
[2]Brain Rehabilitation Research Center, Malcom Randall VA Medical Center, Gainesville, FL, USA
*Corresponding author's email: kevin.dames@cortland.edu

Introduction: Linear associations between body size and biomechanical dependent variables are commonly assumed [1,2]. These linear relationships are useful in normalization schemes, where variability due to anthropometric characteristics is removed and any remaining differences between groups or conditions can be explained by the intrinsic control paradigms enacted to complete the task. For example, the inverted pendulum model of balance considers the centre of mass (CoM) to be a point mass oscillating atop a stationary base of support (BoS) [4], with greater centre of pressure (CoP) motion associated with aging or disease [3]. However, a taller person would have a greater vertical separation of their CoM from the feet (which are also likely larger), resulting in greater torques about the ankle for a given lateral CoM displacement. Yet, the variability due to height or BoS area across persons is not typically accounted for in traditional balance outcomes such as path length or sway area [3].

Time to Boundary (TtB) is a balance measurement that accounts for BoS area. It is calculated by dividing the instantaneous CoP velocity into the distance from the CoP to the edge of the BoS it is approaching, representing the time available to generate postural adjustments to prevent the CoP from exceeding the BoS [5]. As such, while a taller person may exhibit larger path lengths (and, consequently, faster instantaneous CoP velocity), this greater CoP motion may be proportional to their larger BoS area. This study aims to explore the relationship between height and postural stability. Under the assumptions of the inverted pendulum model, we hypothesized that height would be correlated with CoP path length but independent of TtB.

Methods: Ninety-seven healthy adults (68 men and 29 women; 22 ± 6 years, 1.8 ± 0.1 m, 83.0 ± 17.4 kg, body mass index 26.6 ± 4.2 kg m^2) stood quietly with feet together and eyes open on a force platform (Fs = 100 Hz) for 150 seconds. CoP data were smoothed with a dual-pass digital low pass Butterworth filter at 4 Hz and centred. Feet length and width were measured to determine the BoS. BoS width was the sum of the two feet widths and length was taken as the longer of the two feet. Path length was calculated as the sum of absolute point-to-point displacements of the CoP trajectory in anterior-posterior (AP), medial-lateral (ML), and resultant (R) directions [3]. A TtB series was generated by dividing the instantaneous CoP velocity vector elementwise into the distance to the edge of the BoS the CoP was approaching. From this continuous series, the minimum events were indexed according to recommended methods [5] for AP and ML directions. Simple linear correlations were calculated between height and all postural stability measures. For simplicity, only the absolute minimum TtB correlations with height are presented here, with similar outcomes found when correlating the average and standard deviation of the TtB series with height. Alpha was set at .05.

Results & Discussion: The main result of this study is that CoP path length is positively correlated with height (Fig. 1). While the variation in path length explained by height is small (5.29% for R PL, 8.47% for ML PL), observing this relationship in young, healthy adults suggests anthropometrics may contribute to the limitations of displacement-only CoP measures in fall prediction models [6]. Given CoP path length (and consequently velocity) and BoS area are both positively correlated with body size, then considering the CoP velocity within the BoS framework when calculating TtB effectively normalizes the measurement. While not the initial intention of the TtB variable, a *de facto* normalization component is a novel aspect of TtB in contrast to the traditional measures (e.g., path length, sway area) which neglect anthropometric factors.

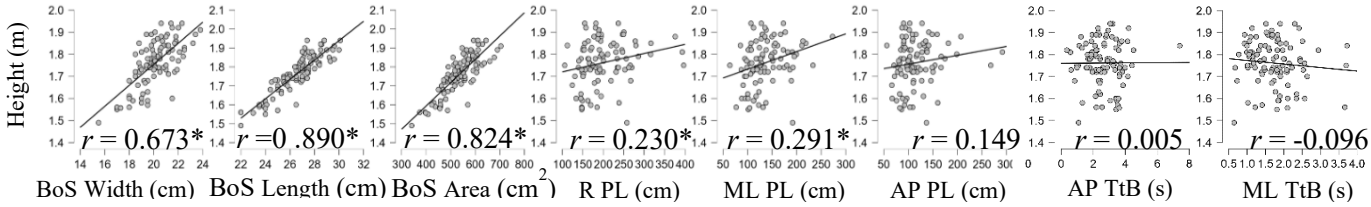

Figure 1: Scatterplots illustrating height's (vertical axis of each image) relationship with base of support (BoS) dimensions, CoP Path Length (PL) as Resultant (R), Medial-Lateral (ML), and Anterior-Posterior (AP), and Minimum Time to Boundary (TtB) for AP and ML. * indicates a significant correlation (p<.05).

Significance: If experimental groups differ greatly in height, then any significant differences in position-based CoP measures, such as path length, may be an artifact of body size inequality rather than indicators of disease progression, aging, or imposed interventions. In contrast, TtB is not related to height and may be used to discern the effects of clinical conditions and fall risk without concern for anthropometric inequalities.

References: [1] Hof (1996), *Gait Posture* 4; [2] Wannop et al. (2012), *J Applied Biomech* 28. [3] Prieto et al. (1996), *IEEE* 43(9); [4] Peterka (2003), *IEEE* 22(2); [5] Dames & Richmond (2023), *Hum Mov Sci* 92; [6] Topper et al. (1993), *J American Ger Soc* 41(5).

DESIGN AND VALIDATION OF A DEVICE TO MEASURE THE IMPACT OF DOG WALKING ON GAIT STABILITY

Samantha Morrison[1], Julio Ramirez-Reyes[2], Nicole Arnold[1], Lara Thompson[1,2] and Alex Peebles[2]
[1]Biomedical Engineering Program, University of the District of Columbia
[2]Department of Mechanical Engineering, University of the District of Columbia
*Corresponding author's email: alexander.peebles@udc.edu

Introduction: Between 2001 and 2020, it was estimated that 422,659 adults visited an emergency department for a leash-dependent dog walking injury in the US, with 55% of these cases being the result of an accidental fall [1]. Living with a dog is common, and while there are health benefits associated with living with a dog, there are also risks. One study found that 37 people reported to a single hospital over a two-month period with dog-walking related injuries, with 26 being fractures, 10 soft tissue injuries, and one head injury; being pulled over while walking was the most common injury mechanism [2]. Despite the established epidemiology of dog-walking related injuries, there has been limited academic research on how dog walking impacts fall risk or the risk for soft-tissue injuries. Thus, the purpose of this project was to design and validate a system to simultaneously measure dog leash tension and human gait stability.

Methods: Shown in Figure 1, a 500 kg S-type load cell was chosen to measure leash tension, which was outfitted with eye bolts and carabiners to connect inline between the dogs' leash and harness. The load cell was wired into an instrumentation amplifier circuit constructed using four operational amplifiers (LM358-N), which produced a voltage signal that is measured using a microcontroller (Arduino Nano Every). The system also contains an inertial measurement unit (MPU6050) which measures triaxial accelerations and transmits data to the microcontroller. The microcontroller stores force and acceleration data on a micro-SD card at 200 Hz. A push button and LED were added for human-computer interaction. The device logs data for research only. A readout for the dog walker may be included in future iterations of the device. All components were soldered into a prototype board and fit inside a custom 3D printed enclosure which is fixed to the participants low back using an elastic strap and Velcro. The device was brought to our campus weight room for calibration and validation testing. Weights were suspended from the device in regular intervals up to 180 lbs, a load comparable to the expected maximum force a dog could pull. Bland-Altman plots were used to visualize and analyze measure error (true relative to measured) across the range of loads tested. Paired t-tests and linear regression analyses were used to quantify the agreement and measurement error.

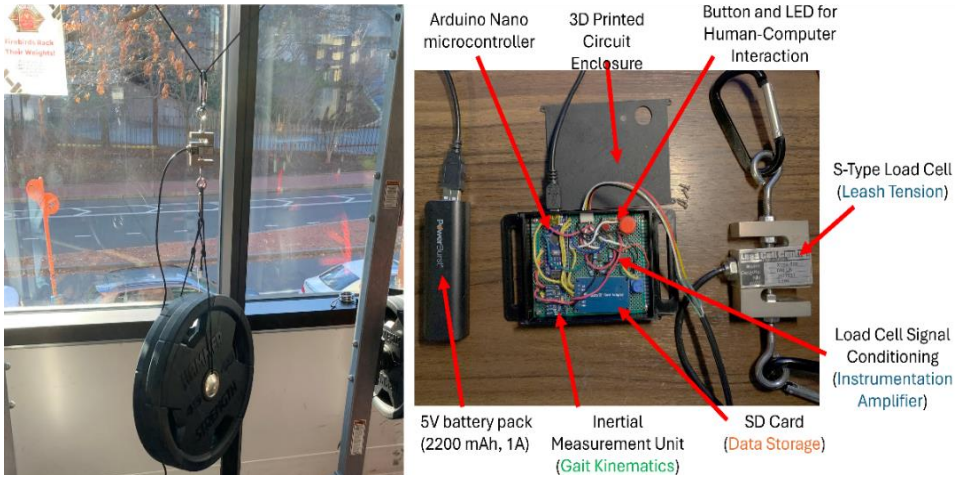

Figure 1: Leash tension validation procedure (left) and device components/assembly (right)

Results & Discussion: There was a very strong correlation between measured and true values ($r = 0.99$, $p < 0.01$), with an average bias of -0.002 lbs ($p = 0.98$). The Bland-Altman plot shown in Figure 2 demonstrates that the measurement error is constrained to less than ± 5 lbs across the measurement range of 0 – 180 lbs, and that error does increase in an unexpected manner with increasing weight. We believe these results could be further improved through a refined validation procedure. The exercise weights used as our known standard were not calibrated to NIST standards and were suspended from a lightweight cable thus any swinging that occurred would influence force readings. Future iterations of the device will be wireless and lower profile than the current system.

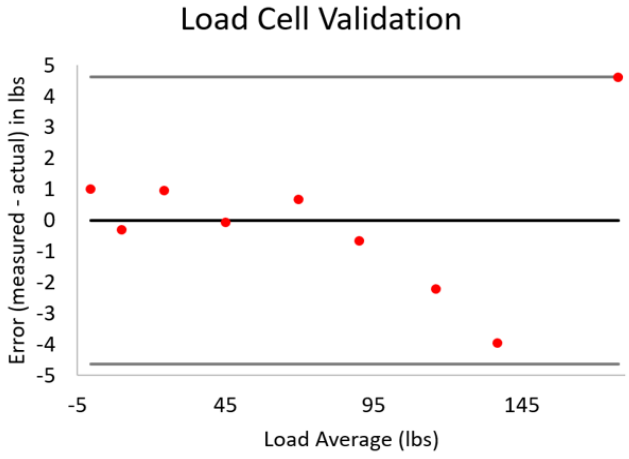

Figure 2: Bland-Altman plots visualizing measurement error.

Significance: The system developed and validated in this project will allow us to conduct future experiments to determine the impact that dog walking has on gait stability. This line of research could help us understand and prevent dog-walking related injuries.

Acknowledgments: Funding support was received from NIH (Award Number R25AG067896) and NSF (Award Number: 2229575).

References: [1] Maxson et al. (2023), *MSSE* ; [2] Willmott et al. (2012), *Accident Analysis and Prevention* 46.

FOR MoS, THE *MARGIN* IS WHAT MATTERS – WHY WE NEED PROBABILITY OF INSTABILITY: PoI

Jonathan B. Dingwell[1*], Joseph P. Cusumano[2], Meghan E. Kazanski[3]
[1] Department of Kinesiology, Pennsylvania State University, University Park, PA, USA
[2] Department of Engineering Science & Mechanics, Pennsylvania State University, University Park, PA, USA
[3] Department of Medicine, Division of Geriatrics and Gerontology, Emory University School of Medicine, Atlanta, GA, USA
*Corresponding author's email: dingwell@psu.edu

Introduction: At a given instant, smaller lateral Margin of Stability (MoS_L) indicates a smaller impulse is needed to knock a person off balance [1,2]: they are "*less* stable". However, averaging MoS_L over multiple steps, $\mu(MoS_L)$, yields perplexing results. Persons at high fall risk [3], or who experience destabilizing perturbations [4], exhibit larger (supposedly "*more* stable") $\mu(MoS_L)$, despite clearly being *de*stabilized. We assert MoS_L is a sound instantaneous mechanical quantity, but computing $\mu(MoS_L)$ is the wrong statistic.

When people walk, most steps are stable: occasional unstable steps are *un*likely (rare) events. Conversely, the mean of any set of values quantifies (by definition) *very* likely events: for normal Gaussian distributions, the value observed *most* often. This is why computing MoS_L on a single step is mechanically sound, while computing $\mu(MoS_L)$ over multiple steps yields contradictory interpretations.

By definition [1,2], MoS_L quantifies a *margin* (distance) from a *threshold* ($MoS_L = 0$) above which stability holds. Over many steps, people exhibit a *range* of MoS_L values. But they only violate Hof's condition [1] on those (few) steps when $MoS_L < 0$; regardless of their mean, $\mu(MoS_L)$. The relevant statistical metric to compute should thus instead quantify, from any sequence of steps, the likelihood a walker will violate Hof's condition [5]. We proposed the lateral Probability of Instability (PoI_L) [5] to do this. Here, we describe how to compute PoI_L and demonstrate how and why it helps resolve the paradoxical findings of prior studies (e.g., [3,4], etc.).

Methods: Given any mean and standard deviation, (here, $\mu(MoS_L)$ & $\sigma(MoS_L)$ from some sequence of steps), PoI_L is calculated as [5]:

$$PoI_L = \mathrm{P}\left(MoS_{Ln} < 0\right) = \frac{1}{2}\left[1 - erf\left(\frac{\mu\left(MoS_{Ln}\right)}{\sigma\left(MoS_{Ln}\right)} \cdot \frac{1}{\sqrt{2}}\right)\right] \times 100\%, \quad (1)$$

which is easily computed (e.g., just use 'erf' function in Matlab!). We first computed probability density functions (PDF) for various μ & σ (Fig. 1A-C), and used Eq. (1) to compute their *resultant* PoI_L. We then computed PoI_L across a range of μ for different σ, and across a range of σ for different μ (Fig. 1D-E).

These analyses demonstrate that one cannot infer a walker's likelihood of violating Hof's dynamic stability condition [1] knowing either $\mu(MoS_L)$, or $\sigma(MoS_L)$, or both separately, but only via PoI_L. We propose PoI_L can thus explain & resolve paradoxical findings.

Results & Discussion: We nominally chose μ = 4cm ± σ = 2cm (Fig. 1A). With *no* change to μ, increasing σ *in*creases PoI_L (Fig. 1B). Then, holding σ constant, increasing μ *de*creases PoI_L (Fig. 1C).

Over $0 \le \mu \le 10$cm, we computed PoI_L for $\sigma \in \{2,4,6\}$cm. For any mean (μ), PoI_L *in*creases for larger σ (Fig. 1D). Over $0 \le \sigma \le 10$cm, we computed PoI_L for $\mu \in \{2,4,6\}$cm. For any standard deviation (σ), PoI_L *de*creases for increased μ (Fig. 1E). Thus, knowing either μ or σ independently, or both simultaneously, cannot indicate PoI_L.

For walking, we expect impaired or perturbed persons to exhibit more variability [4,5] (e.g., Fig. 1B). But we also expect they may adapt, e.g., take wider steps that would *in*crease their $\mu(MoS_L)$, but mitigate their instability risk by *de*creasing PoI_L (e.g., Fig. 1C).

This explains why calculating $\mu(MoS_L)$ yields paradoxical results: $\mu(MoS_L)$ is statistically not consistent with Hof's condition [1,2]. It does not quantify *risk* of instability, $\mathrm{P}(MoS_L) < 0$, whereas PoI_L does.

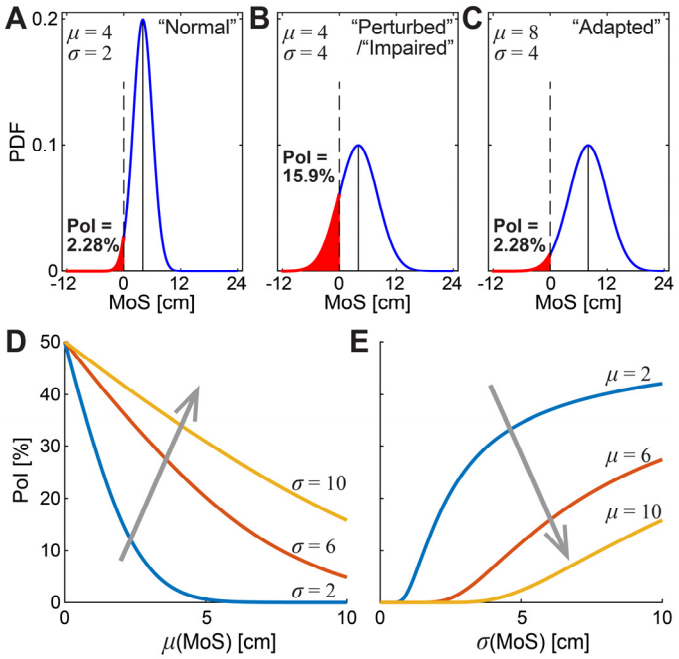

Figure 1: A) Suppose a hypothetical distribution (PDF) of *MoS* values for "normal" walking. **B)** If perturbed, we expect steps to become more variable. With *no* change in $\mu(MoS)$, this would greatly increase *PoI*. **C)** However, if people adapt (e.g., take wider steps), this would increase $\mu(MoS)$, but *decrease PoI*. **D)** For any $\mu(MoS)$, any ↑ $\sigma(MoS)$ will ↑ *PoI*. **E)** But for any $\sigma(MoS)$, any ↑ $\mu(MoS)$ will ↓ *PoI*.

Significance: MoS_L itself quantifies [1,2] (by definition) a person's instantaneous *margin* away from their instability *threshold* (MoS_L = 0). For any sequence of steps, PoI_L quantifies the probability with which a person will cross that threshold. Hence, PoI_L is the only statistical metric that is consistent with the original mechanical principles underlying Hof's derivation of MoS_L.

Moreover, most researchers already compute $\mu(MoS_L)$ and $\sigma(MoS_L)$. Adding one simple extra calculation (i.e., 1 line of Matlab code) to compute PoI_L is easy [5] and can resolve many long-standing paradoxical interpretations in the current literature (e.g., [3,4], etc.).

Acknowledgements: Partly supported by NIH / NIA Grants # R01-AG049735 & R21-AG053470.

References: [1] Hof et al. (2005) *J Biomech* 38(1); [2] Hof (2008) *Hum Mov Sci* 27(1); [3] Watson et al. (2021) *BMC Musc Disord* 22(1); [4] Onushko et al. (2019) *PLoS ONE* 14; [5] Kazanski et al. (2022) *J Biomech* 144.

DOES PROLONGED EXPOSURE TO A SOFT EXOSKELETON AFFECT KINEMATICS AND FALL RISK WHILE WALKING?

Duleepa Subasinghe[1*], Jessica Aviles[1], Divya Srinivasan[1]
[1]Department of Industrial Engineering, Clemson University
*Corresponding author's email: dsubasi@clemson.edu

Introduction: Occupational back-support exoskeletons (BSEs) are expected to reduce the risk of overexertion injuries to the back that are common in physically demanding tasks, such as manual material handling [1]. A common mechanism by which passive BSEs assist lifting motion is to provide external hip extension torques that are transferred to the torso through supportive frames, straps, or bands. However, these devices add extra weight to the body and may restrict torso/hip motions while walking, which, in turn, may impose balance constraints on users and increase fall risk. Previous studies with rigid BSEs found modest negative effects on postural balance during gait [2][3][4]. However, BSE designs are evolving, and we now have viable textile-based designs that use elastic elements to provide assistance. It is unclear whether such soft BSEs also have unintended effects on gait and if/how users adapt to such changes over time.

Therefore, the objective of this study was to evaluate changes in gait with prolonged use of a soft, passive BSE. The BSE used for this study was the Herowear Apex (Apex 1, HeroWear, Nashville, TN, USA), which provides assistance to the torso through the energy (re)stored in elastic bands connecting the upper body to the back of the thighs. The Apex uses a mechanistically different approach to assistance compared to rigid BSEs and is lighter and does not include rigid frames. Hence our hypothesis was that there may be small changes in gait kinematics on initial exposure to the BSE, however, these differences would be attenuated with time (as users adapted to using the device).

Methods: A repeated-measures design was used, where each participant completed a single four-hour session that included a battery of industrially relevant tasks with no-exoskeleton (noEXO), exoskeleton (EXO), and no-exoskeleton trials in an A-B-A protocol. The first noEXO assessment was followed by 90 minutes of exoskeleton exposure (Figure 1), where participants performed a range of simulated manual material handling tasks (lifting, lowering, and carrying boxes with low load levels to avoid fatigue). Over the 90-minute exposure, three EXO assessments were conducted, which included walking trials along a straight, and level, 10 m walkway.

A convenience sample of twelve healthy young adults (6M, 6F), with no prior experience in using BSEs, were recruited for this study. BSE assistance level was fixed at the middle level (strong) across participants to eliminate any effects of varying assistance levels on adaptation rates.

Outcome measures included hip, knee, and ankle range of motion (ROM) and peak angular velocity, as well as step length (normalized to participant height), step width, and minimum toe clearance (MTC) during gait. For this analysis, we only explored changes in the initial and final EXO assessments ($EXO_{initial}$ and EXO_{final}) compared to the initial noEXO assessment. A two-way, mixed-factor analysis of variance (ANOVA) was performed on each outcome measure with EXO as a within-subject factor and gender (GEN) as a between-subjects factor.


(a) (b)

Figure 1: Illustration of the experimental setup for the 90-minute exoskeleton exposure consisting of (a) lifting and (b) carrying. Walking assessments (with no boxes) were conducted at the beginning, middle, and end of the exposure.

Results: EXO use decreased hip ROM ($p = 0.001$), decreased ankle ROM ($p = 0.009$), decreased step length ($p = 0.023$), and increased step width ($p = 0.038$) compared to the initial noEXO assessment. Some of these changes were observed at both initial and final EXO assessments. Specifically, hip ROM decreased by 4% at $EXO_{initial}$ and was still significantly decreased by ~2% at EXO_{final}, step length decreased by 2% and step width increased by 9% at $EXO_{initial}$ and these changes persisted (to the same magnitude) at $EXO_{final.}$, compared to the initial noEXO assessment.

Discussion: Use of the Herowear Apex BSE led to small but significant reduction in hip and ankle ROM as well as decreased step length and increased step width, suggesting a more cautious or restricted gait pattern. Most changes persisted after prolonged (90-minute) EXO exposure, indicating that users do not return to their normative gait patterns during EXO use. While MTC did not differ, previous research suggests that an increased step width (comparable to the magnitude of change seen here) can lead to increased fall risk among the elderly. Finally, despite using a soft BSE, our findings agree with prior work on rigid hip-torque BSEs (e.g., BackX) [2][4].

Significance: We investigated user adaptions to a soft-BSE and found that changes in gait appeared during EXO use and persisted throughout a 90-minute session. Further understanding of prolonged BSE use should be considered to enable the successful translation of exoskeletons for practical implementation.

References: [1] Kingma et al. (2010), *Ergonomics* 53; [2] Park et al. (2022), *J Ann Biomed Eng 50*; [3] Baltrusch et al. (2018), *Applied Ergonomics* 72; [4] Park et al. (2022), *Gait & Posture 92.*

ACCURATE LOWER BODY KINEMATICS USING A HANDHELD SMARTPHONE

J.D. Peiffer[1,2*], R. James Cotton[1,3]
[1]Center for Bionic Medicine, Shirley Ryan AbilityLab
[2]Department of Biomedical Engineering, Northwestern University
[3]Department of Physical Medicine and Rehabilitation, Northwestern University
*Corresponding author's email: jpeiffer@sralab.org

Introduction: Despite the diagnostic and prognostic utility of biomechanics, its use in clinical practice is minimal due to time constraints for busy clinicians and the technical knowledge needed to use motion capture technology. Markerless motion capture using a smartphone camera overcomes these barriers. However, integrating vision algorithms that provide 3D joint angles with biomechanically grounded models remains a critical gap to harnessing modern computer vision advances for clinical practice. In this work, we introduce and validate a technique for accurately measuring lower-body joint movements using just a handheld smartphone.

Methods: We recruited 36 clinical participants—19 with a history of stroke and 17 lower limb prosthesis users—and 26 control participants for this study. Participants walked across a room measuring 8 × 10 m and were recorded using two systems: (1) a markerless multi-camera system consisting of 12 cameras, as detailed in [1] and (2) a smartphone collecting RGB video at 30 Hz [2]. For each system, we estimated 3D and 2D keypoints for every frame using MeTRAbs-ACAE [3]. We jointly optimized the scale parameters of a biomechanical model based on LocoMuJoCo [4] and an implicit function $f_\phi: t \rightarrow \theta$ mapping time (t) to biomechanical joint angles (θ), where ϕ are the learned parameters of a multi-layer perceptron [5]. The implicit function is unique to each trial and is trained to produce joint angles that when pose the biomechanical model, aligns with the detected 3D and 2D keypoints, weighted by their confidence. Additionally, we estimated the global orientation of the smartphone and refine this estimate using the smartphone's internal gyroscope.

To evaluate the accuracy of these methods, we compared the mean angular error (MAE) of the lower body joint angles between the portable smartphone and multi-camera system. We also report Pearson's correlation coefficient to examine the temporal correlation in the joint angles.

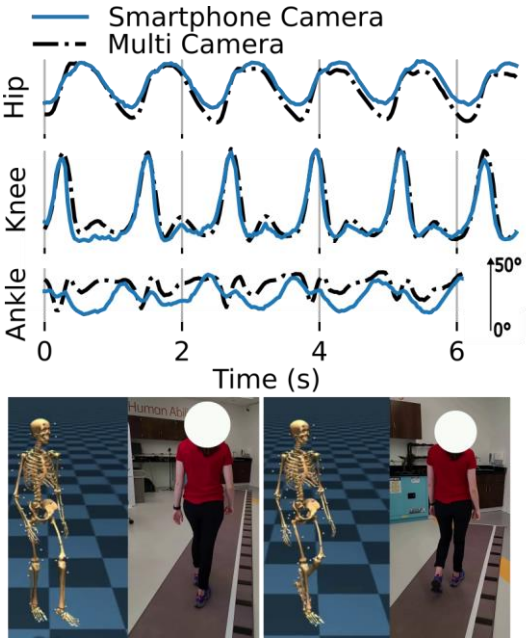

Figure 1: Example joint angles (degrees) from a subject walking across a room followed by a researcher holding a smartphone.

Group	↓MAE (deg)			↑Pearson's r		
	Knee	Hip	Ankle	Knee	Hip	Ankle
Stroke	5.84	5.83	4.66	0.93	0.96	0.64
Control	6.06	3.57	5.77	0.96	0.98	0.69
Prosthetic	7.08	5.25	6.39	0.93	0.97	0.60

Table 1: Median metrics across all runs separated by subject cohort.

Results & Discussion: Subjects completed an average of 3 trials leading to a total of 179 trials evaluated here. Figure 1 shows an example comparison between the biomechanical fits found from the multi-camera and smartphone camera system. Table 1 shows moderate agreement between the smartphone system and the multi-camera ground truth. Ankle MAE was lowest for the stroke group while hip MAE was lowest for the control and prosthetic groups. Prosthetic knee flexion had the highest MAE—an expected result as keypoint detectors often fail on prosthetic limbs not covered by clothing. Pearson correlations were high for the knee and hip indicating good temporal agreement between the two systems. While ankle MAE was low, this likely reflects the decreased range of motion of that joint. Pearson correlations for the ankle are significantly lower than the hip and knee. One possible reason for this is the ankle being occluded during parts of walking, particularly as videos were typically in frontal plane from behind (Figure 1) and difficulty in detecting small changes in ankle movement.

Significance: Modern computer vision makes human pose estimation much more accessible—now possible using only a handheld smartphone. However, state-of-the-art models rarely output joint angles for biomechanically valid models. We present a method to fit a biomechanical model to smartphone videos and validate it against a multi-camera system, finding an agreement of around 4-7 degrees for different clinical populations. This work bridges a critical gap between the computer vision and biomechanics community by introducing a method to link state-of-the-art keypoint detection to biomechanically interpretable results.

Acknowledgments: This work was generously supported by the American Neurological Foundation, the Restore Center P2C (NIH P2CHD101913), and the Research Accelerator Program of the Shirley Ryan AbilityLab. JDP is supported by the National Science Foundation Graduate Research Fellowship Program under Grant No. DGE-2234667

References: [1] Cotton et al. (2023), arXiv:2303.10654 [2] Cimorelli et al. (2024), Sci Rep 14(1) [3] Sárándi et al. (2023), *IEEE/CVF WACV*, pp. 2956-2966 [4] Al-Hafez et al. (2023), arXiv:2311.02496 [5] Cotton (2024), arXiv:2402.17192

OPENCAP MONOCULAR: HUMAN MOVEMENT DYNAMICS FROM A SINGLE SMARTPHONE VIDEO

Scott D. Uhlrich[1,2*], Shardul Sapkota[1], Antoine Falisse[1], Scott L. Delp[1]
[1]Stanford University, Stanford, CA; [2]University of Utah, Salt Lake City, UT
*Corresponding author's email: suhlrich@stanford.edu

Introduction: The ability to easily measure the kinematics and kinetics of human movement could improve the prevention and treatment of neurological and musculoskeletal diseases. The time and expertise required to measure movement with marker-based motion capture has limited its adoption in the clinic and in large-scale research studies. We recently developed OpenCap, open-source software that estimates kinematics and kinetics using two smartphone videos [1]. OpenCap and other markerless motion capture technologies [2] lower the time and cost barriers to movement analysis by orders of magnitude [1]; however, they require multiple cameras. If we can achieve similar accuracy from a single video, the >4 billion smartphone owners around the world would have access to 3D motion capture. The computer vision field has made advances in estimating the global pose of a human mesh from a single video [3], but these algorithms are not designed for or evaluated on their biomedical utility. This study aims to develop and evaluate a pipeline for estimating kinematics and kinetics of common human movements (walking and squatting) from a single video.

Methods: Here we introduce OpenCap Monocular, which combines 3D human pose estimation, biomechanical modeling, and dynamic musculoskeletal simulation to estimate kinematics and kinetics from monocular video (Figure 1a). We evaluate the pipeline on walking and squatting trials with synchronously recorded video (45° from front-facing), marker-based motion capture, and force plate data [1] for one individual (33-year-old female). First, we estimate foot contact probability and the global pose of an SMPL model [4] using WHAM [3], a state-of-the-art regression-based 3D pose estimation algorithm. Using the WHAM results as the initial guess, we perform a two-stage optimization to solve for camera parameters and global human pose. The first optimization solves for camera parameters and SMPL shape parameters (i.e., anthropometry) by minimizing reprojection error assuming a fixed camera and known subject height. After fixing camera and SMPL parameters, the second optimization solves for the global SMPL pose by minimizing reprojection error, foot position variance during contact, and joint velocity. We then extract anatomical landmarks from SMPL vertices, scale a musculoskeletal model [1], and run Inverse Kinematics using OpenSim 4.4 [5]. We generate a muscle-driven dynamic simulation that tracks the kinematics to estimate ground forces [1,6]. To evaluate accuracy, we compute mean absolute differences between OpenCap Monocular and marker-based motion capture and force plates and average across trials.

Figure 1: (a) The OpenCap Monocular pipeline for estimating kinematics and kinetics from video. **(b)** Optimizing pose after regression-based pose estimation reduces drift over five repetitions of squatting (translational error reduced from 96mm to 46mm).

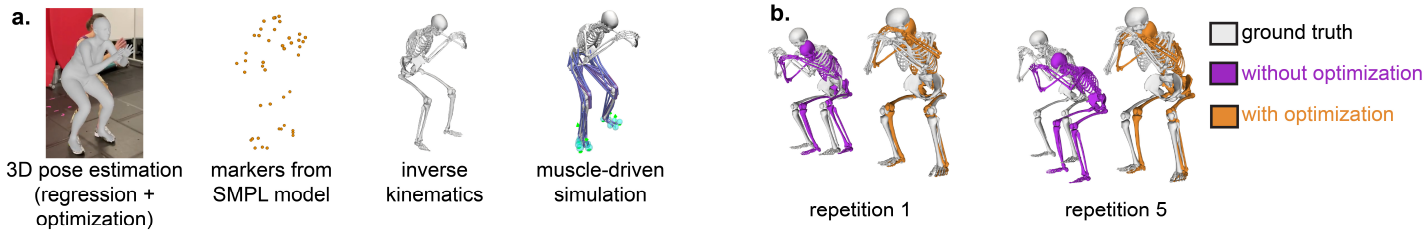

Results & Discussion: For walking and squatting, OpenCap Monocular had mean absolute differences from marker-based motion capture and force plates of 6.6° and 37mm (pelvis translation) for kinematics, and 7.7%bodyweight for reaction forces (Table 1). The joint angle differences during walking (5.6°) are comparable to the two-camera OpenCap system (5.2°), an eight-camera markerless motion capture system (5°) [2], and a 17-sensor IMU suit (5°) [7]; however, translational differences (27mm) are greater than two-camera OpenCap (7mm). Ground reaction force accuracy during walking (medio-lateral: 1.3% bodyweight, anterior-posterior: 4.9%, vertical: 21.5%) is worse than two-camera OpenCap (1.5–11.1% bodyweight) [1] and IMUs (1.7–9.3% bodyweight) [8], likely due to larger errors in pelvis translation. The pose optimization reduces drift from the regression-based pose estimation model (Figure 1b).

Table 1: Mean absolute differences between OpenCap and marker-based motion capture. Kinematic differences are averaged across 24 rotational and three translational degrees of freedom, and ground forces are averaged across three directions.

	Kinematics (rotations, °)	Kinematics (translations, mm)	Ground forces (% bodyweight)
Opencap Monocular	6.6	37	7.7
OpenCap two-camera	4.9	7	4.2

Significance OpenCap Monocular estimates kinematics and kinetics in two activities for a single individual with similar but slightly worse accuracy than two-camera OpenCap; further validation across individuals and activities is needed. Biomechanical analysis from a single video will dramatically expand the frequency and ease with which we can quantify movement in the home, clinic, and field. Rigorous analysis in the context of biomechanical assessments is a necessary step in this expansion.

References: [1] Uhlrich et al. (2023), *Plos Comput Biol* 19(10). [2] Kanko et al. (2021), *J Biomech* 127. [3] Shin et al. (2024), *Proc CVPR*. [4] Loper et al, (2015), *Proc SIGGRAPH Asia*. [5] Seth et al. (2018) *Plos Comput Biol* 14(7). [6] Falisse et al. (2019) *J R Soc Interface* 16. [7] Al Borno et al. (2022), *J Neuroeng Rehabil* 19(11). [8] Karatsidis et al. (2019), *Med Eng Phys* 65.

SMARTPHONE-BASED DIGITIZED NEUROLOGICAL EXAMINATION TOOLBOX FOR MULTI-TEST NEUROLOGICAL ABNORMALITY DETECTION AND DOCUMENTATION

Trung-Hieu Hoang[1*], Christopher Zallek[2], Minh N. Do[1]
[1] Department of Electrical and Computer Engineering, University of Illinois at Urbana-Champaign, IL, USA
[2] OSF HealthCare Illinois Neurological Institute – Neurology, IL, USA
*Corresponding author's email: hthieu@illinois.edu

Introduction: One in five people will be 65 years or older by 2030. Many of them will develop neurological conditions, e.g., Parkinson's disease (PD) [1], or experience aging-related neurohealth deterioration. Primary care limitations and the growing shortage of neurologists [2] are worsening barriers to primary neurological care access for screening and symptom triage. Screening consistency, quality, and documentation are exacerbating factors within this care bottleneck. These lead to delays in diagnosis and treatment and inefficient use of healthcare resources. In this study, we provide a modular set of toolboxes for recording and extracting contactless screening digitized neurological examination (DNE) biomarkers and analyzing their capability for detecting and documenting abnormal exam features on PD and other neurological disorders (OD). Specifically, we study a *DNE record* with five neurological tests: finger tapping (FT), finger to finger (FTF), forearm roll (FR), stand-up and walk (SAW), and facial activation (FA).

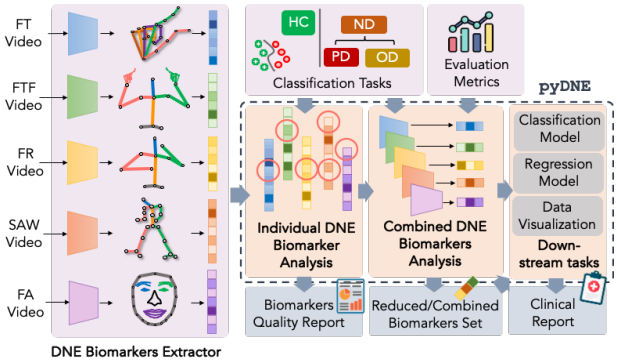

Figure 1: Overview of our proposed digitized neurological examination (DNE) and the *pyDNE*

Methods: Our *DNE Recorder* software [3] allows recording each exam while giving audio and visual instructions using an iPhone/iPad device. All recordings are synchronized to a cloud storage for later processing. Using off-the-shelf pose estimators, the major 2D/3D human keypoints are detected. Following, DNE Biomarker Extractor module (Fig. 1-left) extracts a set of 75 *DNE biomarkers* for all tests, capturing the kinematic characteristics of individual movements. These digital biomarkers quantify the movement symmetry - left versus right side, and the consistency across cycles for periodic movements. Additionally, the amplitude, period, velocity, and acceleration of major joints are also computed. Following, *pyDNE* – an open-source Python framework (Fig. 1-right) represents those biomarkers into a unified platform for in-depth feature quality analysis, considered both separately (Individual DNE Biomarker Analysis) and collectively (Combined DNE Biomarker Analysis). Here, we support simple statistical tests (e.g., Mann-Whitney U Test), and feature importance analysis (recursive feature elimination). In addition, the digital biomarkers can be incorporated into several downstream binary/multi-class classification tasks with deep learning/machine learning models in *pyDNE*. Noticing the hierarchical structure of the classification task between healthy controls (HC) and ND, which can be further sub-categorized to PD and OD, a *hierarchical classifier* [4] is adopted. We also consider the classification tasks at single test- and record- level (multi-test).

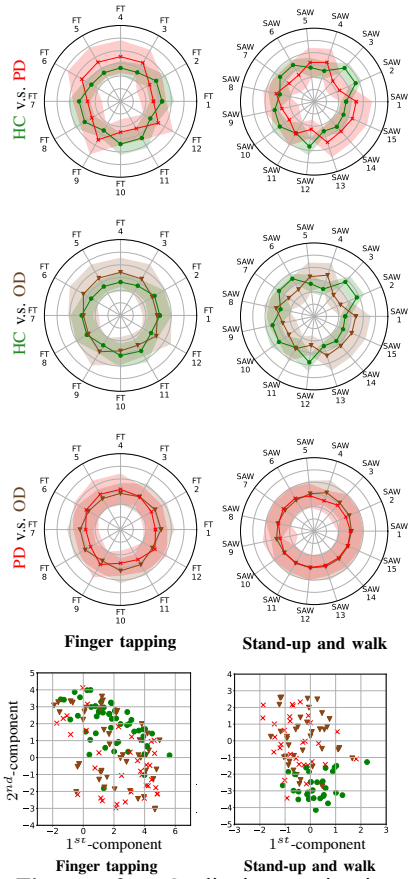

Figure 2: Qualitative pair-wise comparison between DNE biomarkers from the HC (●), PD (×) and OD (▼) groups. Mean *(solid line)* and variance *(shaded area)* of the normalized DNE biomarkers (*top rows)*. Dimensionality reduction analysis of concatenated features *(last row)*. For space constraints, only FT, SAW are shown.

Results & Discussion: DNE 113 – *a multi-test DNE database* containing 643 videos with five neurological examinations are recorded on a population of 113 subjects (55 males; age 64.1±14.3; disease duration 2.2±5.1; PD/OD/HC=34/33/46), covering a broader range of abnormalities (beyond PD/OD) as in previous works. Many measured DNE biomarkers are statistically significantly different ($p<0.05$, *two-tailed*) between HC versus (vs.) PD/OD, while the differentiation between PD vs. OD is limited. Fig. 2-top illustrates these observations qualitatively on the mean/variance of the normalized DNE biomarkers of the FT, SAW tests. Generally, combining information from multiple features within a single test gives better discrimination across groups, as visualized in Fig. 2-bottom using t-SNE [5]. Furthermore, multi-test input classification gives the highest performance. We achieved an accuracy above 90% for the task of HC vs. PD/OD and 64% for PD vs. OD. We highlighted the difficulties in distinguishing PD from OD. Noteworthy, this task presents similar challenges for humans as the diagnosis of PD must include a complete clinical history and non-motor examinations. Hence, we position DNE as a *contactless screening neurological exam abnormality detector*.

Significance: This study provides a *proof-of-concept* for a comprehensive DNE solution, streamlining the *entire process* from data acquisition to a final analysis and validating its ability on *real patients*. The open-source software will serve a broader spectrum of use cases. We also emphasize the role of *examining the quality of digital biomarkers* in vision-based human motion analysis, not only for interpreting the computer-aided exam results but also for advancing the next generation of digital health toolboxes. Our *pyDNE* facilitates this process.

Acknowledgments: This project has been funded by the Jump ARCHES endowment through the Health Care Engineering Systems Center and the Innovation for Health (IFH) Collaboration with Bradley University and OSF HealthCare.

References: [1] C. Marras *et al.*, npj Parkinson's Disease (2018); [2] J. J. Majersik *et al.*, Neurology (2021); [3] T.-H Hoang *et al.,* IEEE-JBHI (2022); [4] F. M. Miranda *et al.*, JMLR (2023); [5] L. van der Maaten *et al.,* JMLR (2008).

IMPROVING GAIT IN OLDER ADULTS USING A SMARTPHONE-BASED HAPTIC FEEDBACK SYSTEM

Ehsan Sharafian M.*, Colby Ellis, Babak Hejrati
The Biorobotics and Biomechanics Laboratory, University of Maine, Orono, ME
*Corresponding author's email: ehsan.sharafian@maine.edu

Introduction: Walking is a fundamental aspect of daily life, essential for maintaining independence and quality of life, particularly among older adults. However, challenges often arise with aging in maintaining mobility. Gait speed emerges as a critical factor in achieving and sustaining an optimal gait pattern in this population. This research focuses on improving gait of older adults through the use of a novel haptic feedback system. The hypothesis to test was that using haptic feedback to increase the thigh extension (PTE) in older adults could lead to increase in stride length (SL) and gait speed. Two haptic feedback approaches of (1) error feedback (EF) and (2) positive feedback (PF) were explored. In the EF approach, participants adjusted their thigh movements to avoid receiving feedback, while in the PF approach participants adjusted their thigh movements to receive feedback as rewards. To compare the two algorithms, improvements in participants' PTE, height-normalized gait speed, and height-normalized SL were investigated. Both approaches show that subjects were able to significantly improve their walking in PTE and SL compared to their normal walking pace ($p<0.05$) and EF could improve speed significantly ($p< 0.05$).

Methods: In this study, 10 participants 65 years and older (73.9 ± 7.0), who could walk independently without using assistive devices, were recruited, and assigned to each feedback group ($n_{EF}=n_{PF}=5$). As it is shown in Figure 1, four inertial measurement units (IMUs) were used to measure the thigh and foot angles, and the feedback algorithms and real-time data processing were implemented on a smartphone using a custom Android application [1]. The users' PTE were evaluated and compared in real-time with individualized target values for this parameter [2]. Upon receiving commands from the smartphone, the vibrotactile cells, controlled by Arduinos, applied tactile feedback on the posterior sides of the participants' thighs.

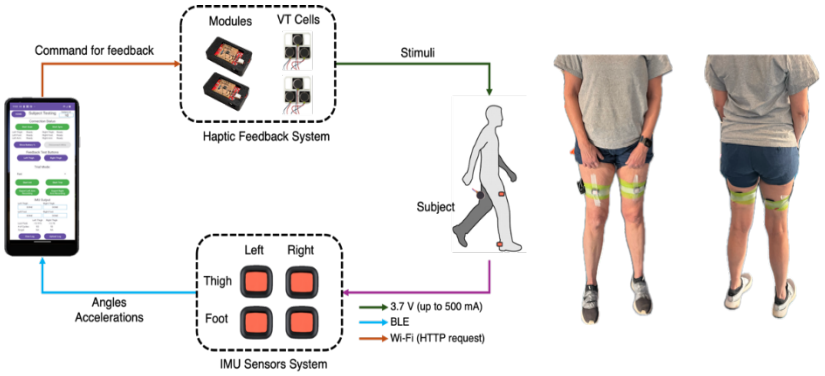

Figure 1: Components of the haptic feedback system

Two experimental conditions included (1) walking at a self-selected normal (N) speed without any feedback and (2) walking while receiving haptic feedback (FB) under either of the two algorithms. In the EF, participants received feedback on their thighs if their PTE were below the targets. In the PF, participants received feedback if their PTEs were greater than or equal the targets.

Results & Discussion: Figure 2 illustrates the changes in PTE, height-normalized SL and speed for the normal (N) and feedback (FB) trials of EF and PF approaches. Improvements in these key gait parameters are concluded compared to the N trial. Analysis of the results using paired samples T-test revealed that PF approach significantly improved PTE, SL, and speed ($p < 0.05$). In contrast, while PTA and SL significantly improved with EF approach ($p < 0.05$), speed did not show a significant improvement ($p = 0.2$). Independent sample T-test showed there were no statistically significant differences between these EF and PF approaches in PTE ($p = 0.3$), SL ($p = 0.541$) and speeds ($p = 0.849$). A case-wise analysis showed that for 9 out of 10 participants all the PTE, SL, and speed significantly improved ($p < 0.001$).

The system and approaches significantly improved walking, where PF approach showed slightly better performance in terms of speed improvement. Although there was not a significant difference between the effects of the two approaches, more participants are still needed to investigate which approach can have better improvement.

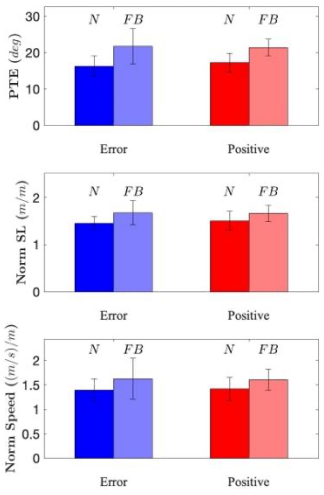

Figure 2: Comparison of parameters in N and FB trials for the EF and PF approaches

Significance: EF and PF significantly improved the walking speed of 9 older subjects above 65, with no instability observed in their walking. The results suggest that the system can be utilized as gait training for older adults to enhance their walking pattern. Moreover, PF and EF had almost the same improvement in walking for subjects, which means that both can be used as the haptic feedback method for training. In the future, this system could potentially be used outside of the lab setting, allowing for home-based long-term training.

Acknowledgments: The National Institute on Aging of the National Institutes of Health (NIH/NIA) under the Award Number 1R15AG078865-01A1.

References:

[1]: Noghani, Mohsen Alizadeh, "Modulation of arm swing frequency and gait using rhythmic tactile feedback."
[2]: Hossain, Md Tanzid, "Investigating the efficacy of a tactile feedback system to increase the gait speed of older adults."

How Low Can you Go? Refining an Algorithm for Assessing Freezing of Gait in Parkinson Disease

Allison M Haussler[1*], Lauren E Tueth[1], David S May[1], Gammon M Earhart[1], Pietro Mazzoni[2]
[1] Program in Physical Therapy, Washington University in St. Louis School of Medicine, St. Louis, MO, USA
[2] Department of Neurology, The Ohio State University College of Medicine, Columbus, OH, USA
*Corresponding author's email: a.haussler@wustl.edu

Introduction: Freezing of Gait (FOG), characterized by sudden involuntary arrests of the feet while walking, is a debilitating symptom of Parkinson disease (PD), leading to reduced independence and increased risk of falls.[1] Up to 80% of individuals with PD are expected to experience FOG over the course of the disease,[2] but it is still one of the most poorly understood symptoms. FOG episodes occur episodically and inconsistently, making assessment difficult. Current methods for measuring FOG include self-report questionnaires, which may be biased, and expert video review, which is quite time consuming and tedious. Developing additional methods to detect and evaluate FOG objectively is a high research priority in PD.[3] A leading approach is using wearable sensors in combination with proprietary algorithms, as these sensors provide objective data on how a person is moving before, during, and after a FOG episode. Previous work by our group demonstrated the utility of wearable sensors to measure FOG both in lab and at home using our Probability of Freezing of Gait (pFOG) algorithm.[4] The purpose of this study is to refine our current pFOG algorithm using previously collected data[5] to identify the lowest possible sampling rate for maintaining FOG detection and to identify which task(s) elicit FOG most consistently across participants for improved assessment. Lower sampling frequencies may prolong battery life and reduce user burden in terms of needing to recharge devices, and identification of specific tasks that can evoke freezing consistently could inform a standardized test battery for us at home and in clinic.

Methods: Nineteen participants with PD and FOG completed walking tasks (both single and dual task) and simulated instrumental activities of daily living (IADLs) while wearing three inertial measurement sensors (IMUs) sampling at 100 Hz. Three sensors were worn: one at the top of each foot and one on the left hip (Physilog 6 (n=6) or ActiGraph GT9X Link (n=13)). For the sampling rate analysis, raw IMU data from the participants who wore Actigraph GT9X Link sensors (n = 13) were down-sampled to both 60 Hz and 30 Hz. Following down-sampling, each participant's data was then re-processed using the pFOG algorithm to detect FOG events. The algorithm defines an FOG event when the probability rating ≥ 0.7. Video review of the in-lab session to mark FOG events was also performed by a licensed physical therapist and considered the "gold standard." Accuracy at the different sampling rates (100, 60, 30Hz) was calculated as the ratio of amount of time defined as true positive FOG and true negative FOG (sensor and human rater agree) divided by the total length of time during the in-lab session. Accuracy as well as sensor-based percentage of active walking time spent freezing were calculated for the whole in-lab visit (walking tasks plus simulated IADLs). Accuracy was compared using a one-way ANOVA ($p<.05$) and Tukey HSD post-hoc tests. As a secondary analysis, expert video review of the whole sample (Physilog plus ActiGraph wearers) was used to determine which task(s) elicited FOG events in the most participants and which task led to the longest FOG duration to understand better what types of tasks reliably provoke FOG.

Results & Discussion: Mean (SD) accuracy for all of the in-lab tasks combined for 100 Hz, 60 Hz, and 30 Hz was 90% (8.31), 87% (7.24), and 71% (5.80) respectively. A one-way ANOVA revealed a significant difference in overall accuracy between sampling rates ($F_{2, 36} = 26.76$, $p <.001$). Post-hoc Tukey HSD tests revealed significant accuracy differences between 30 Hz and 100 Hz ($p <.001$) and 30 Hz and 60 Hz ($p <.001$), but no significant accuracy differences between 60 Hz and 100 Hz ($p = .55$). The lack of a significant difference between 60 Hz and 100 Hz suggests FOG event detection is not hindered by lowering the sampling frequency to 60 Hz. In general, accuracy percentages were higher for the IADL tasks vs. the walking tasks. This is promising as the IADL tasks are meant to represent the home environment and illustrate that this sensor method may be a helpful way to assess FOG without a clinician present. For the walking tests, the 'Go Outside and Turn' dual task, involving walking through an open door into a hallway, making a 180 degree turn within a marked box and then walking around the perimeter of the box while counting backwards by threes, provoked FOG events in the highest number of participants (n= 16/19). The 360 dual task, involving standing in place and turning 360 degrees both directions while also counting backwards by threes, elicited the longest duration of FOG summed across participants (78 seconds total).

Significance: This work is an important step in refining the pFOG algorithm for increased practical use. The ability to use a lower sampling frequency without compromising accuracy may save battery life, allowing for the collection of more data, particularly in the home setting. Additionally, wearable sensors that sample at lower frequencies may be less expensive, allowing for wider implementation and the potential use of consumer-grade IMUs (i.e. smartwatches) to gather motion data and assess FOG. Both of the tasks that elicited the most FOG episodes and the longest duration of FOG involve turning, a common trigger for FOG, suggesting that some type of turning assessment is particularly useful in reliably eliciting and assessing FOG.

Acknowledgements: This project was supported by the Encompass Health/Washington University grant program for Central Nervous System Recovery and Restoration (CNSRR) (author PM) as well as the National Center For Advancing Translational Sciences of the National Institutes of Health under Award Number TL1TR002344 (author AH).

References: [1] Dorsey et al. (2018). *J Park Dis*. 19(8); [2] Giladi et al. (2008) *Mov Disord Off J Mov Disord Soc*. 23(Suppl 2); [3] Bohnen et al. (2022) *Mov Disord Off J Mov Disord Soc* 37(2); [4] Prateek et al. (2018) *IEEE Trans Biomed Eng*. 65(10); [5] May et al. (2023) *Bioeng Basel Switz*. 2023 10(3)

Two weeks of Achilles tendon loading monitored by instrumented insole is associated with plantarflexor function

Ke Song[1*], Michelle P. Kwon[1], Andy K. Smith[2], Karin Grävare Silbernagel[2], Josh R. Baxter[1]
[1]University of Pennsylvania, Philadelphia, PA; [2]University of Delaware, Newark, DE
*Corresponding author's email: ke.song@pennmedicine.upenn.edu

Introduction: Achilles tendinopathy is debilitating for physically active adults [1]. Exercises with load progression are a gold standard for rehabilitation [2] but do not consider the heterogeneous functional status among patient subgroups with different clinical traits [3]. Rehabilitation programs aim to promote function by adjusting daily living activity based on patient-reported pain and activity level [4,5], yet monitoring Achilles tendon loading progression and patient adherence out of the clinic remains a major technical challenge. Without knowing how Achilles tendon load in daily living relates to function, it is unclear if physically active patients can resume high-loading activity if they present with weakness. Our group is developing wearable sensor strategies to monitor real-world tendon load [6,7]. Our goal was to quantify cumulative tendon load in Achilles tendinopathy patients and determine its correlations with plantarflexor function.

Methods: We enrolled 15 Achilles tendinopathy patients after informed consent in this IRB-approved study. They performed isometric and isokinetic (slow: 30°/s, fast: 150°/s) plantarflexor maximal voluntary contractions (MVCs) to determine their plantarflexor function. Patients then worn an instrumented force-sensing insole (Loadsol) for 2 weeks, and we estimated Achilles tendon loads from insole data using our validated physics-based algorithm [6]. We categorized the 2-week Achilles tendon loads at two threshold levels: *overall* load ≥ 0.3×body weight (×BW) that results from all daily living activities, and *high-level* load ≥ 3×BW that results exclusively from dynamic exercises [2]. We computed cumulative tendon loads at these 2 levels to be the impulse of *overall* and *high-level* loads over their loading time (**Fig. 1A**, inset). We normalized cumulative loads by the total hours of *overall* load to control for the varied insole wear time across patients. We computed Pearson correlations between cumulative tendon load and plantarflexor moment, power, and work during MVCs. We also correlated the MVC metrics with survey scores on Achilles tendinopathy symptoms (VISA-A) and self-reported current activity level on the Physical Activity Scale [4]. We defined a correlation of $|r| \geq 0.6$ as strong, 0.4 – 0.6 as moderate, and < 0.4 as weak [8].

Results: 15 patients (46.7±12.0 y/o, BMI: 32.9±9.9 kg/m^2) wore an insole sensor for 10.1±2.2 (6–14) days and accumulated 0.98±0.18 ×BW (0.69–1.27) of *overall* tendon load *per hour*. As a subset of *overall* load, we found a larger variation in *high-level* load *per hour* (0.08±0.07 ×BW, 0–0.21). *Overall* load had a moderate positive correlation to isometric plantarflexor moment (r = 0.543) and weak correlations to isokinetic metrics (0.327< r <0.413). *High-level* load was positively and strongly correlated to fast MVC plantarflexor moment (r = 0.625; **Fig. 1A**) and moderately to other MVC metrics (0.475< r <0.592). Finally, plantarflexor function during MVCs was weakly correlated to symptoms (0.217< r <0.301; **Fig. 1B**) and weak-to-moderately to self-reported activity (0.329< r <0.491; **Fig. 1C**).

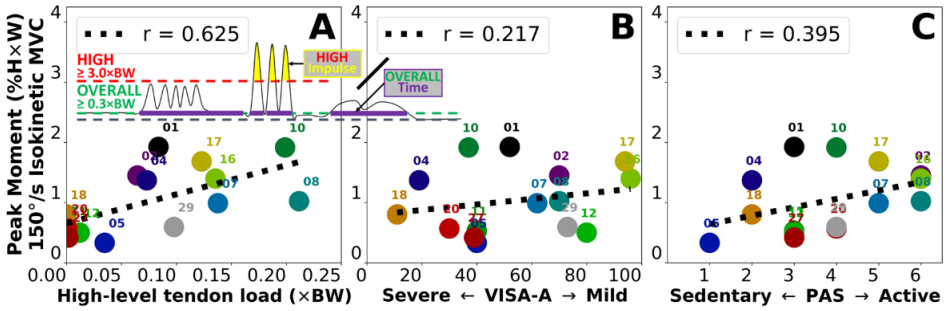

Figure 1: Peak plantarflexor moment during fast isokinetic MVC (150°/s) versus 2 weeks of cumulative Achilles tendon load monitored by a force-sensing insole (**A**). *High-level* Achilles tendon load (≥ 3×BW) per hour was strongly correlated to peak plantarflexor moment during the fast MVC. In contrast, peak moment during the fast MVC was only weakly correlated to patient self-reported symptom severity (VISA-A; **B**) and current level of physical activity (PAS, Physical Activity Scale; **C**).

Discussion: Our study is the first to continuously monitor Achilles tendon load in daily living for 2 weeks and link it with experimentally measured plantarflexor function. We found that plantarflexor strength had stronger correlations with the *high-level* Achilles tendon load than *overall* load, suggesting that functional capacity is better defined by the ability to perform high-loading exercises rather than routine activities. We also found that patients with plantarflexor weakness had less cumulative *high-level* load, suggesting muscle weakness and symptoms may limit patients' *high-level* tendon loading capacity. Yet, we found weak correlations between plantarflexor strength and self-reported symptoms and activity, indicating self-reported pain or inactivity may not suggest functional deficit in all patient subgroups [3]. Sensor-monitored Achilles tendon load shows promise as a reliable biomarker of functional recovery in physically active patients. Our ongoing research is acquiring wearable sensor data in larger cohorts to compare these novel metrics against muscle-tendon structure.

Significance: Our findings reveal that plantarflexor function is more strongly correlated with cumulative Achilles tendon load than self-reported symptoms or activity. Because patients with more *high-level* tendon load show better plantarflexor strength, treatment for this group might be better aimed at daily living load management rather than strengthening. Our sensor data are defining real-world Achilles tendon loading profiles that are better functional biomarkers for specific patient subgroups [3], which will help clinicians personalize rehabilitation and monitor its impacts out of the clinic to optimize therapeutic loading. Biomechanics researchers should improve the fidelity and practicality of wearable sensing, so clinicians can leverage real-world data to promote functional recovery in more patients.

Acknowledgments: Funding was supported by the National Institutes of Health R01AR078898, P50AR080581, and R01AR072034.

References: [1] Shaikh et al. 2017 *IJSM*. [2] Baxter et al. 2020 *MSSE*. [3] Hanlon et al. 2023 *JOSPT*. [4] Silbernagel et al. 2007 *AJSM*. [5] Stevens & Tan 2014 *JOSPT*. [6] Hullfish & Baxter 2020 *Gait Posture*. [7] Kwon et al. 2023 *Sci Rep*. [8] Evans 1996 *APA Book*.

THE EFFECTS OF AGE AND ANTICIPATION ON PROACTIVE AND REACTIVE BALANCE RESPONSES TO TREADMILL BELT PERTURBATIONS DURING WALKING

Emily Eichenlaub[1*], Jessica Allen[2], Vicki Mercer[3], Jeremy Crenshaw[4] and Jason R. Franz[1]
[1]Joint Dept. of BME, UNC Chapel Hill and NC State, USA, [2]Dept. of Mechanical and Aerospace Engineering, UF, USA, [3]Division of PT, UNC Chapel Hill, USA [4]Dept. of Kinesiology and Applied Physiology, UD, USA
*Corresponding author's email: emeich@email.unc.edu

Introduction: Our older adult population is at an exceptional risk of falls, with injuries that can be devastating and contribute to reduced independence and quality of life and significant personal and financial costs. Compared to younger adults, older adults have worse reactive balance responses and are thus more vulnerable to balance challenges [1-2]. Conversely, anticipatory proactive adjustments, such as changing step kinematics, may be used to prepare for and better respond to balance challenges [3-4]. The purpose of this study was to investigate the effects of age on preparing for and responding to rapid treadmill belt accelerations and decelerations designed to elicit instability during walking. We hypothesized that: (1) independent of age, unanticipated perturbations would elicit larger changes in step kinematics (i.e., shorter but wider steps) and margins of stability (MoS) than anticipated balance challenges and (2) older adults would exhibit greater vulnerability to perturbations than young adults, with disproportionate effects when unanticipated.

Methods: 20 young adults (8 M/12 F; mean ± standard deviation; age: 22.8±3.3 years; preferred walking speed: 1.39±0.14 m/s) and 18 older adults (9 M/9 F; age: 73.7±5.2 years; preferred walking speed: 1.31±0.19 m/s) participated. Participants walked unperturbed on the treadmill at their preferred walking speed for 2 minutes. Then, participants responded to treadmill belt perturbations delivered at the instant of heel-strike in which the belt accelerated or decelerated over 200 ms at 6 m/s^2 controlled using a custom MATLAB script. We delivered perturbations either unexpectedly (i.e., unanticipated) or at the end of a three-second verbal countdown (i.e., anticipated). We recorded 3D motion capture from the arms, trunk, pelvis, and legs. We calculated steps widths, step lengths, and anterior-posterior (MoS_{AP}) and mediolateral (MoS_{ML}) margins of stability using standard procedures [5-6]. Values were extracted at the instant of heel strike on the leg contralateral to the perturbation: the step preceding (Preceding), the step immediately following (Perturbed), and two steps after the perturbation (Recovery). We used multifactorial ANOVAs with age (i.e., younger vs. older) as a between-subjects factor and condition (i.e., unperturbed, anticipated, and unanticipated) as a within-subjects factor for each direction.

Results & Discussion: We primarily focus here on age and age×condition interaction effects (Fig. 1). Preceding step – Independent of direction or age, anticipation elicited increased MoS_{ML} compared to unperturbed walking (p-values≤0.013). A significant main effect of age revealed that older adults took shorter steps than younger adults preceding belt accelerations (p=0.032). A significant age × condition interaction (p=0.017) revealed that anticipation caused only younger adults to take shorter steps preceding decelerations. Perturbed step – Independent of age, anticipated accelerations elicited increased MoS_{ML} and wider step lengths than unanticipated perturbations (p-values≤0.022). A significant age × condition interaction (p=0.007) revealed that, independent of anticipation, accelerations elicited shorter steps in older adults compared to unperturbed walking; decelerations elicited shorter and wider steps in both groups (p-values≤0.014). Recovery step – Independent of anticipation, an age × condition interaction (p≤0.014) revealed that decelerations elicited decreased MoS_{AP} and MoS_{ML} for older adults compared to unperturbed walking (p-values<0.024). Independent of anticipation, accelerations elicited shorter steps in older versus younger adults (p=0.028) though, independent of age, anticipation permitted narrower step widths following decelerations (p=0.009). Cumulatively, our results show that age affects proactive adjustments to anticipated balance perturbations and may especially affect one's ability to recover from a balance challenge that elicits a backwards fall (i.e., decelerations).

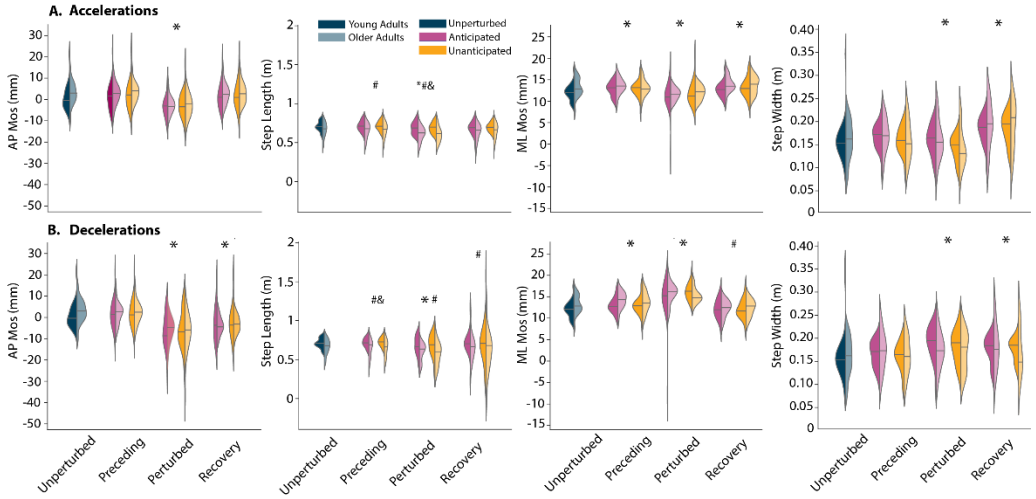

Figure 1. Margin of stability and step kinematic outcomes for the unperturbed walking and preceding, perturbed, and recovery steps in response to (A) accelerations and (B) decelerations. Asterisks (*) denote main effects of condition (unperturbed, anticipated, and unanticipated), pounds (#) denote main effects of age, and ampersands (&) denote age × condition interactions.

Significance: Given the complexity of environmental interactions that can precipitate falls, this is an important step toward understanding predisposing factors for and the ecological impact of age-related instability.

Acknowledgments: Supported by NIH (R21AG067388).

References: [1] Lord et al. (1994), *J Am Ger Soc*; [2] Thompson et al. (2018), *Clin Biomech*; [3] Stokes et al. (2017), *Sci Rep*; [4] Wu et al. (2015), *PLoS One*; [5] Hof et al. (2005), *J Biomech;* [6] McAndrew Young et al. (2012), *J Biomech*
[1] Eichenlaub et al. (2023), *Hum Move Sci*; [2] Eichenlaub et al. (2023), BMES 2023.

THE ROLE OF TENDON STIFFNESS IN GOVERNING LEG MUSCLE RESPONSIVENESS TO UNANTICIPATED SLIPS IN YOUNGER AND OLDER ADULTS

[1]Ross E. Smith*, [1]Andrew D. Shelton, [2]Gregory S. Sawicki, [1]Jason R. Franz
[1]Biomedical Engineering, UNC Chapel Hill and NC State University, Chapel Hill, NC, USA
[2]George W. Woodruff School of Mechanical Engineering, Georgia Institute of Technology, Atlanta, USA
*Corresponding author's email: rsmit@ad.unc.edu

Introduction: Fall-related injuries among older adults are a large public health burden. One factor increasing both fall incidence and injury severity among older adults is the decline in proprioceptive acuity [1]. Delays in sensory feedback immediately following a balance perturbation would hinder both the detection of instability and the deployment of a subsequent recovery strategy via muscle action. Previous authors have found older adults have delayed agonist muscle activity onset, at least after a trip-like perturbation [2]. However, we have recently discovered that the instability elicited by perturbations are highly context specific [3]. Further, age-related decreases in the size, sensitivity, and number of muscle spindles, which are proprioceptive mechanoreceptors that rapidly relay length and velocity changes of muscle fibers, are well documented among older adults. Older adults also experience age-related reductions in tendon stiffness and increases in passive muscle stiffness, which during a rapid, unanticipated joint position change, could act to delay and decrease the velocity of muscle spindle stretch and hinder perturbation detection. However, the relation between age-related decreases in tendon stiffness and muscle responses following balance perturbations is currently unknown. As such perturbations act by disrupting the foot, the ankle joint would be immediately impacted, providing an ideal location to measure both series elastic stiffness and muscle responses. Thus, the purpose of our study was to determine whether soleus (SOL), medial gastrocnemius (MG), and tibialis anterior (TA) muscle response times are delayed following treadmill-induced slip perturbations in older versus younger adults and if that delay is associated with reduced tendon stiffness. We used Achilles tendon stiffness (k_{AT}) as a surrogate for generalized tendon changes due to age. We hypothesized that (1) older adults would exhibit slower muscle responses and lesser k_{AT} than younger adults, and (2) across our cohort, slower muscle responses would negatively correlate with k_{AT}. Data in support of these hypotheses would indicate a target for intervention to increase resiliency to falls among older adults.

Methods: 22 younger (21.59 ± 2.10 yrs, 66.39 ± 8.62 kg) and 19 older (74.05 ± 6.02 yrs, 68.87 ± 20.18 kg) adults participated. Participants completed treadmill walking trials at their preferred speed while responding to 5 randomly-applied treadmill-induced slip perturbations at heel-strike (200 ms duration, 6 m/s^2). All perturbations were separated by at least 10 consecutive unperturbed steps. Surface electromyography (EMG) measured excitation of the SOL, MG, and TA muscles after perturbations. EMG signals were processed using a Teager Kaiser energy operator to amplify the signal-to-noise ratio [4]. All muscle onset times were manually identified as the first burst of muscle activity following perturbation onset. Passive k_{AT} was measured during passive, isokinetic ankle rotations from 20° plantarflexion to 30° dorsiflexion. The musculotendinous junction of the MG was captured using ultrasound and its position was manually tracked and transformed into a common coordinate system with a marker on the posterior calcaneus to estimate AT length change. AT force was calculated by dividing net ankle moment during the passive rotations by a generalized moment arm length [4]. Finally, k_{AT} was calculated as the slope of the linear best fit relationship between AT force and elongation between 0-80% of passive range.

Results & Discussion: Older adults exhibited lesser k_{AT} than younger adults (4.44 ± 1.87 vs. 6.12 ± 2.82 N/mm, p=0.033). In partial agreement with our hypotheses, TA onset time averaged 8% slower in older versus younger adults (143.93 ± 10.37 vs. 132.76 ± 21.71 ms, p=0.019). Given that TA onset occurred within 50 ms of early stance phase peak plantarflexion (full foot contact following heel-strike), these results imply a delay in TA stretch reflex activity in older adults following a slip perturbation. Conversely, MG (234.99 ± 77.35 vs. 310.25 ± 64.61 ms, p<0.001) and SOL (161.01 ± 67.54 vs 204.13 ± 71.17, p=0.027) onset times occurred earlier for older adults than for younger adults. We suspect here that, for older adults, earlier plantarflexor onset later in stance may be required to generate additional push-off moments in the face of delayed TA excitation, whereas faster TA excitation in younger adults may better arrest momentum following a treadmill-induce slip. Finally, we discovered that greater k_{AT} correlated with earlier MG onset times – an observation we found only for younger adults (r=-0.447, p=0.037).

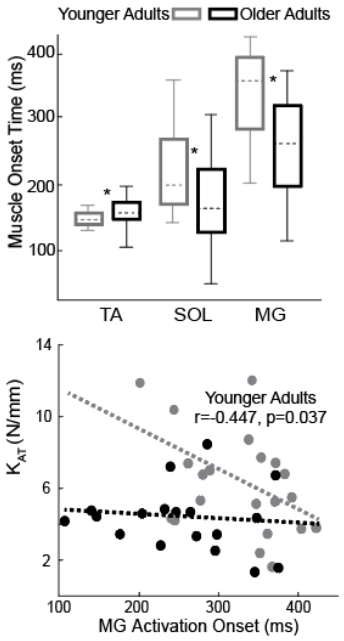

Figure 1. Shank muscle onset times (top) and Achilles tendon stiffness (k_{AT}) versus medial gastrocnemius (MG) onset time (bottom) in younger and older adults. * denotes significant group differences for t-tests, and significant correlations denoted by r-values. (a=0.05)

Significance: Collectively, delayed muscle responsiveness in aging appears to generalize across several contexts of instability and may contribute to increased vulnerability to perturbations. In addition, associations between greater tendon stiffness and improved muscle responsiveness – identified here for younger adults – warrant further study as a potentially modifiable factor.

Acknowledgements: This study was supported by grants from the NIH (R21AG067388, R01AG058615).

References: [1] Ferlinc, et al. (2019), *Materia Soci Medica*; [2] Pijnappels, et al. (2005), *Exp Brain Res*; [3] Shelton, et al. (2024), *Hum Mov Sci;* [4] Solnik, et al (2010), *Eur J Appl Phys*; [5] Raske & Franz, 2018, *J Biomech.*

RESPONSES TO WALKING PERTURBATIONS IN PEOPLE WITH VESTIBULAR HYPOFUNCTION

Michelle J. Karabin[1*], Richard W. Smith[1], Patrick J. Sparto[2], Joseph M. Furman[3], Mark S. Redfern[1]
[1]*University of Pittsburgh, Department of Bioengineering* [2]*University of Pittsburgh, Department of Physical Therapy*
[3]*University of Pittsburgh, Department of Otolaryngology* *Corresponding author's email: mjk160@pitt.edu

Introduction: Maintaining stability during walking is a challenge for some people with vestibular hypofunction (PwVH). PwVH often experience postural and gait instability, which leads to significantly increased fall risk [1]. While some PwVH are able to compensate for their sensory loss, approximately 20% of PwVH demonstrate chronic instability [2]. Their poor walking stability may be due to deficient execution of the major stabilization strategies used in walking, including the regulation of foot placement, lateral ankle roll, ankle push-off, and trunk posture [3]. A rigorous biomechanical analysis of these strategies is lacking in PwVH, particularly in perturbed walking where more valuable insights regarding balance control can be gained. Thus, the purpose of this work was to identify differences in stability and the execution of stabilization strategies in unperturbed and perturbed walking between healthy controls (HCs) and PwVH across a range of compensation levels with a long-term goal of developing ways to improve walking stability in this population.

Methods: Fifteen HCs (40.5 ± 15.0 y.o.; 9F) and 8 PwVH (43.1 ± 11.9 y.o.; 5F) performed overground walking trials with and without ground shift perturbations while kinematics were captured (Vicon). Perturbations occurred on the third right heel strike in the medial or lateral direction (displacement: 6.5cm; peak velocity 0.65m/s). Three repetitions of each perturbation type were completed. Outcomes were assessed on the stride following the perturbation (or corresponding stride for unperturbed walking). Stability was assessed using the minimum margin of stability (MoS_{min}) and four stabilization strategies were evaluated. Foot placement was evaluated by step width. The lateral ankle strategy was assessed using the ankle inversion excursion of the perturbed leg during single support. The ankle push-off strategy was evaluated by the ankle plantarflexion excursion of the perturbed leg during double support. The trunk strategy was quantified by the peak-to-peak lateral trunk sway. Differences in stability and strategies were evaluated using linear mixed models and Sidak post hoc comparisons (SPSS) with effects for trial type (unperturbed, medial and lateral perturbation), group (HC, PwVH), and their interaction. Participants also completed a ten-item clinical gait assessment (Functional Gait Assessment or FGA [4]) to identify if balance recovery was different based on functional compensation.

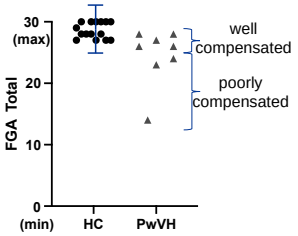

Figure 1: FGA scores for HCs and PwVH.

Results & Discussion: There was a significant interaction effect of trial type and group on MoS_{min}, with PwVH showing decreased stability following medial perturbations (interaction: p=0.02; pairwise: p<0.01). Both groups used strategies to respond to perturbations in a manner consistent with restoring stability (see [5] for explanation), but there were no significant differences between groups. FGA performance was worse and more variable in PwVH (Fig. 1). Three PwVH had FGA scores significantly worse than HCs. Therefore, the models were rerun considering three groups: HC, well compensated PwVH, and poorly compensated PwVH (FGA score < 3 S.D.s below HC average FGA score). This analysis again revealed a significant interaction effect on MoS_{min}, but with only poorly compensated PwVH showing worse stability than HCs following medial perturbations (interaction: p=0.02; pairwise: p<0.01). Thus, the poorer stability seen in the whole PwVH group was likely driven by the poorly compensated individuals. Poorly compensated PwVH showed exaggerated responses in several strategies following medial perturbations, which are considered more destabilizing than lateral perturbations [3]. Poorly compensated PwVH had increased plantarflexion excursion (interaction: p<0.01; pairwise: p<0.01) and tendency toward increased trunk sway (interaction: p = 0.03; pairwise: p=0.21) compared to HCs following medial perturbations (Fig 2a,b). There was a trend toward increased ankle inversion excursion in this subgroup (Fig 2c), but the interaction was not significant. Step width was not different across groups (Fig 2d). These results suggest that poor stability in this subgroup may be related to exaggerated, not deficient, use of these strategies. Additionally, poorly compensated PwVH walked more slowly (1.00 m/s) than HCs (1.33 m/s, p=0.03) and well compensated PwVH (1.25m/s, p=0.24), but including gait speed in the models did not change the significant interactions.

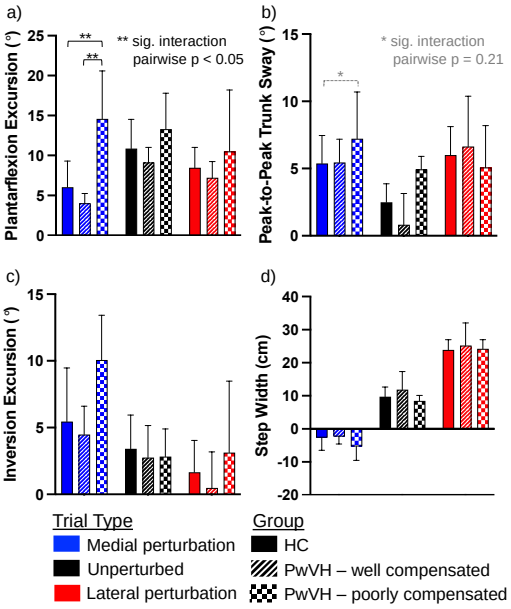

Figure 2: Strategy responses to perturbations across HC and PwVH who are well and poorly compensated.

Significance: This work highlights how balance recovery in walking in PwVH varies based on level of compensation, as defined by FGA score. Specifically, poorly compensated PwVH show exaggerated responses to perturbations, consistent with hypermetria previously seen in this population [6]. Rehabilitation focused on reducing hypermetric responses may be beneficial. Furthermore, the slower speed in this subgroup suggests that PwVH who walk slowly may benefit most from such rehabilitation efforts.

Acknowledgments: NIDCD: F31DC020110. Thanks to CJ Shores & Kshitija Koli for assistance with data collection/processing.

References: [1] Agrawal et al. (2020). *J. Gerontology: Series A, 75*(12). [2] Halmagyi et al. (2010). *Restorative neurology & neuroscience*, 28(1). [3] Reimann et al. (2018). *Kinesiology Review*, 7(1). [4] Wrisely et al. (2004). *Physical Therapy*, 84(10). [5] Karabin et al. (2024). *J Biomech* 162, 111898. [6] Horak et al. (2009). *Annals NY Academy Science*, 1164.

IDENTIFICATION AND PREDICTION OF INTRINSIC TRIP DETERMINANTS IN PEOPLE POST-STROKE

Austin L. Mituniewicz[1], He (Helen) Huang [1], Michael D. Lewek[1,2]
[1] Joint Department of Biomedical Engineering, University of North Carolina at Chapel Hill and North Carolina State University
[2] Division of Physical Therapy, Department of Health Sciences, University of North Carolina at Chapel Hill
*Corresponding author's email: amituniewicz@unc.edu

Introduction: In people recovering from stroke, many falls result from an internally generated trip during walking [1], in which the foot does not successfully clear the ground during swing [2]. Although training strength, balance, and specific reactive responses can reduce fall prevalence in otherwise healthy older adults [3], the presence of altered muscle control in people post-stroke limits the potential benefit of these interventions [4]. Rather than reacting to a trip, we propose a proactive approach, which can identify the gait-related trip before it happens. Zhang et al. developed a fully generalized outlier detection method, using only two features to predict trips in people post-stroke [5]. Impressively, this method was able to accurately predict, at toe-off, more than 90% of the internally generated trips in 75% of the participants. However, the binary outcome (trip vs non trip) and the late timing of the decision limits intervention decision-making and options, respectively. Therefore, the purpose of this work was two-fold: 1) to quantify the critical factors of a trip and 2) to accurately predict these components prior to the end of stance.

Methods: Twelve people with chronic hemiparesis post-stroke walked on a split-belt instrumented treadmill at a range of speeds, with and without cognitive dual tasks (e.g. conversation, counting backwards) and other distractions to increase the likelihood of gait-related trips. While participants walked, we collected motion capture and ground reaction force (GRF) data that we processed in Visual3D. We defined "normal" steps as ones where the slope of the vertical GRF's (vGRF) descending limb was always negative (Figure 1a) and where slope of a real-time gait phase estimator [6] (Figure 1b), over the same period, was always positive (i.e., no disruption to foot progression). Kinetic and kinematic deviations could therefore be determined from the vGRF and gait phase estimator, respectively (Figure 2). Using this approach, four classes arose: 1) normal – no deviation from normative kinematics or kinetics, 2) only kinetic disturbance, 3) only kinematic disturbance, 4) trip – deviation from both normative kinematics and kinetics. Using an 80-20 training-testing split, a support vector machine (SVM) was trained to discriminate between normal, kinetic, and kinematic classes. To ensure that predictions were made with adequate time for a future intervention to prevent a trip, only data preceding a 200N threshold on the vGRF's descending limb were considered. Model performance was assessed through both its ability to accurately predict these classes in the testing set and to identify trips as different from normal. Because even one trip could lead to a fall, "correct" classifications for the first three classes were those with an average posterior probability greater than 50%.

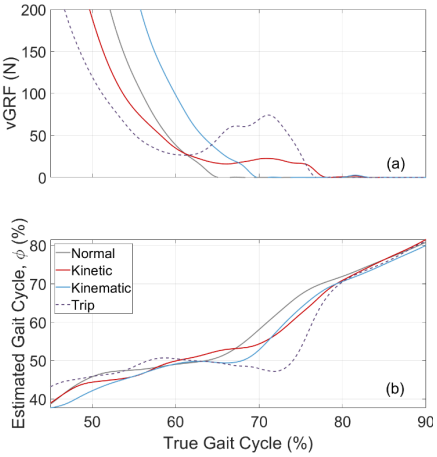

Figure 1: Representative vGRF (a) and phase estimator (b) data from each of the four classes from one participant.

Results & Discussion: SVM correctly predicted 74.7%, 76.7%, and 81.6% of all normal, kinetic, and kinematic classes tested. Impressively, it accurately identified 94.1% of trips as different from normal steps. This strong result indicates that despite not being directly trained on *any* trip observations, our SVM extrapolated the kinetic and kinematic information used in its training. Of the trips incorrectly classified as normal (i.e. false negative), nearly half came from one participant's data. Closer inspection revealed in all of these instances "normal" posterior probability dropped under 50% in the samples just preceding the decision threshold. However, averaging these points with earlier data caused improper classification. Future work should therefore examine if a more accurate prediction can be made by either weighting the data closer to the decision more highly than earlier time points or by reducing the window that data is examined. Another strength of this work is its practical feature set. Unlike prior work which considered kinematic features from all body segments in their initial feature selection [5], our SVM used only features that could be collected from inertial measurement units placed on the thigh and shank (shank angle, knee angle, vertical position of the ankle relative to the body, and the phase estimator).

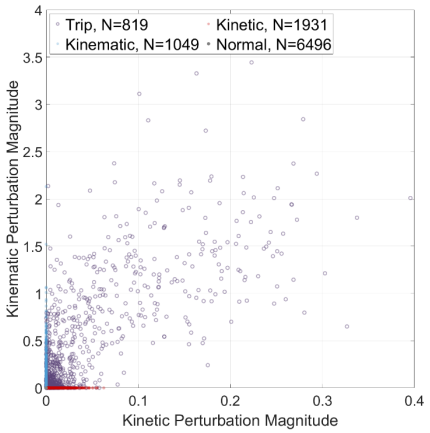

Figure 2: Integrals of the foot clearance archetypes used to train the classification algorithm.

Significance: In this work, we quantified both the kinematic and kinetic contributions to abnormal foot clearance events and were highly accurate in predicting which steps would lead to such events, well before they occurred. By unifying this work with that from our gait phase estimator and an assistive device such as a functional electrical stimulator or exoskeleton, we are primed to prevent trips and eliminate their disastrous results.

Acknowledgments: NSF Graduate Research Fellowship, NIH Grant # R21 HD098570

References

[1] Jørgensen et al. (2008), *Stroke* 33(2); [2] Burpee & Lewek (1993), *Clin. Biomech.* 30(10); [3] Marigold et al. (2005), *J. Am. Geriatr. Soc.* 53(3); [4] Klein et al. (2013), *Motor Control* 17(3); [5] Zhang et al. (2017), *TNSRE 25*(8); [6] Mituniewicz et al (2023), *ASB*

THE INFLUENCE OF STROKE ON PROACTIVE BALANCE CONTROL DURING WALKING

Tara Cornwell[1*] and James M. Finley[1-2]
[1]Department of Biomedical Engineering, University of Southern California, Los Angeles, CA
[2]Division of Biokinesiology and Physical Therapy, University of Southern California, Los Angeles, CA
*Corresponding author's email: tara.cornwell@usc.edu

Introduction: Awareness of an upcoming gait perturbation allows people to proactively plan a response to prevent a fall. Young adults can use auditory warnings to proactively widen their step widths in preparation for inversion/eversion perturbations [1]. However, it remains to be seen if people with neuromotor impairments resulting from a stroke can use proactive strategies when warned of impending perturbations. People post-stroke have impaired reactive balance during walking [2], so we may expect them to use timing information about an impending perturbation to inform proactive strategies that reduce their reliance on reactive responses. Yet, in an obstacle avoidance task that allows for proactive control, people post-stroke have more collisions than their neurotypical peers, suggesting that they may have deficits in planning or executing proactive stepping behaviors [3]. Here, we had neurotypical people and people post-stroke respond to treadmill trips under different audiovisual cueing conditions to determine how they use information about perturbation timing to modulate proactive versus reactive control. We hypothesized that more precise timing cues would prompt proactive strategies that reduce the destabilizing effects of perturbations in both groups but that these strategies would be less effective in people post-stroke.

Methods: Fourteen people with chronic stroke and 14 age-/sex-matched neurotypical adults walked on a dual-belt treadmill while responding to single-belt accelerations with No, General (3-8 steps prior), Exact (2 steps prior), and Countdown (6 steps prior) audiovisual cues. We hypothesized that participants would use these cues to make proactive kinematic adjustments by increasing the extent to which their center of mass (COM) is within their base of support, known as the margin of stability (MOS), and proactive kinetic adjustments by generating less positive work before and during the trip to prevent the COM from rapidly moving out of the base of support. To quantify the effectiveness of these strategies, we evaluated the change in peak COM velocity magnitude during the perturbation steps with versus without cues. We used linear mixed-effects models to evaluate the effects of cue condition, group, and the interaction between the two on the difference in each outcome measure from the No cue condition (alpha=0.05).

Results & Discussion: Participants reduced their peak COM velocity magnitudes during perturbation steps (Figure 1A; p=0.008) by approximately 6% with Exact (p=0.003) and 5% with Countdown cues (p=0.005) relative to 0.40 and 0.34 m/s with No cues for the neurotypical and post-stroke groups, respectively. Neither group used a proactive kinematic strategy to reduce peak COM speed, as there were no significant changes in MOS with cues (p=0.068). Instead, participants appeared to rely on kinetic strategies, reducing positive work performed by the trailing leg contralateral to the perturbation (Figure 1B; p=0.001) by approximately 3% with Exact versus No cues (p=0.010). Participants also reduced positive work performed by the leading leg with cues (Figure 1C; p<0.001), but this reduction was greatest in the neurotypical group by approximately 13% (p=0.011). Neurotypical participants reduced positive work performed by the leading leg by 10% with General (p=0.002), 18% with Exact (p<0.001), and 19% with Countdown (p<0.001) versus No cues. In summary, both groups used audiovisual cues to reduce the destabilizing effects of trips on their COM dynamics, but neurotypical participants had larger reductions in leading leg positive work.

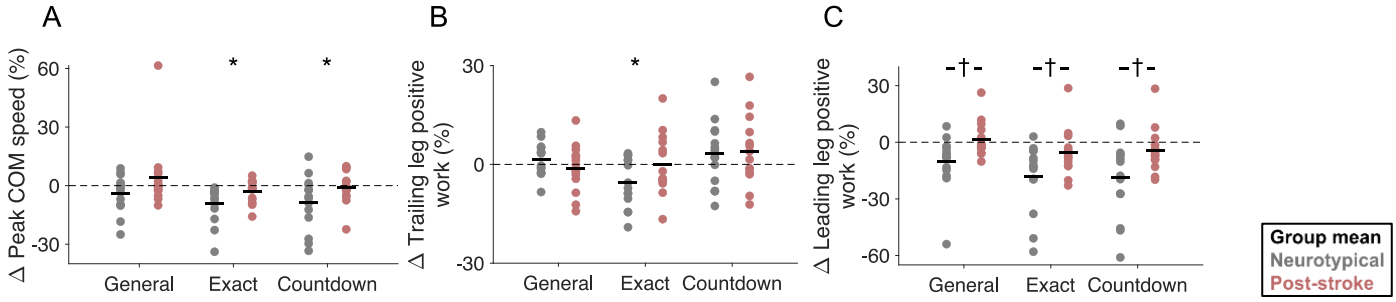

Figure 1: Compared to trips with No cues, both groups (A) reduced their center of mass (COM) speeds with Exact and Countdown cues and (B) reduced trailing leg positive work prior to trips with Exact cues. (C) Cues also allowed people – particularly in the neurotypical group – to reduce leading leg positive work. Subject data is presented with circles and group means are presented with black lines. Significant effects of cue condition or group within conditions (p<0.05) are presented with asterisks and crosses, respectively.

Significance: Real-world perturbations vary in predictability, allowing for both proactive and reactive control strategies. However, most work thus far has evaluated proactive control in neurotypical young adults who may be more confident in their reactive strategies than populations with fall risk. Identifying how neuromotor impairments influence the use of proactive strategies, as presented here, could inform our understanding of balance control during walking and the design of interventions to address fall risk in people post-stroke.

Acknowledgments: American Heart Association Predoctoral Fellowship 23PRE1012432

References: [1] Kreter et al. 2021. *J Exp Biol* 90, 105496. [2] Liu et al. 2022. *Front Neurol* 13. [3] Den Otter et al. 2004. *Exp Brain Res* 161, 180-92.

TASK-SPECIFIC EXERCISE TRAINING: A CLINICALLY TRANSLATABLE AND COST-EFFECTIVE PARADIGM TO REDUCE SLIP-FALL RISK

Jessica Pitts[1*], Tanvi Bhatt[1]
[1]Department of Physical Therapy, University of Illinois at Chicago, Chicago, IL, USA
*Corresponding author's email: jpitts5@uic.edu

Introduction: Falls occur in at least 30% of older adults each year and can often be attributed to external, environmental perturbations experienced while walking, such as slips [1]. Fall prevention programs in clinics and communities typically include conventional exercises for volitional balance control and strength, although these exercises have limited transfer to reactive balance control when exposed to external perturbations [2]. An alternative fall prevention paradigm is perturbation training, which is known to improve reactive balance through repeated perturbation exposure in a safe, laboratory environment. A single session of overground perturbation training can reduce fall rate by ~45-50%, via improvements in two key biomechanical determinants which account for 90-100% of slip-falls: 1) reactive center of mass (COM) stability and 2) vertical limb support [3,4]. Improvements in these key variables may be attributed to improved control of the slipping limb and more effective recovery stepping [5]. Despite these robust effects, overground perturbation training has limited clinical translatability due to complex technology and equipment requirements. Thus, we designed a novel series of task-specific exercises which target the key mechanistic factors that contribute to slip-falls, while using minimal equipment, cost, and technology. On a novel, unexpected post-training slip, we hypothesized that those who completed a single session of task-specific exercise training would have lower fall rate and backward loss of balance (BLOB) rate than a control group, resulting from training-induced improvements to reactive COM stability, reactive vertical limb support, and slip intensity control.

Methods: 24 participants (26.5±5.8 yrs) participated in the study, including 12 in the task-specific exercise training group and 12 in the control group. The task-specific exercise training group completed 6 progressive exercises that targeted 4 main components of slip recovery: controlling COM stability, maintaining limb support, decreasing slip intensity, and optimal recovery step landing. We included volitional-based exercises focused on agility, reaction time, and power generation (e.g., lunges, agility stepping) to facilitate components of a successful perturbation response, such as improving control of the slipping limb under frictionless conditions and rapid recovery stepping. Additionally, we included reactive-based exercises in the form of predictable perturbation exposures (e.g., stepping onto a movable sliding plate). Training lasted ~45 minutes. After training, both the training group and control group (who completed no training) were exposed to an unexpected overground slip perturbation, induced by releasing a pair of side-by-side, low friction platforms that were embedded midway along a 7-m walkway, allowing them to freely slide up to 100 cm forward.

Results & Discussion: In support of our hypothesis, we found that task-specific exercise training reduced BLOB rate (i.e., need to take a backward recovery step) on the unexpected, post-training slip. Only 42% of the training group experienced a BLOB, which was significantly lower than 100% BLOB rate in the control group ($p=0.005$). No one (0%) fell in the training group and 25% of the control group fell, although this difference was not significant ($p=0.217$). Task-specific exercise training also improved key slip-fall determinants. There were no group differences in pre-slip margin of stability (MOS) or hip height ($p>0.136$), although the training group had higher post-slip MOS than the control group at both liftoff and touchdown of recovery stepping ($p<0.001$) (**Fig. 1A**). The training group also had significantly higher post-slip hip height than the control group ($p=0.002$) (**Fig. 1B**). Improvements in MOS and hip height were associated with a more anterior COM position, greater COM velocity in the anterior direction, and reduction in slip intensity (i.e., smaller slip distance) in the training group (Pearson's r>0.6, $p<0.05$). Our results show that just a single session of task-specific exercise training could significantly reduce slip-related fall risk when an unpredictable environmental perturbation is experienced, potentially due to improved control over the slipping limb and more effective recovery stepping.

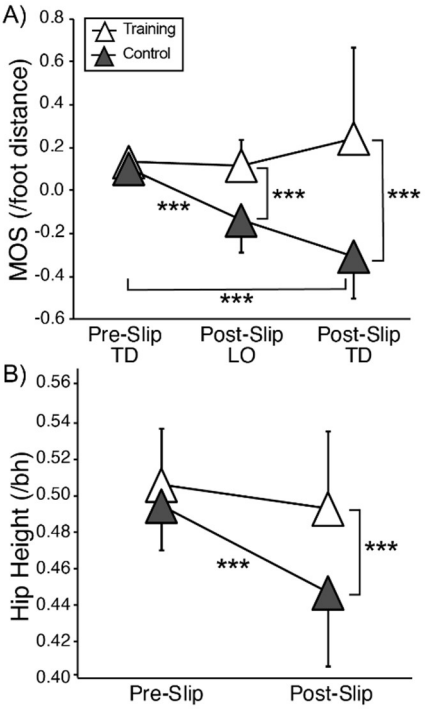

Figure 1: Key biomechanical slip-fall determinants on a novel, post-training overground slip in the task-specific exercise training and control groups. **A)** shows the Margin of Stability (MOS) at pre-slip touchdown (TD) and post-slip at recovery step liftoff (LO) and TD. **B)** shows pre- and post-slip hip height. MOS was normalized to foot distance and hip height was normalized to body height (bh). ***indicates p<0.001.

Significance: Task-specific exercise training could have similar effects on fall risk reduction as perturbation training, although without the need for complex technology or expensive costs. In the future, task-specific exercise training could be translated into clinics and communities to increase the accessibility of effective fall prevention training, especially for older populations. Future studies should examine the effects of task-specific exercise training for additional types of perturbations and in more fall-prone populations.

Acknowledgments: The Cognitive, Motor, Balance Rehabilitation Lab, and Department of Physical Therapy at the University of Illinois at Chicago.

References: [1] Bergen (2016), *JSTOR* 65(37); [2] Kannan et al. (2020), *Brain Sciences* 11(2); [3] Pai et al. (2014), *Archives of Physical Medicine and Rehab* 69(12); [4] Bhatt et al. (2006), EBR 170; [5] Wang et al. (2020), *J. Applied Biomechanics* 36(4).

REMOTE MONITORING OF SPATIOTEMPORAL GAIT PARAMETERS ACROSS THE MENSTRUAL CYCLE: IMPACT OF TIME OF DAY AND SLEEP PRESSURE

Lara Weed[1], Brandon Nguyen, Serena Thompson, Reed Gurchiek, Renske Lok, Marcia Stefanik, Emily Kraus, Scott Delp, Jamie Zeitzer

[1]Department of Bioengineering, Schools of Engineering & Medicine, Stanford University, Stanford, CA 94305

*Corresponding author's email: Weed@stanford.edu

Introduction: Women experience complex physiological and behavioral fluctuations across the menstrual cycle and have a limited understanding of its impact on physical performance. Measurement over a full menstrual cycle (~28 days) poses challenges due to limitations of either in-lab (e.g., time and cost) or remote monitoring (e.g., battery life, memory, consistent sensor placement). Moreover, the interconnected nature of daily and monthly biological rhythms [1] and behavioral disturbances, such as in sleep [2], require measurement and data fusion across multiple physiological systems. With recent advances in wearable sensing technologies for continuous, passive monitoring, we can simultaneously measure relevant systems enabling the quantification of the menstrual cycle's impact on performance. The purpose of this preliminary work was to examine real-world spatiotemporal gait characteristics during walking across the menstrual cycle in young, healthy women, accounting for the contribution of diurnal rhythms (time-of-day) and sleep (homeostatic pressure). This work seeks to uncover the individual and interconnected contributions of each of these phenomena to self-selected stride time.

Methods: After obtaining informed consent, 48 young, healthy, eumenorrheic women (age: 23.6±3.0 years, BMI: 23.3±3.6 kg/m^2, self-reported menstrual cycle length: 29.3±2.9 days) not on hormonal contraceptives were instrumented with inertial measurement units (100 Hz, ±8g, ±2000°/s, AX6, Axivity, Newcastle upon Tyne, UK) adhered (SimPatch, Seoul, Republic of Korea) to the bilateral shanks and a wrist-worn wearable (ActLumus, Condor Instruments, São Paulo, Brazil) measuring arm movement (1-min epochs). Participants wore all sensors for 28 days with weekly changes while simultaneously tracking the menstrual cycle via self-reported menstruation onset and urine-based luteinizing hormone testing (MomMed, Kowloon, China) as an ovulation marker. There were no behavioral constraints during this month. Stride times were computed for each leg following detection of heel-strike events from the mediolateral axis gyroscope signal [3]. Defining walking strides as between 0.8s and 1.6s, we isolated 5,461,766 strides among all participants. Sleep timing was estimated using standard algorithms [4] (ActStudio, Condor Instruments, São Paulo, Brazil), and homeostatic pressure, a measure of sleep drive accumulation, was calculated according to [5]. Menstrual cycle phase was characterized as a percentage using the onset of menstruation and self-reported cycle length. Linear mixed-effect modelling quantified the impact and interaction of menstrual cycle phase, time-of-day, and homeostatic pressure on stride time, accounting for random effects due to participant.

Results & Discussion: Menstruation was observed in all participants with ovulation observed in 75%, consistent with previous literature [6]. Participants had variable sleep timing and duration allowing us to examine a variety of combinations among sleep, circadian, and menstrual phases. Stride time during walking was sensitive to time-of-day, menstrual phase, and homeostatic sleep pressure accumulation (Figure 1). Stride time was decreased during daytime hours (7 am – 8 pm) with a diurnal fluctuation of 6.6%. When homeostatic pressure exceeded ~200 (equivalent to ~15 h awake), stride times decreased 4.8%. Stride time was 0.9% longer during the follicular phase compared to the mean, and the amplitude of fluctuation across the menstrual cycle was 2.8%. Linear mixed-effect modelling indicates a significant interaction between time-of-day, menstrual phase, and homeostatic sleep pressure ($F_{(8,\ 5461766)} = 33.443$, $p<<0.01$).

Walking stride time is sensitive to time-of-day, homeostatic pressure, and menstrual phase, though more so to the first two. As expected, there is a longer stride time during the night as well as with extended time awake. Increased stride time during the night appears mitigated during the luteal phase. Future work will examine whether these findings extrapolate to other spatiotemporal measures of neuromuscular control of gait, as well as a more precise assessment of circadian phase.

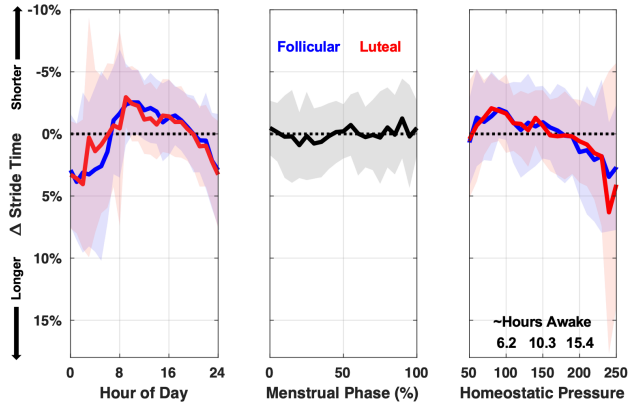

Figure 1: Walking stride time relative change by hour of day (left), menstrual cycle (middle), and under homeostatic sleep pressure (right). Means (solid lines) and standard deviations (shaded regions) are represented. Follicular (blue, <50% of menstrual cycle) and luteal (red, >50%) phases are displayed for hour of day and homeostatic pressure.

Significance: This is the largest study using passive, high sampling rate remote monitoring to examine fluctuations in gait across the menstrual cycle, accounting for both circadian timing and homeostatic pressure. This work focuses on women, who have been understudied, and fluctuations across the menstrual cycle, which have frequently been ignored in research. We hope that this work will provide insights into normal fluctuations across the menstrual cycle in young, healthy women.

Acknowledgments: We would like to thank the Wu Tsai Human Performance Alliance and NeuroTech Training program (NSF Grant No. 1828993) for providing support and the Stanford Research Computing Center for providing computational resources.

References: [1] Baker & Driver (2007) *Sleep* 8(6); [2] Baker & Lee (2018) *Sleep* 13(3); [3] Aminian et al. (2002) *J Biomech* 35(5); [4] Cole et al. (1992) *Sleep* 15(5); [5] Rusterholz et al. (2010) *Sleep* 33(4); [6] Metcalf & Mackenzie (2008) *J BioSocial Sci* 12(3).

AGE- AND SEX-RELATED DIFFERENCES IN MUSCLE AND GAIT BIOMECHANICS DURING INCLINE WALKING

Yujin Kwon[1*], Yunbeom Nam[1], Gwanseob Shin[1]
[1]Department of Biomedical Engineering, Ulsan National Institute of Science and Technology, Ulsan, South Korea
*Corresponding author's email: ekwon@unist.ac.kr

Introduction: Age-related neuromuscular changes such as reduced muscle function contribute to a decline in mobility. While adequate ankle dorsiflexion (DF) range of motion (ROM) is required for efficient push-off during walking [1], older adults exhibit reduced ankle ROM and push-off power during walking, which may lead to gait adaptations. The issue can be more noticeable during incline walking where the slope angle is added to the ankle DF. Our previous study found that individuals with limited DF ROM walked with a larger plantarflexor muscle activity on inclined surfaces [1]. In another study, older adults were found to have reduced Achilles tendon stiffness and therefore walk at shorter muscle length, which results in less efficient power generation [2]. Since ankle flexion and plantarflexor muscle length increase on inclined surfaces, older adults with altered muscle function may find incline walking more challenging compared to young adults and walk with different biomechanical adaptations. In this study, we have included age and sex as independent variables that have been associated with ankle joint flexibility. We hypothesized that older adults/males would operate at shorter plantarflexor fascicle length and walk with smaller ankle plantarflexion angle and higher shank muscle activity than young/female adults.

Methods: Sixteen healthy young (8YM, Young Male; 8YF, Young Female) and 16 older adults (8OM, Older Male; 8OF, Older Female) who are 65 years old or older participated in this study. They conducted ankle plantarflexion (PF) maximum voluntary contraction (MVC) trials on an isokinetic dynamometer at seven ankle joint angles in a randomized order from -15° (PF) to 15° (DF) separated by 5°. Then they performed 2-min incline walking trials at four slope angles (level, 5°, 10°, 15°) at the same preferred waling speed for walking on the highest slope. In each slope condition, they performed a normal stride and then a longer stride walking trial to modify plantarflexor muscle mechanics. During the MVC and walking trials, an ultrasound probe was placed to the gastrocnemius medialis muscle to track muscle fascicles. Two IMUs were attached on the foot and shank to calculate ankle joint angle, and six surface EMG electrodes synchronously recorded activities of following muscles at 2,000 Hz: Tibialis Anterior (TA), Gastrocnemius Medialis (GM), Vastus Lateralis (VL), Rectus Femoris (RF), Biceps Femoris (BF), Gluteus Maximus (GMAX). From the MVC trials, muscle fascicles were tracked using UltraTrack from the ultrasound images [3]. GM muscle-tendon moment arm and muscle force were estimated [4] to establish individual muscle force-length curve and find the optimal length at which the maximum force is generated. All calculated variables were compared between age and sex groups using four-way mixed ANOVA ($p<0.05$).

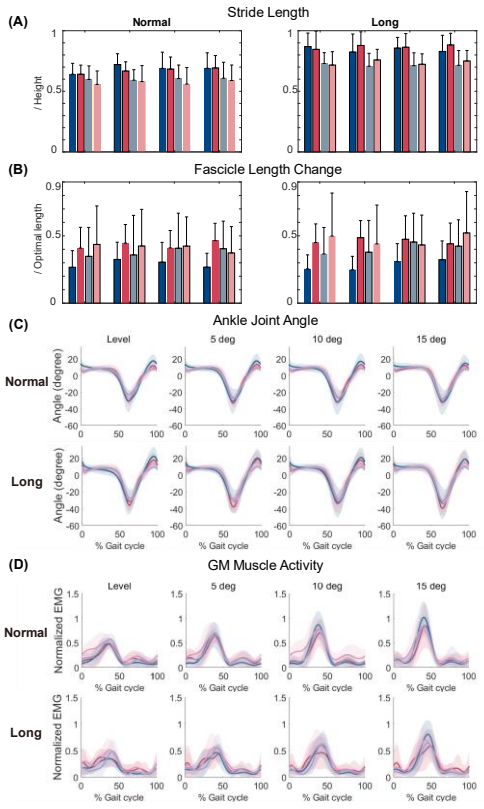

Figure 1: Representative graphs showing results of each group (navy: YM, red: YF, blue: OM, pink: OF).

Results & Discussion: All participants successfully increased the stride length in the longer stride condition by 25.2% on average ($p<0.001$). GM fascicle length change normalized to their optimal length was longer for YF than YM in the normal stride condition ($p=0.004$). The operating range of GM muscle of older adults was significantly shorter than that of young adults ($p=0.001$), which could affect older adults' inefficient power generation during walking with increased muscle activation and metabolic cost. The peak PF angle during push-off significantly increased with slope ($p<0.001$) and stride ($p<0.001$). Participants might have increased ankle PF to increase stride length by increasing toe flexion, utilizing the energy stored in the plantar and toe flexor tendon to generate propulsive force [5]. The strategy might have helped them walk with a lower plantarflexor muscular load even on higher slopes, which was confirmed by older adults' significantly lower GM muscle activity in the longer stride condition ($p<0.001$). While mean activity of all muscles increased with slopes, RF was the only muscle that showed a significant age effect where young adults showed larger muscle activity than older adults ($p<0.001$). Young adults increased RF and GMAX activity with stride ($p=0.013$), suggesting a different neuromuscular adaptation following stride length change between age groups. Taken together, we interpret our results to suggest older adults can walk with lower muscular load by increasing ankle excursion. This way, older adults could walk with longer stride length on higher slopes while compensating for their limited force-generating capacity.

Significance: Research on the effect of ankle mobility on lower leg muscle mechanics and then gait biomechanics is needed to suggest a safer and more efficient walking strategy for individuals with different physical capacities. The results suggest the efficacy of the method to be used as a guideline during gait training. For example, males or older adults with limited ankle joint flexibility compared to females or young adults, respectively, may be prescribed to adopt a strategy to increase ankle ROM and ankle PF during walking to increase stride length. With stride length associated with walking speed, it may be used to improve walking performance for older adults.

References: [1] Kwon and Shin. (2022), *Gait Posture* 92; [2] Krupenevich et al. (2022), *Gerontology* 68; [3] Farris and Lichtwark. (2016), *Comput. Methods Programs Biomed* 128; [4] Bobbert et al. (1986), *J Biomech* 19; [5] Fuller. (2000), *J Am Podiatr Med Assoc* 90

ASSOCIATION BETWEEN JOINT RANGE OF MOTION AND MINIMUM TOE CLEARANCE IN WOMEN WITH HIP AND KNEE OSTEOARTHRITIS

Joy O. Itodo, Steven A. Garcia, Kharma C. Foucher
Biomechanics and Clinical Outcomes Laboratory, University of Illinois, Chicago
jitodo2@uic.edu

Introduction: People with hip and knee osteoarthritis (OA) have higher rates of falls compared to their healthy counterparts [1]. Further, women are at higher risk for both OA [2][3] and for falls compared to men regardless of OA status. In addition, individuals with knee and hip OA likely exhibit distinct disease symptoms and adaptations that uniquely contribute to fall risk between groups. Therefore, understanding the causes of falls in women, who are already vulnerable due to a diagnosis of hip or knee OA is important for development of tailored interventions.

We have previously observed that recurrent falls is associated with lower minimum toe clearance (MTC) during walking at self-selected speeds in people with OA [4]. As a next step, we sought to understand how other aspects of OA gait mechanics contribute to MTC. In this study, we investigated the role of sagittal plane joint ranges of motion (ROM) during walking, since achieving adequate toe clearance requires flexion of the ankle, knee, and hip and because reduced ROM is a common impairment in both hip and knee OA. Further, since people with hip and knee OA may exhibit different types of gait compensations, it is important to understand how any association varies by the affected joint (i.e., hip or knee). Accordingly, we hypothesized that (i) decreased hip, knee, and ankle ROM are associated with decreased MTC in women with OA and (ii) that women with knee and hip OA would use varying joint techniques to clear the toe as evidenced by different associations between ROM at each joint and MTC.

Methods: We evaluated walking biomechanics on a treadmill in 35 women with hip or knee OA (Hip OA = 18, age 58 ± 8 years, and BMI 31.87 ± 6.33 kg/m^2). Participants walked for 2.5 minutes at their self-selected speed on an instrumented split-belt treadmill (Treadmetrix). Visual 3D (C-Motion) was used for model building and marker trajectories were filtered using a 6 Hz lowpass filter. Gait outcomes computed included sagittal plane joint angles for the ankle, knee, and hip. ROM for each joint were calculated as the maximum sagittal plane ROM during the gait cycle. For further analysis, the average of 10 clean consecutive steps was utilized. Self-reported pain symptoms were assessed via the Hip Disability and Osteoarthritis Outcome Score (HOOS) and Knee Disability and Osteoarthritis Outcome Score (KOOS) – Pain subscales. Statistical analyses were conducted using R statistical software version 2023. We used multiple linear regression controlling for pain to evaluate the relationship between joint ROM and MTC separately in hip and knee OA groups. The predictor variables were the hip, knee, and ankle ROM and pain and the response variable was MTC. The alpha level was set as $\alpha = 0.05$ for all analyses.

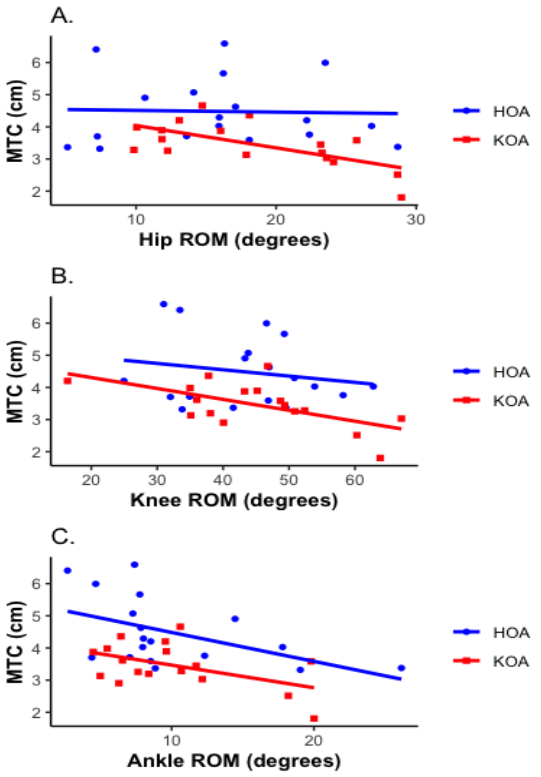

Figure 1: Relationships between (A) hip range of motion (ROM), (B) knee ROM, (C) ankle ROM, and minimum toe clearance (MTC) in women with hip and knee osteoarthritis (KOA).

Results & Discussion: In women with knee OA, lower limb joint ROMs together were associated with MTC (adj. $R^2 = 0.438$, $p = 0.025$). However, hip ROM was the only significant coefficient, with a reduced hip ROM being associated with a higher MTC ($r = -0.650$, $p = 0.037$). By contrast, in women with hip OA, the lower limb joint ROMs were not associated with MTC (adj. $R^2 = 0.092$, $p = 0.278$). However, individually, decreased ankle ROM was significantly associated with a higher MTC ($r = -0.498$, $p = 0.045$).

We found the association between lower limb joint ROM and MTC was the opposite of that hypothesized. Contrary to our hypothesis, decreased lower limb joint ROM was associated with increased toe clearance – not decreased. We speculate that pelvic or truncal deviations are being used to maintain toe clearance rather than modifications of hip, knee, and ankle ROM. The statistical results supported our second hypothesis of varying joint techniques being used between affected joints. Women with knee OA had decreased proximal hip joint ROM when the toe clearance was higher while women with hip OA had decreased ankle joint ROM. This suggests that there may be joint-specific adaptations employed to reduce fall risk depending on the affected joint.

Significance: Identifying disease specific biomechanical factors associated with better toe clearance will aid in the prioritization of interventions to prevent falls. Since our results show different joint involvement in clearing the toe between women with knee and hip OA, it suggests that management strategies should be tailored to joint affectation.

Acknowledgments: R21AG052111 and Pilot funding through UL1TR002003

References: [1] Dore, A.L. *et al.,* (2015) *Arthritis Care & Research* 67 (633-639); [2] Srikanth V.K *et al.*, (2005) *Osteoarthritis Cartilage*; 13(9); [3] Maradit Kremers *H et al.*, (2015) *J Bone Joint Surg Am* 97(17); [4] Itodo J.O *et al.*, (2024) *ACSM*

COMPARISON OF LOWER EXTREMITY JOINTS' KINEMATICS COORDINATION AT GAIT PHASES BETWEEN MALES AND FEMALES IN FRONTAL AND TRANSVERSE PLANES

Abed Khosrojerdi[1], Nathan Q. Holland[1], Hunter J. Bennett[1], Stacie I. Ringleb[1*]
[1]Old Dominion University, Norfolk, VA, USA
*Corresponding author's email: sringleb@odu.edu

Introduction: Evidence suggests that differences exist between males' and females' lower extremities, including a less prominent anterior condyle [1], a reduced medial-lateral to anterior-posterior dimension aspect ratio of the knee joint, and rounder and wider pelvises in females [2]. These differences lead to different joint kinematics patterns such as greater hip adduction and internal rotation for females during walking [3] which can increase the risk of musculoskeletal injuries and pain [4]. Despite a rich literature on sex effects on skeletal and kinematics characteristics, there is a lack of coordination pattern (CP) measures to better understand the neuromuscular control underlying sex differences during walking [5]. A recent study on segmental coordination in frontal and transverse planes reported sex differences in lower extremity segment coordination such as more anti-phase patterns for females during mid-stance [5]. However, considering the sex differences in joint-based coordination can elucidate the interplay at the body system level, whereas segmental coordination emphasizes individual joint coordination. This might be a better way to reveal the interplay of these differences in functional movement, such as walking. Therefore, the current study aims to investigate the sex differences in the lower extremity joints CP in frontal and transverse planes. We hypothesized that lower extremity joint CP differs between males and females.

Methods: Five females with an average age of 23.6±3.64 years, a mass of 73.99±21.61 kg, and a height of 167±4.5 cm, and five males with an average age of 20.2±2.16 years, a mass of 87.74±24.5 kg, and a height of 184±1.2 cm were instructed to walk on a walkway five times. A nine-camera VICON motion capture system (Oxford, UK) was utilized to record the kinematics of lower extremity joints. For each participant, three gait cycles were manually separated into seven phases: loading response (LR), mid-stance (MSt), terminal stance (TSt), pre-swing (PS), initial swing (ISw), mid-swing (MSw), and terminal swing (TSw). The kinematics data was processed using Visual 3D (C-motion, Inc.) and a custom MATLAB code (The Mathworks, Natick, MA) to compute ankle/knee, knee/hip, and ankle/hip kinematics CP in frontal and transverse planes using a modified vector coding method. The average CP for each gait phase was then extracted for statistical analysis. Differences between sexes were investigated using an independent t-test in IBM SPSS 27.

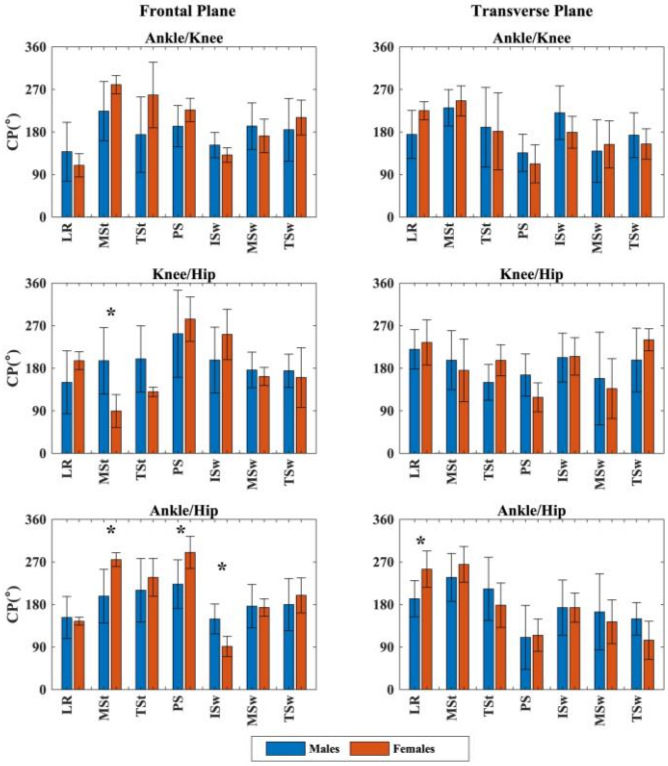

Figure 1: The first and second columns show the average CPs of ankle/knee, knee/hip, and ankle/hip during each phase of the gait cycle in frontal and transverse planes, respectively.
* indicates the significant difference between males and females.

Results & Discussion: There was no significant effect of sex in ankle/knee CP in the frontal plane. Females showed antiphase CP (knee abduction/hip adduction) with knee dominancy while males had in-phase CP (adduction) with hip dominancy during MSt for knee/hip CP ($p=0.01$). Females showed antiphase CP (ankle eversion/hip abduction) with ankle dominancy while males had in-phase CP (ankle eversion/hip adduction) with hip dominancy during MSt and PS (p's<0.05). Further, females had in-phase CP (ankle inversion/hip abduction) with ankle dominancy while males demonstrated antiphase CP (ankle inversion/hip adduction) during ISw for ankle/hip CP ($p=0.01$) (Fig 1. First column). In the transverse plane, there was no significant effect of sex for ankle/knee and knee/hip CPs. However, females showed in-phase CP (internal rotation) with ankle dominancy while males had the same CP with hip dominancy during LR ($p=0.03$) for ankle/hip CP (Fig 1. Second column). The results revealed that the major effect of sex on CP is on joint dominancy, in which females have higher motion in the distal joint of the coordination couples while males have higher motion in the proximal joint. These results aligned with previous investigations conducted in the sagittal plane [6], in which it was observed that females displayed distal joint dominancy while males had proximal joint dominancy. These differences can be because of anatomical factors such as greater pelvic width [7] and greater femoral anteversion angle [8] than the males.

Significance: The results showed that females employ different CPs than males during MSt and ISw. These differences can be applied to injury prevention strategies, rehabilitation protocols, sports performance optimization, and orthopedic interventions.

References: [1] Poilvache et al. (1996), *Clin Orthop Relat Res* 331(35-46); [2] Hitt et al. (2003), *JBJS* 85(4); [3] Hurd et al. (2004), *J Clin Biomech* 19(5); [4] Neal et al. (2016), *Gait & Posture* 45; [5] Konishi et al. (2024), *J Biomech* 162(111891); [6] Khosrojerdi et al. (2023), *ASB Conf*; [7] Lewis et al. (2017), *Anatomical Record* 300(4); [8] Braten et al. (1992), *Acta Orthop Scandinavica* 63(1).

INFLUENCE OF SEX AND BODY SIZE ON MARKER AND MARKERLESS MOTION CAPTURE DURING GAIT

Neil Wills[1], Derek N Pamukoff [1,*]
[1]School of Kinesiology, Western University, London ON
*Corresponding author's email: dpamukof@uwo.ca

Introduction: Three-dimensional motion using reflective markers is a common method to evaluate individual movement patterns, but there are limitations to the use of physical markers. For example, manual marker placement on anatomical landmarks introduces errors in segment endpoint estimation. Secondly, marker motion artifact during dynamic tasks confounds the measurement of rigid segments. Anatomical differences between males and females and between individuals with diverse body size may contribute to additional error in model construction. Markerless motion capture is an alternative that negates the use of physical markers and removes human error in marker placement on precise anatomical landmarks. While markerless motion capture has moderate to good agreement with marker-based motion capture during dynamic tasks [1,2], the influence of sex and body size has not been explored, and it is unclear of markerless motion capture methods should utilize sex- or body size- specific modeling procedures. Therefore, the purpose of the study was to evaluate the influence of sex, body size, and motion capture method on sagittal and frontal plane knee and hip kinematics during gait.

Methods: 40 healthy young adults (18-30 years old) participated and were divided into 4 groups of 10: females and males with body mass index between 18.5-24.9, and with body mass index between 30.0-40.0. Participants completed 2 sessions separated by 2-7 days with identical procedures to obtain gait biomechanics, and marker-based and markerless data were obtained simultaneously from the same trials using synchronized motion capture systems. Marker-based data were obtained using a 6-camera system (Qualisys Miqus 1), and markerless data were obtained using an 8-camera system (Qualisys Miqus 3-Hybrid). Marker-based cameras were mounted on tripods between 0.5-2m high and positioned to optimize marker coverage of the right limb (i.e. foot to pelvis). Markerless cameras were ceiling mounted approximately 3m high. 5 gait trials were recorded over a 10m walkway over 2 inground force plates at a self-selected speed (±5%) that was maintained via timing gates. A full gait cycle (i.e. right foot to right foot) was obtained for each trial. Motion capture and force plate data were sampled at 60Hz and 1200Hz, respectively. Data were recorded using Qualisys Track Manager, and markerless data were exported to Theia 3D (version 2023). All data were exported to Visual 3D to extract joint angles during the gait cycle and time-normalized from 0-100%. Inverse kinematics derived all knee and hip angles with analogous joint constraints for marker and markerless data. A 2 (sex), by 2 (body size), by 2 (motion capture method) ANOVA with repeated measures was used to evaluate hip and knee kinematics using statistical parametric mapping with data averaged from both days. As we were primarily interested in how sex and body size affected methods comparisons, post hoc evaluations were only completed where significant interactions or main effects pertained to motion capture method (i.e. interactions or main effects including only body size or sex were not further evaluated).

Results & Discussion: Consistent main effects of method were observed for knee and hip kinematics in both planes indicating that markerless produces lower amplitude kinematics than marker-based methods (all $p<0.001$), which is consistent with previous published work [1]. There were unique interactions between sex, body size, and method in both planes at the hip joint. In the sagittal plane hip angle, females had a more flexed hip throughout 100% of the gait cycle compared with males, but this was only identified with marker-based methods ($p<0.01$). Moreover, those with lower body size had a more extended hip near terminal stance (87-100%) compared with those with larger body size but this was only found using markerless methods ($p<0.01$). In the frontal plane, females had larger hip adduction angles during stance (2%) and swing (14%) with marker-based compared with markerless data ($p=0.03$), but only during swing in males ($p<0.01$). There were also unique interactions between sex, body size, and method in the frontal plane knee joint angle. Males had a larger knee adduction angle during swing compared with females, but this was only found with markerless methods ($p=0.04$). Secondly, a larger knee abduction angle during stance (1-31%) was found in those higher body size compared to those with lower body size, but only with marker-based methods ($p<0.001$). Furthermore, a larger knee abduction angle was found during marker-based compared with marker-less methods in those with high body size, but the opposite was found in those with low body size ($p<0.001$). Collectively, data indicate that sex and body size have unique influences on gait outcomes derived with different motion capture methods and should be considered when comparing biomechanical data obtained with different systems using diverse samples. The hip centre estimation technique influences hip and knee kinematics as it determines the location of the proximal endpoint of the thigh segment [3]. Error in hip joint centre location can be amplified during marker-based motion capture due to marker placement that is further confounded by additional pelvis mass and sex. Females and adults with obesity may have additional mass surrounding bone landmarks that are commonly used for pelvis construction. As such, the effects of body size and sex on motion capture method observed in our study may be due to error in calibration marker placement, additional motion artifact of tracking targets on the sacrum, or difference in hip joint estimation technique used between methods.

Significance: Sex and body size influence knee and hip kinematics during gait assessed with marker and markerless motion capture. Future algorithms utilizing a markerless approach may consider unique models that are specific to sex and body anthropometrics. Studies are needed to provide validation of markerless approaches to gold standards (e.g. video fluoroscopy) in addition to further comparisons to traditional marker-based methods.

Acknowledgments: This project received funding from the Natural Sciences and Engineering Research Council of Canada (RGPIN-2022-04804) and Canadian Foundation for Innovation John R. Evans Leader Fund (Project ID: 42110)

References: [1] Kanko et al. (2021), *J Biomech*; [2] Wren et al, (2023), *Gait and Posture;* [3] Hara et al, (2016), *Scientific Reports*

SENSITIVITY OF GAIT VARIABLES TO SEX-SPECIFIC PELVIS GEOMETRY IN MUSCULOSKELETAL MODELS

Sheeba Davis[1*], Russell T. Johnson[2], Matthew C. O'Neill[3], Brian R. Umberger[1]
[1]School of Kinesiology, University of Michigan, Ann Arbor, MI
[2]Department of Physical Medicine and Rehabilitation, Northwestern University, Chicago, IL
[3]Department of Anatomy, College of Graduate Studies, Midwestern University, Glendale, AZ
*Corresponding author's email: sheeba@umich.edu

Introduction: Musculoskeletal modeling and simulation are widely used to study the mechanics and energetics of locomotion. Musculoskeletal models are valuable for quantifying variables such as joint kinematics and moments, muscle forces, and joint contact loads. However, model outputs are sensitive to the assumptions underlying them. Among the many aspects of biomechanical modeling, musculoskeletal geometry is an important factor that affects joint center and muscle attachment locations. Most human musculoskeletal models are derived from adult male specimens [e.g., 1] and are commonly used to study both males and females, ignoring potential sex differences. Very few female-specific musculoskeletal models exist [e.g., 2], and none are available for use as a standard gait musculoskeletal model in OpenSim. Hence, it is unclear to what extent gait analysis results obtained for female subjects are affected by using generic musculoskeletal models that are based on male anatomical data. Generic musculoskeletal models are typically scaled either uniformly or non-uniformly to adjust the anthropometry to a specific subject. However, the effects of these scaling methods on sex-specific musculoskeletal geometry is unknown. The pelvis is the skeletal element with the most pronounced sex-specific differences within the locomotor anatomy [3], likely affecting muscle function and joint loading. Therefore, the purpose of this study was to investigate the effects of using musculoskeletal models with male- and female-specific pelvis geometries that are scaled uniformly and non-uniformly on the estimation of joint kinematics and moments, hip muscle forces, and joint contact forces for females during walking.

Methods: A 'generic' 3-D musculoskeletal model [4] (14 rigid body segments, 37 degrees of freedom and 80 muscle actuators) based on an adult male specimen was used and is referred to as male-specific. A female-specific model was created by replacing the male pelvis with a female pelvis geometry [2]. Hip joint locations and muscle attachments in the female-specific model were adjusted to align with the female pelvis geometry using OpenSim Creator [5]. 3-D marker trajectories and ground reaction forces (GRF) from five female subjects (28±1 yr, 1.63±0.04 m, 61±8 kg) walking at preferred speeds (1.3±0.15 m/s) were used for analysis [6]. Male- and female-specific models were scaled uniformly and non-uniformly in OpenSim [7]. In uniform scaling, one scale factor was used for all three dimensions for each segment. In non-uniform scaling, distinct scale factors were used for the antero-posterior, medio-lateral, and supero-inferior dimensions. The four scaled models were used to calculate 3-D joint angles and moments, muscle forces, and hip joint contact forces. Similarities in waveform patterns and differences in the magnitudes of output variables across the four conditions were assessed using zero-lag cross-correlations (r) and root-mean-square deviations (RMSD). Differences in the peak values of hip joint contact forces were tested using one-way repeated measures ANOVA.

Results & Discussion: All gait variables were similar in pattern ($r > 0.97$) across the four conditions, except for slight differences in joint angles between female- and male-specific pelvis conditions ($r = 0.90$). In most cases, there were greater differences in magnitude (RMSD values) for sex-specific musculoskeletal geometry than for the scaling approach (exemplar results in Fig. 1). A wider distance between hip joint centers in the female-specific model increased the moment arm of the vertical GRF, resulting in a greater hip ab-ad moment (Fig. 1B) than in the male-specific model. Similarly, wider pelvis geometry altered the muscle attachments in the female-specific pelvis reducing muscle moment arms; thus, increasing the hip abductor muscle forces (Fig. 1C) required to compensate for the larger hip ab-ad moment. In addition, larger hip abductor muscle forces lead to greater vertical hip joint contact forces (Fig. 1D). Particularly, peak vertical hip joint contact forces were significantly greater ($p = 0.0002$) with the female-specific pelvis, but were not different between scaling conditions ($p = 0.7442$). Overall, sex-specific musculoskeletal geometry had a greater effect on gait variables than the scaling approach. An important limitation is that the only female-specific element in the model was the pelvis. Future studies should consider other sex-specific aspects of musculoskeletal geometry.

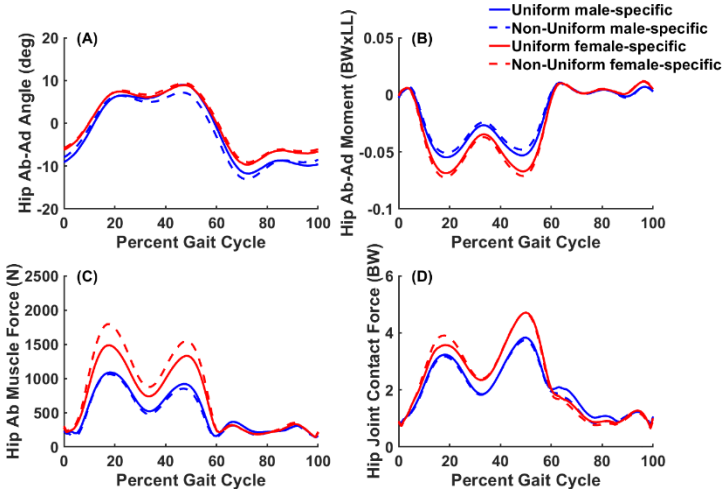

Figure 1: Hip abduction-adduction angles (A) and moments (normalized to body weight and limb length) (B), hip abductor muscle forces (C), and hip joint contact forces (normalized to body weight) (D) across the four sex-specific pelvis and model scaling conditions.

Significance: This study provides preliminary evidence that models with sex-specific musculoskeletal geometry will be needed to fully understand sex differences in human gait.

Acknowledgments: Supported by NSF BCS 2018523, 2018436.

References: [1] Delp & Loan (1990), *Comput Sci Eng* 2(5); [2] Modenese & Renault (2021), *J Biomech* 116; [3] Stewart (1954), *Am J Phys Anthropol* 12; [4] Lai et al. (2017), *Ann Biomed Eng* 45(12); [5] Kewley & Seth (2022), *TU Delft - 4TU.ResearchData*; [6] Johnson et al. (2022), *J Exp Biol* 225(5); [7] Seth et al. (2018), *PLoS Comput Biol* 14(7).

AUTOMATED TRACKING OF INFANT REACHING: EVALUATING A POSE ESTIMATION TOOL

Ipsita Sahin[1], Tristan McCarty[1], Georgia Kouvoutsakis[2], Elena Kokkoni[1]*
[1]Dept. of Bioengineering, University of California, Riverside, Riverside, CA 92521, USA
[2]Dept. of Electrical and Computer Engineering, University of California, Riverside, Riverside, CA 92521, USA
*Corresponding author's email: elena.kokkoni@ucr.edu

Introduction: Vision-based motion tracking is becoming a popular tool for studying and evaluating human motion. Compared to traditional marker-based systems and manual tracking, automated pose estimation tools offer a promising alternative for efficient and reliable motion capture and analysis outside of the controlled environment of a lab. More specifically, these tools have been designed to automatically detect facial and other key points of the human body from video recordings, which can be a great solution when working with young populations, such as infants. Nevertheless, these tools are trained on adult data, and may not accurately capture infant behavior, because of differences in poses and movement patterns between the two populations. Prior work has examined the use of such a tool, OpenPose [1], with infants, to evaluate spontaneous limb movement while lying in a supine position [2]. However, it is unknown if this applies to tracking other types of movement that may of interest to evaluate during infancy. The goal of this work was to examine the validity of OpenPose to track infant arm movement during reaching actions. The findings from this work will contribute to a better understanding of the use of this tool to track infant reaching and inform strategies for improving its accuracy through post-processing.

Methods: In this work, data from 36 infants (including 7 with neurodevelopmental conditions) under 12 months old were analyzed. The data came from 42 videos collected from publicly available sources and captured the infants reaching for objects across various everyday settings, such as homes and clinics. Out of these videos, a total of 434 reaching actions (6806 frames) were identified and segmented. The analysis involved two parts; manual (www.kinovea.org) and automatic tracking (OpenPose) of the wrist joint of the arm reaching for an object. For 18 reaching actions (4.15% of the dataset), the position of the wrist joint was not detected at all (detection confidence, $c = 0$) by OpenPose for more than 60% of the reaching duration. Subsequently, these 18 reaching actions were excluded from further analysis and only the 416 reaching actions were analyzed and used for comparison, spanning 6483 frames. In 247 frames (3.81%), where the wrist was not detected, the missing data underwent linear interpolation and finally applied a moving average filter to smooth the data [2]. To evaluate the agreement between the two tracking methods, non-parametric correlation, and Bland-Altman (B&A) analyses were performed (violation of normality was confirmed using the Kolmogorov-Smirnov test). Additionally, the Lock-Step Euclidean Distance (LSED) was computed to compare the trajectories obtained from both tracking methods. LSED measures the total distance between all pairs of corresponding points in two trajectories [4]. A custom script was used for computations and the significance level was set at 0.05 for all analyses. The results are reported in pixels (px), as calibration was not possible for all videos.

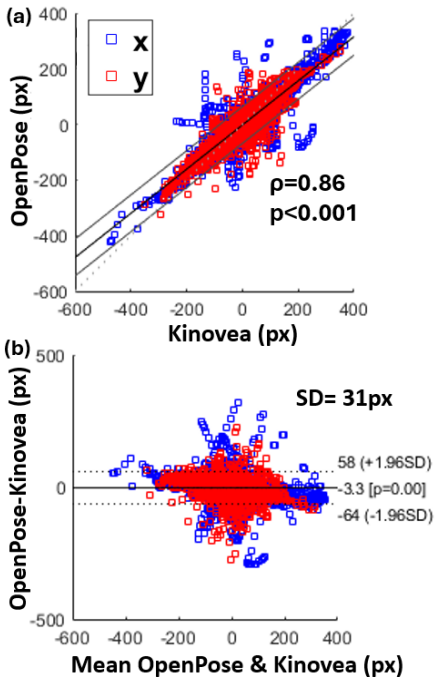

Figure 1: **(a)** The Spearman correlation plot; and **(b)** The B&A plot for the x-y coordinate of wrist detected using OpenPose and Kinovea. The solid and dashed black lines denote bias and 95% LOA.

Results & Discussion: A strong and significant positive correlation between the 2D coordinates of the two tracking methods (Spearman's $\rho = 0.86$, $p < 0.001$) was found (Fig. 1a). The B&A analysis revealed a mean difference (bias) of $-3.3px$ between the two methods. The standard deviation (SD) of the differences was found to be $31px$. The limits of agreement, LOA, (95% confidence interval (CI)) were calculated as $54.7px$ above and $60.7px$ below the mean difference. When the mean difference is closer to zero, the line representing zero falls inside the CI and/or the LOA is narrow, these indicate relatively close agreement between the methods [4] (Fig. 1b). Additionally, the LSED value (mean $\pm$ SD) was $25.45 \pm 24.28px$ with a coefficient of variation (CV) of 95%, where the LSED values of the reaching trajectories varied between [$2.52px$ $199.77px$]. The high SD, CV, and maximum value, coupled with the low average and minimum value, indicated that while some trajectories exhibit close agreement, others demonstrate discrepancies between the methods.

Significance: By assessing the validity of OpenPose in tracking infant arm movements during reaching actions, this study contributes to understanding the feasibility and reliability of using automated tracking solutions (primarily trained with adult data) for the infant population. The strong positive correlation and low bias emphasize the potential of OpenPose as a valuable tool for characterizing infant reaching motion. This work highlights the effectiveness of OpenPose as an automated tracking tool in select scenarios while showing that additional training data is needed before it can be applied for use in all pediatric reaching tasks.

References: [1] Cao et al. (2019), *IEEE Trans Pattern Anal Mach Intell* 43:172-186; [2] Chambers et al. (2020), *IEEE Trans Neural Syst Rehabil Eng* 28:2431-2442; [3] Tao et al. (2021), *GISci Remote Sens* 58:643-669; [4] Parampreet et al. (2017), *Int J Acad Med* 3:110-111.

TWO FEET, ONE FORCE PLATE: A NOVEL MACHINE LEARNING APPROACH SOLVES FOR BILATERAL GROUND REACTION FORCES ON A SINGLE FORCE PLATE

Jennifer K. Leestma[1,2*#], Ryan C. Emadi[3#], Gregory S. Sawicki[1,2,4], Aaron J. Young[1,2]
[1]George W. Woodruff School of Mechanical Engineering, [2]Institute for Robotics and Intelligent Machines, [3]School of Electrical and Computer Engineering, [3]School of Biological Sciences, Georgia Institute of Technology (*[#]Indicates equal contribution*)
*Corresponding author's email: jleestma@gatech.edu

Introduction: For decades prior to the invention of split-belt treadmills, solving for bilateral ground reaction forces (GRFs) during the double stance phase of walking proved to be a prominent challenge. Though the popularization of split-belt treadmills largely mitigated this concern, the recent rise in research focused on perturbed and unsteady gait may have resurrected the "two feet, one force plate" conundrum. In this area of research where mediolateral stability is often a focus, participants frequently cross over onto a single force plate in the steps immediately following a perturbation; this renders subsequent and valuable double stance joint dynamics data useless. We developed a novel data-driven approach that combines an existing machine learning framework with cutting-edge deep learning architectures to solve for bilateral GRFs during double stance on a single force plate.

Methods: We used our previously collected open-source data set that was approved by the Georgia Institute of Technology Institutional Review Board [1]. In this study, we perturbed 11 participants using 96 different perturbation conditions that varied in magnitude, direction, and timing. We corrected for GRFs during platform movement using a method adapted from [2]. During initial development of this method, we are not considering any double stance data in which participants crossed over onto a single force plate. For remaining double stances, we calculated total force plate data to replicate data had the participant crossed onto a single force plate.

We sought to combine two concepts from the artificial intelligence field to solve for bilateral GRFs. ***Supervised machine learning*** allows us to train models that map biomechanical data to GRFs, but does not consider force plate-based constraints that we know must be true (e.g., bilateral GRFs must sum to total GRF). ***Constraint satisfaction***, on the other hand, allows you to define relationships between variables, but does not provide a method to choose from the many solutions that satisfy the defined relationship (e.g., many combinations of bilateral GRFs can sum to total GRF). We combined these concepts through a framework called ensemble learning; instead of attempting to train one near-perfect model of bilateral GRFs, ensemble learning trains many imperfect models, where the mean output is typically a reasonable estimate. Rather than taking the mean of models, we used the ensembles to generate probability distributions of bilateral GRF component estimates. We then applied our set of constraints and chose the highest probability combination of components that satisfied the constraints. Constraints are applied for all forces and centers of pressure (COP) (Fig. 1).

We implemented this approach for one participant through subject-dependent ensembles of temporal convolutional networks (TCNs), which are uniquely suited for biomechanical applications [3]. The TCN takes in the total GRF data and lower limb joint centers and outputs bilateral GRF components. We trained five types of two-headed models, with each type being a TCN for the GRF and COP components with two heads estimating the right and left force plates. We trained 20 TCNs for each GRF or COP component.

Results & Discussion: The mean absolute error (MAE) for mediolateral (ML), vertical (VERT), and anteroposterior (AP) forces were 1.18, 0.45, and 0.55% of the participant's steady state peak to peak (SSP2P), respectively. The MAE for ML and AP COP were 0.18 and 0.55 cm, respectively. We are exploring various avenues to improve the accuracy of this approach, including evaluating what additional biomechanical input data may improve accuracy. One of the challenges associated with this approach is validating the outputs during invalid double stance trials. Our future work will include collecting data from instrumented insoles during diversely perturbed trials to validate the vertical GRF as well as ML and AP COP estimates against this additional experimental data.

Significance: The goal of this work is to provide an approach for the biomechanics community that enables the recovery of valuable inverse dynamics data during locomotion on a single force plate. If, after further development, our approach is consistent, accurate, and capable of subject-independent estimates, we plan to provide an open-source framework with trained models to the research community.

Acknowledgments: This work was supported by the NSF GRFP Award #1324585 and NIH Award DP2-HD111709.

References: [1] Leestma et al. (2023), *J Exp Biol*. [2] Hnat et al. (2018) *J Biomech*. [3] Molinaro et al. (2022), *IEEE TMRB*.

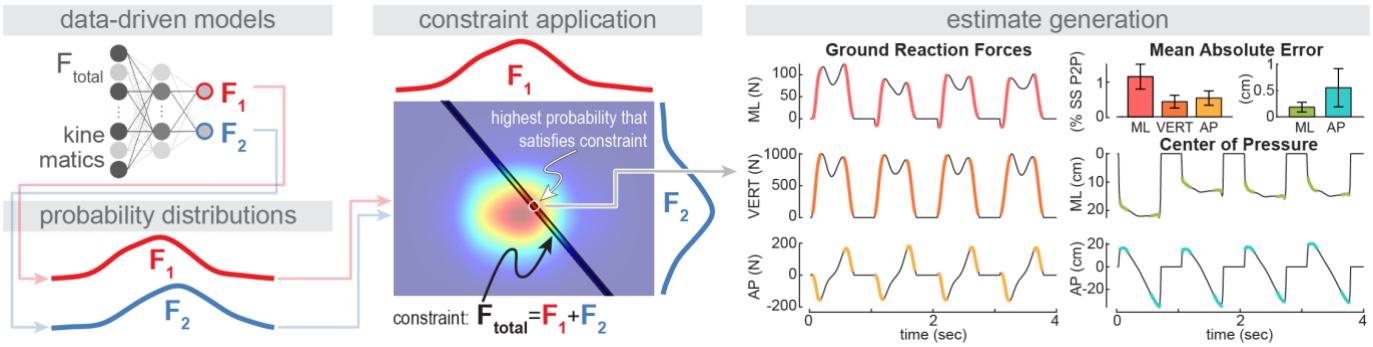

Figure 1: We used 20 TCN models to generate bilateral force estimate probability distributions. We then applied various constrains to the multi-dimensional probability distribution and chose the highest probability estimate that satisfied the constraints. All MAE results are shown.

CONCURRENT VALIDITY AND RELIABILITY OF IN-STADIUM MARKERLESS MOTION CAPTURE IN ESTIMATING JOINT KINEMATICS DURING BASEBALL PITCHING

Arnel L. Aguinaldo[1*], Tyler K. Cardinale[1], Taylor La Salle[1], James H. Buffi[2]
[1]Padres Biomechanics Laboratory, Point Loma Nazarene University, San Diego, CA
[2]Reboot Motion, Inc.
*Corresponding author's email: arnelaguinaldo@pointloma.edu

Introduction: Markerless motion capture systems allow for the estimation of 3D segmental pose of human movement without the encumbrance of markers used in traditional motion capture. Machine-vision based technologies facilitate the collection of kinematic data across diverse settings in which subjects perform movements such as walking, running, and throwing [1]. Recently, in-stadium markerless motion capture has been the primary modality for ball tracking, video assistant referring, player tracking, and human pose estimation of athletic movements at sporting events [2]. However, the criterion validity of baseball pitching kinematics using this emerging markerless motion capture technology remains unclear. Therefore, this study aimed to examine the concurrent validity and reliability of baseball pitching kinematics estimated by an in-stadium markerless motion capture system compared to an "in-lab" markerless system using marker-based motion capture as the ground truth.

Methods: This analysis is based on a sample of 18 collegiate baseball players (height = 1.83 ± 0.02 m, mass = 86 ± 18 kg, fastball velocity = 84.3 ± 4.1 mph), all of whom provided written informed consent to participate in this study. Each pitcher threw 10 fastballs off a regulation mound while their segment motions were concurrently recorded with a 5-camera in-stadium markerless motion capture system (Hawk-Eye, Basingstoke, UK), 10-camera in-lab markerless motion capture system (*Miqus*, Qualisys, Göteborg, Sweden), and an 8-camera marker-based motion capture system (*Arqus*, Qualisys, Göteborg, Sweden) at a sampling rate of 300 Hz. The marker-based system recorded the locations of passive markers placed over specific anatomical landmarks [2]. Thirty-eight of the over 100 body key points predicted by *Theia3D* (v. 2023.1.0.3160, Theia Markerless, Kingston, ON) were spatially aligned with the marker-based targets using the *theia_merge* pipeline command in *Visual3D* (HAS Motion, Canada). A separate, customized pipeline was used to transform the 29 key points estimated by Hawk-Eye (v. 2024.1.26.3) into the Qualisys reference frame using the mid-hip point to spatially align the data from both systems. Data from all systems were low-pass filtered at 18 Hz and subsequently processed through the same IK model in *Visual3D*. The concurrent validity of markerless raw position data was measured using the Mean Per Joint Positional Error (MPJPE). The concordance correlation coefficient (CCC) [3] and a nested Bland-Altman analysis were used to assess the validity and reliability of relevant segment lengths and discrete kinematic data using 7 to 10 trials per pitcher (n=98). The 95% confidence intervals (CI) around the systematic bias and each limit of agreement (LoA) were estimated using the method of variance estimates recovery (MOVER) [4]. All data agreement analyses were performed with the *simplyagree* package in R (4.3).

Results & Discussion: To date, this is the first report on the validity and reliability of the Hawk-Eye in-stadium markerless system in estimating pitching kinematics. The MPJPEs for the Hawk-Eye and Theia systems were 0.058 ± 0.010 m and 0.038 ± 0.008 m, respectively (Figure 1, left). Hawk-Eye overestimated pelvic width by 0.040 m while Theia overestimated it by 0.048 m (Figure 1, center). Similarly, maximum external rotation (MER) of the throwing shoulder was overestimated by both markerless systems (Figure 1, right). Hawk-Eye estimated selected discrete kinematics with moderate inter-system reliability (CCC = 0.464, CI [0.356, 0.561]), which indicates that the systematic bias between motion capture modalities varies throughout the relevant kinematic ranges.

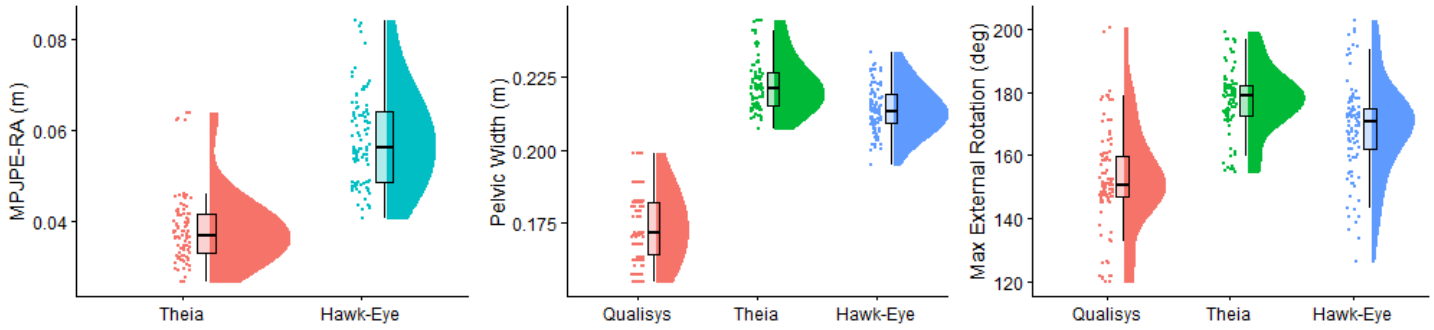

Figure 1: Raincloud plots for the MPJPE (left), pelvic width (center), and MER (right) estimated by the marker-based and markerless systems

Significance: Due to the inferential differences between systems, it is highly improbable that perfect concordance in all metrics can be achieved. Although the feasibility of markerlessly capturing kinematics in more natural baseball settings has important implications for player health and performance, more equivalence analyses that include pitchers with higher ball velocities should be performed to add to the validity evidence of in-stadium motion capture technology established by this study.

Acknowledgments: The authors thank the San Diego Padres for allowing us to collect the data in their home stadium for this study.

References: [1] Kanko, R. M., et al. (2021). *Journal of Biomechanics*, *127*(July), 110665; [2] Naik et al. (2022). *Applied Sciences, 12*(9), 4429. [3] Carrasco, J. L., et al. (2013). *Computer Methods and Programs in Biomedicine, 109*(3), 293–304; [4] Zou, (2013). *Stat Methods in Med Res, 22*(6), 630.

Leveraging a complete, manually segmented upper limb muscle MRI dataset for convolutional neural network training

Samuel Gillespie[1,2*], Pouyan Firouzabadi[1,2], Maximilian Carvajal[1,2], Haley Geithner[4], Marta García[3,5], Katherine Saul[4], Wendy M. Murray[1,2]
[1]Northwestern University, Evanston, IL, [2]Shirley Ryan AbilityLab, Chicago, IL, [3]Argonne National Laboratory, Lemont, IL, [4]North Carolina State University, Raleigh, NC, [5]Northwestern-Argonne Institute of Science and Engineering, Evanston, IL
*Corresponding author's email: samuelgillespie2023@u.northwestern.edu

Introduction: In-vivo quantification of muscle volume is of interest for both researchers and clinicians. Manual segmentation of muscles from magnetic resonance (MR) images is established as an accurate muscle volume measurement technique, but is inherently time consuming and requires a trained expert to perform [1]. Automatic muscle segmentation using a deep convolutional neural network (DCNN) trained on a dataset of manually segmented images has been implemented for lower limb [2] and shoulder muscles [3]. Automatic segmentation can have lower accuracy for smaller muscles [2] and feasibility of these approaches for upper limb muscles beyond those that cross the shoulder has yet to be evaluated. Leveraging a dataset containing manual segmentations of all arm muscles crossing the glenohumeral, elbow, and wrist joints [1], the long-term goal of this project is the creation of open-source models for automatic segmentation and computation of volumes for muscles throughout the upper limb.

Methods: An existing dataset of MR images from 10 subjects containing manual segmentations of all muscles (Palmaris longus excluded) that cross the shoulder, elbow, or wrist [1] was pre-processed and curated for DCNN training, with FAIR [4] principles in mind. Two image sets are present for every subject; one collected with a body coil for the shoulder and upper arm muscles (12 total), and the other with an arm coil for the forearm muscles (19 total). Manual segmentation was performed on original DICOM images using 3D Doctor (Able Software Corp., Lexington, MA). Segmentations were exported as boundary files and converted with Python (Python Software Foundation) to DICOM mask files co-registered with the corresponding images. Images and masks were then converted to NIfTI format and organized for use with the self-configuring nnUNet [5] python library, which generates 2D, 3D, and 3D-cascaded UNet architectures for a given dataset. The 2D and 3D self-configured nnUNet models were generated and trained for 100 epochs with 5-folds in binary (single muscle) and multiclass (all muscles) configurations. Validation Dice and Intersection-Over-Union (IoU) metrics and volume error of the model predictions compared to original manual segmentations were assessed and calculated as the means of the values for the 5 training folds. Results for a sample of 4 muscles that span different sizes (65.1 - 380.5cm^3), anatomical locations within the limb, and image sets are presented here.

3D Multiclass Models (Sample Muscles)

Image Coil	Muscle	Dice	IoU	Volume % Error	Volume (cm^3)
Arm	BRD	0.809	0.683	7.49%	65.1
	FDP	0.900	0.818	4.23%	91.6
Body	DELT	0.911	0.838	0.72%	380.5
	TRI	0.912	0.842	2.19%	372.1

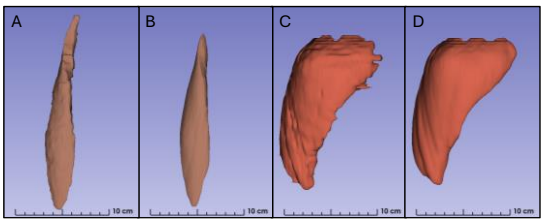

Figure 1: (**Top**) Validation Dice, IoU, and Volume error of trained model predictions compared to original manual segmentations for Deltoid (DELT), Triceps Brachii (TRI), Brachioradialis (BRD), and Flexor Digitorum Profundus (FDP), with mean manual segmentation volumes in the last column [1] (**Bottom**) Example **A&C)** manually segmented and **B&D)** model predicted BRD & DELT volumes visualized with Slicer (slicer.org)

Results & Discussion: The multiclass 3D UNet approach achieved the highest performance and was consistently high performing across the sample muscles (Fig. 1). Volume errors are comparable to reported maximum inter-segmenter variations, which were directly assessed in the manual segmentations for both the deltoid (1.2%) and brachioradialis (4.4%) [1]. Future work will involve curation of more datasets [6–8] for both training and testing, as well as longer training (>100 epochs) to improve model performance.

Significance: We demonstrate promising early results for the feasibility of developing high-performing DCNN models for automatic segmentation of muscles throughout the upper limb. The time and effort reduction of automatic muscle segmentation, which thus far has not been realized beyond muscles that cross the shoulder, can greatly facilitate the quantitative study of muscle volume with MRI.

Acknowledgments: This work is supported by NIH R21AR080953. The project used resources of the Argonne Leadership Computing Facility, a U.S. Department of Energy (DOE) Office of Science user facility at Argonne National Laboratory and is based on research supported by the U.S. DOE Office of Science-Advanced Scientific Computing Research Program, under Contract No. DE-AC02-06CH11357. Computational resources and staff contributions provided for the Quest high performance computing facility at Northwestern University is jointly supported by Office of the Provost, the Office for Research, and NUIT.

References: [1] K. R. S. Holzbaur *et al.*, *J. Biomech.* 40 (2007) [2] R. Ni *et al.*, *J. Med. Imaging*. 6 (2019) [3] L. Riem *et al.*, *Radiol. Artif. Intell.* 5 (2023) [4] M. D. Wilkinson *et al.*, *Sci. Data*. 3 (2016) [5] F. Isensee *et al.*, *Nat. Methods*. 18 (2021) [6] K. R. Saul *et al.*, *J. Appl. Biomech.* 31 (2015) [7] M. E. Vidt *et al.*, *J. Biomech.* 45 (2012) [8] M. E. Vidt *et al.*, *Arthrosc. J. Arthrosc. Relat. Surg.* 32 (2016)

MIDTARSAL JOINT WORK DOES NOT EXPLAIN THE INFLUENCE OF MIDTARSAL JOINT STIFFNESS ON THE METABOLIC COST OF SIMULATED RUNNING

Daniel J. Davis[1*], John H. Challis[2]
[1]Sayu Lab for Biomechanics and Locomotion, University of Utah, Salt Lake City, UT
[2]Biomechanics Laboratory, The Pennsylvania State University, University Park, PA
*Corresponding author's email: Daniel.J.Davis@utah.edu

Introduction: The function of the human foot's arch is thought to be beneficial in gait in that in addition to storing and returning energy itself it allows for efficient use of the energy generated by musculotendinous structures for propulsion. The spring-like nature of some structures crossing the human lower limb joints has been proposed to provide an evolutionary advantage which aids in efficient bipedal running [1]. The foot's arch has been demonstrated to store and return energy in a spring-like manner as well [2], and thus may contribute to the efficiency of gait by reducing active energy generation requirements. The amount of energy stored and returned by spring-like structures is in part a function of their stiffness, and it has been proposed that humans have benefited from a stiffer arch compared with our evolutionary relatives [3]. Should arch stiffness impact the efficiency of human running, this would then highlight the role of the foot's arch, and have far-reaching implications on our understanding of the benefits of the human arch.

It is difficult to independently examine the effects of changes in foot arch stiffness *in vivo*. However, with the use of computational musculoskeletal modeling, multiple foot arch stiffness values can be tested for a given 'individual' to examine arch stiffness' influence more directly. The purpose of this study is therefore to determine if foot arch stiffness influences the metabolic cost of steady state running between two different running foot strike types.

Methods: To simulate the right stance phase of rearfoot (RF) and non-rearfoot (NRF) strike running, a previous planar 13-segment, 26-muscle model [4] developed in OpenSim [5] was used. The foot model comprised a rearfoot and forefoot segment connected by the midtarsal joint and a metatarsophalangeal joint which connected the forefoot and toe segments. A torsional spring at the midtarsal joint (stiffnesses: 200, 400, 600, 800, and 1,000 Nm/rad) was used to alter the passive stiffness such that the joint had a representative range of a range of *in vivo* quasi-stiffness values [6]. A path spring along the plantar surface of the foot represented the plantar aponeurosis.

Computational musculoskeletal simulations of steady-state running were performed in OpenSim Moco [7] based on running data from 15 participants [8]. Inverse kinematics was used to generate joint angles from the stance phase of experimental rearfoot and non-rearfoot strike running. Simulations were performed which minimized the sum of muscle excitations squared, and the discrepancies with experimental joint angles, joint angular velocities, and ground reaction forces [4]. The metabolic cost of the muscles of the right leg during the stance phase was estimated using the model of Umberger [9].

Results & Discussion: The positive, negative, and net mechanical work performed about the midtarsal joint as midtarsal joint torsional spring stiffness increased followed a similar decreasing pattern in both running foot strike conditions (Fig 1). However, the metabolic cost of transport decreased by ~5% relative to the lowest stiffness condition in rearfoot strike running with increasing stiffness but increased by ~10% in non-rearfoot strike running (Fig 1), suggesting that mechanisms beyond foot energy storage and return were responsible for the alterations in metabolic economy. The MCoT of the triceps surae, which were altered the most out of any modeled muscle, together followed a similar pattern to the stance limb MCoT in each foot strike condition. This is likely due to changes in muscle fiber shortening velocity, as at the timing of peak muscle fiber force, the shortening velocity of the triceps surae muscles also followed a pattern similar to the stance limb MCoT.

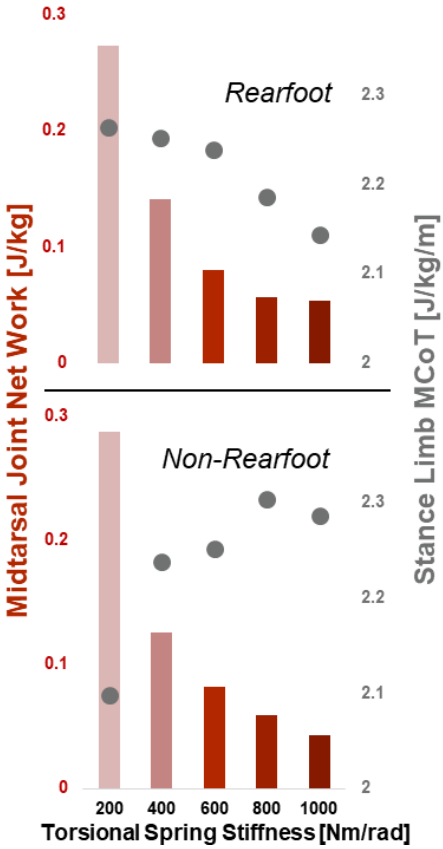

Figure 1: Increasing the midtarsal joint torsional spring stiffness decreased the net midtarsal joint work in both rearfoot and non-rearfoot running, however, increased stiffness decreased the stance limb metabolic cost of transport (MCoT) in rearfoot strike running and increased the MCoT in non-rearfoot strike running.

Significance: These simulations demonstrate that midtarsal joint stiffness modulates the MCoT of human running. That the difference in metabolic cost was sensitive to the foot strike type provides evidence that the spring-like function of the foot's arch, which also varies according to gait mode [8], influences the metabolic cost of locomotion. However, foot arch stiffness did not alter running MCoT via changes in the amount of energy storage and return *per se*, but rather by altering the behavior of ankle joint musculature. Researchers aiming to uncover the mechanisms underlying locomotor energetics should consider the influence of the foot's arch when employing computational musculoskeletal models.

References: [1] Bramble & Lieberman (2004), *Nature* 432(7015); [2] Ker et al. (1987), *Nature* 325(6100); [3] McNutt et al. (2018), *Evol Anthropol* 27(5); [4] Davis & Challis (*in press*) *Comput Methods Biomech Biomed Engin*; [5] Delp et al. (2007), *IEEE Trans Biomed Eng* 54(11); [6] Holowka et al. (2021), *J Exp Biol* 224; [7] Dembia et al. (2020), *PLoS Comput Biol* 16(12); [8] Davis & Challis (2023), *J Biomechanics* 151; [9] Umberger (2010), *J Roc Soc Interface* 7(50).

HOW DOES ADDITION OF A LATERAL EXTRA-ARTICULAR TENODESIS DURING ANTERIOR CRUCIATE LIGAMENT RECONSTRUCTION ALTER LOAD SHARING WITHIN THE KNEE?

Sarah C. Edwards[1], Matthew B. Blomquist*[1], Molly A. Day[1], Pamela J. Lang[1], Joshua D. Roth[1]
[1] University of Wisconsin-Madison, Madison, WI
*mbblomquist@wisc.edu

Introduction: There is debate about whether a lateral extra-articular tenodesis (LET) should be added during anterior cruciate ligament reconstruction (ACLR) in high-risk individuals[1]. Prior studies have shown that adding an LET during ACLR leads to load sharing between the LET and ACL grafts[3-5], which helps explain the high graft survival and good patient reported outcomes[2]. However, these studies vary widely in two key surgical parameters: (1) location of the femur anchor of the LET graft and (2) knee flexion angle at time of graft tensioning. Therefore, it is critical to understand how these surgical parameters alter load sharing between key knee structures (i.e., ACL and LET grafts, and menisci). Accordingly, ***our objective*** was to determine how the addition of an LET graft alters load sharing between key knee structures across a range of femoral anchor locations of the LET graft and flexion angles for graft tensioning.

Methods: We generated a virtual cohort of 1000 models by randomly sampling the linear stiffness and slack length of all ligaments in a validated, 12-degree-of-freedom, musculoskeletal model of the knee[6] to account for the wide range of laxity patterns in the population (***Fig. 1a***). We assumed the ACL in the model represented an ACL graft. To replicate an LET procedure, we created an additional graft strand with the same properties as the iliotibial (IT) band. This graft maintained its distal insertion point of the IT band at Gerdy's tubercle and was wrapped underneath the LCL. To account for differing surgical parameters, we tensioned the LET graft to 20 N at 30°, 45°, and 90° for each model. We also varied the femoral anchor location of the graft ±15 mm in both the anterior-posterior and superior-inferior directions from the baseline anchor location on the postero-lateral aspect of the femur (***Fig. 1a***). We then performed forward dynamic simulations in OpenSim JAM of anterior (100 N) and internal rotation (10 Nm) laxity assessments at 30° flexion (***Fig. 1b***). We computed (1) the percent contribution of the LET and ACL graft tensions to restraining against the applied load for both laxity tests, and (2) the change in peak contact forces on the posterior lateral meniscus between the ACLR + LET and ACLR conditions. We analyzed these values using descriptive statistics (i.e., mean and standard deviation) instead of traditional statistical hypothesis tests because of the large sample size of this probabilistic, computational study.

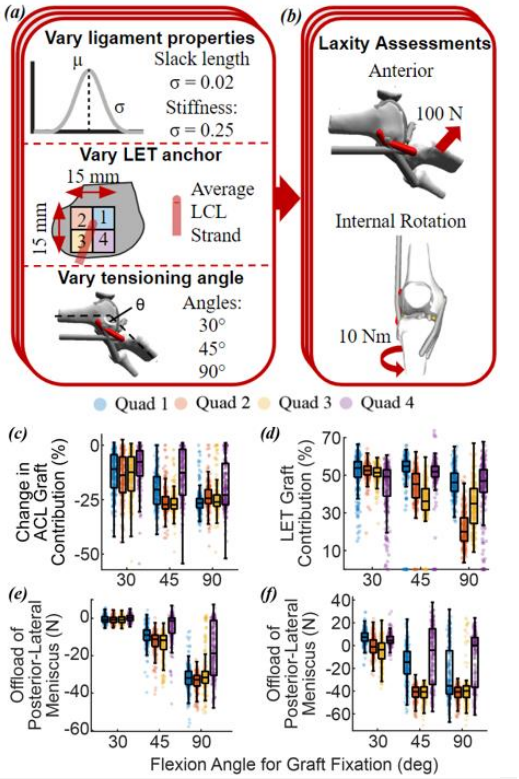

Figure 1: ***(a)*** We created 1000 models and varied ligament properties and femoral anchor locations and tensioning angles of the LET graft. ***(b)*** We then performed anterior and internal rotation laxity tests on each model. Box plots (***left, c and e***) show the % change in ACL graft contribution **(c)** and offloading of the posterior-lateral meniscus **(e)** during the anterior laxity tests. Box plots (***right, d and f***) show the % change in LET graft contribution **(d)** and offloading of the posterior-lateral meniscus **(f)** during the internal rotation laxity tests.

Results & Discussion: Addition of the LET graft generally offloaded the ACL graft during anterior laxity tests across all combinations of surgical parameters (mean ± standard deviation = -21± 10%, ***Fig. 1c***). The greatest reduction in ACL graft tension occurred when the LET graft was tensioned at 90° flexion (-27 ± 14%, ***Fig. 1c***). During the internal rotation laxity tests, the percent contribution of the LET graft was highest when it was tensioned at 30° (50 ± 9%, ***Fig. 1d***). The presence of the LET graft also offloaded the posterior aspect of the lateral meniscus for both anterior and internal rotation laxity assessments (-13± 5 N and -18 ± 7 N respectively, ***Figs. 1e and 1f***). The offloading of the lateral meniscus was greatest when the graft was tensioned at 90° and most consistent when the graft was placed in quadrants 2 and 3 (***Figs. 1e and 1f***). In general, the percent contributions of the ACL and LET during the anterior laxity tests were similar across graft fixation locations except for LET contributions during internal rotation laxity tests when the LET graft was tensioned at 90° of flexion. When the LET graft was tensioned at 90° of flexion, the lowest (21 ± 9%) and highest (46 ± 8%) LET contributions occurred when the femoral anchor location was in quadrant 2 (superior-posterior) and quadrant 1 (superior-anterior), respectively (***Fig. 1d***). Our data indicates that the ACL graft and posterior lateral meniscus are most consistently offloaded when the LET graft is tensioned at 90° flexion. While the LET is able to best offload the ACL graft when tensioned at 90° flexion, the percent contribution of the LET graft was lowest when placed in quadrant 2 (superior-posterior, ***Fig. 1d***). These findings demonstrate that surgeons should consider patient-specific characteristics when deciding at which angle to tension the LET graft and where to anchor it to the femur. Additionally, the effects of the LET on load sharing varies widely within our cohort which suggests that considerations for the other secondary restraints is important when personalizing an ACLR + LET for a particular patient.

Significance: These findings highlight that load sharing within the knee is highly sensitive to modifiable surgical decisions during an ACLR + LET procedure. Thus, personalizing these decisions may further improve outcomes after ACLR+LET in high-risk patients.

References: 1. Getgood, Arthroscopy, 2022. 2. Mahmoud, Arthroscopy, 2022. 3. Draganich, AJSM, 1990. 4. Engebretsen, AJSM, 1990. 5. Marom, AJSM, 2020. 6. Lenhart, Ann Biomed Eng, 2015.

THREE-DIMENSIONAL OPTIMAL CONTROL SIMULATION OF HUMAN-LIKE AND CHIMPANZEE-LIKE BIPEDAL WALKING IN *AUSTRALOPITHECUS AFARENSIS*

Brian R. Umberger [1*], Aravind Sundararajan[2], Matthew C. O'Neill [2]
[1]School of Kinesiology, University of Michigan, Ann Arbor, MI, USA
[2]Department of Anatomy, College of Graduate Studies, Midwestern University, Glendale, AZ, USA
*Corresponding author's email: umberger@umich.edu

Introduction: Understanding how musculoskeletal trait evolution facilitated the development of walking capabilities in our hominin ancestors is a major goal in human evolutionary biology. The emergence of *Australopithecus* (*A.*) *afarensis* about 3.9 million years ago is argued to represent a major adaptive shift in bipedal walking capabilities as compared to the last common ancestor of modern humans and chimpanzees. Yet, as a species, *A. afarensis* exhibits a suite of skeletal traits in the pelvis, lower limb, and foot that differentiate it from both living human and chimpanzee species. How this unique combination of traits interacts to determine locomotor function has been an area of longstanding interest and disagreement [1,2].

Musculoskeletal simulation is a powerful approach to evaluate the simultaneous, interacting effects of pelvis and lower limb skeletal traits, since they are directly parameterized in musculoskeletal models and optimal control simulations permit identification of their effects on locomotor performance. Here, we test the hypothesis that the *A. afarensis* musculoskeletal structure can reproduce the three-dimensional (3-D) kinematics and ground reaction forces (GRF) of both human and bipedal chimpanzee walking using optimal control simulation. The failure to reproduce either species gait is taken as evidence rejecting the hypothesis for that species.

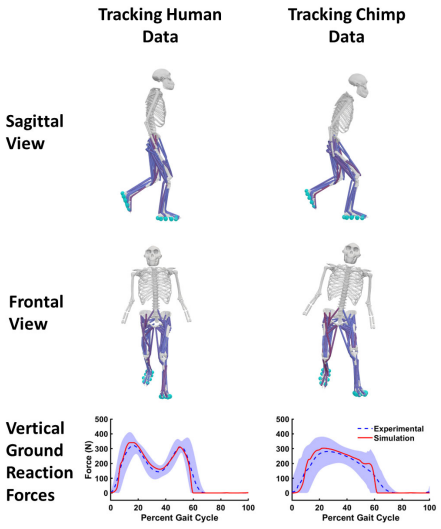

Figure 1: Body postures and GRFs for bipedal walking in the *A. afarensis* model at dimensionless speeds of 0.56 (1.23 m/s) while tracking human (left) and chimpanzee (right) experimental data.

Methods: Optimal control simulations of bipedal walking were generated in OpenSim Moco using a newly developed 3-D musculoskeletal model of *A. afarensis* [3] (Fig. 1). The model has 19 degrees of freedom, 86 muscles, and a mass of 26.5 kg. The optimal control problem was defined to minimize an objective function that consisted of a tracking term and an effort term. The tracking term was the squared differences in 3-D kinematic and GRF data, and the effort term was cubed muscle excitations. Simulations were generated that tracked speed-matched, species-specific human and chimpanzee experimental gait data [4,5]. GRF data were scaled to account for inter-specific body mass differences. The neuromuscular effort of walking was characterized as integrated muscle activation, summed across muscles.

Results & Discussion: *A. afarensis* gait simulations reproduced the salient kinematic and kinetic features of both human-like and chimpanzee-like walking (Fig. 1). The human data were tracked more closely than the chimpanzee data, and neuromuscular effort was lower for human-like walking (Table 1). Chimpanzee walking patterns were matched as well, but with greater tracking error due to a slightly less flexed and abducted limb than in the chimpanzee data. Muscle activation patterns were generally similar between datasets, with greater effort for chimpanzee-like walking primarily associated with elevated or prolonged activation of several muscles.

	RMSE		
	KIN	GRF	ACT
Tracking Human Data	4.3	0.060	0.072
Tracking Chimp Data	8.1	0.080	0.086

Table 1: Root mean square error (RMSE) for tracking 3-D kinematics (KIN, degrees) and ground reaction forces (GRF, proportion of body weight). Neuromuscular effort (ACT, integrated muscle activation).

While neither hypothesis was rejected based on these results, differences in performance between the datasets provide a weaker form of evidence that *A. afarensis* musculoskeletal structure was less well suited to chimpanzee-like bipedal walking, consistent with *a priori* expectations for a habitual biped. While the tracking quality was better for the human data, chimpanzee data-tracking produced a gait that was distinctly more ape-like than human-like. Tracking simulations are therefore insufficient to resolve the 3-D gait patterns for *A. afarensis*; instead, a predictive simulation approach based on optimality criteria that are robust for both habitual (e.g., human) and facultative (e.g., chimpanzees) bipedal walking is needed.

Significance: The present results demonstrate the general compatibility of *A. afarensis* locomotor anatomy with both human-like and chimpanzee-like walking. This indicates that tracking simulation are, by themselves, insufficient to determine the bipedal gait of this fossil hominin species. A deeper understanding of walking capabilities in this species will require an integrated set of human, chimpanzee, and *A. afarensis* predictive simulations.

Acknowledgments: This research was funded by NSF grants BCS 2018523 and 2018436.

References: [1] Lovejoy (1981) *Science* 211; [2] Stern & Susman (1983) *Am J Phys Anthro* 60, (1983); [3] O'Neill et al. (2024) *Am J Biol Anthro* 183; [4] O'Neill et al. (2015) *J Hum Evol* 86; [5] O'Neill et al. (2022) *J Hum Evol* 168.

MODELING RESIDUAL LIMB MUSCLE WEAKNESS IN GAIT FOR INDIVIDUALS WITH UNILATERAL TRANSTIBIAL AMPUTATION

Wenxin Zhou*, Matthew Mulligan, Brian R. Umberger
School of Kinesiology, University of Michigan, Ann Arbor, MI
*Corresponding author's email: wxzhou@umich.edu

Introduction: People with unilateral transtibial amputation (TTA) typically adopt compensatory strategies during gait due to the loss of musculoskeletal structures below the knee and the use of a prosthesis [1]. These compensatory strategies are characterized by changes in stride parameters, kinematics, kinetics, and muscle activation patterns for the residual and intact limbs. For example, individuals with TTA tend to walk with greater hip extension, knee flexion, and ankle dorsiflexion in the intact limb, as well as greater hip and knee flexion during stance in the residual limb [2]. Spatiotemporal asymmetries, such as shorter stance time for the residual limb, are also reported in literature [3]. Furthermore, peak isometric and isokinetic knee extension/flexion torques have been reported to be 30-75% lower in the residual than the intact limb of transtibial prosthesis users [4]. Besides the physical asymmetries in people with TTA, strength asymmetries might independently contribute to altered walking performance [5], but this is difficult to tease out empirically. Musculoskeletal models that represent people with TTA who possess full muscle strength can reproduce able-bodied gait mechanics with minimal deviations [6]. A modeling and simulation approach could also be useful in understanding how residual limb muscle weakness affects gait mechanics. Therefore, the purpose of this study was to isolate the effects of residual limb muscle weakness on walking performance in simulations of individuals with TTA. We predicted that gait simulations with greater residual limb muscle weakness would increasingly deviate from able-bodied gait in ways that mirror those observed in people with TTA.

Methods: The TTA model was adapted from a two-dimensional able-bodied musculoskeletal model [7] with 11 degrees of freedom and 18 muscles in the lower limbs. To represent TTA, the left ankle muscle were removed and a passive prosthesis was modeled by adding linear torsional springs to the left ankle and metatarsophalangeal joints [6]. Maximum isometric muscle forces in the residual limb were scaled in decrements of 10%, resulting in ten models representing 0% (full strength) to 90% residual limb muscle weakness compared with the intact limb. Optimal control simulations of a full stride of walking at 1.3 m/s were generated using OpenSim Moco. The objective function consisted of a tracking term (squared differences in kinematics and ground reaction forces from able-bodied gait data [7]) and an effort term (cubed muscle excitations). We identified the minimum weight on the tracking term that reasonably reproduced the experimental data in the full-strength case, which permitted the weaker models to deviate from the experimental data. Similarities in pattern and differences in magnitude for the kinematic and GRF data between able-bodied gait and simulated gait at each strength level were evaluated using zero-lag cross-correlation (r) and root-mean-square deviations (RMSD). Stance time asymmetry was expressed as a percent difference between the limbs, and the neuromuscular effort of walking was characterized as the integrated muscle activation, summed across muscles.

Results & Discussion: The optimal control simulations converged for all residual limb weakness levels except 90%, indicating that the 90% weakness model was too weak to walk. On average, GRFs were close to the experimental data from 0-50% residual limb weakness (RMSD < 27 N, $r \geq 0.98$), with larger deviations in magnitude at greater levels of weakness (RMSD = 42 N at 80% weakness). The kinematic results were more complicated, with offsetting joint-specific changes across different weakness levels. The kinematic changes with residual limb weakness included adaptations reported in the literature, such as greater residual limb knee flexion in stance phase [2].

Stance time asymmetry was 2.4% in the full strength condition, with more time spent on the intact limb, and increased steadily with the level of residual limb muscle weakness to a maximum of 4.3% in the 80% weakness condition (Fig. 1A). The range of stance time asymmetries agreed well with those reported in the literature for people with TTA [3]. Neuromuscular effort also increased steadily with greater residual limb muscle weakness (Fig. 1B), consistent with the finding that people with more of a residual limb strength deficit have greater perceived exertion in walking [5]. Counterintuitively, there was a disproportionate increase in *intact* limb effort at greater degrees of residual limb weakness (Fig. 1B), as the model relied more upon the stronger limb in those cases. Overall, the model of residual limb muscle weakness reproduced many of the gait adaptions observed in people with unilateral TTA who use a prosthesis to walk.

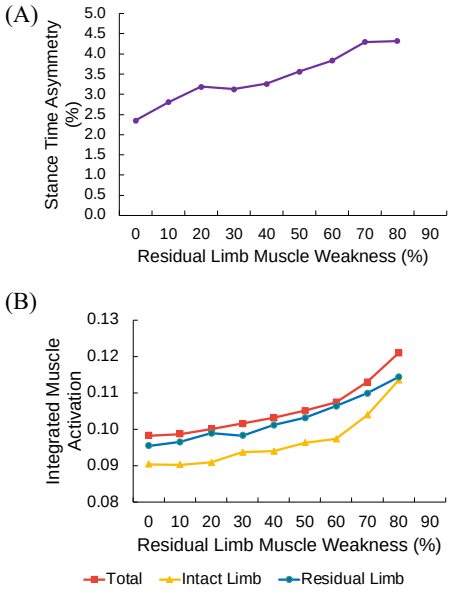

Figure 1. (A) Stance time asymmetry and (B) neuromuscular effort with increasing residual limb muscle weakness from 0-80%.

Significance: While gait adaptations in people with TTA are a complex phenomenon, the present results indicate that weakness in the residual limb relative to the intact limb may be an independent contributor to these gait changes. Further investigation using predictive simulation will enhance our understanding of the compensatory strategies adopted by unilateral transtibial prosthesis users and inform potential strength training goals for post-TTA rehabilitation programs.

References: [1] De Marchis et al. (2022*), Front. Rehabilit. Sci* 3; [2] Bateni & Olney (2002), *J Prosthet Orthot* 14(1); [3] Isakov et al. (2000), *Prosthet Orthot Int* 24(3); [4] Hewson et al. (2020), *Prosthet Orthot Int* 44(5); [5] Ihmels et al. (2022), *Gait Posture* 97; [6] Russell Esposito & Miller (2018), *PLoS One* 13(1); [7] Nguyen et al. (2019), *IEEE Trans. Neural Syst. Rehabil. Eng* 27(7).

SEX DIFFERENCES IN SCALING OF LOWER LIMB MUSCLE MOMENT ARMS AS DEMONSTRATED BY MRI-BASED MUSCULOSKELETAL MODELS

Kimberly M. Steininger[1*], Emily M. McCain[1], Mario E. Garcia[1], Allen Luk[1], Silvia S. Blemker[1]
[1]University of Virginia, Charlottesville, VA, USA
*Corresponding author's email: fma5br@virginia.edu

Introduction: Current musculoskeletal models are based upon limited data sets that are not representative of the general population: models are typically based on the geometry of male subjects, exclude known sex differences in musculoskeletal geometry, incorporate biased scaling relationships that are not sex-specific, and likely provide predictions not representative of female subjects [1]. Computational modeling can be used to construct high fidelity subject-specific models, ultimately improving understanding of how geometric differences impact muscle function. Furthermore, advances in magnetic resonance imaging (MRI) segmentation of muscle and bone allow for definitions of precise, subject-specific muscle origin and insertion points [2]. This thus allows us to elucidate the effects of variations in subject geometry and sex on muscle moment arm: **This research aims to use subject-specific MRI-based models to determine if scaling relationships between body dimensions and moment arms of adductor brevis and adductor longus muscles differ between healthy male and female subjects.**

Methods: Ten male and ten female subjects were recruited between the ages of 20-47 (27.4±8.39 years) within five height (1.72±0.11 m) and mass (74.8±19.59 kg) categories [3], and MRI data was collected to produce lower body bone and muscle segmentations for each subject. Muscle segmentation: Subjects were scanned supine using a 3T Siemens (Munich, Germany) Trio MRI Scanner in a two-point Dixon sequence with a field of view: 280 mm x 450 mm, slice thickness: 5mm, and in-plane spatial resolution: 1.1 mm × 1.1 mm. The scans were processed using a deep convolution neural network-based segmentation method (Springbok Analytics, Charlottesville, VA), producing 3D models of all bones and muscles of the lower extremities [4]. Model building: Pelvis and femur geometries were imported into MATLAB (MathWorks) as reference point clouds, and adductor brevis and longus geometries were imported as query point clouds to determine their location respective to the bone references. Muscle origin and insertion areas were then located using the k-nearest neighbor algorithm, using minimum Euclidean distance measurements to classify data groupings [5]. Using these areas, the origin and insertion points of each muscle were calculated from the center point of each region. OpenSim [6] models were created in OpenSim Creator [7] by importing bone and muscle STL files, defining hip joints, and attaching muscles to the origin and insertion points defined previously. Analysis: Peak hip adduction moment arm values were extracted from subject-specific OpenSim models. Anatomical dimensions—subject height, inter-anterior superior iliac spine (ASIS) distance, ASIS-greater trochanter distance, leg length, and greater trochanter-tibial plateau distance—as a predictor of peak moment arm were then analyzed for each sex using linear regressions (MATLAB).

Results & Discussion: In female subjects, adductor brevis moment arms correlated most strongly with the greater trochanter-tibial plateau distance (R^2 = 0.51) and adductor longus moment arms correlated most strongly with inter-ASIS distance (R^2 = 0.55). Male subjects, in contrast, showed that both adductor brevis and adductor longus moment arms most strongly correlated with height (adductor brevis: R^2 = 0.80, adductor longus: R^2 = 0.75). These results suggest that sex differences in musculoskeletal geometry leads to differential scaling relationships between muscle moment arms and body dimensions. Future work will incorporate additional muscles into the analysis and examine the functional implications of these differential scaling relationships.

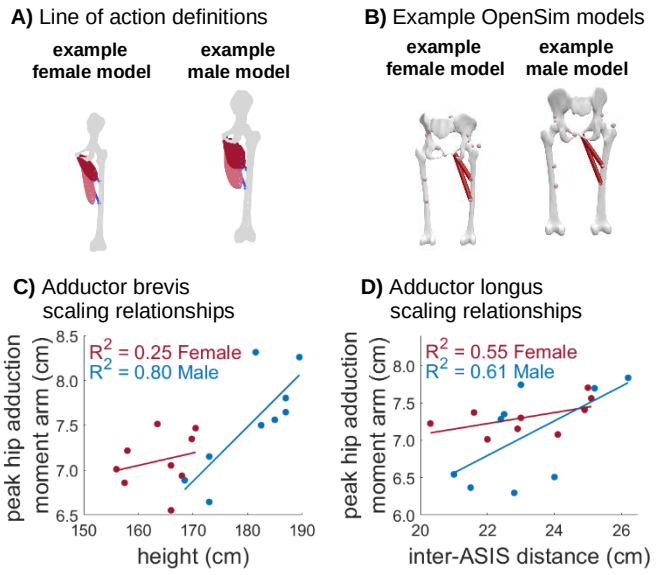

Figure 1: A) Musculoskeletal geometry of right hip with calculated adductor brevis and adductor longus origin and insertion points for two representative subjects. **B)** OpenSim models of the same two subjects (left to right) **C)** Peak adductor brevis moment arm plotted against subject height **D)** Peak adductor longus moment arm plotted against subject inter-ASIS distance.

Significance: Identifying new, geometrically-derived sex-specific scaling laws can lead to musculoskeletal models that eliminate bias, allow for higher precision calculations, and apply to a broad range of individuals inclusive of varied height, weight, and sex. Sex-specific geometric differences and their impact on muscle function have not been studied in-depth, party due to the lack of modeling frameworks that inadequately address sex differences. Our ultimate goal is to create a framework for rigorously addressing sex as a biological variable in musculoskeletal modeling and simulation research.

Acknowledgments: Research funded by NIH Grant #R01AR078396.

References: [1] Rajagopal et al. (2016), *Trans Biomed Eng*; [2] Smale et al. (2019), *J Biomechanics*; [3] Fryar et al. (2016), *Vital Health Stat*; [4] Ni et al. (2019), *J Med Imaging*; [5] T.M. Cover and P.E. Hart (1967), *IEEE Information Theory*; [6] https://simtk.org/projects/opensim/; [7] https://opensimcreator.com/

JOINT PERSONALIZATION OF A NOVEL SHOULDER MODEL PRODUCES HIGH-PRECISION KINEMATICS ACROSS AGE AND GENDER

Claire V. Hammond[1*], Heath B. Henninger[2], Benjamin J. Fregly[1], and Jonathan A. Gustafson[3]
[1]Rice University, Houston, TX. [2]University of Utah, Salt Lake City, UT. [3]Rush University Medical Center, Chicago, IL.
Correspondence to: Claire V. Hammond, cvhammond@rice.edu

Introduction: One in two adults will suffer a debilitating chronic or acute shoulder injury in their lifetime. Existing treatments for shoulder injuries result in highly variable post-treatment shoulder function. Personalized neuromusculoskeletal models offer the ability to investigate "what if" scenarios while accounting for functional, morphological, and neural control differences between individuals. Existing shoulder models use generalized coordinates that are difficult to personalize, largely because the shoulder is not modelled as a closed kinematic chain. An improved shoulder model is needed to support computational treatment design methods that seek to maximize functional outcome for each patient. The objective of this work was to employ a novel Joint Model Personalization (JMP) tool, part of the Neuromusculoskeletal Modeling (NMSM) Pipeline (nmsm.rice.edu), combined with a new close-chain kinematic shoulder model to investigate the accuracy of scapular joint tracking from older and younger healthy adults. We assessed kinematic accuracy by quantifying the model's ability to reproduce biplane fluoroscopy data across four subjects and eight clinical tasks.

Methods: Experimental Data for this work consisted of patient-specific (2 males / 2 females), age split (2 over 45 y/o, 2 under 35 y/o), high-resolution CT-images and biplane fluoroscopy kinematic data of the shoulder from an open-source repository [1]. Briefly, subject-specific 3D reconstructions of the scapula and humerus were created from CT-images, and anatomical landmarks were identified for the scapula (glenoid center, inferior angle, trigonum spinae, posterolateral acromion, acromioclavicular joint) and the humerus (humeral head center, elbow lateral epicondyle, and medial epicondyle) using published methods [2]. Model-based markerless tracking was used with the biplane fluoroscopic data to generate accurate kinematics of the scapulothoracic joint and glenohumeral joint following standard decomposition techniques to generate Euler angles [3]. Activities included both weighted and unweighted overhead tasks during shoulder flexion, scaption, abduction, and internal/external humeral rotation (n=8).
Computational Model. A closed-chain kinematic shoulder model was developed in OpenSim[4] using standard OpenSim joint types (e.g., pin/ball/custom) enabling personalization of joint parameters—a major limitation of existing models. First, a subject-specific OpenSim model was developed using subject model geometry described above. The scapulothoracic joint was modelled with 5 degrees of freedom (DoFs) - 2 rotations about a spherical coordinate system, 1 translation about an intermediate body, and 2 additional rotations about a scapula-based rotation center. The clavicle was attached to the thorax as a 2 DoF universal joint and to the scapula at the AC marker location as a point constraint—producing a closed-chain kinematic shoulder model.

Exact marker data was created for each landmark on an unconstrained model with 6 DoFs per body. This marker data was used to personalized a shoulder model for each subject (n=4) using JMP. The JMP tool personalizes joint parameters (positions/orientations in body segments), scales bodies, and moves markers based on user-provided settings to minimize the normalized mean squared distance between experimental and model markers on the bodies of interest via a bi-level optimization technique [5]. All eight overhead tasks were used to personalize the shoulder models, where normalized mean squared distances were calculated between landmarks and model markers across all subjects.

Results & Discussion: All models were successfully personalized by the novel JMP-based personalization methodology. The average error for each subject was small (1.2mm) and the maximum error remained low (7.8mm). These results (Figure 1) indicate that the novel closed-chain shoulder model developed with standard joint types is effective to model high-precision kinematics of the shoulder complex.

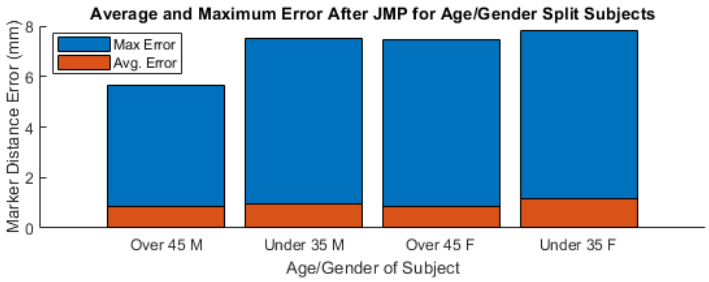

Figure 1: Average and maximum error after JMP-based personalization.

Effective personalization of kinematic models enables subject-specific modeling by allowing a patient's unique movement and anatomic structure to be built into the model for future analysis. Personalized kinematic shoulder models could facilitate further personalization of the muscles and neural control systems underlying the shoulder complex. The shoulder model and code to create a personalized shoulder model can be found at simtk.org/projects/shoulder-model.

Significance: The development of a personalization technique that produces high-precision kinematics across age and gender can allow researchers to investigate high quality computational models of the shoulder even if the subject differs from the original model. Research in areas focusing on shoulder kinematics in traditionally underrepresented groups, such as women, may be able to more easily generate kinematics from markered and markerless motion capture. This research could also help facilitate more research in neuromusculoskeletal pathologies by increasing the quality of subsequent muscle and neural control modeling.

Acknowledgments: The NMSM Pipeline is supported by the US National Institutes of Health (R01 EB030520).

References: [1] Kolz et al., *J Biomech*, 2021. [2] Kolz et al., *Gait Posture*, 2020. [3] Wu et al., *J Biomech*, 2005. [4] Seth et al., PloS, 2018. [5] Reinbolt et al., *J Biomech*, 2005.

FUNCTIONAL RECOVERY TIMECOURSE IN A PRECLINICAL MODEL OF ACHILLES TENDON INJURY

Jarod M. Forer[1,2*], Kaitlyn Link[1], Bella Yannello[1], Yan Carlos Pacheco[1], Michael E. Hahn[2], Nick J. Willett[1]
[1]Department of Bioengineering, Knight Campus for Accelerating Scientific Impact, University of Oregon, Eugene, OR, USA
[2]Bowerman Sports Science Center, Department of Human Physiology, University of Oregon, Eugene, OR, USA
*Corresponding author's email: jforer@uoregon.edu

Introduction: Tendons are integral components of the musculoskeletal system, transmitting forces from the muscles to the skeleton to create movement. Additionally, tendons are minimally vascularized compared to other peripheral tissues, resulting in poor healing outcomes [1]. Considering tendon injuries make up 45% of the more than 60 million musculoskeletal injuries that occur annually in the United States, an obvious need exists to investigate and improve functional recovery [2]. A plethora of preclinical models on tendon injury exist in the literature; most studies implementing these models have investigated the effects of different treatments on healing. However, many do not study the effects of injury to the point of full recovery, and fewer still measure functional outcomes to quantify recovery. von Frey (VF), a method of testing tactile allodynia, is used broadly in the field of orthopedic research, but has not been used in a model of complete tendon rupture and repair or measured more than two weeks after tendon injury. We used electronic VF (Bioseb) and Dynamic Weight Bearing (DWB, Bioseb) (an assessment of spontaneous limb function) to quantify full functional recovery from a surgically induced Achilles tendon rupture over a period of two months. Structural outcomes including tendon cross-sectional area, mass, and fluid content, as well as tracer clearance were measured at a timepoint before full recovery to further describe the consequences of this injury model. We hypothesized that full Achilles tendon rupture and suture repair would lead to increased sensitivity and offloading of the injured limb as shown by VF and DWB, and that both metrics would recover to baseline levels over a period of two months.

Methods: All procedures were conducted in accordance with IACUC protocol. Female Sprague-Dawley rats received a unilateral complete transection of the Achilles tendon followed immediately by suture repair. In a cohort of 12 animals, VF and DWB tests were conducted one day before injury, and 4-, 7-, 14-, 28-, and 56-days post injury. A second cohort of 6 animals was euthanized at 14 days to collect data about tendon morphology. Images of the tendon were taken *in situ* following removal of surrounding tissue and analyzed with ImageJ (FIJI) to determine cross-sectional area. Mass was measured immediately post-excision, and fluid content was calculated from the ratio of mass after and before 72 hours of lyophilization. Prior to euthanasia, 5 µL injections of near-infrared tracer dye were delivered to injured and contralateral tendons of three animals 1-week post injury. Tracer clearance analyses were conducted via an IVIS Spectrum (Revvity). VF and DWB data were analyzed with two-way ANOVA (Tukey's posthoc) and structural and clearance data were analyzed with paired t-test in Prism (Graphpad), with an alpha level of 0.05.

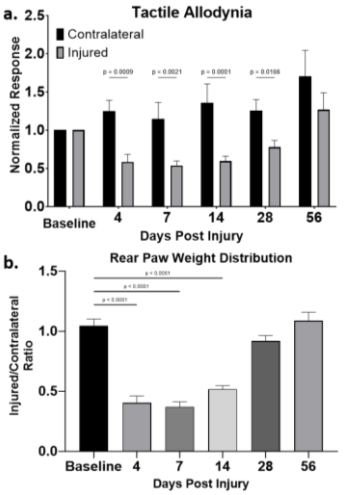

Figure 1: a) VF and b) DWB normalized to baseline. n=12 for all timepoints other than 56 days post injury, where n=6. Data shown as mean ± SEM.

Results: VF measurements showed an initial increase in sensitivity (decrease in withdrawal force) of the injured leg that returns to baseline four weeks after injury (Fig 1a). At four weeks post-injury, there was still a significant difference between the injured and contralateral limbs, which was not present at eight weeks. DWB measurements showed significant offloading of the injured limb after injury that fully recovered at four weeks post injury (Fig 1b). Two weeks post-injury tendon cross sectional area ($p=0.0002$), fluid content ($p=0.0052$), and mass ($p=0.0223$) were all significantly increased in the injured limbs compared to the contralateral limbs. Functional tracer clearance measurements showed faster clearance with significantly lower time constants in the injured limbs ($p=0.0258$).

Discussion: Both VF and DWB demonstrated loss of function followed by functional recovery from a full Achilles tendon transection over a two-month period. The results between the two differed however, with DWB showing full recovery by 4 weeks while VF still showed differences between contralateral and injured legs at that timepoint. The incorporation of multiple functional tests represents a holistic picture of the healing response. The structural changes shown two weeks after injury are consistent with the lack of full functional recovery at that time. Measurement of functional tracer clearance from the injury site showed that the injury model had significantly accelerated clearance when compared to contralateral limbs. Limitations of this study include a lack of multiple timepoints for the structural measurements and functional clearance parameters, and the lack of a sham control group for the functional testing cohort. These findings motivate investigation into how these structural changes and functional clearance parameters differ with time since injury.

Significance: Treatments of tendon injury depend on how much is known about the healing mechanisms of the tissue. This study investigates areas of functional recovery and fluid clearance, that are undescribed as of yet, and therefore provides a new avenue for researchers and practitioners alike to investigate potentially new strategies.

Acknowledgments: This work is supported by the Wu Tsai Human Performance Alliance and the Joe and Clara Tsai Foundation.

References: [1] Chen, T. M. et al. *Clin. Anat.* 22: 377-385, 2009. [2] Smallcomb, M., et al. *Am. J. Phys. Med. & Rehab.* 101: 801, 2022.

DONOR SITE ULTRASOUND CHARACTERISTICS DO NOT INFLUENCE GAIT BIOMECHANICS SIX MONTHS AFTER ANTERIOR CRUCIATE LIGAMENT RECONSTRUCTION

Alex Nilius[1*], Justin Dennis[1], Thomas Birchmeier[1], Troy Blackburn[1]
[1]University of North Carolina at Chapel Hill, Chapel Hill, NC
*Corresponding author's email: ahewson@unc.edu

Introduction: Aberrant gait biomechanics are common following anterior cruciate ligament reconstruction (ACLR) and are associated with development of post-traumatic knee osteoarthritis (PTOA).[1] Individuals with ACLR display smaller peak knee flexion angles (PKFA), internal knee extension moments (PKEM), and vertical ground reaction forces (vGRF)[2] during gait compared to healthy controls and the contralateral limb,[3] all which have been linked to cartilage degeneration.[4,5] The central third of the patellar tendon is commonly harvested as a graft source for ACLR, and donor site morbidity contributes to persistent discomfort and pain.[6] Persistent knee pain may contribute to aberrant gait biomechanics, as those who experience clinically significant pain as identified by the Knee Injury and Osteoarthritis Outcomes Score (KOOS) subscales walk with lower peak vGRF early following ACLR.[2] Ultrasound imaging can be used post-operatively to monitor donor-site healing (Figure 1). Complete regeneration of the donor site occurs within 6 months in approximately 70% of patients, while the remaining 30% recover after 12 months.[7] However, it is unclear whether regeneration of donor site tissue influences gait biomechanics associated with development of PTOA. Therefore, the purpose of this study was to evaluate correlations between ultrasound measures of patellar tendon characteristics (cross-sectional area [CSA] and echo intensity (EI, mean pixel brightness and a measure of tissue quality) and gait biomechanics outcomes and KOOS pain scores in individuals 6 months post-ACLR. Due to donor site morbidity and the association between pain and aberrant gain biomechanics, we hypothesized that lesser regeneration of the patellar tendon would be associated with smaller PKEM, PKFA, vGRF and lower (worse) KOOS Pain scores.

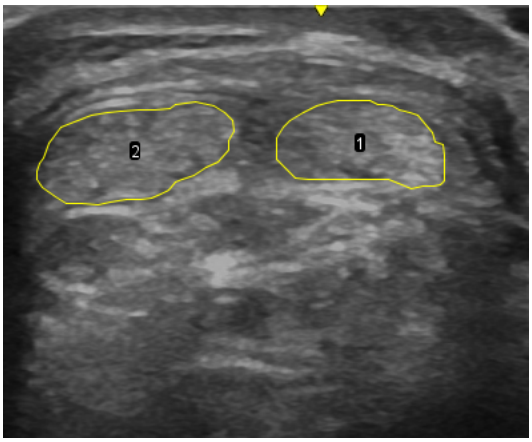

Figure 1: Binocular pattern of patellar tendon displayed 6 months after ACLR

Methods: Gait biomechanics were assessed in 16 participants with primary, unilateral ACLR using a patellar tendon autograft 6.0 ± 0.3 months post-ACLR. Gait outcomes (peak KEM, KFA, and vGRF) were assessed during the loading response phase while participants walked at their preferred speed. Transverse plane ultrasound images of the patellar tendon were obtained from the ACLR and contralateral limbs from which patellar tendon CSA and EI (i.e., mean gray scale brightness value [range 0-255 arbitrary units]) were assessed. CSA of the ACLR limb was expressed as a percentage of the contralateral limb to estimate % regeneration. Partial correlations were used to evaluate associations between patellar tendon CSA and EI and gait biomechanics outcomes, controlling for gait speed ($\alpha = 0.05$). Simple correlations were used to evaluate associations between patellar tendon CSA and EI and KOOS pain scores.

Results & Discussion:
Contrary to our hypothesis, only weak correlations were observed between patellar tendon CSA or EI and all of the gait biomechanics measures and KOOS pain scores, none of which were statistically significant (Table 1). These data suggest it is unlikely that healing status of the graft site influences gait biomechanics 6 months post-ACLR.

Gait Biomechanics Outcomes	Ultrasound Measures	
	CSA	EI
PKEM	0.252 (p = 0.365)	0.017 (p = 0.953)
PKFA	0.260 (p = 0.350)	-0.020 (p = 0.942)
vGRF	0.187 (p = 0.504)	0.031 (p = 0.913)
KOOS Pain	-0.356 (p = 0.175)	-0.133 (p = 0.624)

Table 1: Correlations between patellar tendon characteristics, gait biomechanics outcomes, and KOOS pain scores

Significance: Donor site morbidity is a clinically significant problem following ACLR. Despite persistent discomfort and pain, it is unlikely that the status of healing as represented by cross-sectional area or echo intensity influences gait biomechanics associated with the development of PTOA. Future research should investigate rehabilitation interventions aimed at improving other aspects of the knee extensor mechanism, such as decreasing graft site morbidity and improving quadriceps muscle function.

Acknowledgments: This study was supported by the Department of Defence Award Number W81XWH21C00490011582719.

References: [1] Khandha A, et. al.*J Orthop Res*. 2017;35.; [2] Pietrosimone B, et. al. *Med Sci Sport Exerc*. 2019;51(2):246-254 [3] Slater L V, et. al.J Athl Train. 2017;52(9); [4] Scanlan S, et. al. *Proc Am Soc Biomech*. 2007;252:3-4; [5] Mundermann A, et. al. *Arthritis Rheum*. 2005;52(9); [6] Shelbourne KD, et. al. *Knee Surgery, Sport Traumatol Arthrosc*. 1997;5(3). [7] Yazdanshenas H, et. al. *J Orthop*. 2015;12(4)

LANDING BIOMECHANICS IMPROVE 6 TO 12 MONTHS FOLLOWING ANTERIOR CRUCIATE LIGAMENT RECONSTRUCTION DESITE PERSISTENT KINESIOPHOBIA

Thomas Birchmeier[1*], Nathan Lopus[1], Alex Nilius[1], Justin Dennis[1], Troy Blackburn[1]
[1]University of North Carolina, Chapel Hill, NC
*Corresponding author's email: tbirchmeier@unc.edu

Introduction: Individuals with anterior cruciate ligament reconstruction (ACLR) and who score greater than 19 on the Tampa Scale for Kinesiophobia-11 (TSK-11) are 13 times more likely sustain an ACL injury to either limb within 2 years of returning to sport.[1] In those with ACLR, higher TSK-11 scores are associated with smaller knee flexion angles (KFA)[2] and lesser vertical ground reaction forces (vGRF)[3] in the ACLR limb during a drop vertical jump (DVJ). During landing, knee extension moment (KEM) is responsible for eccentric control of KFA. Thus, landing with limited KFA and KEM while shifting weight-bearing to the uninvolved limb increases ACL loading in the uninvolved limb, which can lead to injury.[4] There is limited prospective evidence that changes in TSK-11 scores correlate with changes in landing biomechanics from 6 to 12 months following ACLR when patients are transitioning into sport. The purpose of this study was to compare TSK-11 score, peak KFA, KEM, and vGRF during a DVJ between 6 and 12 months post-ACLR. We hypothesized that KFA and KEM would increase bilaterally; vGRF would increase in the ACLR limb but decrease in the uninvolved limb; and TSK-11 score would decrease from 6 to 12 months post-ACLR. The secondary purpose was to assess the relationship between percent change in TSK-11 score from 6 to 12 months post-ACLR and the percent change in KFA, KEM, and vGRF. We hypothesized that percent change in TSK-11 score would positively associate with percent change in KFA, KEM, and vGRF.

Methods: Twelve participants (50% female) enrolled in this prospective laboratory study. Data were collected at 6.0±0.2 months and 12.2±0.3 months post-ACLR. A 10-camera motion capture system interfaced with two embedded force plates were used to collect biomechanical data. A 30-cm box was positioned half the participant's height from the force plates. Participants jumped from the box to the force plates then jumped vertically for maximal height. Peak KFA (°), KEM (Nm) and vGRF (N) were identified between initial contact (vGRF>10 N) of the first landing and take-off (vGRF<10 N) of the vertical jump and averaged across 5 trials. Peak vGRF was normalized to body weight (xBW) and KEM was normalized to the product of body weight and height (xBW*height). Percent change was calculated as the difference between the 6-month and 12-month values divided by the 6-month value. Participants completed the TSK-11, an 11-item questionnaire with scores ranging from 11-44, for which higher scores indicate greater fear of movement and injury. TSK-11 scores >17 are considered high, while scores of >19 are associated with greater ACL injury risk. Separate 2x2 (Limb x Time) repeated measures ANOVA with partial η^2 effect sizes ($p\eta^2$) and Bonferroni Post Hoc test were used to assess differences in biomechanical variables. A repeated measures ANOVA was used to assess differences in TSK-11 score between time points. The relationship between percent change in TSK-11 and percent change in KFA, KEM and vGRF were assessed with Pearson Correlations (*a-priori* alpha 0.05).

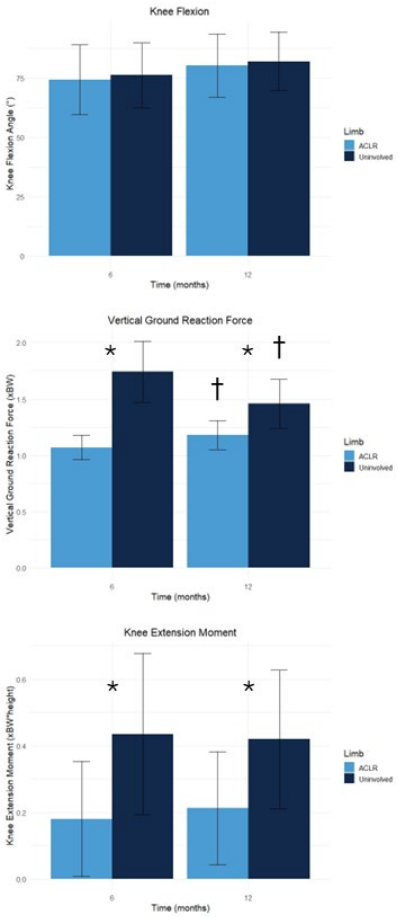

Figure 1. Drop vertical jump landing biomechanics. *Indicates significant between limb differences. †Indicates significant differences between 6 and 12 months post-ACLR.

Results & Discussion: Contrary to our hypothesis, KFA and KEM did not significantly increase from 6 to 12 months post-ACLR (Figure 1). At 6 months (p <0.001) and 12 months (p < 0.001), the uninvolved limb KEM was greater than that of the ACLR limb. Potentially, the ACLR limb was experiencing persistent quadriceps strength deficits, common in individuals with ACLR, and was unable to adequately dissipate eccentric loading during landing. Despite the lack of change in KFA and KEM, ACLR limb vGRF (p = 0.03) increased, while uninvolved limb vGRF decreased (p <0.001) from 6 to 12 months post-surgical. Notably, ACLR vGRF was lesser at 6 months (p < 0.001) and 12 months (p = 0.04) compared to the uninvolved limb. At 6 months post-ACLR, participants were off-loading the ACLR limb as protective mechanism, but regained more symmetrical loading 12 months post-ACLR. TSK-11 scores improved over time from 21.3±5.6 to 18.8±4.2 (p = 0.034, $p\eta^2$ = 0.347), but remained high (>17) at follow up indicating greater kinesiophiba and potentially higher risk of ACL injury. Unlike previous studies, percent change in TSK-11 did not associate with percent change in KFA (r = 0.231, p = 0.470), KEM (r = -0.040, p = 0.901), or vGRF (r = -0.237, p = 0.458). Based on these results, the magnitude of change in TSK-11 score, is not related to the magnitude of the change in landing biomechanics.

Significance: Despite improvement in landing biomechanics, TSK-11scores remained high (>17) 12 months post-ACLR. The percent change in TSK-11score did not associate with the percent change in landing biomechanics, whereas previous cross-sectional studies have reported a relationship between TSK-11 score and landing biomechanics.[2,3] Further research is warranted to determine whether the magnitude of the change in TSK-11score influences landing biomechanics following ACLR.

Acknowledgments: This study was supported by the National Institute of Arthritis and Musculoskeletal and Skin Diseases Award Number F32AR081708 and the Department of Defence Award Number W81XWH21C00490011582719.

References: [1] Paterno et al. *Sports Health.*2018;10(3); [2] Trigsted et al. *Knee Surgery, Sport Traumatol Arthrosc.*2018;26(12); [3]Noehren et al. *Orthop J Sport Med.*2017;5(7_suppl6). [4] Yu and Garret. *Br J Sports Med*.2007;41(suppl 1)

Alterations in Patellofemoral Cartilage Composition are not Associated with Quadriceps Size or Strength following ACL Reconstruction

McKenzie S. White[1*], Steven A. Garcia[1], Yuxi Pang[2], Claire M. Casey[1], Riann M. Palmieri-Smith[1], Lindsey K. Lepley[1]
[1]School of Kinesiology, University of Michigan; Ann Arbor, MI, USA
[2]Department of Diagnostic Imaging, St. Jude Children's Research Hospital; Memphis, TN, USA
*Corresponding author's email: mckwhite@umich.edu

Introduction: Persistent muscle weakness following anterior cruciate ligament reconstruction (ACLR) is thought to contribute to the increased prevalence of post-traumatic osteoarthritis (PTOA). However, studies between muscle weakness and PTOA have primarily used indirect measurements of joint health such as the Kellgren-Lawrence grading system and joint space narrowing. [1,2] Further work is needed to uncover the relationship between muscle strength and early cartilage changes that may occur prior to structural deterioration. $T_{1\rho}$ relaxation times from quantitative magnetic resonance imaging (MRI) provide a direct measure of proteoglycan, collagen orientation, and water content in the cartilage extracellular matrix. Increases in $T_{1\rho}$ are thought to indicate early PTOA-related degeneration. Previous data has shown vasti weakness is associated with changes in $T_{1\rho}$ 6 months after ACLR [3], but whether muscle weakness is linked with poorer cartilage health at further time points after surgery or if other clinical markers such as muscle size or self-reported function are associated with early alterations in cartilage composition remains unclear. Our main objectives were to I) characterize self-reported function, quadriceps size, strength, and cartilage composition utilizing $T_{1\rho}$ and II) determine the associations between self-reported function, quadriceps size, strength, and cartilage composition in those with a history of ACLR and in Controls.

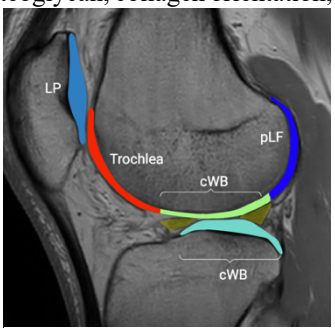

Figure 1. Representative Regions of Interest. Abbreviations: LP, lateral patella; cWB, combined weight bearing; pLF, posterior lateral femur

Methods: Twenty-four individuals with a primary ACLR via patella tendon autograft (male/female = 15/9, Age = 22.8 ± 3.6 years, body mass index = 23.2 ± 1.9 kg/m^2, time since surgery = 3.3 ± 0.9 years), and 24 healthy controls (male/female = 14/10, Age = 22.0 ± 3.1 years, body mass index = 23.3 ± 2.6 kg/m^2) underwent a single testing session. Patients completed self-reported function through the Knee Injury and Osteoarthritis Outcome Score (KOOS). Quadriceps strength was assessed on an isokinetic dynamometer during maximal isometric and isokinetic contractions. Quadriceps muscle volume and $T_{1\rho}$ were quantified in regions of interest (Figure 1) on a 3-Tesla MRI Philips Ingenia scanner. Independent t-tests compared KOOS scores between ACLR and Control subjects. Linear mixed effects models assessed (I) quadriceps muscle volume (II) strength and (III) $T_{1\rho}$ relaxation times between the ACLR, Contralateral, and Control Limbs. Linear regressions determined associations between quadriceps muscle volume, strength, and $T_{1\rho}$ in the ROI's and limbs that were found to be significant in linear mixed effects models.

Results & Discussion: The ACLR individuals scored significantly lower on KOOS symptoms, pain, quality of life, and function in sport and recreation ($p < 0.05$). The quadriceps were on average 7.6% smaller in the ACLR limbs than the Contralateral limbs ($p < 0.001$). No differences in peak isometric strength ($p = 0.237$) or rate of torque development ($p = 0.234$) were found between limbs. ACLR limbs had significantly increased $T_{1\rho}$ in the medial and lateral patella (estimate = 5.87-10.20, t = 2.43-3.84, p = 0.001-0.045) compared to both the Contralateral and Control limbs (Figure 2A/2B) and in the trochlea (estimate = 5.19, t = 2.52, p = 0.037) compared to the Control limbs (Figure 2C). No between limb differences were found in the weight bearing or posterior regions of the femur or tibia ($p > 0.05$). Quadriceps muscle volume and strength in ACLR limbs were not associated with $T_{1\rho}$ in any region of interest (p =0.254-0.921). KOOS pain was positively associated with $T_{1\rho}$ in the trochlea in the ACLR limbs (estimate = 0.74, t = 2.19, p = 0.04).

Significance: Overall, cartilage alterations were largely localized to patellofemoral regions in ACLR limbs and patients reporting more pain symptoms exhibited longer $T_{1\rho}$ relaxation times. These observations may reflect an ongoing process of cartilage matrix remodeling or degradation that may progress irrespective of muscle size and strength. These results contribute to our understanding of factors that may precipitate early joint degeneration following ACLR.

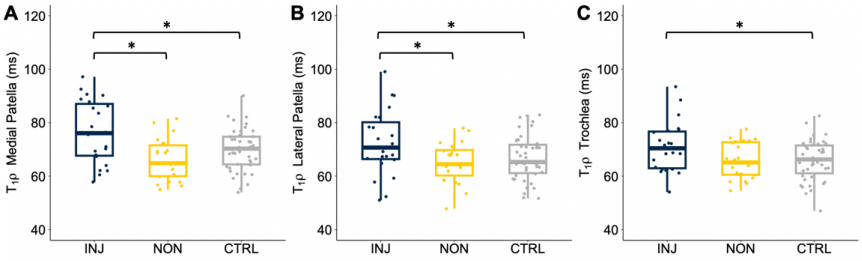

Figure 2. Comparison of $T_{1\rho}$ in the Patella and Femoral Trochlea in the ACLR, Contralateral, and Control limbs. $T_{1\rho}$ relaxation times of the medial and lateral patella in the ACLR limbs showed a significant increase of 108-116% (or 5.7-10.3 m/s) compared to the Contralateral and Control limbs (p = 0.001-0.045). The $T_{1\rho}$ relaxation times of the femoral trochlea in the ACLR limbs showed a significant increase of 108% (or 5.0 m/s) compared to the Control limbs (p = 0.037) and was trending toward significance when compared to the Contralateral limbs (p = 0.056).

References: [1] Keays et al (2010), Am J Sports Med, 38(3); [2] Tourville et al. (2014), Am J Sports Med, 42(2); [3] Pietrosimone et al (2019), Knee Surg Sports Traumatol Arthrosc, 27(8).

Pain isn't everything: Pain pressure threshold does not correlate with graft-site characteristics following BPTB autograft

Claudia Kacmarcik PT, DPT[1], Naoaki Ito, PT, DPT, PhD[2] Karin Grävare Silbernagel, PT, PhD, ATC[1]
[1]University of Delaware, Newark, DE; [2]University of Wisconsin-Madison, Madison, WI
kgs@udel.edu

Introduction: During anterior cruciate ligament reconstruction (ACLR) using a bone-patellar tendon-bone (BPTB) autograft, the central third of the patellar tendon is harvested. Individuals with this graft type have increased intensity and duration of anterior knee pain, compared to those with alternative graft types [1]. Following graft harvest, the patellar tendon exhibits characteristics similar to what has been described after Achilles tendon rupture [2], including early formation of a large tendon callus followed by remodeling and a decrease in tendon size over time [3]. One month after graft harvest, larger patellar tendon CSA is related to stronger knee extensor torque [4]; however, the relationship between structural changes and pain following patellar tendon graft harvest is not known. The purpose of this investigation was to assess the relationship between donor-site pain-pressure threshold (PPT) and patellar tendon structure including cross-sectional area (CSA), thickness, shear modulus, and viscosity.

Methods: Thirty-four participants (15 females | 19 males), were included in this secondary analysis of a prospective cohort study assessing graft-site recovery at 1, 3-4, and 6-9 months following ACLR. (age [mean ± SD] = 22.6 ± 7.2 years, BMI = 25.0 ± 3.5, IKDC (International Knee Documentation Committee subjective knee form) at 1 month (45.1 ± 11.8), 3-4 months (65.5 ± 9.0), and 6-9 months (79.9 ± 8.2)). Patellar tendon thickness and CSA were captured in supine with 30º of knee flexion using B-mode ultrasound (GE Healthcare; LOGIQ e, Chicago, IL). PPT was measured with a pressure algometer (SBMedic) at 50% length of the patellar tendon in the same position. Continuous shear wave elastography (cSWE) was performed with participants seated in 90º of hip and knee flexion. cSWE measures tendon shear modulus (kPa) and viscosity (Pa-s) using the Voigt model for viscoelasticity. Shear waves of 11 different frequencies are propagated through the quadriceps tendon by an external actuator (Minshaker Type 4810, Bruel and Kjaer, Norcross, GA, USA) and measured at the patellar tendon using high-framerate ultrasound to perform calculations (Ultrasonix, Vancouver, BC, Canada). Limb symmetry index (LSI) was calculated for all measures ([involved/uninvolved] × 100), and Pearson correlations were computed to assess the relationship between symmetry in PPT and structure variables (Table 1).

	1 Month		3-4 Months		6-9 Months	
Variable	**Mean**	**SD**	**Mean**	**SD**	**Mean**	**SD**
Time from surgery (months)	1.33	0.29	3.43	0.26	6.76	0.67
UN PPT (kPa)	951.64	441.81	850.65	344.37	754.99	196.72
IN PPT (kPa)	581.62	245.89	622.65	217.31	574.72	202.20
UN Central Thickness (cm)	0.42	0.10	0.42	0.10	0.43	0.10
IN Central Thickness (cm)	0.90	0.19	0.83	0.16	0.80	0.19
UN CSA (cm^2)	0.88	0.15	0.91	0.18	0.92	0.17
IN CSA (cm^2)	1.80	0.53	1.73	0.50	1.67	0.55
UN Central Shear Modulus (kPa)	62.38	16.29	61.32	18.66	63.91	18.41
IN Central Shear Modulus (kPa)	75.28	23.17	59.75	18.52	61.59	20.02
UN Central Viscosity (Pa-s)	22.54	7.45	22.72	5.64	23.76	6.25
IN Central Viscosity (Pa-s)	24.48	7.22	23.35	5.84	19.85	6.13

Table 1: Uninvolved (UN) and involved (IN) limb tendon pain pressure threshold (PPT), and structure. (SD = standard deviation)

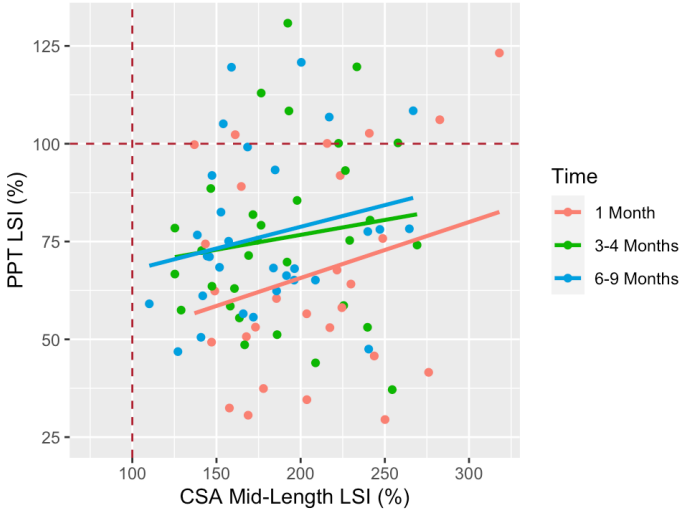

Figure 1: Scatter plot with trend lines of PPT LSI and CSA LSI at 50% tendon length at each time point. Dotted lines represent 100% LSI with values below and to the right indicating higher pain sensitivity and larger CSA in the involved (surgical) versus uninvolved limb, respectively.

Results and Discussion: PPT LSI was not correlated with tendon structure LSIs at any time point [R = -0.37 – 0.33; p = 0.056 – 0.977], despite PPT LSI values indicating higher surgical-limb pain pressure sensitivity (lower PPT) throughout the course of rehabilitation (Fig. 1). These findings demonstrate that symmetry in tendon pain sensitivity may not reflect symmetry in structural recovery after BPTB autograft harvest. A limitation of this study is the spread of raw PPT values, prompting the use of LSIs (Table 1). A larger sample size may enable the use of raw values and generation of a more robust model considering the impact of additional demographic factors such as body mass index or patient reported outcomes.

Significance: These results indicate that clinicians should not rely on patellar tendon pain as a meaningful metric for assessing graft-site recovery in patients with BPTB autograft.

References: [1] Marques et al. (2020), *Orthop J Sports Med*; [2] Rendek et al. (2022), *AJSM, 50*(12); [3] Ito et al. (2024), *JOR;* [4] Ito et al. (2024), *KSSTA*

ESTIMATING IN VIVO MUSCLE SHEAR MODULI USING MICRO-INDENTATION

Daniel Ludvig[1,4], Qifeng Wang[2], Ridhi Sahani[1,4], Kenneth R. Shull[2], Eric J. Perreault[1,3,4]
Departments of [1]Biomedical Engineering, [2]Material Science and Engineering, [3]Physical Medicine and Rehabilitation, Northwestern University, Evanston, IL [4]Shirley Ryan AbilityLab, Chicago, IL,
*Corresponding author's email: daniel.ludvig@northwestern.edu

Introduction: The mechanical properties of skeletal muscle are essential for generating the forces required for human movement. While tensile properties have been extensively studied in skeletal muscle, few have characterized shear properties, and none have done so *in vivo.* The shear modulus of skeletal muscle is highly relevant to force transmission and function, as shearing between muscle fibers and the surrounding extracellular matrix is implicated in lateral force transmission [1,2] and shearing is a common mode of muscle injury [3]. Studies in which shear properties are characterized are limited [4–6] to *ex vivo* conditions, as shear loading is difficult to implement experimentally on an intact muscle. To our knowledge shear modulus has not been previously characterized in active muscle, a more functional state where the mechanical properties of the muscle are very different. The objective of this study was to develop a methodology that could quantify shear modulus in the direction parallel and perpendicular to muscle fibers in an *in vivo* muscle and test the validity of this method in a gel phantom replicating the transversely isotropic material properties of skeletal muscle.

Methods: To solve the challenge of measuring shear properties of an intact and active muscle we used micro-indentation [7] with a highly asymmetric rectangular blade indenter. To assess the viability of this method we 1) quantified the accuracy of the micro-indentation on custom made organogel phantoms in which shear moduli could be directly measured with rheometery and 2) tested the feasibility on *in vivo* cat soleus muscle at two muscle lengths under both passive and active conditions (Fig. 1). A rectangular blade with a width of 0.14 mm and a length of 20 mm was used for indentation and was oriented either parallel or perpendicular to muscle fibers/direction of transverse isotropy. The indenter applied an indentation that combined linear (2 mm at 2 mm/s) and sinusoidal indentation (0.2 mm at 10 Hz). The slow linear indentation was used to compute the static mechanical properties (the results shown here), but future work will also look at the dynamic mechanical properties that can be estimated using the sinusoidal indentation component. Shear moduli in both directions were computed by optimizing a transversely isotropic finite element model given the forces resulting from the indentation in both directions.

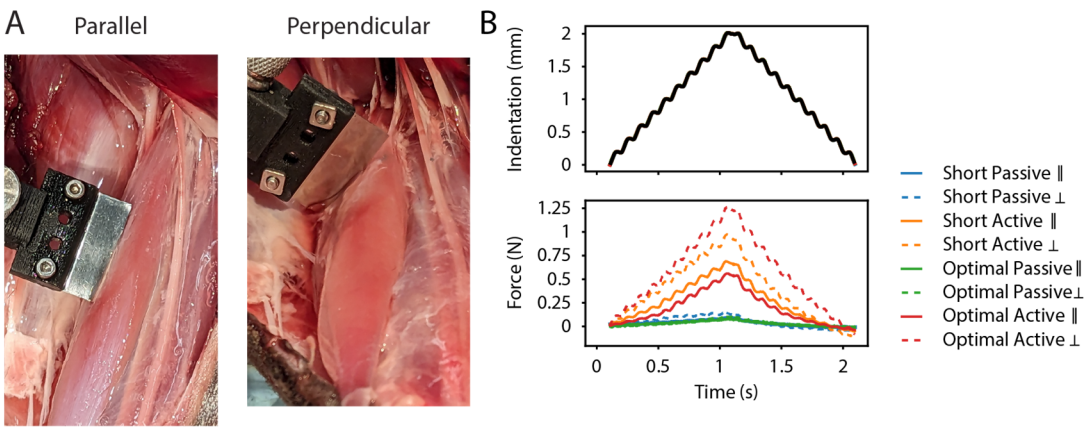

Figure 1. A) Micro-indentation of cat soleus muscle oriented both parallel and perpendicular to the muscle fibers. B) Micro-indentation displacement, (top) and force (bottom) of live cat soleus muscle with indenter parallel (solid lines) and perpendicular (dashed lines) to the muscle fiber direction at optimal (length where active force is maximal) and short (length where active force is 50% maximal) lengths when the muscle is passive and active.

Results & Discussion: The micro-indentation method was able to generate shear moduli estimates within 10% of the values estimated with traditional approaches in the gel phantom. The calculated shear moduli of the gel phantom using the micro-indentation method were 5.0 kPA (parallel) and 5.7 kPA (perpendicular) which closely matched the shear moduli computed using a rheometer (parallel: 4.9 kPa; perpendicular 5.2 kPa). We were able to successfully indent the cat soleus muscle during both active and passive conditions (Fig. 1). As expected, the resistance to indentation was much greater when the muscle was active compared to when the muscle was passive. The resistance to indentation was greater when the indenter was perpendicular to the muscle fibers as compared to when it was parallel.

Significance: This method will allow for *in vivo* estimation of two-dimensional shear moduli for the first time. Given the vast difference in Young's moduli between passive and active conditions, it is likely that the shear moduli also drastically differ between active and passive conditions (which agrees with our single muscle measure presented here). Quantitative estimates of shear moduli during active conditions will be key to developing more accurate biomechanical models of muscle and interpreting the metrics provided by shear-wave elastography.

Acknowledgements: NIH R01 AR071162

References: [1] Street (1983), *J Cell Physiol* 114; [2] Sharafi & Blemker (2011), *J Biomech* 44; [3] Järvinen et al. (2014), *Muscles Ligaments Tendons* 3; [4] Morrow et al (2010) *J Mech Behav Biomed Mater* 3; [5] Hashemi et al (2020) *Proc Inst Mech Eng* 234; [6] Moreira & Nunes (2022) *J Braz Soc Mech Sci Eng* 44 [7] Li et al. (2006*) J. Biomed. Mater. Res.* 80B

TENDON SLACK LENGTH IS A MODELING MISNOMER: THE "ANATOMICAL" PARAMETERS CALCULATED DO NOT REFLECT ANATOMICAL REALITY

Richard L. Lieber[1], Zheng Wang[2], Benjamin I. Binder-Markey[3], Lomas Persad[2], Alexander Y. Shin[2], *Kenton R. Kaufman[2]

1 Shirley Ryan Ability Lab, Chicago, IL, USA.

2 Department of Orthopedic Surgery, Mayo Clinic, Rochester, MN, USA.

3 Departments of Physical Therapy and Biomedical Engineering, Drexel University, Philadelphia, PA, USA

*Correspondence: rlieber@sralab.org

Introduction: Musculoskeletal modeling of joint moments requires knowledge of muscle, tendon and joint properties. One component in this chain is the length of tendon between the muscle fibers and their insertions. In his classic paper, Felix Zajac coined the term "tendon slack length" as an anatomical term that reflected the length of tendon in series with the muscle fibers that had a stress-strain relationship whereby, at peak muscle force, tendon strain was 3.3% [1]. This term served both to shift the muscle length-tension relationship and to allow appropriate amounts of sarcomere shortening. However, with the advent of advanced computing, this value has lost its anatomical meaning, and models are rarely, if ever, validated against actual anatomical values [2]. Here, we take advantage of the opportunity to directly measure the tendon length in a slack human gracilis muscle [3], as well as other anatomical parameters, and compare these measured values to the modeled parameters.

Methods: Human gracilis muscles were harvested during muscle transfer surgery in brachial plexus injury patients (n=16) [3]. Active muscle force was measured at four joint configurations using a buckle transducer and electrical stimulation [4]. After the gracilis was excised from the body, it was laid untethered onto a sterile towel (i.e., "slack") and resting muscle-tendon unit (MTU) length measured. The muscle experimental optimal fiber length was calculated based on the full width at half maximum of the active muscle length-tension curve [5]. To match the current definition of "tendon slack length," experimental tendon slack length was calculated as resting MTU (measured directly) minus optimal fiber length determined experimentally. Modeling parameters used were from the gracilis muscle model published by Hamner *et al.* [6] in the OpenSim 4.4 software package, scaled to each subject's body segment length. Experimental anatomical parameters were compared to modeled parameters using a paired t-test. Significance level (α) was set to $p<0.05$

Results & Discussion: All three measured anatomical values were significantly different compared to their modeled counterparts (Fig. 1). Modeled MTU length exceeded measured MTU length by ~50% (Fig. 1A) while modeled optimal fiber length exceeded measured optimal fiber length by over 100% (Fig. 1C). Modeled "tendon slack length" was ~50% of the actual experimental value (Fig. 1B). All differences were highly significant ($p<0.01$) and physiological meaningful. Interestingly, the modeling software produced a reasonable fit to the experimental data but did so with muscle and tendon parameters that were vastly different from those obtained experimentally. These data demonstrate that, given the current state-of-the-art in biomechanical modeling, it is possible to fit experimental data using parameters that bear little resemblance to the actual underlying anatomy. Thus, we opine that the term "tendon slack length" as used in musculoskeletal modeling is a misnomer that implies the user has some idea of the length of the tendon in the muscle-tendon unit.

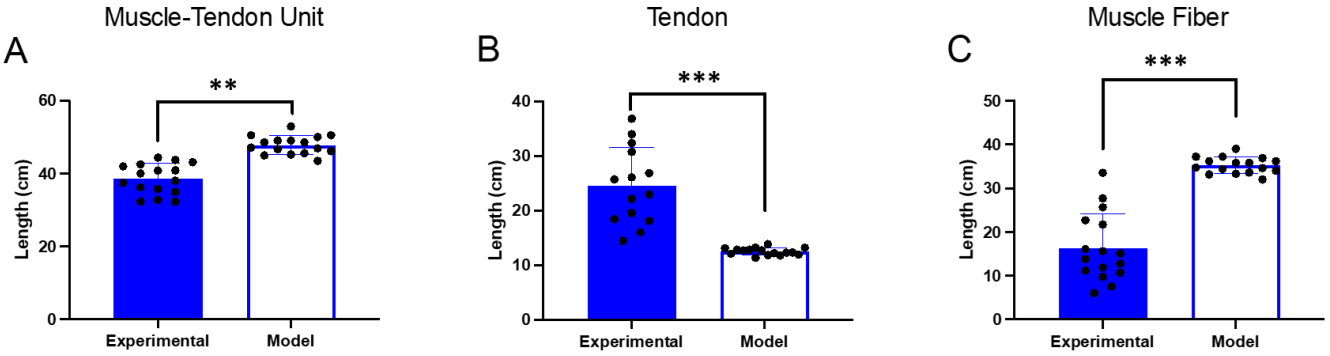

FIGURE 1: (A) Muscle-tendon unit length measured experimentally (filled blue bar) and modeled (open bar). (B) Tendon length measured experimentally (filled blue bar) and modeled as "tendon slack length" (open bar). (C) Optimal muscle fiber length calculated from the experimental length-tension curve (filled blue bar) and modeled (open bar). Data for each bar represent mean±SD (n=16 patients). Statistical comparison symbols: **-$p<0.01$; ***-$p<0.001$

Significance: The fact that a good fit to experimental data can be obtained from biomechanical modeling software despite the fact that the underlying anatomical parameters are nowhere near the actual measured values is concerning for musculoskeletal modeling. This experiment shows that even some of the simplest parameters are very poorly determined by current modeling software.

Acknowledgments: This work was supported by VA funding 1 I01 RX002462 and Research Career Scientist Award Number IK6 RX003351 from the United States (U.S.) Department of Veterans Affairs Rehabilitation R&D (Rehab RD) Service.

References:

[1] Zajac (1989), *CRC Crit Rev Biomed Eng* **17**:359. [2] Hicks *et al.* (2015) *J Biomech Eng* doi: 10.1115/1.4029304. [3] Binder-Markey *et al.* (2023), *J Physiol* **601**:1817. [4] Persad *et al.* (2022) *Sci Report* 12:1. [5] Winters *et al.* (2011), *J Biomech* **44**:109. [6] Hamner *et al.* (2010), *J Biomech* **43**:2709.

CHANGES IN THE PASSIVE MECHANICS OF SKELETAL MUSCLE FOLLOWING BOTULINUM TOXIN TYPE A INJECTION

Timothy McGinley[1] and Benjamin I Binder-Markey[1,2]
[1]School of Biomedical Engineering, Science and Health Systems & [2]Department of Physical Therapy & Rehabilitation Sciences, Drexel University, Philadelphia Pa
Corresponding email: tm3292@drexel.edu

Introduction: Following a stroke, a decrease in descending neuromuscular drive results in muscle weakness, poor motor control, and motor neuron hyperexcitability. The motor neuron hyperexcitability results in persistent signals to the muscle, leading to muscle hyperactivity, commonly referred to as spasticity. To prevent this muscle hyperactivity and increase physical function, Botulinum Neurotoxin Type A (BoNT-A) is used as a treatment. The usage of BoNT-A causes chemical denervation at the neuromuscular junctions that partially paralyzes the muscle decreasing spasticity, increasing the range of motion, and causing muscle atrophy [4]. We found that in individuals with chronic stroke who received BoNT-A demonstrated long-term increases in passive muscle stiffness [1]. Whereas in those individuals who never received BoNT-A, the passive skeletal muscle mechanics remained unaffected following a stroke [1]. However, the timeline for the progression of increased passive muscle mechanics remains unknown. Therefore, the purpose of this study was to begin to understand the timeline of how BoNT-A affects skeletal muscle's passive mechanical properties using a pre-clinical animal model. We hypothesize that we will observe higher passive forces and stresses in skeletal muscle that increase with time.

Methods: Passive mechanical characteristics of BoNT-A injected, and non-injected tibialis anterior (TA) muscles were collected from 20 male and 20 female Sprague-Dawley rats over the course of a 6-week period. Rats aged 13 to 15 weeks were injected with 2 units/kg of BoNT-A in a single TA, and contralateral non-injected TA served as the control. Bilateral TA muscles were dissected and tested at 1-, 2-, 4-, 5-, & 6-weeks post-injection. The muscles were dissected from distal to proximal insertions, placed in a physiological bath, and mechanically tested. For mechanical testing, the samples were fastened to a 5N force transducer and muscle slack length was determined. Each muscle was lengthened in ~5% whole muscle strain increments from 0%-50% in a step-wise function with a 3-minute hold at each strain. Force and displacement at the end of each hold were recorded. Following testing, we recorded the sample's muscle mass. Muscle passive forces were normalized to physiological cross-sectional area (PCSA) [3]. The force-strain data and normalized passive stress-strain data were fit to a non-linear regression due to the nature of whole muscle mechanical data [2]. The normalized stiffness and mass were compared across injected and non-injected samples.

Results & Discussion: Muscles injected with BoNT-A demonstrated significantly lower mass post-testing (Table 1). Normalized stress-strain curves showed significantly higher stress profiles in the affected samples (Fig. 1). This difference increased with time, becoming the largest at 6 weeks post-injection.

However, when comparing the force vs. strain curves, no significant differences were seen between the injected and non-injected muscles. Thus, in these early time points, within the first month and a half following BoNT-A injections, the increase in muscle stiffness post-injection is likely a result of decreased mass and PCSA due to muscle atrophy and contractile tissue rather than an increase in connective tissue.

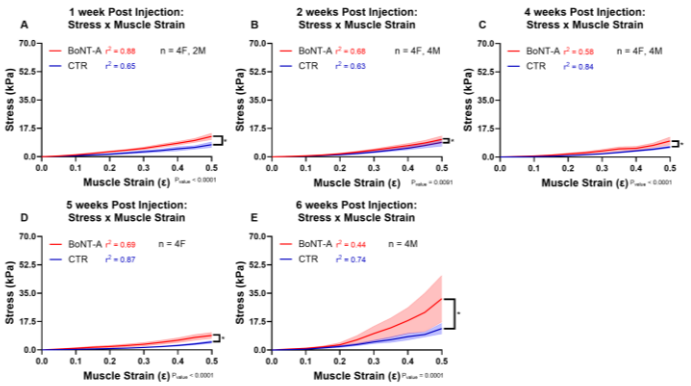

Figure 1: Normalized stress-strain curves for BoNT-A injected (red) and contralateral (CTR) (blue) of Tibailis Anterior at A) 1-week, B) 2-week, C) 4-week, D)5-week, & E) 6-week post injection. Data shown as averages±SD. Overall r^2 for each condition. * *and bracket indicate p<0.05*

Significance: Within the first 6-weeks post BoNT-A injection, the normalized passive mechanics of the tibialis anterior whole muscle was altered. In these early time points following the injection, the muscles demonstrated a reduction in mass and PSCA, likely resulting in an increase in passive muscle stress but not of passive muscle force. Future studies will explore the long-term effects of BoNT-A by increasing the time-period post-injection. Additionally, collagen content analysis will be performed to determine the changes in connective tissue content over time. Understanding the long-term effects of BoNT-A will aid in determining the optimal treatment of spastic muscles, maximizing these individuals' physical function and quality of life.

*Table 1: Averaged physiological properties of BoNT-A injected and contralateral muscle *=p<0.05 compared to contralateral muscle*

	Mass (mg)		
	Female		
	BoNT-A	Contralateral	% Difference
1WK	542.78 ± 21.98*	681.93 ± 42.94	-20%
2WK	371.03 ± 29.46*	669.37 ± 35.17	-45%
4WK	267.78 ± 06.16*	694.78 ± 03.95	-61%
5WK	266.73 ± 06.02*	569.18 ± 19.77	-53%
6WK	—		
	Male		
	BoNT-A	Contralateral	% Difference
1WK	672.33 ± 63.82*	907.73 ± 91.16	-26%
2WK	554.88 ± 72.47*	1013.2 ± 119.2	-45%
4WK	532.03 ± 13.43*	1182.2 ± 41.86	-55%
5WK	—		
6WK	539.5 ± 29.56*	1296.75 ± 44.55	-58%

Acknowledgments: Individual Researcher Biomedical Award from The Hartwell Foundation and Foundation for Physical Therapy Research

References:

[1] Binder-Markey et al. (2021), *Front Neurol* 12; [2] Binder-Markey et al. (2021), *J Biomech* 129; [3] Ward et al. (2020), *Front Physiol* 11; [4] Dutta et al. (2016), *J Maxillofac Surg* 7.

REPLICATING *IN VIVO* MUSCLE MECHANICS IN CONTROLLED *EX VIVO* EXPERIMENTS OF SEVERAL SPECIES AND MUSCLES

Caitlin Bemis[1,2*], Monica Daley[1], and Kiisa Nishikawa[2]
[1]Department of Ecology and Evolutionary Biology, University of California, Irvine, CA
[2]Department of Biological Sciences, Northern Arizona University, Flagstaff, AZ
*Corresponding author's email: caitlin@iblackburn.com

Introduction: Muscles have been viewed as motors producing force depending on their activation, strain, and velocity under isometric and isotonic conditions [1]. However, understanding and predicting intrinsic muscle mechanics (i.e., activation-dependent force response of muscles to strain and velocity transients), remains challenging. These challenges persist in part because the current paradigm of muscle function – the sliding filament and swinging cross bridge theory – is commonly represented by 'Hill-type' muscle models that predict force depending on quasi-static isometric force-length and isotonic force-velocity relationships [2]. 'Hill-type' model parameters do not capture the mechanical effects that time-varying loads impose on muscle force and work during dynamic *in vivo* movements[3,4]. To understand the contributions of intrinsic muscle properties to *in vivo* force production, elucidation of muscle's *dynamic* force-length and force-velocity relationships are required.

Traditional work loop techniques drive muscles through predefined strain trajectories, frequencies, and stimulation patterns and measure the resulting force, work, and power output[5]. However, muscle force, work and power output are determined not only by neural activation, but also by interactions between strain and activation. Load transitions can have complex effects on strain dynamics, muscle gearing and deformation[6]. Here we present a method to investigate unconstrained time varying force production, using *in vivo* muscle fascicle length and timing of activation, in controlled *ex vivo* experiments with a well characterized *"avatar"* muscle, mouse extensor digitorum longus (EDL).

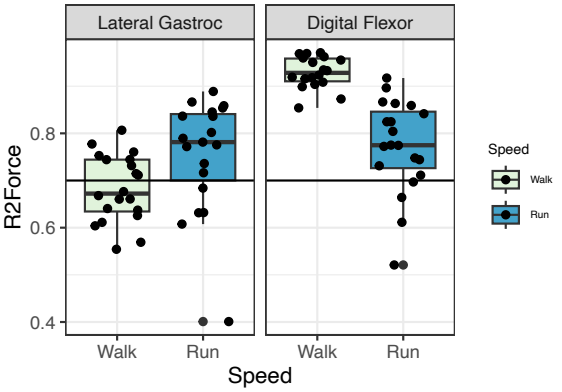

Figure 1: R^2 values comparing time-varying force between *in vivo* guinea fowl and *ex vivo* mouse muscles. Both lateral gastrocnemius and digital flexor strain trajectories comparisons are shown at both speeds. Individual stretch-shortening cycles R^2 values of mouse EDL shown. Black line average results from models that use "Hill-type" models to predict *in vivo* time-varying force.

Methods: One stride was selected from guinea fowl *in vivo* fascicle length trajectories of lateral gastrocnemius (LG) and digital flexor-IV (DF-IV)[7] muscles during walking and running on a level treadmill. *In vivo* length trajectories and timing of activation were used as length and stimulation inputs during *ex vivo* work loops using mouse EDL (n = 156). Amplitudes of *ex vivo* length trajectories were scaled to match *in vivo* passive force rise. For each strain trajectory at both speeds, time varying force was measured and compared to *in vivo* production. Both *in vivo* and *ex vivo* time-varying force were scaled to compare to account for differences in muscle physiological cross-sectional area (PCSA).

Results & Discussion: Our *ex vivo* "avatar" work loop experiments accurately replicated force production and work output in several conditions guinea fowl muscles at varying speeds. *Ex vivo* experiments using *in vivo* guinea fowl length trajectories and timing of stimulation resulted in accurate R^2 (mean $R^2 = 0.61 – 0.97$) for both LG and DF length changes during walk and run (Figure 1). Results of "*avatar*" experiments demonstrate that viscoelastic responses to deformation from applied loads can be represented by strain and velocity transients in fasicles. These transients have large effects on muscle force production[6]. Several studies using Hill-type models to predict *in vivo* time varying force[8–10] results were averaged and compared directly to R^2 values produced in our physical *"avatar"* muscle model (Figure 1). Our "*avatar*" experiments outperform several Hill-type models when replicating *in vivo* time-varying force with varying species and muscles, especially as stride frequency increases.

Significance: The results of this study support an emerging new perspective that considers muscles not just as motors that produce force in response to activation, but also as actively tunable materials in which force arises from resistance to deformation by applied loads [6]. This study demonstrates that strain trajectories and stimulation patterns derived from *in vivo* measurements and imposed on *ex vivo* mouse EDL muscles accurately represent time-varying force production of *in vivo* guinea fowl LG and DF. Our results are consistent with the idea that muscles rely on intrinsic properties to produce time-varying force and regulate work output [4–6] that are tuned by strain and stimulation interactions [6]. Additionally, we demonstrate that the *avatar* method can capture the complexity of time-varying force production during *in vivo* locomotion in muscles with large variation in compliance and muscle-tendon architecture.

Acknowledgments: Funding secured by Monica Daley and Kiisa Nishikawa from NSF (IOS-2016049 and DBI-2021832)

References: [1] Seth et al., (2011) *Procedia IUTAM* 2 [2] Ahn (2012) *J. Exp Bio* 215 [3] Biewener & Daley (2007) *J. Exp. Biol.* 210. [4] Sponberg & Sawicki (2023) *J. Exp. Biol.* 226 [5] Josephson (1999) *J. Exp. Biol* 202 [6] Rice et al., (2023) *J. Exp. Biol* 226 [7] Daley & Biewener (2011) *Phil. Trans. R. Soc* 366 [8] Wakeling et al., (2021) *J. Exp Biol* 117 [9] Dick et al., (2017) *J. Exp. Biol.* 220 [10] Lee et al., (2013) *J. Exp. Biol.* 46

THE LESS-AFFECTED SIDE IN SPASTIC HEMIPLEGIA: IS IT THE SAME AS TYPICALLY DEVELOPING? A STUDY OF MUSCLE PROPERTIES AND FUNCTION

Rachel L. Lenhart[1], Diego Caban-Rivera[2], Chris Church[1], Curtis Johnson[1], Arianna Trionfo[1], M. Wade Shrader[1], Jason J. Howard[1]
[1]Nemours Children's Hospital, Wilmington, Delaware
[2]University of Delaware, Newark, Delaware
*Corresponding author's email: rachellenhart@gmail.com

Introduction: Muscle anatomy and function in unilateral cerebral palsy (CP) are known to be altered in the more affected (MA) lower extremity. The contralateral less-affected (LA) limb is thought to function as in typically developing (TD) children, but it is unclear if this holds true. The objective of this study was to use magnetic resonance elastography (MRE) and physical testing to determine if LA limbs in spastic hemiplegia have similar anatomic and functional relationships compared to TD children.

Methods: Children with spastic hemiplegia, GMFCS I or II, with no spasticity-altering injections in the previous 6 months, and TD children, aged 5-18 years, were recruited from a tertiary level children's hospital. Exclusion criteria were prior lower extremity fractures or surgery. Shear wave modulus (stiffness) and anatomic characteristics [cross sectional area (CSA), fat fraction], were determined with MRE and standard MR of the gastrocnemius and soleus for dominant TD and LA CP limbs, respectively. Ankle dorsiflexion (DF, Silfverskiöld test) by goniometry and plantarflexion (PF) force by dynamometer were measured by a subspecialized physical therapist from our gait laboratory. Student t-tests were used to compare MRE/MR measures between groups. Regression equations were used to correlate MRE/MR measures to force and DF range.

Results & Discussion: 11 children with hemiplegic CP [mean age 11 (range 5-17) years] and 15 TD children [13 (5-18) years] were included. TD limbs had similar DF range to LA limbs in CP [DF with knee flexed mean(±SD) degrees: 15(6) vs 15(8), p=0.85; DF with knee extended: 9(4) vs 6(6), p=0.11]. TD children had greater PF force compared to the LA limb in CP [35.8(14.8) vs 24.9(9) kgf, p=0.04], despite no significant difference in CSA for the gastrocnemius [7.79(4.01) vs 6.47(2.63) cm2, p=0.32] or soleus [13.35(6.38) vs 13.52(4.20), p=0.93] between groups. A robust correlation existed between PF force and CSA for TD limbs (R2=0.66, p<0.001) which did not exist for LA limbs in CP (R2=0.007, p=0.8). A weak but statistically significant correlation existed between TD soleus stiffness and DF with knee flexed (R2=0.28, p=0.04) that was not found for LA limbs in CP (R2=0.03, p=0.58). There was no relationship between gastrocnemius stiffness and DF with knee extended in either group (TD R2=0.05, p=0.39; LA R2=0.001, p=0.91).

Significance: Despite similar ankle range of motion and calf CSA, LA limbs in CP exhibited decreased PF force compared to TD limbs. Unlike TD limbs, force was also not correlated to CSA for LA limbs in CP. These findings suggest that the LA limb in CP should not be considered typically functioning, with possible explanations rooted in differences in motor control and/or intrinsic muscle properties (e.g., DNA methylation abnormalities, sarcomeric dysfunction), requiring further study.

Acknowledgments: Funding from ACCEL DE-CTR pilot grant under NIH U54-GM104941.

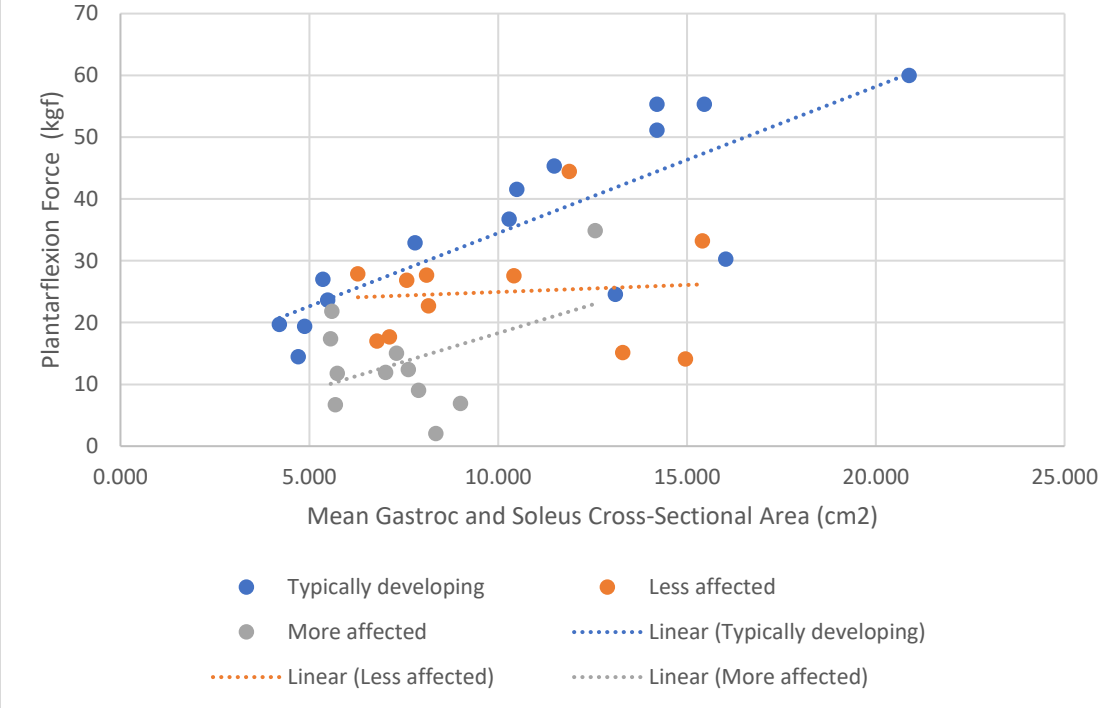

Figure: Relationship of ankle plantarflexion force to mean gastrocnemius and soleus cross-sectional area. Note the positive relationship for typically developing limbs (blue) vs less affected limbs in CP (orange). The more affected side is also represented (grey).

Do muscle moment arms adapt to chronic limb loading during growth?

Roberto Castro Jr.[1*], Kavya Katugam-Dechene[1], Talayah Johnson[1], Timothy Ryan[2], Stephen J. Piazza[1], Jonas Rubenson[1]

[1]Dept. of Kinesiology, The Pennsylvania State University, University Park, PA, USA
[2]Dept. of Anthropology, The Pennsylvania State University, University Park, PA, USA
*Email: CastroRoberto@psu.edu

Introduction:

A muscle's moment arm is one of the most important determinants of its function in movement. For example, Effective Mechanical Advantage (EMA; the ratio of the muscle moment arm to the moment arm of the applied load), and it's inverse, the Gear Ratio, have been used to explain a broad range of performance characteristics such as the energetics of walking and running and the ability to accelerate the body center of mass [1,2]. Although much is known about muscle tissue adaptation to load stimulus, whether moment arms are also plastic remains largely unknown. This is an important question, not only for understanding the basic biology of muscle, but also because a lack of physical activity in humans, in particular in growing children, may present a risk to musculoskeletal health. To overcome the practical and ethical limitations of studying human participants, we examined this question in an avian bipedal model (guinea fowl; *Numida meleagris*). Previously we found indication that guinea fowl subjected to high-acceleration training during growth presented with a larger Achilles tendon moment arm [3]. To test developmental plasticity of muscle moment arms more precisely, we subjected animals to a more pronounced chronic limb loading stimulus that targeted a single ankle flexor muscle, the *tibialis cranialis* (TC). Based on our pervious observations, we hypothesized that this load stimulus would likewise result in a larger muscle moment arm.

Methods:

Twenty guinea fowl were obtained as day-old keets and randomly assigned to a control group (CON; n=10) and a limb loaded group (LL; n = 10). From 2 wks to 16 wks of age, LL animals' tarsometatarsus were unilaterally loaded with a mass equal to 3.5% body mass. All animals underwent 20 minutes running training 3x/wk. Animals were euthanized at 16wks of age. The TC moment arm was measured using the tendon travel method. Limb specimens were secured using two Lowman bone clamps (Fig.1). A cluster of four retroreflective markers were fastened in the femur, tibiotarsus and tarsometatarsus segments using bone pins (Fig.1) and tracked using a 6-camera motion analysis system (Kestrel 300; MAC). A constant force (10N) linear transducer (LVDT) was connected to the TC tendon via 3.0 monofilament suture to measure tendon travel. For each limb (loaded and unloaded limbs) the ankle joint was cycled through its range of motion five times while simultaneously recording limb motion and tendon travel (d). A combination of static and dynamic trials was used to establish anatomical coordinate systems used to compute ankle joint angles (θ). Moment arm was computed as over the range of ankle angles from $^{\Delta d}/_{\Delta \theta}$. To validate our system, a phantom limb was 3-D printed with known moment arm dimensions. Moment arm differences were detected at a resolution of 0.2mm.

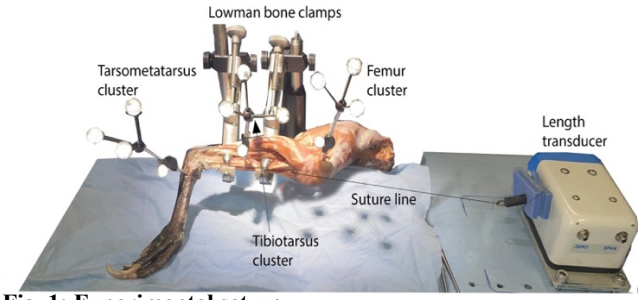

Fig. 1: Experimental set-up.

Results & Discussion:

To date, we have performed preliminary analyses on two specimens. In both specimens, we observed an increase in muscle moment arm with increasing ankle flexion (Fig. 2). The average moment arms (across joint angles) did not differ more than one mm between specimens (the average moment arm in the chronic loaded limbs were 11.88mm and 12.19, and in the unloaded limbs were 10.57 and 11.52). In both specimens, we found the average moment arm was larger in the chronically loaded limb (by 11.0 and 5.5 percent). The larger moment arm in the chronically loaded limbs is suggestive of developmental plasticity and agrees with our hypothesis. In our previous study on the same experimental animals, we found that the TC fiber architecture adapts in ways that can decrease fiber velocity (by alleviating force-velocity constraints) and thus may improve muscle work capacity. Combined, these and our current data suggest a mechanism by which the moment arm responds plastically to increases torque capacity while changes in muscle architecture modulate fiber velocity. We note this is highly speculative, especially considering our limited sample size to date. Further analyses of the remaining specimens are required to draw any firm conclusions.

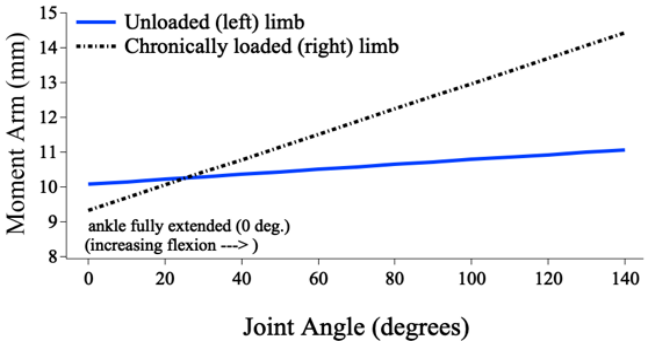

Fig. 2: Example moment arm from the loaded and unloaded limb of one specimen

Significance:

Our study is among the first to explore plasticity of muscle moment arms during growth. The findings from our work will reveal the extent to which muscle moment arms should be considered when investigating how the structure and function of the musculoskeletal system adapts to variation in load stimulus and physical activity.

Acknowledgments:

This study was supported by NIH grants R21AR071588 and R01AR080711.

References:

[1] Biewener (1991), Journal of Biomechanics, 1, 19–29; [2] Carrier et al. (1994) *Science*, 265(5172), 651–653; [3] Matthew Q. Salzano (2020), *Pennsylvania State University.*; [4] Katugam-Dechene (2023), *Pennsylvania State University.*

WALKING INDUCED COMPRESSIVE STRAIN RECOVERY IN ARTICULAR CARTILAGE

Axel C. Moore[1*], JiYeon A. Hong[1], Tejus Surendran[1], Daniel K. White[2]
[1]Department of Biomedical Engineering, Carnegie Mellon University
[2]Department of Physical Therapy, University of Delaware
*Corresponding author's email: axelm@andrew.cmu.edu

Introduction: Articular cartilage lines the ends of long bones in synovial joints and functions to provide load-bearing and low-friction articulation. These biomechanical functions are largely driven by the poroelastic mechanics (fluid pressurization) of the articular cartilage [1]. Unfortunately, the same poroelastic pressures that lead to load-bearing and lubrication also drive fluid exudation and concurrent tissue strain. Static loading in vivo (e.g., standing) produces as much as -30% strain in 60 min. Interestingly, active loading during daily activities (e.g., walking, squatting, cycling, running) in vivo produces an initial period of fluid exudation and strain (~ -5%) [2]; after which, active loading arrests further fluid loss and tissue strain [3]. While static and active loading drive fluid exudation and cartilage strain, static unloading (e.g., lying down) provides recovery, and to date, is the only in vivo recovery mechanism [3]. Previous work by our team and others have shown that excised cartilage specimens are capable of strain recovery during simulated activity [4]. Therefore, we hypothesize that active loading is capable of cartilage strain recovery in vivo. To test our hypothesis, we use magnetic resonance imaging (MRI) to evaluate the in vivo strain of the articular cartilage in young adult knees following a series of tasks (**Fig 1**).

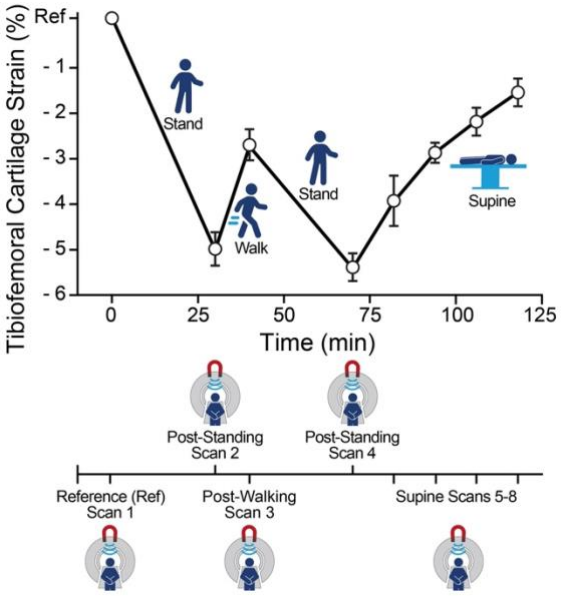

Figure 1: Tibiofemoral cartilage strain (mean ± 95% confidence interval) as a function of task. MRI's are taken following each task.

Methods: Participants. Following IRB approval, we recruited N=8 asymptomatic young adults to participate in the study. Participant age (29 ± 3 years of age, mean ± 95% confidence interval), biological gender (4 male, 4 female), and BMI (23 ± 2) were recorded. Up to 5 days prior to MRI scanning, participants were given a wrist worn activity monitor (13 ± 5k steps/day). MRI Scanning. Participants arrived at the MRI facility on the day of scanning and were positioned within the scanner (3T MAGNETOM Prisma, Siemens) with a 15 channel Tx/Rx knee coil around their right knee. Participants were scanned in the following fixed order: (1) reference, and immediately after (2) 30 min of standing, (3) walking for 10 min at 110 steps/min, (4) 30 min of standing, and (5-8) 12, 24, 36, and 48 min of lying down in supine (**Fig 1**). A proton density weighted turbo spin echo (PD-TSE) was used to assess the morphology and thickness of the articular cartilage. The in-plane resolution and slice thickness were 0.3 and 1.5 mm respectively. Data Analysis. Cartilage thickness is measured as the tibiofemoral bone-to-bone distance within the medial and lateral compartments, in the region of cartilage-cartilage contact. MRI scans were registered to the reference scan to ensure the same region was measured. We calculate cartilage strain as the change in cartilage thickness divided by the reference thickness. All values are reported as the mean ± 95% confidence interval unless stated otherwise.

Results: The compressive strain for both the medial and lateral compartments is shown in **Fig 1**. Note that all strain measures are calculated relative to the reference (Ref) value. After 30 min of static loading (standing), there is a clear thinning of the articular cartilage to an average -5.0 ± 0.4 and -5.3 ± 0.6% strain in the medial and lateral compartments. Following a 10 min walk (active loading), the cartilage thickness recovers 2.3 ± 0.3 and 2.6 ± 0.6% strain, which confirms our hypothesis that active loading is capable of in vivo strain recovery. Following a second bout of static loading to approximately the same strain (-5.4 ± 0.3 medial and -5.1 ± 0.5% lateral) the participant lies supine (static unloading), and the cartilage thickness and strain progressively recover. Following 48 min of unloaded recovery the cartilage recovered 3.8 and 3.6% strain in the medial and lateral compartments.

Discussion: In agreement with prior literature, static loading causes cartilage strain [5] while static unloading causes strain recovery [3]. These dynamics are driven by fluid flow out of and into the articular cartilage (changes in composition) [6]. Counter to the existing in vivo literature, we have shown that active loading (walking) is not simply an exudative and arresting mechanism [3,7] but also a mechanism of recovery, which we hypothesize is driven by fluid flow back into the articular cartilage. In future work, we will further assess this fluid flow hypothesis using T2-w imaging.

Significance: The implications of activity driven cartilage strain recovery may be significant. While epidemiological studies have documented the chondroprotective nature of joint activity, we have yet to identify the mechanism. Based on the findings of this work, activity may protect the cartilage through the recovery and maintenance of compressive strain. Furthermore, it may be the loss of this recovery mechanism that leads to or contributes to the development of cartilage degeneration.

References: [1] G.A. Ateshian et al, J. Biomech. (2009), [2] F. Eckstein et al, J. Anat. (2006), [3] F. Eckstein et al, Anat. Embryol. (1999)., [4] A.C. Moore et al, OA&C. (2017), [5] S. Uzuner et al, J. Mech. Behav. Biomed. Mater. (2021)., [6] R.B. Souza et al, Osteoarthr. Cartil. (2014)., [7] C.S. Paranjape et al, Sci. Rep. (2019).

FEMORAL SHEAR STRAIN LINKED TO SYMPTOMATIC KNEE OSTEOARTHRITIS TWELVE MONTHS POST-ACL RECONSTRUCTIVE SURGERY

Emily Y. Miller[1*], Timothy Lowe[2], Hongtian Zhu[2], Danielle Dresdner[1], James Kelly[1], Corey P. Neu[1,2]
[1]University of Colorado Boulder Biomedical Engineering Program
[2]University of Colorado Mechanical Engineering Department
*Corresponding author's email: emily.y.miller@colorado.edu

Introduction: Knee Osteoarthritis (OA) effects more than 86 million adults worldwide and lacks both approved therapeutic interventions and disease-modifying treatments**.** After an anterior cruciate ligament (ACL) tear nearly one half of individuals develop post-traumatic OA within 10 years [1]. Therefore, joint injury cohorts comprised of subjects who have torn an ACL and undergone a subsequent reconstructive surgery provide a unique opportunity to study and characterize the development of OA at its earliest stages. Early post-traumatic OA is characterized by biochemical and mechanical property changes to the articular cartilage, which could be early indicators of OA. Recently, DENSE MRI sequences have been used to calculate pixel level full field mechanical displacement and strain maps of cartilage under repetitive motion [2], which provides insights into mechanical property changes to articular cartilage. In this study, we utilized DENSE MRI to quantify mechanical strain in the medial articular cartilage and examined associations between strain and clinically relevant knee symptoms in a cohort of participants twelve months following ACL reconstructive surgery.

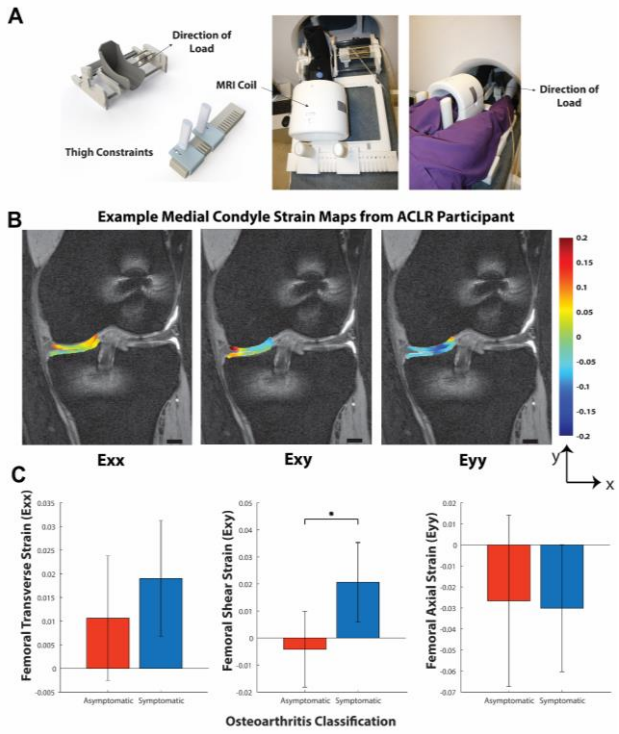

Figure 1A: MRI compatible loading device**. B.** Example strain maps. **C.** Average strains by KOOS classification

Methods: Ten participants (time from surgery: 12±1 months, 18 to 40 years of age), having received either a bone-patella tendon-bone autograft or quadriceps tendon autograft with one of three collaborating surgeons underwent 3D double echo steady state (DESS) acquisition to visualize morphology, and DENSE MRI acquisition during cyclic varus loading on the knee joint [4-6]. All DENSE images were acquired while the knee underwent a cyclic load mimicking the walking cycle provided by an exogenous loading device (Figure 1A). Participants completed the Knee Osteoarthritis Outcome Score (KOOS) at the time of MRI scan and were classified as having clinically relevant knee symptoms (symptomatic vs asymptomatic) if Quality of Life score <87.5, and two or more of pain <86.1, symptoms <85.7, ADL <86.8, sports/rec <85.8 [3]. All MRI measurements were segmented via a semi-automatic segmentation algorithm into two regions of interest (ROI) based on the anatomical regions of the knee (i.e., medial femur, medial tibia). Displacements from DENSE MRI were further processed to derive in-plane Green-Lagrange strains (Figure 1B) [2]. The mean value for each MRI metric within each ROI (femoral and tibial) was then calculated. We then evaluated the relationship between OA symptomatic status vs MRI metrics of strain using an independent t-test. (Figure 1C).

Results & Discussion: Five participants were classified as symptomatic and five were classified as asymptomatic for OA. The average KOOS score of the symptomatic group was 75.2±SE compared to 91.5±SE for the asymptomatic group. DENSE MRI of *in vivo* medial articular cartilage provided measures of cartilage biomechanics in our joint injury cohort. Within our cohort of ten participants, we found that femoral shear strain (Exy) was significantly higher in the participant pool that was symptomatic for OA ($p = 0.04$, Fig. 1C), which provides insight into pre-osteoarthritic mechanical property changes to articular cartilage. This is consistent with our prior work in cartilage explants [1] where we found that shear strain was significantly correlated to OA score as determined by histological scoring [1]. No differences were observed in either femoral transverse (Exx) or axial (Eyy) strain, and no differences were observed in any tibial strains.

Significance: Non-invasive imaging methods such as MRI are of particular interest for the evaluation of pre-OA conditions. Articular cartilage has been shown to soften with advancing OA, and this study demonstrates the potential ability of *in vivo* DENSE MRI to quantify those mechanical changes. This work demonstrates the potential of femoral shear strain, to identify those patients most at risk of progressing towards an OA disease state before irreversible changes to the knee joint occur.

Acknowledgments: This work was supported by NIH grant 2 R01 AR063712.

References: [1] Griebel A. et al. MRM, 2014. [2]. Chan D. et al., Sci. Rep. 2016. [3] O'Connell D. et al., The Knee. 2023. [4] Lee W. et al., MRM 90(3), 2023. [5] Lee W. et al., MRM 89(2), 2023. [6]. Zhu H. et al., SSRN 4569548

NON-WEIGHT BEARING FOLLOWING INJURY CAN PRESERVE TISSUE HEALTH IN A PRECLINICAL MODEL OF POST-TRAUMATIC OSTEOARTHRITIS

Jarred M. Kaiser[1,2*], Katherine B. Berg[3], Tamera N. Mistry[3], Daniel F. Cottmeyer[3], Young-Hui Chang[4], Liang-Ching Tsai[3]
[1]Emory University, [2]Atlanta VA Medical Center, [3]Georgia State University, [4]Georgia Institute of Technology,
*Corresponding author's email: jarred.kaiser@emory.edu

Introduction: Traumatic joint injuries dramatically increase the risk of developing post-traumatic osteoarthritis (PTOA). Current rehabilitation protocols following injury or reconstructive surgery aim to regain joint function and return the patient to pre-injury activity. Yet, little is known regarding how to optimize rehabilitation protocols to delay or prevent PTOA. While rehabilitation protocols often include early rest following injury and surgery, these protocols vary widely in non-weight bearing periods, ranging from 2 to 12 weeks after injury, with little scientific justification. Transitioning to weight-bearing must strike a balance between resolving injury-induced inflammation and preventing adverse effects of disuse. Specific to articular cartilage, even normal levels of mechanical loading through weight-bearing in inflamed post-injury conditions can lead to tissue degradation (1). Conversely, sustained non-weight bearing leads to proteoglycan loss (2) and may predispose the tissue to injury upon activity return. Longitudinal mechanistic or interventional studies on the effect of weight-bearing after injury on cartilage health is highly challenging and complex in humans due to the slow disease progression and complex interactions among patient factors. Thus, here we present a preclinical study using a standardized model of meniscal injuries in rats to examine the effects of varying non-weight bearing durations on knee tissue health following injury. We hypothesized that non-weight bearing following injury would preserve joint tissue health in both male and female rats.

Methods: We used a standard preclinical model of PTOA– the medial meniscal transection (MMT) model. Eight-week-old male (N=20 total) and female (N=26 total) Lewis rats received either a sham surgery (transection of only the medial collateral ligament, which does not progress to joint degradation) or MMT (which progresses to early PTOA by three weeks). MMT rats were randomly allocated to a group: immediate weight-bearing (no suspension) or hindlimb suspension for one, two or three weeks. The sham rats were suspended for 3 weeks. The study is on-going, with current enrolments of 3-6 rats per sex/group. Hindlimb suspension is a common technique to reduce weight-bearing in rats, mimicking the non-weightbearing phase of clinical care. We lowered rats from suspension after their pre-determined duration and they were allowed to freely ambulate until the study ended at 8 weeks, where we expected to see full cartilage lesions and large osteophytes in the untreated MMT rats. Tibiae were imaged using contrast enhanced micro-computed tomography and were assessed for cartilage composition (CT attenuation is inversely proportional to proteoglycan content) and cartilage and osteophyte morphology. As this study is on-going, we first pooled outcomes from both male and female rats together and used a linear mixed model with or without a weight as a co-variate to detect for differences in joint morphological parameters among groups.

Results & Discussion: MMT resulted in significant knee degradation. Compared to shams, MMT resulted in a significant loss of proteoglycans (increased CT attenuation), large cartilage lesions, and large osteophytes (**Fig. 1A**). These findings were consistent in male and female rats, though progression rate may differ with lesions first appearing in male rats at week 4 and in female rats at week 6 (data not shown). Non-weight bearing after injury reduced tissue degeneration in a dose-dependent manner (**Fig. 1A**). Two and three weeks of suspension reduced cartilage surface roughness (**Fig. 1B**, $p<0.001$) and osteophyte size (**Fig. E**, $p<0.003$). Lesions were reduced with at least two weeks of suspension in female rats but required three weeks of suspension in male rats (**Fig. 1C**). Unloading did not improve cartilage composition (**Fig. 1D**), suggesting that the cartilage in these rehabilitated rats may have residual mechanical deficiencies. Our future studies will focus on the safe transition from non-weight bearing to normal activity. One week of suspension was insufficient to slow joint degradation in all rats. While we observed an effect of sex on tissue morphology, this effect did not remain once accounting for body mass.

Significance: Our preclinical experiments provide scientific support for the importance of joint unloading following injury to slow PTOA. The effects of unloading may be dose-dependent, indicating the need for determining the optimal duration of non-weight bearing and a safe transition to activity following traumatic knee injuries.

Acknowledgments: R01AR080154

References: (1) Nam, J et al. PLoS One 2009. (2) Souza RB et al. J Ortho Sports Phys Ther. 2012

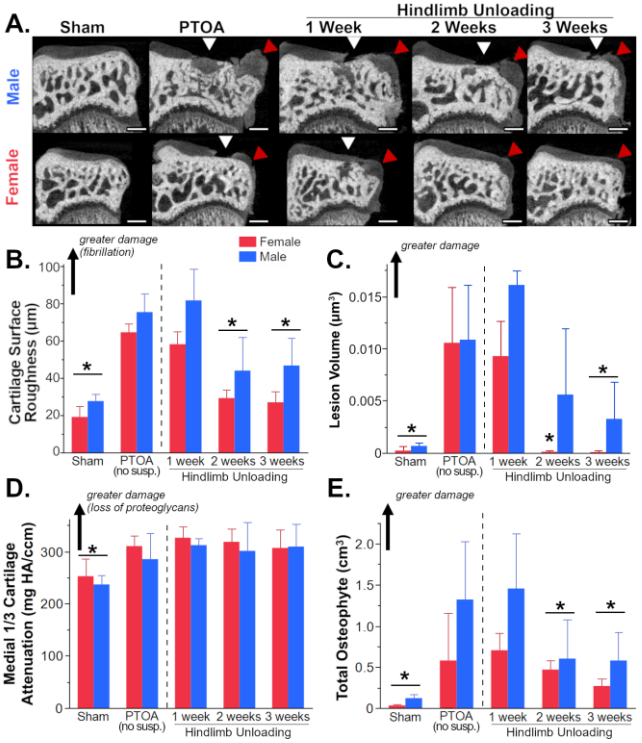

Figure 1: Coronal contrast-enhanced microCT images of the medial tibia (A). Cartilage damage (white arrow) and osteophytes (red) were observed in the untreated PTOA rat but decreased with suspension duration. Two and three weeks of non-weight bearing decreased cartilage fibrillation (B), and osteophyte volume (D) but did not preserve proteoglycan content (C). * significant difference with no-suspension.

EFFECT OF GRADIENT ON WALKING BIOMECHANICS IN ADULTS WITH KNEE OSTEOARTHRITIS

Samantha K. Price[1*], Joshua J. Stefanik[2], Cara L. Lewis[3], Irene S. Davis[4], David T. Felson[3], Patrick Corrigan[1]
[1]Saint Louis University, [2]Northeastern University, [3]Boston University, [4]University of South Florida
*samantha.price@slu.edu

Introduction: Evidence-based guidelines for non-surgical, non-pharmacologic management of knee osteoarthritis (OA) highly recommend exercise as a first-line strategy for managing pain and preventing functional decline [1-2]. Walking continues to be the most common form of exercise for adults with knee OA [3]. However, for individuals with knee OA, starting a walking program without guidance could worsen pain and perpetuate disease. Biomechanical measures, such as external knee flexion moments (KFM) and knee adduction moments (KAM), have been associated with knee OA progression [4-5]. Yet, current studies that evaluate KFM and KAM in adults with knee OA typically only include flat walking [6], which is not representative of real-world walking environments. Expanding current research by evaluating knee joint kinetics during different types of walking could enhance our understanding of knee joint loading in adults with knee OA and improve the prescription of walking. Previous studies have assessed knee joint loading during inclined or declined walking in adults with knee osteoarthritis [7-8]. However, these studies do not directly compare differences in knee joint loading between flat, inclined, and declined walking. The purpose of this study was to determine the effect of gradient on KFM, KEM, and KAM during flat, inclined, and declined walking in adults with knee OA.

Methods: Adults with clinically defined symptomatic unilateral knee OA completed this study. Inclusion was based on the National Institute for Heath and Care Excellence (NICE) criteria (≥ 45 years, knee pain lasting >3 months, knee pain ≥ 3/10 with walking, and knee stiffness lasting < 30 minutes in one knee). The painful limb was defined as the symptomatic limb and the nonpainful limb was defined as the asymptomatic limb. Participants completed three 2-minute walking conditions at a constant self-selected speed (0.91(0.1) m/s) on a force-instrumented split-belt treadmill (Bertec Inc., Columbus, OH, USA) in a 3D motion analysis environment (Qualisys AB; Gotenburg, Sweden). Three gradient conditions were collected: 0° (flat), +4.8° (inclined), and -4.8° (declined). A gradient of 4.8° was chosen because it is the maximum gradient for public ramps set by the Americans with Disabilities Act [9]. Ground reaction forces and kinematic data (2160 and 180 Hz, respectively) were collected in the second minute of each condition. Using inverse dynamics, the KAM, KEM and KFM were calculated across 10 gait cycles. The KFM, KEM, and KAM impulse (scaled to body weight and mass), were determined for each step (Figure 1). For statistical analysis, 2x3 (limb-by-condition) repeated measures ANCOVAs compared average knee joint moment impulses between the limbs for the three different walking conditions, while adjusting for gait speed.

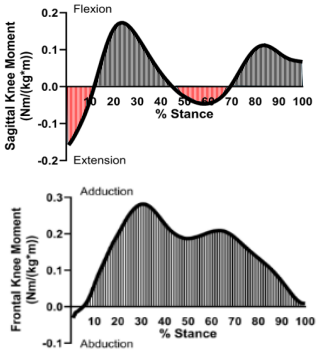

Figure 1: Sagittal and frontal plane knee moment impulses measured from heel strike to toe off.

Results & Discussion: 22 participants were included (13 F; age=60(7) years; height=170(10) cm; body mass=82.3(20.5) kg). Average pain (SD) with walking, on an 11-point scale, was 2(1) during both flat walking and inclined walking, and 2(2) during declined walking. There was a significant main effect of condition ($p<0.0001$) for KFM impulse, with increased impulse during declined walking (Figure 2a). There was also a significant main effect of condition ($p<0.0001$) for KEM impulse, with increased impulse during inclined walking (Figure 2b). However, there were no significant effects of condition on KAM impulse ($p\geq0.09$, Figure 2c).

Overall, there was a significant effect of gradient on sagittal-plane knee joint moment impulses. Declined walking increased knee flexion moment impulse and inclined walking increased knee extension moment impulse. KAM impulse did not change for any gradient. This is not surprising given the change of gradient was in the sagittal plane. There were no main effects of limb with the painful and nonpainful limbs demonstrating similar knee joint loading regardless of gradient.

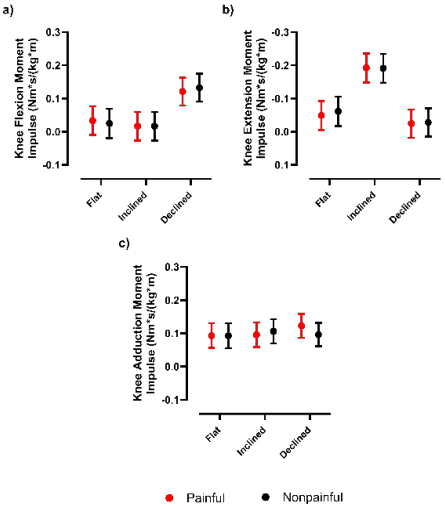

Figure 2: Mean (95% CI) knee joint loading of the painful and nonpainful limb during each type of walking.

Significance: Walking gradient appears to affect sagittal-plane knee joint loading in adults with knee OA. Considering KFM has been associated with the progression of knee OA, including inclined walking, and avoiding declined walking in the prescription of walking programs may reduce knee joint loading and prevent the progression of knee OA.

Acknowledgments: Funding for the study was provided by the Rheumatology Research Foundation and Academy of Orthopaedic Physical Therapy.

References: [1] Bannuru et al. (2019), *Osteoarthritis Cartilage* 27(11); [2] Kolasinski et al. (2020), *Arthritis Rheumatol* 72(2); [3] Dai et al. (2015), *Journal of physical activity & health* 12 Suppl 1:S128-40; [4] Chehab et al. (2014), *Osteoarthritis and Cartilage* 27(11); [5] Miyazaki et al. (2002), *Annals of the Rheumatic Diseases* 61(7); [6] D'Souza et al. (2021), *Osteoarthritis and cartilage 30(3);* [7] Haggerty et al. (2014), *Gait and Posture* 39(4); [8] Gustafson et al. (2015) *Clin Biomech* 30(5); [9] Americans with Disabilities Act (ADA) (2000), *Fed Regist* 65(202)

Knee Extensor Fatigue Impacts Gait Mechanics in Individuals with Knee Osteoarthritis

Skylar C. Holmes[1], Athulya Simon[1], Jane A. Kent[1], Katherine A. Boyer[1]
[1]University of Massachusetts, Amherst
*Corresponding author's email: scholmes@umass.edu

Introduction: In healthy older adults, muscle fatigue has been proposed as a contributor to poorer mobility [1]. There is evidence that older healthy (OH) adults experience measurable knee extensor (KE) fatigue with a treadmill walk protocol as compared to younger adults [2]. This study also found decreased ankle dorsiflexion moments and KE torque post treadmill walk in older adults, suggesting an impact of KE fatigue on gait mechanics [2]. With older age, loss of muscle strength may exceed that of muscle mass, resulting in lower specific torque. KE muscle dysfunction, including lower isometric and isokinetic torques, are also common with KOA [3]. In people with KOA, specific torque may be even lower due to due to voluntary activation deficits [4,5]. To date, there is limited evidence to explain whether and how muscle fatigue may alter control and coordination of movement in KOA. Therefore, the purpose of this study is to 1) characterize knee extensor fatigue in response to a 30-min treadmill walk (30MTW) in individuals with and without KOA, and 2) determine the impact of KE fatigue on gait mechanics. We hypothesize that individuals with KOA will have greater fatigue (decrease in maximum isometric torque; MVIC), and that this fatigue will be exacerbated in those with lower KE specific torque (MVIC/fat-free muscle size). We also hypothesize that in KOA there will be greater reductions in sagittal plane range of motion (ROM) and peak joint power for all lower extremity joints.

Methods: Seven adults with symptomatic KOA (5F, age: 70±4y, BMI: 25.9±3, MVPA: 227±45min) and 7 healthy older adults (5F, age: 73±4y, BMI: 23±4, MVPA: 237±45min) participated in this study after completing the informed consent process approved by the University of Massachusetts Amherst IRB. Overground gait analysis and isokinetic knee extensor testing were completed before and after participants completed a 30MTW at preferred speed. Five overground walking trials were captured pre and post 30MTW, from which stance phase joint kinematics were calculated using the point cluster marker technique, and joint powers were calculated using an inverse dynamics approach. Primary outcomes were hip, knee, and ankle range of motion and peak positive joint power. MVIC (Nm) at 70 degrees of flexion was quantified by isokinetic dynamometer (Biodex System 4 Pro, Shirley, NY). Axial images of the thigh were obtained in a 3T MRI system using a multi-echo (6-point) Dixon sequence (3 stacks, 8 mm slice thickness, 24 slices per stack, TR=35 ms, TE=2.46 ms, voxel volume: 1.25x1.25x8). A region of interest was drawn around the KE muscle group on each slice [6]. Peak fat-free muscle cross-sectional area (CSA, cm^2) and fat fraction (%) were quantified using a custom-written MATLAB script. Specific torque was calculated as the ratio of peak torque and maximum CSA. Linear regression was used to analyze the associations between specific torque and KE fatigue (α= 0.10). Independent samples t-tests were used to compare the change in gait mechanics and strength from pre to post 30MTW (α= 0.10) and paired t tests evaluated within-group changes in response to the 30MTW.

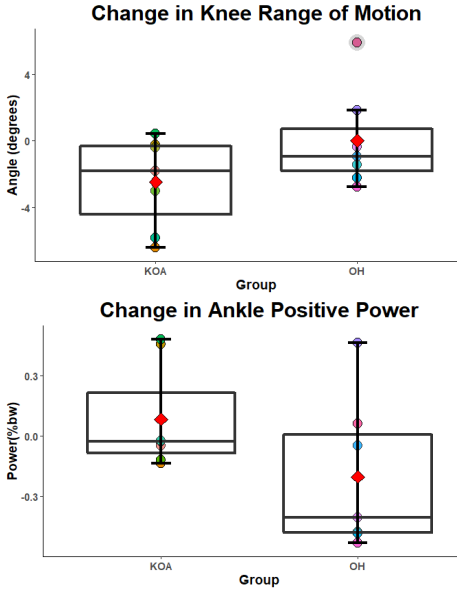

Figure 1: Group differences with 30MTW in knee flexion ROM (*top*) and ankle joint power (*bottom*). Negative values indicate a decrease post 30MTW while positive values indicate an increase post 30MTW.

Results & Discussion: Baseline MVIC (KOA: 129.3±29 Nm; OH: 142.1±42Nm, mean±SD) and gait speed (KOA: 1.37 m/s OH: 1.43 m/s) did not differ between groups (all $p \geq 0.10$), indicating that our individuals with KOA had relatively high mobility function. KOA and OH both fatigued in response to the treadmill walk (KOA Change: 80 %baseline MVIC, OH Change: 83%baseline MVIC, all $p<0.05$), with no difference by group in fatigue. Specific torque did not predict muscle fatigue (r^2 = -0.07, p=0.64). There were significant differences in the change in knee ROM (p= 0.067, Cohen's d= 2.86, Fig 1A) and ankle joint power (p= 0.063, Cohen's d =0.33, Fig 1B) between KOA and OH. The larger decrease in ankle positive power in OH suggests a redistribution of joint power in OH that was not observed in people with KOA, consistent with previous work showing a redistribution in joint powers in older adults [7]. In contrast, KOA decreased knee ROM, suggesting a quadriceps avoidance pattern, which is common in KOA and may be implemented to shift demand away from the KE [8].

Significance: Despite similar baseline characteristics and KE fatigue, the biomechanical responses to walking in individuals with KOA were different from healthy, age- and sex-matched adults. In combination, these differences suggest sub-clinical limitations in "biomechanical flexibility" even in highly functioning individuals with KOA.

Acknowledgments: This research was supported by the National Institute of Aging under Award Numbers F31AG079538 and R01AG068102 and by an ISB Matching Dissertation Grant.

References: [1] Foulis et al. (2017) *PLoS One*, 12(9); [2] Hafer et al. (2020) *J Appl Biomech* 36(3); [3] Slemenda, C., et al. (1997) *Ann Intern Med* 127(2) [4] Kent-Braun et al. (1999) *J Appl Physiol* 87:1 [5] Lewek et al., (2004) J Orthop Res. Jan;22; [6] Fitzgerald et al. (2021) *J Physiol.* 599(12) [7] Devita et al. (2000) *J Appl Physiol* 88 [8] Favre J et al. (2014) *Osteoarthritis Cartilage* 22(3)

KNEE KINEMATICS DURING STAIR ASCENT ARE ASSOCIATED WITH STRENGTH AND PATIENT REPORTED OUTCOMES AFTER TOTAL KNEE ARTHROPLASTY

Shelley Oliveira Barbosa[1], Tom Gale[1], Clarissa LeVasseur[1], Paige Paulus[1], Marit Johnson[1], Raghav Ramraj[1], Emma Scarton[1], Yuuka Tanabe[1], Kal Byrapogu[1], Elizabeth Copp[1], Kenneth Urish[1], William Anderst[1]
[1]Department of Orthopaedic Surgery, University of Pittsburgh, Pittsburgh, PA
*Corresponding author's email: shelleyob@pitt.edu

Introduction: Approximately 1 million primary total knee arthroplasties (TKA) are completed in the U.S. each year, yet 20% of patients are dissatisfied following their primary TKA [1-2]. The exact cause of patient dissatisfaction post-TKA is unknown; possible causes include sociodemographic factors and patient function [2-4]. Although highly accurate post-TKA kinematics have been measured using biplane radiography [5-6], associations between knee kinematics and clinical outcome measures are lacking. The objective of this interim analysis was to investigate the relationship between *in vivo* knee kinematics, patient-reported outcomes (PROs), and functional testing in patients who received TKA. We hypothesized (a) post-surgery PROs and functional testing scores would be correlated to TKA knee kinematics, and (b) pre- to post-surgery changes in PROs and functional testing scores would be correlated to changes in kinematics.

Methods: All participants provided written informed consent to participate in this ongoing IRB-approved study. Participants underwent unilateral TKAs (Journey II BCS, Smith & Nephew) which were completed by the same surgeon and robotic system. All participants attended pre-surgery (PRE) and 1-year post-surgery (POST) motion testing, completed PROs (Knee Injury and Osteoarthritis Outcome Score (KOOS)), and completed functional testing (lateral step-down test [7], hip abductor strength, and quadriceps strength). KOOS was split into Pain, Symptoms, function in daily living (ADL), function in Sport and Recreation (Sport/Rec), and knee-related Quality of Life (QOL) subscales [8]. Hip and quad strength were measured with a handheld dynamometer during maximum voluntary isometric contraction testing (MVIC). Participants were recorded while performing the lateral step-down test and videos were later graded by a licensed physical therapist. For the motion testing, three trials of stair ascent were imaged using synchronized biplane radiographs at 100 images/s for 1 second each trial (80 kV, 125 mA, 1 ms exposure per image). The femur and tibia motion were tracked using a previously validated model-based tracking technique with an accuracy of 0.7 mm, 0.9° [9]. Coordinate systems were constructed on the contralateral side and were mirrored onto the operated side [10]. Tibiofemoral kinematics were calculated and interpolated to every degree of flexion and averaged across trials. The averages and ranges of four kinematic variables (abduction/adduction, internal/external rotation, lateral/medial translation, anterior/posterior translation) for PRE and POST were calculated, and differences between test dates (CHG) were also calculated. Spearman correlation was used to identify associations between the kinematics and KOOS, maximum hip and knee MVIC force output, or lateral step-down numeric score, for both POST and CHG, with significance set at $p < 0.05$.

Results: Data from 13 of 29 subjects (6F, age 65±6.1 years, BMI 31.3±9.1 kg/cm^2) who have completed POST testing are included in this interim analysis. POST hip abductor, quad strength, and KOOS subscales were correlated with POST kinematic parameters (Table 1). For CHG, only KOOS subscales were correlated with kinematics changes (Table 1). No correlations were found with the lateral step-down test or abduction/abduction rotation.

Table 1. Correlations between KOOS or functional testing scores and kinematics.

	KOOS and Functional Scores	Kinematics	p-value, rho
POST	Greater hip abductor strength	Greater tibial internal rotation	p=0.014, ρ=-0.660
		Greater range of anterior/posterior translation	p=0.028, ρ=-0.605
	Greater quad strength	Greater tibial medial position	p=0.010, ρ=0.687
	Better Pain Score		p=0.022, ρ=0.625
	Better ADL Score		p=0.015, ρ= 0.657
CHG	Improved ADL Score	Decreased medial position of tibia	p=0.031, ρ=0.597
	Improved QOL Score		p=0.006, ρ=0.714
	Improved QOL Score	Increased posterior position of tibia	p=0.040, ρ=0.574

Discussion: These interim results suggest that specific knee kinematics are associated with post-TKA strength and KOOS scores, and pre- to post-surgery changes in knee kinematics are associated with changes in KOOS subscales. This believed to be the first report to link changes in tibiofemoral kinematics after TKA with functional outcomes and patient-reported outcomes after TKA. Additional movements of daily living (e.g., walking, chair rise, and stair descent) are being investigated to confirm these relationships hold for different loading conditions.

Significance: Identification of associations between kinematics and PROs or function may be beneficial for the direction of post-surgery physical therapy, future device design and development, and improving patient satisfaction post-TKA.

Acknowledgments: This work was supported by a research grant from Smith & Nephew.

References: [1] Siddiqi et al. (2022) *Arthroplast Today*; [2] Gunaratne et al. (2017) *J of Arthroplasty*; [3] Jacobs and Christensen (2014) *J of Arthroplasty*; [4] Young-Shand et al. (2021) *J of Arthroplasty*; [5] Guan et al. (2016) *JOR*; [6] Schutz et al. (2019) *J R Society Interface*; [7] Piva et al. (2006) *BMC Musculoskeletal Disorders*; [8] Roos and Lohmander (2003) *Health and Quality of Life Outcomes*; [9] Tashman and Anderst (2003) *J Biomech Eng*; [10] Gale et al. (2019) *JOR*.

Running Biomechanics Vary by Sport in Division I Collegiate Athletes

Victoria A. Heiligenthal[1,2], Mikel R. Joachim[1], Bryan C. Heiderscheit[1,2]
[1]Department of Orthopedics and Rehabilitation, Badger Athletic Performance, University of Wisconsin-Madison
[2]Department of Biomedical Engineering, University of Wisconsin-Madison
joachim@ortho.wisc.edu

Introduction: Running is a core athletic task that is relevant to most sports; however, the role running plays may differ based on the structure and objective of the sport. Technical-based or multi-directional sports often require athletes to accelerate quickly when performing additional tasks while athletes in uni-directional sports rely solely on straight-line running. Biomechanical differences have been shown in athletes in different sports when completing tasks like cutting, landing, and sprinting [1, 2, 3], but differences in straight-line running mechanics at submaximal speeds have yet to be studied. Characterizing biomechanical differences in variables known to influence submaximal running performance, such as cadence, propulsive impulse, peak vertical ground reaction force (VGRF), and duty factor, may be relevant for training, injury prevention and recovery, as most athletes train at submaximal speeds. The purpose of this study was to assess differences in running biomechanics among collegiate athletes from varied sports across submaximal running speeds.
Methods: Running gait data were obtained per a standardized protocol as part of routine institutional procedure and stored within the Badger Athletic Performance database [4]. Records were extracted if the athlete was cleared for participation at time of testing, had data available at 2.68, 3.35, and 4.47m/s, and had no history of lower extremity surgery. Variables of interest included cadence, duty factor (% stance phase), peak VGRF, and propulsive impulse. Separate linear mixed effect models were used to assess sport and speed effects within each sex, accounting for repeated observations across limbs, with least square means and 95% confidence intervals reported.
Results: A total of 271 unique athletes from men's and women's cross country (MCC, N=54, WCC, N=60) and basketball (MBB, N=12, WBB, N=13), women's soccer (WSC, N=43), and men's football (MFB, N=77) met inclusion criteria. Males demonstrated a sport-by-speed interaction for all variables ($p<0.001$, Table 1). Females demonstrated significant interactions for all variables ($p<0.04$, Table 1) except cadence, which did not demonstrate a significant interaction ($p=0.67$), but did demonstrate significant sport and speed main effects ($p<0.001$). Post-hoc comparisons are described in Table 1.
Discussion: Sport and running speed significantly influenced running mechanics among both men and women. For both sexes, all sports responded to an increase in running speed as expected with cadence, propulsive impulse, and peak VGRF increasing and duty factor decreasing. At the same speed, CC athletes generally demonstrated greater cadence, propulsive impulse, and peak VGRF compared to other sports within their respective sex, except at 4.47 m/s where football athletes had the greatest cadence. These differences in running biomechanics may reflect sport-specific adaptations, with CC athletes demonstrating mechanics associated with improved straight-line running performance, such as increased propulsive impulse and peak VGRF.
Significance: This study provides initial evidence that running biomechanics vary in male and female athletes competing in differing sports at submaximal speeds. Our findings may inform strength and conditioning professionals and sports medicine clinicians about additional athlete-specific variables to consider (sex and sport) when assessing running mechanics for optimizing training, implementing injury prevention programs, and monitoring post-injury recovery. Future studies including athletes from additional sports, testing at different speeds, and analyzing more variables should be conducted to further verify the results of this study.
Table 1. Least square means (95% confidence interval) for each variable of interest by sport and speed. Significant differences across sports within a speed are reported.

	Cadence (steps/min)				Propulsive Impulse (Ns/ kg)						Peak VGRF (N/kg)						Duty Factor (% gait cycle)					
Running Speed (m/s)	MCC	MBB	MFB	All Female Sports	MCC	MBB	MFB	WCC	WBB	WSC	MCC	MBB	MFB	WCC	WBB	WSC	MCC	MBB	MFB	WCC	WBB	WSC
2.68	161* (160, 163)	156 (152, 159)	157^ (155, 158)	164 (162, 165)	0.166 (0.161, 0.171)	0.169 (0.159, 0.180)	0.183^ (0.178, 0.187)	0.167 (0.162, 0.172)	0.185‡ (0.173, 0.196)	0.165 (0.159, 0.172)	24.4* (24.0, 24.7)	21.0 (20.2, 21.7)	22.7^ (22.4, 23.0)	23.4 (23.1, 23.8)	22.1 (21.3, 22.8)	22.6# (22.2, 23.0)	34.3 (33.9, 34.8)	40.1† (39.1, 41.0)	37.9 (37.4 38.2)	34.6 (34.2, 35.0)	37.8 (36.9, 38.7)	36.2 (35.7, 36.6)
3.35	165* (163, 166)	161 (163, 166)	162^ (160, 163)	168 (167, 170)	0.195 (0.190, 0.200)	0.191 (0.180, 0.201)	0.205^ (0.201, 0.209)	0.193 (0.188, 0.199)	0.207‡ (0.196, 0.219)	0.188 (0.182, 0.195)	26.2* (25.9, 26.6)	23.8 (23.1, 24.5)	24.7^ (24.4, 25.0)	24.9 (24.6, 25.2)	24.0 (23.3, 24.7)	24.2# (23.8, 24.6)	31.1 (30.9, 31.7)	35.0† (34.1, 35.9)	34.1 (33.8, 34.5)	31.9 (31.5, 32.3)	34.0 (33.1, 34.8)	32.9 (32.5, 33.4)
4.47	173 (171, 175)	172 (168, 175)	174+ (173, 176)	181 (179, 182)	0.232 (0.227, 0.237)	0.223 (0.212, 0.234)	0.230^ (0.226, 0.234)	0.226 (0.220, 0.231)	0.240‡ (0.227, 0.253)	0.212 (0.206, 0.218)	28.3* (27.9, 28.6)	25.2 (24.5, 26.0)	26.3^ (26.0, 26.6)	26.4 (26.1, 26.8)	25.0 (24.2, 25.9)	25.6# (25.2, 26.0)	28.4 (28.0, 28.8)	31.6† (30.6, 32.5)	30.8 (30.5, 31.2)	29.0 (28.6, 29.4)	30.8 (29.8, 31.8)	29.9 (29.4, 30.4)

Abbreviations: MCC – men's cross country, MFB – men's football, MBB – men's basketball, WCC – women's cross country, WBB – women's basketball, WSC – women's soccer.
*MCC significantly greater than all other sports. +MFB significantly greater than all other sports. ^MFB is greater than MBB. †MBB is greater than all other sports. ‡WBB is greater than all other sports. #WSC is greater than WBB.

Acknowledgments: The authors acknowledge the Sports Medicine staff at the University of Wisconsin-Madison Division of Athletics for their commitment to the welfare of the student athletes and for their contributions to the Badger Athletic Performance Program.

References: 1. Cowley et al. (2006), J Athl Train 41(1): 67-73. **2.** Huang et al. (2019), ISBS 37(1). **3.** Haugen et al. (2019), PLoS ONE 14(7): e0215551. **4.** Stiffler-Joachim et al. (2019), Med Sci Sports Exerc 51(10).

FREE MOMENT INCREASES WHILE RUNNING WITH A STROLLER

Joseph M. Mahoney[1,2,3,*], Amy Lista[1], Diego Carbajal[1], Naomi Fay[1], Benjamin W. Infantolino[1], Allison R. Altman-Singles[1,2]
[1]Kinesiology, Penn State Berks, Reading PA 19610
[2]Mechanical Engineering, Penn State Berks, Reading PA 19610
[3]Mechanical Engineering, Alvernia University, Reading PA 19601
*Corresponding author's email: joseph.m.mahoney@gmail.com

Introduction: Running with a stroller can be beneficial for physical and mental health, parent-child bonding, and instilling values in young children. Little research has been done to examine the mechanics of running with a stroller to determine how it affects the mechanical risks for running-related injuries. Previous work in the lab has indicated that vertical impact loading and loading rates are reduced while running with a stroller [1], which may be protective against overuse injuries in runners [2]. However, kinematic analysis showed increased dynamic hip and knee valgus and kinematic changes consistent with constrained foot placement [3].

Previous work has shown a correlation between Free Moment (FM), the torsional moment produced between the foot and ground, and injury risk in runners [4,5]. Specifically, runners who had a history of tibial stress fractures (TSF) had increased peak absolute FM ($|FM|_{max}$), peak adduction FM (ADDFM), FM at time of peak braking force (FMBRAK), and the area under their FM curve (IMP) compared to uninjured controls [4]. In addition, $|FM|_{max}$, in conjunction with hip adduction and ankle eversion, was able to predict a history of TSF in a large cohort of runners [5]. Furthermore, studies of increased load carriage during running observed increased FM characteristics [6].

Due to the kinematic changes observed while running with a stroller and the implications of added load, it is important to evaluate the torsional profile of the GRF in this population. Thus, the purpose of this study was to compare FM parameters in individuals running with and without a stroller.

Methods: 38 healthy local runners (aged 18-45, running > 8 km/week) were recruited. Runners ran across an 18 m runway with embedded force plates (Bertec, Columbus, OH). A self-selected speed was determined after a warmup, then maintained within 10% for 5-10 satisfactory trials with and without a running stroller (Expedition, BabyTrend, Fontana, CA) loaded with 11 kg. Force and moments (sampled at 2000 Hz) from the force plate were recorded using Nexus (Vicon, Centennial, CO). All data were zero-lag LP filtered using a 4th-order Butterworth with a 70 Hz cutoff. Data were then trimmed to stance phase based on footstrike as onset of vertical GRF above 0.001% bodyweight and toe-off at GRF below that threshold.

FM values were calculated during stance phase using the definition put forth in [4,5]. All FM values were normalized by the subject's bodyweight (BW) and stature (St). The ADDFM, FMBRAK, IMP, and $|FM|_{max}$ were calculated for each subject, condition, and trial. The median value over all a subject's trials was found. The means of these distributions were compared using a two-tailed bootstrap t-test with 10^6 resamples. Significance threshold was set *a priori* to $\alpha = 0.05$. All analysis and statistics were performed in MATLAB (R2023b, Mathworks, Natick, MA).

Results & Discussion: 11 male and 27 female subjects (29.8±8.9 years, 1.69±0.17 m, 64.9±10.2 kg) who ran 26.4±19.5 km/wk participated in this study.

A significant difference in means was found for all three FM variables (Fig. 1). The ADDFM increased by 64.6% ($p<0.001$). The FMBRAK increased by 47.3% ($p<0.001$). Net impulse increased by 146% ($p<0.001$), absolute maximum FM increased by 72.6% ($p<0.001$).

This increase in FM characteristics may be indicative of an increased risk of TSF and other torsion-related running injuries [4,5]. The effect observed while pushing a stroller is similar to runners with a history of TSF [4,5], and running while carrying a heavy load [6].

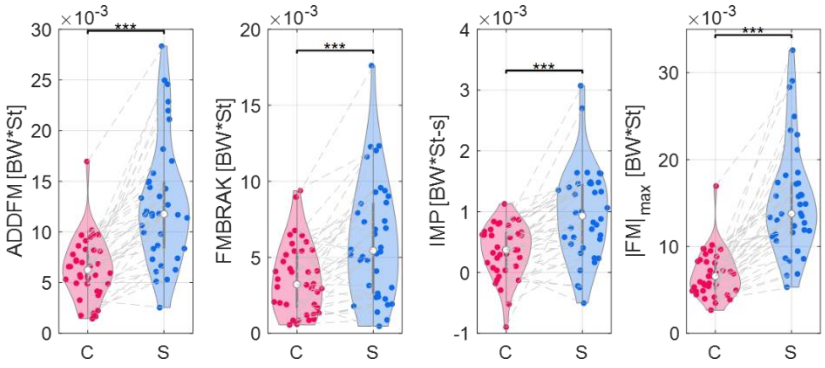

Figure 1. Maximum FM Adduction (ADDFM), FM at braking peak (FMBRAK), Impulse (IMP) under the FM curve, and absolute maximum FM ($|FM|_{max}$). Means were compared using two-sided bootstrapped t-test. *** indicates $p < 0.001$.

Significance: The increase in these FM characteristics when running with a stroller *could* indicate increased risk of injury, specifically TSF [4,5]. This risk could be partly mitigated by minimizing the load in the stroller [6] and utilizing a motion control shoe [7].

Acknowledgements: This work received funding from the Franco, Cohen-Hammel, MC REU, and RDG Awards from PSU.

References: [1] Mahoney (2022) *NACOB*, Ottawa, ON; [2] Davis (2016) *Br J Sports Med*, 50; [3] Lista (2023) *ASB*, Knoxville, TN; [4] Milner (2006) *J BioMech* 39; [5] Pohl (2008) *J BioMech*, 41; [6] Baggaley (2020) *Gait Posture*, 77; [7] Jafarnezhadgero (2019) *Gait Posture*, 73.

GAIT ASYMMETRY AND MOOD STATE AFTER MULTIPLE DAYS OF RUNNING: A DESCRIPTIVE ANALYSIS

Marni G. Wasserman[1*], James J. McDonnell[1], Kai-Wen Chien[1], Ali Boolani[2], John S. Raglin[1], Edward Nyman[3], Jennifer Sumner[3], Allison H. Gruber[1]
[1]Department of Kinesiology, Indiana University, Bloomington, IN, USA
[2]Department of Aeronautical and Mechanical Engineering, Clarkson University, Potsdam, NY, USA
[3]Brooks Sports, Inc., Seattle, WA, USA
*Corresponding author's email: marnwass@iu.edu

Introduction: Running gait asymmetry has been studied in relation to lower limb load distribution and its implications for running-related injuries (RRI) [1,2]. While some evidence suggests that the nature of the variability is injury-specific [1,3], there is conflicting support for association with RRI [1,2], and it remains unclear how changes in symmetry over time may compound or protect against RRI risk. Likewise, running gait variability is influenced by exhaustion, but research is limited to its effects during a single prolonged run [4,5] and has not accounted for the potential effects of mental fatigue elicited by exhaustive exercise. The purposes of this analysis were therefore to (A) descriptively assess the effect(s) of multiple days of prolonged running on gait asymmetry and mental mood state, and (B) determine functional groups according to directional change in asymmetry, mental fatigue, and mental energy.

Methods: Eight recreational runners (3M/6F; mean±1SD: age: 30.4±6.9 years) performed three consecutive days of running on an instrumented treadmill (Treadmetrix) at a fixed speed (3.2±0.4 m/s) previously identified as their first ventilatory threshold. Runs were terminated when the subject reported a Borg rate of perceived exertion (6-20) of 17 or greater (23.0±10.2 min). 3D gait was collected for 30 seconds of each minute of each run. Asymmetry measures for average ground contact time (GCT) and peak vertical ground reaction force (vGRF) were examined as indicators of lower limb load distribution [2]. Subjects also completed a mental fatigue and mental energy index [6] before and after runs to assess change in mood state. Left (L) vs. right (R) asymmetry for lower limb GCT and vGRF for the baseline (minute 3) and end of each run was calculated using the Symmetry Index (SI) [1]. Paired t-tests were used to compare L vs. R and baseline vs. end SI for each run; baseline and end SI scores were then combined into a single average run SI score. A repeated measures ANOVA with Tukey's post-hoc comparisons was used to assess differences in run duration and baseline, end, and change in average SI, R, L, and mood state ($p \leq 0.05$). Pearson's correlations were used to determine relationships between mood states and SI. Data exploration revealed subject-level trends in mood state that allowed for grouping of participants by change in baseline mental fatigue from run 1-2. Independent t-tests and Cohen's *d* effect size were used to compare outcomes between groups.

Results & Discussion: L vs. R vGRF and baseline vs. end SI were similar between runs ($p>0.05$). GCT varied for L vs. R during run 2 ($p=0.023$, $d=-1.02$), and post-hoc testing revealed an increase in R baseline GCT between runs 2-3 ($p=0.034$). These findings support the postulation that some degree of asymmetry may act to increase variability in load distribution [3], thereby reducing RRI risk [2]. Runners tended to increase asymmetry from run 1-2, but whether individual SI continued to increase in run 3 varied in relation to mood state. Mental energy and mental fatigue were significantly correlated during run 1 at baseline ($r=-0.932$, $p=0.001$), at the end of run 1 ($r=-0.839$, $p=0.009$), and during run 2 between baseline energy and post-run fatigue ($r=-0.841$, $p=0.009$). Mental fatigue and mental energy have been defined as separate but related constructs [7], the correlational magnitude of which appeared to decrease with subsequent runs; however, due to incomplete run 3 mood state data for two subjects, we were unable to statistically confirm this. Group-level differences existed between subjects whose baseline mental fatigue increased ($p=0.012$; INC, N=3) vs. those who remained constant (CO, N=5) from run 1-2 ($p=0.003$, $d=-3.5$; Fig. 1), but this change in mental fatigue was not significantly correlated with change in mental energy. Compared to CO, INC had lower run 1 baseline mental fatigue ($p=0.023$, $d=2.2$), longer run 1 duration ($p=0.009$, $d=-2.8$), and greater relative increase in average GRF SI from run 2-3 (i.e., increased asymmetry; $p<0.001$, $d=-6.1$) (Fig. 1). Given that lower mental fatigue may prolong time to exhaustion [8], it is plausible that INC ran longer during run 1 due to lower baseline mental fatigue, but that this greater initial stressor precipitated a larger increase in run 2 baseline mental fatigue and run 3 average GRF SI.

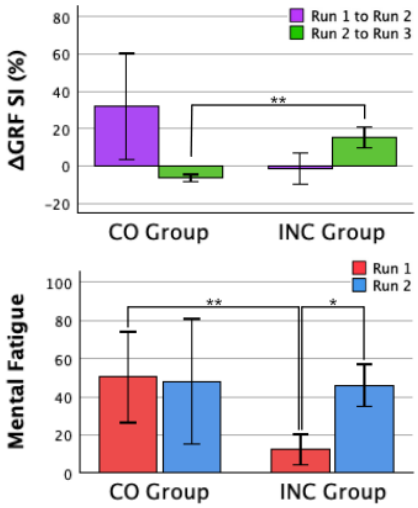

Fig. 1: Group-level comparisons of relative change in ensemble-averaged peak vGRF SI baseline mental fatigue for CO and INC by run. Significance shown at $p \leq 0.05$ (*) and $p \leq 0.01$ (**). Error bars = ±1 SD.

Significance: Runners with significant fluctuations in baseline mental fatigue became more asymmetrical with each run, while those with more stable mental fatigue maintained or increased symmetry. The nature of individual change in symmetry in response to additional days of running may indicate predisposition to a particular type of RRI mechanism; tracking trends in SI and mood state may serve to inform modifications to training load for RRI-rate reduction. Future research should explore whether the magnitude and direction of asymmetry deviation from baseline across runs is a stronger predictor of RRI than baseline asymmetry alone.

Acknowledgments: This study was funded by Brooks Sports, Inc.

References: [1] Zifchock et al. (2006), *J Biomech* 39(15); [2] Bredeweg et al. (2013), *Gait & Posture* 38(4); [3] Hamill et al. (1999), *Clin Biomech* 14(5); [4] Meardon et al. (2011), *Gait & Posture* 33(1); [5] Radzak et al. (2017), *Gait & Posture*; [6] Boolani et al. (2019), *Fatigue* 7(1); [7] Loy et al. (2018), *Med Hypotheses* 113:46–51; [8] Lopes et al. (2006), *Med Sci Sports Exerc*. 52(10).

MECHANISMS FOR INCREASING RUNNING SPEED ON LEVEL GROUND, UPHILL, AND DOWNHILL GRADES

Rachel M. Robinson[1*], Seth R. Donahue[2], Aida Chebbi[1], Michael E. Hahn[1]
[1]Department of Human Physiology, University of Oregon, Eugene, OR, USA
[2]Northwestern University Prosthetics-Orthotics Center, Northwestern University, Chicago, IL, USA
*Corresponding author's email: rrobins3@uoregon.edu

Introduction: When running on level ground (LG), faster submaximal speeds are achieved by increasing stride length, stance phase positive hip and ankle work, and swing phase positive hip work.[1,2] Fewer studies have evaluated the mechanisms for increasing speed when running uphill (UH) and downhill (DH).[3] By evaluating spatiotemporal variables and joint kinetics during stance and swing phases of running, the purpose of this study was to determine whether the mechanical strategies to increase speed are different between LG, UH and DH running. Due to greater changes in step frequency when increasing UH speed, it was hypothesized that increasing UH speed would elicit greater increases in swing phase positive hip flexor work and smaller changes in stance phase work than LG.[4] Due to similar spatiotemporal changes with speed for LG and DH running, no differences were expected between LG and DH strategies.

Methods: Twelve recreational runners (7 female, age: 24.4 ± 7.7 yr., mass: 63.2 ± 10.0 kg, height: 171.0 ± 9.65 cm) completed 30s running trials at 5 speeds on LG, 7.5° UH, and 7.5° DH. Kinematic data were collected at 200 Hz using an 8-camera motion capture system (Motion Analysis Corp.) and kinetic data were collected at 1000 Hz using a force-instrumented treadmill (Bertec). Running speed was based on each participant's self-reported 5k pace. Speed categories were defined as Speed 1 (1:30 min/mile slower than 5k pace), Speed 2 (1:00 min/mile slower than 5k pace), and Speed 3 (:30 min/mile slower than 5k pace), Speed 4 (5k pace), and Speed 5 (:30 min/mile faster than 5k pace). Since not all subjects were able to complete the UH trial at 5k pace, only Speeds 1-3 were analysed. Sagittal hip, knee, and ankle power were calculated using inverse dynamics in Visual 3D (C-Motion, Inc.). Joint work was calculated as the time integral of the of the power-time curves. Positive and negative work for stance and swing phase were calculated separately. Two-way repeated measures ANOVAs (3 grades x 3 speeds) were performed in SPSS (IBM Corp.) to test for within-subject differences in spatiotemporal and joint work variables.

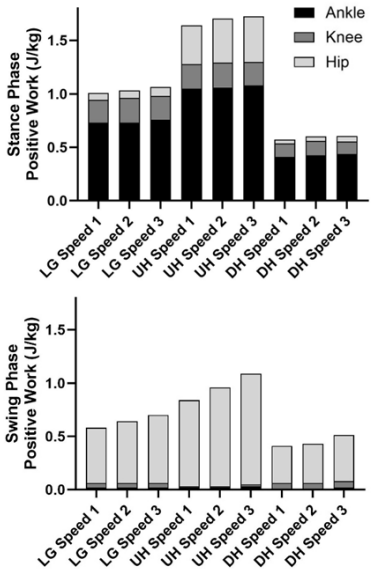

Figure 1: Stance (top) and swing phase (bottom) positive joint work for each speed and grade condition. Error bars omitted for clarity.

Results: The average running velocity for speed categories 1, 2, and 3 were 3.23 ± 0.38, 3.44 ± 0.43, and 3.68 ± 0.49 m/s, respectively. Average stance and swing phase positive joint work for each grade and speed are displayed in Figure 1. The only spatiotemporal variable with a significant interaction effect ($p < 0.05$) was swing time. While swing time was not significantly different between speeds during LG running, swing time was shorter for faster speeds during UH and DH running. Significant main effects of speed ($p < 0.05$) were detected for step frequency, step length, and contact time. No significant interaction effects were observed for stance phase joint work. Significant main effects of speed ($p < 0.05$) were detected for stance phase positive and negative hip work and negative ankle work, all of which increased with speed. Significant interaction effects ($p < 0.05$) were observed for all swing phase joint work variables except for positive knee work. For all grades, increasing speed required greater swing phase positive hip, negative hip, and negative knee work. Swing phase positive hip work increased by 25% on LG, 29% on UH, and 24% on DH from Speed 1 to 3. Swing phase negative hip work increased by 32% on LG, 41% on UH, and 54% on DH from Speed 1 to 3. Swing phase negative knee work increased by 21% on LG, 29% on UH, and 20% on DH. While significant interaction effects were detected for swing phase positive and negative ankle work, the magnitude of these variables was near zero (Fig. 1).

Discussion: A significant interaction effect for swing phase positive hip work with a greater increase during UH running supports our hypothesis. Contrary to our hypothesis and previous work, which reported significant grade-by-speed interaction effects for stance phase work, no significant interaction effects were observed for stance phase kinetics.[3] This difference may be attributed to the previous study's 0.84 m/s difference between test speeds compared to the current study's .21-.24 m/s difference. The significant reduction in swing time while running UH at faster speeds may be a strategy to minimize stance phase energy generation. Rather than generating more energy per step to increase speed, the leg swings forward more quickly to take the next step sooner. Despite the increased positive hip work required to swing the leg during faster UH running, body weight support is more costly than leg swing, and this may be a worthwhile trade-off.[5] Reduced swing time while running DH at faster speeds may reflect participant comfort levels running DH on a treadmill. Participants may limit their step length and contact the ground early if uncomfortable with a steep DH grade, thus limiting swing time.

Significance: This study expands on previous investigations into the combined effects of speed and grade on running mechanics by including swing phase joint kinetics. Understanding the mechanical demands of UH and DH running at common training speeds may guide selection of rehabilitation and training techniques for runners who train or compete on hilly terrain.

Acknowledgments: This work was supported by the Wu Tsai Human Performance Alliance and the Joe and Clara Tsai Foundation.

References: [1] Weyand (2000), *J Appl Physiol* 89; [2] Jin (2018), *Hum Mov Sci* 58; [3] Khassetarash (2020), *Scand J Med Sci Sports* 30(9); [4] Vernillo (2020), *Scand J Med Sci Sports* 30(9); [5] Arellano (2014), *ICB* 54(6)

EFFECTS OF SIX WEEKS OF ROMANIAN DEADLIFT ECCENTRIC TRAINING ON TERMINAL SWING KINEMATICS DURING MAXIMAL SPRINTS

Scott K. Crawford[1,2*], Jack A. Martin[2], Jessica Vlisides[1], Quinlan Thompson[1], Bryan C. Heiderscheit[2]
University of Wisconsin-Madison Departments of [1]Kinesiology and [2]Orthopedics & Rehabilitation
*Corresponding author's email: skrawford2@wisc.edu

Introduction: The negative work performed by the hamstrings during the swing phase of running significantly increases as an athlete nears top end speed [1]. Due to the large excursions and high peak eccentric loads encountered during swing, the hamstrings are also highly susceptible to injury during sprinting [2]. Exercises that eccentrically train the hamstrings may reduce injury risk.

One exercise shown to be effective in reducing hamstring strain injury risk (HSI) is the Nordic hamstring exercise (NHE). The hamstrings are exposed to high eccentric demand during the NHE [3]. However, the NHE typically loads the knee flexors at relatively short muscle lengths, which may not translate to sprint kinematics during late swing. Hip dominant exercises such as the Romanian deadlift (RDL) can load the hamstrings through a full range of motion [4].

The impact of eccentrically biased RDL training (mimicking the NHE) through a full range of motion on improving sprint performance and kinematics has not been described. Joint kinematics acquired during overground sprinting may provide more nuanced data than sprint performance times alone. Inertial measurement units (IMUs) allow for sprint kinematics to be measured on-field where athletes can reach and maintain maximal speed throughout the sprinting duration. Therefore, the purpose of this study is to investigate the effects of a 6-week RDL eccentric training program on terminal swing knee extension and hip flexion during sprinting.

Methods: Eight participants underwent 60 m sprint testing before and after the 6 week RDL training intervention which consisted of twice weekly supervised training sessions. IMUs (Xsens Technologies) were placed on the sternum, sacrum, thighs, legs, and feet. Each participant performed 3 maximal effort trials with 90 seconds rest between trials.

Kinematic data from the fastest trial were exported for analysis in MATLAB. Running speed was determined based on pelvis segment velocity, and kinematic data were cropped to the time in which speed was greater than 90% of the maximum speed during the sprint. Individual strides were identified based on the knee joint angle with foot-ground contact being approximated to occur just after peak knee extension in late swing. Joint angles were normalized to percent gait cycle and averaged across strides for each participant.

Peak hip flexion and knee extension angles during terminal swing (defined as 55-100% of the running cycle) were extracted for each participant. Comparisons of peak knee extension and hip flexion between time points were made using separate linear mixed effects models. Data are presented as least square mean [95% confidence interval].

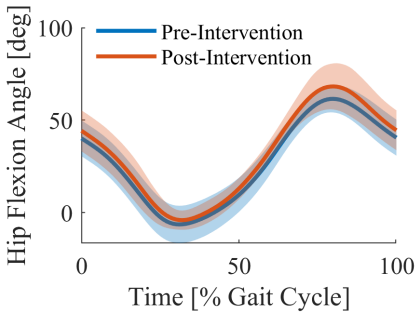

Figure 1: Mean (±SD) hip flexion angle across participants at each time point.

Results & Discussion: The eight participants (2 females) had a mean (standard deviation) age of 23.7 (2.0) years, body mass 71.8 (6.4) kg, height 174.2 (9.4) cm, and body mass index 23.7 (2.0) kg/m^2. Maximum strength in the RDL increased 16.0 (6.5)% after training. There were significant differences between pre- and post-training sprint kinematics in peak hip flexion angle ($p < 0.01$) but not in peak knee extension angle ($p = 0.61$) during terminal swing. Peak hip flexion increased 6.9° [2.1, 11.6] (Fig. 1) whereas peak knee extension had changes of -0.6° [-3.1, 1.9] following the eccentric training.

Previous work calculated minimal detectable changes (MDC) of 3.7° and 5° for peak hip flexion and knee flexion, respectively, during submaximal treadmill running (3.2 m/s) [5]. Moreover, a fatiguing protocol induced reductions in peak hip flexion of 2.1° with a large effect size associated with this value (Cohen's d = 0.97) [6]. Though direct comparisons of MDC between submaximal and maximal running should be interpreted with caution, our results suggest increases in peak hip flexion angle are both indicative of true change and of meaningful magnitude.

These findings indicate that eccentric training with the RDL through a full range of motion may induce kinematic changes during terminal swing of maximal sprinting. Increased hip flexion without changes in knee extension during terminal swing induces greater proximal hamstrings stretch. Previous investigations have suggested hip-dominant exercises target the often-injured biceps femoris long head (BFlh) muscle and greater hip flexion increases stretch in the BFlh during running [1, 4]. This stretch coupled with high activation of the hamstrings in terminal swing [1, 7] may indicate participants are better able to handle the high negative work in this phase of the sprint and changes in kinematics are exercise-specific [8]. Larger sample sizes and different exercises (e.g., NHE) are needed to confirm our findings.

Significance: Preliminary findings suggest eccentrically biased RDL training can induce meaningful changes in hip and knee kinematics during sprinting. Future work will investigate if changes in hip and knee kinematics are dependent upon specific eccentric exercises.

Acknowledgments: Funding provided by the Wisconsin Alumni Research Foundation and Clinical and Translational Science Award Program, through the NIH National Center for Advancing Translational Sciences, grant UL1TR002373 and KL2TR002374 (SKC).

References: [1] Chumanov ES et al (2007). *J Biomech* 40:3555–3562. [2] Ekstrand J et al (2022). *Br J Sports Med* 6:292–298. [3] Van Dyk N et al (2019). *Br J Sports Med* 53:1362–1370. [4] Bourne MN et al (2017). *Br J Sports Med* 51:1021–1028. [5] Bramah C et al (2021). *Gait Posture* 85:211–216. [6] Wilmes E et al (2021). *Med Sci Sports Exerc* 53:2586–2595. [7] Van Den Tillaar R et al (2017). *Int J Sports Phys Ther* 12:718–727. [8] Chumanov ES et al (2011). *Med Sci Sport Exerc* 43:525–32.

COMPARING SAGITTAL PLANE RUNNING KINEMATICS BETWEEN TRAIL AND ROAD SURFACES IN MAXIMAL AND TRADITIONAL FOOTWEAR

J.J. Hannigan[1*], Megan Dailey[1], Collier Lawrence[1], Christa Shipman[1], Zivit Spector[1], Kathy Reyes[2]
[1]Program in Physical Therapy, College of Health, Oregon State University – Cascades, Bend, OR USA
[2]Program in Kinesiology, College of Health, Oregon State University, Corvallis, OR USA
*Corresponding author's email: jj.hannigan@osucascades.edu

Introduction: Trail running participation has increased by over 200% over the past 10 years [1]. However, approximately 40% of trail runners incur a running-related injury each year, with ankle sprains being the most common [2]. This suggests that running surface appears to play a factor in running injury risk, as ankle sprains are far less common during road running [2]. While trail running injuries appears to be associated with technical terrain, a high number of ankle sprains were still reported on smooth, groomed trail surfaces, suggesting that trail technicality is not the only factor in trail running injury risk.

Footwear is also likely an important consideration in trail running injury prevention, as cushioning was identified as the most important aspect of trail shoe design among injured and uninjured runners [2]. Maximal running shoes, loosely defined by higher midsole stack height than traditional shoes, have recently increased in popularity among road and trail runners. However, maximal running shoes may affect ankle kinematics [3], potentially increasing the risk of developing a running-related injury.

No research to date has explored the effect of surface and shoe type on trail running biomechanics. Due to the increased trail running participation, as well as the potential effect of running surface and shoe on trail running injury rates, investigating the effect of running surface and shoe on trail running biomechanics appears warranted. Therefore, the purpose of this study was to compare running kinematics between trail and road surfaces in a maximal and traditional shoe. Based on previous research [3], it was hypothesized that runners would display significantly less dorsiflexion at initial contact in the maximal shoe condition on both surfaces, but that sagittal plane knee and hip kinematics would be unaffected by shoe or surface.

Methods: Seven healthy distance runners have participated in this study to date (6F, 1 M). Each participant ran 5 trials at their easy run pace on a paved trail surface, and 5 trials on a single-track crushed gravel trail surface at a local park. Participants wore either a maximal shoe (Hoka Bondi v7) or traditional shoe (New Balance 880 v11) for these initial 10 trials, and then switched to the other shoe condition for 5 additional trials per surface.

Kinematic data for this study was collected using markerless motion capture. Ten Sony RX0 II cameras were positioned around these adjacent trail surfaces. Each camera was connected to a PoE switch and laptop computer, and synchronized using Sony control boxes. Video data was synchronously collected from each camera at 120 Hz using the Sony web portal. Raw video data was then processed with Theia3D software (Theia Markerless), which uses 3D pose estimates from the synchronized video data to compute lower limb joint angles. Kinematic data were smoothed in Theia3D using a 12 Hz GCVSPL filter and then exported to Visual3D for final analysis. Based on currently available reliability data, this investigation focused on sagittal plane hip, knee and ankle kinematics (angle at initial contact, peak angle, angular excursion). This data was compared using a 2x2 repeated measures ANOVA to investigate the effect of surface and shoe ($\alpha = .05$)

Results & Discussion: At the hip, no interaction effects nor main effect of shoe was noted ($p > .05$). For the main effect of surface, the hip flexion angle at initial contact was significantly higher on the trail surface compared to the road surface (road: 33.2 ± 2.7°, trail: 36.1 ± 2.4°, $p < .001$), while hip extension excursion was significantly higher on the trail surface compared to the road surface (road: 46.0 ± 2.7°, trail: 48.1 ± 4.5°, $p = .004$),

At the knee, there was a main effect of surface on the knee flexion at initial contact, with the trail surface higher than the road surface (road: 17.6 ± 3.5°, trail: 19.7 ± 5.2°, $p = .039$). An interaction effect was also noted for knee flexion excursion ($p = .022$), which was significantly higher on the road surface (27.2 ± 4.4°) compared to the trail surface (23.9 ± 5.3°) in the maximal shoe condition. No significant interaction effects, nor main effect of surface or shoe, were noted for any measure of sagittal plane ankle kinematics ($p > .05$).

The differences in angle at initial contact and angular excursion at the hip and knee in the sagittal plane may suggest different limb stiffening strategies between trail surfaces. While the angle at initial contact was higher on the trail surface at both the hip and knee, opposite effects were observed for excursion. At the hip, excursion was higher in the trail condition, while at the knee, excursion was higher in the road condition, albeit only in the maximal shoe condition.

Significance: Trail runners are injured at very high rates with different injury distributions compared to road runners [2]. While trail technicality may be a factor, trail running injuries also occur frequently on flat, groomed surfaces, suggesting that other factors may be related to injury risk. The current results from this preliminary study suggest that sagittal plane hip and knee kinematics may be affected by trail surface, which is worthy of further investigation. However, the most common injury in trail runners appears to be at the ankle, where no differences in sagittal plane kinematics were observed. Future studies should investigate frontal plane ankle kinematics during trail running, although this measure is complicated by lower reliability during markerless motion capture.

Acknowledgments: The authors would like to acknowledge Shea Hasselbach for her assistance with data collection and processing.

References: [1] Andersen (2022), *The State of Trail Running*; [2] Hamill et al. (2022), *Foot Sci* 14(2); [3] Hannigan & Pollard (2019), *Am J Sport Med* 47(4).

EFFECTS OF CHANGING FOOT-GROUND STIFFNESS ON STANDING WEIGHT BEARING ASYMMETRY

Mark Price[1,2*], Calder Robbins[1], Banu Abdikadirova[1], Wouter Hoogkamer[2], Meghan E. Huber[1]
[1]Department of Mechanical and Industrial Engineering, University of Massachusetts Amherst
[2] Department of Kinesiology, University of Massachusetts Amherst
*Corresponding author's email: mprice@umass.edu

Introduction: Maintaining standing balance is a challenging task for people who have suffered central nervous system damage, such as from a stroke. This commonly manifests as uneven distribution of weight on the lower limbs [1,2], less synchronized balance control between limbs [3], and increased body sway during quiet standing [1]. These deficiencies are correlated with a higher tendency to fall due to weaker balance control [3]. Conventional stroke rehabilitation has struggled to improve standing balance, even as improvements are made in other measures such as walking speed and step length symmetry [1].

A potential method for altering standing balance behavior may be controlling the foot-ground interaction dynamics via adjustable stiffness. As asymmetric perturbations have been demonstrated to elicit neuromotor adaptation such as with split-belt walking [4], we propose that similar adjustments in weight-bearing symmetry during standing may be made by asymmetrically perturbing the stiffness of the interface between the foot and the ground. To study this effect, we developed robotic footwear in which the foot-ground interface stiffness can be adjusted independently under each foot. We hypothesized that lowering the stiffness under one foot during standing would cause neurologically intact human participants to increasingly bear more weight on the more rigid side as the perturbation continued (H1), and that this effect would be sustained when stiffness was increased again (H2).

Methods: The variable stiffness sole consists of a soft 3D printed mesh housed inside a flexible pressurized plastic air pocket (Fig 1a). Pressure is controlled with a pneumatic system consisting of a microcontroller (Arduino Pro Mini), pressure storage tank, control solenoids, and pressure sensors. Approximate linear stiffness for the loading region experienced in this study is mapped to controlled pressure states from data collected on a force-sensing mechanical testing machine (Instron).

We recruited 5 adults (age: 27.4±7.4 years; height: 169±6 cm; weight: 75.6±10.4 kg) without musculoskeletal or neurological injury or disorder to participate in this study. Participants stood with 17 cm between their heels and a 14° angle between the long axes of their feet [5]. Each foot rested on a separate force plate (AMTI) recording 3D ground reaction forces at 1920 Hz. A variable stiffness sole was fitted to the participant's left foot and a height-matched rigid sole was fitted to their right foot, each over their own shoes. Participants were instructed to stand still and watch a fixed point on the wall for five minutes. We controlled stiffness under their left foot to maintain approximately 50 kN/m for 60 s, then triggered a stiffness change to approximately 18 kN/m, which was maintained for 120 s before increasing back to 50 kN/m again for the remaining 120 s. Each transition took place over ~10 s before the new stiffness stabilized. We calculated weight bearing asymmetry as the ratio of the difference between rigid and variable stiffness vertical ground reaction forces and their sum: $(vGRF_V - vGRF_R)/(vGRF_V + vGRF_R) \times 100\%$. We calculated the average of this ratio over 5 s windows at the end of the initial high stiffness setting (Baseline), the start and end of the low stiffness setting (Perturbation-Early and Perturbation-Late), and the start of the final high stiffness setting (Aftereffect), not including the first 10 s while stiffness was in transition. We performed a repeated measures ANOVA to evaluate the effect of stiffness condition (Baseline, Perturbation-Early, Perturbation-Late, Aftereffect) on weight bearing asymmetry. Planned comparisons in the form of paired t-tests on were used to further evaluate our hypotheses (H1: Perturbation-Early vs Perturbation-Late; H2: Baseline vs Aftereffect).

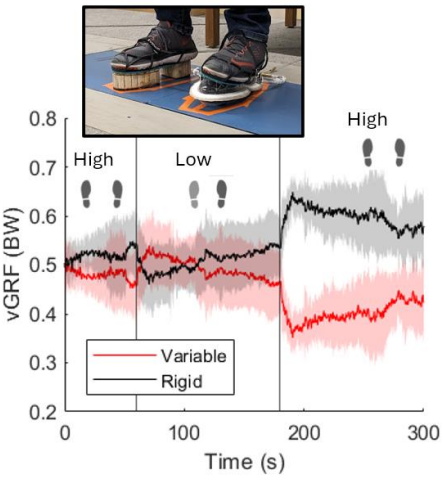

Figure 1: Top: Adjustable stiffness footwear prototype worn next to a height-matched rigid sole on force plates used to capture GRF data. Bottom: Vertical ground reaction force (mean ± SD) for each foot, averaged across participants. Vertical lines indicate a change in stiffness state in the controllable sole.

Results & Discussion: Changing stiffness had a significant effect on weight bearing asymmetry ($p = .0005$). Weight bearing shifted toward the rigid side from Perturbation-Early to Perturbation-Late (Mean difference: -13.2%, $p=.079$) and weight bearing favored the rigid side during the Aftereffect condition relative to Baseline (Mean difference: -18.5%, $p = .028$). Group mean rigid and variable stiffness vGRF over time are illustrated in Fig 1b with stiffness transitions marked. Interestingly, the size of the aftereffect exceeded the perturbation response. Both comparisons support our hypotheses, though the comparison evaluating H1 did not achieve $p<.05$ and will require further investigation with more participants. It is also not clear that changes in weight-bearing have stabilized after 2 minutes, and future experiments may require longer exposures to allow participants to fully adapt.

Significance: These results show that changing foot-ground stiffness during quiet standing can elicit changes in weight bearing strategy during and after the perturbation, suggesting that neuromotor adaptation has occurred. An intervention which can elicit an 18% shift in weight bearing toward one side post-exposure is highly promising for correcting weight-bearing asymmetry. This finding demands further study: do these changes occur in people after stroke, and do they persist with repeated training?

References: [1] Roelofs et al. (2018), *Neurorehabil Neural Repair* 32(11); [2] Genthon et al. (2008), *Stroke* 39(6); [3] Mansfield et al. (2012), *Neurorehabil Neural Repair* 26(6); [4] Reisman et al. (2007), *Brain* 130(7); [5] McIlroy & Maki (1997), *Clin Biomech* 12(1).

DETAILED GAIT KINEMATICS FROM A SINGLE WEARABLE SENSOR: COMPARING FOUR ANKLE-FOOT PROSTHESES IN FREE-LIVING, UNSUPERVISED NEIGHBORHOOD WALKS

Katherine Heidi Fehr[1], Yisen Wang[1], Jennifer Nicole Bartloff[1], Julian C. Acasio, Brad D. Hendershot, Peter G. Adamczyk[1]
[1] Mechanical Engineering Department, University of Wisconsin–Madison, Madison, WI
*Corresponding author's email: kfehr@wisc.edu

Introduction: Following a lower-limb amputation, selecting a suitable prosthetic foot is critical. Objective data is needed to inform clinical decision-making when prescribing an appropriate prosthesis. Most existing studies on device performance are conducted in controlled lab environments—the few that take place outside the lab and are often low-resolution activity estimates [1]. Here, we developed a method to use data from a single prosthesis-mounted sensor and personalized 3D scan to obtain real-world, detailed gait kinematics. In this case study, we compare gait outcomes of a person with transtibial amputation in the real-world during unsupervised neighborhood walks while using prostheses with different features that could affect foot clearance and swing phase kinematics.

Table 1: Summary statistics of key measures of gait kinematics (mean ± s.d.)

	N	MFC	N	WS	SL	SWV	MTX	SWD
units	*count*	*mm*	*count*	*m/s*	*m*	*mm*	*mm*	*score*
LP	673	12.4 ± 5.6	488	1.15 ± 0.04	1.21 ± 0.06	56.0	-56.1 ± 72.1	40
ES	844	15.2 ± 6.9	791	1.08 ± 0.03	1.27 ± 0.06	64.6	-49.4 ± 80.0	39
HA	1046	10.2 ± 7.9	815	1.09 ± 0.03	1.27 ± 0.07	68.4	-72.3 ± 83.8	35
MP	390	21.1 ± 6.4	217	1.15 ± 0.05	1.24 ± 0.07	43.0	-56.7 ± 53.9	29

Methods: One female with unilateral transtibial amputation (age: 44 yrs, time since amputation: 27 yrs, body mass: 71 kg) used four prostheses in everyday life for one week at a time, each outfit with a single sensor: (1) low-profile carbon fiber foot (LP), (2) c-shaped energy storage and return foot (ES), (3) foot with an articulating hydraulic ankle (HA), and (4) microprocessor-controlled damper at the ankle (MP). To have a comparable data set, we used GPS to extract one spontaneous neighborhood walk with each foot from the participants' month-long data collection. Each walk was in the same neighborhood along a similar path. To extract key gait kinematics, we first reconstructed the prosthesis-mounted IMU trajectory [2] and combined it with data from a 3D scan of each corresponding prosthesis (Figure 1). We then calculated minimum foot clearance (MFC), defined as the shortest vertical distance between the shoe—considering all the points from the scan (Figure 1)—and walking surface during forward swing phase. By dividing the points posteriorly and anteriorly, we also calculated minimum hindfoot and forefoot clearance. Stride length (SL) and stride width variability (SWV) were determined [3], defining forward and lateral foot placement as the position of the IMU at each stance phase relative to the local forward direction (best-fit line in a centered moving window of seven strides). Using the position of the toe from the 3D scan, we measured the maximum toe excursion (MTX)—the maximum orthogonal distance between the toe trajectory and the afore-described best-fit line. To further interpret these measures, walking speed (WS) was calculated on a stride-by-stride basis by dividing SL by elapsed time. In addition, the participant scored each foot after the week of use with a "Satisfaction with Device" survey (SWD) [4].

Results & Discussion: MFC was highest when using the MP foot, suggesting a gait less prone to trips. When using the HA foot, MFC was lowest (Figure 1), contrary to the expected behavior of the ankle "lifting" the toes during swing. Use of the MP foot also resulted in the lowest SWV and MTX deviation, which may reflect improved stability [5]. The participant also walked fastest wearing the MP foot (tied with LP); generally, faster self-selected walking speed is positively correlated with functional ability [6]. Based on the SWD score, the participant preferred LP, which coincided with faster walking speed, reduced SWV, and near-average SL deviation and MTX performance (in comparison to the other prostheses). While excelling in many kinematic measures, MP received the lowest SWD score.

Significance: The proposed method offers a multi-dimensional understanding of the participant's gait with each prosthesis. This work demonstrates the potential of a (singular) sensor-based approach for gaining a rich understanding of gait with different prostheses in real-world environments, helping inform prosthetic prescription practices. Additional analyses across multiple environments and terrains, repeated paths, and days of adaptation will further improve the richness of these findings.

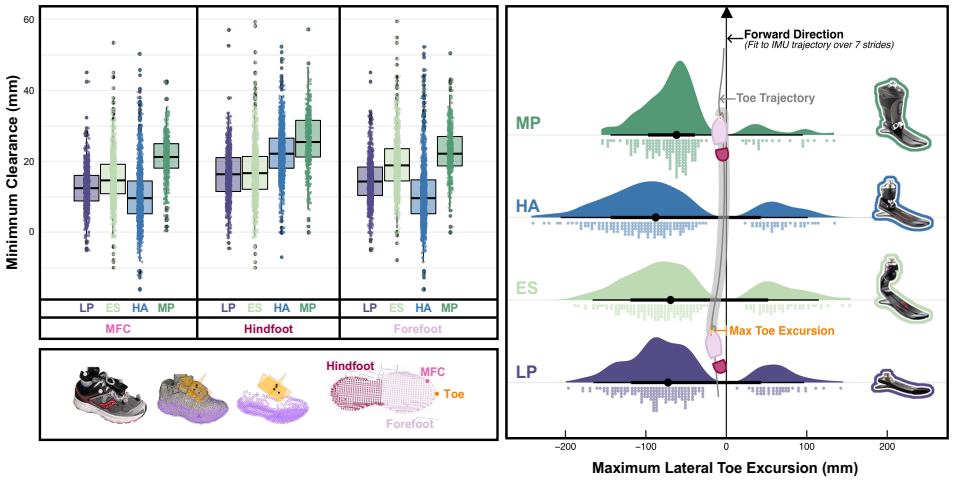

Figure 1: Minimum clearance of the whole-foot, hindfoot and forefoot with each prosthesis, note that some MFC values are negative due to a rigid body assumption made when fusing the IMU reconstruction with the 3D scan (top left), illustration of the 3d scan to whole-foot trajectory reconstruction (bottom left), and maximum lateral toe excursion with each prosthesis.

Acknowledgments: Supported by award W81XWH-19-2-0024. Views do not reflect official policy of nor implied endorsement by the DoD or US Government.

References:

[1] Raschke (2015), *J. Biomech* **[2]** Wang et al. (2024), *Sensors* **[3]** Ojeda et al. (2015), *Med. Eng. Phys.* **[4]** Heinemann et al. (2003) *Prosthet. Orthot. Int.* **[5]** Collins et al. (2013), *PLOS ONE* **[6]** Fritz et al. (2009), *J Geriatr. Phys. Ther.*

A MODEL ON OPTIMIZING THE DESIGN AND SIMULATING THE STIFFNESS, ROLL-OVER SHAPE, AND EFFECTIVE ALIGNMENT OF A SEMI-ACTIVE TWO-KEEL VARIABLE STIFFNESS PROSTHETIC FOOT

Zhengcan Wang[1*], Peter G. Adamczyk[1]
[1]Department of Mechanical Engineering, University of Wisconsin–Madison, Madison, WI 53706, USA
*Corresponding author's email: zwang2272@wisc.edu

Introduction: The adaptability of current commercial lower-limb prostheses (prosthetic feet) is still not satisfactory, lacking in comfort and overall effectiveness. This is mainly constrained by the fact that most commercial prosthetic feet are passive, having constant shape and mechanical characteristics. And the high cost, weight, height, and power of some microprocessor-controlled active protheses limit their adoption by lower-limb prothesis users. To improve the user's experience and reduce complexity and cost, based on the original one-keel design [1], we propose a semi-active Two-Keel Variable Stiffness Prosthetic Foot (VSF-2K), where the stiffness of the forefoot keel and hindfoot keel can be modulated through a motor-actuated moving fulcrum during the swing phase of walking. In this study, we develop a simulation model for the VSF-2K to: (1) optimize the design of the keels to reduce the overall stiffness, as a less stiff prosthesis provides more energy return and a greater range of motion [2]; and (2) simulate the stance phase of walking on level ground with the optimal VSF-2K, at different stiffness settings and ankle alignment angles. We analyze the effects of hindfoot and forefoot stiffness modulation on the prosthetic characteristics—hindfoot, forefoot, and vertical stiffnesses, roll-over shape (ROS), and effective alignment—as outputted by the model. A previous study showed that varying the stiffness of the hindfoot and forefoot components has similar effect to changing the alignments [2]. However, all these effects are primarily empirical and experimental. A theoretical understanding of design – stiffness – alignment interaction is crucial for the practical application of the semi-active prosthetic foot's adaptability. Therefore, we also aim to show that nonzero alignment can be emulated by the change in stiffness.

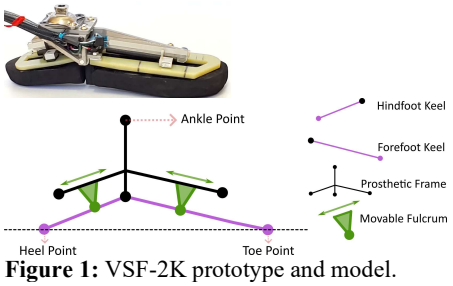

Figure 1: VSF-2K prototype and model.

Methods: The model consists of two submodels: the Design Optimization Model and the Rollover Model. Fig. 1 shows the simplified model of the VSF-2K. The two keels of the VSF-2K are modelled as overhung beams, as shown in Fig. 2. In the Design Optimization Model, we use Euler-Bernoulli beam theory to calculate and maximize the deflection (thereby decreasing the stiffness) of the VSF-2K's keels, by inputting five design parameters (Fig. 2) and calculating the width profile to ensure the design remains within the Flexural Strength of the material (Gordon Composites-67-UBW). We designed for the worst-case scenario, where a high load (1200 N) is applied at the toe/heel, and the fulcrum is at its maximum displacement.

In the Rollover Model, we utilize the load-angle profile (from heel-strike to toe-off) provided by ISO 22675:2016 as the input for vertical load and shank angle. We use Euler-Bernoulli beam theory again to simulate a single step over level ground with the VSF-2K at various stiffness settings and plantarflexed, neutral, and dorsiflexed ankle alignment, identifying the contact point of load for each keel at each shank angle, i.e., the point where the keel becomes tangent to the ground. There are three stages: (1) heel-only, (2) foot-flat, and (3) toe-only contact. First, boundary ankle angles for these three stages are found through geometric analysis. Second, we divide foot-flat into two parts: (2.1) the initial half, ending when the loads on the hindfoot and forefoot equalize, and (2.2) the latter half, ending when the heel lifts off the ground. Third, we assume the heel is stationary at stage (1) and (2.1), and the toe is stationary at stage (2.2) and (3).

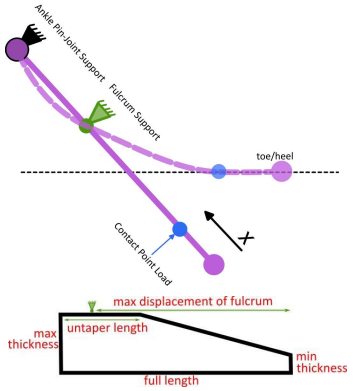

Figure 2: (1) Overhung beam (keel). (2) Front view of the keel.

Results & Discussion: For a specific stiffness setting and alignment of VSF-2K, there are four sets of results from this simulation model: (1) the optimal design, (2) stance phase animation, (3) the ROS, and (4) the heel (ankle angle -15°), toe (angle +20°), and vertical (angle 0°) stiffnesses, similar to standard tests [3]. Fig. 3 shows a pilot result relating roll-over shape and stiffness settings. By changing stiffnesses, the VSF-2K can alter the ROS radius or center position to compensate for nonzero-alignment; this capability could be used to adapt to sloped terrain, as the natural leg does [4].

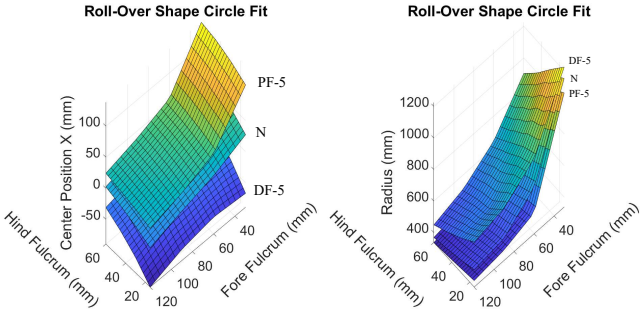

Figure 3: The center position (left) of the ROS circle fit and the radius (right) when ankle alignment is: dorsiflexion 5° (DF-5) – neutral 0° (N) – plantarflexion 5° (PF-5).

Significance: This semi-active prosthesis bridges the gap between passive and active prostheses by adding adaptability while maintaining low height, weight, power, and cost. The model provides a theoretical foundation for understanding how a bending-beam prosthetic foot interacts with the ground and the interplay among design, stiffness, and alignment. The model will also inform control laws for modulating the prosthesis's stiffness during walking over different terrains.

Acknowledgments: Supported by award W81XWH-19-2-0024. Views do not reflect official policy of nor implied endorsement by the DoD or US Government.

References: [1] Glanzer+ 2018 *TNSRE*; [2] Adamczyk+ 2017 *HMS*; [3] AOPA 2010 *Prosth. Foot Proj.*; [4] Hansen+ 2004 *HMS*.

FOOT-ANKLE BIOMECHANICS IN TRANSTIBIAL PROSTHESIS USERS WALKING WITH PROSTHETIC FEET AND CORRESPONDING EMULATED PROSTHETIC FEET

Tyler K. Ho[1*], Elizabeth G. Halsne[1,2], Talia R. Ruxin[1], David C. Morgenroth[1,2]
[1]Center for Limb Loss and MoBility, VA Puget Sound Health Care System, Seattle, WA
[2]University of Washington, Seattle, WA
*Corresponding author's email: tyler.ho@va.gov

Introduction: Selecting an optimal prosthetic foot is an important aspect of maximizing mobility for people with lower limb loss (LLL) [1]. The mechanical properties of prosthetic feet vary across models, yet patients with LLL cannot typically trial different prosthetic feet due to cost and time constraints [2]. A robotic prosthetic foot emulator (PFE) may provide an opportunity for prosthesis users to quickly compare walking with different prosthetic feet in the lab or clinic by mimicking the sagittal-plane mechanical properties of commercially available prosthetic feet [3]. While previous work demonstrated strong agreement between the angular stiffness properties of *Actual* feet and corresponding *Emulated* feet during mechanical testing [4], it is unknown whether this agreement extends to foot-ankle biomechanical outcomes of prosthesis users during walking. Therefore, this study aimed to investigate how the foot-ankle biomechanics of prosthesis users walking with *Actual* and *Emulated* feet compared and, secondly, whether users could correctly identify the *Emulated* feet. We hypothesized that there would be no significant differences in prosthetic foot rollover radius, prosthetic foot-ankle peak power and positive work, step length asymmetry, or step time asymmetry between *Actual* and *Emulated* prosthetic feet.

Methods: Participants: 10 males (50.6±13.9yrs, 102.3±9.7kg, 1.80±0.50m) with unilateral transtibial amputation were recruited and provided informed consent for participation in this IRB-approved study. Procedures: Participants completed two randomized bouts (*Actual* or *Emulated* feet) of treadmill walking trials, with three prosthetic foot type conditions (i.e., Fillauer All-Pro, Rush HiPro, Össur Vari-Flex) randomized within each bout. Participants were blinded to prosthetic foot type throughout study procedures and had accommodated to each *Actual* and *Emulated* foot during previous study visits. Participants trialed each *Emulated* and *Actual* foot by walking on a level, instrumented split-belt treadmill (AMTI; 1200Hz) at a self-selected comfortable walking speed for several minutes. The last 30 seconds were recorded with a 16-camera motion capture system (Vicon Nexus; 120 Hz) using a modified Vicon Plug-In Gait model marker set. After walking trials were completed with all six feet, participants were asked to determine which *Emulated* feet they thought corresponded with each of the *Actual* feet. Data Analysis: Kinematic and kinetic data were passed through a 4th-order Butterworth filter with a cut-off frequency of 6Hz. All biomechanical outcomes were calculated within Visual3D, including using the unified deformable model for prosthetic foot-ankle power, and exported for analysis. Linear mixed-effects regression was used to estimate within-participant differences by condition (*Actual* vs *Emulated*), foot type, and condition*foot type interaction, using Dunn-Sidak correction for multiple comparisons.

Results & Discussion: There was a significant difference in *Emulated* - *Actual* prosthetic foot rollover radius for All-Pro (-3.8±1.4cm) and Vari-Flex (4.8±1.1cm) feet ($p<0.001$). Significant *Emulated* - *Actual* differences were also found in peak ankle push-off power and ankle work for Rush (0.38±0.08W/kg; 0.033±0.005J/kg) and Vari-Flex (0.32±0.09W/kg; 0.039±0.008J/kg) feet ($p<0.001$) (Fig. 1). These differences in foot-ankle biomechanics between *Emulated* and *Actual* feet may be explained by the limitations of our mechanical testing methods. Since we tested each foot only at one fixed angle (i.e., +20°) [5], the feet may have flexed more during loading than they would during typical physiological loading. Thus, the range of motion of *Emulated* feet during mid-to-late stance may have been greater than that of *Actual* feet. Despite these biomechanical differences between *Emulated* and *Actual* feet, we found no differences in step length or step time asymmetry. Additionally, nine out of the ten participants were able to correctly match all three *Emulated* feet to the corresponding *Actual* feet (one participant misidentified the Rush and Vari-Flex feet). These results indicate that the PFE foot profiles may still be distinct enough for prosthesis users to differentiate between foot types despite differences in foot-ankle biomechanics.

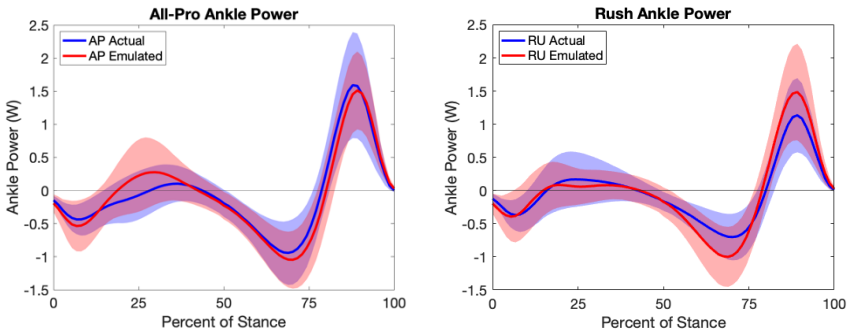

Figure 1. Prosthetic foot-ankle power across stance phase for *Actual* (blue) and *Emulated* (red) feet averaged across participants walking on All-Pro feet (left) and Rush feet (right).

Significance: A PFE may provide an efficient way for prosthesis users to "test drive" several prosthetic feet and allow them to determine their preferences during clinical foot selection. To improve the agreement between the foot-ankle biomechanics of prosthesis users walking with the PFE compared to actual feet, future work should characterize the angular stiffness of prosthetic feet over an entire heel-to-toe rollover and should expand activities beyond level ground walking.

Acknowledgments: This study was funded by an Orthotic and Prosthetic Education and Research Foundation Fellowship Award (E.G. Halsne). Special thanks to Jane Shofer, who performed the statistical analysis for this study.

References: [1] Versluys R, Disabil Rehabil. 4(2):65-75, 2009; [2] Schaffalitzky E, Disabil Rehabil. 3(4):285-94, 2012; [3] Caputo, J, J Biomech Eng, 136(3):035002, 2014; [4] Halsne, EG, J Biomech Eng. 144(11), 2022; [5] ISO 22675:2016a

SOFT WEARABLE ROBOT IMPROVES ARM REACHABLE WORKSPACE FOR INDIVIDUALS WITH ALS

Prabhat Pathak[1], James Arnold[1], Katherine Burke[2], Carolin Lehmacher[1], Connor McCann[1], Yichu Jin[1], Tanguy Lewko[1], Sarah Cavanagh[1], David Pont-Esteban[1], Kelly Rishe[3], John Paul Bonadonna[1], David Lin[3], Sabrina Paganoni[2], Conor Walsh[1*]
[1]John A. Paulson School of Engineering and Applied Sciences, Harvard University, Cambridge, MA, USA
[2]Neurological Clinical Research Institute, Massachusetts General Hospital, Boston, MA, USA
[3]Department of Neurology, Massachusetts General Hospital, Harvard Medical School, Boston, MA, USA
*Corresponding author's email: walsh@seas.harvard.edu

Introduction: Amyotrophic lateral sclerosis (ALS) is a neurodegenerative disease that leads to upper-extremity muscle atrophy and weakness, reducing the reachable workspace of the arm [1]. Offloading the arm against gravity around the shoulder joint, the largest torque-bearing upper-extremity joint, has been proven to be an effective strategy for increasing reachable workspace by improving distal and proximal joint function and movement quality [2]. Recently, our team developed a soft inflatable wearable robot that uses a pneumatic actuator placed under the arm to lift it against gravity and demonstrated its efficacy in improving functional arm use and proximal joint (i.e., shoulder and trunk) movement quality for individuals with ALS [3]. However, we did not assess the efficacy of the wearable robot in extending the area in front of their body where they can functionally use their distal joints, which is essential to effectively perform functional tasks [4]. To this end, we aim to evaluate the efficacy of a soft inflatable wearable robot in increasing reachable workspace and distal joint range of motion (ROM) and reducing pathological joint compensation.

Methods: Two individuals living with ALS were recruited to participate in the study. The two participants (P1 and P2) were 59 and 54-year-old women who were diagnosed with ALS 10 and 25 months before the study, respectively. We used a soft inflatable wearable robot to offload each participant's arm weight, using a textile actuator that is attached to a custom-made shirt and control unit that can be worn by the participants. The robot utilizes signals from inertial measurement units (IMUs) and capacitive deformation sensors attached on the upper limb to decode residual shoulder movement and tune the level of assistance to the arm.

To assess reachable workspace [2], we asked the participants to elevate their arm and simulate drawing the largest possible circle in front of them, while keeping their arm parallel to the ground three times each and repeated this procedure with the robot on and off. We used an optical motion capture system to track upper-limb movement and quantified the reachable workspace by calculating the area within the region drawn by the hand center of mass (COM) trajectory in the horizontal plane, i.e., in anterior posterior (AP) and medial lateral (ML) directions. We calculated elbow flexion/extension range of motion (ROM) to evaluate the distal function and calculated the displacement of trunk COM trajectory in the horizontal plane to evaluate trunk compensation.

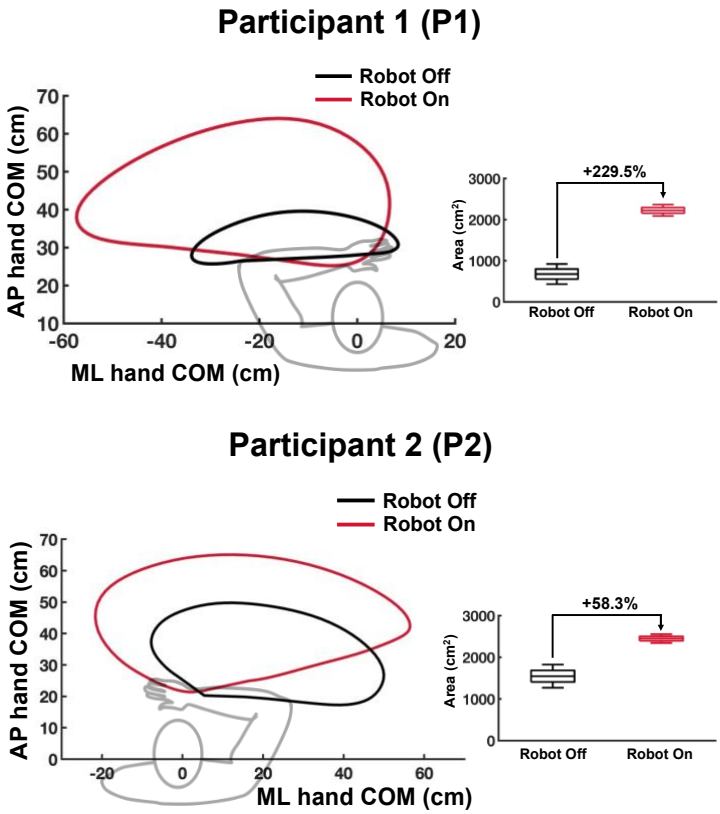

Figure 1: Changes in the reachable workspace area for two individuals living with ALS (P1 and P2) using a soft inflatable wearable robot.

Results & Discussion: We found that the soft inflatable wearable robot, on average, increased horizontal plane workspace area for both P1 and P2 by 229.5 and 58.3%, respectively (Fig. 1). The larger improvement for participant with a smaller workspace area indicates the effectiveness of the wearable robot might be dependent on participant's baseline functional level. Additionally, the wearable robot improved the distal joint function for both participants by increasing the elbow flexion/extension ROM for P1 and P2, on average, by 48.7º and 36.0º, respectively. Furthermore, the robot alleviated pathological trunk compensation by reducing the displacement of trunk COM trajectory for P1 and P2, on average, by 27.5 and 58.0%, respectively.

Significance: Considering the efficacy of the soft wearable robots in improving functional arm use for individuals with ALS over larger workspace, we expect our technology to be beneficial in increasing the ability to perform functional tasks with improved movement quality over larger reachable workspace for individuals with ALS.

Acknowledgments: This study was supported by the National Science Foundation under Awards No. 2236157 and 2345107.

References: [1] Oskarsson et al. (2016), *Muscle Nerve* 53(2); [2] Simpson et al. (2020), *IEEE Trans. Med. Robot. Bionics* 2(3); [3] Proietti et al. (2023), *Sci. Transl. Med.* 15(681); [4] Michaelsen et al. (2004), *Exp. Brain Res.*. 157.

EVALUATION OF A SHARED CONTROLLER FOR OBSTACLE AVOIDANCE OF A BALLBOT WHEELCHAIR

Yu Chen[1], Mahshid Mansouri[1], Ze Wang [1], Chenzhang Xiao[1], João Ramos[1], Elizabeth T. Hsiao-Wecksler[1], and William R. Norris[2]*
[1]Mechanical Science & Engineering, University of Illinois at Urbana-Champaign
[2] Industrial & Enterprise Systems Engineering, University of Illinois at Urbana-Champaign
*Corresponding author's email: wrnorris@illinois.edu

Introduction: Our group has developed a novel self-balancing, riding ball-based robot called PURE (Personalized Unique Rolling Experience) as a revolutionary mobility device for manual wheelchair users [1]. PURE features omnidirectional motion and compact form, enabled by its ballbot drivetrain. The Torso-Dynamics Estimation System (TES), based on an IMU and custom force plate, allows the rider to use torso motions (lean/twist) to intuitively control direction and speed [2]. The device's maneuverability and under-actuated dynamics pose challenges for obstacle avoidance and estimating braking distances and timings, especially for novice users in congested areas. Therefore, a shared-control (S-C) scheme between rider and robot was developed to minimize collision risks and enhance rider's safety and performance. Tests were conducted to understand how and to what extent the S-C scheme can assist users, and to compare its performance to the no S-C case. The study hypothesized that the proposed shared controller could accommodate users with various torso range of motions (ROM) to navigate smoothly and safely through challenging navigation scenarios such as narrow hallways and tight corners.

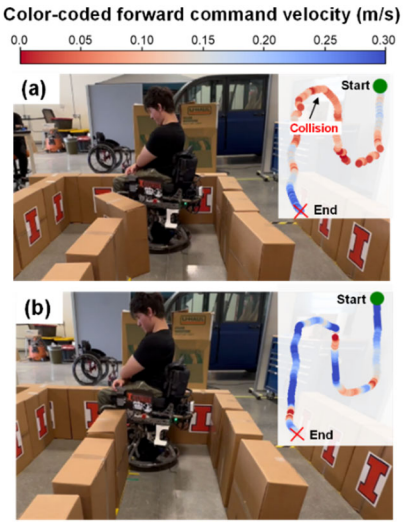

Figure 1: Qualitative analysis of the shared-control system showcasing a trial from S14, a manual wheelchair user with complex spinal conditions and max $ROM_{sagittal} = 32.28^{\circ}$ for the S-Turn course. (a) Without S-C, the path exhibited jittery and erratic movements, with velocities below 0.1 m/s and a collision when making a tight turn. (b) With S-C, the trajectory was smoother, and velocities exceeded 0.2 m/s. without collisions.

Methods: The proposed shared-control approach enables safe and intuitive navigation by providing deceleration assistance and haptic/audio feedback when too close to an obstacle. A vision system, consisting of RGB-D cameras, LiDAR and Time-of-Flight sensors, is used for obstacle detection. The shared controller is based on our novel Passive Artificial Potential Field method, building on traditional Artificial Potential Field formulations [3]. It provides motion resistance when the operator drives PURE towards an obstacle, such that if the user is leaning and getting too close an obstacle, the S-C scheme would apply a resistive force in the opposite direction to slow down the device. An IRB-approved human subject evaluation including 10 manual wheelchair users (mWCU) and 10 able-bodied users (ABU) was conducted to explore the performance and effort of navigating PURE with and without S-C (Table 1). Prior to navigating through the test courses, a maximum ROM test was conducted where the participant was asked to perform a series of torso movements. While seated on the stationary PURE, subjects performed a series of 4 torso movements for 3 cycles per motion starting from their neutral position, i.e., sitting upright and facing front (e.g., leaning forward/backwards, left/right, and twisting to their left/right to their maximum comfortable range). This test was crucial as participants needed to use their torso movements to drive PURE, and the objective was to understand the extent of possible ROMs that the S-C scheme could accommodate. Participants' torso ROM were recorded using the TES (Table 1). Then, participants were asked to go through a training course to get familiar with PURE and its S-C operation. During testing, they were asked to navigate through two obstacle courses (S-Turn and Zigzag shapes), each with wide and narrow width settings, at their comfortable speed while avoiding collisions, with and without the S-C for three trials per test condition. For each test condition, the completion time (T_c) and a collision index (C_i), based on weighted collision types, were recorded.

TABLE 1. SUBJECT DEMOGRAPHICS AND ANTHROPOMETRIC AVERAGE (STANDARD ERROR) DATA

		ABU	mWCU
Number [Male: Female]		10 [5:5]	10 [4:6]
Age (years)		23.6 (1.1)	27.4 (1.6)
Height (m)		1.68 (0.02)	1.62 (0.03)
Weight (kg)		58.1 (2.3)	51.6 (2.6)
Years of using mWC (yrs)		NA	19.4 (2.55)
Torso Range of Motion (°)	frontal	63.1 (4.2)	46.6 (4.5)
	sagittal	58.6 (3.3)	41.1 (3.5)
	transverse	91.3 (4.2)	64.5 (9.5)

Results & Discussion: Repeated-measures MANOVA tests (and subsequent univariate ANOVAs) on T_c and C_i revealed significant effects by test course ($p < 0.001$), shared-control use ($p < 0.001$), and their interaction ($p = 0.005$), but no differences between groups ($p > 0.05$). S-C usage reduced C_i by over 50% across all test courses, from 2.5 to 0.9 ($p < 0.001$); however, it had minimal effect on T_c from 25.9 s to 25.9 s ($p = 0.99$), suggesting that S-C did not significantly alter travel speed. Additionally, the qualitative analysis of participants' movement trajectories in different test courses underlined S-C scheme's effectiveness in reducing motion corrections by offering deceleration assistance. That is, the rider experienced reduced need of continuous back-and-forth leaning for speed adjustment, instead maintaining a stable posture while the device managed obstacle avoidance in challenging environments (Fig 1). Post-test questionnaire results (4 pt Likert scale) consistently found S-C to be intuitive (3.55), natural (3.15), safe (3.5), and non-aggressive (1.5).

Significance: The proposed shared-control approach between rider and device can enhance maneuverability and safety, and benefit users who need to navigate through challenging real-world scenarios such as narrow hallways, tight corners, restroom stalls, etc.

Acknowledgments: NSF NRI #2024905. Thanks to A. Bleakney, J. Elliot, D. McDonagh, P. Malik, K. Driggs-Campbell, Yixiao Liu, Keona Banks, Tianyi Han, ZhanPeng Li, YinTao Zhou, Tommy Nguyen, Maxine He, Jason Robinson, ZhongChun Yu and John Hart.

References: [1] C. Xiao et al. *IROS*, 2023. [2] S.Y. Song et al. *ACM/IEEE HRI*, 2024. [3] O. Khatib, *Int J Rob Res*, 5(1): 90–98, 1986.

SELECTION OF RECOVERY LEG AFTER A STANDING-SLIP IN YOUNG ADULTS

Diane' Brown, MS[1], Jiyun Ahn, MS[1], Caroline Simpkins, MS[1], Feng Yang, PhD[1]*
Department of Kinesiology and Health, Georgia State University, Atlanta, GA USA
*Corresponding author email: fyang@gsu.edu

Introduction: Perturbation-based training, grounded on the motor learning theory, aims to assist the trainees with developing fall-resistant skills, particularly the ability to effectively execute the recovery steps, in response to external postural disturbances. Various modalities, including standing-slips on treadmills (like the ActiveStep treadmill), have yielded promising results across various populations [1,2]. While standing-slip perturbation training is widely used, the selection of the recovery leg between the dominant and non-dominant legs after the slip remains unclear. Given that a slip perturbation could happen to either leg in the real-life situations, it is important to allow both legs to experience the recovery stepping process in a perturbation-based training protocol. To achieve this goal, it is imperative to understand if the trainees have a preference for selecting a particular leg, for example, the dominant leg, as the recovery leg after a slip. This cross-sectional study sought to determine whether young individuals consistently take their dominant leg to recover balance during an unanticipated novel standing-slip on a treadmill. We hypothesized that young adults always favor their dominant side for recovering balance in the event of a slip while standing.

Methods: The data of 86 healthy young adults (61/25 females/males, mean ± standard deviation age: 24.52 ± 4.7 years) were extracted from previous studies [1-3] that administered a treadmill-based standing-slip. All included studies utilized the same inclusion criteria: aged 18-45 years, no musculoskeletal or cardiorespiratory illnesses, and no prior perturbation training. The procedures to induce the standing-slip across all studies were standardized. Participants' leg dominance was self-reported, which has been shown as a reliable way to determine the dominant leg [4]. Fitted with a safety harness, all participants stepped onto an ActiveStep treadmill (Simbex, NH). They were instructed to stand on the treadmill initially and experience a "slip-like" movement later. They were also told to try and recover the balance in case of a slip. After about 5-6 standing trials without slip, participants experienced a standing-slip without knowing when and how it occurred. The standing-slip was induced by suddenly accelerating the treadmill belt forward to a peak speed followed by a deceleration section to diminish the belt speed. Four slip profiles with varying intensities, characterized by the peak belt speed, were adopted: 0.9 (10 subjects), 1.2 (61 subjects), 1.8 (5 subjects), and 2.4 (10 subjects) m/s, respectively. The slip distance was 0.36 m for the first three profiles and 0.48 m for the last one. The recovery leg was the leg moved backward to attempt to reestablish balance after the slip. If the recovery leg was the same as the dominant leg for a participant, this individual was classified into the congruent group. Otherwise, the participant was considered in the conflictive group. The congruence rate was calculated as the ratio of the number of participants in the congruent group to the sample size of each slip intensity or the total sample size across slip profiles. The congruence rate was analyzed by using the χ^2 test. The demographic information and slip intensity metrics (the peak belt speed and slip distance) were compared between groups (congruent vs. conflictive) using independent t-tests. All statistics were performed using SPSS 29.0 (IBM, NY), and $p < 0.05$ was deemed significant.

Results & Discussion: All participants took a backward recovery step after the standing-slip perturbation on the treadmill. Among the 86 participants, 53 took the dominant leg to execute the recovery step (the congruence rate = 61.6%) while 33 used their non-dominant leg to recover balance. All demographic information was comparable between groups ($p > 0.152$ for all) and slip distance was not different between groups ($p = 0.138$). The peak belt speed was significantly faster in the conflictive group than in the congruent group (1.464 ± 0.485 vs. 1.262 ± 0.369 m/s, $p = 0.032$). The congruence rate was 90%, 62.3%, 40%, and 40% for the slip profiles with the peak belt velocity of 0.9, 1.2, 1.8, and 2.4 m/s, respectively (Fig.1). The slip profile with the lowest slip intensity (0.9 m/s) was associated with a larger congruence rate than the other three slip profiles ($p = 0.086$ vs. 1.2 m/s, $p = 0.039$ vs. 1.8 m/s, and $p = 0.019$ vs. 2.4 m/s). The congruence rate for the slip profile of 1.2 m/s was also higher than those for the two higher-intensity profiles ($p = 0.100$ vs. 1.8 m/s and $p = 0.033$ vs. 2.4 m/s). The congruence rate was the same between the two higher-intensity profiles. The findings revealed a notable preference for using the dominant leg (61.6%), but it is not universally consistent, with 38.4% still stepping the non-dominant leg. Slip intensity, especially the peak belt speed, seems to significantly affect the recovery leg selection, with lower intensities favoring the dominant leg choice. This study only involved healthy young adults and tested a limited range of intensity levels. As a result, the generalizability of the findings may be limited. More studies are needed to address this limitation.

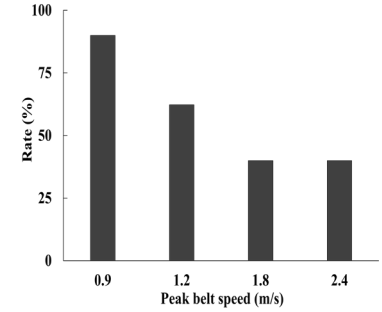

Figure 1: Comparison of the congruence rate between the four intensity levels, quantified by the peak belt speed: 0.9, 1.2, 1.8, and 2.4 m/s.

Significance: This preliminary study provides insight into how healthy adults choose the recovery leg after a standing-slip. The information could inform the design of standing-slip-based perturbation training programs for reducing falls. Our findings could also guide future studies to further investigate how clinical populations pick the recovery step, between dominant and non-dominant or between strong and weak sides, during slips and other types of perturbations.

Acknowledgments: The authors thank Sangwon Shin for assisting with data collection.

References: [1] Yang, F et al. (2018), *J Biomech 72, 1-6*; [2] Simpkins, C et al. (2023), *J Biomech 152, 111572*; [3] Ahn, J et al. (2023), *J Biomech, 164, 111962*; [4] van Melick, N et al. (2017), *PLoS One 12, e0189876.*

Video-based analysis for estimating hip impact velocity and acceleration during a fall using a pose-estimation algorithm

Reese P. Michaels, Yaejin Moon
Syracuse University
Corresponding author's email: yamoon@syr.edu

Introduction: Falls are one of the leading causes of accidental injury and death among the elderly [1]. Since the direct cause of fall-induced injury is an excessive mechanical load applied to the body upon impact [2], previous studies employed kinematic and kinetic parameters, such as fall velocity and impact force [2], to estimate the injury risk of a fall. However, due to safety concerns, these lab-based fall experiments either did not reflect the accidental nature of a fall or were conducted with young individuals. As an alternative approach, previous research has analyzed video footage of real-life falls of older adults [3,4]. These studies extracted kinematic parameters from the video by manually marking landmarks of the body parts in each frame [5], a process that is both time- and labor-intensive. The recent rise of AI-based pose estimation algorithms, which automatically detect and track the position of human body parts, presents a promising approach to efficiently analyze kinematics in video-captured movement. Here, we examined the accuracy of the pose estimation algorithm OpenPose in assessing the kinematic features, including hip impact velocity and acceleration, of video-captured older adult falls.

Methods: We used a secondary dataset containing 110 videos (captured at 30Hz; Fig1.A) of 13 older adults (10 male, age = 64.0 ± 5.9 years) falling sideways in an experimental setting [6]. In the original study, participants were instructed to fall naturally, later classified as "stick-like" and "knee block", and for some trials to perform a "tuck and roll" strategy" [6]. The video data was accompanied by synchronous motion capture (VICON) and inertial measurement unit (IMU; MC10) data, which served as the gold standard reference. OpenPose was applied to each video to generate a time series of the body key points, including the ankle, knee, and hip. Then, a custom MATLAB code analysed the key point outputs extracted from OpenPose to calculate the instantaneous hip velocity and acceleration upon ground impact. To measure agreement between the gold standard measurement (truth value) and OpenPose (estimated value), we examined three validation metrics: 1) accuracy (i.e., mean absolute error = |OpenPose – Gold Standard|), 2) precision (i.e., variance of absolute error), and 3) bias (i.e., mean of error = OpenPose – Gold Standard). For accuracy and bias, the percentage error (i.e., $\frac{Error}{Gold\ Standard\ Measure} \times 100\%$) was also calculated. Additionally, Pearson's correlation analyses were performed to determine associations between reference measurements and OpenPose estimations for both hip velocity and acceleration, respectively.

Results & Discussion: Overall, the hip impact velocity measured by OpenPose had good agreement with the reference standard (Accuracy: 0.17 ± 0.13 m/s; 7.28 ± 5.21%), with a minimum bias (Bias: -.04 m/s; -1.27%; Fig1.C) and there was a strong correlation between measurements (r= 0.83, p<0.01; Fig1.B). The hip impact acceleration measured by OpenPose was much less accurate and precise (Accuracy: 26.3 ± 19.4%) compared to hip impact velocity with a tendency for underestimation compared to the reference standard (Bias: -0.31g, -5.21%), especially for falls where participants employed the stick-like strategy. There was a moderate correlation for hip impact acceleration between OpenPose and the gold standard (IMU) estimations (r=0.67, p<.01).

Our results suggest that OpenPose can accurately (less than 10% error) estimate the hip impact velocity in video-captured falls. The algorithm yielded a greater error in estimating hip impact acceleration, which could originate from the low frame rate of the camera settings or the inherent limitation of taking second derivatives to calculate acceleration from the position data.

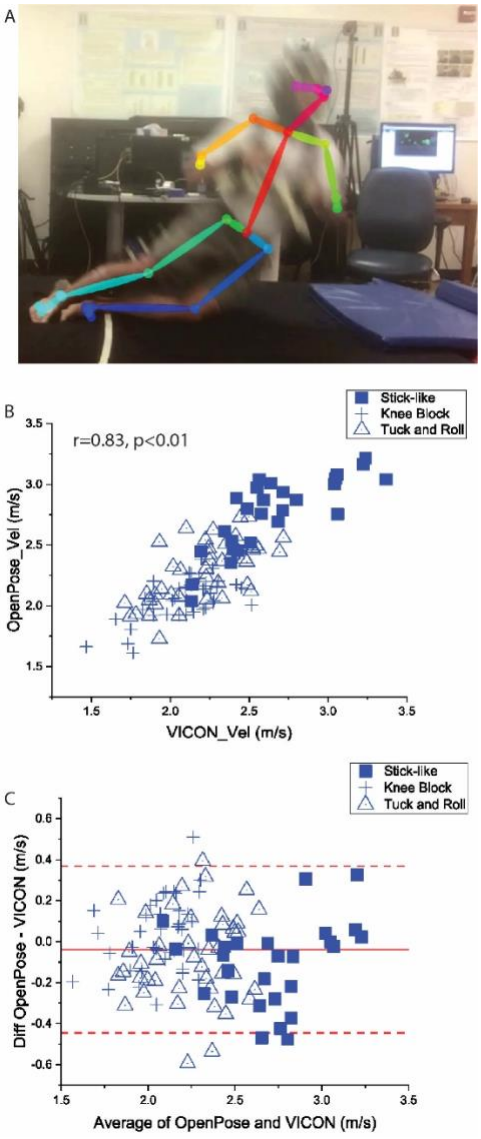

Figure 1. A) Example video frames overlaid with key point detection from OpenPose showing a participant's fall; B) a scatter plot; and C) a Bland-Altman plot of the hip impact velocity comparing VICON (truth value) vs. OpenPose (estimated).

Significance: To our knowledge, this is the first study to apply a pose estimation algorithm, OpenPose, for estimating the biomechanical features of a fall. OpenPose is capable of accurately estimating hip impact velocity, which is the most frequently reported injury-risk parameter for a fall [2]. However, further study is needed to improve the accuracy of estimating hip impact acceleration using the AI algorithm. These results will lay the groundwork for utilizing the AI algorithm when analysing video-captured falls, which will ultimately enable the extraction of biomechanical features from real-life video-captured elderly falls.

References: [1] Centers for Disease Control and Prevention (2020); [2] Moon & Sosnoff (2017), *Arch Phys Med Rehabil.* 98(783-794); [3] Robinovitch et al. (2022), *Age and Ageing* 51(12); [4] Komisar & Robinovitch (2021), *Current Osteoporosis Reports* 19(381-390); [5] Choi et al. (2015), *J of Biomechanics* 48(911-920); [6] Moon et al (2019), *J of Biomechanics* 83(291-297)

WAIST-TO-HEIGHT RATIO, BMI, AND GRIP STRENGTH ARE NOT ASSOCIATED WITH THE REQUIRED FRICTION DURING LADDER DESCENT

Sarah C. Griffin[1*], Violet M. Williams[1], April Chambers[1,2], Rakié Cham[1], Kurt E. Beschorner [1]
[1]University of Pittsburgh, Department of Bioengineering; [2]University of Pittsburgh, Department of Health & Human Development
*Corresponding author's email: scg57@pitt.edu

Introduction: Falls from ladders pose a severe burden on society both at and away from work. Slips from ladders specifically cause around 14% of falls, yet there is a lack of understanding on the mechanistic cause of slips during ladder climbing [1]. The required coefficient of friction (RCOF) is a metric that quantifies the amount of friction that needs to be present for someone to not slip while completing a task and it has been positively associated with slip risk in walking [2]. The use of RCOF in ladder climbing is emergent. RCOF is person-specific and has been shown to be related to obesity in walking, where higher BMI (body mass index) is associated with a higher RCOF [3], but no studies have yet determined the impact of obesity on slip risk during ladder climbing. Because ladder climbing is a rigorous task that requires strength of both the upper and lower body, obesity may influence climbing biomechanics and increase RCOF. Additionally, body composition may affect the mechanics of ladder climbing as body shape may alter how close a person can position their body to the ladder and thus alter their center of mass position relative to the ladder.

BMI is a common yet imperfect metric of obesity. One limitation is that BMI only considers weight and does not consider muscle mass. Other metrics like the waist-to-height ratio can better capture body shape and general health [4]. In this work, we considered both BMI (because of ease of use) and waist-to-height ratio. Additionally, effects of obesity could influence risk via strength because someone with higher strength may be able to climb with more control and thus lower RCOF. Grip strength is commonly used as an estimate of individuals' overall body strength and has previously been shown to be related to fall severity during perturbed ladder climbing [5]. However, the effect of grip strength on RCOF is unknown. The goal of this work is to determine if there is an association between the BMI, waist-to-height ratio, or grip strength and RCOF while someone descends a ladder. We hypothesized that a higher RCOF would be associated with higher obesity metrics and lower normalized strength.

Methods: Twenty healthy adults (10F, height = 1.69±0.06 m, weight = 76.8±16.0 kg, BMI = 26.8±4.9 kg/m^2, age = 43.3±13.3 years, waist-to-height ratio = 0.504±0.075) who regularly climb ladders completed three descending trials on an instrumented ladder oriented at 90 degrees with a round rung. The third rung of the ladder was rigidly attached to a three-dimensional force plate (AMTI Inc, Watertown, MA, USA) which collected the kinetics at the shoe-rung interface. Participants donned 79 reflective markers which were tracked by 12 motion capture cameras (Vicon Motion Systems Ltd., Centennial, CO, USA) to quantify kinematics. Participants were recruited across a wide range of BMI (from healthy to obesity class 1) to ensure spread on this variable. Grip strength was found across three trials for both hands using a hydraulic hand dynamometer (Jamar, Chicago, IL, USA). The single maximum value for each participant was selected and normalized to their weight. One participant was missing grip strength values due to time constraints of their testing session.

The peak RCOF was found for each trial by generating time series coefficients of friction in the plane of the shoe. The peak was chosen as the highest of the first three local maxima during foot contact, excluding the low forces during early stance. Average RCOF peak within each subject was the dependent variable in three separate bivariate regression models which included the BMI, waist-to-height ratio, or normalized strength as the independent variable.

Results & Discussion: None of the considered factors was associated with RCOF: BMI ($F_{1,18}$ = 0.15, p = 0.70, R^2 = 0.008, Fig 1A), waist-to-height ratio ($F_{1,18}$ = 0.71 p = 0.41, R^2 = 0.038, Fig 1B), or the normalized grip strength ($F_{1,17}$ = 2.02, p = 0.173, R^2 = 0.106, Fig 1C). These findings indicate that obesity and grip strength are likely not strongly associated with RCOF and slip risk while descending a ladder. While these results are unexpected, they are promising for the safety of ladder climbers. Other work has shown that a person's biomechanical strategy for climbing ladders has been associated with their RCOF [6]. In conjunction, these findings indicate that anyone *can* climb a ladder safely, they may just need to be taught how to do so. Future work with more participants will confirm these results.

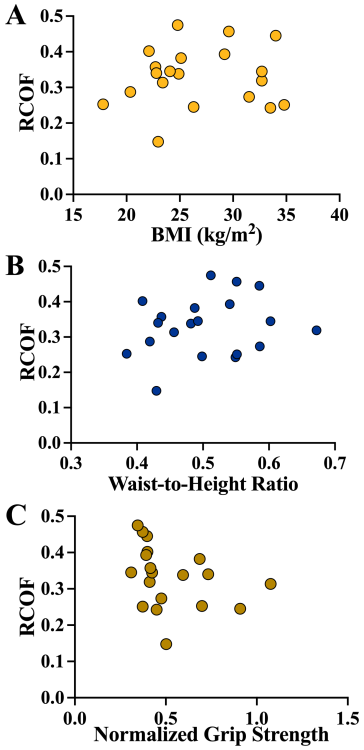

Figure 1: The relationship between RCOF and BMI (A), waist-to-height ratio (B), and grip strength (C).

Significance: These results indicate that, in people with ladder climbing experience, a person's strategy for climbing a ladder is much more important than the person themself. Therefore, it is crucial to improve ladder safety training protocols to encourage safe strategies across all ladder climbers.

Acknowledgments: This research was funded by NIOSH R01OH011799 and NSF GRFP 2139321.

References: [1] Cohen et al. (1991), *J Safety Res* **22**: 31-39. [2] Beschorner et al. (2016), *Gait Posture* **48**: 256-260. [3] Liu. (2010), *Research and Practice for Fall Injury Control in the Workplace*, (81). [4] Ashwell et al. (2009), *Nursing Standard* **23.41**: (49) [5] Pliner et al. (2019) *Gait Posture* **68**: 23-29. [6] Griffin et al. (2024), *ASB, Novel biomech variable, foot-body coupling angle, predicts slip risk*.

VISUAL CUES DELIVERED THROUGH AUGEMENTED REALITY HINDER BALANCE CONTROL AND INCREASE MUSCLE FATIGUE DURING AN EXTENDED SIMULATED OVERHEAD WORK TASK

Wendy T. Pham[1], Makena Savola[1], Jacob W. Hinkel-Lipsker[1]
[1]Department of Kinesiology, California State University, Northridge, CA USA; wendy.pham.285@my.csun.edu

Introduction: Overhead work, where a person has their shoulders flexed and arms above their head, is common in many technical professions such as construction workers and electricians [1]. Long periods of overhead work can cause compensatory mechanisms at the shoulder joint as a means for workers to limit or delay fatigue [2], and may also have more global effects such as diminished standing balance control [3]. Researchers have attributed this effect to muscle fatigue in the cervical spine and shoulders driving impaired proprioception in the cervical spine, a subsequent decrease in head and neck position sense, which may cause a downstream negative effect on overall postural stability and lead to falls, injuries, and lost work time [3,4]. Therefore, to ensure the health and safety of the overhead worker it is of interest to examine means to improve balance control in this population. New developments in augmented reality (AR) technology, which superimposes holographic images over the user's field of view, has the ability to provide visual cues to workers regarding their body sway—providing additional sensory information to counteract proprioceptive changes. Thus, the purpose of this study was to examine how balance control cues provided through AR alter whole-body balance control during an extended overhead work task. We hypothesized that when using AR, participants would exhibit less excursion of their center of pressure (COP) but an increased COP velocity, indicating smaller, more rapid adjustments to the COP as a result of real-time visual cues. We also hypothesized that participants would demonstrate increased leg muscle activity, as measured through surface electromyography (EMG) when using AR, as the visual cues provided would evoke stronger neuromuscular responses to maintain balance.

Methods: Ten healthy participants were recruited to complete two counterbalanced overhead work conditions (AR and no AR) in a random order on two different days. For both conditions, participants completed a simulated overhead work scenario for one hour, in this case a paint-by-numbers task positioned above their head. Following a baseline quiet standing period used to normalize COP and EMG metrics, this hour-long task was completed over 15 work-rest cycles. In the AR condition, participants were equipped with a Microsoft Hololens 2 that used the headset's integrated accelerometers and gyroscopes to display holographic real-time feedback to users regarding head motion. COP data were recorded from two force plates during each of the 15 work cycles, and surface EMG data were recorded from the gluteus medius and lateral gastrocnemius (LG) of each participant's dominant leg. A repeated-measures multivariate analysis of variance (MANOVA) was used to test for the main effect of condition on all dependent variables. Further, a joint analysis of EMG spectrum and amplitude (JASA) was conducted to determine whether shifts in EMG spectra and amplitude between the beginning and end of the overhead work sessions were more related to muscle fatigue or changes in force production [5].

Results & Discussion: The MANOVA revealed a significant main effect of condition ($p < 0.05$). Follow-up pairwise comparisons indicated participants in the AR condition exhibited a significant increase in anterior-posterior (A/P) COP excursion compared to no AR ($p < 0.05$; Figure 1A). This result indicates that the visual cues provided through AR hindered postural sway and does not support our hypothesis. It is possible that participants responded too strongly to the visual cues, which brought postural control more into their attentional focus than typical. While there were no significant pairwise differences between the other COP and EMG variables, the JASA performed on the LG indicated that more shifts in EMG spectrum and amplitude while participants were using AR were related to fatigue than while they were not using AR, and no shifts in the AR condition were related to increases in force (Figure 1B). Taken together, participants demonstrated an increase in A/P COP excursion and greater fatigue of the LG muscle when using AR. As the LG works to control A/P body sway, it is possible that these two outcomes are linked—AR causes greater correction in the A/P direction, resulting in greater LG fatigue.

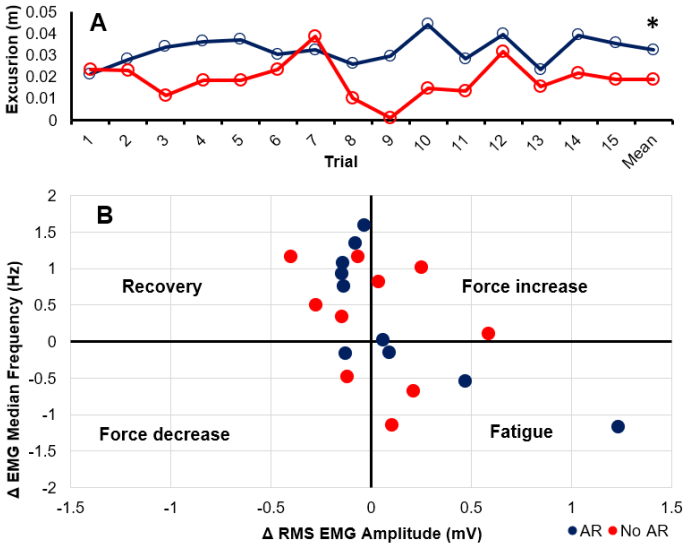

Figure 1. A) A/P COP excursion across the overhead work period, normalized to bilateral quiet standing. B) JASA using the changes in EMG spectrum and amplitude of the LG from the start to the end of the working period.

Significance. AR is becoming more prevalent in society, with major financial investment coming from industry and infinite possible use cases. These cases include the use of AR in the workplace to foster more worker-in-the-loop scenarios, where people are provided with real-time information through technology to make more informed workplace decisions. With the overall negative effects of AR noted in this study, these results caution the applicability of applicability in worker-in-the-loop scenarios. In total, AR technology is advancing at a more rapid pace than scientific understanding of how people interact with it on a physiological and behavioral level, and more research is needed to better elucidate how users respond to the technology before it becomes more fully integrated with society.

Acknowledgements: Thanks to CrossComm, Inc. for development of the custom AR application used in this study.

References: [1] DeBock et al. (2022). *IEEE TBME 69*(10); [2] Grieve & Dickerson (2008). *Occup Ergo 8*(1); [3] Nusbaum (2003) *JOEH 64* (1); [4] Abdelkader et al. (2020). *J Musc Neuron Interact 20*(3); [5] Luttman et al. (2000) *Int J Ind Ergo 25*(6).

A PILOT STUDY OF ON-SITE WORKPLACE REACTIVE BALANCE TRAINING

Gabrielle M. Ferro[1], Youngjae Lee[1], Michael L. Madigan[1*]
[1]Grado Department of Industrial and Systems Engineering, Virginia Tech, Blacksburg, VA, USA
[*] Corresponding author's email: mlm@vt.edu

Introduction: Among workers in the U.S., an average of 19,000 falls on the same level occur each year, with trips preceding 36% of those falls [1]. Reactive balance training (RBT) has been shown to improve trip recovery [2,3] and reduce fall risk [4] among community-dwelling older adults. RBT may also be a viable fall risk reducing strategy for workers in occupations with increased fall risk. Therefore, the purpose of this pilot study was to evaluate the efficacy and feasibility of RBT in an on-site field study among workers at a water treatment facility. We hypothesized that RBT would improve workers' reactive balance after simulated trips based on similar results among older adults [2,3].

Methods: Ten males who worked in the field on the construction and repair of municipal water distribution and wastewater collection facility were initially recruited. Six field workers and one office worker completed the study (age 39.3 ± 10.3 years; height 1.8 ± 0.1 m; mass 96.2 ± 9.5 kg). Participants were randomly assigned to either RBT (n = 4) or a control intervention (n = 3). Over three consecutive days, participants completed a 10-minute reactive balance assessment, two 20-minute intervention sessions, and a second 10-minute reactive balance assessment. RBT sessions involved exposing participants to 24 trip-like perturbations at 1.6-3.6 mph while standing on a treadmill (Fig. 1). The control training consisted of a variety of standing and walking balance exercises. Reactive balance assessments included four trip-like perturbations at different speeds (1.6 mph twice, 2.4 mph, and 3.0 mph). Participant response was assessed with (1) reactive balance rating (RBR) scored 0-8 [2] and (2) maximum trunk flexion angle using an inertial measurement unit placed on the sternum (Opal, APDM Inc., Portland, OR, USA, 128 Hz). No inferential statistics were performed given the small and pilot-nature of the study. Feasibility was evaluated based upon participant exit interviews and scheduling success.

Figure 1: Reactive balance training involved using a modified treadmill to repeatedly apply trip-like perturbations. A foam block simulated a trip obstacle.

Results & Discussion: RBT participants improved their RBR from 7.0 ± 0.8 (mean ± SD) pre-training to the highest possible rating (8.0 ± 0.0) post-training. Only one out of three control participants improved their RBR pre- to post-training. The mean maximum trunk angle decreased for the first perturbation (1.6 mph) after training for both groups. However, the trends in trunk flexion angle did not show obvious benefits of RBT over controls across all four perturbations during assessments (Fig. 2).

All workers were able to recover from all perturbations during assessments without noticeable harness support, resulting in high RBR scores. The RBR scores and minimal improvement in trunk flexion angle across all participants may have resulted from these assessments having not been challenging enough to accurately evaluate reactive balance capacity of the participants. The RBT protocol used was adapted from a training for older adults [2], and it is likely the perturbation speeds during RBT and assessments need to be increased. The study limitations also included a small sample size and group assignment did not balance for age, physical fitness, or job duties. During exit interviews, all workers found the on-site training to be beneficial and worked within their schedule. However, some participants who were originally recruited to participate were unable to attend the sessions due to unexpected changes to their schedules or communication lapses. Future on-site studies would be more successful with clear and frequent communication with participants and a pre-determined schedule with built-in flexibility that accommodates the unpredictable nature of construction and maintenance work.

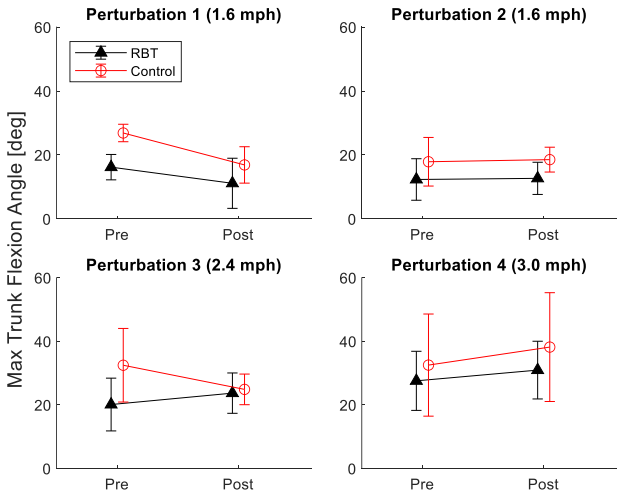

Figure 2: Maximum trunk angle at different treadmill perturbation speeds pre- and post-training.

Significance: RBT has the potential to reduce fall risk among workers in occupations with increased fall risk. This pilot study demonstrated that RBT and balance assessment can be feasibly conducted on-site at industry facilities, and provided valuable lessons learned for the future.

Acknowledgments: We thank Veolia North America and the Haworth, NJ Water Treatment Plant for their partnership. Funding was provided by R21OH012451. The content does not necessarily represent the official views of the CDC.

References: [1] BLS (2019), *Data Retrieval Tool*; [2] Allin, et al. (2020), *BMC Geriatrics* 20(205); [3] Bieryla, et al (2007), *Gait & Posture* 26; [4] Rosenblatt , et al. (2013) *J Am Geriatr Soc.* 61(1)

PERSONALIZED SONIFIED POSTURE BIOFEEDBACK FOR OLDER ADULTS: A PILOT CLINICAL STUDY

Zahava Hirsch[1*], Mitchell Tillman[1], Jun Ming Liu[1], Janine Molino, Antonia Zaferiou[1]
[1]Stevens Institute of Technology, Biomedical Engineering Dept., Hoboken, NJ USA
*Corresponding author's email: zhirsch@stevens.edu

Introduction: Falls are a leading cause of fatal and nonfatal injuries in older adults and carry a heavy quality of life impact [1]. Notably, half of all walking steps are turns, and falls during turns are 7.9 times more likely to result in a hip fracture for older adults [2]. There are many factors that lead to fall-risk, including postural changes in older adults [3]. Research has shown that sound biofeedback can improve proper form through error biofeedback, as well as increased motivation through active engagement and interaction [4]. We performed a pilot study to determine if real-time sonified biofeedback training can improve posture for older adults training twice a week for multiple weeks. We hypothesized that **1)** compared to the baseline trials in the pre-training visit, the baseline trials during the final training visit will have a smaller posture angle (more upright) and **2)** compared to the baseline trials within each training visit, the training trials will have a smaller posture angle for both normal speed and fast speed trials.

Methods: In this pilot study, an older adult (f, 84 years) completed one pre-training visit, four training visits (T1, T2, T3, T4) across two weeks, and a post-training follow-up by phone. A 13-segment whole body kinematic model [5] was built using optical motion capture data (250 fps; OptiTrack, USA). A physical therapist (PT) was present for all lab visits to provide instruction and guard against falling. The participant completed a walking course for each trial, which included walking straight for 4m, a 90˚ left turn, straight 4m, 180˚ turn-and-go, straight 4m, a 90˚ right turn, straight 4m, and a 180˚ turn-and-stop. During the pre-training visit the participant completed written and cognitive assessments, standard balance and muscle strength assessments with the PT, and 10 baseline trials on the walking course: 5 normal speed and 5 fast speed (no PT instruction or sonication). During each of the training visits, 10 baseline trials were performed (5 normal, 5 fast speed). This was followed by 20 training trials, (10 normal and 10 fast speed), all with verbal cues from the PT and sonified biofeedback fading out 20% each visit (i.e.: Training Visit 2 had 2/10 trials without sonification). At the end of each training visit, the participant was given a survey to rate and share their experiences with sonified biofeedback. To calculate "Posture angle" for each trial, a vector was created between the pelvis markers and the head markers. The pelvis-based sagittal-plane was used to provide the posture angle only in the sagittal-plane. A "good posture" trial was recorded each lab visit as the goal angle for the sound design. When the posture angle approached the goal, a "pleasant" low pitch brass (e.g., trumpet) instrument sound was heard. If the posture angle was greater than the goal, a pitch increase informed the participant to become more upright. See the example video.

Results & Discussion: We found a significant decrease in average posture angle in the final training visit (T4) as compared to the pre-training visit for both speeds, supporting hypothesis 1 (**Fig. 1**; $p < 0.0001$ for normal and fast). In addition, we found a significant decrease in the posture angles during training as compared to baseline trials during T1, T3, and T4 – partially supporting hypothesis 2 ($p < 0.0001$ for each comparison). During T2, however, there was a significant *increase* in posture angle during normal speed training trials as compared to the baseline trials ($p < 0.0001$). Overall, this indicates that training with sonified biofeedback and verbal PT cues improved postural control within most visits and across weeks. Interestingly, we found that simply telling the participant that we were going to work on posture resulted in an improvement in posture - posture angle decreased from the pre-training visit baseline trials to the T1 baseline trials, before any training occurred. There are several limitations to this pilot study that we are working to rectify with our current studies. For example, we observed how important it was to have the same PT for all visits, as the PT alternated within this pilot study (PT #1 for pre-training, T2, and T4; PT #2 for T1 and T3). In the survey responses, the participant wrote that "*the coordination of listening to the pitch change and adjusting my posture was challenging*," but that they liked "*becoming aware of my posture and how to correct it*," and found that learning how to make adjustments to their gait to maintain a lower pitch "*gives me more confidence and less anxiety about falling*". During the follow-up phone call, the participnat reiterated that they are more focused on their posture in their day-to-day, and feel more confident in their movements. The participant also shared that they tripped while going down a ramp and were thankful to have had an upright posture because they attributed their ability to avoid a fall to their posture, in this case.

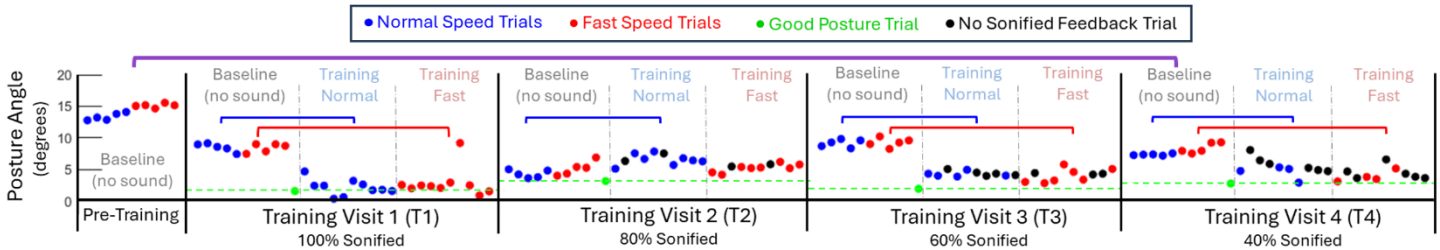

Figure 1: *Average posture angle per turning course trial. Blue and red dots indicate normal and faster speed trials, respectively. Black dots indicate training trials with verbal cues only (no sonification). The purple bar indicates a significant difference in posture angle between the pre-training and T4 visit baseline trials. Blue and red bars indicate significance between the normal and fast speed baseline and training trials within each visit.*

Significance: This study evaluated the feasibility and immediate effects of sonified biofeedback training to help older adults improve postural control. We are expanding this study and improving designs that convey balance and gait measures through musical sounds.

Acknowledgements: National Science Foundation Award #1944207. Special thanks: Allison Clark and Franceah Palencia-Quijano.

References: [1] Moreland et al. (2020), *Morb. Mortal. Wkly Rep*. 69(27); [2] Cumming et al. (1994), *J. Am. Geriatr. Soc.* 42(7); [3] Fernandes et al. (2018), *Fisioter. Mov.* 31; [4] Maes et al. (2016), *Front. Neurosci.* 1; [5] de Leva (1996). *J Biomech.* 29

REDUCED ACHILLES TENDON STIFFNESS IN AGING ASSOCIATES WITH HIGHER METABOLIC COST OF WALKING

Aubrey J. Gray[1*], Rebecca L. Krupenevich[2], Gregory S. Sawicki[3], Jason R. Franz[1]
[1] Joint Dept. of Biomedical Engineering, University of North Carolina at Chapel Hill and NC State University, Chapel Hill, NC
[2] Division of Behavioral and Social Research, National Institutes of Health, Bethesda, MD
[3] George W. Woodruff School of Mechanical Engineering, Georgia Institute of Technology, Atlanta, GA
*Corresponding author's email: graaj@email.unc.edu

Introduction: When walking at the same speed, older adults (≥65 years) consume metabolic energy much faster than younger adults (e.g., 18-35 years), which can accelerate fatigue and reduce independence and quality of life. In particular, neuromechanical interaction between triceps surae muscle function and Achilles tendon stiffness (k_{AT}) is critical for tuning positive power generation during push-off which is in turn responsible for as much as half of the cost of walking [1]. Older and younger adults walk with similar ankle joint kinematics [2] and thus similar triceps surae muscle-tendon unit lengths. Thus, for a given activation, the more compliant Achilles tendon of older adults would compel shorter triceps surae muscle operating lengths, and contribute at least in part to a higher metabolic cost of walking for older adults. The purpose of this study was to *(i)* quantify age-related differences in k_{AT} across a range of matched muscle activations using electromyographic biofeedback and *(ii)* determine the relation between k_{AT} at matched activations and the metabolic cost of walking across age. We hypothesized that: (1) young and older adults would exhibit greater k_{AT} at higher triceps surae activations, consistent with a shift from the nonlinear to linear region of the length tension curve, (2) older adults would exhibit lesser k_{AT} compared to young adults at matched activations, and (3) k_{AT} would positively correlate with a higher metabolic cost of walking.

Methods: We recruited 15 healthy younger adults (23±4 years, 8F/7M, 72.9±14.2 kg, 1.7±0.1 m) and 15 healthy older adults (72±5 years, 9F/6M, 74.6±17.1 kg, 1.69±0.10 m) who participated after providing written, informed consent. We collected *in vivo* cine B-mode ultrasound images of participants' medial gastrocnemius muscle-tendon junction (MTJ) and Achilles free tendon distal to the MTJ and muscle activations from surface recording electrodes on the right soleus and lateral gastrocnemius. We quantified k_{AT} in a dynamometer during an ankle dorsiflexion task performed at rest ("passive") and at 25% and 75% maximum voluntary isometric contraction (MVIC) activation, the latter two prescribed using real-time electromyographic (EMG) biofeedback. We also quantified net metabolic power normalized to participant body mass during a 5-minute walking trial at 1.25 m/s. We assessed between-group differences in net metabolic power using an independent samples t-test. For k_{AT}, we performed a two-way mixed-effects ANOVA to test for a significant effect of age (between-subject effect; older vs. younger) and activation (within-subjects factor; passive, 25%, 75%).

Results & Discussion: Younger and older adults increased k_{AT} with increasing triceps surae activation. Indeed, a significant main effect of activation level ($F_{2,56}$=17.80, p<0.001, η_P^2=0.39) revealed that, across age groups, k_{AT} increased roughly four-fold from passive rotation to 25% MVIC activation, and again by +65% from 25% to 75% MVIC activation (Fig. 1A). This outcome reflects the nonlinear length-tension relation for tendon and demonstrates how the mechanics of a seemingly passive elastic tissue can depend on muscle activation. However, a significant main effect of age ($F_{1,28}$=4.34, p=0.046, η_P^2=0.13) revealed that older adults exhibited, on average, 44% lesser k_{AT} than younger adults across activation conditions (Fig. 1A). This effect appeared to arise not only from altered tendon length-tension relations with age, but also from differences in the operating region of those length-tension relations between younger and older adults. We also found that older adults walked with 17% higher net metabolic power than younger adults (older vs. younger: 3.11±0.36 W/kg vs. 2.66±0.58 W/kg) (p=0.017) (Fig. 1B). We found no correlations between k_{AT} during passive rotation or at 25% MVIC activation and net metabolic power during walking (r≤0.07, p≥0.05). Conversely, we found that k_{AT} measured at 75% MVIC activation significantly and positively correlated with net metabolic power during walking (r=-0.365, p=0.048) (Fig. 1C).

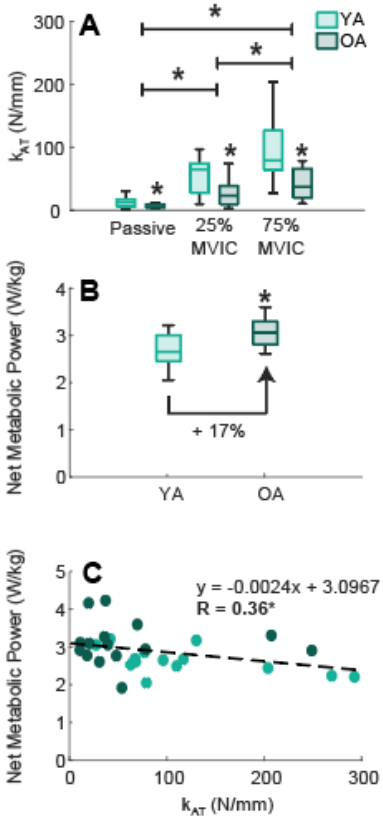

Fig. 1. (A) Age-related differences in k_{AT} across a range of MVIC activations. (B) Age-related differences in net metabolic power during walking. (C) Correlations between 75% MVIC activation k_{AT} and net metabolic power during treadmill walking. Linear fit and statistical outcomes shown for the combined cohort of older and younger adults. Asterisk (*) represents a correlation deemed statistically significant (i.e., p<0.05).

Significance: This study provides the first empirical evidence to our knowledge that age-related decreases in k_{AT} exact a potentially significant metabolic penalty during walking. These results pave the way for interventions focused on restoring ankle muscle-tendon unit structural stiffness to improve walking energetics in aging.

Acknowledgments: This work was supported by grants from the National Institute on Aging (R01AG058615 to JRF and GSS, and F32AG067675 to RLK).

References: [1] Huang, T. W., et. al. (2015) *Journal of Experimental Biology*. [2] Kerrigan, D. C., et. al. (1998) *Archives of physical medicine and rehabilitation*.

THE EFFECT OF SHOE INSOLE STIFFNESS ON WALKING PERFORMANCE IN OLDER ADULTS: A FEASIBILITY STUDY

Logan T. White*[1], Philippe Malcolm[1], Jason R. Franz[3], Kota Z. Takahashi[2]
[1]Department of Biomechanics, University of Nebraska at Omaha, Omaha, NE, USA
[2]Department of Health and Kinesiology, University of Utah, Salt Lake City, UT, USA
[3]Biomedical Engineering, University of North Carolina Chapel Hill and North Carolina State University, Chapel Hill, NC, USA
*Corresponding author's email: whitexlogan@gmail.com

Introduction: Older adults (i.e., ≥ 65 years) characteristically walk slower [1] and with greater metabolic energy cost [2] compared to their younger counterparts. Older adults consume metabolic energy faster due in part to age-related decreases in ankle push-off mechanics [3], yielding a redistribution to stronger but less economical hip muscles [4]. Older individuals also have weaker toe flexors and smaller intrinsic foot muscles than younger adults [5]. Considering that the toe flexors play an important role in modulating stiffness during locomotion [6], interventions capable of restoring function could improve walking outcomes in older adults. For example, footwear with carbon fiber insoles (CFI) can artificially increase foot stiffness and plantarflexor force output during locomotion [7–9] in younger adults. These changes may decrease metabolic cost, however, these effects have yet to be investigated in older adults. Moreover, the effects of CFI are complex; too much added stiffness increases metabolic cost when ankle power demands are low (i.e., slow walking) [9]. Thus, the aim of this study was to investigate the effects of footwear stiffness modifications on walking performance during the 6-Minute Walk Test (6MWT) in older adults. We hypothesized that a medium footwear stiffness condition would elicit the best 6MWT performance (i.e., furthest distance with lowest metabolic cost of transport) compared to lower and higher stiffness conditions. As a secondary aim, we investigated the potential modulating influences of subject-specific factors (toe flexor strength and passive foot compliance) on the effects of CFI during the 6MWT. We hypothesized that individuals with weaker toe flexors and more compliant feet would exhibit greater performance benefits from higher stiffnesses and vice versa.

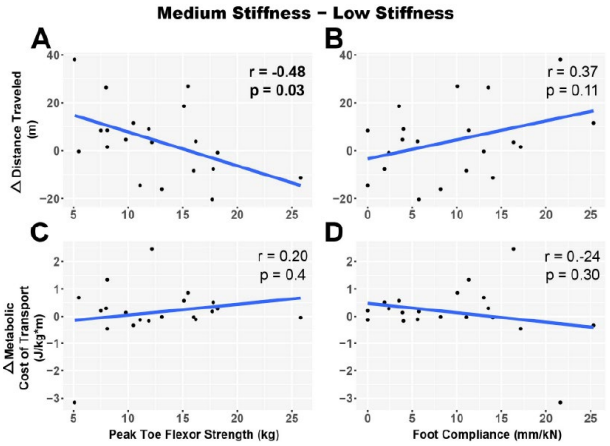

Figure 1: Differences in distance traveled (medium minus low stiffness) as a function of participants' **(A)** peak toe flexor strengths and **(B)** passive foot compliance, and differences metabolic cost of transport as a function of participants' **(C)** peak toe flexor strengths and **(D)** passive foot compliance.

Methods: 20 healthy older adults (10 M/10 F; mean ± sd: age: 76.0 ± 6.0 years, body mass: 79.6 ± 24.7 kg, body height: 166.4 ± 10.3 cm) performed four 6MWTs: three with our standardized footwear conditions normalized by mass (control [*low*], control + 1.6-mm insole [*medium*], control + 3.2-mm insole [*high*]) and one with the participant's own footwear. Participants completed conditions in a randomized order over two days. We recorded 6MWTs in a long hallway between cones spaced 28.96 m. Participants were instructed to walk as far as possible in 6 minutes and were given specific updates throughout the duration of the walk [10]. We recorded distance travelled and derived whole-body metabolic cost of transport using a wearable metabolic system (COSMED, Rome, Italy). To determine toe flexor strength, participants performed a maximum effort contraction with a toe grip dynamometer (Takei Scientific Instruments Co., Niigata City, Niigata). To calculate passive foot compliance, participants performed a barefoot sit-stand test. The dorsal height of the right foot while standing and sitting were subtracted and divided by the difference in body weight applied to the foot [11]. We quantified the effects of footwear condition using a one-way repeated measures ANOVA. Pearson's correlations quantified the change in distance travelled between the medium and low/high and low stiffness conditions with respect to toe flexor strength and passive foot compliance.

Results & Discussion: There were no significant differences across the four shoe conditions for either distance travelled ($F(3,57) = 1.73$, $p = .171$, $\eta 2 = 0.001$) or whole-body net metabolic cost of transport ($F(3,57) = 0.35$, $p = .700$ (H.F.), $\eta 2 = 0.001$). However, there was a significant negative correlation between toe flexor strength and the change in distance travelled between the medium and low stiffness conditions ($t(18) = -2.310$, $p = .033$, $r = -.478$, CI = [-0.760 -0.045]) (Fig. 1A). In other words, weaker toe flexors correlated with further distance travelled in the medium stiffness compared to the low stiffness insoles. No other significant correlations were found ($p > .106$).

Significance: The current findings indicate that toe flexor muscle weakness in older adults may be an important screening factor for identifying individuals who may benefit from interventions designed to augment foot structural stiffness.

Acknowledgments: This work was supported by a grant from the NIH (R01AR081287) awarded to KZT and JRF.

References: [1] Himann et al. (1987), *Med & Sci Sport & Exer,* 20(2); [2] Das Gupta et al. (2019), *Sci Rep*, 9(1); [3] Delabastita et al. (2021), *Scand J Med Sci Sports*, 31(5); [4] DeVita P, Hortobagyi T (2000), *J Appl Physiol*, 88(5); [5] Mickle et al. (2016), *J Orthop Sports Phys Ther*, 46(12); [6] Farris et al. (2020), *J R Soc*, 17(168); [7] Hoogkamer et al. (2018), *J Sports Med*, 48(4); [8] Ray SF, Takahashi KZ (2020), *Sci Rep*, 10(1):8793; [9] Takahashi et al. (2016), *Sci Rep*, 6(1); [10] ATS BOARD OF DIRECTORS (2002) ATS Statement: Guidelines for the Six-Minute Walk Test. 166:111-117; [11] Zifchock et al. (2006), *FAI*, 27(5):367–372.

CHANGES IN WALKING BIOMECHANICS AND DISTAL TO PROXIMAL SHIFT IN MULTI-MUSCLE ACTIVITY PATTERNS OCCUR IN RESPONSE TO KNEE EXTENSOR MUSCLE FATIGUE

Erica M. Casto[1*], Katherine A. Boyer[1]
[1]Department of Kinesiology, University of Massachusetts Amherst, Amherst, MA
*Corresponding author's email: ecasto@umass.edu

Introduction: Aging is associated with slowing gait speeds, a significant clinical marker for all-cause mortality risk. Slowing of gait has been attributed in part to altered biomechanics and muscle activity. One hallmark of aging gait is a reduction in ankle propulsion, and associated compensatory increase in hip kinetics. The underlying mechanisms for why this occurs in some but not all older adults in the absence of pathology are not well understood. Prior work has shown that lower limb strength is related to the distal-to-proximal shift [1], and that plantarflexor strength alone cannot explain reduced propulsion [2]. Knee extensor (KE) function (peak torque) declines with age and has been associated with mobility impairment, yet little is known about the direct role the KE muscles play in age-related changes in biomechanics. Inducing KE muscle fatigue (acute decrement in torque) in young healthy adults provides a mechanism to determine if changes in sagittal plane biomechanics are related to KE function in the absence of other age-related changes or pathology. The aim of this study was to quantify the impact of bilateral KE fatigue on walking mechanics and muscle activity. We hypothesized a decrease in joint range of motion, as well as a distal-to-proximal shift in joint kinetics and muscle activity patterns following fatigue.

Methods: Twenty-nine young healthy adults (18F; Age: 23±45) participated in the study following IRB approved informed consent. Participants completed bilateral KE strength and gait analysis before and after two KE fatigue protocols. Bilateral KE strength was quantified via maximal isometric voluntary contractions (MVIC) on a isokinetic dynamometer (Biodex System 4, NY) with a custom bilateral attachment. The fatigue protocols involved a series of repeated maximum dynamic contractions at 120 deg/sec and differed only by number of repetitions (60 vs 180 reps). KE fatigue was quantified as the percent decline in peak MVIC torque relative to baseline. Gait analysis involved participants walking on a split-belt instrumented treadmill at their preferred speed with 43 retro-reflective markers consistent with the Point Cluster Technique [3] and with electromyography (EMG) sensors placed on 14 muscles following SENIAM guidelines. Those muscles included Gluteus Maximus (GMAX), Gluteus Medius (GMED), Biceps Femoris (BF), Semitendinosus (ST), Tensor Fasciae Latae (TFL), Rectus Femoris (RF), Vastus Lateralis (VL), Vastus Medialis (VM), Lateral Gastrocnemius (LG), Medial Gastrocnemius (MG), Soleus (SOL), Tibialis Anterior (TA), Erector Spinae Longissimus (ESL), and Multifidus (MUL). Multi-muscle patterns (MMPs) were created by using 17 non-linearly scaled wavelets (10-250Hz) to resolve EMG signals in time-frequency space for each muscle and combining them into a single pattern vector as described previously [4]. Kinematics, kinetics, and EMG multi-muscle patterns were averaged over 10 strides and analyzed using principal components (PC) analysis. One-way repeated measures ANOVAs were used to test for within-subjects differences in PC scores between baseline and the 2 fatigued conditions with Tukey's post-hoc testing.

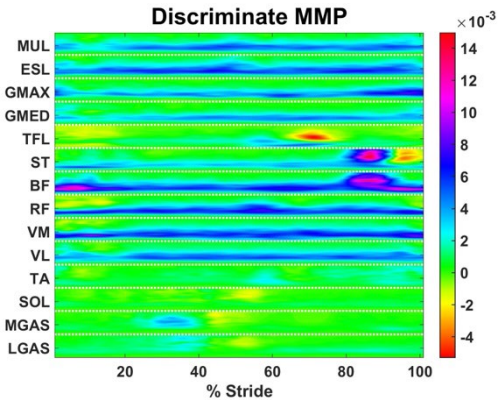

Figure 1: Discriminant MMP representing the weighted linear combination of PC1, PC6, and PC13. Increases in activation post fatigue are shown in blue and pink, while decreases post fatigue are in yellow and red.

Results & Discussion: Muscle fatigue was greater post 180 reps than post 60 reps relative to baseline (Δ19.1 ±14.1%; Δ 9.1 ±10.4%; p=0.003). Differences were found between baseline and post-180 reps for PC2 in both the hip ($p<0.001$, eigenvalue (EV) =8.4) and knee (p=0.001, EV = 17.5) joint angles and knee joint moment (p=0.001, EV =7.8) indicating an overall decrease range of motion, as well as more knee flexion and smaller knee moments throughout stance. No differences in ankle kinematics or kinetics were detected. The scores for PC1 and PC6 for the anterior-posterior (AP) ground reaction force (GRF) were different between baseline and post-180 reps which indicated smaller AP GRF through stance (p=0.001, EV = 39.1). MMP analysis revealed differences in scores between post-180 reps and both baseline ($p<0.001$) and post-60 reps ($p<0.001$) for PC1, PC6, and PC13 that together explain 24.2% of the variance in the data. No differences were found between baseline and post-60 reps MMP scores (p=0.5). These results suggested a general increase in muscle activity throughout the gait cycle for KE, gluteal, and low back muscles with a noted reduction in plantar flexor activity at push off (Figure 1).

Significance: In this study we identified changes in hip and knee mechanics, GRFs, and muscle activity with KE muscle fatigue in young healthy adults. Changes were only detected with the longer protocol where muscle fatigue was greater, suggesting a critical threshold of muscle fatigue or weakness may be required before changes in mechanics occur. Further, we observed a distal-proximal redistribution in muscle activity highlighting that reduced propulsion with age may not be solely a result of plantar flexor dysfunction, but reflective of weakness in more proximal muscles.

Acknowledgments: UMass Amherst Graduate School Dissertation Grant, SPHHS Dean's Dissertation Fellowship, Priscilla Clarkson Graduate Student Scholarship

References: [1] Hortobágyi, et al. (2016), *Eur J Appl Physiol* 116(4); [2] Franz (2016), *ESSR* 44(4); [3] Andriacchi, et al. (1998) *J Biomech.* 120(6); [4] von Tscharner (2000), *J Electromyogr Kinesiol.* 10(6).

FATIGUE-INDUCED CHANGES IN MUSCLE FUNCTION AND KNEE MECHANICS DURING GAIT

Millissia A. Murro[1]*, Katherine A. Boyer[2] and Jocelyn F. Hafer[1]
[1]Kinesiology & Applied Physiology, University of Delaware,[2] Kinesiology, University of Massachusetts Amherst
*Corresponding author's email: murrom@udel.edu

Introduction: Compared to younger adults, older adults tend to have altered gait patterns such as slower walking speeds, reduced stride lengths, smaller distal, and greater proximal joint ranges of motion and joint moments [1,2]. This altered gait may be due to poorer muscle function in older adults, including lower rate of torque development (RTD), peak torque, and muscle power [3,4]. However, the relationship between muscle function and gait mechanics is poorly understood. Cross-sectional studies across age or levels of muscle function established associations between muscle function and gait but do not reveal whether reduced muscle function is directly responsible for altered gait. Fatigue protocols that induce a decrease in muscle function may allow us to determine the extent to which decreased muscle function drives changes in gait. A better understanding of the relationship between muscle function and gait mechanics may enable better-targeted interventions to improve gait mechanics in older adults. Therefore, the purpose of this study was to determine if there is a relationship between changes in knee extensor muscle function (peak torque, RTD, and peak power) and changes in gait mechanics (knee flexion range of motion (ROM) during stance, knee extension moment during early stance, peak knee flexion moment, and knee flexion at heel strike) in response to a 30-minute treadmill walk meant to induce fatigue in older adults. We hypothesized that decreases in muscle function would be associated with decreased knee extension moments during early stance and increases in knee flexion ROM during stance, knee flexion at heel strike, and peak knee flexion moments.

Methods: Thirty-eight healthy older adults (20M/18F; 62.3±3.8years) were included in this analysis. Individuals performed isometric and high-velocity isokinetic knee extensor muscle testing along with over-ground gait analyses using standard motion capture techniques before and after a 30-minute treadmill walk (30MTW). The 30MTW consisted of walking at a preferred speed on a level treadmill, with periodic one-minute challenge periods (minutes 7, 17, and 27) with a 3% increase in the treadmill incline [4].

The muscle function variables of interest were knee extensor peak isometric torque, RTD, and peak concentric power at 270°/s. The gait mechanics variables of interest were knee flexion angle at heel strike, knee flexion ROM in stance, external knee extension moment in early stance, and peak external knee flexion moment. Muscle function and gait mechanics were compared pre to post-30MTW using a one-tailed paired t-test to determine if the cohort had changed on average in response to the walk. The change in each variable pre-to-post 30MTW was determined (Δ=post-pre). Stepwise linear regression was used to determine the extent to which changes in muscle function variables explained changes in each gait mechanics variable (α=0.05).

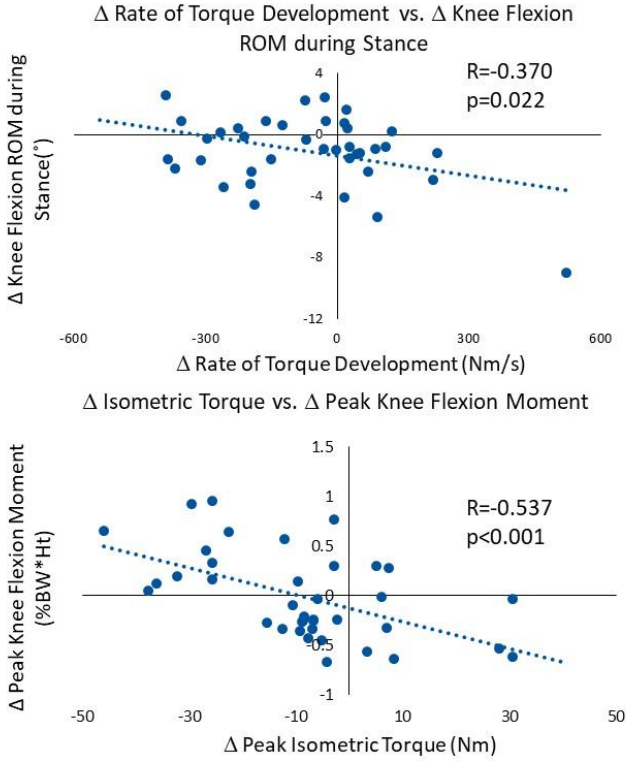

Figure 1. Associations between change in knee flexion ROM during stance and change in rate of torque development (top) and between change in peak knee flexion moment and change in isometric torque (bottom).

Results & Discussion: There were significant ($p<0.05$) declines in muscle performance (peak torque, -8.7±17.5 Nm; RTD, -70.0±195.7 Nm/s; and peak power, -40.1±63.4 W) post-30MWT. There were significant ($p<0.05$) decreases in knee extension moment in early stance (0.1±0.4%BW*Ht) and increases in knee flexion at heel strike (1.4±1.8˚) post-30MWT. No differences were found for knee flexion ROM in stance ($p=0.997$) and peak knee flexion moment ($p=0.544$).

Stepwise linear regressions indicated that the change in the RTD was the only significant predictor of the change in knee flexion ROM during stance, and the change in peak torque was the only significant predictor of the change in peak knee flexion moment (Figure 1). Previous studies found similar declines in muscle torque, RTD, and power in response to fatiguing protocols [4,5]. However, the research regarding kinetic and kinematic changes following fatigue is mixed. Our results suggest that the acute decline in the function of the knee extensors (RTD and peak torque) is directly related to one's ability to control sagittal plane knee movement during gait.

Significance: Typically, fatigue studies associate the changes in gait mechanics with changes in muscle strength or power, but few have assessed whether gait mechanics are associated with RTD. This work suggests that aspects of muscle function other than torque and power may provide insight into gait. Future research should focus on further exploration of the impact of RTD on gait mechanics in the older adult population.

References:

[1] Devita and Hortobagyi, *J Appl Physiol* 2000, 88(5):1804-1811 [2] Murray et al., *J Gerontol* 1969, 24(2):169-178 [3] Thompson BJ et al., *AGE*. 2014;36(2):839-849 [4] Hafer et al., *Gait Posture* 2019, 70:24-29 [5] D'Emanuele, *Front Hum Neurosci* 2021, 15: 701916

MINIMALIST AND ATHLETIC SHOES WITH AND WITHOUT DEFORMABLE FOOT ORTHOSES AFFECT HEALTHY FOOT ENERGETICS

Adrienne Henderson*[1], Dustin Bruening[2], Elisa Arch[1]
[1]University of Delaware, Newark, DE; [2]Brigham Young University, Provo, UT
*Corresponding author's email: ahendo@udel.edu

Introduction: Athletic shoes are a common shoe choice for clinical populations because they are a low-cost option that can work in conjunction with prescribed devices, such as orthoses, to fulfill patients' specific footwear needs. However, athletic-style shoes alter foot and ankle function [1]. Shoe stiffness can also impact foot and ankle function and is commonly manipulated in athletic shoes using deformable foot orthoses (DFOs) made from carbon fiber [2]. A key aspect of DFOs is their ability to store energy as they deform and release it as they rebound [3]. The effects of DFOs on foot energetics during walking, particularly when incorporated into different types of shoes, are not well understood. Therefore, to achieve the ultimate goal of improving patient walking function, we must first gain a basic understanding of how specific foot joints are influenced by DFOs and the shoes used with them. The stiffness of footwear used in this study ranged from the minimalist shoes (compliant), to walking shoes (moderately compliant), to minimalist shoes with DFOs placed inside (moderately stiff), to walking shoes with DFOs placed inside (stiffest). We hypothesized that with increasing shoe stiffness metatarsophalangeal (MTP) positive work would significantly increase (H1), that midtarsal positive work would significantly increase s (H2), and that ankle positive work would decrease(H3).

Methods: 10 healthy participants (28.7 ± 5.3 yrs, 78.4 ± 18.2 kg, 1.76 ± 0.09 m) walked at 0.8 statures/sec under 4 randomized footwear conditions: minimalist shoes (MS), walking shoes (WS), minimalist shoes with DFOs (MS+DFO), and walking shoes with DFOs (WS+DFO). A multi-segment foot marker set was applied through cutouts in WS and WS+DFO conditions, while they were applied directly to the sock-like upper for the MS and MS+DFO conditions. Time normalized 1st MTP, midtarsal, and ankle angles, moments, and power were calculated using Visual 3D. Peak positive and peak negative power were calculated. Positive and negative work for each joint were calculated by integrating the positive and negative areas under the power curve, respectively. Repeated measures ANOVA with a Holm post-hoc test was used to compare calculated metrics for each joint across all four shoe conditions.

Results & Discussion: Results showed that increasing shoe stiffness led to a significant increase in positive work (supporting H1) and peak power at the MTP joint and a significant decrease in MTP negative work and peak power (Figure 1A). This confirms that DFOs are capable of returning stored energy to the foot, specifically to the MTP joints while walking [3]. Additionally, the MTP joint, which is commonly known for its lack of mechanical efficiency in gait due to its large negative work and limited positive work, appears to become more mechanically efficient with increasing footwear stiffness, particularly with DFOs [4,5]. Compared to MS, walking with WS or WS+DFO resulted in significantly decreased negative work and peak power at the midtarsal joint with no change in the positive work (does not support H2), but a decreased peak positive power (Figure 1B). This indicates that active energy generation occurred at this joint, which is in direct contrast to the traditional model of midtarsal mechanics as a passive mechanism, where the amount of energy generated cannot be greater than the amount of energy previously stored [6]. Increasing shoe stiffness led to significantly decreased ankle positive work (supporting H3) and peak power and significantly increased its negative work and peak power (Figure 1C). These results showed that ankle energetics were closely associated with MTP energetics. As MTP peak positive power increased with increasing shoe stiffness, there was a concomitant decrease in ankle peak positive power. This resulted in the ankle becoming less mechanically efficient as the MTP became more mechanically efficient. These findings demonstrate that walking shoes with DFOs placed inside (WS+DFO) may significantly enhance the energy efficiency of the foot, but not the ankle.

Significance: Populations with decreased foot energetic efficiency (e.g., elderly individuals) may benefit from increased efficiency with WS+DFO use. Additional research is warranted to establish whether elevated foot energy efficiency translates to broader systemic benefits.

Acknowledgements: Supported by National Science Foundation (Award # 2032190)

References: [1] Franklin (2015) *Gait Posture* 42(3); [2] Ortega (2021) *Sports Med* 51; [3] Henderson (2021) *J Biomech* 128; [4] Bruening (2016) *Gait Posture* 35(4); [5] Zelik (2018) *J Biomech* 75; [6] Bruening (2018) *J Biomech* 73.

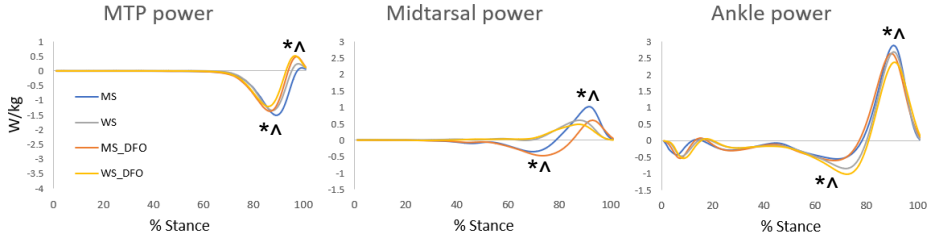

Figure 1: Power profiles for MTP (left), midtarsal (center), and ankle (right joint for all 4 footwear conditions. * Indicates significant main effects difference for work. ^ Indicates significant main effects difference for peak power. Alpha was set at 0.05.

EFFECTS OF AGE-RELATED LOSS OF MUSCLE STRENGTH AND MASS ON PREDICTED GAIT

Varun Joshi[1*], Katherine A Boyer[2], Jane A Kent[2], Brian R Umberger[1]
[1]School of Kinesiology, University of Michigan, Ann Arbor, MI
[2]Department of Kinesiology, University of Massachusetts, Amherst, MA
*Corresponding author's email: varunjos@umich.edu

Introduction: Age-related loss of muscle mass and strength is well documented [1]. Older adults are also known to prefer slower walking speeds and have a greater metabolic cost of transport (MCoT) [2]. Musculoskeletal gait simulations of older adults show similar behaviors [3] and suggest that lower "specific strength," i.e., maximal muscle force or power production per muscle mass, is the dominant factor for these differences. However, reduced specific strength is not always observed in single muscle fiber experiments [4].

We hypothesize that even if specific strength does not change, a non-uniform loss of muscle strength across the lower body might lead to some of the outcomes observed in older adults. We consider a situation reported in the literature where older adults lose nearly 30% mass in their proximal lower-limb muscles, but less than 10% mass in distal muscles like the soleus (SO) and tibialis anterior (TA) [5]. To test this hypothesis, we created a musculoskeletal model of a young adult (YA), and three models of older adults (OA), each with the same total body mass as YA, but representing different combinations of lower-limb muscle strength and mass loss:

1. OA-uniform10/30 – 10% mass loss and 30% strength loss in each muscle (23% loss of specific strength).
2. OA-uniform30/30 – 30% mass loss and 30% strength loss in each muscle (no loss in specific strength).
3. OA-specific – Muscle-specific mass loss [5] (no loss in specific strength, SO and TA 10% mass loss, others 30% mass loss).

For each model we solve for the optimal, symmetric, stride-periodic gait with the lowest MCoT and compare the resulting cost across OA models, as well as with the results for the YA model.

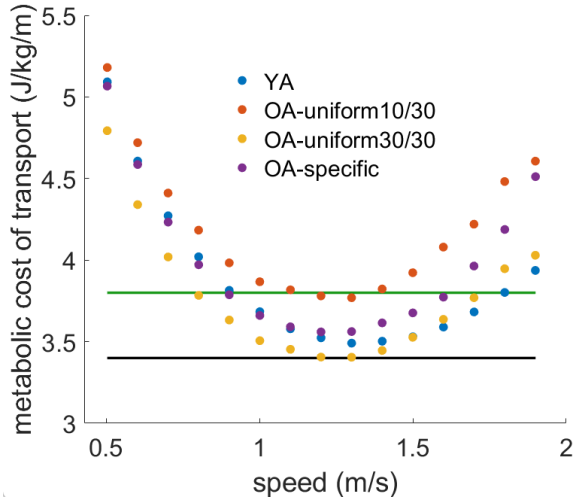

Figure 1: Predicted MCoT across walking speeds for three older adult models and a younger adult model. Solid horizontal lines represent the experimentally measured metabolic cost of transport for healthy young adults (black) and older adults (green) [9].

Methods: We developed an 18 muscle, 9 degree-of-freedom, sagittal-plane musculoskeletal model of a young adult human based on previous work [3, 6, 7]. A trajectory optimization problem that minimized a metabolic energy cost-like term was solved to obtain the muscle excitations that generate realistic walking behavior for this YA model [8], as well as variants of the model representing OAs. The objective function was defined as

$$\mathrm{MCoT} = \underset{e(t)}{min} \sum_{i=1}^{n_{\mathrm{mus}}} \int \dot{E}_i(t)\, dt$$

where $e(t)$ is the set of muscle excitations and $\dot{E}_i(t)$ is the metabolic power consumed by the i^{th} muscle at time t. The minimum MCoT was determined across a range of speeds from 0.5 – 1.9 m/s, as well as the speed at which this cost is minimized.

Results & Discussion: Of the three older adult models (OA-uniform10/30, OA-uniform30/30, and OA-specific) only OA-uniform10/30 consistently uses more energy per unit distance than YA at all walking speeds. OA-uniform30/30 counterintuitively uses less energy than YA, while OA-specific, with muscle-specific loss in mass and strength (SO and TA 10% mass loss, others 30% mass loss), leads to energy use equal to YA below 1.1 m/s and greater than YA above 1.1 m/s. We also find that the lowest possible MCoT for OA-specific and OA-30/30 models are lower than for OA-uniform10/30. The minimum-energy walking speeds for the models are- YA: 1.32 m/s, OA-uniform10/30: 1.23 m/s, OA-uniform30/30 and OA-specific: 1.25 m/s.

While specific mass and strength reductions do not lead to increased energy use at all speeds, they match experimental observations of greater energy use by older adults at moderate-to-high speeds, and lower energy-optimal speeds. A model with uniform loss of mass and strength, even though it is effectively weaker than the OA-specific model, uses less energy. While lower muscle strength and mass have been implicated in gait changes in OA [3], other age-related changes in neuro-physiological pathways, control strategies, connective tissue, force transmission mechanisms, and the metabolic efficiency of force production at the single fiber level might also contribute to differences in the metabolic energy cost of walking between OA and YA.

Significance: Older adults generally lose more muscle from their proximal lower limbs than from the distal limbs. This simulation study shows that a non-uniform loss of mass and strength across the lower limb can lead to greater energy use in older adults, and slower optimal walking speeds. Better measurements of the relative loss of mass and strength in the lower limb muscles of older adults would help refine musculoskeletal models of aging. This would lead to a better understanding how these muscle-specific changes contribute to gait outcomes in older adults, which could in turn be used to guide future interventions to preserve and restore mobility.

Acknowledgments: This work was funded by NIH grant 5R01AG068102.

References: [1] Thelen (2003), *J Biomech Eng* 125(1); [2] Martin et al (1992), *J App Physiol* 73(1); [3] Song and Geyer (2018) *J Physiol* 596(7); [4] Grosicki et al (2022) *J Physiol* 600 (23); [5] Naruse et al (2023) *J Appl Physiol* 134(4); [6] Nguyen et al (2019), *IEEE TNSRE* 27 (7); [7] Ong et al (2019) *PloS Comput Biol* 15 (10); [8] Dembia et al (2020) *PLoS Comput Biol* 16 (12); [9] Das Gupta et al (2019) *Sci Rep* 9 (1)

FOOT-SPECIFIC DETERMINANTS OF HABITUAL WALKING SPEED AND ENDURANCE IN YOUNG ADULTS

Ross E. Smith[1*], Aubrey Gray[1], Stephanie Gomez-Palacios[1], Howard Kashefsky[2], Kota Takahashi[3], Jason R. Franz[1]
[1]Biomedical Engineering, UNC Chapel Hill and NC State University, Chapel Hill, NC, USA'
[2]Division of Vascular Surgery, University of North Carolina Medical Center, Chapel Hill, NC, USA
[3]Department of Health and Kinesiology, University of Utah, Salt Lake City, UT, USA

*Corresponding author's email: rsmit@ad.unc.edu

Introduction: Older adults have slower habitual walking speeds and reduced walking endurance compared to younger adults. These phenomena have been in part attributed to reduced propulsion from the plantarflexor muscles. However, with age, propulsive deficits in walking may also manifest at the foot. It is well established that older adults have smaller and weaker intrinsic foot muscles [1], which may in turn require larger magnitudes of intrinsic foot muscle excitation to generate requisite stance-phase forces. Additionally, recent evidence suggests that foot anthropometrics affect gait propulsion; for example, longer heels are related to increased plantarflexor leverage, reduced plantarflexor muscle activity, and reduced metabolic cost in younger adults [2]. Foot anthropometrics may also dictate leverage for push-off, potentially affecting plantar intrinsic muscle (PIM) force-generating capacity and/or requisite activation, in turn affecting habitual gait speed and functional gait capacity (i.e., endurance). However, little is known about these latter associations. Thus, our purpose was to evaluate the extent to which functional gait outcomes - namely, preferred walking speed (PWS) and walking endurance (i.e., 6-minute walk test distance) may be governed by foot-specific neuromechanical (i.e., toe flexor strength, PIM excitation, and PIM thickness) and anthropometrical (i.e., heel and great toe length) factors. To establish a preliminary deterministic model to inform future studies, our study focuses foremost on a cohort of healthy younger adults. We hypothesized that faster PWS and greater 6MWT distance would correlate with: stronger toe flexors, higher PIM EMG, larger PIM thickness, longer heels, and longer toes.

Methods: 15 healthy younger adults (26.5 ± 5.4 years old, 76.6 ± 16.2 kg) participated. We measured 6MWT using published best practices [3] and PWS as the average velocity of three walking trials performed along 30-m walkway. We measured heel and great toe lengths from standing 3D motion capture as the distances between: (i) the posterior calcaneus to a point halfway between the navicular tuberosity and the sustentaculum tali and (ii) the medial aspect of the first metatarsophalangeal (MTP) joint to the distal phalange of the great toe, respectively. We quantified toe flexor strength during maximal voluntary isometric contractions using a custom foot dynamometer with the ankle and MTP joints at neutral anatomical positions. In this same position, B-mode ultrasound images of the flexor digitorum brevis (FDB), a large PIM, were used to calculate FDB thickness. Finally, we collected stance phase electromyographic records (EMG) during treadmill walking (1.2 m/s) from an indwelling electrode placed in the belly of the FDB. Multivariate linear regression models assessed the relationships between functional gait outcomes and foot-specific gait determinants.

Results & Discussion: Overall regression models for 6MWT distance [$F(5,9)=0.868$] and PWS [$F(5,9)=2.331$] were not significant (Table 1), indicating factors outside of foot dimensions and PIM function are needed to fully explain habitual walking speed and endurance in healthy, young adults. However, stronger ($r=0.588$, $p=0.011$) and shorter toes ($r=-0.455$, $p=0.048$) were each independently associated with greater 6MWT distances (Figure 1). Our interpretations are thus far speculative. Stronger toe flexors may enable increased net propulsion capacity during walking, allowing farther 6MWT distances in younger adults. Additionally, shorter toes – by reducing the net external moment arm of the ground reaction force vector and thereby requisite peak ankle plantarflexor demand on a per step basis – may delay the onset of fatigue and thereby improve walking endurance.

Significance: We have discovered novel evidence that two determinants of foot function – stronger but shorter toes – associated with improved walking endurance in younger adults. Using this framework in populations with foot dysfunction may provide useful clinical diagnostics and targets for training and footwear interventions.

Table 1. Linear regression model results and individual correlations for gait outcomes and foot-specific determinants.

	6MWT			PWS		
	r	p	Model	r	p	Model
Toe Strength (N/kg)	**0.588**	**0.011**	r=0.564	0.431	0.055	r=0.570
FDB EMG (% MVIC)	-0.153	0.293		-0.043	0.440	
FDB Thickness (Norm)	-0.094	0.370	*p*=0.128	0.088	0.378	*p*=0.568
Heel Length (Norm)	-0.408	0.065	F=2.331	-0.121	0.679	F=0.868
Toe Length (Norm)	**-0.445**	**0.048**		0.116	0.341	

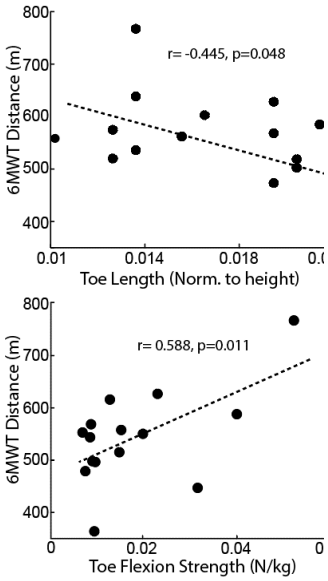

Figure 1. Toe length (top) and toe flexion strength (bottom) versus six-minute walk test distance. Significant effects denoted by correlation results in text. (a=0.05)

Acknowledgements: This study was supported by grants from the NIH (R01AR081287).

References: [1] Menz, et al. (2005). *J Gerontol*. [2] Papachatzis, et al. (2023). *J Exp Biol*. [3] American Thoracic Society (2002). *AJRCCM*.

WHAT CAN 350 MILES OF OVERGROUND WALKING TELL US ABOUT THE INDIVIDUALITY OF GAIT?

Tyler M. Wiles[1*], Seung Kyeom Kim[1], Nick Stergiou[1,2], Aaron D. Likens[1]
[1]Department of Biomechanics, University of Nebraska at Omaha
[2]Department of Physical Education & Sports Science, Aristotle University, Thessaloniki
*Corresponding author's email: tylerwiles@unomaha.edu

Introduction: Most humans have a fingerprint that is unique and persists throughout life. Although fingerprints may not radically change throughout life, experiences such as extreme burns, skin diseases, or trauma will change their appearance. Similarly, facial features, vocal tone, vernacular, style, and personality change with age or significant life experiences, but fundamental features remain constant. The same is true for gait. Each person is composed of unique physiological, biomechanical, and psychological characteristics that define who they are, and may be evident in the way we walk. Like fingerprints, gait has been used to accurately identify individuals based on fundamental phenotypes [1-4]. In fingerprints, a significant identifier is the layout of the finger's ridges, facial features for mugshots, or potentially, spatiotemporal characteristics of gait [5]. We hypothesized that there are gait characteristics intrinsic and unique to everyone, so that everyone has a unique "gaitprint", similar to humans possessing unique fingerprints with identifiable ridges. We further hypothesized that common gait features would provide answers to uncovering this gaitprint [6]. Our team expected to, and accurately, found unique gaitprints using basic gait kinematics.

Methods: Twenty-six young (12 female, 24.5 ± 2.1 years old, 174.5 ± 7.0 cm tall, weighing 72.3 ± 15.6 kg), 28 middle (24 female, 46.4 ± 6.1 years old, 170.5 ± 7.4 cm tall, weighing 80.9 ± 14.6 kg), and 27 older adults (12 female, 64.3 ± 6.2 years old, 172.2 ± 9.3 cm tall, weighing 80.6 ± 15.9 kg) were sampled from the NONAN GaitPrint dataset [7]. Lower body kinematic data was collected using inertial measurement units recording at 200Hz. Participants completed 18, four-minute overground walking bouts, evenly split into two days. A total of 74 variables were then calculated including bilateral spatiotemporal variables consisting of distance traveled, average speed, cadence, stride and step lengths, widths, and times, supplemented by percentage of stance, swing, and support phases. Bilateral lower body joint angles (hip, knee, ankle) were also calculated as mean and standard deviations of peak flexion, extension, range of motion, and velocity. Approximately 350 miles (n = 1,458 trials) of walking data were used to train four methods of identification under different data splits: Euclidean distance (ED), cosine similarity (CS), random forest (RF), and support vector machine (SVM) classifiers. Each method was trained on a random 70% of the data (70%/30%), trials from day 1 (Day 1), or the first trial (Trial 1), and tested on the remainder of all trials, per data split, for identification (Table 1). Rank 1/5/10 use the top 1/5/10 most similar trials for identification.

Results & Discussion: Identification performance was best in the 70/30 split with the RF approach generating the best Rank 1 Accuracy, followed by SVM, CS, and ED, in that order. Our results also demonstrated that the simple approach of comparing gait feature vectors (ED and CS) resulted in relatively good identification, with the CS method outperforming the ED method. Accuracy deteriorates when less training data is used, especially in the Trial 1 condition, where most notably ED drops below chance levels. Machine learning approaches (RF & SVM) fared better, although performance still dropped, especially for Trial 1 SVM performance. Secondary identification tests found that the removal of distance traveled increased accuracy (by nearly 20% in some cases), and that an optimized collection of gait features can reach at least 90% accuracy in as little as 15 features (70/30 Rank 1 ED) or 90% in seven features (70/30 SVM). Considering our results, a general implication is that a person's identity is indeed related to patterns of gait variability produced when walking overground. Potential limitations of the current work include the lack of middle-aged men as of February 2024, and the initial restriction to only use linear measures of variability of the angular and spatiotemporal features of gait. The investigation of strictly nonlinear measures of gait variability is underway and expected to provide similar identification accuracy compared to this report [6,8].

Table 1: Percentage of correct identifications per data split and algorithm including using the Rank 1,5,10 most similar trials.

Distribution	ED Rank 1	ED Rank 5	ED Rank 10	CS Rank 1	CS Rank 5	CS Rank 10	SVM	RF
70/30	91.55%	94.75%	96.35%	95.66%	97.49%	98.40%	98.49%	98.63%
Day 1	74.07%	87.79%	91.49%	80.25%	91.91%	95.47%	92.59%	91.08%
Trial 1	42.99%	60.35%	67.90%	58.17%	74.80%	84.02%	65.94%	70.66%

Significance: We provide evidence that the way we walk is a distinguishable biometric, a gaitprint, with results supporting nearly 99% identification accuracy. The exceptional identification accuracy is rooted in simplicity and reliance on long standing features of gait and its variability. For example, the hip and ankle provide almost the entirety of the work to walk forward [9]. The importance of the hip and ankle, and their subsequent use as a unique identifier, are supported as highly weighted features in our methodology. In addition, almost all gait features involving standard deviations were commonly found to be the most important identifiers.

Acknowledgements: NSF 212491, NIH P20GM109090, R01NS114282, University of Nebraska Collaboration Initiative, the Center for Research in Human Movement Variability at the University of Nebraska at Omaha, NASA EPSCoR, IARPA.

References: [1] Wang et al. (2010), *DICTA.* 320-327; [2] Cao et al. (2018), *IET Radar Sonar Navig.* 12(7); [3] Nixon (2005), *Human Identification Based on Gait*.; [4] Świtoński et al. (2011), 7th *ISPA.* Dubrovnik, Croatia.; [5] Jain et al. (2002), *Pattern Recognit.* 35(11).; [6] Stergiou & Decker (2011), *Hum. Mov. Sci.* 30(5); [7] Wiles et al. (2023), *Sci. Data*. 10, 867; [8] Gibbons et al. (2020) *Motor Control*. 24(1).; [9] Eng & Winter (1995), *J. Biomech.* 28(6).

EVALUATING JOINT KINEMATICS AND MOBILITY ACROSS PROSTHETIC FEET IN REAL-WORLD ACTIVITIES

Yisen Wang[1*], Katherine H. Fehr[1], Julian C. Acasio, Brad D. Hendershot, Madeleine E. Beauvais[1], Peter G. Adamczyk[1]
[1]University of Wisconsin-Madison, Madison, WI, USA
*Corresponding author's email: ywang2557@wisc.edu

Introduction: Comparative evaluation of how different prosthetic feet affect movement is common in the laboratory but rare in other settings. Motion reconstruction using wearable inertial sensors facilitates such real-world gait analysis. With improvement in methods and sensor system design, more abundant information can be recorded and extracted from real-world dataset. In this study, we used a suite of prosthesis-mounted inertial sensors to perform weeks-long movement monitoring of persons with transtibial amputation as they wore different prosthetic feet for a week each during real-world, everyday living. We evaluated mobility and joint kinematics in terms of bouts of walking and joint ranges of motion (ROM), and adaptation over time.

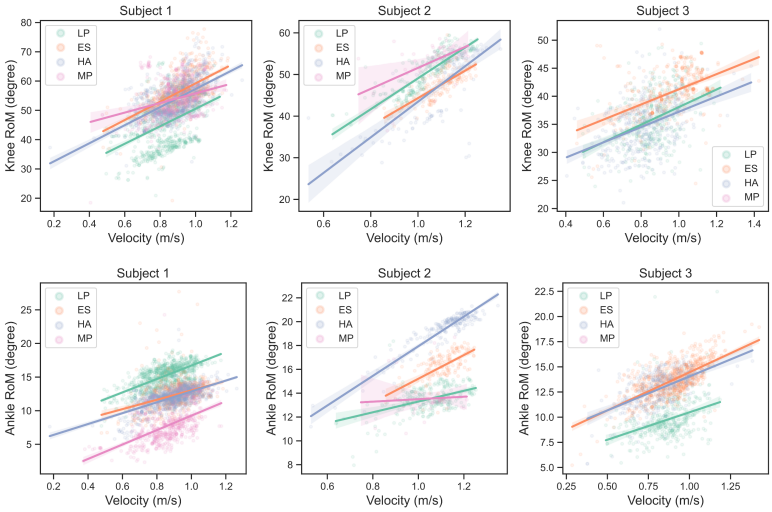

Figure 1: Linear fit for knee and ankle joint ranges of motion (RoM) vs. speed.

Methods: Three participants (2F/1M, 80.2±27.5 kg, 58±12.2 yr) were equipped with three or four prosthetic feet in a random order: (1) low-profile carbon fiber foot (LP), (2) c-shaped energy storage and return foot (ES), (3) foot with hydraulic damper ankle (HA), (4) foot with microprocessor-controlled damper ankle (MP). A customized sensor suite containing multiple IMUs on the foot, shank, and thigh and a GPS module were attached to the prosthetic-side leg. The real-world walking trajectory was reconstructed from the foot-mounted IMU data using strap-down integration [1]. The knee joint and angle joint motions were reconstructed from shank vs. thigh IMUs and shank vs. foot IMUs, respectively, using drift-free self-alignment methods [2]. Ankle and knee joint sagittal ROM and average walking speed were computed for each steady walking bout [3]. Relationships by foot between ROM and speed were fitted by linear regression.

Results & Discussion: Walking speed increased with bout duration (Table 1), in concurrence with [4]. Participant 2 demonstrated faster average walking speeds in each bout, consistent with this participant being younger and more active than the other two. Participant 1 was an older and more hesitant walker, and showed the largest range of motion and relatively slow speed (Figure 1). Participant 2 showed distinct ankle and knee ROM vs. speed trends across different feet, with more significant differences than the other two subjects (Figure 1). The LP foot in general led to decreased knee ROM, perhaps as a result of higher stiffness compared with the ES foot [5]. However, a surprising result was that participant 1 had the largest ankle ROM using the LP foot. Over time, the general trend for ROM vs. speed shifted downwards (Figure 2), indicating an adaptation process on PC foot where reduced knee ROM was used despite achieving the same speeds. However, we only observed this adaptation on subject 1, perhaps due to being older and less active and thus may have adapted to the new foot more slowly [6].

Table 1: Walking speed (strides) for bouts of walking, binned by duration.

	ID	Bouts Duration (seconds)					
		<10	>10	10-30	30-60	60-120	>120
Average Walking Speed (m/s)	1	0.49±0.17 (n=3131)	0.70±0.16 (n=2020)	0.65±0.15 (n=1367)	0.78±0.14 (n=326)	0.86±0.12 (n=183)	0.87±0.09 (n=144)
	2	0.49±0.22 (n=540)	0.75±0.26 (n=280)	0.63±0.22 (n=180)	0.93±0.19 (n=46)	0.97±0.15 (n=24)	1.06±0.09 (n=30)
	3	0.47±0.19 (n=3962)	0.65±0.16 (n=2178)	0.63±0.16 (n=1800)	0.71±0.16 (n=306)	0.80±0.14 (n=63)	0.83±0.09 (n=9)

Significance: These results begin to demonstrate the potential of high-resolution, long-term real-world motion tracking. Such rich information aids in understanding overall mobility outcomes and more specific joint-level mechanisms, with potential to elucidate how different devices and environments affect movement. Moreover, capturing subject-specific responses to different prosthetic feet and adaptation over time, which is rarely captured in literature [6], further enhances the value of wearable sensor-based approaches for real-world studies.

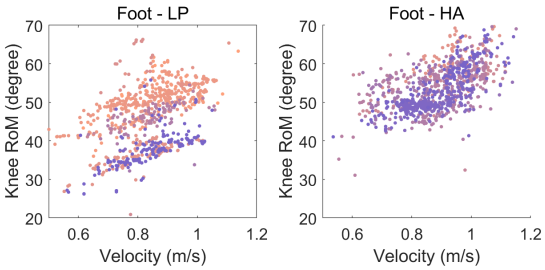

Figure 2: Adaptation of knee angle range of motion (ROM) in participant 1, from light red (day 1) to light blue (day 7).

Acknowledgements: Supported by DoD award W81XWH-19-2-0024. Views do not reflect official policy of nor implied endorsement by the DoD or US Government.

References: Wang+ 2024 *Sensors* 24(5). Potter+ 2022 *Sensors* 22(21). Dubbeldam+ 2010 *Clin Biom* 25(8). Kirk+ 2024 *Sci Rep* 14(1). Shepherd+ 2017 *TNSRE* 25(12). Wanamaker+ 2017 *POI* 41(5).

DETAILED GAIT KINEMATICS FROM A SINGLE WEARABLE SENSOR: COMPARING FOUR ANKLE-FOOT PROSTHESES IN FREE-LIVING, UNSUPERVISED NEIGHBORHOOD WALKS

Katherine Heidi Fehr[1], Yisen Wang[1], Jennifer Nicole Bartloff[1], Julian C. Acasio, Brad D. Hendershot, Peter G. Adamczyk[1]
[1] Mechanical Engineering Department, University of Wisconsin–Madison, Madison, WI
*Corresponding author's email: kfehr@wisc.edu

Introduction: Following a lower-limb amputation, selecting a suitable prosthetic foot is critical. Objective data is needed to inform clinical decision-making when prescribing an appropriate prosthesis. Most existing studies on device performance are conducted in controlled lab environments—the few that take place outside the lab and are often low-resolution activity estimates [1]. Here, we developed a method to use data from a single prosthesis-mounted sensor and personalized 3D scan to obtain real-world, detailed gait kinematics. In this case study, we compare gait outcomes of a person with transtibial amputation in the real-world during unsupervised neighborhood walks while using prostheses with different features that could affect foot clearance and swing phase kinematics.

Table 1: Summary statistics of key measures of gait kinematics (mean ± s.d.)

	N	MFC	N	WS	SL	SWV	MTX	SWD
units	*count*	*mm*	*count*	*m/s*	*m*	*mm*	*mm*	*score*
LP	673	12.4 ± 5.6	488	1.15 ± 0.04	1.21 ± 0.06	56.0	-56.1 ± 72.1	40
ES	844	15.2 ± 6.9	791	1.08 ± 0.03	1.27 ± 0.06	64.6	-49.4 ± 80.0	39
HA	1046	10.2 ± 7.9	815	1.09 ± 0.03	1.27 ± 0.07	68.4	-72.3 ± 83.8	35
MP	390	21.1 ± 6.4	217	1.15 ± 0.05	1.24 ± 0.07	43.0	-56.7 ± 53.9	29

Methods: One female with unilateral transtibial amputation (age: 44 yrs, time since amputation: 27 yrs, body mass: 71 kg) used four prostheses in everyday life for one week at a time, each outfit with a single sensor: (1) low-profile carbon fiber foot (LP), (2) c-shaped energy storage and return foot (ES), (3) foot with an articulating hydraulic ankle (HA), and (4) microprocessor-controlled damper at the ankle (MP). To have a comparable data set, we used GPS to extract one spontaneous neighborhood walk with each foot from the participants' month-long data collection. Each walk was in the same neighborhood along a similar path. To extract key gait kinematics, we first reconstructed the prosthesis-mounted IMU trajectory [2] and combined it with data from a 3D scan of each corresponding prosthesis (Figure 1). We then calculated minimum foot clearance (MFC), defined as the shortest vertical distance between the shoe—considering all the points from the scan (Figure 1)—and walking surface during forward swing phase. By dividing the points posteriorly and anteriorly, we also calculated minimum hindfoot and forefoot clearance. Stride length (SL) and stride width variability (SWV) were determined [3], defining forward and lateral foot placement as the position of the IMU at each stance phase relative to the local forward direction (best-fit line in a centered moving window of seven strides). Using the position of the toe from the 3D scan, we measured the maximum toe excursion (MTX)—the maximum orthogonal distance between the toe trajectory and the afore-described best-fit line. To further interpret these measures, walking speed (WS) was calculated on a stride-by-stride basis by dividing SL by elapsed time. In addition, the participant scored each foot after the week of use with a "Satisfaction with Device" survey (SWD) [4].

Results & Discussion: MFC was highest when using the MP foot, suggesting a gait less prone to trips. When using the HA foot, MFC was lowest (Figure 1), contrary to the expected behavior of the ankle "lifting" the toes during swing. Use of the MP foot also resulted in the lowest SWV and MTX deviation, which may reflect improved stability [5]. The participant also walked fastest wearing the MP foot (tied with LP); generally, faster self-selected walking speed is positively correlated with functional ability [6]. Based on the SWD score, the participant preferred LP, which coincided with faster walking speed, reduced SWV, and near-average SL deviation and MTX performance (in comparison to the other prostheses). While excelling in many kinematic measures, MP received the lowest SWD score.

Significance: The proposed method offers a multi-dimensional understanding of the participant's gait with each prosthesis. This work demonstrates the potential of a (singular) sensor-based approach for gaining a rich understanding of gait with different prostheses in real-world environments, helping inform prosthetic prescription practices. Additional analyses across multiple environments and terrains, repeated paths, and days of adaptation will further improve the richness of these findings.

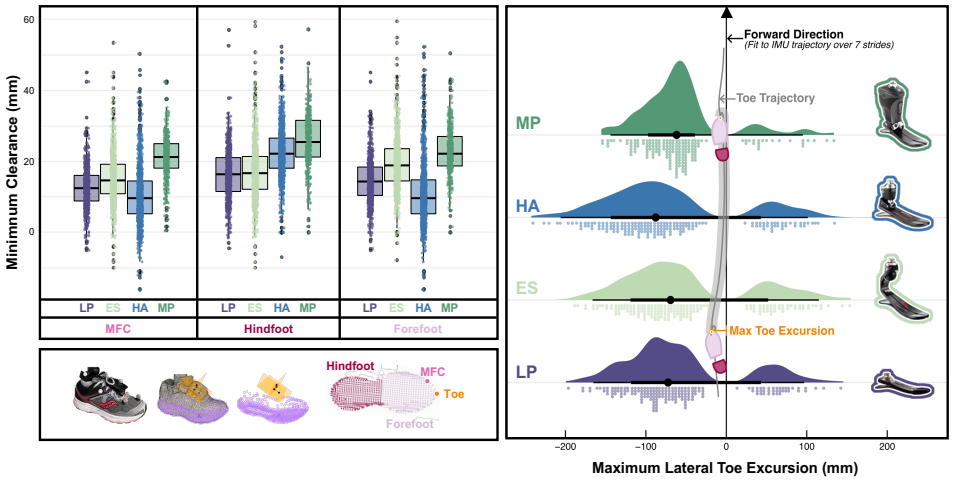

Figure 1: Minimum clearance of the whole-foot, hindfoot and forefoot with each prosthesis, note that some MFC values are negative due to a rigid body assumption made when fusing the IMU reconstruction with the 3D scan (top left), illustration of the 3d scan to whole-foot trajectory reconstruction (bottom left), and maximum lateral toe excursion with each prosthesis.

Acknowledgments: Supported by award W81XWH-19-2-0024. Views do not reflect official policy of nor implied endorsement by the DoD or US Government.

References:

[1] Raschke (2015), *J. Biomech* **[2]** Wang et al. (2024), *Sensors* **[3]** Ojeda et al. (2015), *Med. Eng. Phys.* **[4]** Heinemann et al. (2003) *Prosthet. Orthot. Int.* **[5]** Collins et al. (2013), *PLOS ONE* **[6]** Fritz et al. (2009), *J Geriatr. Phys. Ther.*

AGE AND TASK INFLUENCE ANTERIOR-POSTERIOR FOOT PLACEMENTS IN HUMAN LOCOMOTION

Ashwini Kulkarni[1*], Chuyi Cui[2], Shirley Rietdyk[3], Satyajit Ambike[3]
[1]Old Dominion University, Norfolk, VA; [2]Stanford University, CA; [3]Purdue University, IN, USA
*Corresponding author's email: a1kulkar@odu.edu

Introduction: Maintaining stable walking requires consistent positioning of the extrapolated center of mass relative to the feet (base of support) [1]. This dictates our anterior-posterior (AP) foot placement at each step. However, obstacles force us to place our feet at precise locations relative to the obstacle to avoid tripping [2]. These demands on AP foot placement are antagonistic, and we must prioritize one constraint over the other. Our previous work indicates a shift towards prioritizing the environment-induced constraint as we approach and step over visible obstacles [3].

To delve deeper into real-world walking, we examined how young and older adults manage AP foot placement when encountering sequential constraints. People typically plan upcoming foot placements two steps ahead [4], so we disrupted this process by introducing a visual target two steps before the obstacle and measured its impact on foot placement coordination. We predicted that both age groups would prioritize the two environmental constraints on foot placement. However, the visual target, posing no threat to balance, may elicit a weaker response from older adults. This target is expected to disrupt the natural approach to the obstacle, and older adults might be less willing to deviate from their established strategy for crossing the obstacle.

Methods: Fifteen younger (24±3 years) and fourteen older adults (64±5 years) walked on an 8 m walkway and crossed an obstacle placed midway in the walkway. They performed a control task with just the obstacle, and a task with a visual target at their preferred foot location that they stepped on during the approach (Fig. 1A). Each task was performed 20 times. The across-trial covariance in the distances of the trail and lead heel from the obstacle was quantified using the inter-step covariation (ISC) index [3] for multiple steps. A lower ISC index simultaneously indicates more variable step length, a greater priority for the environmental rather than the body-centric constraint, and vice versa. A Task × Step × Age ANOVA on the ISC index was conducted.

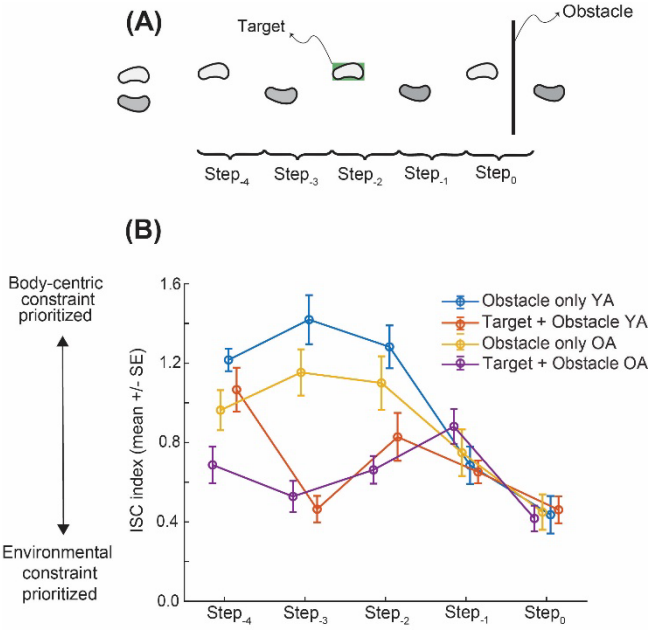

Figure 1. (A) Bird's eye view of the walkway with target and obstacle. (B) Mean + SE of the inter-step covariance index (ISC).

Results & Discussion: The ANOVA revealed a Task × Step interaction ($p < 0.001$). The ISC index changed systematically with step, and this pattern was influenced by Task. Thus, including the stepping target impacted the covariance in the foot placements before and at the target; this resulted in lower ISC value for $Step_{-3}$ (Fig. 1B).

Our key finding is a significant Age × Step interaction ($p = 0.002$). Foot placement coordination index (ISC) over multiple steps differed between age groups. Older adults exhibited a lower ISC at the obstacle crossing step ($Step_0$) compared to all preceding steps. Younger adults, on the other hand, showed a dip in ISC at both the crossing step and the preceding step ($Step_{-1}$). Both age groups minimized ISC at the crossing step and the step involving the visual target ($Step_{-3}$). This confirms our prediction that both groups prioritized environmental constraints. However, the visual target's effect across age was not what we had predicted. Older adults lowered ISC across all approach steps, suggesting a more consistent and cautious approach. Younger adults displayed more flexibility, switching between prioritizing consistent step length and precise foot placement (compare Fig. 1B, purple and red curves, $Step_{-4}$ to $Step_{-2}$). This difference might reflect older adults' aversion to task switching, which is known to demand greater cognitive resources. Alternatively, the target might have prompted them to initiate the process of lowering ISC earlier to reach the optimal level for obstacle crossing. This also means that older adults tolerated the higher inconsistency in step length caused by their focus on precise foot placement. This suggests they perceived the potential instability from variable step length as less threatening than a trip over the obstacle.

Significance: Foot placement control is critical for maintaining balance while walking. Traditionally, researchers believed that medial-lateral foot placement is actively controlled, whereas AP placement is dictated by sagittal-plane passive dynamics of gait [5]. Although this view holds during straight-line walking on level surfaces, it may likely fail in complex environments. Our work suggests active supra-spinal control arising from vision and motor centers in the brain governing AP control when humans navigate cluttered environments. This active control becomes evident when humans approach and cross visible stationary obstacles.

Studying active AP foot placement control is important because tripping, a significant cause of falls (17-59% of falls) [6], primarily occurs in the sagittal plane. The sensitivity of the ISC index to age and task variations suggests that our methods could be valuable tools to identify whether trips occur due to deficits in active AP foot placement control during complex navigation.

References: [1] Hof, 2005, *J Biomech*, 38(1); [2] Chen et al., 1991, *J Gerontology*, 46(6); [3] Kulkarni et al., 2023, *Motor Control.* 27(1); [4] Matthis and Fajen, 2014, *J Exp. Psych*, 40(1); [5] Kuo and Donelan, 2010, *Phys Ther*, 90 (2); [6] Berg et al., 1997, *Age Ageing*, 26(4).

ASYMMETRIC WALKING PRODUCES IMPROVEMENTS IN LIMB LOADING RATE VARIABILITY

Noah Davidson[1*], Ainsley Svetek[1], Kristin D. Morgan[1]
[1]Department of Biomedical Engineering, University of Connecticut, Storrs, CT 06269
*Corresponding author's email: noah.davidson@uconn.edu

Introduction: Individuals following post-anterior cruciate ligament reconstruction (ACLR) have been shown to demonstrate altered motor control, leading to more variable and pathological limb loading characteristics [1]. Continual exposure to these irregular biomechanics, observed as increased loading rate variability (LRV), can then contribute to the development of degenerative conditions like knee osteoarthritis (OA) [2,3]. Furthermore, despite extensive rehabilitation protocols, between-limb asymmetries persist. One such enduring asymmetry is between-limb loading rates; this interlimb discrepancy demonstrates the inability to efficiently attenuate forces propagating through the limb, contributing to higher likelihoods of developing knee OA. However, a recent study demonstrated how purposely induced asymmetric walking can be effective in restoring healthy motor control [4], therefore this study sought to utilize Poincaré analysis to investigate if LRV is improved following asymmetric walking.

Here, asymmetric walking was utilized to initialize therapeutic gait adaptations. However, rather than comparing loading rate means, we investigated the ability of purposefully induced asymmetric walking to reduce pathological LRV in the overloaded limb of post-ACLR individuals using Poincaré analysis. Poincaré analysis, which is a technique that can capture the dynamic stride-to-stride variability during walking, served to quantitatively and graphically evaluated short- and long-term limb LRV as it is a valuable measure of motor control. We hypothesize that both the short- and long-term LRV in the overloaded limb of post-ACLR individuals would decrease after asymmetric walking when the overloaded limb is moving slower than the underloaded limb indicating the adoption of healthy motor control.

Methods: Six post-ACLR individuals (age: 21.2 ± 1.5 years; height: 1.69 ± 0.06 m, mass: 68.5 ± 14.7 kg, time since surgery: 52.0 ± 22.6 months) completed a walking protocol on an instrumented Bertec split-belt treadmill. Participants first performed baseline symmetric walking trials at 1.0 m/s and 1.5 m/s to determine their overloaded limb; defined by a between-limb loading rate percent difference of >4% [5]. Participants then performed 10-minute asymmetric walking trials where one limb was set at 1.0 m/s and the other at 1.5 m/s, followed immediately by 3-minute post-adaptation 1.0 m/s and 1.5 m/s symmetric walking trials. The order of the post-adaptation symmetric walking trials was randomized. To evaluate if there was a positive adaptation in limb LRV in response to asymmetric walking, Poincaré analysis was used to compute the short- (SD1) and long- (SD2) term LRV for each limb during the symmetric walking trials. Wilcoxon signed rank tests was performed to compare baseline and post-adaptation limb LRV ($\alpha < 0.05$).

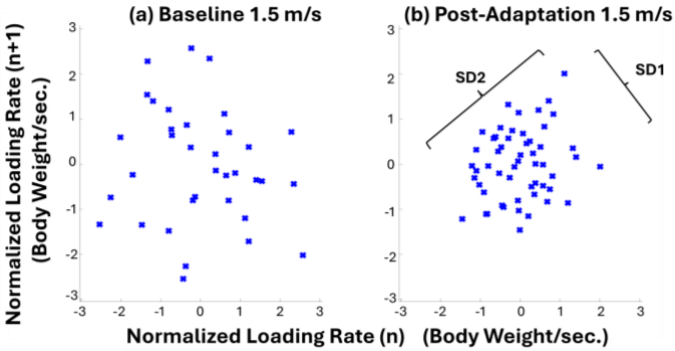

Figure 1: Poincaré plots of loading rate data from a post-ACLR participant's overloaded limb during the symmetric (a) baseline 1.5 m/s trial and the (b) post-adaptation 1.5 m/s walking trial that followed the asymmetric walking trial where the overloaded limb was set at the slower speed.

Results & Discussion: Poincaré analysis demonstrated that post-ACLR individuals decreased their limb LRV following asymmetric walking. Despite only having six available participants, short-term LRV was significantly different ($p=0.036$) between the 1.5 m/s baseline and the 1.5 m/s post-adaptation walking trials with mean SD1 values decreasing by 0.21 following asymmetric walking. There was also a strong trend towards significance ($p=0.093$) as SD2 values, which represent long-term variability, also decreased following the asymmetric walking trial where the overloaded limb was set at the slower speed. Additionally, the Poincaré plots graphically highlighted the positive adaptation in motor control as both SD1 and SD2 decreased indicating a reduction in limb LRV (Fig. 1). These results of this preliminary analysis demonstrate that while post-ACLR individuals continue to suffer impaired motor control that alters their ability to maintain consistent loading mechanics, they continue to possess the ability to adopt improved and more stable biomechanics.

Significance: The pathological limb loading variability often seen in post-ACLR individuals can predispose them to higher likelihoods of reinjury or development of knee OA, which makes correcting any lingering motor control deficits a topmost priority. Here, Poincaré analysis was able to quantitatively and graphically demonstrate how asymmetric walking could lead to the adoption of healthy limb loading dynamics measured by a decrease in both short- and long-term LRV. Fortunately, the reduction in LRV following asymmetric walking suggests that subject-specific, targeted asymmetric walking can be a viable post-ACLR rehabilitative strategy.

Table 1: Comparison of mean short- (SD1) and long- (SD2) term limb loading rate variability (LRV) in the overloaded limb during the 1.5 m/s baseline and post-adaptation symmetric walking trials. *Indicates significant difference (p-value <0.05)

Variable	Baseline Trial	Post-Adaptation Trial	p-value
SD1	0.78 ± 0.36	0.57 ± 0.14	0.036*
SD2	0.81 ± 0.40	0.54 ± 0.17	0.093

References: [1] Davidson et al. (2024), *Gait & Posture*; [2] Moraiti et al. (2013), *J Arthrosc. Rel. Surg.* 25(7); [3] Luc et al. (2014), *J Ath. Train.* 49(6); [4] Halkiadakis et al. (2023), *Ortho. J Sports Med.* 11(11); Herzog et al. (1989), *Med. & Sci. in Sports Exers.* 21(1).

THE EFFECT OF TRANSFEMORAL AMPUTATION ON HIP MUSCLE QUICKNESS

Kristin A. Perrin[1*], Noah J. Rosenblatt[2], and Deanna H. Gates[1]
[1] School of Kinesiology, University of Michigan, Ann Arbor, MI 48103
[2]Rosalind Franklin University of Medicine and Science, North Chicago, IL, USA
*Corresponding author's email: kperrin@umich.edu

Introduction: Over 50% of people with amputation fall annually [1]. To avoid falling when laterally perturbed, it is necessary to generate a rapid response from hip musculature [2]. While it is generally believed that people with transfemoral amputation (TFA) have weaker hip musculature [3], no studies have explored how quickly this strength can be accessed. Measures of neuromuscular quickness have been shown to have a stronger relationship with fall risk than overall strength in older adults [4]. Therefore, the purpose of this study is to compare hip neuromuscular quickness between people with and without TFA.

Methods: Four individuals with TFA and three healthy sex-, age-, weight-, height-, and activity-level matched controls participated after providing written informed consent. Potential TFA participants were included if they had a unilateral amputation and at least six months of prosthesis use. Participants performed 1-2 days of testing, separated by at least 48 hrs. On each day, we tested hip strength in abduction and flexion during maximum voluntary isometric contraction (MVC) using a computerized dynamometer (Humac Norm, CSMi, Stoughton, MA) sampling at 1250 Hz. Participants then performed 100 rapid, sub-maximal contractions where they were instructed to "contract as explosively as possible and to relax immediately." [5] Trials were divided into 5 blocks of 20 contractions. Each block consisted of 5 contractions, 4- seconds apart, at four intensities (20%, 40%, 60%, 80% of MVC), presented in ascending order. Target zones of ± 10% of the target intensity were displayed on a screen. Participants were given a one-minute break between blocks. The first block was used as practice and not included in analyses. All participants completed testing with both limbs, in random order. The residual limb was assessed with the prosthesis off. Torque data were filtered using a 5th order low-pass Butterworth filter. For each contraction we extracted the peak torque and the peak rate of torque development (RTD), calculated as the derivative of the filtered torque signal. After plotting the peak torque (%MVC) versus peak RTD (%MVC/s) for each contraction, the rate of torque development scaling factor (RTD-SF) was obtained as the slope of the best fit line (Fig.1). The residual and intact limb for participants with TFA were compared to the dominant limbs for controls as there were no differences between dominant and non-dominant limbs. Hedges' g was used for comparison with reporting of medium effect size > 0.5 and a large effect size > 0.8.

Results & Discussion: The intact limb was weaker than controls in both hip abduction (g= 1.75) and flexion (g= 2.47). The residual limb was weaker than controls in abduction (g= 0.75) and intact limb in flexion (g= 0.71). Participants with TFA had decreased neuromusuclar quickness on their residual compared to intact limb in abduction (g= 1.35) and flexion (g= 4.67). Both limbs had decreased quickness compared to controls in both abduction (RL g= 0.75, IL g= 1.75) and flexion (RL g= 4.51, IL g= 0.52). R^2 values were lower for the residual limb, indicating that participants had less consistent responses. Decreased consistency could be the result of impaired proprioception of the residual limb, which decreases the ability to accurately control submaximal contractions. The results are limited by the small sample size. We will continue collecting data in a larger sample to determine if amputation broadly has an impact on muscle function and similarly if factors such as amputation etiology, and/or K-level might explain individual differences.

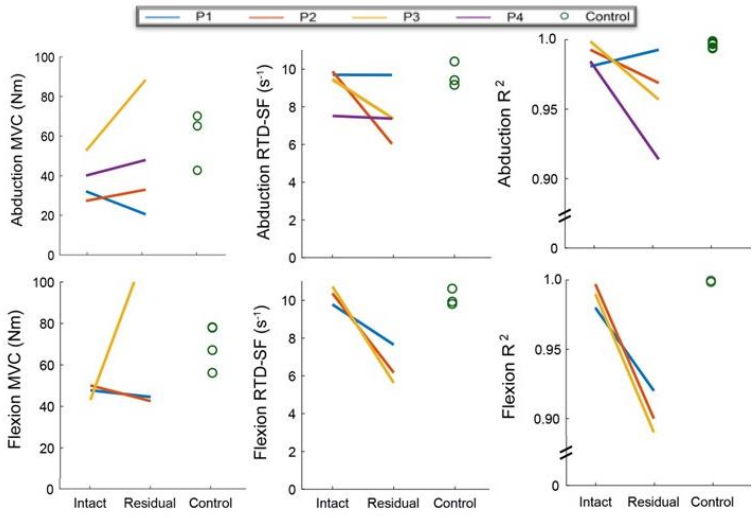

Figure 1: Right) Maximum Voluntary Contraction (MVC) for hip abduction (top) and flexion (bottom). Middle) Rate of torque development scaling factor (RTD-SF) limbs in hip abduction and flexion. Left) R^2 for the fit between peak RTD and MVC. Data are shown for the intact and residual limb of participants with TFA and dominant limb of control participants.

Significance: Preliminary evidence suggests amputation affects hip muscular strength and potentially neuromuscular quickness, however more data is required. Deficits of hip musculature quickness for individuals with TFA, if observed in a larger sample size, could be improved through training [6].

Acknowledgments: This work is funded by the Department of Defense under Award #W81XWH-22-1-0140.

References: [1] Miller, WC (2001) *Arch Phys Med Rehabil*. 82; [2] Inacio, M. (2019) *J. Biomech* 82; [3] James, U. Scand J. Rehabil Med. 5(2), 55-66, 1973 [4] Lanza, MB. (2020) *J. Electromyogr Kinesiol.* 55:; [4] Kozinc, Z. (2022) *Eur J Appl Physiol*. 122(4). [6] van Cutsem M. J Physiol. 513, 295-305, 1998.

POSTURAL CONTROL IN PATIENTS WITH ANKLE SPRAINS AND CONTROLS BEFORE REHABILITATION

Isaiah McNeilly[1*], Caroline Althouse[1], Paige McHenry, MS, ATC[2], Jamie Morris, PT, DPT, DSc[2], Erin Florkiewicz PhD, ATC [2], Eliot Thomasma PT, DPT, DSc[2], Will Pitt PT, DPT, PhD[3], Michael Crowell DPT, DSc[4], Gregory Freisinger, PhD[1*]
[1]United States Military Academy Dept of Civil and Mechanical Engineering, [2]Baylor University - Keller Army Community Hospital Sports Physical Therapy Fellowship, [3]Army-Baylor Doctor of Physical Therapy Program, [4]University of Scranton DPT Program
*Corresponding author's email: gregory.freisinger@westpoint.edu

Introduction: Ankle sprains are one of the most common musculoskeletal injuries at the United States Military Academy at West Point (USMA), similar to that of the broader physically active population. Nearly 30% of sports-related injuries are attributed to ankle sprains, which often lead to recurring injuries and residual symptoms [1]. Consistent with high ankle reinjury rates is Chronic Ankle Instability (CAI), a condition characterized by continual damage to mechanoreceptors in the ligamentous and capsular tissues of the ankle that affects stability, strength, joint position sense (JPS), associated with increased reinjury rates [2]. Without mechanisms to quantitatively assess postural control and sensorimotor function, it is challenging for clinicians to determine recovery status after ankle injury. Our research aims to investigate whether there are variations in linear metrics of postural control, calculated using center of pressure data, between the injured limb of individuals suffering from acute lateral ankle sprains, the non-injured limb of the same individuals, and a healthy control group. Due to weakened support structures surrounding the ankle and associated severity-dependent pain of ankle sprains, we expected that there would be significant differences in mediolateral (ML) and anterior-posterior range (AP), mean velocity (VEL), and 95% ellipse area (95% EA) when comparing the injured limb (INJ) with healthy controls (CONT). Further, we expected no significant difference in any postural control metrics between the uninjured limbs (UNINJ) and controls.

Methods: The study consisted of 42 total participants, [Injured n = 17m:5f, (20.6±2.0 yrs, 1.7±0.1 m, 80.7 ± 15.0 kg) and Control n=15m:5f, (20.8±1.3 yrs, 1.7±0.1 m, 81.5 ± 15.9 kg)]. Center of pressure position was collected from a force platform during the single-limb static task of the modified balance error scoring system (mBESS) with eyes closed. For the injured population, data was collected 6.1 ± 3.2 days following injury. The following linear metrics were calculated from center of pressure data using custom MATLAB code: ML range, AP range, mean VEL, and 95% EA. Ensemble averages were then calculated from approximately 3 trials per participant, and utilized in subsequent statistical analyses. Paired or unpaired t-tests were used to assess the differences between INJ limbs, UNINJ limbs, and CONT limbs, with significance level set at $\alpha = 0.05$.

Results & Discussion: Linear metrics of postural control for INJ, UNINJ, and CONT limbs are shown in Table 1. We found statistically significant increases in AP range and 95% EA for the patient's INJ limb and UNINJ limb when compared to controls. However, we found no significant difference between INJ and UNINJ limbs for any metric. Increased values for AP and 95% EA between the INJ limb and controls are consistent with our hypothesis. This increase may be due to pain or a change in the sensorimotor pathways that provide proprioception; however, we also identified a significant difference between the UNINJ limb and controls for both AP and 95%EA. Contrary to our hypothesis, there was no significant difference between INJ and UNINJ limbs.

TABLE 1: Linear Metrics of Postural Control for Patients Before Rehabilitation

					P Value		
	INJ (n = 22)	UNINJ (n=22)	CONT(R) (n=20)	CONT(L) (n=20)	INJ-CONT(L)	UNINJ-CONT(L)	INJ – UNINJ
Mediolateral Range, mm	44.4 ± 12.1	41.4 ± 10.1	43.1 ± 24.6	37.4 ± 14.6	0.06	0.12	0.37
Anteroposterior Range, mm	45.7 ± 15.0	44.4 ± 18.0	31.5 ± 18.6	28.5 ± 10.5	**< 0.001**	**< 0.01**	0.48
Velocity, mm/s	75.7 ± 19.7	71.0 ± 22.7	78.2 ± 33.9	75.2 ± 23.7	0.53	0.92	0.32
95% Ellipse Area (mm^2)	3366 ± 1421	3243 ± 1925	1995 ± 1950	1719 ± 1257	**< 0.001**	**< 0.01**	0.78

[a]Values presented as mean ± SD. Metrics calculated from center of pressure position data.

Significance: With consistently high rates of ankle sprain injuries and resulting CAI diagnoses, providing clinicians with quantifiable data to gauge function can assist in their return to duty decision-making and guide rehabilitation protocols. These metrics can further provide data throughout the rehabilitation process to quantify the improvement of postural control nearing clearance considerations. Statistical significance between non-injured limbs compared to controls is less intuitive but has been reported previously through research on bilateral balance impairments. A significant difference in balance is suggested to be attributable to acute inflammation that leads to neuromuscular inhibition for both limbs [3][4]. Further, statistically significant differences in the AP range but not in the ML range could signify that compensation occurs in the anterior-posterior direction due to mediolateral vulnerability associated with lateral ankle sprains.

Acknowledgments:
This work was funded by the Telemedicine and Advanced Technology Research Center at the U.S. Army Medical Research and Development Command through the Advanced Medical Technology Initiative

References: [1] Kirby et al. (2016) *The Foot 28* (1); [2] Moisan et al. (2021) *Journal of Foot and Ankle Research* (1). [3] Evans et al. (2004) *American Orthopeadic Foot & Ankle Society* (837). [4] Wilkstrom et al. (2010) *Gait and Posture* (3).

OLDER BALLET DANCERS SHOW LOWER FALL RISK THAN OLDER NON-DANCERS

Caroline Simpkins[1*] and Feng Yang[1]
[1]Georgia State University
*Corresponding author's email: claubacher1@gsu.edu

Introduction: Falls are a serious health concern with severe adverse consequences in older adults [1], and it is essential to develop effective fall prevention interventions for these individuals. Ballet has been applied to older adults with some health benefits [2]. However, previous studies have focused on the effects of ballet practice on improving fall risk factors, instead of on improving falls. Therefore, it remains unclear whether ballet could indeed reduce falls in older adults. The purposes of this study were to 1) determine how older ballet dancers respond to an unexpected and standardized standing-slip and 2) examine their physical and cognitive fall risk factors relative to non-dancers. We hypothesized that older ballet dancers would 1) have a lower fall rate than non-dancers when exposed to a slip and 2) demonstrate better physical and cognitive functions compared to their non-dancer peers.

Methods: Forty-three older adults were recruited: 20 ballet dancers (currently training in ballet 2.25 ± 1.25 days/week for 81.00 ± 14.10 min/day) and 23 age/sex-matched non-dancers. After completing physical and cognitive function tests, participants donned a safety harness and stepped onto the ActiveStep treadmill (Simbex, NH). The harness was connected to a loadcell and an overhead arch through dynamic ropes. After 3 standing trials (informed no belt movement would occur), participants were told a slip may or may not occur on the subsequent trials. Following 3 more standing trials where participants anticipated a slip, but no slip occurred, the unexpected slip took place. The standardized slip was generated by suddenly accelerating the belt forward to 1.2 m/s over 300 ms, and then diminishing the belt to zero over another 300 ms [3]. The total belt slip distance was 36 cm. The primary outcome was the slip faller rate. Secondary outcomes included dynamic balance, leg muscle power and strength, physical activity (PA) level, and cognitive function. The slip outcome was classified as a fall if the peak loadcell force exceeded 30% of the body weight [4]. The slip-faller rate was the ratio of fallers to the total participant number per group. Dynamic balance was assessed with the Timed-Up-and-Go (TUG) test. Leg muscle power was examined with the Five Times Sit-To-Stand (5×STS) test. The time (in sec) to complete the TUG and 5×STS was recorded (shorter time = better balance/power). The dominant knee extensors and ankle plantar-flexors muscular strength (in Nm/kg) was measured on an isokinetic dynamometer (Biodex System 4, NY). The Rapid Assessment of Physical Activity questionnaire measured PA level (max score of 10, higher score = higher activity), and cognitive function was measured with the Montreal Cognitive Assessment (MOCA; max score of 30, higher score = better cognition). Dichotomous variables (slip fall and sex) were analyzed using Fisher's exact test. Continuous variables meeting or violating normality assumptions were compared between groups by using independent *t*-tests and Mann-Whitney *U* test, respectively. All analyses were conducted using SPSS 29.0 (IBM, NY) with an α of 0.05.

Results & Discussion: The results support our first hypothesis as significantly fewer dancers fell than non-dancers after the slip (9 out of 20 dancers vs. 19 out of 23 non-dancers, $p = 0.013$, Table 1). Our second hypothesis was partially supported. The dancers were faster than non-dancers to perform the TUG ($p = 0.003$) and 5×STS ($p < 0.001$) tests. Dancers also displayed stronger knee extensors ($p = 0.010$) and ankle plantar-flexors ($p = 0.031$). The dancers were more physically active than their non-dancer counterparts ($p < 0.001$). However, MOCA scores were similar between groups ($p = 0.205$), implying comparable cognitive functions between them. The findings indicate that ballet dancers have a lower fall risk than non-dancers when exposed to an identical standing-slip. The lower slip-fall risk in dancers could be related to their better dynamic balance, greater leg muscle power, and stronger knee extensors and ankle plantar-flexors. Although PA scores differed statistically between groups, both groups were active older adults (as opposed to sedentary). Thus, the lower slip fall risk and better physical functions in dancers could be attributed to their ballet practice. Our findings reinforce the notion that ballet practice reduces fall risk in older adults.

Parameter	Group		*p*-value
	Dancers	*Non-Dancers*	
Age (years)	63.85 ± 7.60	67.48 ± 6.40	0.097
Sex (M/F)	3/17	4/19	1.000
Mass (kg)	61.39 ± 11.28	72.29 ± 15.71	0.014
Height (m)	1.62 ± 0.08	1.65 ± 0.10	0.325
Faller rate (%)	45%	83%	0.013
TUG (sec)	9.59 ± 2.11	11.48 ± 2.16	0.003
5×STS (sec)	11.41 ± 2.18	14.57 ± 2.90	< 0.001
Knee extensor (Nm/kg)	1.54 ± 0.37	1.27 ± 0.28	0.010
Ankle plantar-flexor (Nm/kg)	1.07 ± 0.24	0.86 ± 0.35	0.031
MOCA (/30)	28.47 ± 1.58	27.73 ± 1.88	0.205
PA (/10)	9.30 ± 0.86	7.26 ± 2.24	< 0.001

Table 1: Demographic and outcome comparisons (mean ± SD) between dancers ($n = 20$) and non-dancers ($n = 23$).

Significance: Our study suggests that older ballet dancers have a significantly lower fall risk than non-dancers when exposed to an unexpected standing-slip. The lower fall risk among dancers could be due to their better physical functions which are established fall risk factors for older adults. The dancers' better physical functions may result from ballet practice. Therefore, our results indicate that ballet practice has the potential to reduce fall risk for older adults. More studies are needed to further examine how ballet affects falls in daily living conditions and physical and cognitive functions in various populations with heightened fall risk.

Acknowledgments: This project was supported by the American Society of Biomechanics Grant-in-Aid Award, Scott Lilienfeld Injury Prevention Scholarship (Emory University), and Dissertation Grant (Georgia State University).

References: [1] Salari, N. et al., *J Orthop Surg Res* 17: 334, 2022. [2] Letton, M.E. et al., *J. Phys. Act. Health* 17: 566-574, 2020. [3] Simpkins, C., et al., *J Biomech* 145: 111366, 2022. [4] Yang, F. & Pai, Y.-C., *J Biomech* 44: 2243-2249, 2011.

COMPARATIVE ASSESSMENT OF POSTURAL BALANCE CONTROL IN MULTIPLE SCLEROSIS PATIENTS USING VIRTUAL TIME-TO-CONTACT AND TRADITIONAL BALANCE METRICS

Soubhagya Nayak[1], Daniel Peterson[2], Jessie Huisinga[3], and Hyunglae Lee[1,*]
[1]School for Engineering of Matter, Transport and Energy, Arizona State University, Tempe, AZ, USA
*Corresponding author's email: Hyunglae.Lee@asu.edu

Introduction: Multiple sclerosis (MS), a progressive neurological disorder that leads to the degeneration of nerve fibers in the central nervous system, often results in impaired balance and an increased risk of falls. Given the extensive physical, psychological, and social repercussions of falls on MS patients, it is crucial to investigate how MS affects postural balance control and the consequent heightened risk of falls. Previous studies on postural balance in individuals with MS have shown increased postural sway compared to healthy controls during quiet standing, especially with eyes closed, although some studies reported no significant differences in sway between MS patients and controls under similar conditions. The discrepancies in findings may stem from an oversight of how traditional balance control metrics, like Path length and Sway area, fail to consider the critical relationship between the center-of-pressure or mass (CoP or CoM) and the base-of-support (BoS). Other measures like virtual time-to-contact (VTC) and time-to-boundary dynamically assess the time needed for the CoP/CoM to reach the BOS by modeling CoP/CoM kinematics, offering a more detailed evaluation of postural balance [1]. These measures, emphasizing the CoP/CoM-BoS relationship, have shown greater robustness in identifying balance control differences among healthy and neurodegenerative populations compared to traditional balance metrics. This study aims to assess the effectiveness and robustness of VTC in evaluating balance control in MS patients compared to traditional metrics, such as Path length and Sway area. We hypothesize that VTC effectively evaluates postural balance and is more robust than traditional metrics in differentiating balance control under various task conditions.

Methods: The study included 119 MS patients (93 females, 26 males; average age: 45.4 years; height: 1.67 m; weight: 79.5 kg; 10.8 years since diagnosis; EDSS: 2.2; ABC: 80.5; 25 feet walk: 5.3 seconds) and 48 healthy controls (38 females, 10 males; average age: 43.8 years; height: 1.66 m; weight: 72.6 kg; ABC: 95.5; 25 feet walk: 4.3 seconds). The MS patients and controls underwent quiet standing assessments under three conditions (Eyes open, Eyes closed, Foam surface), with each condition involving three 30-second trials, while participants maintained a consistent initial stance with feet outlined on a force-plate, in comfortable shoes, looking at a picture, arms crossed, and a heel-to-heel distance of 10 cm. Quantitative balance measures were captured with 33 body markers placed on anatomical positions for detailed analysis. Marker data collected from the toes, metatarsophalangeal joints, and heels plotted the BoS, while markers on key pelvic and sacral points allowed for the calculation of the CoM coordinates on the transverse plane. The study utilized CoM data and calculated VTC, Path length, and Sway area metrics to assess postural balance across conditions and employed the coefficient of variation (CV) for robustness analysis. Mixed model ANOVAs were used to evaluate differences in balance across Eyes open, Eyes closed, and Foam surface conditions between MS and control groups using VTC, Path length, and Sway area metrics. Additionally, paired t-tests and Wilcoxon signed rank tests (when data normality is not satisfied) were performed to evaluate differences in CV of three metrics for each experimental condition.

Results & Discussion: Experimental results demonstrated that the new balance metric, VTC, was effective in assessing balance control among MS patients, showing a significant decrease in VTC when transitioning from Eyes open to Eyes closed ($p < 0.001$) and from Eyes closed to Foam surface ($p < 0.001$) conditions (Fig. 1A). This trend was also evident in the postural balance assessments in the control group ($p < 0.001$ for same comparisons). All metrics reached statistical significance in all pairwise comparisons, except Sway area for the comparison between Eyes open and Eyes closed conditions for MS ($p = 0.06$) and control ($p = 1.0$). However, Path length and Sway area metrics showed greater variability than VTC in MS patients (Fig. 1A-C). Importantly, VTC demonstrated the lowest CV in any task conditions compared to traditional balance metrics ($p < 0.001$ for Eyes open, Eyes closed and Foam surface in both MS and Control groups), highlighting its consistency and superior robustness in evaluating postural balance control for participants in both the MS and control groups (Fig. 1D & 1E).

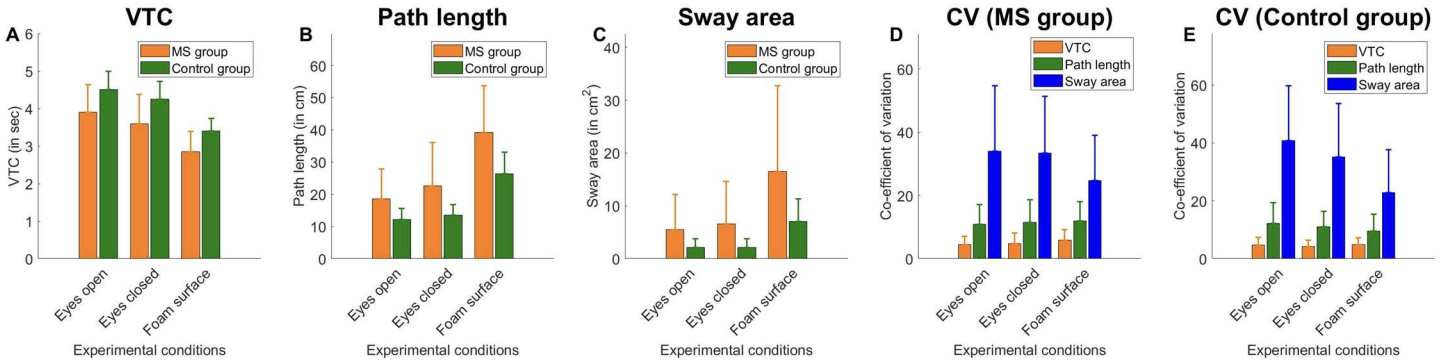

Figure 1: Postural balance control assessment using A) VTC, B) Path length, C) Sway area. Robustness analysis using CV for D) MS group and E) Control group.

Significance: The study illustrates two key findings: VTC is effective in assessing balance control in MS patients and control groups under various task conditions and the most robust metric compared to traditional balance metrics used in this study. This can be attributed to VTC's emphasis on the CoM-BoS relationship, an aspect overlooked by traditional balance metrics.

Acknowledgement: Informed consent was obtained for all participants with oversight from Kansas University Medical Center IRB.

References: [1] Slobounov, S. M., Moss, S. A., Slobounova, E. S., & Newell, K. M. (1998). Aging and time to instability in posture. *The Journals of Gerontology Series A: Biological Sciences and Medical Sciences*, *53*(1), B71-B80.

POSTURAL ADJUSTMENTS DURING ACTIVITIES OF DAILY LIVING WITH AN UPPER LIMB PROSTHESIS

Mira E. Mutnick[1*], Alec McKheen[1], Christina Lee[1], Susannah M. Engdahl[1], Deanna H. Gates[1]
[1]University of Michigan
*Corresponding author's email: mmutnick@umich.edu

Introduction: Use of an upper limb prosthesis is associated with increased compensatory movements [1] and altered balance during standing [2]. As many daily activities are performed while standing, individuals with upper limb differences (ULD) who use prostheses may face challenges in maintaining balance. Only two prior studies have explored center of pressure (COP) in people with ULD and found that people with ULD have greater COP excursion than non-amputee controls during quiet standing [2] and standard assessments of dexterity [3]. However, little is known about how individuals with ULD maintain balance during activities of daily living (ADLs). Based on observed association between prosthesis use and COP excursion, we hypothesized that people with ULD would have greater COP excursion across ADLs when using their prosthesis, compared to non-amputee controls. Additionally, given the finding of large COP excursion during quiet standing even without using the prosthesis for a task, we also hypothesized that people with ULD would demonstrate greater COP excursion during unimanual tasks when using their intact limb compared to non-amputee controls using their dominant limb.

Methods: Nine participants with transradial limb absence (4 female/5 male, 3 congenital/6 acquired, age: 48 ± 16 years) and nine age/sex-match controls (4 female/5 male, age: 45 ± 16 years) without amputation participated. Four participants used body-powered prostheses, three used myoelectric prostheses, and two used both. While standing on a single force plate (AMTI, Watertown, MA) collecting ground reaction forces at 1200 Hz, participants performed a series of ADLs including applying deodorant (DEO), moving a can or box from a low to high shelf (CAN, BOX), and putting a pin in a small target (PIN). ADLs were classified as unimanual (CAN, PIN), bimanual asymmetric (DEO), or bimanual symmetric (BOX). COP data were filtered using a 4th-order low-pass Butterworth filter with a 50Hz cutoff frequency. We excluded any trials where participants stepped or moved such that their feet were not fully on the force plate. We defined the beginning and end of each trial by a 5cm/s velocity threshold of the write joint center and visually verified [1]. We calculated the COP sway path (SP) length, mean velocity (MV), 95% prediction ellipse area (EA), and principal direction of the ellipse independently for each trial and then averaged across all five trials for each limb. Given the small and unequal sample, we calculated Hedges' g effect size for pairwise comparisons (i.e., intact v. prosthetic, intact v. control). Effect sizes were considered small for $|g| \geq 0.2$, moderate for $|g| \geq 0.5$, and large for $|g| \geq 0.8$ [4]. Only moderate and large effect sizes are reported.

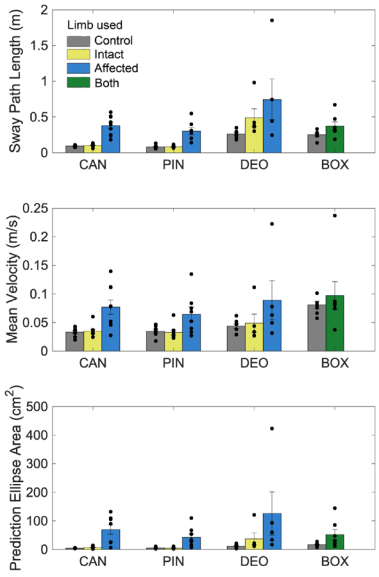

Figure 1: Sway path length (m), mean COP velocity (m/s), and 95% prediction ellipse area (cm^2) for all limb conditions and ADLs.

Results & Discussion: *Unimanual (CAN, PIN).* Participants with ULD had a larger SP, MV, and EA when using their prosthetic limb compared to intact limb for both CAN and PIN ($g_{SP} > 2.06$, $g_{MV} > 1.14$, $g_{EA} > 1.53$) (Fig. 1). These results are consistent with prior studies in which people with ULD had greater COP motion compared to non-amputee controls while completing dexterity assessments with their prosthesis [4]. Compared to controls, people with ULD using their intact limb had a larger EA for CAN ($g_{EA} = 7.22$), but a smaller EA for PIN ($g_{EA} = 2.65$). Differences in EA may reflect the different task demands as the PIN task is a precision task, while CAN is not. People with ULD may have needed to apply tighter control (smaller ellipse area) when using their intact limb to account for prosthetic disturbances.

Bimanual Asymmetric (DEO). People with ULD had a larger MV and EA, when using their prosthetic limb to apply the deodorant compared to when using the intact limb ($g_{MV} = 0.61$, $g_{EA} = 0.64$). People with ULD using their intact limb had larger SP and EA compared to the control limb ($g_{SP} = 1.21$, $g_{EA} = 1.90$). Because the prosthesis is still used in opening the deodorant stick when applying it with the intact limb, there is added task difficulty which may increase the duration of the intact trial, leading to a larger sway path compared to non-amputee controls.

Bimanual Symmetric (BOX). People with ULD had larger SP ($g_{SP} = 0.98$) and EA ($g_{EA} = 3.57$) compared to non-amputee controls. There was a large effect for principal direction where people with ULD tended to lean more toward their intact side, while non-amputee controls tended to lean more toward their non-dominant side ($g_{Dir} = 1.77$). Future work will investigate the influence of the heterogeneity of the amputee population on COP metrics, such as the etiology of limb difference (congenital or acquired), type of prosthesis (body-powered or myoelectric), and prosthesis experience.

Significance: This study provides insight into the increase in postural control demands of people with ULD compared to non-amputee controls in dynamic tasks that are representative of activities people routinely engage in. The results suggest that postural demands are affected by a range of tasks, but particularly those in which the prosthesis is engaged.

Acknowledgments: Funded by the Department of Defense under Award No. W81XWH-16-1-06548.

References: [1] Engdahl et al. (2022), *Clinical Biomechanics*, 92. [2] Major et al. (2020) *Am J Phys Med Rehabil* 99. [3] Vujaklija et al. (2023). *IEEE Trans. BME*, 70. [4] Cohen (1998), *Stat Power Analysis*.

ESTIMATING REACTIVE-STEPPING ROTATIONAL VELOCITY FROM FORCE PLATES ALONE

Michael Christensen* and Jeremy Crenshaw
University of Delaware
email: mschris@udel.edu

Introduction: Reactive balance, the body's rapid response to maintain stability after a perturbation, refers to a domain of balance that has been linked to increased fall risk [1]. In research settings, perturbations are elicited with computer-controlled treadmills, cable pulls, and translatable platforms, and key kinematic outcomes are determined from motion-capture recordings [2]. Such specialized equipment limits the feasibility of assessing reactive balance outside of the research setting. Conversely, tests used in clinical settings, such as the Push-and-Release Test (PRT), can quickly assess reactive balance with minimal equipment. With no instrumentation, these tests have limited precision and repeatability [3].

Simple force-plate instrumentation can address these concerns—allowing for a clinically-feasible test with minimal instrumentation that quantifies key biomechanical measures of the response. Previously, we have shown that by using force-plates we can estimate the contributions of kinematic outcomes describing individual components of the stepping response (e.g. step length and time) [4]. Here, we attempt to use force-plate data to quantify peak lean angular velocity, a kinematic outcome that is key to the success of a reactive step [5].

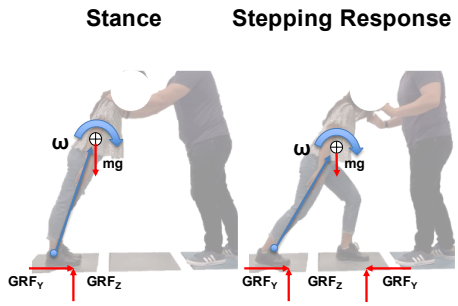

Figure 1: Example of the force-plate instrumented Push-and-Release test administered in the anterior direction. Kinetic variables of note and peak lean angular velocity (ω) are indicated.

Methods: Five participants with neurotypical function (4M/1F; mean (SD) Age: 28.6 (2.3) years; BMI: 25.4 (2.4) kg/m^2) years) underwent the instrumented Push-and-Release Test in the anterior (Figure 1), lateral, and posterior directions captured by two force plates (1200 Hz). Full-body motion-capture data (120 Hz) were also recorded to estimate ankle-joint center and whole-body center of mass (COM). Each participant completed 18 to 24 trials at a range of perturbation difficulties. Peak lean angular velocity (ω) was defined using motion capture data to determine the greatest rotational velocity of a vector from the trail limb ankle-joint center at perturbation onset to the whole-body center of mass at a given point in time in the sagittal or frontal plane. A mechanically determined ω was estimated from force plate data, as seen in Eq. 1 – 3 [6]. Agreement between the force-plate estimated ω and motion-capture determined ω between 94 to 105 trials per direction were assessed using Intraclass Correlation Coefficients (ICC 2,1) and Bland-Altman Plots.

$$vCOM_Y = vCOM_0 + \int_{t_0}^{t_n} \frac{GRF_{Net-Y}(t_n)}{m}$$

$$vCOM_Z = vCOM_0 + \int_{t_0}^{t_n} \frac{GRF_{Net-Z}(t_n) - mg}{m}$$

$$\omega = \frac{\sqrt{vCOM_Y{}^2 + vCOM_Z{}^2}}{l}$$

Eq. 1 – 3: Assuming the participant starts in a static position, linear COM velocity (vCOM) at a given point in time (t_n) can be determined from force data and then converted to an angular velocity (ω) using a known pendulum length (l). Pendulum length was defined as greater trochanter height multiplied by a scale factor [7].

Results & Discussion: Mechanically estimated ω showed weak-to-moderate agreement with the motion-capture determined ω (Fig. 2). The force-plate-determined ω consistently underestimated lean angular velocity. For the posterior and lateral perturbations, this underestimation was more evident for larger values (i.e. larger perturbations). We suggest that this bias in ω estimation is due to an assumed pendulum length (***l***) that is too large. In addition, an assumed constant pendulum length does not capture a shortening that may occur at larger-magnitude perturbations, possibly due to stance-limb knee flexion. Linear vCOM alone may represent a kinematic outcome that is a valid metric of reactive-balance skill. Preliminary analysis suggests that we can assess this variable with force plates only, as mechanically estimated linear vCOM, the numerator in Eq. 3, showed strong agreement with its motion capture equivalent (Anterior: 0.90, Posterior: 0.92, Lateral: 0.82). Further work is needed to determine if such an outcome is sensitive to the effects of neuromuscular impairment or beneficial intervention.

Significance: We can reasonably estimate peak lean angular velocity using force-plate-derived measures. This is a promising indicator that we can use force plates to mechanically assess reactive balance during the clinically feasible push-and-release test. An assumed, constant pendulum length is a weakness of our approach that must be addressed to improve the validity of our measure.

References: [1] Mansfield et al., 2015. *Phys Ther.* 101; [2] Devasahayam et al., 2023. *Phys Ther*. 103; [3] Smith BA, et al., 2016, *Physiother Res Int.* 21; [4] Christensen et al., 2023 *ASB Abstract*; [5] Crenshaw et al., 2012. *J Biomec.* 45. [6] Buurke et al., 2023. *J Biomec*. 146. [7]. Hof et al., 2005. *J Biomec*. 38.

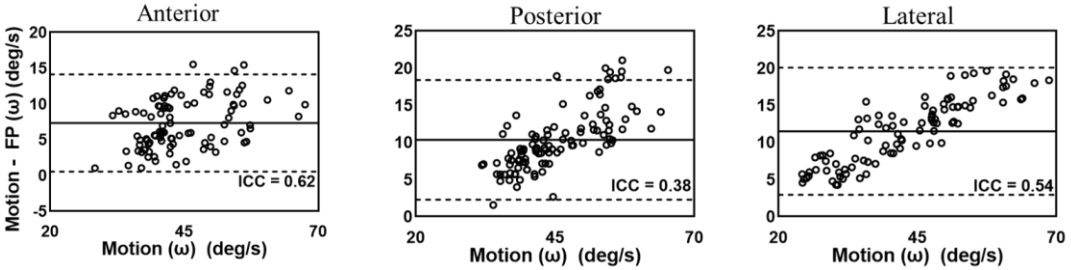

Figure 2. Bland-Altman plots showing motion-capture determined peak lean angular velocity (ω) versus the difference between actual and estimated ω. Horizontal lines represent the mean difference (solid) and the 95% limits of agreement (dashed).

THE EFFECTS OF GLUTEUS MEDIUS FATIGABILITY ON GAIT INSTABILITY IN OLDER ADULTS

Andrew D. Shelton[1*], Vicki S. Mercer[2], Katherine R. Saul[3], and Jason R. Franz[1]
[1] Joint Dept of Biomedical Eng., UNC Chapel Hill & NC State University, Chapel Hill, NC, USA, [2]Div of Physical Therapy, UNC Chapel Hill, Chapel Hill, NC, USA, [3]Dept of Mechanical and Aerospace Eng., NC State University, Raleigh, NC, USA
*Corresponding author's email: adshelt@email.unc.edu

Introduction: As we age, a variety of factors are associated with an increased fall risk. Those that affect balance and stability include multi-factorial declines in sensory, motor, and cognitive-motor acuity [1-3]. Fatigue is an independent and critical factor for responding to balance challenges [4,5]. Our primary focus on objective muscle fatigue is to establish mechanistic links between the decline in a muscle's ability to generate force following fatigue and performance on tasks that have a high risk for falls. The majority of past studies on fatigue in older adults have used isometric tasks likely to lack ecological validity to the circumstances that precipitate falls. Mediolateral stability, in particular, is crucial for older adults to safely navigate their daily environments and compared to anteroposterior stability, disproportionally requires active control; the gluteus medius (GMed) is the key muscle in regulating lateral foot placement and thereby mediolateral stability. Our study aimed to characterize the effects of local GMed fatigue on gait instability in a cohort of older adults. We hypothesized that GMed fatigue would compromise mediolateral walking balance control – evidenced by larger vulnerability to lateral waist-pull perturbations and decreased speed and accuracy when responding to prescribed changes in lateral foot placement.

Methods: 15 older adults (7 females, age: 73.3±6.7 yrs, height: 1.75±0.09 m, mass: 80.1±17.9 kg) participated in this research study. To represent daily environmental balance challenges, participants completed two walking balance tasks before and after GMed fatigue. Specifically, participants walked while responding to lateral waist-pull perturbations (i.e., a reactive response task) and targeted lateral stepping (i.e., a proactive, goal-directed task) before and after GMed fatigue. Fatigue was induced through a continuous lateral side-stepping task at 40 Hz between targets of 50% leg length while wearing a resistance band delivering 50% maximum isometric GMed strength (as measured at 50% leg length elongation). Stepping continued until either the participant slowed by >20% of the metronome speed or deviated by >20% from the step target. We confirmed GMed fatigue via decreases in maximum isometric force and median frequency from surface electromyography. Using 3D motion capture data, we calculated: (*i*) center of mass displacement (CoM) and mediolateral margin of stability during the lateral waist pull and (*ii*) foot placement accuracy and time of leg swing deviation during targeted lateral stepping.

Results & Discussion: Continuous lateral stepping induced significant GMed fatigue; on average, EMG median frequency decreased by 16% (66.3±19.5 Hz vs 78.6±21.9 Hz, $p<0.001$, Fig. 1A) and maximum isometric force decreased by 9% (110.5±37.3 N vs 121.7±38.5 N, $p<0.001$). As hypothesized, repeated measures comparisons revealed a significant effect of fatigue on vulnerability to lateral waist-pull perturbations. Here, GMed fatigue elicited 14% larger lateral CoM displacement (12.7±3.6 cm vs. 11.1±3.7 cm, $p=0.01$, Fig. 1B) requiring 11% larger margins of stability during recovery (13.6±3.8 vs. 12.3±2.7 cm, $p=0.004$, Fig. 1C). Conversely, and in contrast to our hypothesis and despite also being regulated via GMed muscle action, performance on the proactive, goal-directed task (i.e., lateral stepping) was unaffected by GM fatigue (e.g., Fig. 1D-E). There are at least two potential explanations for these contrasting results. The first is that the reactive response task (i.e., lateral waist pulls) is likely to have required faster and more vigorous GMed muscle actions compared to the goal-directed task. The second is that, although provided only a single stride duration, participants could have potentially modified their strategy to meet the task demands – something they would have been less capable of doing during the reactive response task.

Significance: This study is the first to draw a mechanistic link between GMed muscle fatigue and its compromising effect when called upon to preserve stability in response to an unexpected lateral walking balance disturbance. These findings point to the importance of targeted preventative strategies to reduce GMed muscle fatigability to preserve older adults' ability to respond to unexpected environmental perturbations where falls are likely. As an important next step, we are interrogating musculoskeletal simulations to determine muscle compensations to mitigate perturbation-induced instability in the presence of GMed fatigue.

Acknowledgments: Supported by a pre-doctoral fellowship from the National Institutes of Health (F31AG079499).

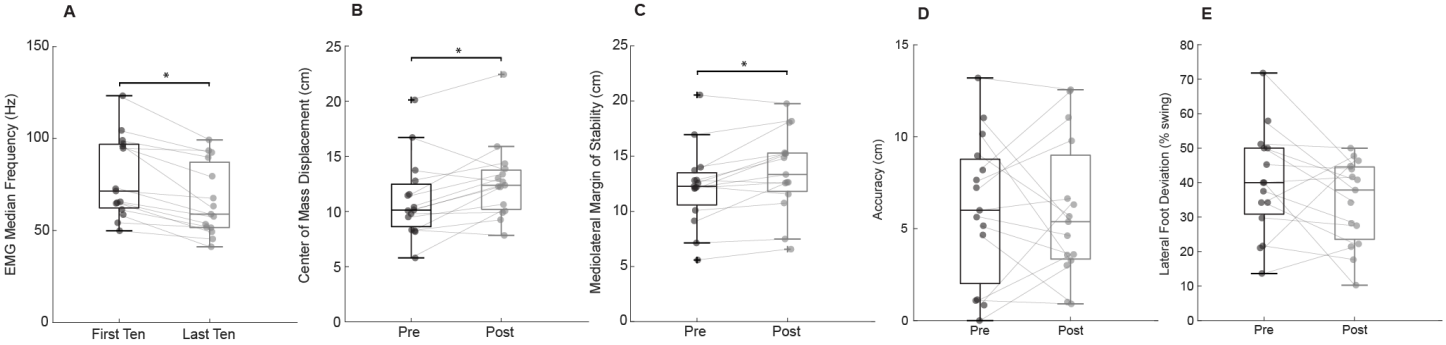

Figure 1: (A) Evidence of gluteus medius (GMed) fatigue from the first to the last ten cycles of the side-stepping task. Effect of fatigue on (B) center of mass displacement and (C) margin of stability when responding to lateral waist-pull perturbations. Effect of GM fatigue on the (D) accuracy and (E) timing when performing the goal-directed lateral stepping task. Asterisks (*) indicate significant differences ($p<0.05$).

References: 1. Melzer et al. 2004 2. Springer et al. 2006 3. Thelen et al. 1996 4. Tinetti et al. 1988 5. Helbostad et al. 2010

EFFECTS OF TRANSTIBIAL LIMB LOSS AND REPEATED TREADMILL-INDUCED PERTURBATIONS ON MOTOR LEARNING OF DYNAMIC BALANCE IN OLDER INDIVIDUALS

Lawrence Chung[1*], Matthew J. Major[2] and Nicholas P. Fey[1]
[1]Walker Department of Mechanical Engineering, The University of Texas at Austin, Austin, TX 78712 USA
[2]Department of Physical Medicine & Rehabilitation, Jesse Brown VA Medical Center, Chicago, IL 60611 USA
Lchung1287@utexas.edu

Introduction: Older individuals and wearers of leg prostheses experience compromised dynamic balance, as quantified through changes in whole-body and segmental contributions to angular momentum. Older individuals with limb loss experience compounded effects of natural neuromotor decline and use of current prosthetic technologies. Even in average aged individuals with limb loss who use standard-of-care prostheses there exist differences in metabolic cost and walking patterns relative to able-bodied (AB) persons [1]. As a form of scientific and clinical inquiry, repeated exposure to perturbations is one method to induce learning during certain scenarios of disturbance during gait. This paradigm has been studied for individuals with limb loss as well as other clinical groups such using either single or split-belt treadmills [e.g., 2]. However, how these sagittal-plane treadmill-induced perturbations disrupt peak whole-body measures of balance and center-of-mass velocity is less understood. Furthermore, how these measures change across repeated exposures to quantify motor learning within an individual have not been examined. This study assessed effects of transtibial limb loss and repeated gait perturbation exposure on whole-body angular momentum (*H*) and velocity in older individuals. We hypothesized that older individuals with transtibial limb loss will exhibit signs of motor learning, resulting in reduced peak magnitudes of *H* and center-of-mass velocities during successive perturbations. We also hypothesized that these relationships would differ relative to age-matched AB controls.

Methods: Twelve participants were enrolled in this study, 7 unilateral transtibial prosthesis users (73±5 years, 83±11 kg, 176±7 cm, all traumatic etiology) and 5 AB controls (74±4 years , 82±6 kg, 172±5 cm). The Activities-specific Balance Confidence (ABC) Scale was administered to each participant. Two prosthesis users could not complete the perturbation protocol; thus 10 participants were evaluated. Participants were fit with a full-body custom marker set and then completed two 30-second steady-state baseline walking trials for accommodation followed by twelve perturbation trials on an instrumented treadmill (Motek). Perturbations involved walking at 0.8 m/s until perturbation onset (6.5 m/s^2 belt acceleration to 3.3 m/s and then immediate deceleration) triggered at initial contact of a random step between 21 and 40. Perturbations were delivered during single-limb stance of either the dominant/sound or non-dominant/prosthetic limb at random. Kinematic data were captured at 120 Hz and analyzed in Visual3D to estimate 3D whole-body *H*. Peak positive and negative whole-body center of mass *H* and velocities were extracted from all perturbation trials. Data were grouped according to stance limb when the perturbation occurred. Linear regression (α=0.05) was applied on a per-subject basis to predict either peak *H* or velocity versus the trial exposure. Separate analyses were conducted within an individual and within the subset of perturbations applied to each limb. The relationship between peak *H* and velocity across perturbations was also analyzed using a similar statistical method.

Results & Discussion: Generally, our hypotheses regarding the perceived evidence of motor learning was supported. We observed statistically significant trends for both groups (Fig.1). There was a stronger relationship (learning rate) within the limb loss group when significant motor learning trends were detected. Most learning of dynamic balance in both groups was observed within the sagittal and transverse planes, and little evidence of motor learning was observed in the frontal plane. Within the sagittal plane (Fig. 1), the control subjects (grey points) exhibited motor learning in their negative i.e., forward *H*, shown by their progression towards zero, while the prosthesis users tended to progress their backward *H* toward decreasing momentum values with repeated exposures when perturbed during stance of the prosthetic leg, highlighting a unique difference between these groups. Two individuals with limb loss in particular (green and magenta, Fig. 1) showed the most evidence of learning. These individuals differed substantially having used a prosthesis for 54 years (green) and 2 years (magenta). Yet, these two shared the highest ABC scores of the group compared to the two participants with limb loss that did not complete the protocol who had the lowest ABC scores.

Significance: Our study adds to the continued efforts to understand why some older people with and without limb loss exhibit evidence of motor learning and some do not, as well as the connection between perceived and performance results. Treadmill-induced perturbations is one method that should be further researched to promote motor learning during specific balance-challenging tasks to understand the role of balance confidence, age and prosthesis design.

Acknowledgements: This work is partially supported by the US Dept of Veterans Affairs (#1IK2RX001322, granted to MJ Major). Contents do not reflect those of the US Department of Veterans Affairs or the US Government.

References: [1] Chu, V. W. T., Hornby, T. G., & Schmit, B. D. (2018) Journal of Neurophysiology, 120(2), 497–508.
[2] Price, M. A., Beckerle, P., & Sup, F. C. (2019) IEEE Transactions on Neural Systems and Rehabilitation Engineering, 27(8).

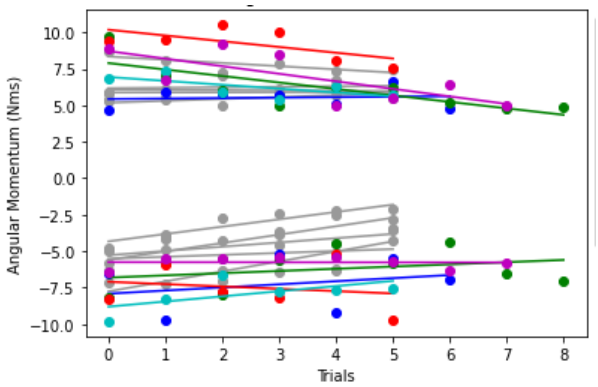

Figure 1: Peak positive (i.e., backward) and negative (forward) whole-body *H* in the sagittal plane during perturbations. Individual prosthesis user participants are shown as separate colors, and AB controls are shown in gray. Linear trendlines or each outcome versus sequential exposures are also shown for each person.

NEURAL OR MUSCULOSKELETAL: WHICH SYSTEM DRIVES THE AGE-RELATED DECLINE IN WALKING ECONOMY?

Brooke Measeles*, Negin Fallah, Ahan Mistry, Owen N. Beck
The Department of Kinesiology & Health Education, University of Texas at Austin
*Corresponding author's email: bmeaseles@utexas.edu

Introduction: Older adults (OA) typically consume 10 to 20% more metabolic energy than young adults (YA) while walking (decreased walking economy) [1]. The age-related decline in walking economy impairs quality of life [2] and is thus important to mitigate (or reverse). Yet, it is unestablished which factor(s) govern the age-related decline in the walking economy.

Perhaps the age-related decline in walking economy is governed by the aging musculoskeletal system. Compared to YA, OA typically have less stiff tendons, greater intermuscular fat, and less dense muscles than YA [3]. OA also have lower mitochondrial-coupling efficiency compared to YA, which may contribute to their decreased walking economy. Collectively, these musculoskeletal characteristics may contribute to the age-related decline in the walking economy.

On the contrary, many studies indicate that the economy of producing the same joint mechanics may not differ between YA and OA [*e.g.,* 1]. These studies suggest that musculoskeletal changes may not govern the walking economy decline in OA vs. YA. Here, we sought to help identify the factors governing the age-related decline in the walking economy. To do so, we quantified YA and OA economy during walking and while producing isolated locomotor-like leg joint moment cycles. We hypothesized that OA would consume more metabolic energy than YA during walking, but not during isolated leg joint torque production. If our hypothesis is supported, the age-related decline in walking economy may be primarily attributed to other systems of the body (*e.g.,* nervous system) – not directly due to aging muscle-tendon properties.

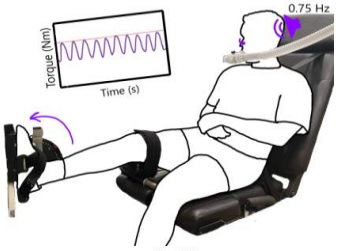

Figure 1: Participant sitting in dynamometer chair producing ankle plantar flexion cycles following auditory and visual feedback.

Methods: We studied 2 OA and 10 YA after obtaining informed written consent. This protocol involved two days of data collection. On the first day, we conducted two 5-min treadmill walking familiarization trials at 0.8 and 1.3 m/s. Next, participants walked again at the same two speeds in a random order for the experimental trials.

On the second day, participants sat on a chair with their right leg secured in a fixed position: ankle at 90° and knee at 165° (90° = perpendicular segments) (Fig. 1). In this position, participants performed 5-min trials where they cyclically produced fixed-end ankle extension moments following visual and audio feedback (0.75 Hz, 0.5 duty, 20 and 30 Nm peak moment) (Fig. 1). Next, participants performed the same 5-min trials using their hip extensors while laying with their hip joint at 160°. We randomized the order of ankle and hip trials. We quantified net $\dot{V}o_2$ uptake and $\dot{V}co_2$ production via open-circuit spirometry during all trials and used a standard equation [4] to compute net metabolic power.

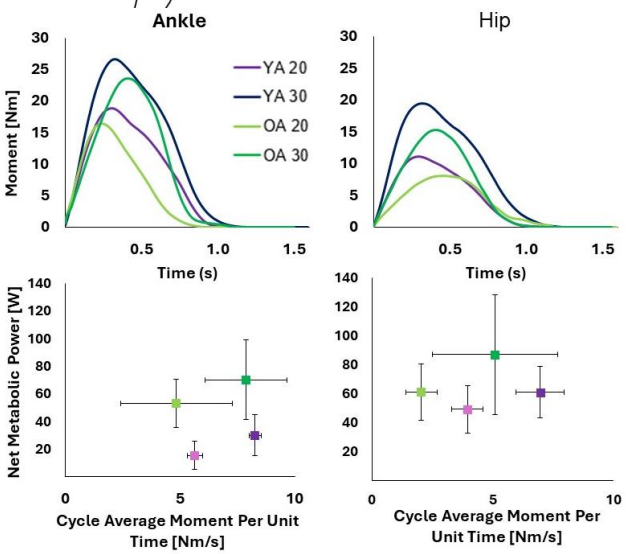

Figure 2: Top row: Avg moment cycles vs. time for ankle and hip joints. Bottom row: Avg (± SE) net metabolic power vs. cycle Avg moment per sec for ankle and hip joints. Purple = young adults (YA n=10) & green = older adults (OA n=2). Lighter color = 20 Nm target peak torque & darker color = 30 Nm target peak torque.

Results & Discussion: OA required more net metabolic power during walking and to produce leg-joint moments (Fig. 1). Numerically, OA consumed, on average, 36% and 32% more net metabolic power than YA during walking at 0.8 and 1.3 m/s, respectively. To control for aging neural control strategies (*e.g.,* distal-to-proximal redistribution of joint mechanics), we assessed metabolic power during isolated leg-joint moment production cycles. During these trials, OA consumed 12 to 40 Watts to produce ankle and hip extension moments than YA, respectively (Fig. 2); rejecting our hypothesis. These greater joint-level metabolic values occurred despite OA producing 14% & 5% lower cycle average moments compared to YA across ankle trials, and 48% & 27% lower cycle average moments across hip trials (Fig. 2). Consistent with the literature, all participants consumed more net metabolic power when they produced greater moments at each joint.

Significance: The primary factors governing the age-related decline in walking economy lack consensus. Based on recent findings that aging neural control strategies likely increase metabolic rate during walking in older vs. young adults [5], we tested whether aging musculoskeletal properties also detectibly influence metabolic rate. Based on our preliminary findings, it is likely that the aging musculoskeletal system measurably contributes to the age-related decline in the walking economy. Therefore, interventions aimed at maintaining youthful musculoskeletal health are warranted to maintain youthful metabolism in older adults.

References: [1]Ortega et al., 2007. *J Appl Physiol*; [2] Martin et al., 1992. *Med Sci Sports Exerc*; [3] Frontera et al., 2008. *J Appl Physiol*; [4] Péronnet, F. et al., 1991. *Canadian J of Sport Sci*; [5] Fallah & Beck., 2023 *ASB Tenn*

THE EFFECTS OF AGE AND FALLS RISK ON MUSCLE COORDINATION COMPLEXITY DURING EVERYDAY WALKING TASKS

Grant T Maddox[1*], Andrew D Shelton[2,3], Vicki S Mercer[2], Jeremy R Crenshaw[4], Jason R Franz[2,3], Jessica L Allen[1]
[1] University of Florida, USA, [2] UNC Chapel Hill, USA, [3] NC State University, USA, [4] University of Delaware, USA
email: grantmaddox@ufl.edu

Introduction: Approximately one-third of older adults fall each year, with many occurring while walking. We previously found that older adult fallers exhibited reduced complexity of muscle coordination during walking [1] and that this reduction was associated with increased instability [2]. However, navigating everyday life requires walking under varying task demands not captured in our previous studies, such as stepping or turning. Therefore, this study aimed to investigate how age and fall risk impact the complexity of muscle coordination during a series of everyday walking tasks. We examined two different but complementary aspects of muscle coordination complexity: (1) complexity *within* each task to gain insight into individual task control. Here, we hypothesized that both age and fall risk would lead to reduced muscle coordination complexity of individual task control. (2) Complexity *across* all tasks to gain insight into how the modulation of muscle coordination across tasks is affected by age and fall risk. Here, we hypothesized that age and fall risk would result in less modulation of muscle activity across tasks, leading to reduced muscle coordination complexity.

Methods: 26 young adults (YA, 15F; 21.74±2.05yrs), 24 older adult non-fallers (NF, 14F;70.88±5.0yrs), and 5 older adult fallers (OF, 2F; 81.1±5.3yrs; at least 2 falls in the last year, a slowed timed up & go test, and reduced self-reported physical function) walked under 4 different conditions at their preferred speed: (1) overground walking, (2) treadmill walking, (3) figure eight walking to assess turning mobility, and (4) a precision stepping task to assess the adjustment of lateral foot placement [3]. Surface electromyography (EMG) was collected from eight lower-limb muscles on the right leg spanning the hip, knee, and ankle: tibialis anterior, soleus, medial gastrocnemius, rectus femoris, vastus lateralis, medial hamstring, gluteus medius, and gluteus maximus. Muscle coordination complexity was quantified using motor module (a.k.a. muscle synergy) analysis. Motor modules were extracted from EMG data using non-negative matrix factorization, and muscle coordination complexity was defined as 100 – the variance accounted for by one motor module (100 – VAFby1) [4]. To test our first hypothesis that older adults would have reduced complexity (lower 100 – VAFby1) *within* each task, 100-VAFby1 was separately identified from the muscle activity from each task. A two-way repeated measures ANOVA was run to compare the 100 – VAFby1 in each task across groups (YA, NF, and OA) with Sidak corrections for multiple comparisons. To test our second hypothesis that older adults would have less modulation of muscle recruitment *across* tasks, we calculated 100-VAFby1 from a matrix in which muscle activity from 10 right leg gait cycles from each task were concatenated together. Differences between groups were identified with unpaired t-tests and Bonferroni corrections for multiple comparisons.

Results & Discussion: We found between-group differences in muscle coordination complexity both within and across walking tasks; particularly during and between straight-line walking and lateral stepping (Fig. 1). Consistent with our first hypothesis, we found that older adult fallers exhibited less complexity than non-fallers during treadmill walking (TM, p=0.01) and than younger adults for the stance limb during precision stepping (PS_{st}, p=0.08). Reduced muscle coordination complexity in older adult fallers likely reflects a balance strategy involving heightened muscle co-activation [5]. It is possible as we increase the number of older adult fallers that more differences within other tasks will emerge. Interestingly, we found older adult non-fallers were *more* complex than younger adults during overground walking (OG, p=0.02). This contrasts previous work in which young adults and older adult non-fallers were of similar complexity when walking on a treadmill [1], pointing to a potential difference in how older adults walk on a treadmill versus overground. For example, this finding is consistent with increased step-to-step variability in overground walking that occurs with age [6]. Finally, consistent with our second hypothesis, we found older adult fallers were less complex than non-fallers across all tasks (Fig. 1B, p<0.01). Here, reduced complexity may be due to older adult fallers being less flexible in their muscle recruitment across tasks, whereas older adult non-fallers and younger adults better modulate their muscle coordination and recruitment to meet the different task demands.

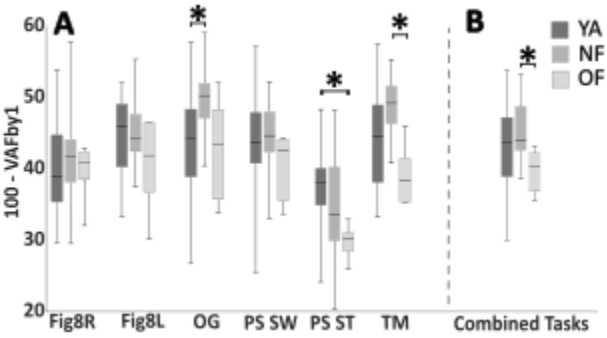

Figure 1 Between-group differences (A) within each walking task and (B) across all walking tasks. (Fig8R – figure 8 right turn; Fig8L – figure 8 left turn; OG – overground walking at preferred speed; PS SW – precision stepping when swing leg; PS ST – precision stepping when stance leg; TM – treadmill walking at preferred speed; * p<0.05, # p<0.1)

Significance: Our results confirm that muscle recruitment for walking is less complex in older adult fallers compared to those who have not fallen. Moreover, we observed this reduction across various walking tasks, potentially reflecting an inability to modulate muscle recruitment to accommodate different task demands. These findings underscore the importance of incorporating task-specific efforts to retrain appropriate muscle coordination, particularly those at risk for falls.

Acknowledgments: Supported by a grant from NIH R21AG067388.

References: [1] Allen and Franz (2018), *J Neurophysiol* 120(5), [2] Maddox et al. (2023), *American Society of Biomechanics*, [3] Selgrade et al. (2020), *J. of Biomechanics* 109710(104), [4] Steele et al. (2015), *Dev Med Child Neurol* 57(2), [5] Chambers et al. (2007), *Gait Posture* 25(4), [6] Callisaya et al. (2020), *Age Ageing* 39(2)

RAPID FORCE PERFORMANCE DISTINGUISHES PEOPLE WITH PARKINSON'S DISEASE FROM HEALTHY AGING

Rebecca J. Daniels[1*], Christopher A. Knight[1]
[1]Kinesiology and Applied Physiology, University of Delaware, Newark, DE
*Corresponding Author: rdaniels@udel.edu

Introduction: Clinical research in Parkinson's disease (PD) needs objective, easy-to-implement measures to quantify the underlying pathophysiology and progression of motor symptoms. Rapid isometric contractions have been used to study disease-related slowing in people with PD. During experiments of rapid isometric force production in healthy adults, the time to peak force is kept relatively constant, regardless of the amplitude [1]. The nervous system achieves this by modulating the rate of force development (RFD), so that higher RFD accompanies larger contractions [1]. The slope of the linear relationship between peak force amplitude and peak RFD (rate of force development scaling factor, RFD-SF) and its R^2 can be quantified, and provides us with a measure of neural control of rapid movements. In PD, people lose the ability to modulate their RFD, such that larger contractions have a prolonged time to PF. Additionally, some people with PD have interruptions in their neuromuscular excitation (segmentation) which result in greater reductions and variability in their RFD, and a disjointed appearing force-time curve [2]. RFD-SF and segmentation are reliable [2,3] measures derived form a non-invasive, time-efficient protocol that precisely identifies impairments and causes of slowing in people with PD compared to healthy older adults [2], and may provide a potential biomarker of PD. Thus, the first aim of this study was to determine whether RFD-SF, R^2 or segmentation could ascertain whether a person has PD. We hypothesized that all dependent measures would significantly determine PD from healthy aging. The second aim of this study was to determine which measure was best able to differentiate people with PD from healthy older adults. We hypothesized that R^2 would best differentiate between groups.

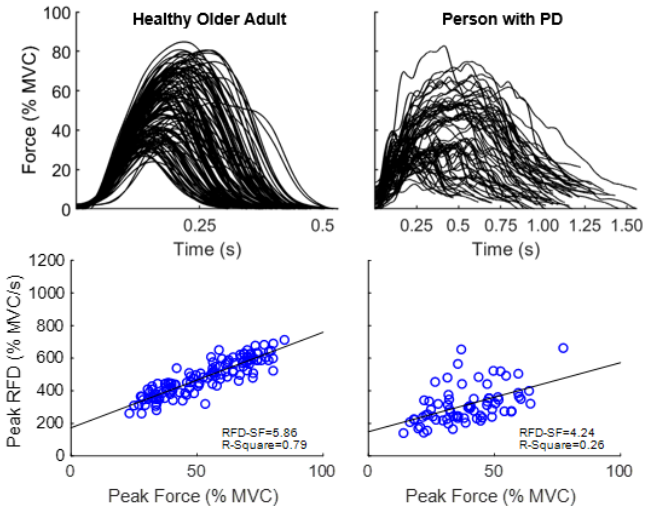

Fig. 1: Force pulse overlay (top) and rate of force development scaling factor plot (bottom) for a healthy older adult subject (left) and person with Parkinson's disease (right).

Methods: This study included 45 people with Parkinson's disease (aged 68.3±7.9 years, 5.1±3.8 years since diagnosis, Levodopa equivalent daily lose=547.2±355.7 mg, Hoehn and Yahr stage 1-4) and nine healthy older adults (aged 77.5±8.8 years). Subjects performed approximately 75 rapid isometric finger abduction force pulses to 20-80% of their maximal voluntary contraction force (MVC) against a force transducer while they viewed feedback of their force on a computer monitor. The first (RFD) and second-time derivatives of force (F"(t)) were calculated using a moving slope function with an overlapping 50 ms window. An RFD threshold of 20% MVC/s determined the start and end of each force pulse. Peak force and the peak RFD were determined for each force pulse. Linear regression was used to quantify the relationship between peak force and peak RFD. Dependent measures included from the regression include the slope (rate of force development scaling factor, RFD-SF), and its R^2. The number of force segments was also calculated from the number of zero crossings in F"(t) from force initiation to 90% of peak force [2]. The median number of force segments for force pulses between 30-50% MVC was used for analysis. Binary logistic regression was used to determine if RFD-SF, R^2 or segmentation were able to predict group membership.

Results & Discussion: Logistic regression models for RFD-SF ($\chi^2(1)=9.19$, p=0.002, Nagelkerke $R^2=0.26$, 85.2% of subjects correctly classified), R^2 ($\chi^2(1)=9.34$, p=0.002, Nagelkerke $R^2=0.27$, 81.5% of subjects correctly classified), and segmentation ($\chi^2(1)=17.87$, p<0.001, Nagelkerke $R^2=0.47$, 83.3% of subjects correctly classified) were all significant, though the model for RFD-SF had the best overall performance correctly predicting 97.8% of people with PD and 22.2% of healthy older adults. All models were more successful at identifying people with PD compared to healthy adults, though our healthy adult sample was older than the PD sample (t=3.12, p=0.001) and small. Considering that aging affects RFD-SF and R^2 [4], and there are instances of very old adults having segmentation [2], the performance of these models may improve by more age-matched subjects in the healthy group. Overall, these findings indicate that our force measures may be promising biomarkers for Parkinson's disease.

Significance: RFD-SF, R^2, and motor segmentation provide comprehensive and precise measures of neuromuscular control impairments during rapid movement that contribute to slowing in people with PD. These measures significantly distinguish PD from healthy aging and may provide potential disease markers or outcome measures during intervention studies.

Acknowledgements: This research was funded by Shake It Off Inc., West Chester, PA.

References: [1] Büdingen & Freund (1976), *Eur J Physiol* 35(2); [2] Howard et al (2022), *Exp Brain Res* 240(7-8); [3] Bellumori et al (2011), *Exp Brain Res* 212(3); [4] Bellmori, et al (2013), *Motor Control* 17(4).

OLDER ADULTS WALK WITH KNEE JOINT MOTION THAT IS MORE DYNAMICALLY STABLE WITH HIGHER DIMENSIONALITY THAN YOUNG ADULTS

Elham Alijanpour[1], Daniel M. Russell[1*]
[1]Kinesiology and Rehabilitation Ph.D. Program, Old Dominion University
*Corresponding author's email: dmrussel@odu.edu

Introduction: Walking, a fundamental human movement requires dynamic stability to be maintained [1]. However, older adults appear to be less stable [2-4] and more susceptible to falls while walking [5]. Previous studies found decreased stability of lower extremity muscle activity [6] and joint velocity [4,7], angle, and displacement [4] in older adults. Contrary to these results some studies found no effect of age on stability of hip joint acceleration [8-9]. These different findings could stem from different measures of stability or indicate differences between joints. In the current study we quantified dynamic stability as the rate of divergence of nearby trajectories in state space (Lyapunov exponent, LyE) and hypothesized aging compromises stability of lower extremity joint motion during walking. Aging may also impact complexity of the joint motion state space, which can be quantified through correlation dimension (CD) [3]. We hypothesized that increased joint motion dimensionality (complexity) with age may co-occur with reduced stability. As walking speed may impact stability and dimensionality differentially with age, we investigated young and older adults walking at five different speeds as a percentage of their preferred walking speed (PWS).

Methods: Ten young (f= 5, age= 25.2±3.2 years, height= 1.72±0.8 m, weight= 74.0±12.2 kg, PWS= 1.32±0.10 m/s) and nine older (f= 4, age= 71.57±4.54 years, height= 1.75±0.09 m, weight= 73.82±12.56 kg, PWS= 1.23±0.11 m/s) healthy adults with no history of falls participated in the study. They were asked to walk on an instrumented mat (Protokinetics, USA) to calculate PWS as an average of five trials. A CGM2.4 marker model and a ten-camera Vicon motion capture system recorded lower extremity joint angle data while participants walked on an instrumented treadmill at five different speeds (80%, 90%, 100%, 110%, and 120% of their PWS), for three minutes at each. Stability and dimensionality of ankle, knee, hip, and pelvis sagittal plane angles were computed using LyE and CD, respectively. Mixed design ANOVA tests were used to investigate the effects of speed and age on joint motion stability and dimensionality.

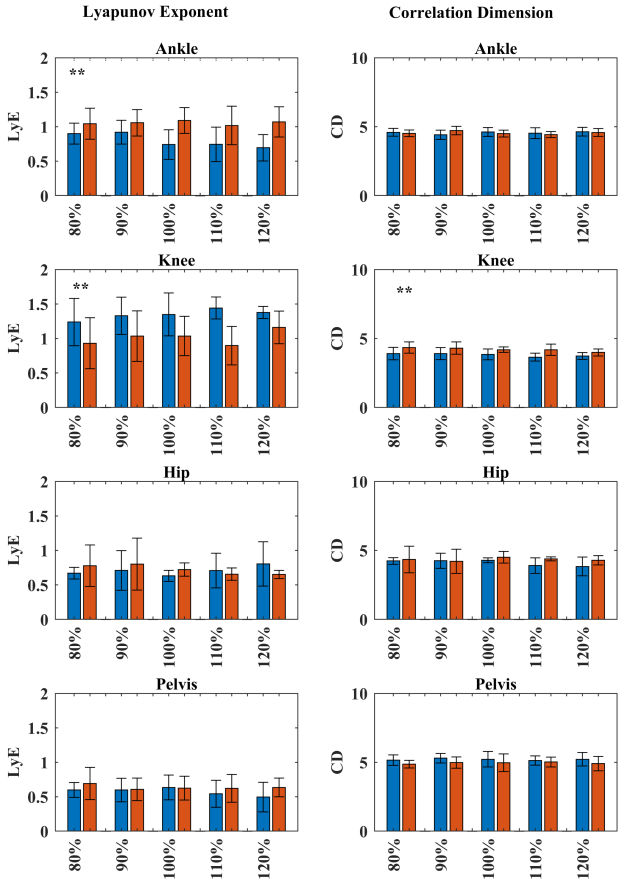

Figure 1: Results of short term Lyapunov Exponent (LyE) (first column) and correlation dimension (CD) (second column) for lower extremity joints. ** shows group differences. There was no significant effect of speed on the measured variables. Blue and orange bars represent young and older groups, respectively.

Results & Discussion: Results revealed age-related differences in joint motion stability (see first column of Fig. 1). Specifically, older adults exhibited decreased stability (greater LyE) in the ankle joint ($F\ (1,17) = 12.61,\ p < 0.002,\ \eta^2 = 0.426$) but increased stability (lower LyE) in the knee joint ($F\ (1,17) = 13.83,\ p < 0.002,\ \eta^2 = 0.435$) compared to the young group. There were no speed and interaction effects on joint motion stability and no age-related effect on the stability of the hip and pelvis motion. Only knee motion dimensionality differed between age groups. Older adults exhibited higher correlation dimension in the knee joint ($F\ (1,17) = 8.28,\ p < 0.01,\ \eta^2 = 0.328$) compared to young adults. Rather than older adults producing more complex and less stable joint motions, these findings highlight that the effects of age on stability and complexity of joint motion during walking depends on the joint being considered. Increased stability and dimensionality of knee motion is consistent with Buchanan et al. [10] and Fink et al. [11], who demonstrated that additional degrees-of-freedom (dimensionality) can be recruited to enhance stability.

Significance: Joint motions in older adults are not uniformly less stable and more complex than young adults. Instead, the findings here suggest that older adults emphasize stabilizing knee over ankle joint motion during walking, which may be achieved by recruiting more active degrees-of-freedom (increased dimensionality). Understanding these changes with age could lead to targeted interventions and rehabilitation approaches tailored to preserving knee function, potentially reshaping research priorities in the field of aging.

References: [1] Holt et al. (1995), *J Motor Behavior,* 27, 164-178; [2] Terrier et al. (2015), *Gait and Posture*, 41(1), 170-174; [3] Buzzi et al. (2003), *J Clinical Biomechanics* 18.5, 435-443; [4] Peterson et al. (2020), *J Parkinson's Disease*, 10(1), 245-253; [5] Boyer et al. (2023), *Experimental Gerontology* 173; [6] Kang et al. (2009), *J Biomechanics*, 42(14): 2231-2237; [7] Hollander et al. (2022), *Gait & Posture*, 95: 284-291; [8] Lockhart et al. (2008), *Ergonomics*, 51(12): 1860-1872; [9] Qiao et al. (2018), *Gait & Posture*, 62: 80-85; [10] Buchanan et al. (1999), *J Motor Behavior*, 31(2): 126-144; [11] Fink et al. (2000), *Physical Review E*, 61(5): 5080.

EFFECTS OF TREADMILL PERTURBATION TRAINING ON LOCAL ORBITAL STABILITY IN CHIARI MALFORMATION

Brittany N. Sommers[1*], Antonie J. van den Bogert[1], Brian L. Davis[1]
[1]Cleveland State University, Cleveland, Ohio, Center for Human Machine Systems
*b.n.sommers@vikes.csuohio.edu

Introduction: Chiari Malformation (CM) is a congenital condition of the cerebellum resulting from herniation of the cerebellar tonsils into the spinal canal. CM symptoms are commonly defined as severe headaches, lack of balance control, poor joint coordination, and muscular weakness. There is no cure for CM, but a decompression surgery is used to maintain headache severity and tonsil herniation. Cerebellar damage is hypothesized to impair the ability to adapt and retain new movement information. This is due to adaptive responses stemming from cerebellar functioning [1]. Since CM is an anatomical malformation of the cerebellum, and not a neurodegenerative condition, it was hypothesized that there may be an ability to develop adaptive or retention responses in CM following perturbation training.

This hypothesis was tested with Floquet multipliers (FMs), a local orbital stability measure. FMs measure cycle-to-cycle stability in response to small internal perturbations. FMs are calculated at one specific, well-defined point of the gait cycle, such as heel strike or toe off, from a Poincaré map. The Poincaré map is a state space representation of 3D positions and velocities of interest [2,3].
Since CM is an anatomical cerebellar malformation, it was hypothesized that there would be improvements in local stability following treadmill perturbation training. This would suggest the ability to adapt to new movement patterns and retain this information, which drives the motivation that neuromuscular rehabilitation efforts are needed in CM, regardless of decompression surgery.

Methods: Data were collected on 12 adult CM participants, and 12 age and weight matched controls. The study was conducted in accordance with an IRB approved protocol at Cleveland State University. All participants completed five walking trials on a split-belt MOTEK M-Gait treadmill. Three of the trials were perturbation intervention trials. Prior to and after perturbation training unperturbed walking trials were performed. The unperturbed walking trials were used in the assessment to test for changes in local orbital stability (FMs). Unperturbed walking trials were 5-minutes each in duration and are denoted as "baseline" (before perturbation training), and "aftereffect" (after all three perturbation trials). 20-minute breaks were required between the final perturbation trial and the aftereffect trial. Perturbation trials were 7-minutes each in duration, with six left and six right perturbations delivered at mid-stance during each perturbed trial. Perturbations were delivered as rapid accelerations of the respective belt. Perturbation magnitudes were fixed to 0.4 m/s for all participants.

State space representations were taken as the 3D positions and velocities of the ankle, knee, and hip (***X***). Two state space matrices were created for left and right limb data. The matrices were time normalized from 0-101 points between each step. From the matrices, the heel strike instances for each step were used as the Poincaré section for the FM analysis. FMs were calculated according to the methods described by McAndrew et al [2] and Hurmuzlu et al [3]. FMs for each trial were calculated as the average magnitude of the 18 eigenvalues [3]. FMs < 1 represent stability for gait, with lower values indicating greater stability. [2,3]

Results & Discussion: One-sample t-tests were used to test for significant differences between baseline and aftereffect FM values *within* groups. For each group, Bonferroni corrections were used to account for the two t-tests, thus $\alpha = 0.025$. The control group displayed significant reductions in average FM for both the right ($p = 0.019$) and left ($p = 0.0072$) heel strike instances. In the CM group, reductions were only significant for the right heel strike instances ($p = 0.024$) (Table 1). No significant differences were found *between* group baseline and aftereffect values. Improvements in gait stability were seen in reduced average FM values following perturbation training. For three instances, these improvements were significant. Participants were required to take a 20-minute break to test for any signs of retention to the training. These results suggest that, at least on a short-term time frame, there are retention effects for gait stability seen in both non-impaired controls and individuals with CM. This supports the hypothesis that Chiari being an *anatomical* cerebellar malformation, and not a *degenerative* condition, may allow for a level of adaptation and retention not previously recognized.

Table 1: *Average FMs at heel strike. B = Baseline, A = Aftereffect, and significant differences are indicated with bold p-values.*

Group	***Equilibrium Point***	***Average FMs***	***Significance (α = 0.025)***
Chiari	Right heel strike	B: 0.336 ± 0.0345 A: 0.313 ± 0.0115	***p = 0.024****
Chiari	Left heel strike	B: 0.327 ± 0.0218 A: 0.309 ± 0.0201	*p = 0.028*
Control	Right heel strike	B: 0.324 ± 0.0164 A: 0.310 ± 0.0181	***p = 0.019****
Control	Left heel strike	B: 0.326 ± 0.0336 A: 0.293 ± 0.0277	***p = 0.0072****

Significance: There is no cure for CM, or standard rehabilitation practices for the neuromuscular symptoms. This study showed that individuals with CM do have the ability to improve adaptive movement performance. It is the goal that this further drives the need for rehabilitation efforts in CM, regardless of surgical intervention, and that dynamic movement trainings will be implemented routinely by clinicians and physical therapists.

Acknowledgments: Acknowledgements are made to the Conquer Chiari Research Center for participant recruitment.

References: [1] Bastian A. *Curr Opin Neurobiol.* (16):645-9. 2006; [2] McAndrew P, et al. *J Biomech.* (44):644-9. 2011 [3] Hurmuzlu Y, et al. *J Biomech Eng* (116):30-6. 1994.

EFFECT OF SPINAL STIMULATION AND INTERVAL TREADMILL TRAINING ON GAIT MECHANICS IN CHILDREN WITH CEREBRAL PALSY

Charlotte D. Caskey[1]*, Siddhi Shrivastav, Victoria M. Landrum[1], Kristie Bjornson, Desiree Roge, Chet Moritz, Katherine M. Steele[1]
[1]Department of Mechanical Engineering, University of Washington, Seattle, WA
*Corresponding author's email: cdcaskey@uw.edu

Introduction: Children with cerebral palsy (CP) have a brain injury around the time of birth that affects the development of neuromuscular motor control and integration of sensory information. Many children with CP have spasticity, an exaggerated stretch reflex, which is thought to contribute to altered gait mechanics [1]. Transcutaneous spinal cord stimulation (tSCS) is a novel, non-invasive neuromodulation technique that activates sensory pathways to amplify communication in the nervous system [2]. Our prior work has shown that pairing tSCS with short-burst interval locomotor treadmill training (SBLTT) reduced spasticity more than SBLTT alone and may lead to increases in peak hip and knee extension and total joint excursion during overground walking [3]. This study sought to evaluate the effects tSCS paired with SBLTT on the coordination of hip and knee extension and subsequent muscle-tendon lengths (MTLs) throughout the gait cycle. Due to the reductions in spasticity from tSCS and SBLTT, we hypothesized that hip and knee kinematic trajectories will be more extended throughout the gait cycle with an increase in peak operating MTLs during gait.

Methods: Four children ages 4-13 years old with spastic CP received 24 sessions each of intervention, first SBLTT only followed by tSCS + SBLTT. There was an 8-week follow-up after each intervention. Spasticity and biomechanical walking assessments were collected the week before and after each intervention and at the end of each 8-week follow-up. Spasticity was evaluated using the Modified Ashworth Scale for the quadriceps, hamstrings, gastrocnemius, and soleus muscles bilaterally. Optical motion capture data were also collected during barefoot, overground, self-selected walking on a 10-meter walkway. Data were processed using custom MATLAB scripts (MathWorks, Natick, MA, USA) and OpenSim v4.3 (Stanford, USA). Statistical parametric mapping was used to compare changes in joint kinematics during each phase and at follow-up timepoints with respect to the timepoint corresponding to the start of that phase. A Bayesian Additive Regression Trees (BART) model was built to isolate the direct effect of spasticity on MTLs, while controlling for participant, muscle, side of the body, study timepoint, and walking speed.

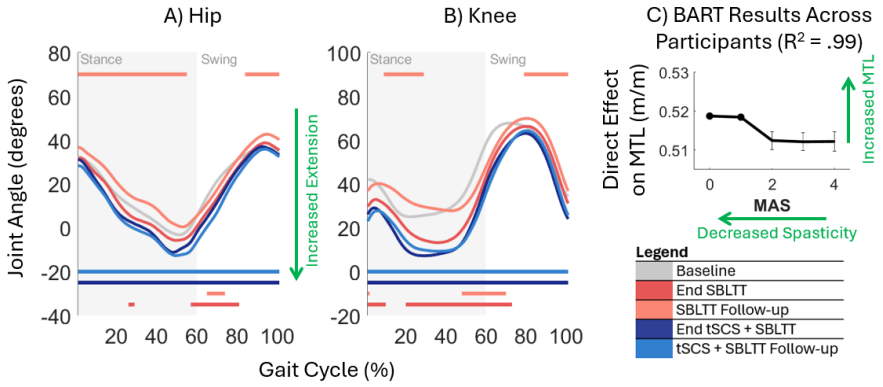

Figure 1: A) Hip and B) knee kinematics during the gait cycle from an example participant. Horizontal colored lines indicate where there were significant changes in kinematics over each phase of the study based on statistical parametric mapping ($p<0.05$). Lines on top indicate locations of significant increases, while lines on the bottom indicate points of significant decreases. C) Bayesian Additive Regression Trees (BART) results quantify direct effects of spasticity as measured by the Modified Ashworth Scale on muscle-tendon lengths (MTL) across muscles. Results are visualized using Accumulated Local Effects Plots.

Results & Discussion: All four participants exhibited the greatest improvements in hip and knee extension after tSCS + SBLTT at 8-month follow-up after tSCS + SBLTT (Figure 1A and B; example from one participant). For the example participant, both the hip and knee were more extended throughout the entire gait cycle after tSCS + SBLTT. This increased extension was maintained into the 8-week follow-up period (Figure 1A and 1B). The BART model using all participants' spasticity data and peak operating MTL had high model fit (R^2 = 0.99) with reductions in spasticity corresponding to a 7.7 mm/m increase in MTL, after controlling for participant, muscle, side of the body, study timepoint, and walking speed (Figure 1C). Current spasticity treatments reduce spasticity but do not consistently translate to improved walking function without extensive additional rehabilitation [4]. These results suggest that tSCS + SBLTT may be able to reduce spasticity while maintaining walking mechanics. Future work should consider by what mechanisms joint extension increases, while MTLs have minimal change.

Significance: This pilot study provides foundational work for developing our understanding of the mechanisms behind which tSCS affects movement for children with CP and how the observed reductions in spasticity with tSCS may affect gait. We highlight the importance of quantifying clinical assessments, such as those for spasticity, with biomechanical outcomes to better understand how novel treatment options translate to changes in function that impact daily life.

Acknowledgments: This work was supported by Seattle Children's Hospital CP Research Pilot Study Fund 2020 Award, UW Rehabilitation Medicine Walter C. and Anita C. Stolov 2021 Research Fund, and NSF Graduate Research Fellowship Program Award DGE-1762114.

References: [1] van der Krogt et al. (2009), *Gait Posture* (29)2009; [2] Edgerton et al. (2021) *Front. Hum. Neurosci.* (15)643463; [3] Shrivastav, Caskey, et al. (2023) *Preprint: medRxiv*; [4] MacWilliams et al. (2022) *DMCN* (64)5

DOES BALANCE CONFIDENCE PREDICT WALKING ACTIVITY POST-STROKE? A DOMAIN-SPECIFIC APPROACH

Grace K. Kellaher[1*], Allison Miller[2], Ryan T. Pohlig[1], Tamara Wright[1], Henry Wright[1], Darcy S. Reisman[1], and Jeremy R. Crenshaw[1]
[1]University of Delaware, Newark, DE; [2]Washington University School of Medicine, St. Louis, MO
*Corresponding author's email: gkk@udel.edu

Introduction: The low balance confidence that is characteristic of persons with chronic stroke[1] is an underlying influence on the limited walking activity levels in this population[2,3]. Balance confidence can be assessed with the Activities-Specific Balance Confidence (ABC) scale, which specifically assesses confidence in performing tasks within the domains of anticipatory control, walking balance, and reactive balance (Table 1). We consider these domains to be functionally distinct[4,5], as improving function in one balance domain does not necessarily translate to improvements in another[5]. The current measures of balance confidence are not domain specific, and therefore are limited in their capacity to inform the targets for domain-specific balance interventions. The purpose of this study was to identify the specific aspects of balance confidence that predict walking activity after stroke in the free-living environment. Doing so will inform the candidate targets for domain-specific balance interventions to improve walking activity, as mediated by improvements in balance confidence.

"How confident are you that you will not lose your balance or become unsteady when you…"	Score (%) Mean(SD)	Proposed Balance Domain
…walk around the house?	87.73(18.24)	walking
…walk up or down stairs?	79.54(23.74)	walking
…walk outside the house to a car parked in the driveway?	80.37(24.46)	walking
…walk across a parking lot to the mall?	93.99(12.78)	walking
…walk up or down a ramp?	71.97(29.14)	walking
…walk in a crowded mall where people rapidly walk past you?	44.56(36.55)	walking
Walking Balance Confidence	**84.41(17.23)**	-
…bend over and pick up a slipper from the front of a closet floor?	81.87(27.22)	anticipatory
…reach for a small can off a shelf at eye level?	89.90(17.60)	anticipatory
…get into or out of a car?	90.25(17.48)	anticipatory
…sweep the floor?	86.28(20.71)	anticipatory
…stand on your tip toes and reach for something above your head?	84.54(20.86)	anticipatory
…stand on a chair and reach for something?	78.49(25.24)	anticipatory
Anticipatory Balance Confidence	**77.15(17.79)**	-
…are bumped into by people as you walk through the mall?	70.92(28.32)	reactive
…step onto or off of an escalator while holding onto a railing?	75.27(30.72)	reactive
…step onto or off an escalator while holding onto parcels such that you cannot hold onto the railing?	51.80(35.65)	reactive
…walk outside on icy sidewalks?	40.26(32.90)	reactive
Reactive Balance Confidence	**59.56(27.15)**	-
Total ABC Score	**75.48(17.92)**	-

Table 1. Domain categorization of ABC Scale.

Methods: This study is a secondary analysis of baseline balance confidence and walking activity data collected as part of a multi-site clinical trial (PI: Reisman, NIH R01HD086362). Participants six or more months post-stroke between 21-85 years of age were included (n = 399; 210M/189F; age: 63.8(12.4) years; time since stroke: 3.6(4.7) years). To measure balance confidence, participants completed the ABC scale. The questions of the ABC scale were then categorized into three different domains of balance (walking, anticipatory, reactive) that align with the domains defined in the Mini-BESTest, a clinical balance test[6] (Table 1). A domain-specific average ABC sub-score was then calculated. Walking activity was monitored with a worn sensor on participant's non-paretic ankle for a minimum of three days. Walking-activity data were recorded and processed as described previously[7]. Four walking activity measures were calculated from the sensor data: activity volume (steps per day), activity frequency (bouts per day), activity intensity (average bout cadence), and sedentary behavior (percent sedentary time). Separate multiple linear regressions were conducted to determine the relationships between domain-specific balance confidence and walking-activity measures.

Results & Discussion: All models moderately predicted walking activity (R^2=0.08-0.11, $p<0.01$), confirming the general relationship between balance confidence and walking activity. Confidence with anticipatory control (β=24.7, $p=0.047$) and reactive balance (β=18.2, $p=0.010$) predicted activity volume. Confidence with anticipatory control (β=0.35, $p<0.01$) predicted activity frequency. Confidence with reactive balance (β=0.045, $p<0.01$) predicted activity intensity. Confidence with anticipatory control (β=-0.11, $p<0.01$) and reactive balance (β=-0.04, $p=0.04$) predicted sedentary behavior.

These results suggest domain-specific links between balance confidence and walking activity. Counterintuitively, walking balance confidence did not predict walking activity measures. Anticipatory-control confidence may influence activity frequency (i.e., the number of bouts) due to the influence of gait initiation, a skill that is altered after stroke[8]. Reactive-balance confidence may influence activity intensity (i.e., cadence) as people walk slower (and therefore have lower cadences) to protect against a fall from a trip[9] or slip[10].

Significance: We have identified specific domains within the ABC scale that correspond with activity volume, frequency, intensity, and sedentary behavior in individuals with chronic stroke. These results provide experimental targets for determining how changes in balance confidence relate to changes in walking activity. Balance confidence can be improved through skill mastery[11], so specifically targeting anticipatory and reactive balance may be key to improving walking activity in post-stroke individuals.

Acknowledgments: This work was supported, in part, by NIH Grant NIH R01HD086362.

References: [1] Salbach et al. (2006, *Arch Phys Med Rehabil* 87(364); [2] Schmidd et al. (2012), *Arch Phys Med Rehabil* 93(1101); [3] Danks et al. (2016), *J Neuro Phys Ther* 40(232); [4] Gill-Body et al. (2021), *Phys Ther* 101(153); [5] Grabiner et al. (2014), *Exer and Sport Sci Reviews* 42(161); [6] Franchigoni et al. (2010), *J Rehabil Med* 42(323); [7] Miller et al. (2022), *J NeuroEngineering Rehabil* 19(111); [8] Sousa et al. (2015), *Clin Biomech* 30(960); [9] van Dieën et al. (2005), *Safety Sci* 43(437); [10] Chambers et al. (2013), *IISE Transactions on Occupational Ergonomics and Human Factors* 1(166); [11] Feltz et al. (2005), *Quest* 57(24)

STEADY EARWORMS: WITHIN TRIAL DIFFERENCES OF MUSIC VS MENTAL SINGING DURING GAIT IN PD

Sidney T Baudendistel[1*], Allison M. Haussler[1], Lauren E. Tueth[1], Elinor C. Harrison, PhD[2], Gammon M. Earhart[1,3,4]
[1]Washington University in St. Louis School of Medicine, Program in Physical Therapy
*Corresponding author's email: bsidney@wustl.edu

Introduction: Parkinson disease (PD) is a neurodegenerative disease that significantly impairs walking ability. People with PD walk with slower, shorter, and with more variables steps than their peers [1]. These spatiotemporal variables are significantly related to falls, community independence, and ultimately mortality [1,2]. Rhythmic auditory stimulation (RAS) is one type of cue-based rehabilitation demonstrated to improve multiple aspects of walking in PD [2]. Our group previously investigated the potential benefits of external cueing (listening to music) compared to internal cueing (i.e. mental singing a song in one's head). While both external and internal cues improve gait velocity and stride length compared to no cue [2], only internal cueing reduces variability [3]. Importantly, these results are based on the combined average of the steps during multiple, 30-second trials. It is unknown how well individuals with PD can maintain a stable rhythm within trials and if there is a difference in pace stabilization between cue types. Therefore, the purpose of this investigation was to compare cadence during the first ten seconds and the last ten seconds of cued gait to determine if cadence degrades over time. As the mental singing trials were done in silence, we hypothesized that cadence would degrade more during mental singing than music, in which the cue was given externally throughout the duration of the trial. As beat detection, generation, and continuation are impaired in PD [4,5], we also hypothesized that cadence would degrade more for people with PD than healthy, older adult controls.

Methods: Individuals with PD (N = 52) and controls (N = 66) first completed trials of preferred walking while wearing six APDM sensors on the wrists, ankles, sternum, and lumbar spine. The average cadence of these three trials was used to calculate four cue rates, performed in random order: 90%, 100%, 110%, and 120% of preferred walking cadence. For each cue rate, two types of cues were performed also in random order: walking while listening to music ("Music") and walking while mentally singing the same song ("Mental"). Participants individually selected their cue song from a standardized catalogue. During the Music trials, one chorus of the cue song was played aloud at the specified tempo before participants began walking and then continued throughout the trial. During the Mental trials, one chorus of the cue song at the specific tempo was played prior to the beginning of the trial, allowing for the participant to internalize the tempo. The song stopped playing prior to the participant walking. All conditions included three, 30-seconds trials.

Following data collection, the average stride length of the Music and Mental conditions were combined at each cue rate for each participant. The cue rate with the longest combined stride length was determined as the "optimal" cue rate allowing for personalization of cues for each individual, similar to [6]. Only the "optimal tempo" trials were analysed for each person in this particular analysis. Within each trial, individual step data was divided into three, ten-second bins, and averaged within each bin. To investigate the changes of cadence within trial, we conducted a three-way analysis of variance (ANOVA) [(Condition: Mental, Music) × (Time: first ten seconds of trial, last ten seconds of trial) x (Group: PD, controls)] to compare mean cadence for each condition across time and between groups at the personalized, optimized cueing tempo. Significance was set to $p \leq 0.05$.

Results & Discussion: We rejected our initial hypothesis that there would be significant differences in cadence between the steps in the first ten seconds compared to the last ten seconds of a 30-second walking trial. None of the individual effects were significant within the model including Condition ($p = .450$), Time ($p = .163$), and Group ($p = .371$). The interactions of Condition × Time ($p = .957$), Condition × Group ($p = .665$), Time × Group ($p = .866$), and Condition × Time × Group ($p = .845$) were also not significant (Figure 1). We chose each individual's optimized cue rate in this analysis and did not consider the percentage from their preferred walking baseline. Covarying for the cue rate chosen as optimal (i.e., 90%, 100%, 110%, 120%) had no effect on the results. Collectively, these results indicate that both people with PD and controls were able to maintain similar levels of cadence at the beginning and end of the trial regardless of cue type. Future studies investigating longer trial times, synchronization rate, and longitudinal training of mental singing as a form as RAS would be of particular interest.

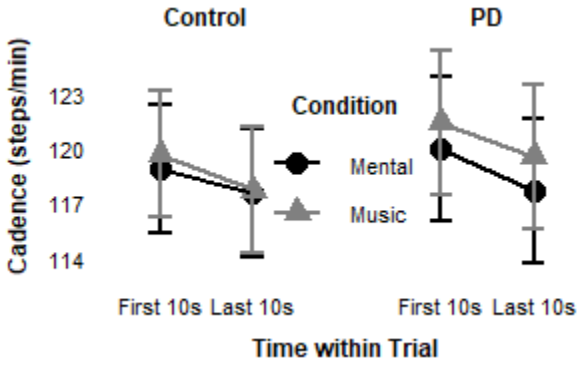

Fig. 1. Average cadence of individuals with and without PD within 30 second trials using two different cues. Error bars represent 95% confidence intervals.

Significance: These results provide further evidence that mental singing may be a viable type of RAS that can be maintained over time. Mentally singing a song can be completed without any devices or aids and may be undetectable to bystanders, potentially reducing stigma of using these tools during their everyday life.

Acknowledgments: This study was funded by the National Institutes of Health [T32HD007434, TL1TR002344, R61AT010753, R33AT010753] and supported by the Greater St. Louis American Parkinson Disease Association (APDA), the APDA Advanced Center for Parkinson Research, and the GRAMMY Museum Grant Program.

References: [1] Mirelman et al. (2019), *Lancet Neurol* 18(697-708); [2] Horin et al. (2020), *Gait Posture* 82(161-166); [3] Harrison et al. (2019), *J Neurol Phys Ther* 43(204-211); [4] Grahn et al. (2009), *Cortex* 45(54-61); [5] Bella et al. (2014), *Front Hum Neurosci* 8(494); [6] Bella et al. (2017), *Sci Rep* 7(42005).

TRANSFERRING INCREASED MOVEMENT AMPLITUDE ACROSS GAIT TASKS IN PARKINSON DISEASE

Chelsea "CJ" Duppen[1], Nina Browner[2], Michael D Lewek[1,3]
[1]Human Movement Science Curriculum, University of North Carolina at Chapel Hill
*Corresponding author's email: chelsea_parker@med.unc.edu

Introduction: People with Parkinson disease (PD) demonstrate small magnitude movements (hypokinesia) when initiating gait, as evidenced by shortened step lengths and smaller anticipatory postural adjustment (APA) sizes [1,2]. These small magnitude movements mirror the shortened step lengths seen during continuous walking [3] and are associated with a heightened risk for falls and reduced functional independence [4,5]. Addressing *gait initiation* impairment is especially pertinent, given its role as the necessary precursor to safe and independent ambulation. Gait initiation and continuous walking share similarities (such as reduced step lengths), which may allow for a transfer of improved movement amplitude between the two tasks. However, the unique requirement of APAs in gait initiation may not be addressed by continuous walking training alone. The purpose of this study was to determine whether a single session of *continuous walking* training for increased movement amplitude would translate to larger movement amplitudes during *gait initiation*. Based on the similarities in step length impairment between the two tasks, we hypothesized that training for increased step lengths during continuous walking would result in longer first steps during gait initiation. However, given the diminished postural control requirements during continuous walking, we hypothesized this training would yield no change in APA size during gait initiation.

Methods: Eleven adults with idiopathic PD (Hoehn & Yahr stages I-III) completed five trials of gait initiation before and after ten minutes of treadmill walking. The treadmill was set to comfortable overground gait speed while participants timed their steps to a metronome beeping at 85% of their comfortable overground cadence to elicit increased step lengths [6]. All gait initiation trials were completed without external cueing. First step length was measured from heel to heel when the initial stepping extremity made initial contact with the ground. Anticipatory postural adjustments were measured as the maximum posterior (anteroposterior) and lateral (mediolateral) center of pressure shift towards the initial stepping limb prior to toe-off. To determine the effects of a single session of training for increased movement amplitude during continuous walking on gait initiation metrics, paired samples t-tests were performed for first step length, mediolateral and anteroposterior APA size ($\alpha = 0.05$).

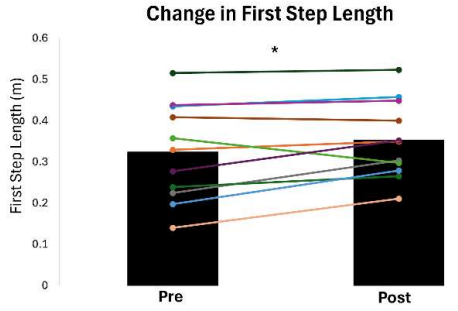

Figure 1: First step length during gait initiation before and after 10 minutes of continuous walking performed while cued for increased movement amplitude (p=0.048; d=0.678). The bar graphs denote average values.

Results & Discussion: After a single session of practicing increased step amplitude during continuous walking, participants demonstrated an increase in first step length during gait initiation ($p = 0.048$, $d = 0.678$) (Figure 1). However, no differences were noted in mediolateral ($p = 0.995$, $d = 0.002$) or anteroposterior ($p = 0.621$, $d = 0.154$) APA sizes (Figure 2). This supports the hypothesis that step amplitude magnitude successfully transfers from continuous walking to gait initiation. Furthermore, these data highlight a lack of association between mediolateral ($r = 0.380$, $p = 0.250$) and anteroposterior ($r = -0.555$, $p = 0.076$) APA sizes and first step performance, consistent with recent literature [7]. Future research should investigate the relative importance of APAs and other postural control metrics in successful gait initiation.

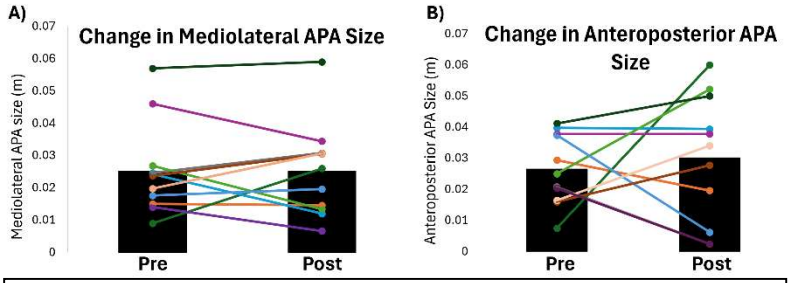

Figure 2: Mediolateral (A) and anteroposterior (B) APA sizes before and after training for increased movement amplitude during continuous walking. The bar graphs denote average values.

Significance: Difficulty initiating and maintaining gait are grouped under the umbrella term "freezing of gait", which is associated with high risk for falls and injury for people with PD [4,5]. The substantial time and financial burden of recurrent rehabilitation for people with PD [8] necessitates identifying the most effective and most efficient interventions. Historically, clinicians and researchers have adapted interventions used for continuous walking to address gait initiation impairments (such as laser canes and metronomes), while still treating them independently [9]. Our results suggest that a single session of training for increased step lengths during continuous walking may lead to increased first step lengths during gait initiation, despite having no bearing on APA sizes.

Acknowledgments: This work was supported in part by the National Center for Advancing Translational Sciences, National Institutes of Health TL1 Postdoctoral Training Program [5TL1TR002491-05] and the Foundation for Physical Therapy Research Promotion of Doctoral Studies I Award.

References: [1] Roemmich et al. (2012), *Gait Posture* 36(3); [2] Halliday et al. (1998), *Gait Posture* 8(1); [3] Galna et al. (2015), *Mov Disord* 30(3); [4] Okuma et al. (2014), *J Parkinsons Dis* 4(2); [5] Santos-Garcia et al. (2020) *Neurol Sci* Vol 41; [6] Chawla et al. (2020), *Motor Control* 25(1); [7] Suethe et al. (2024), *PLOS ONE* [8] Yang et al. (2020) *NPJParkD* 6(15); [9] McCandless et al. (2015) *Gait Posture* 44

Thank you to our Sponsors

AMTI
FORCE AND MOTION

Grainger Institute for Engineering
UNIVERSITY OF WISCONSIN–MADISON

destination madison

novel

QUALISYS

OptiTrack

THEIA
Markerless

Department of Mechanical Engineering
UNIVERSITY OF WISCONSIN–MADISON

COLLEGE OF ENGINEERING
BIOMEDICAL ENGINEERING AND MECHANICS
VIRGINIA TECH

XSENSOR
Intelligent Dynamic Sensing